CIRCUIT THEORY OF ELECTRON DEVICES

BOONE

WILLY

CIRCUIT THEORY
OF
ELECTRON DEVICES

CIRCUIT THEORY
OF
ELECTRON DEVICES

E. MILTON BOONE

PROFESSOR OF ELECTRICAL ENGINEERING
THE OHIO STATE UNIVERSITY

NEW YORK · JOHN WILEY & SONS, INC.
LONDON · CHAPMAN & HALL, LIMITED

Library of Congress Catalog Card Number: 53–7067

PRINTED IN THE UNITED STATES OF AMERICA

PREFACE

THIS BOOK HAS BEEN WRITTEN PRIMARILY FOR COLLEGE AND UNIVERSITY students. Most of the material included in the book has been used during the past ten years in note form by students enrolled in the electrical engineering and engineering physics curricula at The Ohio State University. Course prerequisites have included mathematics through differential and integral calculus, one year of physics at the sophomore level, and one year of work in circuit theory including some treatment of differential equations, transients, and Fourier series. The material is sufficient for a two-semester course and has been used at The Ohio State University during the last quarter of the third year and the first quarter of the fourth year of the electrical engineering curriculum.

The fundamental emphasis of this book is devoted to the circuit theory and not to the physics of electron devices. It is believed that analysis for the beginning student of electron devices should be limited *at first* to the circuit properties of the device, properties that can be determined by measurements at available terminals. Analysis of more difficult internal complexities may be deferred until circuit experience, confidence, and additional maturity have been developed by the student. The usual background of mathematics, physics, and electric circuit theory available to the third- or fourth-year engineering student serves quite well as preparation for the initial linear circuit theory of electron devices, but is inadequate for a thorough appreciation of an analysis carried to the level of electron dynamics and electron emission theory. These ideas based upon experience in years of teaching have led to the arrangement of this book. Some electron and ion physics is, of course, necessary, but this material has been integrated in the circuit theory where needed and is usually sufficient to satisfy the natural curiosity of the thorough student. At The Ohio State University, the material of this book is followed by course material devoted primarily to the physics of electron devices including field theory, electron dynamics, kinetic theory of gases, noise phenomena, and electron emission theory. By the time this more difficult material is presented the student has made con-

siderable progress in his understanding of the electron device as a circuit component and is prepared to appreciate an analysis of the internal complexities of the device.

The vacuum tube and the transistor as operated in the linear region of their characteristics have been treated in this book as four-terminal networks using the generalized admittance or impedance parameters of four-pole theory. This method was suggested to me by Mr. J. A. Morton of the Bell Telephone Laboratories. Much of the philosophy of presentation of the material of this book and some of the material as well have resulted from conferences and correspondence with Mr. Morton. It is a pleasure to acknowledge my indebtedness to him.

I am sincerely grateful to my colleagues at The Ohio State University for their many constructive criticisms and suggestions, and to students whose questions have often led to an improvement in presentation. Professor E. E. Dreese, chairman of the department of electrical engineering, has consistently encouraged the completion of the book and has offered valuable suggestions for its improvement. I am indebted to Professor W. G. Dow of the University of Michigan for introducing me to the field of electronics and for his continued interest in and appraisal of this book. All of the typing and processing of notes and manuscript involved in the preparation of this book has been done by Genevieve E. Bohrman whose skillful assistance has been invaluable and is gratefully acknowledged. It also seems appropriate to acknowledge my debt of gratitude to my wife, Nevada, for her encouragement and for her patient acceptance of the encroachment of manuscript preparation upon free time.

E. MILTON BOONE

Columbus, Ohio
April 1953

CONTENTS

1 ·	Diodes, Triodes, and Equivalent Circuits	1
2 ·	Tetrodes, Pentodes, and Equivalent Circuits	53
3 ·	Audio-Frequency Voltage Amplifiers	76
4 ·	The Audio-Amplifier Power Stage	149
5 ·	Gas-Filled Tubes as Circuit Elements	168
6 ·	Single-Phase Rectifiers and Power Supplies	188
7 ·	Polyphase Rectifiers	226
8 ·	Tuned Radio-Frequency and Band-Pass Amplifiers	249
9 ·	Radio-Frequency Power Amplifiers	290
10 ·	Vacuum-Tube Oscillators	321
11 ·	Modulation and Demodulation	355
12 ·	Circuit Theory of Transistors	415
	Index	471

CHAPTER 1

DIODES, TRIODES, AND EQUIVALENT CIRCUITS

Introduction

The study of electron devices has become an important and an essential part of any curriculum in electrical engineering. The uses of electron tubes are so numerous and so varied in complicated communication and industrial-control systems that it becomes necessary to consider the electron tube in rather general terms as a circuit element of certain particular properties. These circuit properties of electron tubes and other electron devices may be analyzed in their dependence upon the design of the component elements of the device, or they may be determined for practical application by a consideration of the device in its envelope as a "black box" from which extend certain terminals at which energy, force, voltage, etc. may be impressed and the resulting response measured. The latter point of view has the distinct advantage of permitting the intelligent use of the electron device as a circuit component without a prior knowledge of its interior complexities.

Engineering consists of a combination of the processes of analysis and synthesis. Analysis usually precedes synthesis, but it is of extreme importance that analysis be carried only so far as may be required for intelligent and efficient synthesis. For example, one may analyze a building designed to be a home in terms of its functional parts—kitchen, living room, bedrooms, bath, laundry, furnace room, and so on. The analysis may proceed much further, however, to include the concrete block, brick, cement, lumber, nails, pipes, and other components. The degree to which the analysis is carried depends upon the purpose to be served. Most electrical engineers who use electron tubes are concerned with the utilization of these tubes as component parts of systems. For such use, it is unnecessary to carry analysis to the level of complexity that becomes essential when the synthetic product is the tube itself. The tube engineer and the physicist must analyze the electron tube in terms of its dependence upon the materials of which it is built, the physical nature of these materials, and the effect of electric and mag-

netic field forces upon the motion of electrons within the device. Such analysis is complicated and difficult and may be postponed until the student has become familiar with the circuit behavior of electron tubes as determined at the available terminals of the tube.

1-1. Electron-Tube Definitions

Before proceeding with the circuit analysis of electron tubes, it is important to define certain terms in common use. It is assumed that the word "electron" has a definite meaning to the student from previous study or reading in physics, but it is not proposed to define the electron in this book.

The standard definitions proposed by the Institute of Radio Engineers for several important terms are given in the following list:

Electron tube. An electron tube is a device in which conduction of electricity takes place between two or more electrodes through an enclosed vacuum, gas, or vapor.

Vacuum tube. A vacuum tube is an electron tube evacuated to such a degree that its electrical characteristics are essentially unaffected by the presence of residual gas or vapor.

Gas tube. A gas tube is an electron tube in which the electrical characteristics are substantially affected by the presence of an enclosed gas or vapor.

Element (of an electron tube). An element of an electron tube is an integral part of the tube which contributes to its operation.

Electrode (of an electron tube). An electrode of an electron tube is a conducting element that performs one or more of the functions of emitting, collecting, or controlling by an electric field the movements of electrons or ions.

Thermionic tube. A thermionic tube is an electron tube in which one of the electrodes is heated for the purpose of causing electron or ion emission from that electrode.

Cathode. A cathode of an electron tube is an electrode through which a primary stream of electrons enters the interelectrode space.

Anode. An anode of an electron tube is an electrode through which a principal stream of electrons leaves the interelectrode space.

Grid. The grid of an electron tube is an electrode having one or more openings for the passage of electrons or ions. (ASA* definition, 1941) It is the function of the grid to control the flow of electrons between electrodes by controlling the electric field in the interelectrode space.

* American Standards Association.

1-2. Vacuum-Tube Symbols

Vacuum tubes are designated in circuit diagrams by certain standard symbols. A few of these, essential for present use, are shown in the accompanying diagrams.

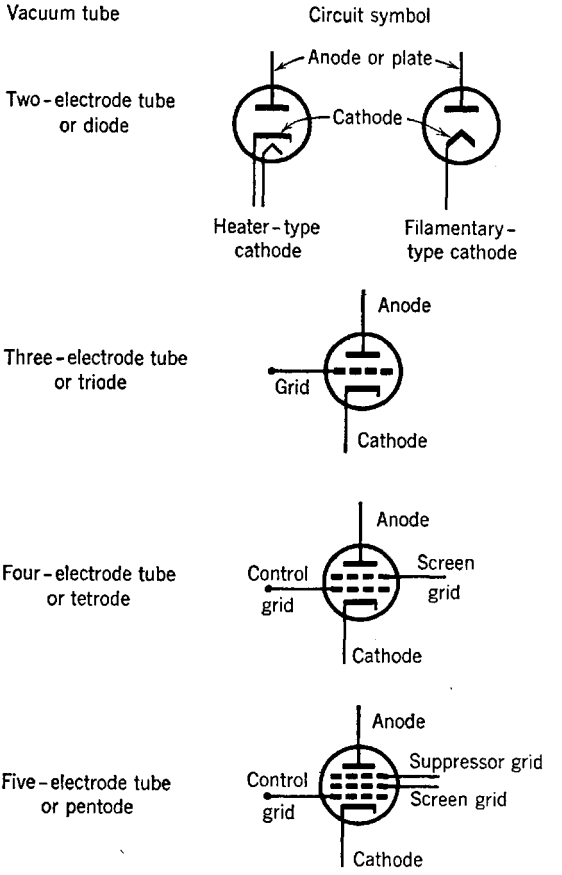

The first part of this text is devoted to the study of the high-vacuum tube and its circuit behavior. Later chapters will be concerned with the gas tube and associated circuits.

A considerable knowledge of the circuit behavior of vacuum tubes may be developed from data obtained by measurements made at the available terminals of the tube if it is assumed that: (1) The electrons set free at a hot cathode are free to move through the interelectrode space under the influence of electric-field forces present in that space; (2) the electron current to or from an electrode under *normal operating*

conditions of the vacuum tube is dependent only upon electrode potentials and not upon the nature of the heated cathode. The last statement is true for tubes operated in accordance with usual design specifications.

1-3. Vacuum-Tube Static Characteristics

"The electrode current * of an electron tube is the current passing to or from an electrode through the interelectrode space. Note. The terms cathode current, grid current, anode current, plate current, etc. are used to designate electrode currents for these specific electrodes. Unless otherwise stated, it is understood that an electrode current is measured at the available terminal."

The measured values of electrode currents as dependent upon voltages applied to the tube electrodes may be plotted, and the resulting curves are termed the tube static characteristics. The word "static" refers to the fact that the changes in electrode voltages are made so slowly that the capacitance existing between electrodes has a negligible effect upon electrode currents.

1-4. The Diode Current-Voltage Characteristic

With a thermionic diode connected as shown in Fig. 1-1, and with the cathode or filament heated to the rated temperature by adjusting the filament current, the volt-ampere tube characteristic may be ob-

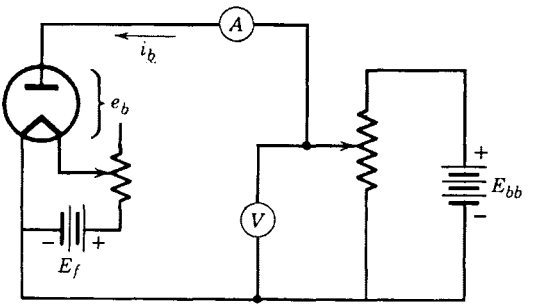

FIG. 1-1. Circuit for obtaining the diode characteristic.

tained by varying the anode voltage and reading the anode current by means of the milliammeter A. A typical volt-ampere characteristic is shown in Fig. 1-2, in which the anode or plate voltage e_b is plotted as abscissa, and the plate current i_b as ordinate. This curve is referred to as a *plate characteristic.*

* IRE Standard definition.

It is evident from Fig. 1-2 that the diode is a nonlinear circuit element, since the derivative di_b/de_b is not constant. The characteristic of a linear circuit element such as a resistor is a straight line through the origin. The slope of the line, di_b/de_b, is constant for a linear circuit element and equal to the variational conductance of the element. For

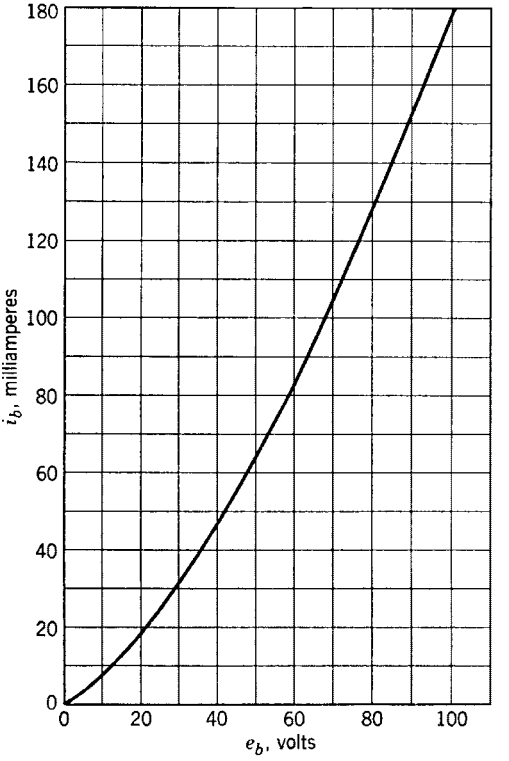

FIG. 1-2. Diode characteristic, type-81 rectifier.

the diode, the quantity di_b/de_b is a function of e_b and is called the *plate conductance* g_p. Its reciprocal is defined as the *plate resistance*, or

$$(de_b/di_b) = r_p$$

The plate resistance r_p as just defined is sometimes referred to as the a-c or variational plate resistance. It is used as a circuit constant when the anode voltage varies by such small amounts above and below a steady average value that the portion of the characteristic involved is approximately a straight line. For a fixed direct voltage, the d-c plate

resistance would be used, and is defined as

$$R_b = E_b/I_b$$

where E_b is any plate voltage and I_b is the corresponding value of plate current. From the diode characteristics of Fig. 1-2, the a-c plate resistance of the type 81 at 80 volts is given exactly by the slope of the curve at 80 volts and is found to be approximately 410 ohms. At the same plate voltage the d-c plate resistance is $R_b = 80/(130 \cdot 10^{-3}) = 615$ ohms.

If a diode is connected in an a-c circuit as shown in Fig. 1-3, the anode will remain positive with respect to the cathode only during the positive half-cycle of the supply voltage. When the anode becomes negative the cathode becomes positive, restraining electrons from leaving the cathode. (Heater connections are not shown in the diagram.) Thus, current flows when the anode is positive and does not flow when the anode is negative. The direction of positive sense of current flow as indicated by the arrow (Fig. 1-3) is opposite to the direction of negative electron flow. The diode in Fig. 1-3 is then acting as a rectifier, and a battery inserted between a and b with its positive terminal at a will receive a pulsating charging current which flows only in the direction a to b. If the applied-voltage wave form is shown and is plotted to the same voltage scale as used for e_b, the current wave form may be obtained by use of the *plate characteristic*, as shown in Fig. 1-4. Point 1 on the plate voltage wave corresponds to point 1′ on the plate current wave. The time axes are plotted to the same scale. The tube current corresponding to the voltage at point 1 is determined by projecting vertically upward from point 1 to the tube characteristic and thence horizontally to the current axis. This current is then properly located on the time axis by laying off the angular distance θ as shown in Fig. 1-4.

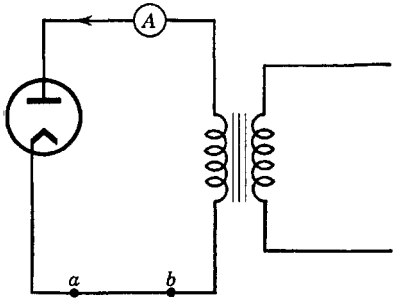

FIG. 1-3. Diode rectifier circuit.

If a resistance load is inserted in series with the diode of Fig. 1-3, the plate current wave form can be obtained by a technique similar to that employed in Fig. 1-4 if the d-c characteristic for the combined tube and load is first found. The new d-c characteristic is determined by the voltage drops in both tube and resistance load, and it may be defined as the *composite characteristic*. Since an exact mathematical expression is

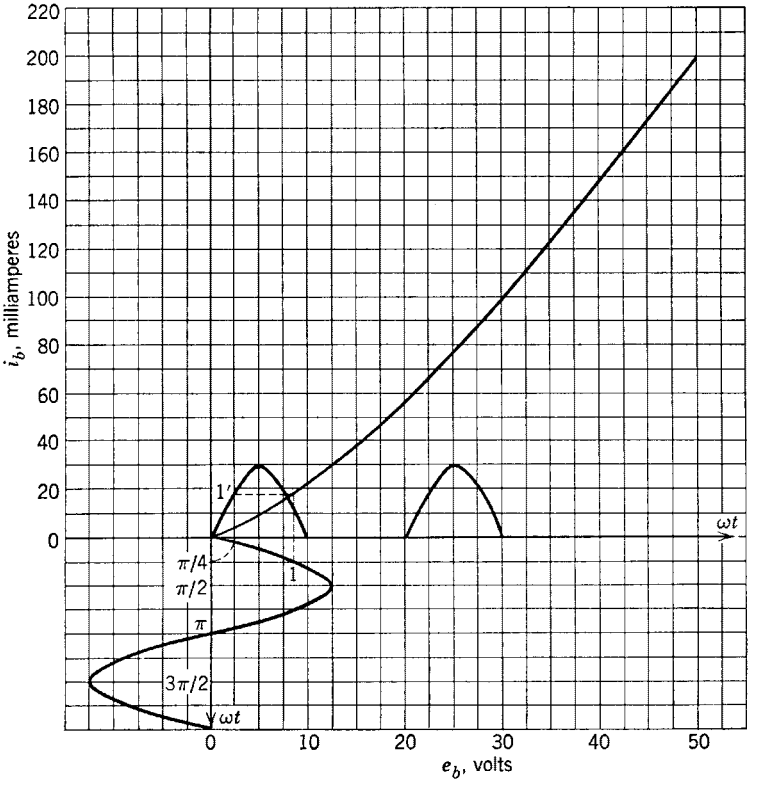

FIG. 1-4. Graphical determination of plate-current wave form.

not available for the nonlinear tube characteristic, the *composite* tube-and-circuit characteristic is determined graphically, as shown in Fig. 1-5, in which the tube voltage e_b is added to the voltage drop across the resistor for a given i_b in obtaining a point on the composite characteristic. Thus, the applied voltage is $e = i_b R + e_b$ for points on the composite characteristic. The tube characteristic must first be obtained experimentally. For a given applied alternating plate voltage, the resulting plate current wave form may now be determined point by point from the composite characteristic as previously shown in Fig. 1-4.

In Fig. 1-6 is shown a circuit similar to that of Fig. 1-5 except that a battery has been included. The effect of the battery, as shown, has been to shift the origin of the alternating plate voltage to point Q on the composite characteristic. The instantaneous value of the a-c component of applied voltage referred to the origin at Q is represented by the symbol e, and the corresponding instantaneous value of the a-c com-

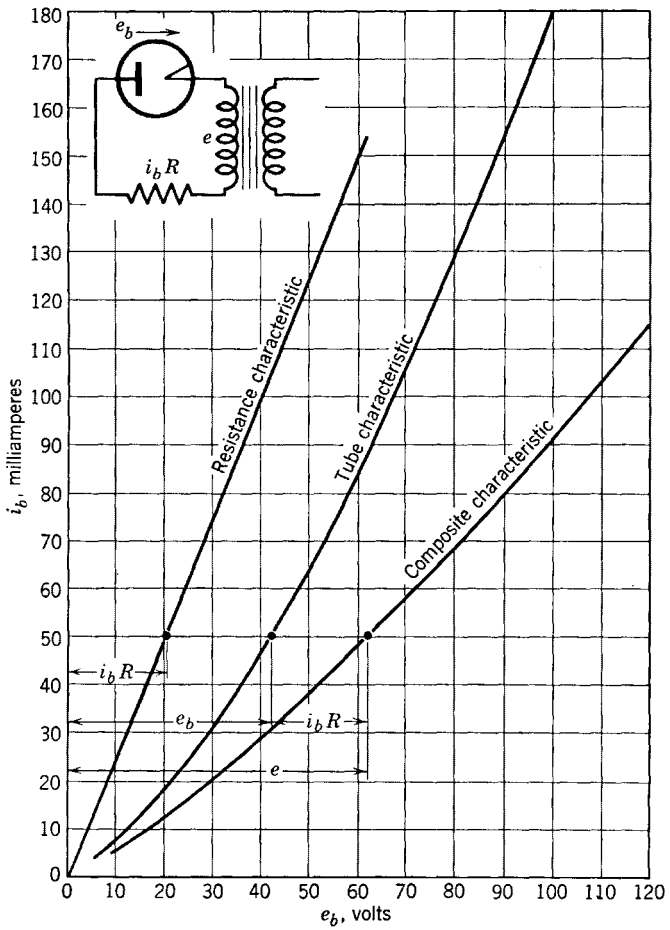

FIG. 1-5. Construction of the composite characteristic.

ponent of plate current referred to the same origin is represented by i_p. The resulting plate current now consists of two components, one alternating, one direct. The value of the d-c component if e is made zero is I_Q; I_{avg} is the average or d-c component resulting from the application of $e + E_{bb}$; I_{avg} and I_Q differ from each other because the tube-and-circuit characteristic is not linear. If the maximum value of the alternating plate voltage is small, the used portion of the characteristic approximates a straight line, and $I_Q \cong I_{avg}$. As far as the superposed alternating voltage is concerned, the approximately linear characteristic is described by an a-c resistance given by the reciprocal of its slope. If R were zero, this a-c resistance would be r_p.

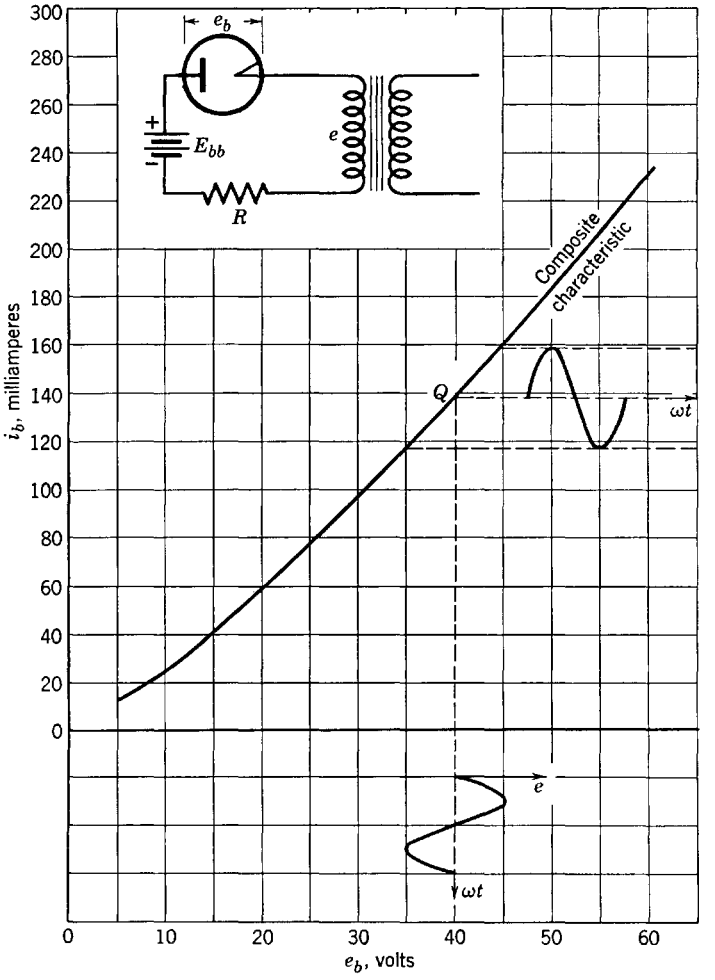

FIG. 1-6. Use of the composite characteristic.

1-5. Triode Static Characteristics

The diode current-voltage characteristic $i_b = f(e_b)$ of Section 1-4 may be described mathematically from a consideration of the motion of electrons in the electric field in the tube. The derivation of an equation for the curve $i_b = f(e_b)$ will be postponed until the circuit properties of the tube have been studied. It should be evident from the experimental data, however, that the diode behaves as a variable resistance of value depending upon the magnitude of the applied anode voltage, provided: (1) that the frequencies of any a-c components of plate voltage are low

enough that the quantity $j\omega C_{pk}e$ is negligible compared with the electron conduction current flowing in the interelectrode space; (e is the instantaneous a-c component of voltage, plate to cathode; C_{pk} is the capacitance between anode and cathode of the tube, and $\omega = 2\pi f$ is the angular frequency of the a-c component of plate voltage); (2) that the cathode is capable of supplying at least as many electrons to the plate as are called for by the voltages applied. Under these conditions it is found that the relation

$$i_b = ke_b^{3/2} \text{ amperes} \tag{1-1}$$

where k is a constant, is a good approximation for the diode static characteristic.

The use of a third electrode between the cathode and the anode of the high-vacuum electron tube was introduced by De Forest in 1907. In modern three-electrode tubes or triodes, the third electrode consists of a grid of fine wires which permit free passage of the electrons through the spaces between the wires. The electric field at the cathode surface is controlled by controlling the electric potential of the grid relative to the cathode, with the result that the anode current is dependent upon the grid voltage, and can be varied by changing either the plate or grid voltage. The anode current i_b now becomes a function of two voltages or, symbolically,

$$i_b = f(e_b, e_c) \tag{1-2}$$

where e_b is the anode voltage and e_c the grid voltage, each referred to the cathode as reference. With three variables involved, a plot of the function i_b would be a surface of three dimensions. Because a surface is rather inconvenient to sketch, it is perhaps preferable to hold one variable constant while plotting the variation of another variable as a function of the third. In this way three families of curves characteristic of the triode are obtained:

(*a*) The plate characteristics, $i_b = F_1(e_b)$, with e_c constant.
(*b*) The mutual or transfer characteristics, $i_b = F_2(e_c)$, with e_b constant.
(*c*) The anode-voltage–grid-voltage characteristics, $e_b = F_3(e_c)$, with i_b constant.

Typical plate, mutual, and anode-grid families for the type-6C5 tube are shown in the sketches (Figs. 1-7, 1-8, and 1-9).

1-6. The Triode Coefficients

The slopes of the families of triode characteristics are significant in tube and circuit analysis. From the plate family (Fig. 1-7) the *plate*

conductance g_p is defined by the relation

$$g_p = \partial i_b / \partial e_b \tag{1-3}$$

and the *plate resistance*

$$r_p = 1/g_p = 1/(\partial i_b / \partial e_b) \tag{1-4}$$

Examination of the curves shows that, as for the diode, these quantities

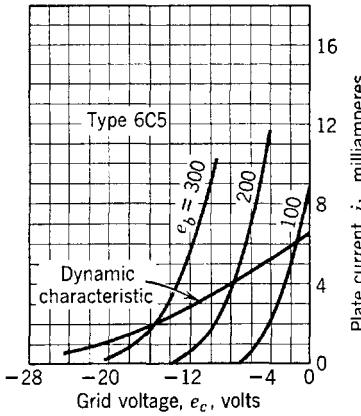

FIG. 1-8. Mutual characteristics.

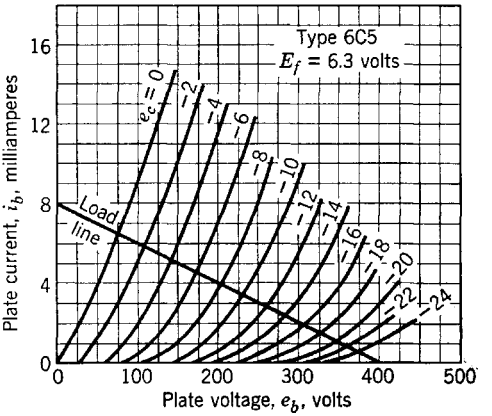

FIG. 1-7. Plate characteristics.

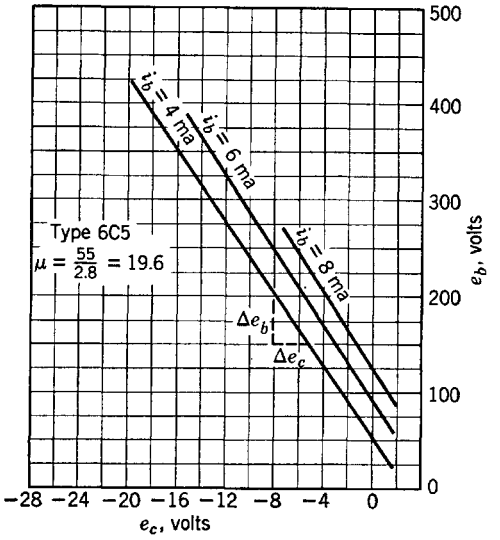

FIG. 1-9. Anode voltage–grid voltage characteristics.

are not constant. From the mutual family (Fig. 1-8) the slope

$$\partial i_b/\partial e_c = g_m \tag{1-5}$$

is defined as the *grid-plate transconductance.* In regard to the grid-anode family of Fig. 1-9, it is evident that the slope is a pure numeric, and the ratio $\partial e_b/\partial e_c$, for one of the curves at constant i_b, is a measure of the relative effectiveness of the grid and anode in controlling the plate current i_b. Thus, for a change Δe_c in increasingly negative grid voltage a positive change Δe_b in anode voltage is required if the current is to remain constant. Since the grid wires are much closer to the cathode than is the anode, $\Delta e_b \gg \Delta e_c$ and the ratio is greater than 1. The quantity

$$-\partial e_b/\partial e_c = \mu \tag{1-6}$$

is defined as the tube *amplification factor* and is fairly constant for negative grid voltages.

The similarity in shape of the triode plate characteristics with the diode characteristic should be noted. In the triode the anode current is found to depend on an equivalent anode voltage $(e_b + \mu e_c)$. Both theoretical and experimental justification exist for the following equation applying to triode plate current:

$$i_b = B(e_b + \mu e_c)^n \tag{1-7}$$

The quantities B and n are constants which are easily determined experimentally. For triodes with indirectly heated, equipotential cathodes, n is approximately 1.5. The quantity $(e_b + \mu e_c)$ is called the *equivalent diode voltage:* diode current-voltage equations are found to apply quite well to triodes if the diode plate voltage is replaced by $(e_b + \mu e_c)$. It should be noted that $i_b = 0$ for $e_c = -e_b/\mu$, which is a convenient relation for determining the required negative grid voltage for effective plate current *cutoff,* or conversely, for determining μ (approximately) if the cutoff voltage is determined experimentally.

1-7. Relation between the Triode Coefficients

Equation 1-2 states that the plate current is simultaneously dependent upon values of the plate voltage and the grid voltage. The effect of changes of plate and of grid voltages upon the plate current may be predicted graphically by the following procedure, as illustrated in

Fig. 1-10. First, an initial value of plate current is chosen at Q on the plate diagram. With grid voltage held constant, the plate voltage is increased by the amount Δe_b, and the plate current is seen to increase by an amount Δi_{b1} to point M on the $e_c = E_c$ plate characteristic. The corresponding points Q and M are located on separate mutual characteristics on the mutual diagram. Next, with e_b held constant at the new value of $E_b + \Delta e_b$ on the mutual diagram, e_c is increased in a positive

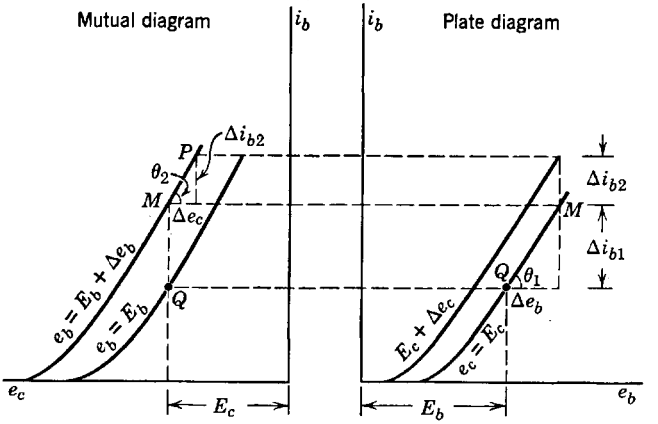

FIG. 1-10. Changes in plate current of a triode resulting from a change, first, in plate voltage with grid voltage constant and, second, in grid voltage with plate voltage constant.

direction (made less negative) by an amount Δe_c. The result is a second increase in plate current Δi_{b2} to point P on the mutual diagram. The total change in plate current is then

$$\Delta i_b = \Delta i_{b1} + \Delta i_{b2}$$

and may be computed from Fig. 1-10. Thus,

$$\Delta i_{b1} = \Delta e_b \tan \theta_1 = \Delta e_b \frac{\partial i_b}{\partial e_b}$$

and

$$\Delta i_{b2} = \Delta e_c \tan \theta_2 = \Delta e_c \frac{\partial i_b}{\partial e_c}$$

Then

$$\Delta i_b = \Delta i_{b1} + \Delta i_{b2} = \frac{\partial i_b}{\partial e_b} \Delta e_b + \frac{\partial i_b}{\partial e_c} \Delta e_c$$

a relation that is, of course, just the statement of the approximate total increment of a function of two independent variables. The relation

$$di_b = \frac{\partial i_b}{\partial e_b} de_b + \frac{\partial i_b}{\partial e_c} de_c \tag{1-8}$$

is the total differential of the plate current obtained from Eq. 1-2. It is the graphical significance of this relation for the triode that has just been illustrated in Fig. 1-10.

If now the changes Δe_b and Δe_c are chosen such that i_b is held constant, as in Fig. 1-9, $di_b = 0$, and, from Eq. 1-8,

$$\left(\frac{de_b}{de_c}\right)_{(i_b \text{ constant})} = \frac{\partial e_b}{\partial e_c} = -\frac{\partial i_b / \partial e_c}{\partial i_b / \partial e_b} \tag{1-9}$$

or the relation between the triode coefficients becomes

$$\mu = g_m r_p \tag{1-10}$$

The most obvious method of obtaining values for the individual triode coefficients is to plot from the experimental data the families of

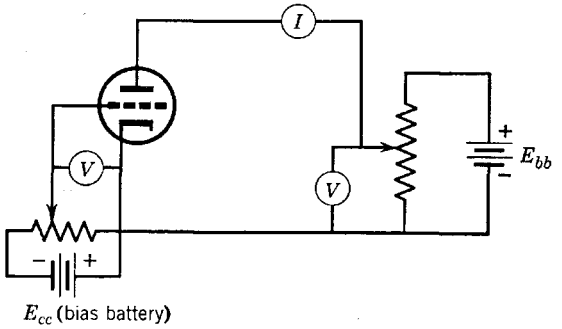

FIG. 1-11. Circuit connections for obtaining triode characteristics.

characteristics and to measure their slopes. The data for plotting such tube characteristics may be obtained by connecting tube and meters as shown in Fig. 1-11.

Numerous other methods for determining triode coefficients have been worked out and are described in detail in the literature and in books on electron tubes. Useful bridge methods of determining μ, r_p, and g_m will be described in Section 1-14. For use in problems, values of μ, r_p, and g_m may be obtained from the plate characteristics or from manufacturer's data books.

1-8. The Load Line. The Dynamic Characteristic

If the tube whose static plate characteristics were given in Fig. 1-7 is connected in a circuit as indicated in Fig. 1-12, the voltage e_b is the instantaneous total voltage of the anode and e_g is the instantaneous a-c component of the grid voltage, each referred to the cathode as reference. As shown, e_g is the instantaneous voltage of an a-c generator connected at the tube input terminals in series with the bias battery. For the present, attention should be focused on the plate (or anode) mesh only. The drop of voltage in the *load resistor* R_L may be shown on the sheet

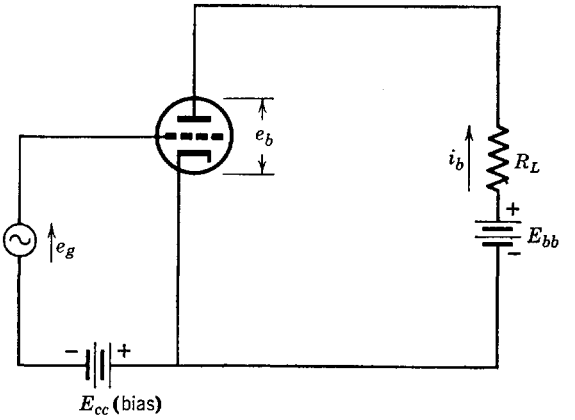

FIG. 1-12. Amplifier circuit.

with the plate characteristics in a manner analogous to that in which the composite characteristic was obtained for the diode. In the plate circuit of Fig. 1-12, Kirchhoff's voltage law requires that

$$E_{bb} = i_b R_L + e_b \tag{1-11}$$

or

$$e_b = E_{bb} - i_b R_L$$

Now if the relation $e = i_b R_L$ is plotted on $i_b - e$ rectangular coordinate paper the result is a straight line, of slope $1/R_L$, passing through the origin of coordinates. This is the method used for the diode (Fig. 1-5) in combining the characteristic curves of circuit and tube to obtain the composite characteristic. Again the objective is to obtain a composite characteristic for tube and circuit, but for the triode the method used differs slightly from the diode method *because of the fact that the plate-supply voltage for the triode is usually fixed, and plate current is controlled by variations in grid voltage.* Therefore, it is customary to *subtract* the

voltage drop in the load resistor $i_b R_L$ from the fixed plate-supply voltage E_{bb} to obtain the voltage across the tube e_b. The process is represented by Eq. 1-11. A plot of Eq. 1-11 is shown in Fig. 1-13. The values of e_b represented by points on the line of Fig. 1-13 are the voltages that would be measured between plate and cathode of an electron tube connected in series with load resistor R_L when the currents through R_L are the corresponding values of i_b.

The *load line* (Eq. 1-11) may be readily sketched by finding the intercepts on the coordinate axes, or by using any known point and the slope of the load line, $di_b/de_b = -1/R_L$. Such a typical *load line* has been

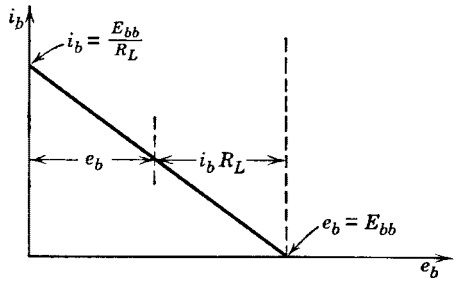

FIG. 1-13. Sketch of the load line $e_b = E_{bb} - i_b R_L$.

sketched on Fig. 1-7, for $E_{bb} = 400$ volts, $R_L = 50{,}000$ ohms. It should be carefully noted that the load line is completely independent of the tube and its characteristics. It is the load resistance characteristic analogous to the resistance characteristic used in Fig. 1-5 with the diode.

Intersections of the load line with the plate characteristics of Fig. 1-7 represent points for which the plate current is such that the sum of the voltage across the tube, plate to cathode, plus the voltage drop across the resistor is equal to the plate battery voltage. If all such points are transferred to the mutual characteristic graph of Fig. 1-8, the resulting locus is truly a tube-and-circuit characteristic and is called the *dynamic characteristic.** At an intersection of the load line with the tube characteristic, i_b and e_c for the particular characteristic will be known and may be transferred to the mutual characteristic graph. Load line and dynamic characteristic will be used in the tube-and-circuit analysis to follow.

* The term "dynamic" as used here is somewhat misleading, although it is in common use. Actually the so-called dynamic characteristic includes those points (on the mutual diagram) which are composite to tube and circuit resistance in the same sense as used already for the diode.

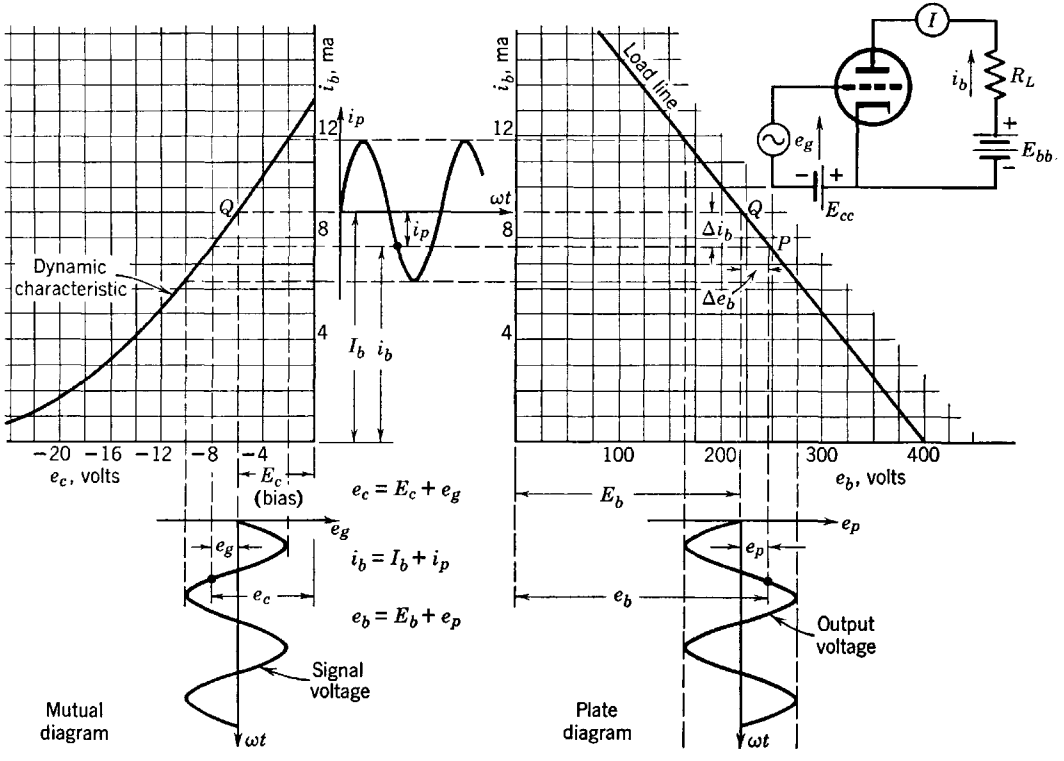

FIG. 1-14. Standard IRE symbols and amplifier operation.

1-9. IRE Standard Symbols

The Institute of Radio Engineers in 1938 adopted a standard system of letter symbols for electron-tube currents, voltages, and parameters. The diagram of Fig. 1-14 and Table 1-1 illustrate the use of the standard

TABLE 1-1

Quantity	Letter		Subscript	
Voltage	E	d-c, rms a-c, average, quiescent, or maximum value (with extra subscript m)	b	plate: total, d-c, or quiescent
			bb	plate battery
	e	Instantaneous component or total value	p	plate: instantaneous a-c component or rms value
Current	I	d-c, rms a-c, average, quiescent, or maximum value (with extra subscript m)	c	grid: total, d-c, or quiescent
			cc	grid battery
	i	Instantaneous component or total value	g	grid: instantaneous a-c component or rms value

symbols. The complete definitions of current and voltage symbols are also given in detail on pages 17 and 19. All voltages are referred to the cathode as reference.

The circuit diagram of Fig. 1-14 shows a triode connected as an amplifier. A source of alternating voltage is connected in series with the grid-bias battery in the grid circuit, and there is a load resistance R_L in the plate circuit in series with the plate battery. The latter is frequently referred to as the B supply. Static characteristics of the tube and the load resistance characteristic or load line are shown on the $i_b - e_b$ or plate diagram, and the dynamic characteristic has been drawn from points transferred to the mutual from the plate diagram. Time axes for the plotting of instantaneous values of grid voltage, plate current, and plate voltage are shown, and the two latter quantities have been obtained by graphical methods identical with those used for the diode rectifier in Fig. 1-4.

Definitions of Standard Symbols. Shown in the diagram (Fig. 1-14) are the load line and dynamic characteristics for a triode connected as a simple amplifier with resistance load R_L. The input, signal, or excitation voltage is the alternating voltage e_g in series with the grid-bias battery, of voltage E_{cc}. The plate battery voltage is E_{bb}. The significance of the various symbols is shown, and the relations between total values and their components are given. The definitions follow:

E_{bb} = plate-supply voltage
E_{cc} = grid-supply voltage
e_c = instantaneous total grid voltage
e_b = instantaneous total plate voltage
i_c = instantaneous total grid current
i_b = instantaneous total plate current
E_c = average or quiescent value of grid voltage
E_b = average or quiescent value of plate voltage
I_c = average or quiescent value of grid current
I_b = average or quiescent value of plate current
e_g = instantaneous value of the a-c component of grid voltage
e_p = instantaneous value of the a-c component of plate voltage
i_g = instantaneous value of the a-c component of grid current
i_p = instantaneous value of the a-c component of plate current
E_g = rms value of the a-c component of grid voltage
E_p = rms value of the a-c component of plate voltage
I_g = rms value of the a-c component of grid current
I_p = rms value of the a-c component of plate current
r_p = a-c plate resistance
g_m = grid-plate transconductance
μ = amplification factor

1-10. Slope of the Load Line. Resistance Load

The equation of the load line is $e_b = E_{bb} - i_b R_L$; the slope di_b/de_b of the load line is $-1/R_L$. At any point P (Fig. 1-14) within the range of operation along the load line, the slope of the line can be obtained as follows:

$$\text{Slope} = \Delta i_b/\Delta e_b = i_p/e_p = -1/R_L \tag{1-12}$$

In Eq. 1-12, Δi_b and Δe_b are the instantaneous changes in plate current and plate voltage from their zero signal values and are therefore identical with the instantaneous a-c values, i_p and e_p. Then,

$$e_p = -i_p R_L \tag{1-13}$$

or, in terms of the rms values, for sinusoids,

$$E_p = -I_p R_L \tag{1-14}$$

Evidently e_p and i_p are 180° out of phase; since i_p increases with increasing e_g, while e_p decreases, i_p is in phase with e_g, and therefore e_p and e_g also differ in phase by 180°. An examination of Fig. 1-14 will show that a positive increase of grid voltage is accompanied by a proportional increase in plate current in the positive direction, if the dynamic characteristic is linear. By positive direction of increase of plate cur-

rent is meant an increase of actual, instantaneous plate current flowing from anode to cathode as shown on the sketch of plate current (Fig. 1-14). Referring to the circuit diagram and to the load line, it is evident that an increase (in the positive direction) of i_b, or of i_p, will result in an increased voltage drop in load resistor R_L and in a corresponding *decrease* in plate voltage. For a pure resistance load, the result is the *phase reversal* of Eq. 1-13 or Eq. 1-14. An important interpretation of these equations is simply this: They show that *an alternating component* of plate voltage appears across the load resistor.

The following relations illustrate the behavior of an amplifier operating in the linear region of its dynamic characteristic:

For a sinusoidal input voltage,

$$e_g = \sqrt{2}\, E_g \sin \omega t \tag{1-15}$$

The total grid voltage is then

$$e_c = E_c + \sqrt{2}\, E_g \sin \omega t \tag{1-16}$$

The instantaneous alternating plate current is (for linear dynamic characteristic)

$$i_p = \sqrt{2}\, I_p \sin \omega t \tag{1-17}$$

The instantaneous total current is

$$i_b = I_b + \sqrt{2}\, I_p \sin \omega t \tag{1-18}$$

The instantaneous alternating component of plate voltage appearing across R_L is then

$$e_p = -i_p R_L = -\sqrt{2}\, I_p R_L \sin \omega t \tag{1-19}$$

The instantaneous total plate voltage is

$$e_b = E_b + e_p = E_b - \sqrt{2}\, I_p R_L \sin \omega t \tag{1-20}$$

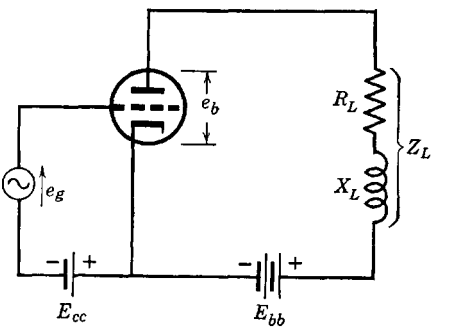

FIG. 1-15. Circuit with inductive load.

1-11. Effect of Load Impedance. Reactive Load

In the following analysis, sinusoidal a-c components of voltage and current are assumed. If the load impedance (Fig. 1-15) is $Z_L = R_L + jX_L$, the voltage across Z_L will depend upon both the rate of change and the magnitude of the plate current, and the operating locus on both plate and mutual diagrams becomes more complicated. From Kirchhoff's law,

$$E_{bb} = i_b R_L + L\frac{di_b}{dt} + e_b \tag{1-21}$$

Since $i_b = I_b + i_p$ and $dI_b/dt = 0$

Eq. 1-21 solved for e_b becomes

$$e_b = E_{bb} - I_b R_L - L\frac{di_p}{dt} - i_p R_L \tag{1-22}$$

Also $$E_b = E_{bb} - I_b R_L \tag{1-23}$$

so that $e_b = E_b - i_p R_L - L di_p/dt = E_b + e_p$ (by definition) (1-24)

Hence, $$e_p = -\left(i_p R_L + L\frac{di_p}{dt}\right) \tag{1-25}$$

Let $i_p = \sqrt{2}\, I_p \sin \omega t$.

Then,
$$\begin{aligned} e_p &= -(\sqrt{2}\, I_p R_L \sin \omega t + \sqrt{2}\, \omega L I_p \cos \omega t) \\ &= -\sqrt{2}\, I_p \sqrt{R_L^2 + (\omega_L)^2} \sin(\omega t + \theta) \\ &= -\sqrt{2}\, I_p |\, Z_L \,| \sin(\omega t + \theta) \end{aligned} \tag{1-26}$$

where $\theta = \tan^{-1} \omega L/R_L$, as shown in the sketch which defines θ.

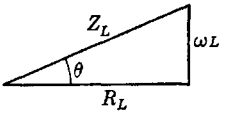

Now the load locus is given by the two equations (see 1-24, 1-25, and 1-21):

$$\begin{aligned} e_b &= E_b - \sqrt{2}\, I_p |\, Z_L \,| \sin(\omega t + \theta) \\ i_b &= I_b + \sqrt{2}\, I_p \sin \omega t \end{aligned} \tag{1-27}$$

Equations 1-27 are the parametric equations of an ellipse. The operating locus on both plate and mutual diagrams is an ellipse provided that μ, r_p, and g_m are constants over the operating range. Such an elliptical operating locus is undesirable in amplifiers because it indicates phase

shift and thus frequency discrimination. An example of the determination of the load locus for an inductive load impedance is given in an example problem solution at the end of Section 1-14.

1-12. The A-C Equivalent Anode Circuit of a Triode Amplifier

The plate current in a vacuum-tube circuit usually consists of one or more a-c sinusoidal components of different frequencies superposed upon a d-c component. The purpose of the direct components of current and voltage is to establish *operating points* and to supply power for operation. The useful output in the vacuum-tube circuit is usually alternating current or voltage, or a-c (average) power. For these reasons, it is convenient and important to reduce the actual vacuum-tube circuits wherever possible to equivalent a-c circuits. This is accomplished by applying the idea of the superposition principle. The equivalent a-c circuit applies only to the sinusoidal a-c components of current and voltage. The results of analysis of the equivalent a-c circuit may be superposed upon the d-c components to obtain the over-all or total values of current and voltage.

If a vacuum triode is operated with negative grid bias and positive anode voltage of such values that the operating point is located on the straight portion of the dynamic characteristic, and if the alternating input grid voltage is of such value that the grid does not swing positive or beyond the linear range of the dynamic characteristic, then the plate current of the tube will have a linear dependence upon the grid voltage and an a-c equivalent circuit can be obtained and used. The conditions shown graphically in Fig. 1-14 comply with these requirements.

There are several methods of obtaining a mathematical expression for the sinusoidal alternating component of plate current. One such method assumes that the plate characteristics are a family of parallel straight lines and utilizes an equivalent diode voltage and applies the superposition principle to separate a-c components from d-c components. Perhaps the simplest method of all utilizes the relation $i_b = f(e_b, e_c)$ which may be expanded about the operating point in a Taylor's series. Only two terms of the series are needed if operation is confined to the linear portion of the dynamic characteristic. Then,

$$\Delta i_b = \frac{\partial i_b}{\partial e_b}\Delta e_b + \frac{\partial i_b}{\partial e_c}\Delta e_c \tag{1-28}$$

in which $\partial i_b/\partial e_b$ and $\partial i_b/\partial e_c$ are constant, and where Δi_b, Δe_b, and Δe_c may be as large as may be desired so long as the requirement of linearity, as specified in the preceding paragraph, is maintained.

When a signal voltage is applied at the input of the amplifier of

Fig. 1-14, the values of e_c, i_b, and e_b change from their quiescent values. The *change* from quiescence of any of these quantities is its instantaneous a-c value, where the origins of the coordinates e_g, i_p, and e_p are taken at the quiescent points on the mutual and plate diagrams. Thus,

$$\Delta i_b = i_p, \qquad \Delta e_b = e_p = e_{KP}, \qquad \Delta e_c = e_g = e_{KG}$$

where the symbols e_{KP} and e_{KG} are used to explain specifically the assumed direction of the instantaneous values of voltage rise. Also,

$$\partial i_b/\partial e_b = 1/r_p, \qquad \partial i_b/\partial e_c = g_m = \mu/r_p$$

Equation 1-28 then becomes

$$i_p = \frac{e_{KP}}{r_p} + \frac{\mu}{r_p} e_{KG} \tag{1-29}$$

For a load resistance R_L, the alternating component of plate voltage e_p becomes (see Eq. 1-13)

$$e_{KP} = -i_p R_L \tag{1-13}$$

Equivalent relations for sinusoids may be written using the effective values of current and voltage instead of the instantaneous values. Equation 1-29 written with effective values is

$$I_p = \frac{E_{KP}}{r_p} + \frac{\mu}{r_p} E_{KG} = \frac{-I_p R_L}{r_p} + \frac{\mu}{r_p} E_{KG} \tag{1-30}$$

using Eq. 1-14. From Eq. 1-30, the effective value of the *alternating component of plate current* is

$$I_p = \frac{\mu E_{KG}}{r_p + R_L} \tag{1-31}$$

The form of Eq. 1-31 suggests that, so far as the *alternating* current is concerned, the actual tube circuit of Fig. 1-16 may be replaced by the equivalent circuit of Fig. 1-17 in which a generator of effective voltage

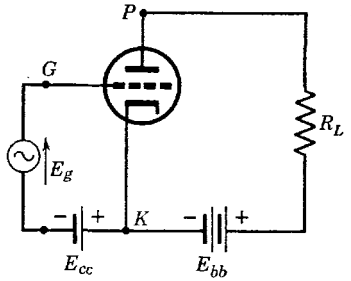

FIG. 1-16. Amplifier circuit.

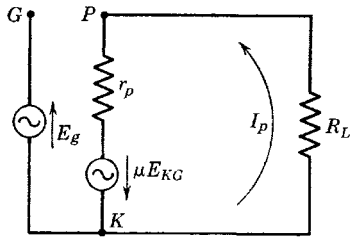

FIG. 1-17. Equivalent a-c circuit.

μE_{KG} and internal impedance r_p is connected to a resistance R_L. The batteries are not shown since their impedances are negligible compared to r_p and R_L. The grid-circuit generator is connected on one side only, since, with negative grid bias, the grid current is negligible and the grid-circuit input impedance infinite.

By the use of the a-c equivalent circuit of Fig. 1-17, the tools of a-c circuit theory are made available for solving tube circuit problems, provided operation is restricted to the region in which the tube characteristics are linear. Equation 1-31 has been written as a vector relation using the effective values of current and voltage, but may be expressed in terms of instantaneous values as

$$i_p = \frac{\mu e_{KG}}{r_p + R_L} \tag{1-32}$$

The circuit of Fig. 1-16 is that of a voltage amplifier. The output voltage of the amplifier is the a-c component of voltage across the load resistor R_L; the input voltage is the voltage E_g. The *voltage gain* of the amplifier may now be obtained from the equivalent plate circuit. In the circuit of Fig. 1-16 with the load resistance R_L replaced (for greater generality) by a load impedance Z_L, the voltage drop across Z_L is I_pZ_L, the output voltage.* The voltage gain may be defined as

$$\text{Voltage gain} = A = \frac{\text{alternating voltage drop across the load impedance}}{\text{alternating voltage drop across the input}}$$

Then, $A = I_pZ_L/-E_g$, and I_p may be obtained from the equivalent a-c circuit (Fig. 1-17) where $E_{KG} = E_g$. Thus,

$$I_p = \frac{\mu E_{KG}}{r_p + Z_L} = \frac{\mu E_g}{(r_p + R_L) + jX_L} \tag{1-33}$$

where $Z_L = R_L + jX_L$ and it is to be understood that these relations have meaning only for sinusoidal voltages and currents. The voltage gain then becomes

$$A = -\frac{\mu Z_L}{r_p + Z_L} \tag{1-34}$$

Equation 1-34 is a convenient one for gain calculations. It should be noticed that the gain as defined is a vector quantity. It is customary to take the voltage drops in the gain equation as from cathode to plate

* It is here assumed, as will be shown later, that the equivalent a-c anode circuit may be used for any linear load impedance and is not restricted to circuits using pure resistance loads.

and from cathode to grid. This accounts for the negative sign before the grid voltage E_g; since E_g is the rms value of the a-c component of voltage *rise* from cathode to grid, $-E_g$ is the corresponding value of voltage drop.

1-13. Use of the A-C Equivalent Plate Circuit

It is very important to observe that the voltage of the generator in the equivalent plate circuit of Fig. 1-17 is μ *times the voltage rise between the cathode terminal K and the grid terminal G* in the external circuit of the tube. The voltage E_g, in Fig. 1-17, is also the voltage rise due to excitation, between cathode and grid inside the tube. Only a-c components are shown on the equivalent circuit, since it represents variations of current and voltage around the operating point which has been used as origin of coordinates on the plate and mutual diagrams. All batteries are deleted. The tube is replaced by the plate resistance r_p and a constant-voltage generator of generated voltage μE_{KG}. Now the symbol E_{KG} is used to call attention to the fact that the actual voltage rise between cathode and grid electrodes inside the tube is the cause of a change in plate current. In the circuit of Fig. 1-16, $E_{KG} = E_g$, the voltage of the generator connected to the input terminals of the amplifier. In general, however, E_{KG} is *not the same as* E_g. Frequently, the voltage between cathode and grid may involve a voltage drop across, for example, a resistor used to supply bias to the grid. In any case an inspection of the actual circuit or of the equivalent a-c circuit will disclose the presence of any alternating voltage other than that of the input excitation between K and G. It is the resultant vector voltage rise between K and G which must *always* be used as the voltage E_{KG} in the expression μE_{KG} for the generated voltage of the equivalent plate-circuit generator.

The recommended procedure in drawing the a-c equivalent plate circuit is the following:

1. Designate the terminals of the tube as P, K, and G as in Fig. 1-16.
2. Draw the plate circuit between P and K *outside* the tube exactly as in the actual circuit, and omit batteries or d-c sources except for associated impedances, if any.
3. Replace the tube between P and K by a constant-voltage generator of internal impedance r_p and generated voltage μE_{KG}.
4. Place arrows on the diagram to show the assumed positive sense of current flow and voltage rise of the generator. In this text the positive sense of current is taken toward the plate, and the positive sense of voltage rise in the equivalent plate-circuit generator is accordingly from P to K.

5. Show the external source of voltage excitation, if any, as a generator of voltage rise E_g connected exactly as in the actual circuit except that the G terminal is left unconnected to the plate circuit, as in Fig. 1-17 (except for conditions to be described later). Any connection between G and the plate circuit may be omitted since it has been assumed that the grid is negatively biased and that conduction and displacement grid currents are negligible.

Examples of the use of the equivalent plate circuit are given in Section 1-14. The symbol V with appropriate double subscripts is used for voltage drop, E for voltage rise.

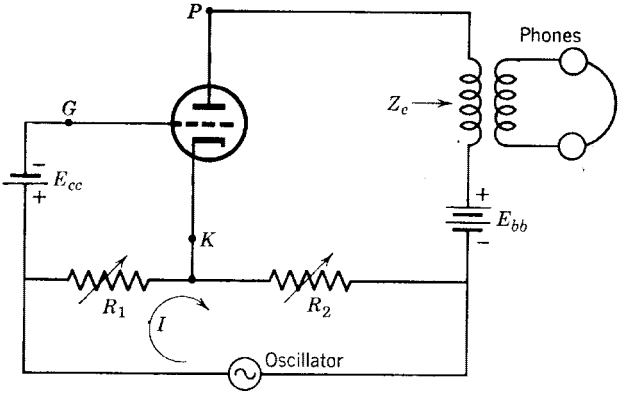

(a) Actual circuit

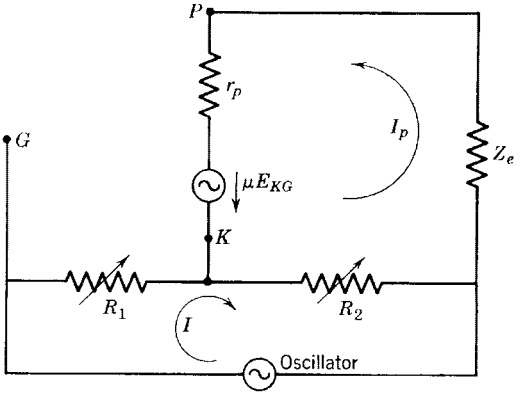

(b) Equivalent circuit

FIG. 1-18. Miller bridge and equivalent a-c circuits.

1-14. Applications of the A-C Equivalent Plate Circuit

A. Measurement of μ. The circuit shown in Fig. 1-18 has been used in the measurement of μ. The impedance Z_e is the impedance looking into the terminals of the transformer which couples the headphones into the anode circuit. It should be observed that in drawing the equivalent a-c plate circuit all batteries are deleted. Points marked P, K, and G refer to plate, cathode, and grid, respectively. The tube is replaced by the equivalent plate-circuit generator with its internal resistance r_p. The assumed positive sense of current flow is shown. The drop in

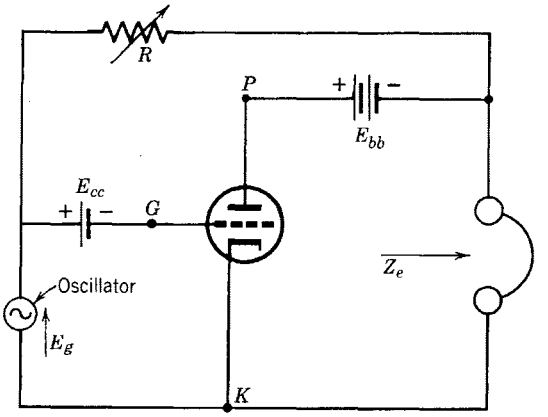

(a) Actual circuit

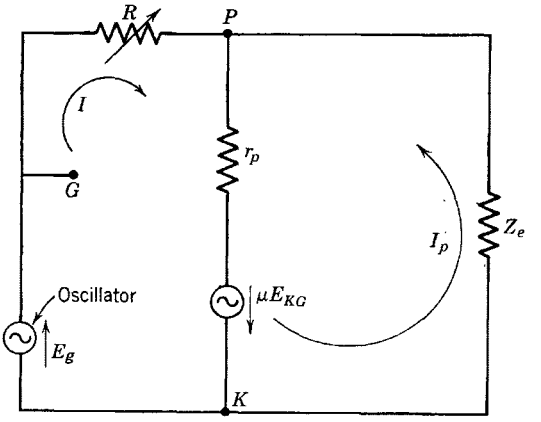

(b) Equivalent a-c circuit

FIG. 1-19. Circuit for the measurement of g_m.

voltage between cathode and grid is $V_{KG} = -IR_1$; the voltage rise, cathode to grid, is $E_{KG} = -V_{KG} = IR_1$. In the plate circuit,

$$\mu E_{KG} = \mu IR_1 = (I_p + I)R_2 + I_p(Z_e + r_p) \tag{1-35}$$

From Eq. 1-35,
$$I_p = \frac{(\mu R_1 - R_2)I}{R_2 + r_p + Z_e} \tag{1-36}$$

If R_1 and R_2 are so adjusted that $I_p = 0$, there will be no sound in the headphones. From Eq. 1-36, $I_p = 0$ if $\mu R_1 - R_2 = 0$, or

$$\mu = R_2/R_1 \tag{1-37}$$

when a balance is obtained.

B. Measurement of g_m. The circuit shown in Fig. 1-19 may be used for the measurement of g_m. For a balance, I_p must be zero. From the equivalent circuit (Fig. 1-19), since $E_{KG} = E_g$,

$$E_g = IR + (I + I_p)r_p - \mu E_g \tag{1-38}$$

$$\mu E_g = I_p Z_e + (I_p + I)r_p \tag{1-39}$$

From Eqs. 1-38 and 1-39,

$$I_p = \frac{E_g(\mu R - r_p)}{[(R + r_p)(r_p + Z_e) - r_p^2]} \tag{1-40}$$

For a balance, $I_p = 0$, $R = r_p/\mu = 1/g_m$, or

$$g_m = 1/R \tag{1-41}$$

C. Amplifier with Inductive Load. In the circuit of Fig. 1-15, let $Z_L = 20{,}000 + j40{,}000 = 44{,}700/\underline{63.4°}$ ohms, $E_{bb} = 400$ volts, $E_{cc} = -8$ volts. It is possible, as follows, to obtain the load locus on both plate and mutual diagrams with the help of the equivalent a-c plate

circuit which has been drawn in Fig. 1-20*a*. For

$$e_g = 2 \sin \omega t, \qquad \sqrt{2}\, E_g = 2 \text{ volts}, \qquad \sqrt{2}\, I_p = \frac{\mu \sqrt{2}\, E_g}{r_p + Z_L}$$

If the tube is a 6C5 for which $\mu = 20$, $r_p = 10{,}000$ ohms,

$$\sqrt{2}\, I_p = \frac{40}{30{,}000 + j40{,}000} = 0.8 \cdot 10^{-3} \underline{/-53.2} \text{ amp}$$

Then, $$\sqrt{2}\, I_p Z_L = (0.8 \cdot 10^{-3} \underline{/-53.2})(44.7 \cdot 10^{3} \underline{/63.4})$$

$$= 35.76 \underline{/10.2} \text{ volts}$$

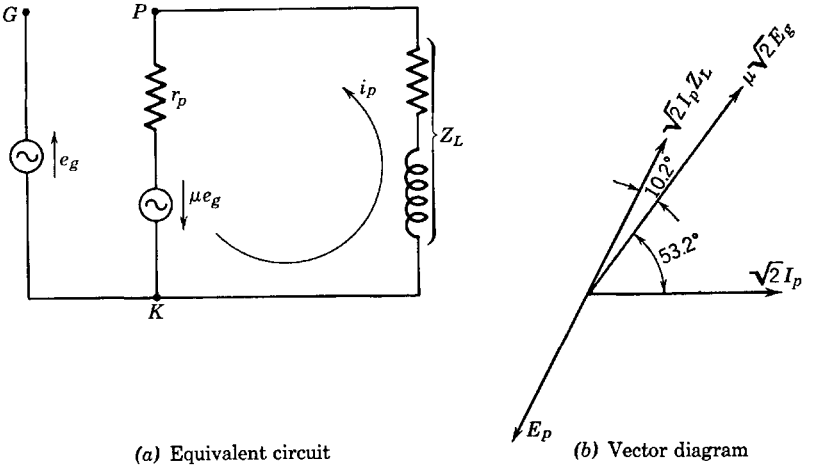

(a) Equivalent circuit *(b)* Vector diagram

FIG. 1-20. Equivalent a-c circuit and vector diagram for the circuit of Fig. 1-15.

These values are shown on the vector diagram of Fig. 1-20*b*, with $\sqrt{2}\, I_p$ as reference vector; however, they were computed with E_g as reference vector.

In agreement with the theory of Section 1-11, where $\sqrt{2}\, I_p$ was used as the reference vector, the parametric equations of the elliptical operating locus are

$$i_b = I_b + \sqrt{2}\, I_p \sin \omega t$$

$$e_b = E_b - \sqrt{2}\, I_p(|\, Z_L \,|) \sin (\omega t + 63.4°)$$

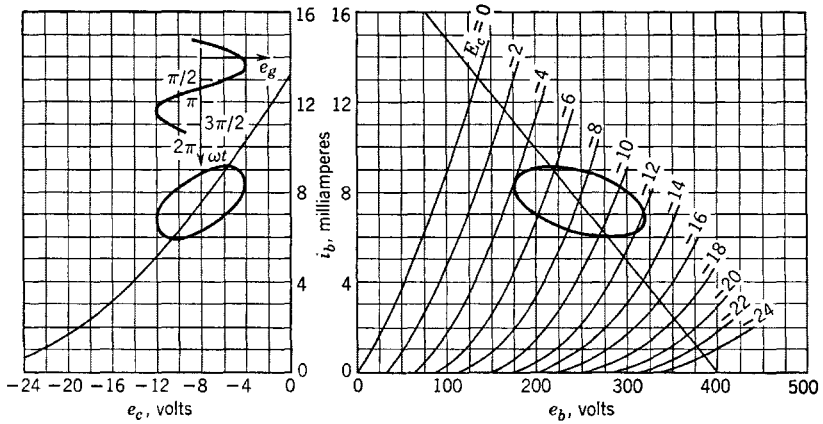

FIG. 1-21. Elliptical load locus, reactive load.

For direct current only, the load line would be determined by the plate battery voltage $E_{bb} = 400$, and the slope of the load line, $-1/20{,}000$. This load line has been drawn on the graph of Fig. 1-21. From the graph the operating point is

$$I_b = 7.6 \text{ milliamperes}$$

$$E_b = 247 \text{ volts}$$

The instantaneous total values of plate current and of plate and grid voltage then are as follows:

$$i_b = 7.6 + 0.8 \sin \omega t \quad \text{(milliamperes)}$$

$$e_b = 247 - 35.8 \sin (\omega t + 63.4°) \quad \text{(volts)}$$

$$e_c = -8 + 2 \sin (\omega t + 53.2°) \quad \text{(volts)}$$

The elliptical load locus shown in Fig. 1-21 has been obtained from the equations for i_b, e_b, e_c by assigning values to ωt. Table 1-2 gives these calculations which have been plotted in Fig. 1-21.

TABLE 1-2. VALUES FOR PLOTTING (FIG. 1-21)

ωt	e_b	i_b	e_g	e_c
90°	231	8.4	1.2	−6.8
270°	263	6.8	−1.2	−9.2
0	215	7.6	1.6	−6.4
180°	279	7.6	−1.6	−9.6
−63.4	247	6.88	−0.354	−8.354
(180 − 63.4)	247	8.32	+0.354	−7.646
206.6	283	7.24	−1.97	−9.97
26.6	211	7.96	1.97	−6.03

1-15. The Constant-Current-Generator Equivalent Circuit

The equivalent tube circuits of Sections 1-12, 1-13, and 1-14 have used a *constant-voltage generator* in the equivalent a-c plate circuit because, in general, the student is better acquainted with the constant-voltage generator than with the *constant-current* generator. An equivalent a-c circuit using the constant-current generator may be obtained from the same fundamental relation,

$$\Delta i_b = \frac{\partial i_b}{\partial e_b}\Delta e_b + \frac{\partial i_b}{\partial e_c}\Delta e_c \tag{1-28}$$

from which the circuit of Section 1-12 was derived.* It will be found that the constant-current-generator equivalent circuit used with Kirchhoff's current or node equations often simplifies the analysis of tube circuits.

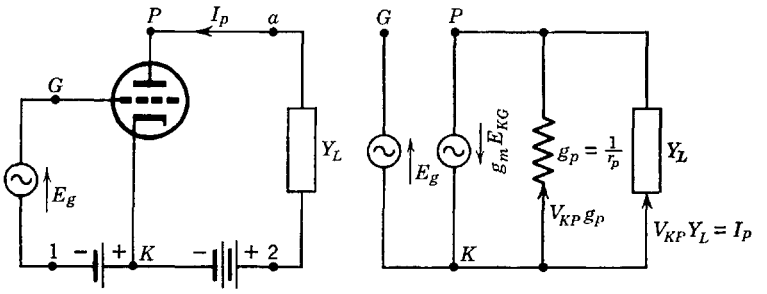

(a) Actual circuit *(b)* Equivalent a-c circuit

FIG. 1-22. Current source equivalent a-c circuit.

In Eq. 1-28, for linear operation, as explained in Section 1-12,

$$\Delta i_b = i_p, \quad \Delta e_b = e_{KP}, \quad \Delta e_c = e_{KG}, \quad \frac{\partial i_b}{\partial e_b} = g_p = \frac{1}{r_p}, \quad \frac{\partial i_b}{\partial e_c} = g_m$$

The resulting expression may then be written as

$$i_p = g_p e_{KP} + g_m e_{KG}$$

or

$$g_m e_{KG} = i_p - g_p e_{KP} \tag{1-42}$$

and this relation may be applied to the triode circuit of Fig. 1-22 in

* It is simpler to obtain the constant-current generator from the constant-voltage circuit of Fig. 1-17 by applying Norton's theorem, but the approach through the interpretation of Eq. 1-42 is preferred because it shows that the constant-current-generator equivalent circuit follows from the same fundamental considerations that were applied in obtaining the constant-voltage circuit.

which the load admittance is

$$Y_L = 1/Z_L$$

and where e_{KG}, i_p, and e_{KP} have been replaced by the corresponding effective or rms values. In Fig. 1-22*b*, $E_{KG} = E_g$, and $E_{KP} = E_p$. Then the voltage rise, cathode to plate, is $E_p = -I_p Z_L$ and $I_p = -E_p Y_L$, and Eq. 1-42 becomes

$$g_m E_g = (-E_p)(g_p + Y_L) \tag{1-43}$$

The form of Eq. 1-43 suggests that the plate conductance g_p and the load admittance Y_L are connected in parallel and are fed by a *constant-current generator* of generated current $g_m E_g$. It may be desirable to use the symbol V_p for voltage drop in the direction from the cathode to the plate side of the load impedance, so that

$$V_{KP} = V_p = -E_p \tag{1-44}$$

Then,

$$g_m E_g = V_p(g_p + Y_L) \tag{1-45}$$

The constant-current generator form of the vacuum-tube equivalent circuit is shown in Fig. 1-22*b*, in which the constant-current generator of generated current $g_m E_g$ and shunt resistance r_p has been inserted between terminals P and K. The quantity E_{KG} is again the voltage rise between cathode and grid terminals inside the tube and, for the circuit shown, is equal to E_g.

The voltage gain of the amplifier circuit (Fig. 1-22*a*) may be obtained from the equivalent circuit (Fig. 1-22*b*) by applying the definition. From Eq. 1-45,

$$g_m E_g = V_p(g_p + Y_L)$$

whence

$$A = \frac{V_p}{-E_g} = -\frac{g_m}{g_p + Y_L} \tag{1-46}$$

It may be easily shown that Eq. 1-46 is identical with Eq. 1-34 if g_m is replaced by μ/r_p, g_p by $1/r_p$, and Y_L by $1/Z_L$. In all respects, results obtained by the use of Fig. 1-22*b* will be identical with those obtained from the constant-voltage-generator equivalent circuit if admittances are replaced by the corresponding impedances and g_m by μ/r_p. It is important at this point to emphasize two facts of fundamental importance: (*a*) An equivalent circuit is never a unique representation of an actual network; i.e., there are infinitely many circuits that may be considered equivalent in the sense of having identical input and output voltages and currents; (*b*) in the equivalent circuits thus far used, the grid current has been assumed zero, and this assumption is not generally

true, even for approximately linear operation, especially as the frequency of the input voltage, in the case of the amplifier, is increased.

Example problem. A type-6C5 triode is connected as an amplifier as shown in Fig. 1-16; the load resistance $R_L = 20{,}000$ ohms, $E_b = 250$ volts, $E_{cc} = E_c = -8$ volts; from the tube data book, $I_b = 8$ ma, $E_g = 5$ volts rms effective value.

(*a*) What is the necessary value of E_{bb}?
(*b*) What is the effective value of the a-c component of plate current I_p? Use the constant-current equivalent circuit.
(*c*) Compute the output voltage.

Solution. (*a*) By Kirchhoff's voltage law, $E_{bb} = i_b R_L + e_b$. For direct current only, operating condition with zero signal voltage, $e_b = E_b$, $i_b = I_b = 8 \cdot 10^{-3}$ amp, $E_{bb} = 8 \cdot 10^{-3}(20{,}000) + 250 = 410$ volts.

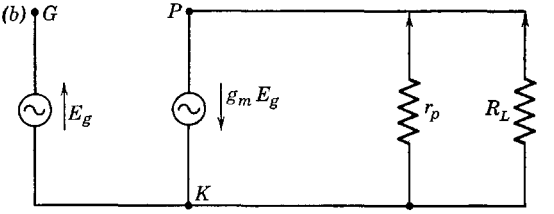

(*b*) From $\Delta i_b = i_p = g_p e_p + g_m e_g$, $i_p = -g_p i_p R_L + g_m e_g$, using Eq. 1-13. In terms of effective values, $I_p = -g_p I_p R_L + g_m E_g$, or $g_m E_g = I_p + I_p R_L / r_p$. Evidently I_p flows in R_L. Then,

$$I_p = \frac{g_m E_g}{1 + R_L/r_p} = \frac{2000 \cdot 10^{-6}(5)}{1 + 2} = \frac{10^{-2}}{3} \text{ amp} = \frac{10}{3} \text{ ma}$$

(*c*) $$V_{KP} = I_p R_L = \tfrac{10}{3} \cdot 10^{-3}(20{,}000) = \tfrac{200}{3} \text{ volts}$$

One may also use the gain equation,

$$A = -\frac{g_m}{g_p + g_L} \quad \text{or} \quad A = -g_m R_{eq} = -g_m \frac{r_p R_L}{r_p + R_L}$$

$$R_{eq} = \frac{10K(20K)}{30K} = \frac{20{,}000}{3}; \qquad A = -2000 \cdot 10^{-6} \frac{20{,}000}{3} = -\frac{40}{3}$$

$$V_{KP} = -\tfrac{40}{3}(-5) = \tfrac{200}{3} \text{ volts}$$

1-16. The Four-Terminal Linear Network

A linear network of electric circuit elements is a network for which the response can be expressed as a sum of the excitations, their derivatives and integrals, each one multiplied by a suitable *constant* coefficient. The definition of a linear network may be stated more briefly by considering only the steady-state condition that the effective values of response currents are, in such a network, related to the effective values of the exciting voltages by a linear equation; i.e., one that may be graphed on rectangular coordinate paper as a straight line. The response of such a network may be in the form of either current or voltage and may result from the application somewhere in the network of voltage or of current. The network is said to be bilateral if energy flows equally well in either direction between any two pairs of terminals. Vacuum tubes are not, in general, bilateral circuit elements, but they behave as linear circuit elements if operated in the linear region of their characteristics. Although networks in general may have many pairs of terminals, there are numerous practical applications of networks that have two pairs of terminals, an input pair and an output pair. Examples are the simple T and π sections used in elementary network theory. Such networks are referred to as four-terminal networks or *four-poles.*

In the elementary analysis of four-terminal networks, recourse is made to the fundamental circuit laws of Kirchhoff. The use of the voltage law has, in the past, been preferred, but in recent years it has been found possible to simplify the analysis of many circuit problems by the use of the current law. That junction in a network at which the summation of the currents is to be found is called a *node.* The equation expressing the law that the vector sum of the currents flowing toward a node is equal to the vector sum of the currents flowing away from the node is referred to as a *node equation.* It has been found that important simplifications of vacuum-tube network theory may result where linear four-terminal network theory and node equations are applied.

Linear four-terminal network theory will be applied to vacuum-tube circuits operating in the linear region of their characteristics. A description of a general four-terminal network is needed before the theory is applied to the vacuum tube. The "box" of Fig. 1-23 has two input and two output terminals. The assumed positive sense of current and of voltage drop at the input and at the output terminals are shown by the arrows. If now the network inside the box behaves as a linear network, it can be shown [1,2] that the *complete performance of the network can*

[1] F. Strecker and R. Feldkeller, *ENT*, **6**, 93–112 (1929).

[2] J. A. Morton, paper presented orally before the Winter Convention of the IRE, Jan. 1945.

be predicted in terms of four parameters which can be measured at the available external terminals. The importance of the preceding statement will be appreciated when it is noted that a knowledge of the circuit details and physical complexities of the contents of the box of Fig. 1-23 is entirely unnecessary in predicting the behavior of the four-terminal network, provided the network is linear.

The behavior of such a linear network as that in Fig. 1-23 may be described by any pair of several pairs of equations expressing relations

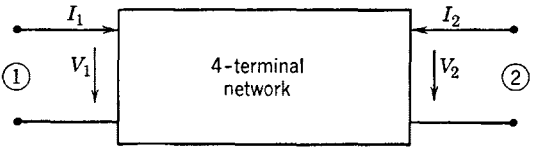

FIG. 1-23.

among the quantities V_1, I_1, V_2, and I_2. These equations may be said to define the properties of the four-terminal linear network. If the network is linear, then a proportionality exists between current I_1 and voltage V_1, between current I_2 and voltage V_2, between voltage V_2 and voltage V_1, and between current I_2 and current I_1. The student has previously encountered examples of such relationships as are proposed for use here in connection with four-terminal networks such as two-winding transformers or T or π arrangements of linear impedances.

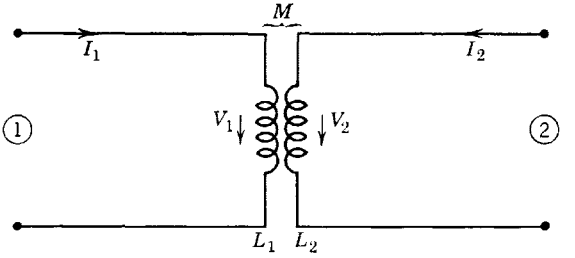

FIG. 1-24. Four-terminal network.

For example, a two-winding transformer (Fig. 1-24) composed of linear elements, has constants $z_{11} = R_1 + j\omega L_1$, $z_{22} = R_2 + j\omega L_2$, $z_{12} = -j\omega M = z_{21}$, where R_1 and L_1, R_2 and L_2 are, respectively, the resistance and inductance of coils 1 and 2 coupled with mutual inductance M. The four-terminal network is described by the equations

$$\begin{aligned} V_1 &= I_1 z_{11} + I_2 z_{12} \\ V_2 &= I_1 z_{21} + I_2 z_{22} \end{aligned} \tag{1-47}$$

where, with terminals 2 open, and a voltage source connected to terminals 1, $I_2 = 0$, and $z_{11} = V_1/I_1$ is defined as the open-circuit driving-point impedance at the input terminals, and $z_{21} = V_2/I_1$ is the open-circuit transfer impedance from 2 to 1. Similarly, with a voltage source connected at 2 and terminals 1 open, $I_1 = 0$, $z_{12} = V_1/I_2$, the open-circuit transfer impedance from 1 to 2, and $z_{22} = V_2/I_2$, the open-circuit driving-point impedance at the output terminals. For a bilateral circuit such as that of Fig. 1-24, $z_{12} = z_{21}$. It is important to remember that V_1, I_1, V_2, and I_2 are variables, and that their values depend upon

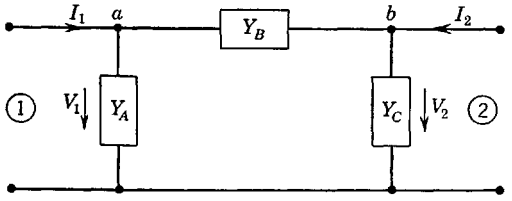

FIG. 1-25. Four-terminal network.

terminating impedances and voltage sources connected to terminals 1 and 2.

Another familiar example of a linear four-pole of general interest is an arrangement of linear impedances or admittances as a π section, as in Fig. 1-25. Since, according to a fundamental theorem of linear networks, any circuit composed of linear, bilateral elements may be replaced at a single frequency by an equivalent T or π section, the circuit of Fig. 1-25 may be used to represent the general four-terminal linear network shown in Fig. 1-23. The behavior of the network may be described as follows, as may be verified by applying Kirchhoff's laws to the circuit of Fig. 1-25. The following node equations are written for nodes a and b:

$$I_1 = V_1 Y_A + (V_1 - V_2)Y_B = V_1(Y_A + Y_B) + V_2(-Y_B)$$

$$I_2 = (V_2 - V_1)Y_B + V_2 Y_C = V_1(-Y_B) + V_2(Y_B + Y_C)$$

Then, by defining

$$y_{11} = Y_A + Y_B$$

$$y_{12} = -Y_B = y_{21}$$

$$y_{22} = Y_B + Y_C$$

it is possible to obtain equations analogous to those of Eqs. 1-47. Then,

$$\begin{aligned} I_1 &= V_1 y_{11} + V_2 y_{12} \\ I_2 &= V_1 y_{21} + V_2 y_{22} \end{aligned} \tag{1-48}$$

are equations that define a linear four-pole and describe its performance.

The admittance y, although related to the components of the equivalent π section as already shown, may be obtained by direct measurement as indicated for the z's of Fig. 1-24. The network behavior is easily predicted if either a set of impedances z or the set of admittances y are known. Lower-case letters are used for the z's and y's to distinguish these quantities from circuit elements connected to terminals external to the box.

1-17. Definitions of the Four-Terminal Network Admittances

Either set of equations 1-47 or 1-48 may be chosen to describe the behavior of the four-terminal network, or four-pole (Fig. 1-23). Equations 1-48 are chosen here because, for vacuum tubes, many circuit problems are greatly simplified when node equations and admittances are used.

The following experimental procedure may be used in the measurement of the y's and therefore as a basis for their definition:

(a) Short-circuit the output terminals, and measure the currents I_1 and I_2 and the voltage V_1 with a driving generator connected to input terminals 1.

(b) Short-circuit the input terminals, and measure the currents I_1 and I_2 and the voltage V_2 with a driving generator connected to output terminals 2.

The following definitions are suggested by the measurements a and b:

$$y_{11} = I_1/V_1 = \text{short-circuit driving-point admittance}$$

$$y_{21} = I_2/V_1 = \text{short-circuit transfer admittance}$$

$$y_{12} = I_1/V_2 = \text{short-circuit feedback admittance}$$

$$y_{22} = I_2/V_2 = \text{short-circuit output admittance}$$

If the measured values of y_{21} and y_{12} are different, then the four-pole is not a reciprocal network. In other words, the reciprocity theorem does not apply.

1-18. Applications of the Four-Pole Theory to Vacuum-Tube Equivalent Circuits

The circuit analysis of a vacuum tube as a linear four-terminal network follows easily from Fig. 1-26, the definitions of Section 1-17, and Eqs. 1-48. Let it be assumed that the tube and batteries, as included between input terminals G-1 and output terminals a-2, are enclosed in a box with only the input and output terminals brought out, as shown in

Fig. 1-26. The external terminating linear admittances are shown as Y_1 and Y_2 in Fig. 1-26, and the circuit is driven by a constant-current generator of generated current I_0. It is required to determine the voltage gain and the driving-point admittances at both input and output

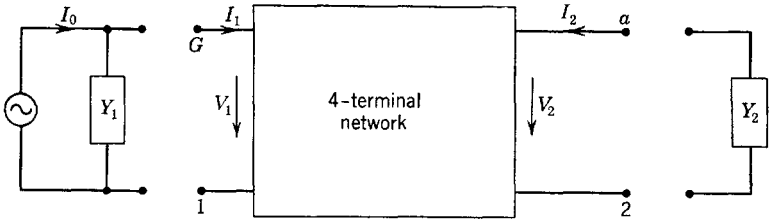

FIG. 1-26. Four-terminal network representing a vacuum tube.

terminals, with the respective output and input terminal admittances connected. In Fig. 1-26,

$$I_2 = -V_2Y_2 = V_1y_{21} + V_2y_{22} \tag{1-49}$$

The *voltage gain* (forward) is obtained from Eq. 1-49 and is

$$\frac{V_2}{V_1} = -\frac{y_{21}}{y_{22} + Y_2} \tag{1-50}$$

Also,

$$I_1 = V_1y_{11} + V_2y_{12} \tag{1-51}$$

Then the *input admittance* of the terminated four-pole is obtained from Eqs. 1-51 and 1-50 and is

$$Y_{11} = \frac{I_1}{V_1} = y_{11} + \frac{V_2}{V_1}y_{12} = y_{11} - \frac{y_{21}y_{12}}{y_{22} + Y_2} \tag{1-52}$$

If the driving generator is removed from the input and connected to the output terminals, then

$$I_1 = -V_1Y_1 = V_1y_{11} + V_2y_{12} \tag{1-53}$$

The *voltage gain* (backward) is obtained from Eq. 1-53 and is

$$\frac{V_1}{V_2} = -\frac{y_{12}}{y_{11} + Y_1} \tag{1-54}$$

The *output admittance* of the terminated four-pole is obtained from Eqs. 1-49 and 1-54 and is

$$Y_{22} = \frac{I_2}{V_2} = y_{22} + \frac{V_1}{V_2}y_{21} = y_{22} - \frac{y_{12}y_{21}}{y_{11} + Y_1} \tag{1-55}$$

The input and output admittances of a vacuum tube connected as an amplifier may be computed, along with the forward and backward voltage gains, according to Eqs. 1-50, 1-52, 1-54, and 1-55, provided that the tube short-circuit admittances y_{ij} and the external terminations Y_1 and Y_2 are known. Several laboratories have made measurements of the y_{ij} admittances using equipment and methods developed originally at Bell Telephone Laboratories by J. A. Morton.[3] The work has not, however, progressed far enough to provide sufficient data for all types of vacuum tubes. It is therefore necessary to identify the y_{ij} admittances with tube and tube-circuit admittances which are already available through manufacturers' ratings of their tube types. Such identification is desirable also in order to permit a comparison of the four-pole theory with older methods of vacuum-tube circuit analysis. In the following section, the four-pole theory will be applied in developing the vacuum tube equivalent circuits in such a way that the relation between the y_{ij} admittances and the tube parameters will be shown for a particular frequency range.

1-19. Relation of the Four-Pole Admittances y_{ij} to Other Tube Parameters

Grid current was neglected in the analysis which led to the anode a-c equivalent circuits of Sections 1-12 and 1-15. Even with negative grid, however, small grid currents may be measured with a sufficiently sensitive microammeter in the grid circuit. At frequencies above the audio range, the capacitances existing between various electrodes in the triode introduce reactances which are comparable with other circuit impedances. In particular, the grid-to-cathode capacitance and the grid-to-plate capacitance result in components of current in the grid circuit which flow even in the absence of any emitted electrons from the cathode. It is therefore necessary to include additional circuit elements in any equivalent a-c circuit of the triode as the operating frequency is increased. In particular, the input circuit of the triode cannot be considered as open at the grid terminal.

The four-pole theory is particularly useful in extending the equivalent circuit to higher-frequency ranges. The analysis to be presented in the following pages will take into account both conduction and capacitive (or displacement) components of grid current. First, the four-pole theory will be applied at such low frequencies that capacitances between electrodes may be neglected. Then the theory will be applied to the array of interelectrode capacitances alone, with the tube cathode cold

[3] The methods of four-pole analysis used here were explained in an oral presentation by J. A. Morton to the Columbus Section of the IRE Apr. 19, 1946.

(no electron emission). The results of the low- and high-frequency analyses will then be combined to obtain a more general equivalent circuit which will describe the behavior of most triodes quite well for frequencies up to about 2 megacycles.

It is found experimentally that conduction grid current depends upon both grid and anode voltages. Therefore, the relations

$$i_c = f_1(e_b, e_c)$$

and

$$i_b = f_2(e_b, e_c)$$

may be used exactly as in Section 1-12 and expanded about operating points in a Taylor series. Again, the first-degree terms only of the expansion are necessary as operation is restricted to the linear region of the tube's characteristics. Then the relations

$$\Delta i_c = \frac{\partial i_c}{\partial e_c}\Delta e_c + \frac{\partial i_c}{\partial e_b}\Delta e_b$$

and

$$\Delta i_b = \frac{\partial i_b}{\partial e_c}\Delta e_c + \frac{\partial i_b}{\partial e_b}\Delta e_b$$

become, for a-c instantaneous components,

$$\begin{aligned} i_g &= g_g e_{KG} + g_{gp} e_{KP} \\ i_p &= g_{pg} e_{KG} + g_p e_{KP} \end{aligned} \tag{1-56}$$

In Eqs. 1-56, $g_g = 1/r_g = \partial i_c/\partial e_c$ is the grid conductance, measurable from the slope of the $i_c - e_c$ grid characteristic.

$g_{gp} = \partial i_c/\partial e_b$ is the plate-to-grid transconductance, measurable from the slope of the $i_c - e_b$ characteristic.

$g_{pg} = g_m = \partial i_b/\partial e_c$ is the grid-to-plate transconductance, measurable from the slope of the $i_b - e_c$ characteristic.

$g_p = \partial i_b/\partial e_b = 1/r_p$ is the plate conductance, measurable from the slope of the $i_b - e_b$ characteristic.

If effective rather than instantaneous values are used in Eqs. 1-56 and the new equations

$$\begin{aligned} I_g &= g_g E_{KG} + g_{gp} E_{KP} \qquad (a) \\ I_p &= g_{pg} E_{KG} + g_p E_{KP} \qquad (b) \end{aligned} \tag{1-57}$$

are compared with Eqs. 1-48, then, with $I_g = I_1$, $E_{KG} = V_1$, $E_{KP} =$

V_2, $I_p = I_2$, the admittances y_{ij} are seen to be related to the tube parameters as follows:

$$\begin{aligned} y_{11} &= g_g = 1/r_g \\ y_{12} &= g_{gp} \\ y_{21} &= g_{pg} = g_m \\ y_{22} &= g_p = 1/r_p \end{aligned} \tag{1-58}$$

The relations of Eqs. 1-58 apply very well for frequencies of the order of 1000 cps or lower. In this frequency range, an equivalent a-c circuit may be based on Eqs. 1-57, as shown in Fig. 1-27. For zero-conduction

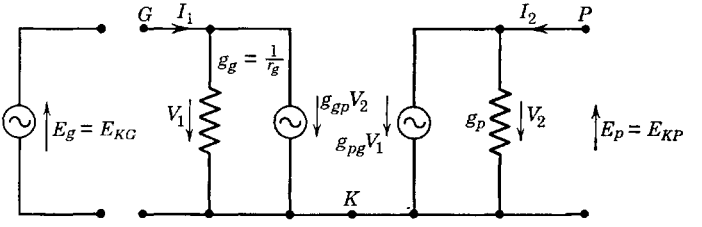

FIG. 1-27. Equivalent a-c circuit for a triode at low frequencies.

grid current, g_g is zero (r_g infinite) and $g_{gp} = 0$, and the circuit of Fig. 1-27 reduces to that previously used in Section 1-15 (Fig. 1-22).

At frequencies of the order of 1000 cps to 1 or 2 Mc per second, capacitive susceptances within the tube are not to be ignored. The *interelectrode capacitances* of themselves constitute a passive, four-terminal network between input and output terminals as shown in Fig. 1-28. The word passive, as used in connection with the network

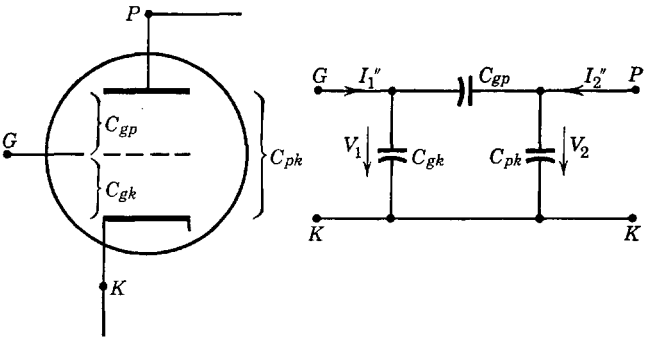

FIG. 1-28. Triode interelectrode capacitances and equivalent passive four-terminal network.

of Fig. 1-28, refers to the fact that there are no generators or sources of energy within the network.

The contributions of the elements of the passive circuit of Fig. 1-28 to the admittances y_{ij} are now obtainable by superposing the currents of the circuit of Fig. 1-28 with the currents of the circuit of Fig. 1-27. Let the currents and admittances of Fig. 1-27 be distinguished from those of Fig. 1-28 by the use of single primes for Fig. 1-27 and double primes for Fig. 1-28. Then, for Fig. 1-27,

$$I_1' = V_1 y_{11}' + V_2 y_{12}'$$
$$I_2' = V_1 y_{21}' + V_2 y_{22}'$$

and, in Fig. 1-28,

$$I_1'' = V_1 y_{11}'' + V_2 y_{12}''$$
$$I_2'' = V_1 y_{21}'' + V_2 y_{22}''$$

When the input currents of the two circuits are superposed, as is physically true with the two circuits connected in parallel,

$$I_1 = I_1' + I_1'' = V_1(y_{11}' + y_{11}'') + V_2(y_{12}' + y_{12}'')$$

and

$$I_2 = I_2' + I_2'' = V_1(y_{21}' + y_{21}'') + V_2(y_{22}' + y_{22}'')$$

Finally, the y_{ij}'s for the complete circuit are given by

$$\begin{aligned} y_{11} &= y_{11}' + y_{11}'' \\ y_{12} &= y_{12}' + y_{12}'' \\ y_{21} &= y_{21}' + y_{21}'' \\ y_{22} &= y_{22}' + y_{22}'' \end{aligned} \tag{1-59}$$

The values of y_{ij}' are given by Eqs. 1-58. The y_{ij}'' admittances of Fig. 1-28 are obtained by applying the fundamental definitions. With a short circuit placed first at the output and next at the input terminals, and with a driving generator connected at the unshort-circuited terminals, the results are as follows:

(*a*) $V_2 = 0$,

$$y_{11}'' = I_1''/V_1 = j\omega(C_{gk} + C_{gp})$$
$$y_{21}'' = I_2''/V_1 = -V_1(j\omega C_{gp}/V_1 = -j\omega C_{gp}$$

(*b*) $V_1 = 0$, (1-60)

$$y_{12}'' = I_1''/V_2 = -V_2(j\omega C_{gp})/V_2 = -j\omega C_{gp}$$
$$y_{22}'' = I_2''/V_2 = j\omega(C_{pk} + C_{gp})$$

The results of Eqs. 1-58 and 1-60 are combined in accordance with Eqs. 1-59 yielding the correct values of y_{ij} to be used in the frequency range 1000 to 2,000,000 cps for standard receiving-type tubes as follows:

$$\begin{aligned} y_{11} &= g_g + j\omega(C_{gk} + C_{gp}) \\ y_{12} &= g_{gp} - j\omega C_{gp} \\ y_{21} &= g_{pg} - j\omega C_{gp} \\ y_{22} &= g_p + j\omega(C_{pk} + C_{gp}) \end{aligned} \tag{1-61}$$

1-20. Gain and Input Admittance of a Triode Amplifier

The relations of Eqs. 1-50, 1-52, and 1-61 provide the information needed to formulate the expressions for forward voltage gain and input admittance of a triode amplifier. A case of particular interest is that for which the grid bias is sufficient to reduce grid conduction current to negligible values. For this case, $g_g = 0$, and $g_{gp} = 0$. The voltage gain (forward) is, from Eq. 1-50,

$$A = -\frac{y_{21}}{y_{22} + Y_2} = -\frac{g_m - j\omega C_{gp}}{g_p + Y_2 + j\omega(C_{pk} + C_{gp})} \tag{1-62}$$

The input admittance, from Eq. 1-52, is

$$\begin{aligned} Y_{11} &= y_{11} + Ay_{12} = j\omega(C_{gk} + C_{gp}) + A(-j\omega C_{gp}) \\ &= j\omega[C_{gk} + (1 - A)C_{gp}] \end{aligned} \tag{1-63}$$

For low frequencies, Eq. 1-62 reduces to Eq. 1-46. Equation 1-63 is frequently referred to as the Miller effect.

A calculation of gain and input admittance for a specific case will illustrate the order of magnitude of A and of Y_{11}. Calculations will be given for the circuit of Fig. 1-22, with the tube assumed to be a type 6C5 for which $g_m = 2000$ micromhos, $r_p = 10{,}000$ ohms, $C_{gp} = 2$, $C_{gk} = 3$, and $C_{pk} = 11$ micromicrofarads. The load impedance $Z_L = 20{,}000$ ohms. Then, $g_p + Y_L = 150 \cdot 10^{-6}$, and Eq. 1-62 becomes

$$A = -\frac{(2000 - j2\omega \cdot 10^{-6})10^{-6}}{(150 + j13\omega \cdot 10^{-6})10^{-6}}$$

If the frequency is 796 cps, $\omega = 5000$ radians per second, and $j2\omega \cdot 10^{-6} = j0.01$ mho; $j130\omega \cdot 10^{-6} = j0.065$ mho. At this low frequency the simpler relation 1-46 applies, and

$$A = -2000/150 = -13.3$$

Also, $$Y_{11} = j5000\{3 \cdot 10^{-12} + [1 - (-13.3)]2 \times 10^{-12}\}$$
$$= j5000(31.6) \cdot 10^{-12}$$
$$= j0.158 \cdot 10^{-6} \text{ mho}$$
$$Z_{11} = 1/Y_{11} = -j6.34 \text{ megohms}$$

The equivalent triode-amplifier input circuit, for 796 cps, is then simply a capacitance of 31.6 $\mu\mu$f. If the frequency is increased to 1593 kilocycles per second, $\omega = 10 \cdot 10^{+6}$, and

$$A = -\frac{2000 - j20}{150 + j130} = -7.6 + j6.67$$
$$= -10.1\underline{/-41.4^\circ}$$
$$Y_{11} = j10 \cdot 10^6[3 + (8.6 - j6.67)2] \cdot 10^{-12}$$
$$= (133.4 + j202) \cdot 10^{-6} \text{ mho}$$

This admittance may be represented by a pure resistance R_{11} in parallel with a pure capacitance C_{11} where

$$R_{11} = \frac{10^6}{133.4} = 7500 \text{ ohms}$$
$$X_{11} = \frac{10^6}{202} = 4950 \text{ ohms}$$
$$C_{11} = 20.2 \ \mu\mu\text{f}$$

To an external voltage source at 1593 kc, this 6C5 amplifier circuit then presents an impedance which is the equivalent of Fig. 1-29.

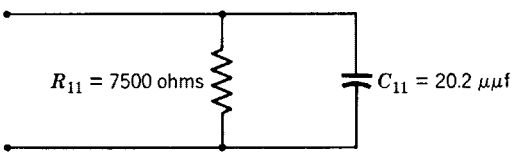

FIG. 1-29. Equivalent input circuit of an amplifier circuit at 1593 kc.

The dependence of the input admittance of the triode amplifier upon C_{gp} is brought out by the foregoing computations. The factor $(1 - A)$ (Eq. 1-63) emphasizes the contribution of the grid-plate capacitance in increasing the input admittance. It is desirable that Y_{11} for an amplifier be as small as possible. This requirement has led to the inclusion of additional grids in vacuum tubes between the plate and the control grid in

order to reduce the control grid to plate capacitance. The characteristics of such multielectrode tubes will be described in Chapter 2.

1-21. A Generalized Equivalent Circuit for Linear Operation

As stated in the preceding section, it becomes necessary to include the tube interelectrode capacitances in equivalent a-c circuits which closely approximate the actual tube behavior in the range of frequency from 1 kc to about 2 Mc per sec. The equivalent circuit applicable in this range of frequencies is shown in Fig. 1-30, which consists of the circuits of Figs. 1-27 and 1-28 superposed.

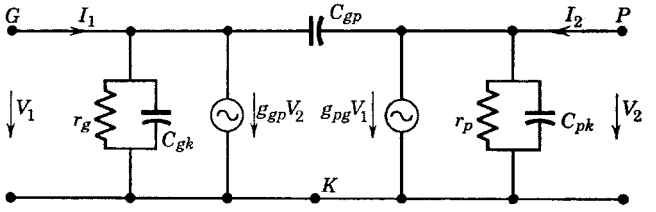

FIG. 1-30. Triode equivalent circuit for frequencies up to 1 or 2 Mc.

The electrodes of a high-vacuum electron tube actually in or adjacent to the electron stream must be connected to the terminals available external to the tube envelope. These connecting leads have distributed inductance and capacitance of such values as to be negligible in the frequency range of applicability of the circuit of Fig. 1-30, but begin to introduce increases in the driving-point, transfer, and feedback admittances for frequencies of the order of 10 to 100 Mc. An attempt to represent those additional circuit complexities is made in Fig. 1-31. It is evident that the circuit has now become very complicated for analysis, but of greater importance is the fact that the new circuit elements can-

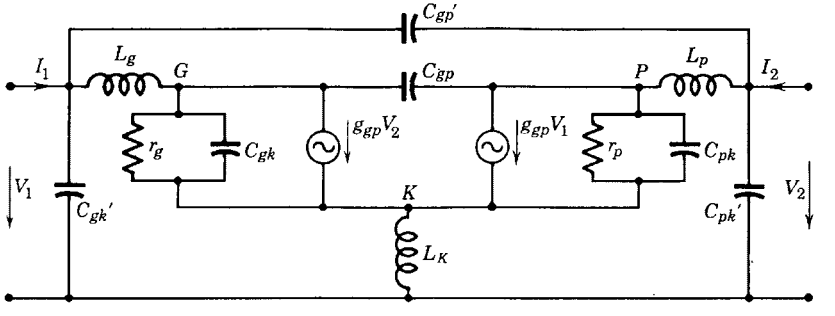

FIG. 1-31. Equivalent a-c circuit as complicated by lead-wire inductances and capacitances for frequencies of the order of 10 to 100 Mc.

not be determined individually from measurements made at the external terminals.

At still higher frequencies of the order of 1000 to 10,000 Mc the circuit admittances y_{ij} become modified by the effects of the finite transit time of the electrons across the interelectrode space, and coupling circuit effects may still be of equal or greater importance in spite of improvements that are of necessity made in the input and output coupling circuits in the higher frequency range above 100 Mc.

It is at this point that the four-pole approach to the tube equivalent circuit offers its most important contribution. The additional circuit complexities are, to a first order of approximation, linear and may be

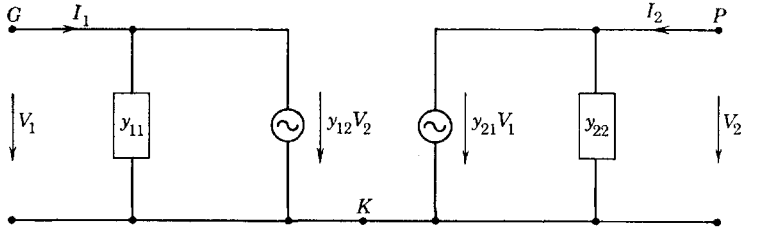

FIG. 1-32. Generalized equivalent a-c circuit.

lumped together into the admittances y_{11}, y_{12}, y_{21}, and y_{22} which may be determined by direct measurement in the frequency range of interest. These admittances as measured at the external terminals contain all coupling circuit and transit-time effects. It is then possible to prepare a generalized equivalent circuit using only the admittances y_{ij}, as shown in Fig. 1-32.

When measurements of the four-pole admittances of electron tubes used in the frequency range 100 to 10,000 Mc are complete, the problem of circuit design and application becomes a straightforward analysis of the circuit of Fig. 1-32 with the values of y_{ij} as dependent upon frequency.

1-22. Photosensitive Devices

Electron tubes which depend for electron emission upon light, of wavelength in the visible spectrum or adjacent to it, are diodes which have many important applications. The static characteristics of photosensitive devices furnish sufficient information for their circuit use. Currents depend upon the available intensity and wavelength of illumination upon the photocathode.

Although several types of photosensitive devices have practical importance, only one has characteristics analogous to the diodes discussed in the present chapter and is known as a *photoemissive* cell. It consists of a cathode which emits electrons when illuminated and an

anode arranged as shown in Fig. 1-33. The cathode is a metal surface of semicylindrical geometry with a coating of the light-sensitive material, usually an alkali metal. The anode is of such form as not to shield the cathode from incident light and may be a straight wire as shown in Fig. 1-33. The electrons released at the cathode as a result of illumination flow from cathode to anode and provide the phototube current. An output voltage depending on the illumination then exists across the resistance R (Fig. 1-33). The tube elements are enclosed in a glass or quartz envelope from which air is evacuated; the resulting tube is considered as a vacuum or gas-filled photocell depending upon the internal pressure.

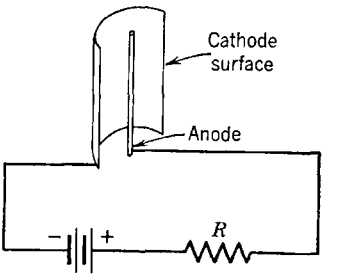

FIG. 1-33. Schematic electrode arrangement of a photocell.

Typical static characteristics of a vacuum photocell are shown in Fig. 1-34. A separate curve is obtained for each value of light flux. A

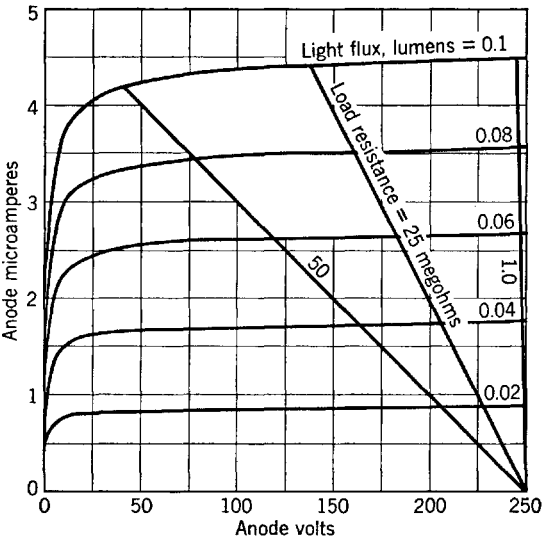

FIG. 1-34. Static characteristics and load lines for a vacuum photocell. (Courtesy RCA)

lumen is equivalent to 0.001496 joule per second or 0.001496 watt. The standard of illumination or luminous intensity is the lumen per square meter which is equal to 0.0929 foot-candle. The lumen per square foot is equal to 1 foot-candle.

The phototube circuit of Fig. 1-35 is suggestive of one application. When light falls on the photocathode, current flows in the phototube circuit as indicated by the arrow. If the triode amplifier has been

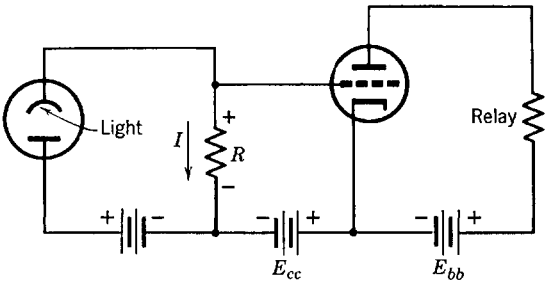

FIG. 1-35. Photocell control of relay.

biased to cutoff by the battery E_{cc}, the voltage drop IR due to the phototube current will provide a positive grid bias such that the triode will conduct. If the triode load resistance is a relay, normally open, the relay may be made to close by the flow of a few milliamperes of triode plate current. If the light is off, the relay will open, since the triode is biased to cutoff. Thus, the relay can be controlled by illumination of the photocathode. The voltage IR available for biasing the triode will depend upon the magnitude of R and also upon the illumination of the photocell, as shown by the load lines of Fig. 1-34.

PROBLEMS

1-1. The tube characteristic of a certain diode is assumed to be linear. It is found that the anode current is 50 ma for an anode voltage of 400 volts.

(*a*) Determine the equation of and sketch the anode-current–anode-voltage characteristic.

(*b*) When the tube is connected in series with the secondary winding of a transformer in which the secondary voltage is given by $e = 300 \sin 377t$, determine the equation of and sketch the anode current as a function of time.

1-2. Solve problem 1-1 if the tube characteristic is assumed to be a parabola, concave up, and if again $i_b = 50$ ma for $e_b = 400$ volts. Compute the plate resistance for $i_b = 10$ and for $i_b = 40$ ma.

1-3. Experimental data on the tube characteristic of a type 81 diode are given in the table. If this diode is connected as shown, determine graphically and sketch

Volts	e_b	20	40	60	80	100
Ma	i_b	18	47	83	129	179

the plate current, given $R = 1000$ ohms, $e = 80 \sin \omega t$.

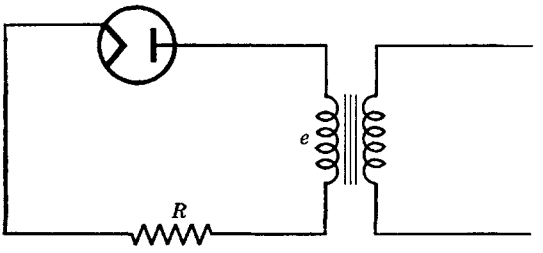

FIG. P1-3.

1-4. The plate current of a certain diode is given by Eq. 1-1 and $i_b = 200$ ma when the plate voltage is 100 volts. Compute the plate resistance at 25 volts and at 100 volts.

1-5. For a certain triode, the plate current is given by

$$i_b = 134 \cdot 10^{-6}(e_c + 0.125e_b)^{1.67}$$

For $e_c = -20$ volts, $e_b = 350$ volts, find:

(*a*) i_b, r_p, g_m, μ.

(*b*) The required plate battery voltage if the operating point is $E_b = 350$, $E_c = -20$ volts, and $R_L = 10{,}000$ ohms.

1-6. Refer to the amplifier circuit of Fig. 1-12. If the tube is a 6C5, its characteristics are given by Figs. 1-7, 1-8, and 1-9, or by the tube manual.

(*a*) Taking $E_{bb} = 400$ volts, $E_{cc} = -8$ volts, and $R_L = 40{,}000$ ohms, draw the load line and the dynamic characteristic, and locate the operating point.

(*b*) If $e_g = 2 \sin \omega t$, $\omega = 5000$ rad per sec, determine graphically the effective value of the alternating component of the plate current assuming linear operation.

(*c*) Sketch e_g on the mutual characteristic, and locate graphically points for sketching the instantaneous values of plate current and plate voltage. Check the phase relation between the alternating components of grid voltage, plate current, and plate voltage.

1-7. For the 6C5 in the circuit of problem 1-6:

(*a*) Obtain data from the tube characteristics for plotting anode-grid voltage characteristics similar to Fig. 1-9 for $I_b = 6$ ma.

(*b*) Determine the tube amplification factor.

(*c*) Find r_p and g_m at the operating point, and check the relation $\mu = r_p g_m$.

(*d*) Find the amplifier voltage gain by graphical methods, and compare the value obtained with that computed from $\mu R_L/(r_p + R_L)$.

1-8. Show that the constant-voltage equivalent circuit of Fig. 1-17 may be converted to the constant-current equivalent circuit of Fig. 1-22 (with $Z_L = 1/Y_L$ replacing R_L) by applying Norton's theorem. Also, show that Eq. 1-46 may be written as

$$A = -g_m Z_{eq}$$

where Z_{eq} is an impedance equivalent to r_p and Z_L in parallel.

1-9. An amplifier circuit is that of Fig. 1-22*a* except that a resistor R_K is inserted in the cathode lead to provide bias voltage equal to the voltage drop $I_b R_K$ due to the d-c component of plate current flowing through R_K. The bias battery E_{cc} is removed. Derive a formula for the gain of the amplifier using (*a*) the constant-voltage equivalent circuit, (*b*) the constant-current equivalent circuit.

1-10. A 6C5 triode is connected as an amplifier with resistance load, $R_L = 40{,}000$ ohms. With conditions identical with those given in problem 1-6, draw the a-c equivalent plate circuit, find the alternating component of plate current (effective value), and compare with the result obtained by graphical means in problem 1-6. Draw the vector diagram, and show the phase relation between E_g and the voltage across R_L.

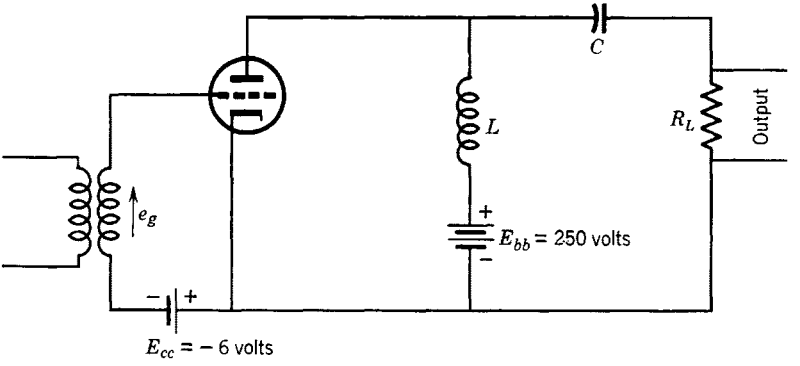

FIG. P1-11.

1-11. The tube in the amplifier circuit shown is a 6J5, $r_p = 7700$ ohms, $\mu = 20$, $C = 0.15\mu f$, $R_L = 10{,}000$ ohms, $L = 5$ henrys.

(*a*) Draw the equivalent a-c plate circuit, neglecting choke resistance.

(*b*) Determine the effective alternating currents in choke and load resistor for $e_g = 4 \sin 5000t$.

(*c*) Find the gain of the amplifier.

(*d*) Draw a complete vector diagram using the voltage across R_L as reference, and find the phase relation between the input and output voltages.

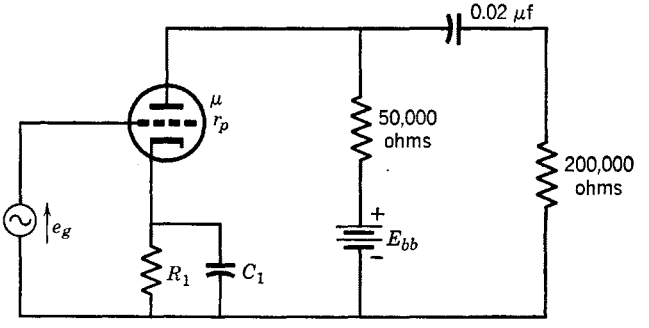

FIG. P1-12.

1-12. In the circuit shown, $\mu = 20$, $r_p = 10{,}000$, $C_1 = 10$ μf. The drop I_bR_1 in the bias resistor R_1 is to be used instead of a battery for grid bias. If the quiescent point is to be $I_b = 5$ ma, $E_c = -6$ volts, determine R_1. Find the voltage gain of the amplifier and the phase angle between input and output voltages if $e_i = 3 \sin 10{,}000t$. Draw a complete vector diagram. $K = 1000$ ohms.

1-13. The accompanying circuit can be used in determining g_m.

(*a*) Draw the equivalent a-c anode circuit.

(*b*) Show that, for silence in the headphones,

$$r_p = R_3(\mu R_1/R_2 - 1)$$

(*c*) If $\mu R_1/R_2 \gg 1$, show that

$$g_m \cong R_2/R_1R_3$$

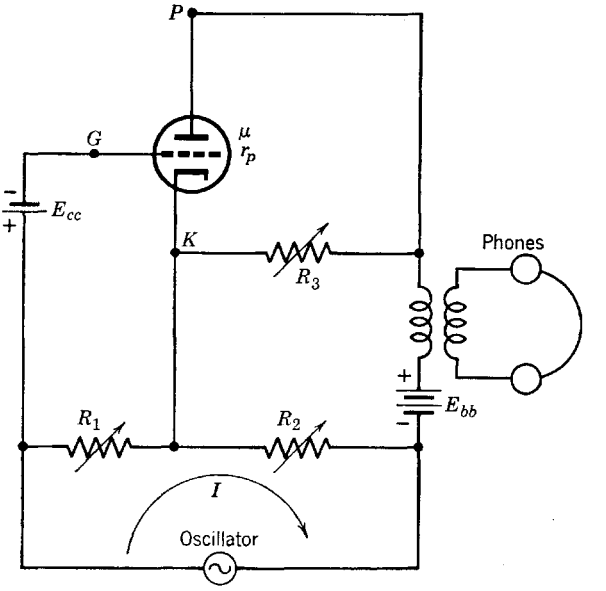

FIG. P1-13.

1-14. Determine the gain of the circuit shown by deriving from the equivalent a-c plate circuit an expression for the gain in terms of μ, R_L, r_p, and R.

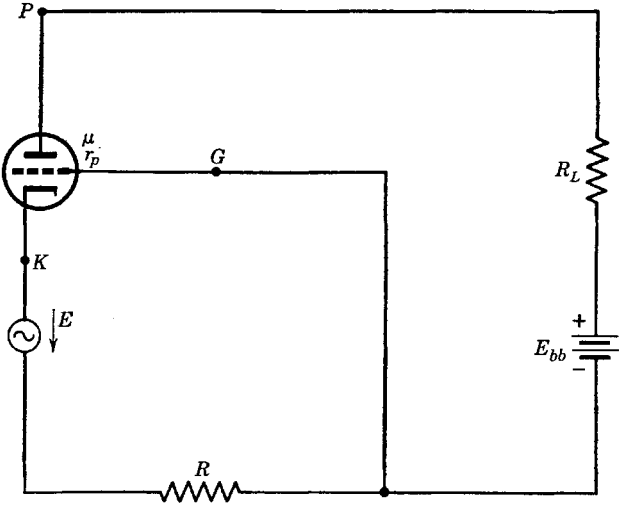

FIG. P1-14.

1-15. A type-2A3 triode is connected as an amplifier with cathode bias resistor (as in problem 1-12), but with no by-pass condenser. The load resistance is 2450

ohms, $r_p = 800$ ohms, $\mu = 4.2$. The tube is to operate at $E_c = -45$ volts, $I_b = 60$ ma, $E_b = 250$ volts.

(*a*) Determine the necessary grid-bias resistor and plate battery voltage.

(*b*) Compute the gain of the amplifier.

1-16. Sketch the complete equivalent circuit of a triode for which $i_c \neq 0$, and include all interelectrode capacitances.

1-17. Sketch the complete equivalent a-c circuit of the amplifier of problem 1-12, including all interelectrode capacitances. Next, draw appropriate simplified a-c equivalent circuits according to the principle that a series impedance may be neglected in a frequency range for which it is equal to or less than 0.1 the magnitude of a fixed impedance with which it is in series, for the following frequency ranges:

(*a*) $0 < \omega < 500$

(*b*) $1500 < \omega < 2500$

(*c*) $5000 < \omega < 50{,}000$

(*d*) $50{,}000 < \omega < 5 \cdot 10^6$

Show only those capacitances in a particular circuit for which the reactances may not be ignored in a numerical computation of circuit currents.

1-18. Assume that the tube in problem 1-17 is a 6J5.

(*a*) Derive a formula for the input admittance of the amplifier at $\omega = 10 \cdot 10^6$ rad per sec, using any appropriate circuit analysis other than the four-pole method.

(*b*) Compute the input *impedance* of the amplifier at $\omega = 10 \cdot 10^6$ rad per sec.

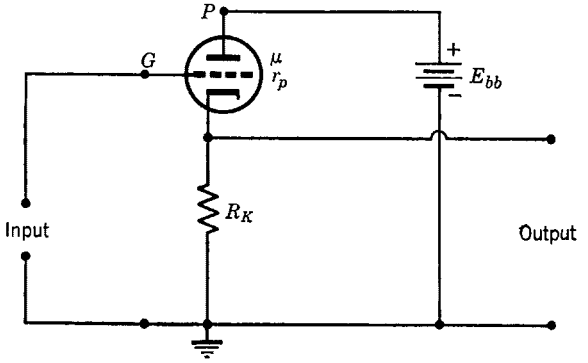

FIG. P1-19.

1-19. (*a*) Sketch the equivalent a-c circuit of the four-terminal network shown, neglecting interelectrode capacitances.

(*b*) Derive expressions for y_{11}, y_{12}, y_{21}, and y_{22} in terms of μ, r_p, g_m, and R_L.

1-20. Repeat problem 1-19, including all interelectrode capacitances.

1-21. Derive an expression for the voltage gain of the circuit of problem 1-19. Include interelectrode capacitances.

1-22. Light flux of 0.06 lumen is incident on a type-929 photocell (Fig. 1-34) in the circuit of Fig. 1-35. The photocell voltage source is 100 volts, and $R = 25$ megohms. Compute the triode bias voltage if $E_{cc} = 20$ volts.

1-23. The photocell of problem 1-22 is illuminated by light of intensity sinusoidally varying from 0.02 to 0.1 lumen at 1000 cps about an average value of 0.06 lumen. If R is 25 megohms, write an expression for the input signal voltage to the amplifier.

CHAPTER 2

TETRODES, PENTODES, AND EQUIVALENT CIRCUITS

2-1. Ideal Plate Characteristics

Triode plate characteristics described in Chapter 1 show the dependence of plate current upon both plate and grid voltages. The plate voltage is ordinarily supplied from a d-c power source of fixed voltage rating, and the control of plate current is, for many applications, desirably a function of the grid voltage only. Ideal characteristics would consist of nearly horizontal, parallel straight lines covering the entire plate diagram. A horizontal anode-current–anode-voltage characteristic indicates that the plate current is independent of anode voltage. Control of plate current in such a case would depend upon grid voltage only.

Plate characteristics approximating the requirement of negligible plate voltage control of plate current may be obtained in vacuum tubes by using additional grids between cathode and plate. The presence of an additional grid between the grid as used in the usual triode arrangement and the anode of the tube greatly reduces the effective grid-plate capacitance. The result of such a reduction of C_{gp} is a very desirable decrease in the tube input admittance, as shown by Eq. 1-63, page 43 of Chapter 1.

2-2. The Tetrode or Screen Grid Tube

An arrangement of two grids in a vacuum tube is shown in Fig. 2-1. The grid nearer to the cathode is now called the *control grid*, and the second grid because of its function of screening the plate from cathode and control grid is called the *screen* grid. It is usually customary to number grids consecutively in multielement tubes beginning with the grid nearest the cathode as number one. Four-electrode high-vacuum tubes are called *tetrodes*.

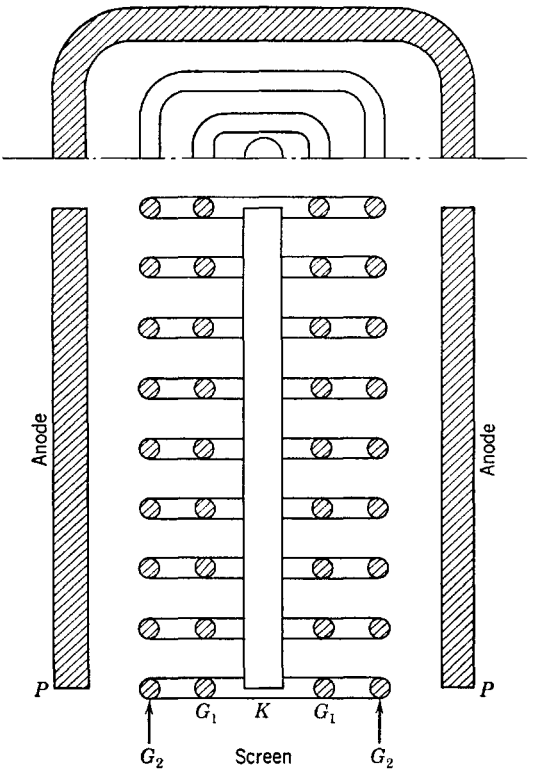

FIG. 2-1. Sectional view of electrode arrangement in a cylindrical tetrode. G_1 and G_2 are control and screen-grid helices.

2-3. Tetrode Static Characteristics

The shielding effect of the two grids between plate and cathode of the tetrode is complete enough so that it becomes necessary to operate the screen grid at high positive voltages in order to obtain appreciable plate current. A connection diagram for a tetrode operated as an amplifier is shown in Fig. 2-2. In connecting a tetrode to its d-c power source, the screen voltage should never be applied until the plate supply is connected, thus avoiding the danger of the entire tube current flowing to the screen and destroying the tube.

Plate and mutual characteristics for a typical screen grid tube are shown in Fig. 2-3. As compared with a triode, the following differences should be observed:

1. The slope, $\partial i_b/\partial e_b$, in the operating region to the right of $e_b = 125$ volts is smaller and therefore the plate resistance is much larger than

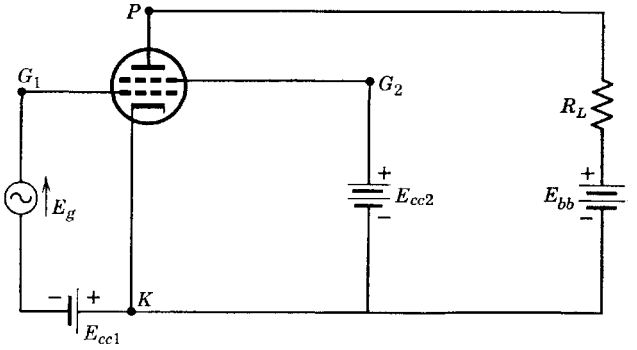

FIG. 2-2. Connection diagram for a tetrode.

that of a triode. For $e_b > 125$ volts, the plate current depends relatively little, compared with the triode, upon the plate voltage.

2. The slope g_m of the mutual characteristics is of the same order of magnitude as for a triode of similar dimensions.

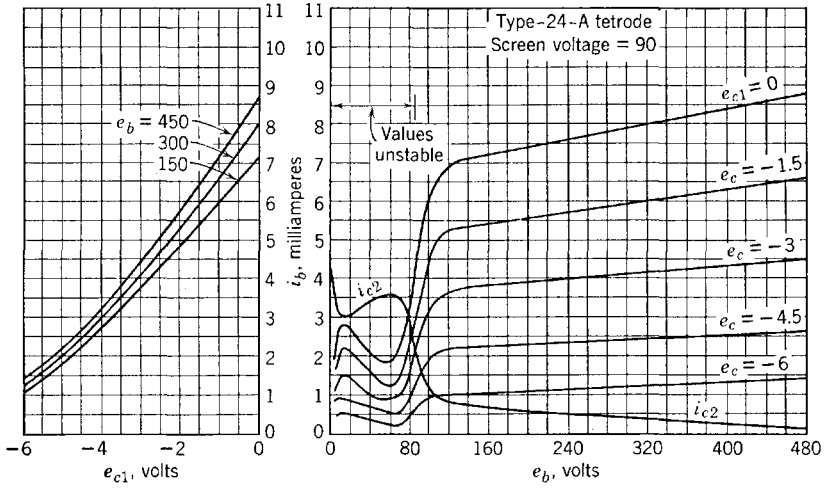

FIG. 2-3. Static characteristics of a tetrode. (Courtesy RCA)

3. For a triode, $i_b = f(e_b, e_c)$. For the screen grid tube, the corresponding relation is

$$i_b = F(e_b, e_{c1}, e_{c2}) \tag{2-1}$$

However, e_{c2} is held constant, and i_b is relatively independent of e_b, so that it may be said that the addition of the fourth electrode has reduced,

rather than increased, the number of independent variables. Approximately, then,

$$i_b = f(e_{c1}) \tag{2-2}$$

The accuracy of the approximation is measured by the closeness of the mutual characteristics, as shown in Fig. 2-3.

It should be observed that the plate characteristic for e_b between 20 and 50 volts has a negative slope, indicating a negative plate resistance. This portion of the tetrode characteristic has had practical application and use as the operating range of a dynatron oscillator. For operation as an amplifier, however, the useful plate voltage range is that above $e_b = 100$ volts. Both instability and distortion would be introduced if operation extends into the region of the plate diagram below 100 volts. The problem of distortion will be considered later in the chapter.

2-4. Secondary Emission in the Tetrode

The plate-current maximum and minimum and the negative plate resistance which are typical of the tetrode plate characteristics at low plate voltages are caused by the occurrence of secondary electron emission from the plate. Secondary electrons are emitted from an electrode only if the incident primary electrons have a certain minimum kinetic energy at impact. For the tetrode of Fig. 2-3, this minimum kinetic energy is attained at approximately 20 volts, at which the screen current begins to increase and the plate current to decrease because secondary electrons from the plate are collected by the screen. With the screen voltage at 90 volts, and the voltage of the plate lower than that of the screen, secondary electrons set free at the anode are accelerated toward the screen. As the plate voltage rises and the secondary emission yield increases, the screen current increases and the plate current decreases, as shown by Fig. 2-3, until the current minimum is reached. At this plate voltage, secondary emission has its maximum effect upon plate current. After the plate voltage reaches equality with the screen grid voltage, secondary electrons leave the plate only because of initial emission velocities. For plate voltages greater than the screen voltage, secondary emission from the plate still occurs, but, since the plate potential is higher than the potential of the screen, secondary electrons return to the plate, and no effects of secondary emission are observable. Secondary electrons may also be released at the screen. At high plate voltage, such secondary electrons would serve to increase the current to the plate and decrease the current to the screen. Occasionally the secondary emission from a screen grid may be enough so that the screen

current actually reverses as the plate voltage increases, showing that a single primary electron may release more than one secondary electron upon collision with the screen. In many of the older tetrode tubes the plate current also reversed at low plate voltage because of a secondary-electron yield ratio (number of secondary electrons released by one primary electron) greater than one. In the modern tubes the anodes are covered with certain surface materials such as graphite which decrease the secondary emission, and thus the effect of secondary emission upon anode current is considerably reduced.

2-5. Tetrode Equivalent A-C Circuit

In the operating range of the tetrode amplifier, the plate characteristics are quite linear. From the functional relation Eq. 2-1, the change in plate current resulting from small changes in electrode voltage is

$$\Delta i_b = \frac{\partial i_b}{\partial e_b}\Delta e_b + \frac{\partial i_b}{\partial e_{c1}}\Delta e_{c1} + \frac{\partial i_b}{\partial e_{c2}}\Delta e_{c2} \tag{2-3}$$

Exactly as for the triode, the change in current or in electrode voltage from quiescence is replaced by the instantaneous a-c component of current or voltage. Accordingly, $\Delta i_b = i_p$, $\Delta e_b = e_{KP}$, $\Delta e_{c1} = e_{KG}$, and, since the screen voltage is held constant, $\Delta e_{c2} = 0$. By definition,

$$\frac{\partial i_b}{\partial e_b} = \left(\frac{di_b}{de_b}\right)_{(e_{c1},\, e_{c2}\ \text{constant})} = \frac{1}{r_p} = g_p \tag{2-4}$$

and

$$\frac{\partial i_b}{\partial e_{c1}} = \left(\frac{di_b}{de_{c1}}\right)_{(e_b,\, e_{c2}\ \text{constant})} = g_m \tag{2-5}$$

As for the triode, if i_b is held constant, $\Delta i_b = 0$, and Eq. 2-3 provides the relation

$$\mu = -\partial e_b/\partial e_{c1} = r_p g_m \tag{2-6}$$

Equation 2-3 then becomes

$$i_p = \frac{1}{r_p} e_{KP} + g_m e_{KG}$$

Now, for sinusoidal voltages and currents, rms or effective values may be used, and, since $E_{KP} = -I_p Z_L$, where Z_L is the equivalent impedance between K and P in the circuit outside the tube,

$$I_p = -I_p Z_L/r_p + g_m E_{KG} \tag{2-7}$$

Equation 2-7 suggests either the voltage-source or current-source

equivalent a-c plate circuit exactly as for the triode. Thus,

$$I_p = \frac{\mu E_{KG}}{r_p + Z_L}$$

suggests an equivalent a-c circuit consisting of a voltage-source generator of voltage μE_{KG} and internal resistance r_p connected across the load impedance Z_L. If, however, Eq. 2-7 is written as

$$g_m E_{KG} = I_p + I_p Z_L / r_p \tag{2-8}$$

it suggests an equivalent a-c circuit consisting of a *current-source* genera-

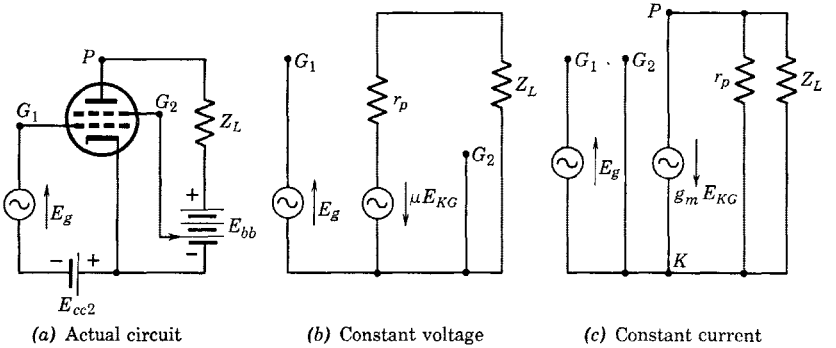

(a) Actual circuit (b) Constant voltage (c) Constant current

FIG. 2-4. Actual and equivalent circuits of a tetrode at audio frequencies.

tor of current $g_m E_{KG}$ supplying current I_p and $I_p Z_L / r_p$ to the impedances Z_L and r_p connected in parallel across the terminals of the generator. The actual and equivalent a-c circuits of the tetrode amplifier are shown in Fig. 2-4. The equivalent circuits of Fig. 2-4 are identical with those used for the triode. Either the voltage-source or the current-source generator may be used in the equivalent a-c plate circuits of both triode and tetrode amplifiers, and the same restrictions as to operation over the region of linearity of the dynamic characteristics apply to both. The plate resistance r_p of the tetrode is ordinarily very large compared with the load resistance; in this case, the plate resistance can be omitted in Fig. 2-4*c*, resulting in a significant simplification.

If all the interelectrode capacitances are included, the equivalent a-c circuit is that of Fig. 2-5. Since the screen-cathode capacitance is short-circuited for alternating current by the screen connection to cathode through the screen supply voltage, C_{g2k} may be omitted. Capacitances C_{pk} and C_{g2p} provide parallel paths from the plate to the cathode and so may be combined. Also C_{g1k} is in parallel with C_{g1g2} through the screen connection to cathode. By combining the parallel capacitances

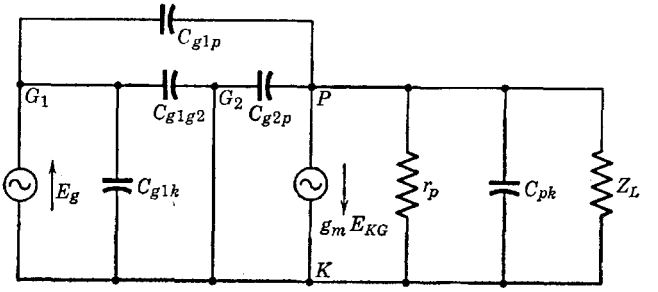

FIG. 2-5. Equivalent a-c circuit of a tetrode amplifier, including interelectrode capacitances.

and neglecting C_{g1p} (which the presence of the grounded screen makes negligibly small), the circuit may be simplified as shown in Fig. 2-6 in which

$$C_{11} = C_{g1k} + C_{g1g2}$$

and

$$C_{22} = C_{pk} + C_{g2p}$$

The input admittance is then

$$Y_{11} = j\omega C_{11}$$

The output capacitance C_{22} is not appreciably different from C_{g2p}, because of the shielding effect of the screen between plate and cathode.

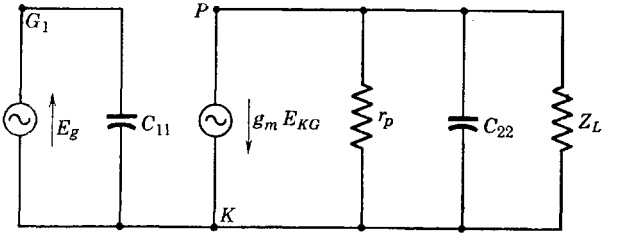

FIG. 2-6. Simplified equivalent tetrode a-c circuit.

The capacitances are now small enough that connecting lead-wire capacitances may become equally important; thus it is necessary to provide adequate shielding for screen grid tubes to realize best results at frequencies much above the audio range.

2-6. Suppression of Secondary Emission. The Pentode

Secondary-emission electrons from the anode are attracted to the screen only for plate voltages that are lower than the fixed voltage applied to the screen grid. The secondary electrons released at the

anode would be forced to return to that electrode if its potential were higher than any potential in the immediate vicinity. Such a *space distribution* of potential between a positive screen grid and a less positive anode can be obtained if a *potential minimum* can be provided between screen and plate. There are two methods in present use which provide the required potential minimum. One of these utilizes a grid of wires aligned with screen and control grid wires, located between screen and anode, and held at zero potential by direct connection to the cathode. The resulting five-electrode tube is called a pentode. The purpose of the third grid is to suppress the secondary-emission current to the

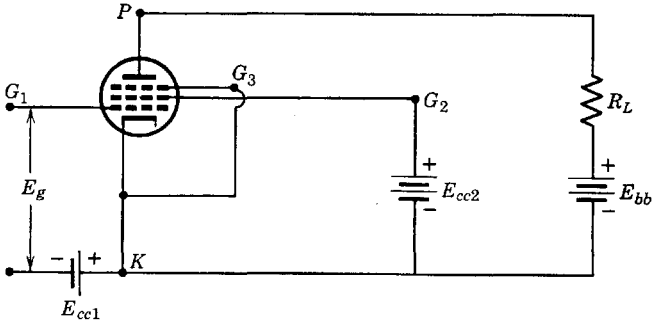

FIG. 2-7. Connection diagram for a pentode amplifier.

screen, and it is called the suppressor grid. The connection diagram of Fig. 2-7 is drawn for a tube in which the suppressor-to-cathode connection is made externally, that is, outside the tube envelope, such as for the type 59, and the 6J7. With the suppressor connection brought out, the tube can be operated as a triode by connecting suppressor grid no. 3 and screen grid no. 2 to the plate. In tubes such as the 6F6 the suppressor grid is connected to the cathode internally. This tube may still be operated as a triode by connecting the screen to the plate.

Suppression of the secondary-emission screen current eliminates the negative resistance range in the plate characteristic of the tetrode. Typical pentode plate characteristics are shown in Fig. 2-8 for the 6F6. The dependence of the plate current upon plate voltage is less evident than for the tetrode. At a control grid bias of -30 or -35 volts, the plate current is virtually independent of plate voltage, and the plate resistance is extremely high. Since the control grid-plate transconductance is approximately the same as for an equivalent triode, the effective amplification factor, $\mu = g_m r_p$, is greatly increased. Depending upon the purpose for which the pentode is designed, r_p for different pentodes varies from about 40,000 to 10^6 ohms, and μ from 100 to 1500. Although

the range of linearity of the pentode plate family extends over a greater area of the i_b–e_b graph sheet, the dynamic characteristic has somewhat the shape of the graph of a cubic equation, and this results in a pronounced third harmonic in the pentode output, to be discussed in Section 2-10. It is chiefly the presence of the third harmonic that limits the undistorted power output of the pentode. It has been shown that the

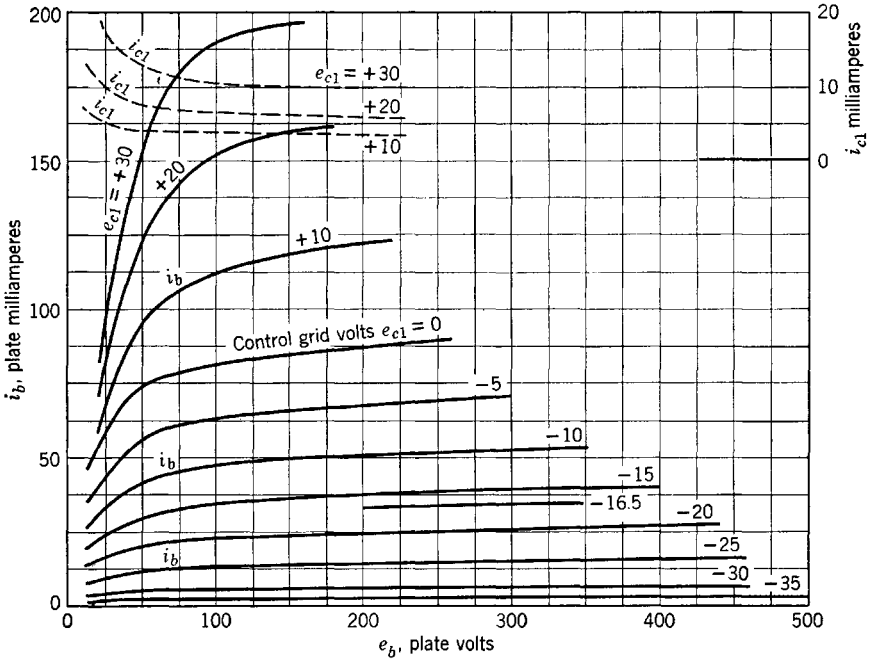

FIG. 2-8. Plate and control grid characteristics of a type-6F6 pentode. (Courtesy RCA)

curved portions of the i_b–e_b characteristics for low plate voltages are responsible for the third harmonic in the pentode output. Since this portion of the characteristic is the result of the suppressor grid action being nonuniform across the path of the electrons, a type of suppressor was sought that did not require a mechanical grid. This research resulted in the *beam-power* [1] or *critical-distance* [2] tube.

2-7. Beam-Power Tube

The beam-power tube is a tetrode in which the effects of secondary emission are largely eliminated by mechanical design of electrodes.

[1] O. H. Schede, *Proc. IRE*, **26**, 137–181 (1938).
[2] H. H. O. Harries, *Wireless Engineer*, **13**, 190–199 (1936).

Suppressor action in the beam-power tube, for example the 6L6, is obtained by the use of the effect of electron space charge in lowering the potential minimum at low plate voltages. Such a potential minimum between screen and plate will result from the presence of electron space charge if a sufficient current flows into this region. By careful alignment of control and screen grid wires and the use of beam-forming plates at cathode potential, a sufficient electron space-charge density is secured between screen and anode to produce a potential minimum in that re-

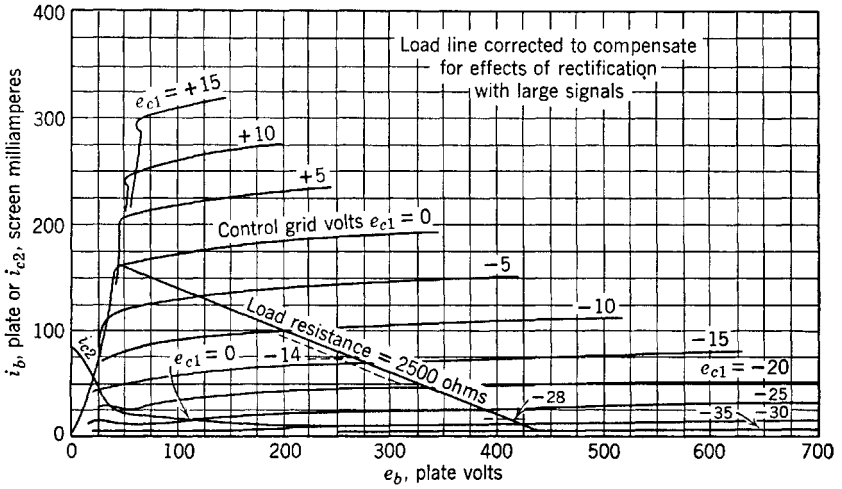

FIG. 2-9. Static characteristics of a type-6L6 beam tetrode. (Courtesy RCA)

gion. In other words, the electrons in transit from screen to plate provide enough negative charge in the interelectrode space between these electrodes to produce a potential minimum. The uniformity of the space-charge density in the plane of the potential minimum provides a much more uniform suppressor effect than a mechanical grid with its inevitable potential variation from grid wire to grid wire.

Typical plate characteristics of the 6L6 beam-power tetrode are shown in Fig. 2-9. Certain values of plate voltage and current in the region of low plate voltage are critical in the operation of beam-power tubes. By this is meant that sudden changes or instabilities occur in the plate-current–plate-voltage relation so that the current in this region is not a single-valued function of the plate voltage. Linear and stable amplifier operation is therefore confined to the region of the flat portions of the characteristics, but, as Fig. 2-9 shows, this occupies the greater part of the plate diagram. The electrode arrangement in a beam-power tube is shown in Fig. 2-10.

The term "critical-distance" tube has been applied to the beam-power tube because the distance between screen and anode, in addition to the electron-beam space-charge density, helps to determine the requisite potential minimum.

The arrangement of electrodes in the beam-power tube permits a considerable increase in the transconductance g_m for tubes of specified size and voltage rating, a fact of importance in the selection of tubes for amplifiers designed to operate over a wide frequency range. The beam-

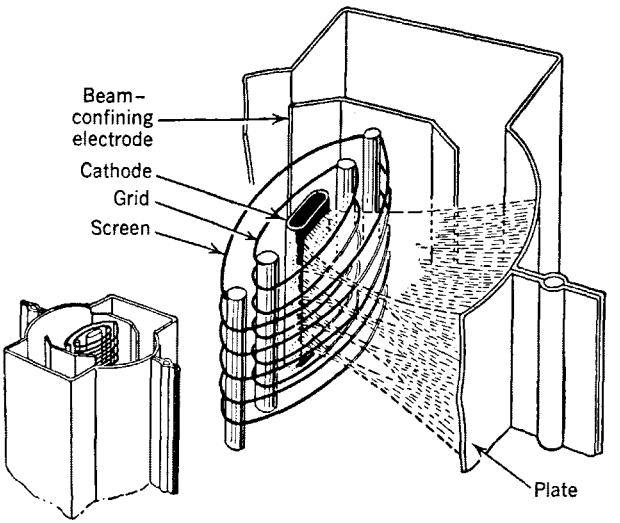

FIG. 2-10. Electrode arrangement in a beam tetrode. (Courtesy RCA)

power tube approaches the ideal power-amplifier tube whose plate characteristics would be flat, parallel, and equally spaced over the entire plate diagram.

2-8. Equivalent Circuits of Pentode and Beam-Power Amplifiers

The relation between plate current and electrode voltages for the pentode is indicated, as was done for triode and tetrode by the relation

$$i_b = f(e_b, e_{c1}, e_{c2}, e_{c3}) \tag{2-9}$$

With screen (e_{c2}) and suppressor (e_{c3}) grid voltages held constant, changes in plate current from the value at quiescence (zero signal voltage) occur for changes in control grid voltage e_{c1} and plate voltage e_b. The result is identical with that for triode and tetrode, so that an identical equivalent circuit results. It is usually more convenient to use the current-source generator, and frequently the pentode plate re-

sistance is so much higher than external circuit resistances that it may be omitted from the equivalent circuit if the current-source generator circuit is used.

Since beam-power tubes are tetrodes, their equivalent circuits are drawn in the same way as for triodes, tetrodes, or pentodes. Therefore, it may be stated that triode, tetrode, pentode, and beam-power amplifiers may be represented in the linear region of their dynamic characteristics by exactly the same type of equivalent a-c plate circuit.

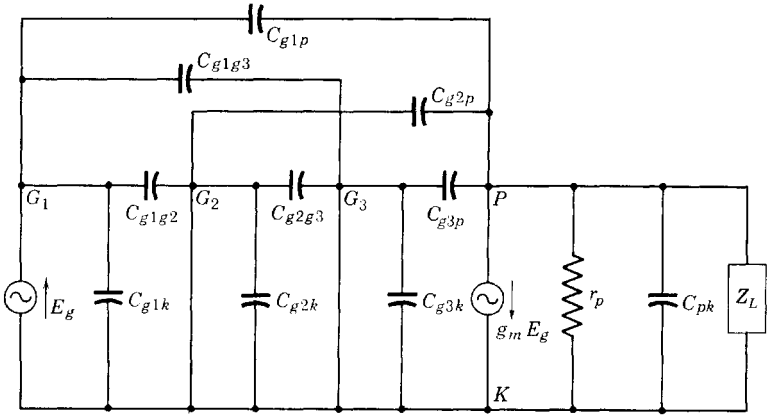

FIG. 2-11. Equivalent a-c circuit of a pentode including all interelectrode capacitances.

For pentodes, the capacitance between any electrode and each of the other four electrodes in the tube results in a total of ten capacitors to be added to the complete equivalent circuit at high frequency. Of the ten capacitances, however, that between control grid and plate is negligible and those between screen and cathode and between suppressor and cathode are short-circuited, as shown in Fig. 2-11. Other capacitors are in parallel, so that they may be replaced by a single capacitor of equivalent capacity. In this manner the circuit of Fig. 2-11 reduces to a simpler circuit with a single input and a single output capacitance as in Fig. 2-6. The relation of C_{11} and C_{22} to the interelectrode capacitances is left as an exercise.

2-9. Applications of Pentodes

Pentode tubes designed for power amplification have fairly low plate resistances, in the range (for receiving-type tubes) of 40,000 to 300,000 ohms. Representative power pentodes are the 6F6 and the 25A6. Voltage amplifier pentodes have much higher values of plate resistance.

Representative types of receiving tubes are: the 1N5-G, plate resistance 1.5 megohms, input capacitance 3.2 $\mu\mu$f, output capacitance 11 $\mu\mu$f, and the 6J7 (see Fig. 2-12): plate resistance 1 megohm. Such tubes are recommended for use in voltage amplifiers and as detectors.

A pentode may be used as a resistance in a circuit to provide a constant current. The type 6J7, for example, if biased to -3 volts, would pass approximately 2 ma for any plate voltage between 100 and 500

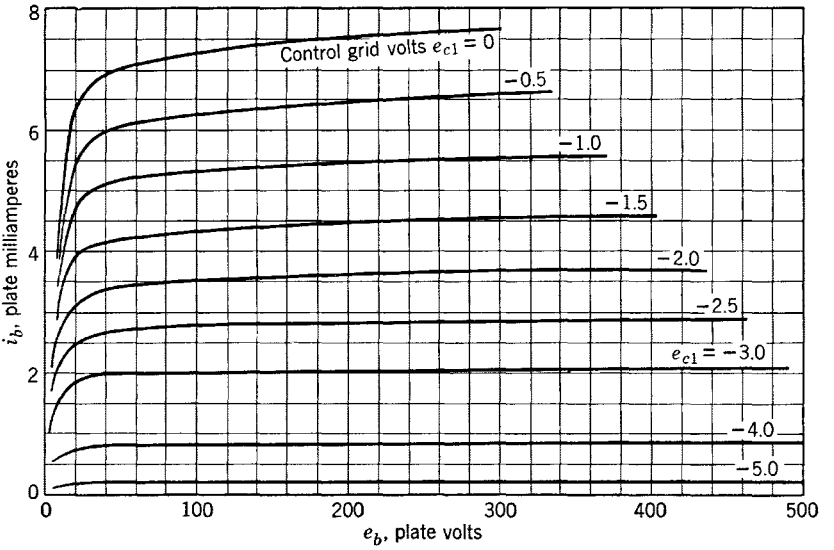

FIG. 2-12. Type-6J7 plate characteristics. (Courtesy RCA)

volts, as an examination of Fig. 2-12 will confirm. This is the basis for a number of applications of the pentode, and reference will be made to this property of the tube in later chapters.

2-10. Distortion

The term "distortion" has been referred to in earlier sections of this chapter. It is now proposed to define the term and to apply it in a further study of the high-vacuum tube and its characteristics as an amplifier.

The location of an operating point on the dynamic characteristic of a triode, tetrode, or pentode determines the possibility and extent of linear operation as already described in Chapter 1. It will now be shown that operation into the nonlinear region of the dynamic characteristic will result in the introduction, into the output of an amplifier, of frequencies not present in the input. These frequencies are harmonics of

fundamental input frequencies, and the presence of such harmonics in the amplifier output is defined as harmonic or amplitude distortion. From the point of view of Fourier analysis, harmonic distortion means that a sinusoidal (single-frequency) input voltage will come out of the amplifier as a nonsinusoidal wave, and this wave will contain harmonic frequencies not present in the input.

The problem of determining the harmonic content of the output of an amplifier with sinusoidal single-frequency input may be approached by analyzing the dynamic characteristic. With the origin of coordinates

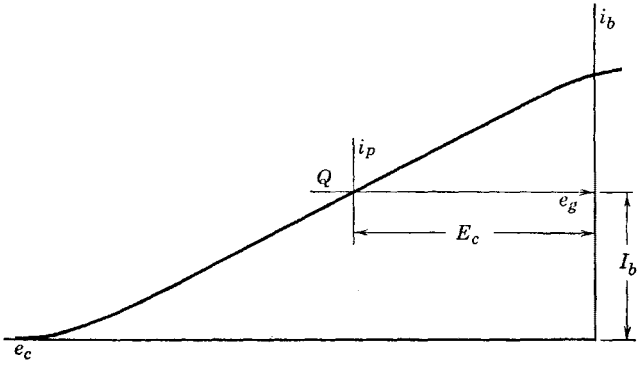

FIG. 2-13. Dynamic characteristic of an amplifier.

at the operating point, the equation of the dynamic characteristic is expressed as

$$i_p = f(e_g) \tag{2-10}$$

Such a relation is possible because the dynamic characteristic is the graphically obtained locus of corresponding values of grid voltage, plate voltage, and plate current. It is drawn on the i_b–e_b mutual characteristics graph, and $i_p = i_b - I_b$, $e_g = e_c - E_c$, as shown by Fig. 1-14. By choosing an origin of coordinates at $e_c = E_c$, $i_b = I_b$, the equation of the dynamic characteristic referred to a set of i_p–e_g coordinate axes may be developed by expressing Eq. 2-10 as a power series. This use of a series approximation may be very simply explained by the statement that the graph of the actual dynamic characteristic is assumed to be expressible mathematically in terms of sums of powers of the signal voltage e_g and that as many terms of the series are used as are necessary to give the desired approximation.

An assumed dynamic characteristic has been drawn for an amplifier as shown in Fig. 2-13. Let it be assumed that the curve of Fig. 2-13 is

represented about the operating point by the infinite series

$$i_p = C_1 e_g + C_2 e_g^2 + C_3 e_g^3 + \cdots + C_n e_g^n + \cdots \qquad (2\text{-}11)$$

in which the constants C_i may be determined as are the coefficients in a Taylor series or by selecting a number of points on the curve of Fig. 2-13 and substituting into Eq. 2-11 the coordinates of such points. Simultaneous equations involving C_1, C_2, C_3, etc., are then obtained from a partial series, and the equations may be solved for the constants C_i. As many terms must be taken as are needed to approximate the actual curve to the desired accuracy, but of course the number of points taken from the actual curve must equal the number of constants to be computed in order to provide sufficient equations.

If the grid input signal voltage is restricted in amplitude to values for which the curve of Fig. 2-13 is a straight line, then Eq. 2-11 becomes simply

$$i_p = C_1 e_g \qquad (2\text{-}12)$$

and, according to the linear circuit analysis of Chapter 1 (Eq. 1-32),

$$i_p = \frac{\mu}{r_p + R_L} e_g$$

Therefore, for linear operation, $C_1 = \mu/(r_p + R_L)$, which is the slope of the dynamic characteristic at the operating point. If the input signal voltage is

$$e_g = E_{gm} \cos \omega t$$

then the a-c component of plate current according to Eq. 2-12 is

$$i_p = C_1 E_{gm} \cos \omega t = \frac{\mu E_{gm}}{r_p + R_L} \cos \omega t = I_{pm} \cos \omega t$$

Now, if E_{gm} $(= \sqrt{2}\, E_g)$ is increased until a region of the dynamic characteristic is involved where the characteristic can no longer be considered to be a straight line, let it be assumed that two terms of Eq. 2-11 more accurately represent the portion of the characteristic that is used than would a single term. Then,

$$\begin{aligned} i_p &= C_1 E_{gm} \cos \omega t + C_2 E_{gm}^2 \cos^2 \omega t \\ &= C_1 E_{gm} \cos \omega t + C_2 E_{gm}^2 (1 + \cos 2\omega t)/2 \\ &= C_2 E_{gm}^2/2 + C_1 E_{gm} \cos \omega t + C_2 E_{gm}^2/2 \cos 2\omega t \end{aligned} \qquad (2\text{-}13)$$

and it is to be noted that the output current now contains a d-c component and a second harmonic not present in the input voltage. These

quantities are distortion components introduced by the nonlinearity of the dynamic characteristic.

In case the characteristic is adequately represented by three terms of Eq. 2-11, and again $e_g = E_{gm} \cos \omega t$,

$$i_p = C_1 E_{gm} \cos \omega t + C_2 {E_{gm}}^2 \cos^2 \omega t + C_3 {E_{gm}}^3 \cos^3 \omega t$$

but $\cos^3 \omega t = \frac{1}{4} \cos 3\omega t + \frac{3}{4} \cos \omega t$, so that

$$i_p = C_2 {E_{gm}}^2/2 + (C_1 E_{gm} + \tfrac{3}{4} C_3 {E_{gm}}^3) \cos \omega t + C_2 {E_{gm}}^2/2 \cos 2\omega t + \tfrac{1}{4} C_3 {E_{gm}}^3 \cos 3\omega t \quad (2\text{-}14)$$

where it should be noted that a third-harmonic component is now present in the output and also that the presence of the cubic term alters the fundamental component.

The foregoing analysis may be indefinitely extended. It is perhaps sufficient to state that, in general, the dynamic characteristic may be represented to any practical desired degree of accuracy by using enough terms of the series of Eq. 2-11. It can be shown that the substitution of $e_g = E_{gm} \cos \omega t$ into Eq. 2-11 yields an expression that may be reduced to

$$i_p = B_0 + B_1 \cos \omega t + B_2 \cos 2\omega t + B_3 \cos 3\omega t + \cdots + B_n \cos n\omega t + \cdots \quad (2\text{-}15)$$

where the B's represent harmonic amplitudes.

The next problem is that of determining the values of B_0, B_1, B_2, etc., from graphical data. It is desirable that all data used be obtainable from the plate diagram. In the method to be used in the following, all measurements may be made on the plate diagram, although the values may be represented more clearly in connection with the dynamic characteristic.

The total plate current is obtained by adding the quiescent value I_b to i_p. Thus Eq. 2-15 becomes

$$i_b = I_b + i_p = I_b + B_0 + \sum_{n=1}^{\infty} B_n \cos n\omega t \quad (2\text{-}16)$$

In practice it is found that the amplitudes of distortion components beyond the fourth harmonic are seldom worth the effort of graphical computation, particularly as harmonic analyzers have been developed and are available for measurement of harmonic amplitudes. Therefore, the analysis and the results given here are included because of use in the interpretation and extension of amplifier theory.

For the case of Eq. 2-13 where two terms only of the series are used, values of B_0, B_1, and B_2 may be computed by reading from the graph

sheet (Fig. 2-14) the values of i_b for particular values of ωt. For this case, Eq. 2-16 becomes

$$i_b = I_b + B_0 + B_1 \cos \omega t + B_2 \cos 2\omega t \tag{2-17}$$

In Fig. 2-14, refer to the curve of grid voltage $e_g = E_{gm} \cos \omega t$. For $\omega t = 0$, $i_b = i_{b\,\max}$; for $\omega t = \pi/2$, $i_b = I_b$; for $\omega t = \pi$, $i_b = i_{b\,\min}$. These

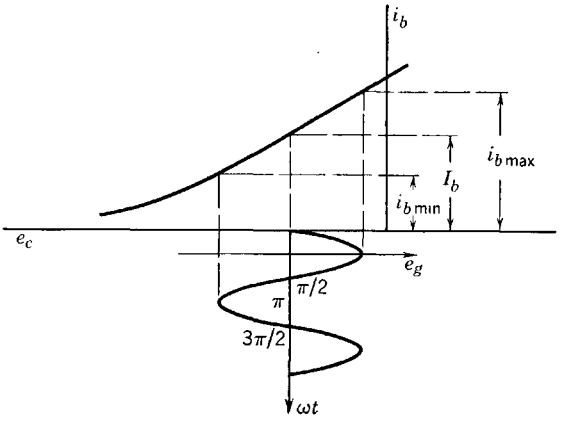

FIG. 2-14. Points for finding second-harmonic distortion.

values may be obtained, also, from Eq. 2-17. Thus, for

$$\omega t = 0, \qquad i_b = i_{b\,\max} = I_b + B_0 + B_1 + B_2$$

$$\omega t = \pi/2, \qquad I_b = I_b \quad = I_b + B_0 \quad - B_2$$

$$\omega t = \pi, \qquad i_b = i_{b\,\min} = I_b + B_0 - B_1 + B_2$$

and these equations may be solved for the harmonic-component amplitudes in terms of the values of i_b determined from the graph. The results are:

$$B_0 = B_2 \tag{2-18}$$

$$B_1 = \frac{i_{b\,\max} - i_{b\,\min}}{2} \tag{2-19}$$

$$B_2 = \frac{i_{b\,\max} + i_{b\,\min} - 2I_b}{4} \tag{2-20}$$

If more components are desired, more terms of Eq. 2-16 may be used, and additional values of ωt introduced, exactly the same procedure being followed as in obtaining Eqs. 2-18, 2-19, and 2-20. A convenient set of values of ωt for determining five harmonic amplitudes are the values for

which e_g is equal to E_{gm}, $\frac{1}{2}E_{gm}$, 0, $-\frac{1}{2}E_{gm}$, and $-E_{gm}$. The corresponding values of i_b obtained graphically from Fig. 2-15 and analytically

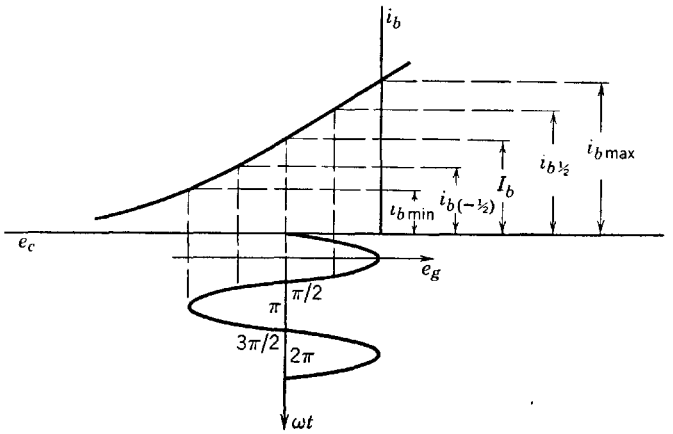

FIG. 2-15. Points for finding harmonic distortion.

from Eq. 2-16 up to and including B_4 are listed in the following tabulation:

ωt	e_g	i_b(graph)	i_b (from Eq. 2-16)	
0	E_{gm}	$i_{b\,\max}$	$= I_b + B_0 + B_1 + B_2 + B_3 + B_4$	
$\pi/3$	$\frac{1}{2}E_{gm}$	$i_{b(1/2)}$	$= I_b + B_0 + \frac{B_1}{2} - \frac{B_2}{2} - B_3 - \frac{B_4}{2}$	
$\pi/2$	0	I	$= I_b + B_0 \quad - B_2 \quad + B_4$	(2-21)
$2\pi/3$	$-\frac{1}{2}E_{gm}$	$i_{b(-1/2)}$	$= I_b + B_0 - \frac{B_1}{2} - \frac{B_2}{2} + B_3 - \frac{B_4}{2}$	
π	$-E_{gm}$	$i_{b\,\min}$	$= I_b + B_0 - B_1 + B_2 - B_3 + B_4$	

The foregoing equations may be solved by determinants or otherwise for the harmonic amplitudes. The final results are:

$$
\begin{aligned}
B_0 &= \tfrac{1}{6}(i_{b\,\max} + 2i_{b(1/2)} + 2i_{b(-1/2)} + i_{b\,\min}) - I_b \\
B_1 &= \tfrac{1}{3}(i_{b\,\max} + i_{b(1/2)} - i_{b(-1/2)} - i_{b\,\min}) \\
B_2 &= (i_{b\,\max} + i_{b\,\min} - 2I_b)/4 \qquad (2\text{-}22) \\
B_3 &= \tfrac{1}{6}(i_{b\,\max} - 2i_{b(1/2)} + 2i_{b(-1/2)} - i_{b\,\min}) \\
B_4 &= \tfrac{1}{12}(i_{b\,\max} - 4i_{b(1/2)} - 4i_{b(-1/2)} + 6I_b + i_{b\,\min})
\end{aligned}
$$

It is possible to determine from the plate diagram or from the dynamic characteristic the values of i_b corresponding to the various selected values of e_g shown in the schedule of Eqs. 2-21, and thus to compute the harmonic-distortion component amplitudes from Eqs. 2-22. The plate diagram is always used to obtain the necessary values of i_b if the plate characteristics corresponding to $e_g = 0$, $\frac{1}{2}E_{gm}$, E_{gm} are available. Harmonic distortion is frequently computed in per cent. For example, the per cent third-harmonic distortion is 100 B_3/B_1. The total per cent harmonic distortion is defined as the square root of the sum of the squares of the individual per cent harmonic distortions. The second harmonic is ordinarily the largest contribution to the total distortion except in the case of push–pull or other systems where it is effectively canceled. The push–pull connection is discussed in Chapter 3. In amplifiers for sound reproduction it is conventional practice to design for less than 5 per cent second harmonic.

2-11. Harmonic Distortion in Tetrodes and Pentodes

As shown in Section 2-10, the criterion for freedom from harmonic distortion of an amplifier tube is the straightness of its dynamic characteristic. Because of the bending of the static characteristics for low plate voltages, pentodes are found to be limited by third-harmonic distortion. It is easy to eliminate the second harmonic in pentodes by a proper choice of load resistance. The amplitude of the second harmonic was given by the relation 2-20 as

$$B_2 = \frac{i_{b\,\max} + i_{b\,\min} - 2I_b}{4}$$

For pentodes and beam tubes with their flat plate characteristics for negative values of control grid voltage, $i_{b\,\min}$ for a fixed-grid swing remains practically constant, regardless of the slope of the load line. For example, if a load line were drawn through an operating point at I_b = 40.0 ma, E_b = 250 volts, $E_{c1} = -15$ volts for the 6F6 of Fig. 2-8, and the control grid swings 15 volts on either side of the bias voltage, then $i_{b\,\min}$ is approximately 8 ma for any load resistance R_L. However, when the grid swing is in the positive direction and reaches zero, $i_{b\,\max}$ will vary rapidly with R_L if the load line intersects the characteristic for $E_{c1} = 0$ near the rounded knee of the curve. Therefore, for a fixed value of $i_{b\,\min}$ and I_b, it is easy to select a value of load resistance, and hence of slope of the load line for which $B_2 = 0$, which requires that

$$i_{b\,\max} = 2I_b - i_{b\,\min}$$

This particular value of maximum plate current is located somewhere along the tube characteristic corresponding to maximum grid swing. For the 6F6 operating point and grid swing suggested,

$$i_{b\,\max} = 80 - 8 = 72 \text{ ma}$$

The slope of the load line through the 72-ma point on the $E_c = 0$ characteristic would then be the negative reciprocal of

$$R_L = \frac{\Delta e_b}{\Delta i_b} \cong \frac{250 - 50}{(72 - 40.0) \cdot 10^{-3}} = \frac{200{,}000}{32.0} \cong 6250 \text{ ohms}$$

If a load resistor of this value were used, the second harmonic would be eliminated.

For power amplifiers, other considerations relating to optimum values of load resistance for best power output impose additional requirements. These will be taken up in the chapter on power amplifiers.

2-12. Variable-Mu Tubes

It is desirable for certain applications to have the amplification factor mu or the control grid-plate transconductance g_m of the tube depend upon the grid bias. Such a result is achieved by making the pitch of the helical control grid winding variable along the length of the grid structure, which amounts to a variable, rather than a fixed, grid-wire spacing along the length of the grid. Control of electron flow from the cathode is dependent upon the field intensity at the cathode, and thus cutoff of plate current occurs for areas of the cathode nearest the closely spaced region of the grid at less negative grid voltages than for areas opposite the more widely spaced grid wires. Such a tube is called a variable-mu, remote cutoff, or supercontrol tube, and is used in radio receivers where the grid bias is made to depend upon the received signal so that the volume of the amplifier is automatically controlled. Cutoff for a variable-mu tube is approached asymptotically as compared with the sharp cutoff of the tube with uniform grid-wire spacing. A typical remote cutoff pentode is the 6K7; a sharp cutoff pentode is the 6J7. The student should compare the plate and mutual characteristics of these tubes.

2-13. Other Multielectrode Tubes

Many multielectrode tubes combine two or more electrode assemblies in the same glass or metal envelope. For example, two triodes or a triode and a pentode may be enclosed in the same bulb. They may or may not use the same cathode, but each has its typical characteristics

independent of the other and so need not be considered as different from similar triode or pentode assemblies in separate envelopes.

Tubes using more than three grids are employed in frequency conversion. Such tubes may have two control grids, two screen grids, and a suppressor and are known as pentagrid mixer amplifiers, as for example the 6L7. The plate current depends upon both control grid signal voltages in a way that involves the product of functions of each voltage. As the signal voltages may be of different frequencies, a *modulation results* and new frequencies appear in the output which were not present in either input. The *pentagrid converter* also uses five grids, including two control grids. One of these is used in an oscillator circuit, and the other obtains signal from a separate source. The two frequencies are effective simultaneously upon the plate current, and frequency conversion results.

2-14. Parallel Feed

In the simple amplifier circuits shown thus far, the direct plate-supply voltage has been fed to the plate of the vacuum tube through the load resistor. The flow of the d-c component of the plate current through the load resistor results in a power loss $I_b^2R_L$, and in a voltage drop, I_bR_L. It is possible to avoid the power loss and to reduce the magnitude of the required plate-supply voltage by supplying the direct current and volt-

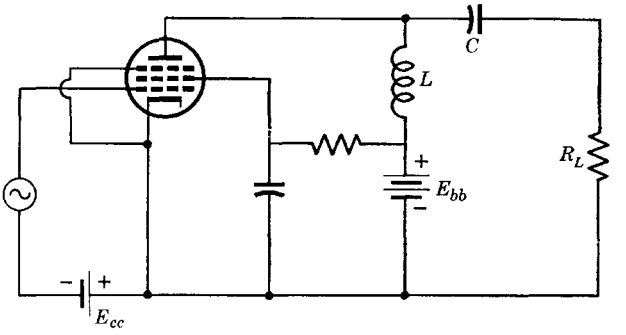

FIG. 2-16. Parallel feed.

age to the plate through an inductance of very low resistance. A blocking condenser is used to prevent direct current from flowing through the load resistance. The reactance of the condenser is negligible compared with the load resistance in the frequency range in which operation is desired. A typical arrangement is shown in Fig. 2-16, in which inductance L is chosen of such size that ωL is very large and C is large enough that $1/(\omega C)$ is very small compared with R_L. Except at very low fre-

quencies neither choke nor condenser need be shown in the equivalent a-c circuit, since the choke is assumed to have such high reactance that it passes negligible alternating current and may be replaced by an open circuit, and since the condenser has such small reactance that it may be replaced by a short circuit. This circuit arrangement is known as parallel feed.

If the resistance of the choke is appreciable, two load lines must be drawn. These are the d-c or static load line for the resistance of the choke, and the a-c or dynamic load line for the resistance of the load. If the resistance of the choke is negligible, the static load line is vertical and the operating plate voltage E_b is equal to the plate-supply voltage. The dynamic load line would then be drawn through the operating point with a slope equal to the negative reciprocal of the resistance of the load.

The static load line is used to locate the operating (quiescent) point. The a-c or dynamic load locus will then be a straight line if $X_c \ll R_L$ and if $X_L \gg R_L$. The dynamic load line is the locus of the a-c components of load voltage.

PROBLEMS

2-1. Using a set of type-24-A plate characteristics, draw a load line to intersect the $E_{c1} = 0$ characteristic at $i_b = 7$ ma and the $E_{c1} = -6$ characteristic at $e_b = 450$ volts. Using parallel feed for the plate circuit and a grid bias of -2 volts and neglecting choke resistance and condenser reactance:

(*a*) Determine the plate battery voltage and load resistance needed.

(*b*) Draw the dynamic characteristic corresponding to your load line, and show the operating range for a grid swing of 1.5 volts (on either side of the bias). Determine the voltage gain graphically. Determine r_p and μ at the operating point, and calculate the gain from the gain formula.

(*c*) Compute the per cent second-harmonic distortion for the amplifier.

2-2. Use the definition of plate resistance to sketch the variation of r_p as a function of e_b, obtaining data from the type-24-A characteristic for $E_{c1} = -3$ volts. Qualitative, rather than quantitative, results are desired.

2-3. An amplifier with resistance load uses a type-6F6 pentode with a load resistance of 5000 ohms; $E_{bb} = 250$ volts, $E_{cc} = -10$ volts.

(*a*) Draw the circuit diagram for parallel feed, showing all grid and battery connections. Draw the equivalent a-c plate circuit.

(*b*) Draw the load line on a set of plate characteristics, and determine the coordinates of the operating point. Obtain the dynamic characteristic.

(*c*) If the grid input voltage has a maximum value of 10 volts, determine the voltage gain graphically.

2-4. Referring to problem 2-3, determine g_m and r_p from the graph sheet at or near the operating point. Determine the slope of the dynamic characteristic at the operating point. Calculate μ and the voltage gain, and compare the latter with the value obtained graphically in problem 2-3.

2-5. Select a load resistance to be used with the amplifier of problem 2-3 so that the second-harmonic amplitude will be zero, and compute the per cent third-harmonic distortion for maximum grid voltages of (*a*) $\sqrt{2}\,E_g = 10$ volts, (*b*) $\sqrt{2}\,E_g = 20$ volts.

2-6. Simplify the circuit of Fig. 2-11 by combining capacitances in parallel and neglecting C_{g1p}. Determine the input and output capacitances in terms of the interelectrode capacitance of the circuit.

2-7. Using the plate characteristics of the 6J7 and 6K7 pentodes, construct mutual characteristics on the same sheet at $e_b = 200$ volts for each tube, and compare the remote and sharp cutoff characteristics. Determine the maximum and minimum values of g_m for each tube in the range of your drawing.

2-8. Draw the connection diagram for a 6J7 pentode amplifier circuit, obtaining the necessary screen supply voltage from a potentiometer across the plate supply. Use a cathode resistor for obtaining grid bias. Show all by-pass condensers. If the pentode operates at $E_b = 240$ volts, $E_{c2} = 100$ volts, $E_{c1} = -2.5$ volts, and the load resistor is 100,000 ohms, find (*a*) the proper size of cathode biasing resistor, (*b*) the plate-supply voltage.

2-9. If the signal voltage at the grid of the tube in problem 2-8 is a sine wave of frequency 800 cycles, amplitude 2.5 volts, compute the output voltage and the per cent harmonic distortion for all harmonics up to and including the fourth. Assume that the cathode biasing resistor is well by-passed.

2-10. Explain, fundamentally, why the insertion of grid wires between control grid and anode in a vacuum tube reduces the effective grid-plate capacitance. Assume that the inserted grid is maintained at a-c ground potential.

CHAPTER 3

AUDIO-FREQUENCY VOLTAGE AMPLIFIERS

THE SINGLE-TUBE OR ONE-STAGE AMPLIFIER CIRCUITS OF CHAPTERS 1 and 2 were introduced to provide examples of tube applications in basic circuits. The present chapter will be devoted to a study of methods of coupling tubes in multistage amplifiers designed for amplification in the audio-frequency range.

3-1. Amplifier Classifications

Amplifiers may be classified in respect to their use as *voltage, current,* or *power* amplifiers.

Amplifiers, as used in this text, are four-terminal networks designed to provide an increase in the amplitude of an alternating voltage. This voltage is referred to as the signal and is applied at the input terminals of the four-pole. If the emphasis is placed upon the production at the output terminals of a higher output voltage, with the magnitude of output current considered unimportant, the amplifier is referred to as a *voltage amplifier,* and certain types of high-vacuum tubes are designed for such use. If the major purpose of the amplifier is to increase the amplitude of a current, then a voltage input proportional to the signal current is fed into the four-pole at its input terminals and is to be increased in amplitude, but the output terminals must be capable of supplying a *current* of amplitude greater than that of the signal current; such an amplifier is referred to as a *current amplifier.* If both current and voltage amplitudes are required to be large at the output terminals, the amplifier is referred to as a *power amplifier.* It is generally true that vacuum-tube amplifiers are voltage-operated devices; that is, they respond to voltage variations at their input terminals. The over-all-output requirement of the amplifier determines the use classification as voltage, current, or power amplifier and dictates the essential circuit properties of tubes and other circuit components which together comprise the composite four-pole.

Amplifiers may also be classified on the basis of frequency range as

audio-, *radio-*, or *video-* (television) frequency amplifiers, each of these requiring circuit elements and tube characteristics to fit the frequency range over which amplification is desired.

An additional standard classification of amplifiers depends upon the portion of the a-c input cycle during which plate current flows, and includes class A, class AB, class B, and class C. The period of plate conduction is determined by the grid bias and the excitation amplitude. Figures 3-1, 3-2, 3-3, and 3-4 illustrate classes A, AB, B, and C, respectively. In each figure, bias and input voltage amplitude typical of the classification are shown, together with a dynamic characteristic and the resulting plate current. It should be particularly noted that class-A

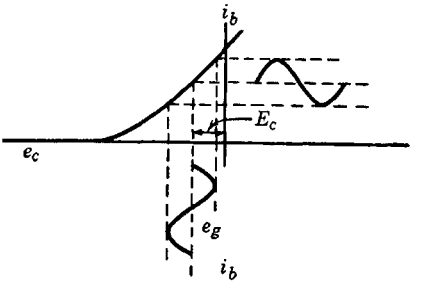

FIG. 3-1. Class-A operation.

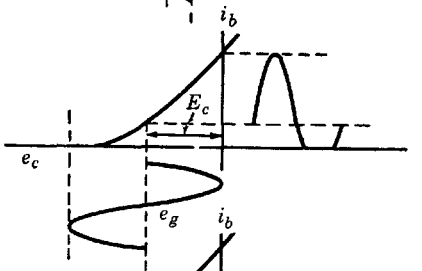

FIG. 3-2. Class-AB operation.

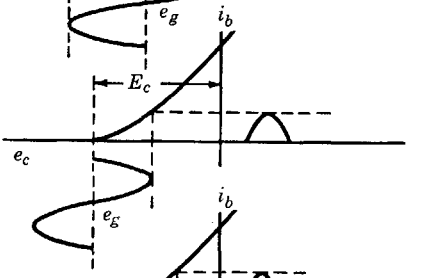

FIG. 3-3. Class-B operation.

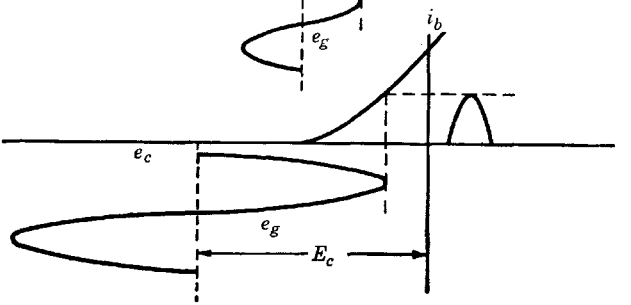

FIG. 3-4. Class-C operation.

operation implies bias on the linear portion of the characteristic and small input amplitude E_{gm} with plate current flowing during the entire grid cycle; for class-B operation the bias is approximately at cutoff, and plate current flows only during one-half the cycle of grid voltage; for class-C operation the bias is below cutoff, and plate current flows only during a period less than half that of the grid cycle. Since audio amplifiers require freedom from distortion, they are always operated class A except for power stages where push–pull operation makes class AB or B operation possible without excessive distortion. Radio-frequency amplifiers employ tuned circuits and may therefore tolerate the distortion inherent in classes other than A. Since plate current flows only with signal voltage in classes B and C, and since the grid amplitude may be much greater than in class A, the B and C amplifiers operate more efficiently than the A class. Class AB is intermediate between classes A and B. A further distinction, depending upon grid swing, is in general use. If the grid swings into the positive region of the mutual characteristics, grid current is expected to flow and the subscript 2 is used. When grid current does not flow, subscript 1 is used. For example, Fig. 3-1 represents a class-A_1 amplifier, Fig. 3-3 a class-B_1. If $E_{g\,max}$ were greater than E_c in Fig. 3-3, the amplifier would operate class B_2.

3-2. Distortion in Amplifiers

In order to describe a sine or cosine wave, three properties of the wave must be known. These properties are amplitude, frequency, and phase. When a given alternating voltage is fed into an amplifier, it is usually desirable that an output voltage of identical frequency but increased amplitude result. As shown in Chapter 1, the phase difference between input and output voltage for amplifiers with pure resistance load circuits * is 180°. When a number of sinusoidal voltages of different amplitudes, frequencies, and phases are simultaneously fed into the input of an amplifier, as for the amplification of music or speech, it is desirable and necessary that: (1) The amplifier output contain exactly the same frequencies as are present in the input; (2) the ratio of the amplitudes of output-to-input voltage components of the same frequency be the same for all frequencies; this is equivalent to requiring that the gain be the same for all frequencies; (3) the relative phase differences between the various frequencies be the same in the output as in the input. The departure of the amplifier from exact conformity with these three conditions is known as distortion. The introduction by the amplifier of frequencies not present in the input results from the non-

* This assumes frequencies are low enough that interelectrode capacitances may be neglected.

linearity of the dynamic characteristic, as discussed in Chapter 2 and is known as *harmonic distortion*. Failure of the amplifier to meet the second requirement of equal gain for all frequencies is known as *frequency distortion* and is caused by circuit or tube reactance values which change with frequency. If the amplifier circuit introduces a phase shift proportional to frequency per stage for all frequencies, requirement 3 is met perfectly, but, since reactance values of tube interelectrode capacitances and circuit inductive and capacitive reactances vary oppositely with frequency, *phase distortion* will result. For speech or music, the ear does not detect small amounts of phase distortion, but it is quite sensitive to harmonic and frequency distortion. If curves of gain are plotted against frequency, the curves will be straight horizontal lines for an ideal amplifier. The departure of the gain from the flat, straight-line characteristic of the ideal amplifier is a measure of the frequency distortion of the actual amplifier.

3-3. Interstage Coupling Circuits

The coupling circuit between two stages of a voltage amplifier may be treated as a four-terminal network. Four coupling circuits that are of importance in voltage amplifiers are:

(*a*) The direct-coupling circuit in which a single resistance serves as the output load of one stage and the input to the following stage. A battery is required to correct the second stage bias.

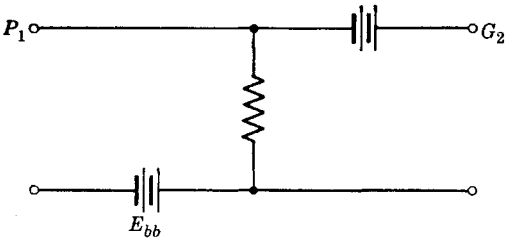

(*b*) The resistance-capacitance coupling circuit is a π network as shown. The plate supply of the first stage is inserted in series with R_L.

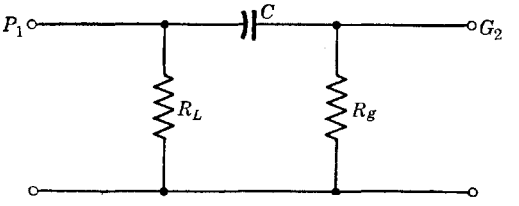

(*c*) The inductance-capacitance circuit is also a π network with an inductance instead of the load resistance R_L used in the R–C circuit. The plate supply for the first stage is connected through the inductance L.

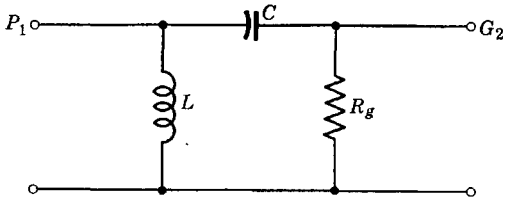

(*d*) The transformer coupling circuit is a transformer of special design, as shown. The plate supply for the first stage is connected either in series with the primary or in shunt by means of parallel feed.

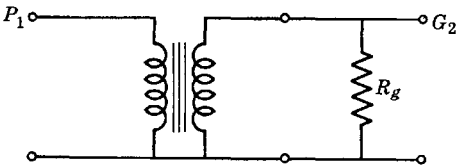

The four coupling circuits are analyzed in the following sections. One method of analysis is to obtain the four-pole admittance parameters of the coupling network, and then to work out the over-all four-pole admittances of tubes and coupling network in tandem. Since the four-pole admittance parameters of tubes and of coupling network are frequency-dependent (except for the direct-coupling network), graphical representation is usually employed. Such methods are convenient for design. For purposes of the present chapter, an elementary circuit analysis of each case is preferred.

3-4. Direct-Coupled Amplifiers

When very low frequencies or small variations in direct voltages are to be amplified, the simplest circuit that may be used for the purpose is that shown in Fig. 3-5. The voltage of the required second-stage bias battery E_{cc2} can be determined if the quiescent current I_{b1} and the load resistor R_1 are known. The direct-voltage drop in R_1 is in such a direction that G_2 is at a lower potential than K_2. In other words, a negative bias already exists on G_2, but in general this voltage would be sufficient to bias the tube T_2 to cutoff unless a battery is connected to correct the bias as shown. The required battery voltage is $E_{cc2} = V_{G2K2} + I_{b1}R_1$, where V_{G2K2} is the required negative bias. For ex-

ample, suppose that $R_1 = 100{,}000$ ohms, $I_{b1} = 2$ ma, $E_{c2} = -10$ volts $= V_{G2K2}$ (desired bias). Then $E_{cc2} = -10 + 200 = 190$ volts. A battery to supply such a voltage is inconvenient and expensive, and,

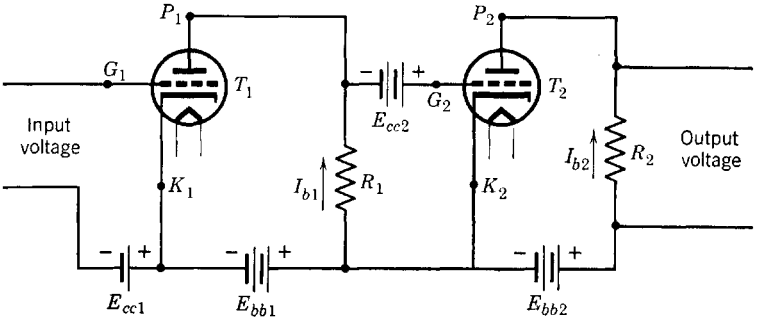

FIG. 3-5. Two-stage, direct-coupled amplifier.

when it is added to the requirement of the two plate batteries of equal or greater voltage, it is obvious that the circuit of Fig. 3-5 is far from ideal.

A circuit utilizing a single plate-voltage power supply and the potentiometer principle was first suggested by Loftin and White.[1] Such a

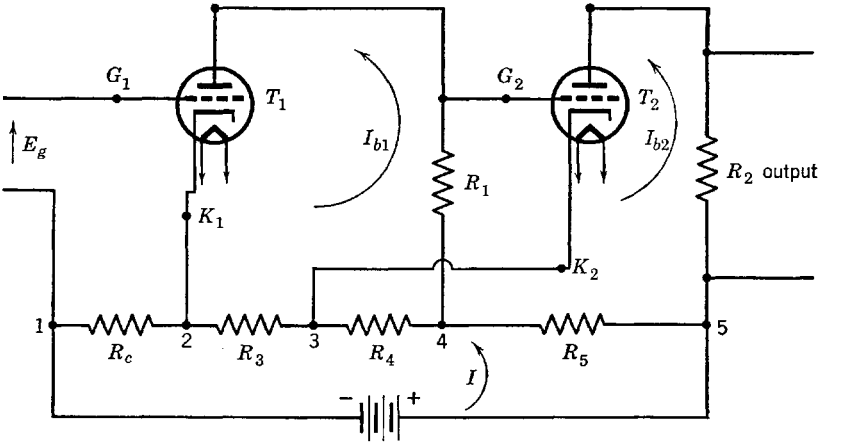

FIG. 3-6. Two-stage, direct-coupled amplifier using a single power source for plate and bias voltages.

circuit is illustrated in Fig. 3-6, in which R_c is the bias resistor for tube 1. With proper choice of power supply voltage and resistors, the voltages required for the circuit of Fig. 3-5 can be supplied as shown in Fig. 3-6.

[1] E. H. Loftin and S. Y. White, *Proc. IRE*, **16**, 281 (1928).

The direction of the direct current in the power-supply circuit is such that K_1 is positive with respect to G_1 by the amount of the drop IR_c. Plate battery voltage E_{bb1}, of Fig. 3-5, has been replaced by E_{24} (voltage rise), E_{bb2} by E_{35}. The bias voltage of the second tube can be obtained from the relation

$$E_{34} = I_{b1}R_1 + V_{G2K2}$$

Here V_{G2K2} = voltage drop, grid to cathode

= E_{c2}, bias voltage (usually a negative number) or voltage rise, d-c component, cathode to grid

Then, $$E_{34} = I_{b1}R_1 + E_{c2} \tag{3-1}$$

For example, if $R_1 = 50{,}000$ ohms, $I_{b1} = 1.8$ ma, $E_{c2} = -5$ volts, the required voltage E_{34} is given by

$$E_{34} = 1.8 \cdot 10^{-3}(50{,}000) - 5 = 90 - 5 = 85 \text{ volts}$$

It should be noted that the cathode of tube 2 is at a higher direct potential than that of tube 1. Either separate heater supplies must be used or the insulation of cathode to heater for each tube must be capable of withstanding the fairly high potential if a common heater source is used for both stages.

Reference again to Fig. 3-6 will show that the d-c supply voltage E will be the sum of $E_{12} + E_{23} + E_{34} + E_{45}$, or

$$E_{15} = E_{12} + E_{23} + E_{35} \tag{3-2}$$

But, for the direct voltage between K_1 and G_1,

$$E_{12} = V_{K1G1}$$

$$E_{23} = E_{24} - E_{34} = E_{24} - (I_bR_1 - V_{K2G2}) \tag{3-3}$$

Equation 3-3 may be written, with $E_{24} = E_{bb1}$, as

$$E_{23} = E_{bb1} - I_bR_1 + V_{K2G2} = E_{b1} + V_{K2G2} \tag{3-4}$$

Further, $$E_{35} = E_{bb2} = E_{b2} + I_{b2}R_2 \tag{3-5}$$

Therefore, the d-c supply voltage is

$$E_{15} = V_{K1G1} + E_{b1} + V_{K2G2} + E_{b2} + I_{b2}R_2 \tag{3-6}$$

or the *numerical* sum of the bias voltages, the plate voltages, and the direct voltage drop through the load resistor of the last tube.

A three-stage direct-coupled amplifier circuit is given in Fig. 3-7. The screen voltage of the input pentode and all bias and plate voltages are obtained by proper selection of a voltage drop in the potential divider circuit. In the third or power stage a pentode is used as a triode. In order to avoid undesirable feedback when audio frequencies in the voice or music range are used, by-pass condensers would be used across all biasing resistors. The capacitances of these condensers are so chosen

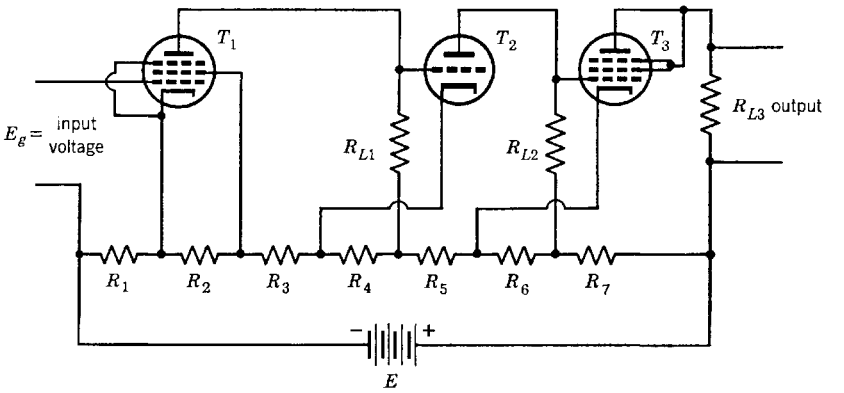

FIG. 3-7. Three-stage, direct-coupled amplifier.

that their reactances in the range of frequencies to be amplified are negligible.

Direct-coupled amplifiers are most useful at low frequencies and have practically zero frequency and phase distortion in their operating range. Such amplifiers also find numerous applications where it is required that a circuit respond to a very small change in voltage, a change that is not necessarily alternating, nor even periodic. Direct-coupled amplifiers have been used in biological studies, for counting purposes, and in experimental psychology in the study of neural response. They have also been used in cathode-ray oscillographs to amplify the input voltage. For this application, frequency and phase distortion must be negligible over a very wide range of frequencies.

Direct-coupled amplifiers are used for measurement purposes as in vacuum-tube voltmeters designed to measure very low frequency or direct voltage. In this, as in most applications of direct-coupled amplifiers, one of the major difficulties is that of zero adjustment, or an adjustment within the amplifier such that with zero input voltage, there will be zero output voltage.

Another important d-c amplifier application is in the field of servomechanisms. Servo amplifiers are frequently required to operate at

very low frequency and may be required to control, for example, the field current of a d-c motor.

Certain disadvantages of the d-c (direct-coupled) amplifier are inherent in the circuit itself. Because of the lack of d-c isolation between stages, small changes in tube characteristics or in battery voltages in one stage are amplified in a succeeding stage so that the tube operating point of the later stage may shift out of the linear region of the dynamic characteristic. There is also a tendency for the amplifier to "drift," which means that a slight change in potential in a given stage may result in a larger change in a succeeding stage, sufficient either to overload that stage or to bias it to cutoff. The tendency to drift [2] is minimized by using small resistors for the potentiometer circuit (Fig. 3-7) which calls for a large-capacity power supply and large "bleeder" current, with attendant power loss. Refinements in the design of direct-coupled amplifiers which eliminate the disadvantages described in the foregoing paragraph are described in the literature and should be referred to before a serious attempt is made to build such an amplifier.

3-5. Resistance-Capacitance Coupling

The d-c coupling existing between stages of the direct-coupled amplifiers which have been described in Section 3-4 is eliminated in the amplifier of Fig. 3-8 by the blocking capacitor C. The equivalent circuit

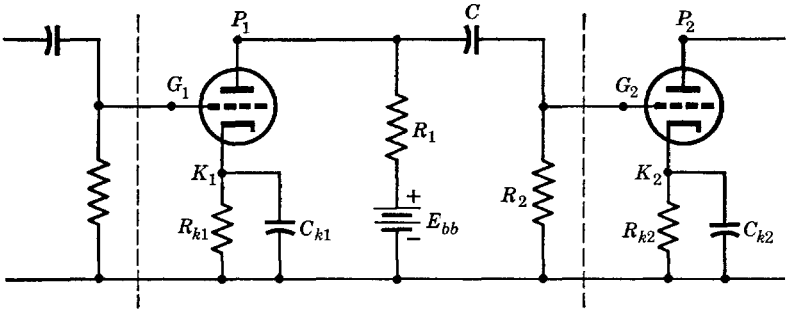

FIG. 3-8. Intermediate stage of an R–C-coupled amplifier.

of Fig. 3-8 is the circuit shown in Fig. 3-9, and R_{11} and C_{11} are the resistive and capacitive components of the input impedance of the next stage. (See Chapter 1, Fig. 1-29.)

Since the grid-to-anode capacitances may be neglected at audio frequencies, each stage of a multistage amplifier may be treated in-

[2] A method of drift correction is given by Loftin and White, *Proc. IRE*, **18**, p. 669 (1930).

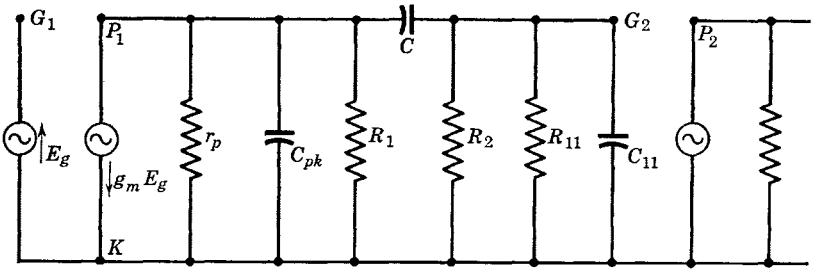

FIG. 3-9. Equivalent a-c circuit of Fig. 3-8.

dependently in finding the gain. If, for example, the amplifier stage of Fig. 3-8 is the mid-stage of a three-stage amplifier, the over-all amplifier gain is given by

$$A = \frac{\text{output voltage of last stage}}{\text{input signal voltage to first stage}}$$

with proper attention as to the use of voltage drops with respect to the common ground terminal. For the separate stages,

$$A_1 = \frac{V_{KG2}}{V_{KG1}}, \qquad A_2 = \frac{V_{KG3}}{V_{KG2}}, \qquad A_3 = \frac{V_{\text{out}}}{V_{KG3}}$$

For the complete amplifier,

$$A = \frac{V_{\text{out}}}{V_{KG1}} = \frac{V_{KG2}}{V_{KG1}} \cdot \frac{V_{KG3}}{V_{KG2}} \cdot \frac{V_{\text{out}}}{V_{KG3}} = A_1 A_2 A_3 \tag{3-7}$$

The importance in many applications of the resistance-capacitance method of amplifier coupling requires that the circuit behavior of R–C-coupled amplifiers be discussed in some detail. In the circuit of Fig. 3-8, resistors R_k are cathode biasing resistors in which the $I_b R_k$ drop provides the proper potential difference E_c between cathode and grid for negative grid bias. The capacitors C_k are chosen of sufficiently large capacitance and correspondingly small reactance to by-pass the a-c components of the plate current around the resistors so that on the a-c equivalent circuit of Fig. 3-9 the equivalent parallel impedance of R_k and C_k is comparatively a short circuit and is therefore not shown. The function of capacitor C is to provide d-c isolation for the following stage. To ensure adequate d-c isolation, the dielectric used in C must be of high-quality material of very high insulation resistance. Any d-c leakage through the capacitor from the plate supply will tend to produce a positive bias on the grid of the next stage. If the amplifier is to have

minimum frequency distortion, the reactance of capacitor C must be negligible. Practically this requirement is met if Xc at the lowest operating frequency is less than one tenth of resistance R_2, for then the alternating voltage across R_2 is approximately equal to that across R_1, and the voltage gain is independent of C; therefore the gain will be independent of frequency in the operating frequency range over which the input admittance of the next stage remains negligible. Resistance R_1 (load resistance) and R_2 (grid-leak resistance) should be as high as possible for maximum gain. The magnitude of R_1 is limited because it must pass the d-c component of load current, and too large a voltage drop I_bR_1 necessitates too large a plate supply E_{bb}. From the circuit of Fig. 3-8,

$$E_{bb} = I_{b1}R_1 + E_{b1} + I_{b1}R_k$$

The magnitude of R_2 is limited because of the flow of grid current to the grid G_2. Usually R_2 is limited to 1 megohm, for even an extremely small grid current would produce an appreciable spurious bias in a resistance of several megohms. Since any charge accumulating on coupling capacitor C must leak off through R_2, the product R_2C is limited in magnitude. Too large a product R_2C means that a sudden positive impulse causing grid current to flow, thus charging the capacitor would affect the grid for too long a time; this phenomenon is known as "blocking." Such conditions limit the size of R_2 and C.

The current-source-generator equivalent circuit has been used in Fig. 3-9, and grid conductance has been assumed to be negligible. All circuit elements have been shown, but, since the capacitor reactances and the magnitude of Y_{11} for the next stage (see Chapter 1, Eqs. 1-62 and 1-63) all depend upon frequency, it is possible to establish frequency ranges within which the circuit may be very much simplified. In the low-frequency range, X_c is greater than one-tenth R_2; also, the reactances of C_{pk} and C_{11} and the resistance R_{11} are so large compared with r_p, R_1, and R_2 that C_{11} and R_{11} may be considered open circuits and omitted

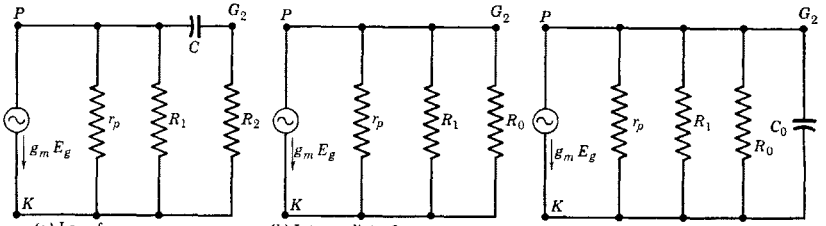

FIG. 3-10. Equivalent circuits in the low-frequency, mid-frequency, and high-frequency range for an R–C-coupled amplifier stage.

from the circuit diagram. The low-frequency circuit is shown in Fig. 3-10*a*. In the mid-frequency range, Fig. 3-10*b*, $X_c < 0.1R_2$ and may be replaced by a short circuit; C_{pk}, C_{11}, and stray wiring capacitances are now in parallel and may be replaced by C_0, but X_{C0} and R_{11} are so large compared with the other circuit elements that they may be considered as open circuits. In the high-frequency range, X_{C0} is small and may not be neglected; $Y_{11} = G_{11} + j\omega C_0$, and it is assumed that $G_{11} \ll \omega C_0$, and may be neglected. The circuit is shown in Fig. 3-10*c*.

Analysis of the gain and phase shift of the *R–C*-coupled amplifier stage of Fig. 3-8 is now greatly simplified by use of the equivalent circuits of Fig. 3-10. In the mid-frequency range, the current $g_m E_g$ flows through an equivalent admittance Y_{eq} given by

$$Y_{eq} = Y_P + Y_1 + Y_2 = 1/R_{eq} \tag{3-8}$$

where $Y_P = 1/r_p, \quad Y_1 = 1/R_1, \quad Y_2 = 1/R_2$

The output voltage drop of the stage is

$$V_{kg2} = g_m E_g R_{eq} \tag{3-9}$$

and the intermediate-frequency voltage gain of the stage is given by the relation

$$A_I = \frac{V_{kg2}}{-E_g} = -g_m R_{eq} = -\frac{g_m}{Y_P + Y_1 + Y_2} \tag{3-10}$$

Since A_I involves only pure resistance elements, the intermediate-frequency gain is independent of frequency. If the following substitutions are made in Eq. 3-10, namely

$$Y_1 + Y_2 = Y_L = 1/R_L$$

where $R_L = R_1R_2/(R_1 + R_2)$ = the equivalent load resistance

and $$g_m = \mu Y_P = \mu/r_p$$

then Eq. 3-10 may be written in the familar form of

$$A_I = \frac{-\mu/r_p}{1/r_p + 1/R_L} = -\frac{\mu R_L}{r_p + R_L} \tag{3-11}$$

In exactly the same manner, the amplifier voltage gain in the high-frequency range may be obtained from the circuit of Fig. 3-10*c*. The high-frequency gain A_H is then given by

$$A_H = \frac{-g_m}{Y_P + Y_1 + Y_2 + Y_{11}} = -\frac{\mu Y_P}{Y_P + Y_1 + Y_2 + Y_{11}} \tag{3-12}$$

For convenience in computation, it is desirable to relate A_H to A_I, which may be accomplished by noting that Eqs. 3-8 and 3-10 may be used in Eq. 3-12, so that

$$A_H = \frac{-g_m}{1/R_{eq} + Y_{11}} = -\frac{g_m R_{eq}}{1 + R_{eq}Y_{11}} = \frac{A_I}{1 + R_{eq}Y_{11}} \tag{3-13}$$

But $Y_{11} = G_{11} + j\omega C_0$, and G_{11} is assumed to be negligible compared with ωC_0. Then $Y_{11} \cong j\omega C_0$, and the quantity $R_{eq}Y_{11}$ may be written as

$$R_{eq}Y_{11} = j2\pi f C_0 R_{eq}$$

If by definition the quantity $1/2\pi C_0 R_{eq}$ be replaced by the *frequency* f_H, then Eq. 3-13 may be written as

$$A_H = \frac{A_I}{1 + jf/f_H} \tag{3-14}$$

where

$$f_H = \frac{1}{2\pi C_0 R_{eq}} = \frac{Y_P + Y_1 + Y_2}{2\pi C_0} \tag{3-15}$$

Equation 3-14 may now be expressed in polar form as follows:

$$A_H = \frac{|A_I| \angle 180°}{\sqrt{1 + (f/f_H)^2} \angle \theta_H} = \frac{|A_I|}{\sqrt{1 + (f/f_H)^2}} \angle 180° - \theta_H \tag{3-16}$$

where

$$\theta_H = \tan^{-1} f/f_H \tag{3-17}$$

As the frequency f increases beyond the intermediate-frequency range, the gain decreases and the phase-shift angle θ_H increases, according to Eqs. 3-16 and 3-17. If f becomes equal to f_H,

$$|A_H| = |A_I|/\sqrt{2} = 0.707|A_I|$$

Therefore, f_H *is that frequency* at which the high-frequency gain falls to 70.7 per cent of the constant gain in the intermediate-frequency range. The angle θ_H is the angle by which the phase difference between output and input voltages fails to be 180°. Therefore, θ_H is a measure of the phase shift in the high-frequency range. At the frequency f_H, $\theta = 45°$.

For the low-frequency gain, the circuit of Fig. 3-10*a* provides an easy method of obtaining A_L. The voltage across r_p (or R_1) is the product of the current $g_m E_g$ and the equivalent single impedance connected across the terminals of the constant-current generator. If the single resistance equivalent to r_p and R_1 in parallel is

$$R = r_p R_1/(r_p + R_1) \tag{3-18}$$

then the voltage across the parallel combination of R and the impedance $R_2 - jX_c$ is

$$V_R = g_m E_g \frac{R(R_2 - jX_c)}{R + R_2 - jX_c} \tag{3-19a}$$

Voltage V_R is also the drop across $(R_2 - jX_c)$, and the output voltage drop across R_2 is therefore

$$V_{kg2} = \left(\frac{V_R}{R_2 - jX_c}\right) R_2 \tag{3-19b}$$

From Eqs. 3-19a and 3-19b the low-frequency gain is

$$A_L = V_{kg2}/-E_g = -g_m R R_2/(R + R_2 - jX_c) \tag{3-20}$$

The numerator and denominator of Eq. 3-20 may be divided by $(R + R_2)$ in order to introduce R_{eq} and thereby also A_I into the expression for A_L. The result is

$$A_L = -\frac{g_m R R_2/(R + R_2)}{1 - jX_c/(R + R_2)} \tag{3-21}$$

From Eq. 3-8, $\quad 1/R_{eq} = 1/r_p + 1/R_1 + 1/R_2$

Use of Eq. 3-18 yields $\quad 1/R_{eq} = 1/R + 1/R_2$

so that
$$R_{eq} = RR_2/(R + R_2) \tag{3-22}$$

If also, $\quad X_c/(R + R_2) = 1/2\pi fC(R + R_2) = f_L/f$

where

$$f_L = 1/2\pi C(R + R_2) = Y_2(Y_1 + Y_P)/2\pi C(Y_2 + Y_1 + Y_P) \tag{3-23}$$

then finally Eq. 3-21 becomes

$$A_L = \frac{A_I}{1 - jf_L/f} \tag{3-24}$$

or
$$A_L = \frac{|A_I|\underline{/180°}}{\sqrt{1 + (f_L/f)^2}\underline{/-\theta_L}} = \frac{A_I}{\sqrt{1 + (f_L/f)^2}}\underline{/180 + \theta_L} \tag{3-25}$$

where
$$\theta_L = \tan^{-1} f_L/f$$

From Eq. 3-25, f_L is the frequency on the low-frequency side of the intermediate range at which the low-frequency gain falls to 70.7 per cent of the gain in the intermediate-frequency region, and θ_L is the measure of the phase shift at low frequencies. Again, $\theta_L = 45°$ at $f = f_L$.

The frequencies f_L and f_H are sometimes referred to as the "half-power" frequencies * by analogy with the criterion for sharpness of resonance in resonance curves. For amplifiers, however, the width of the frequency band $f_H - f_L$ is a measure of the freedom of the amplifier from frequency distortion. A typical R–C-coupled-amplifier gain-frequency curve is plotted in Fig. 3-11. For an amplifier to have the desirable flat region extended over a wide range of frequencies, f_L must be small and f_H large. The requirements are met according to Eq. 3-15

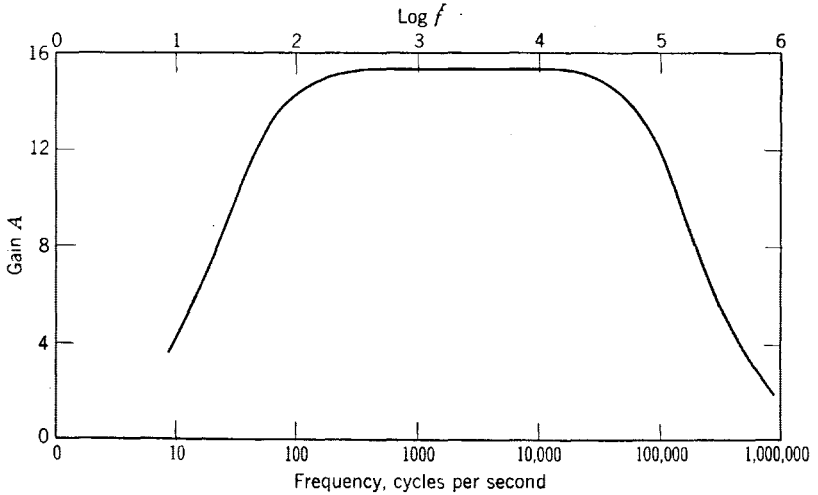

FIG. 3-11. Gain-frequency curve for a typical R–C-coupled amplifier.

and Eq. 3-23 by making C large, C_0 small, and Y_1 and Y_2 large (R_1 and R_2 small). The last adjustment would require a sacrifice of gain and is often justified. For a given set of resistors, R_1 and R_2, it may be stated that the frequency region of constant gain of an R–C-coupled amplifier is limited below by the coupling capacitor C, and above by the capacitor C_0 representing the sum of the input capacitance of the next stage, the output capacitance of the stage itself, and the capacitance between leads. At the high-frequency end, G_{11}, which was neglected, also contributes to the decrease of gain.

Example problem. For an amplifier stage identical with Fig. 3-8, the tube is a 6C5, $R_1 = 50{,}000$ ohms, $R_2 = 100{,}000$ ohms, $C = 0.04$ μf. The total shunt capacitance $C_0 = 150$ $\mu\mu$f, and R_{11} is assumed infinite. Compute the intermediate-frequency gain, and find the frequencies at

* These frequencies are also referred to as the "3 db down" frequencies because the voltage gain as measured in decibels is down 3 db as referred to the mid-frequency gain.

which the gain falls to one fourth the gain in the intermediate range.

Solution. For the 6C5, $g_m = 2000$ micromhos, $r_p = 10{,}000$ ohms, $\mu = 20$.

$$A_I = \frac{-g_m}{Y_P + Y_1 + Y_2} = -\frac{2000 \cdot 10^{-6}}{10^{-4} + 0.2 \cdot 10^{-4} + 0.1 \cdot 10^{-4}}$$

$$= -\frac{20}{1.3} = -15.4$$

$$f_L = \frac{Y_2(Y_1 + Y_P)}{2\pi C(Y_1 + Y_2 + Y_P)} = \frac{0.1 \cdot 10^{-4}(1.2 \cdot 10^{-4})}{6.28(0.04 \cdot 10^{-6})(1.3 \cdot 10^{-4})} = 36.8 \text{ cps}$$

$$f_H = \frac{Y_P + Y_1 + Y_2}{2\pi C_o} = \frac{1.3 \cdot 10^{-4}}{6.28(150 \cdot 10^{-12})} = 138{,}000 \text{ cycles}$$

For
$$\frac{|A_L|}{|A_I|} = \frac{1}{4} = \frac{1}{\sqrt{1 + (36.8/f)^2}}$$

$$(36.8/f)^2 = 15, \qquad f = 36.8/\sqrt{15} = 9.5 \text{ cps}$$

For
$$\frac{|A_H|}{|A_I|} = \frac{1}{4} = \frac{1}{\sqrt{1 + (f/138{,}000)^2}}$$

$$(f/138{,}000)^2 = 15, \qquad f = 138{,}000\sqrt{15} = 535{,}000 \text{ cps}$$

Equations 3-16 and 3-25 provide a basis for computing universal phase shift and gain curves in which the phase shift and the gain ratios

$$\frac{|A_L|}{|A_I|} \quad \text{and} \quad \frac{|A_H|}{|A_I|}$$

are plotted against the frequency ratios f_L/f and f/f_H. Such curves supply data for any R–C-coupled amplifier stage. A tabulation of such data is given in Table 3-1.

TABLE 3-1. PHASE-SHIFT ANGLES AND GAIN RATIOS FOR ANY R–C-COUPLED AMPLIFIER

f_L/f or f/f_H	θ_L or θ_H	f	A/A_I	f
10	84.3	$0.1 f_L$	0.0995	$10 f_H$
5	78.7	$0.2 f_L$	0.196	$5 f_H$
2	63.4	$0.5 f_L$	0.446	$2 f_H$
1	45	$1.0 f_L$	0.707	$1.0 f_H$
0.5	26.6	$2 f_L$	0.893	$0.5 f_H$
0.2	11.3	$5 f_L$	0.980	$0.2 f_H$
0.1	5.8	$10 f_L$	0.995	$0.1 f_H$

The values given in Table 3-1 are plotted in Fig. 3-12. Although the behavior of an ordinary R–C-coupled amplifier may be predicted by use of the curves of Fig. 3-12, it is first necessary to compute f_L and f_H in order to use the curves. Having computed these frequencies, however,

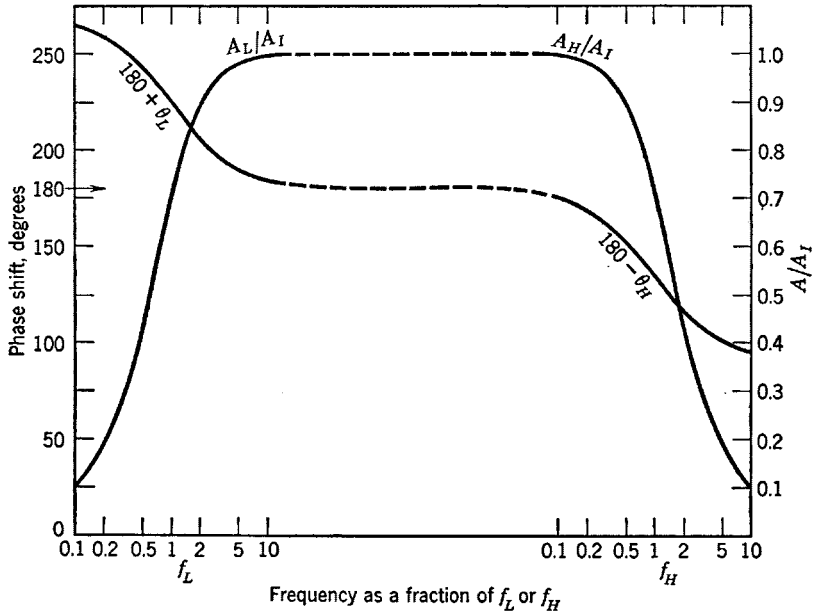

FIG. 3-12. Universal amplification and phase-shift curves for R–C-coupled amplifiers.

it is about as easy and perhaps more accurate to use the gain and phase-shift equations 3-16 and 3-25.

3-6. Inductance-Capacitance Coupling

The method of coupling shown in Fig. 3-13 is termed inductance-capacitance coupling. In the frequency range over which the gain is substantially constant, X_{c1} and X_{c2} are small compared with R_1 and R_2, respectively, and may be neglected; X_{L1} and X_{L2} are very large compared with r_{p1} and R_1,r_{p2} and R_2, so that the equivalent circuit at intermediate frequencies is that of Fig. 3-14. The circuit gain analysis may be carried out in the same way as for the R–C case, and the response curve is similar to that of the R–C-coupled amplifier. Since the frequency range for which the gain is flat is limited by the inductances as well as the capacitances, the range is less extensive than for the R–C amplifier. The chief advantage of the method is that the operating plate battery voltages required are much less as a result of the low direct-voltage drop

in the inductance. Also, the mid-frequency gain for triodes approaches μ. In determining the load line on the plate characteristics, the operating point is approximately the intersection between the vertical line $e_b = E_{bb}$

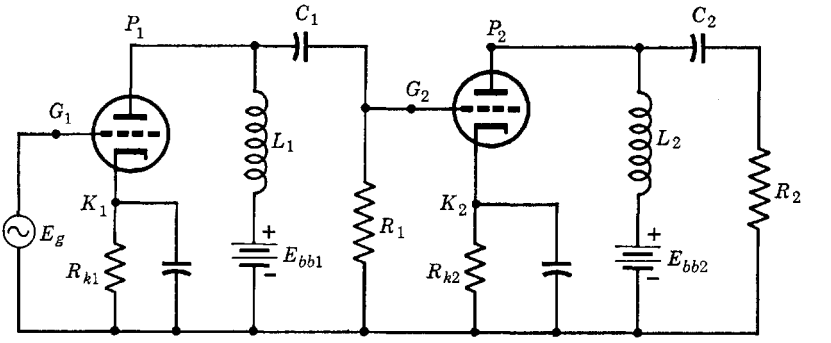

FIG. 3-13. Inductance-capacitance-coupled, two-stage amplifier.

and the characteristic corresponding to the grid bias used. Through the operating point, the load line may be drawn with slope corresponding to the load resistor R_1 (or R_2), of Fig. 3-13.

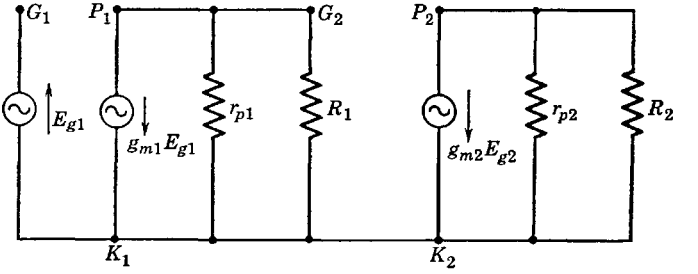

FIG. 3-14. Equivalent a-c circuit of Fig. 3-13 in the intermediate-frequency range.

3-7. Transformer-Coupled Amplifiers

The circuit of Fig. 3-15 uses a transformer as a coupling device between stages. Transformer coupling has a number of advantages, including the following:

1. Each stage has d-c isolation without the use of capacitors.
2. The use of a stepup turns ratio makes possible a voltage gain in excess of μ.
3. Smaller plate supply voltages are required to provide the necessary quiescent operating tube voltage and current, and the I_b^2R losses are greatly reduced, as a result of low primary-winding resistance.

4. Coupling to an output stage involving two tubes in *push–pull* is easily accomplished by using a center-tapped transformer. The push–pull connection will be discussed later in this chapter.

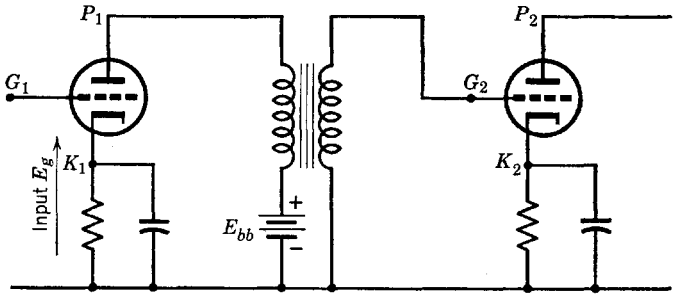

(a) Actual circuit

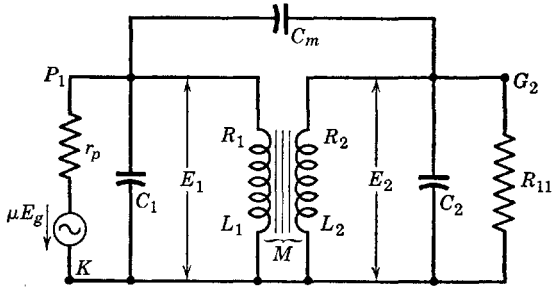

(b) Equivalent a-c circuit

FIG. 3-15. Circuits of a transformer-coupled amplifier.

R_1 and R_2 are, respectively, the primary and secondary effective resistances.

L_1 and L_2 are, respectively, the primary- and secondary-winding inductances.

C_m = capacitance between primary and secondary windings
r_p = plate resistance of tube 1
$C_1 = C_{pk} + C_p$ + lead capacitance
C_{pk} = interelectrode plate-cathode capacitance
C_p = primary distributed winding capacitance
$C_2 = C_s + C_{11}$ + lead capacitance
C_s = secondary distributed capacitance
C_{11} = input capacitance of next stage
R_{11} = input resistance of next stage
M = mutual inductance between windings

The type of transformer used in amplifier coupling and its design are determined by the frequency range over which the amplifier is to be used. Iron-core transformers are used over the audio range; the cores of such transformers are usually constructed of specially designed high-permeability low-loss iron, and the coefficient of coupling is very nearly equal to unity. For frequencies in the radio range, air-core transformers are used. The turns ratio of audio-frequency-coupling transformers does not usually exceed three because of the introduction of secondary distributed capacitance between turns and because of the desirability of having a reasonably high primary inductance.

The principal disadvantages of audio-frequency transformer coupling include the following:

1. Transformers are expensive and bulky.
2. The frequency range in which there is negligible frequency and phase distortion is relatively narrow.
3. Careful shielding is required (contributing to item 1) to prevent coupling due to stray magnetic fields.

Analysis of the equivalent circuit of Fig. 3-15*b*, like that of the *R–C*-coupled-amplifier complete equivalent circuit, is complicated unnecessarily by the presence of circuit elements whose reactances need be considered only in certain frequency ranges. It is, therefore, preferable to make the necessary approximations in setting up the circuit for the low-, intermediate-, and high-frequency ranges rather than to attempt a complete solution in which certain terms would be relatively negligible in the various frequency ranges. The equivalent circuit of Fig. 3-15*b* may then be simplified for approximate analysis as follows:

1. In the audio-frequency range over which iron-core coupling transformers work satisfactorily the reactance of capacitor C_1 and the resistance R_{11} (see Chapter 1, Fig. 1-29) are so high that these elements may be omitted from the equivalent circuit.

2. Capacitance C_m contributes a current component to both primary and secondary circuits. These currents, however, become of practical importance only at the high-frequency end of the useful frequency range of the amplifier because the reactance of C_m is very high in the low- and intermediate-frequency ranges. If the transformer is provided with a grounded shield between primary and secondary windings, C_m may be reduced to a negligible value at all frequencies. A fairly satisfactory approximation for transformers without shielding is to neglect the contribution of C_m to current in the primary circuit and to replace C_m by an equivalent capacitance connected in parallel with C_2. The equivalent capacitance would be equivalent in the sense that it contributes the same current component to the secondary circuit as does the actual

capacitance C_m. The equivalent capacitance C' may be determined as follows: The current through C_m depends upon the voltage across C_m; this voltage, as may be seen from Fig. 3-15*b*, is the vector sum (or difference, depending upon relative winding directions of the transformer primary and secondary) of the voltages E_1 and E_2; the assumed relative positive sense of these voltages on Fig. 3-15*b* is purely arbitrary; since in magnitude $E_2 = nE_1$, where $n = N_2/N_1$, the secondary-to-primary turns ratio, the current through C_m or through C' is given by

$$I = (E_1 \pm nE_1)/-jX_{cm} = nE_1/-jX_{C'}$$

then

$$C_m E_1(1 \pm n) = C'nE_1$$

or

$$C' = \left(\frac{1 \pm n}{n}\right)C_m$$

The secondary capacitance then becomes

$$C_0 = C_2 + C'$$

The use of C' in the secondary to replace C_m is a good approximation to the extent that the coefficient of coupling k may be considered equal to unity. At high enough frequencies, even though $k = 0.98$, the leakage reactances may become appreciable, so that the voltage across C' is not

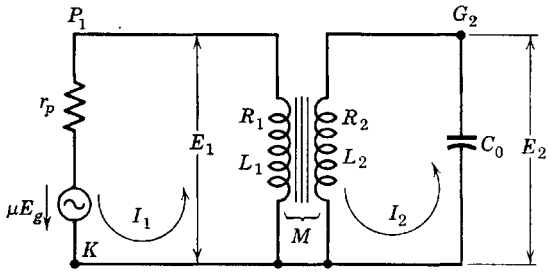

FIG. 3-16. Simplified equivalent circuit of Fig. 3-15.

nE_1 because of the voltage drop and the phase shift in the leakage reactance. The neglect of a corresponding current component introduced by C_m in the primary current is justified because the transformer is an interstage transformer in which the secondary current is negligible. The contribution of C_m to the primary current is negligible compared with the primary a-c component of plate current.

The equivalent circuit of Fig. 3-15*b* may now be replaced by that of Fig. 3-16. Before giving any definitions of the frequency ranges, the

mesh equations of the circuit will be written. From Fig. 3-16,

$$\begin{aligned} \mu E_g &= I_1 Z_{11} + I_2 Z_{12} \\ 0 &= I_1 Z_{21} + I_2 Z_{22} \end{aligned} \tag{3-26}$$ [3]

where

$$Z_{11} = r_p + R_1 + j\omega L_1$$

$$Z_{22} = R_2 + j(\omega L_2 - 1/\omega C_0)$$

$$Z_{12} = Z_{21} = -j\omega M$$

In the low- and intermediate-frequency ranges, X_{C0} is so high that Z_{22} may be considered infinite. Then $I_2 = 0$, and

$$I_1 = \mu E_g / Z_{11}$$

$$E_2 = -I_1 Z_{21} = j\omega M I_1 = \frac{\mu E_g (j\omega M)}{r_p + R_1 + j\omega L_1} \tag{3-27}$$

Now $M = k\sqrt{L_1 L_2}$ and $n = N_2/N_1 = \sqrt{L_2/L_1}$

whence

$$M = kL_1\sqrt{L_2/L_1} = knL_1 \tag{3-28}$$

Since k is very nearly unity, M may be replaced by nL_1. Then,

$$E_2 = \frac{n\mu E_g (j\omega L_1)}{r_p + R_1 + j\omega L_1} \tag{3-29}$$

By definition, the amplifier gain is

$$A_L = \frac{V_{kg2}}{-E_g} = \frac{-n\mu(j\omega L_1)}{r_p + R_1 + j\omega L_1}$$

If numerator and denominator are divided by $j\omega L_1$,

$$A_L = -\frac{n\mu}{1 - j(r_p + R_1)/\omega L_1} \tag{3-30}$$

Equation 3-30 should properly be written with $\pm n\mu$ instead of $n\mu$ in the numerator, since the phase of the secondary voltage depends upon the relative winding directions of primary and secondary. Numerically the

[3] For a discussion of coupled circuits and the use of the double-subscript notation see Chap. VII, W. L. Everitt, *Communication Engineering*, McGraw-Hill Book Co. (1937).

gain is given by

$$A_L = \frac{n\mu}{\sqrt{1 + \left(\frac{r_p + R_1}{\omega L_1}\right)^2}} \tag{3-31}$$

For very low frequencies, ωL_1 is small and $(r_p + R_1)/\omega L_1$ large, so that $| A_L |$ is small. The primary inductance L_1 may be in the neighborhood of 20 henrys. Resistance R_1 is usually small compared to r_p, and, for tubes ordinarily transformer-coupled, r_p is in the range 8000 to 15,000 ohms. As the frequency increases from low values, $\left(\frac{r_p + R_1}{\omega L_1}\right)^2$ decreases and ultimately becomes small compared with unity. The gain then approaches $n\mu$ as f increases.

To distinguish between low- and mid-frequency ranges, the low-frequency range will be defined somewhat arbitrarily as the range of frequency below that frequency for which

$$(r_p + R_1)/\omega L_1 = \tfrac{1}{10}$$

The intermediate or mid-frequency gain will then be given by

$$A_I = -n\mu \tag{3-32}$$

and is independent of frequency. Therefore the gain-frequency curve for the mid-frequency region will be flat and horizontal.

It is possible to determine the gain in the higher-frequency range over which the reactance of C_0 may not be neglected by use of the circuit

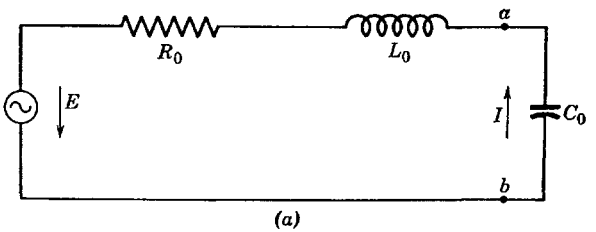

FIG. 3-16a. Circuit equivalent to that of Fig. 3-16 as seen at the terminals of the capacitor C_0.

of Fig. 3-16. If the secondary circuit is opened at terminals a–b, the equivalent circuit looking to the left may be obtained by an application of the mesh equations 3-26 and Thevenin's theorem. If the driving-point impedance as obtained from Eqs. 3-26 is applied to the secondary,

rather than to the primary, the impedance at terminals a–b looking toward the transformer is given by (see Fig. 3-16a)

$$Z_{ab} = R_2 + jX_2 + \frac{(\omega M)^2}{r_p + R_1 + jX_1}$$

$$= R_2 + \frac{(\omega M)^2}{(r_p + R_1)^2 + X_1^2}(r_p + R_1) + j\left[X_2 - \frac{(\omega M)^2}{(r_p + R_1)^2 + X_1^2} X_1\right] \quad (3\text{-}33)$$

If $\omega L_1 \geqq 10(r_p + R_1)$, Eq. 3-33 may be written as

$$Z_{ab} = R_2 + \frac{(\omega M)^2}{X_1^2}(r_p + R_1) + j\left[X_2 - \frac{(\omega M)^2}{X_1}\right] \quad (3\text{-}34)$$

Now

$$(\omega M)^2/X_1 = k^2 X_1 X_2/X_1 = k^2 X_2 = k^2 \omega L_2$$

$$(\omega M)^2/X_1^2 = k^2 X_2/X_1 = k^2 L_2/L_1 = k^2 n^2 \quad (3\text{-}35)$$

Then, let

$$R_0 = R_2 + k^2 n^2 (r_p + R_1) \quad (3\text{-}36a)$$

and

$$L_0 = (1 - k^2) L_2 \quad (3\text{-}36b)$$

so that Eq. 3-34 becomes

$$Z_{ab} = R_0 + j\omega L_0 \quad (3\text{-}34a)$$

The equivalent circuit is shown in Fig. 3-16a. The voltage E, according to Thevenin's theorem, is given by

$$E = \frac{\mu E_g (j\omega M)}{r_p + R_1 + jX_1} \cong \frac{\mu E_g \omega M}{X_1}$$

for

$$\omega \geqq 10(r_p + R_1)/L_1$$

or, using Eq. 3-35,

$$E = kn\mu E_g \cong n\mu E_g \quad (3\text{-}37)$$

The output voltage drop of the amplifier stage is the voltage across the capacitor C_0. The magnitude of the voltage gain at high frequencies is then

$$|A_H| = \left|\frac{IX_{c0}}{E_g}\right|$$

or

$$A_H = -\frac{n\mu}{j\omega C_0[R_0 + j(\omega L_0 - 1/\omega C_0)]} \quad (3\text{-}38)$$

Since $A_I = -n\mu$, Eq. 3-38 may be written as

$$\frac{A_H}{A_I} = \frac{1}{j\omega R_0 C_0 - \omega^2 L_0 C_0 + 1} \tag{3-39}$$

If now an angular frequency ω_0 is defined such that, for $\omega = \omega_0$,

$$\omega_0 L_0 = 1/\omega_0 C_0 \quad \text{or} \quad \omega_0{}^2 = 1/L_0 C_0 \tag{3-40}$$

and if

$$Q_0 = \omega_0 L_0 / R_0 \tag{3-41}$$

then Eq. 3-39 simplifies to

$$\frac{A_H}{A_I} = \frac{1}{j(\omega/\omega_0 Q_0) - \omega^2/\omega_0{}^2 + 1} \tag{3-42a}$$

or

$$\frac{A_H}{A_I} = \frac{1}{\sqrt{(1 - \omega^2/\omega_0{}^2)^2 + (\omega/\omega_0 Q_0)^2}} \angle -\theta_H \tag{3-42b}$$

where

$$\theta_H = \tan^{-1} \frac{(\omega/\omega_0 Q_0)}{(1 - \omega^2/\omega_0{}^2)} \tag{3-43}$$

is the angle by which A_H *lags* A_I.

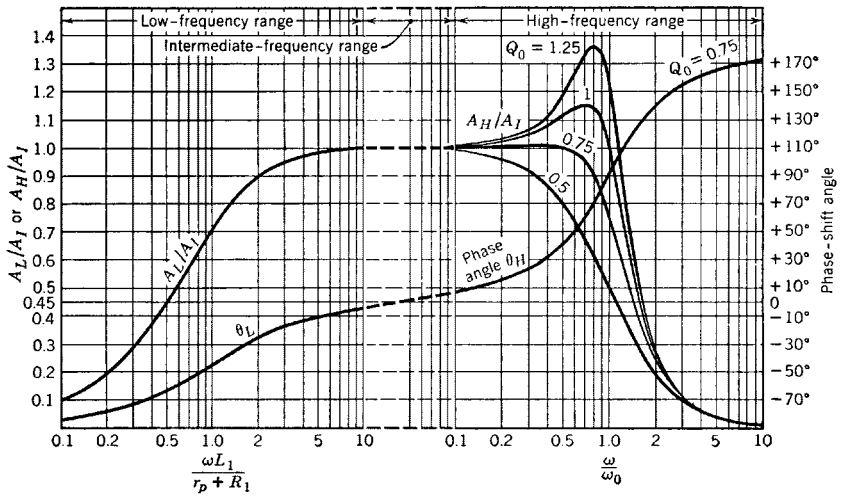

FIG. 3-17. Universal gain and phase-shift versus frequency curves for transformer-coupled amplifiers.

If the ratio $\left|\frac{A_H}{A_I}\right|$ is plotted [4] against $\frac{\omega}{\omega_0}$ for several fixed values of Q_0, as in Fig. 3-17, it is found that peaks in the curves occur in the

[4] F. E. Terman, Universal Amplification Charts, *Electronics*, **10**, 35 (June 1937).

vicinity of $\omega = \omega_0$, and that the magnitude of the rise of the peak above the level $\left|\frac{A_H}{A_I}\right| = 1$ is dependent upon the value of Q_0. Examination of the curves of Fig. 3-17 will show that the flat region of the gain curve may be extended by choosing $Q_0 = 0.75$. At $\omega = \omega_0$, it is evident from Eq. 3-42*b* that

$$\left|\frac{A_H}{A_I}\right| = Q_0$$

The intermediate-frequency range may now be conveniently bounded as follows:

$$10(r_p + R_1)/L_1 < \omega < \omega_0/10 \tag{3-44}$$

The reason for the choice of $\omega = \omega_0/10$ for the upper boundary of the intermediate angular frequency range is found by substituting $\omega = \omega_0/10$ in Eq. 3-42*b*. The result is

$$\left|\frac{A_H}{A_I}\right| = \frac{1}{\sqrt{(1 - 0.01)^2 + (1/10Q_0)^2}}$$

so that, for $Q_0 \geqq 1$, $\quad |A_H| \cong |A_I|$

In the low-frequency range, the gain and phase-angle curves were plotted from Eq. 3-31 by assigning arbitrary values to the ratio $\omega L_1/(r_p + R_1)$. Partial data for the curves are given in Table 3-2.

TABLE 3-2. VALUES FOR $Q_0 = 1.25$ (FIG. 3-17)

$\frac{\omega}{\omega_0}$	$1 - \frac{\omega^2}{\omega_0^2}$	$\frac{\omega}{\omega_0 Q_0}$	θ_H	$\frac{A_H}{A_I}$
0.1	0.99	0.08	4.64°	1.01
0.2	0.96	0.16	9.47°	1.03
0.3	0.91	0.24	14.8°	1.06
0.4	0.84	0.32	20.86°	1.10
0.5	0.75	0.40	28.1°	1.18
0.6	0.64	0.48	36.8°	1.25
0.7	0.51	0.56	47.7°	1.32
0.8	0.36	0.64	60.6°	1.36
0.9	0.19	0.72	75.2°	1.34
1.0	0.00	0.80	90°	1.25
1.2	−0.44	0.96	114.6°	0.945
1.5	−1.25	1.20	136.2°	0.58
2.0	−3.00	1.60	152°	0.29
3.0	−8.00	2.40	163.3°	0.112
5.0	−24	4.00	170.5°	0.041
10.0	−99	8.00	175°	0.01

It is evident from Eqs. 3-31 and 3-42 from which the curves of Fig. 3-17 were prepared that an extension of the region of uniform gain to low frequencies requires that the ratio $(r_p + R_1)/L_1$ be decreased. This requires that $r_p + R_1$ should be reduced and L_1 increased. An extension of the region of uniform gain to higher frequencies requires an increase in the resonant angular frequency ω_0, but to increase ω_0 requires a decrease in L_0 or in C_0, or both. Since $L_0 = L_2(1 - k^2)$, a decrease in L_0 is obtained by (1) decreasing L_2, or (2) decreasing the leakage inductance by increasing k toward 1. Since C_0 depends upon the distributed capacitance, the conditions for widening the range of uniform gain contradict each other, for an increase in L_1 for the purpose of improving the response at the low end requires more turns and introduces more distributed capacitance *for a fixed-turns ratio,* and results in increasing L_0, rather than in decreasing it as required at the high-frequency end. The practical result is that turns ratios for coupling transformers seldom exceed 3, and that triodes of reasonably low values of plate resistance are used in transformer-coupled amplifiers. The low value of $Q_0 = 0.75$ or 0.8 necessary to suppress the resonant peak may be controlled when ω_0 is large by increasing the resistance $R_0 = R_2 + k^2n^2(r_p + R_1)$. This is accomplished by increasing R_2 since the secondary resistance is not involved in determining the low-frequency gain. The secondary resistance may be increased by using high-resistivity wire for the secondary winding. A very complete study of the design of coupling transformers has been made by G. Koehler.[5]

It should be pointed out that the phase angle θ_L of Fig. 3-17 is given by its tangent from the relation (from Eq. 3-30)

$$-\theta_L = \tan^{-1} - (r_p + R_1)/L_1 \tag{3-45}$$

From Eqs. 3-30 and 3-32,

$$\left| \frac{A_L}{A_I} \right| = \frac{1}{\sqrt{1 + \left(\dfrac{r_p + R_1}{\omega L_1}\right)^2}} \underline{/\theta_L} \tag{3-46}$$

so that θ_L is the angle of lead of A_L with respect to A_I. In the same way, from Eq. 3-42*b*, θ_H is the angle of lag of A_H with respect to A_I. In each case the angles are plotted in Fig. 3-17 as computed from their defining equations. The actual angle between output and input voltage depends, as has been stated, upon the relative winding directions of the primary and secondary of the transformer.

[5] G. Koehler, *Proc. IRE*, **16**, 1742 (1928).

The theory of the transformer-coupled amplifier will be illustrated by solving the following sample problem:

Example problem. An amplifier stage consists of a 6C5 coupled by an interstage transformer to a 6F6. The constants of the circuit are: For the 6C5, $\mu = 20$, $r_p = 10{,}000$; for the transformer, $R_1 = 600$ ohms, $R_2 = 25{,}000$ ohms, $L_1 = 20$ henrys, $N_2/N_1 = n = 3$. Assume that the coefficient of coupling is 0.995. If the equivalent secondary capacitance is $C_0 = 80\ \mu\mu$f, determine the gain-frequency characteristics of the 6C5 stage.

Solution. $r_p + R_1 = 10{,}600$ ohms, $\quad |A_I| = n\mu = 60$

for $\quad \omega L_1 = r_p + R_1, \quad |A_L| = 0.707|A_I|$

or $$\omega_L = \frac{r_p + R_1}{L_1} = \frac{10{,}600}{20} = 530 \text{ rad per sec}$$

for $$|A_L| = 0.707|A_I|$$

or $$f_L = \frac{530}{2\pi} = 84.4 \text{ cps} \quad \text{and} \quad |A_L| = 60(0.707) = 42.4$$

at $$\omega = 530 \text{ rad per sec}$$

The beginning of the intermediate-frequency range is determined by

$$(r_p + R_1)/\omega L_1 = 0.1$$

or $$\omega L_1 = 106{,}000 \quad \text{or} \quad f = 5300/6.28 = 844 \text{ cps}$$

$$L_0 = L_2(1 - k^2) \quad \text{where} \quad L_2 = n^2 L_1 = 180 \text{ henrys}$$

Since $k^2 = 0.99$, $\quad L_0 = 0.01(180) = 1.8$ henrys

Then, $\quad \omega_0 = 1/\sqrt{L_0 C_0} = 1/\sqrt{1.8 \times 80 \cdot 10^{-12}}$

$$= \tfrac{1}{12} \cdot 10^6 = 83{,}300 \text{ rad per sec}$$

$$R_0 = R_2 + 0.99(9)(10{,}600) = 25{,}000 + 94{,}400 = 119{,}400 \text{ ohms}$$

Then, $$Q_0 = \omega_0 L_0/R_0 = 83{,}300(1.8)/119{,}400 = 1.25$$

For $\omega = 0.1\omega_0$, $\quad |A_H| = 60/\sqrt{(0.99)^2 + (1/12.5)^2} = 60/0.99 = 60.6$

The corresponding frequency is 8330/6.28 = 1326 cps. Apparently, the region of uniform gain extends only from 844 to 1326 cps and needs to be extended by reducing C_0 or L_0. In addition, according to Fig. 3-17, there will be a high resonant peak, which will occur near $f = 0.8f_0$ or 10,600 cps, and at this frequency the gain will be 1.36(60) = 81.6.

The circuit values necessary for computing the expected behavior of a coupling transformer are best obtained by laboratory measurement.[6] With accurate values of transformer constants, amplifier performance can be predicted with reasonable accuracy consistent with the approximations used in the foregoing theory.

3-8. Push–Pull Operation

Transformer coupling as discussed in the foregoing section or *R–C* coupling as used in voltage amplifiers are usually employed between the first and second or between the second and third stages of a multistage audio-frequency amplifier. The last stage of an amplifier may be expected to deliver the amplified signal at an a-c power level of several

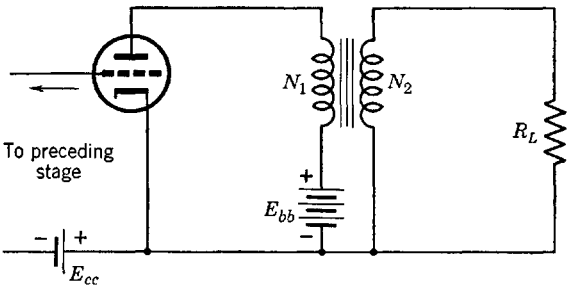

FIG. 3-18. Single-sided output stage.

watts, and so is called the *power stage*. Transformers are used to couple the power stage to the load and are called *output transformers*. Such a transformer should be thought of as an impedance-matching device to match the output impedance of the amplifier to the impedance of a load, such as a loudspeaker. The design of an output transformer obviously differs considerably from that of a coupling transformer.

If a power stage is coupled to a load impedance as shown in Fig. 3-18, the amplifier is said to be *single sided*. A number of distinct advantages are achieved, however, by using the two-tube arrangement of Fig. 3-19, in the power stage. The tubes in the circuit of Fig. 3-19 are said to be connected in push–pull; the advantages of the push–pull amplifier over the single-sided amplifier are: very much less harmonic distortion, more

[6] F. E. Terman, *Radio Engineering*, 3d Ed., McGraw-Hill Book Co.

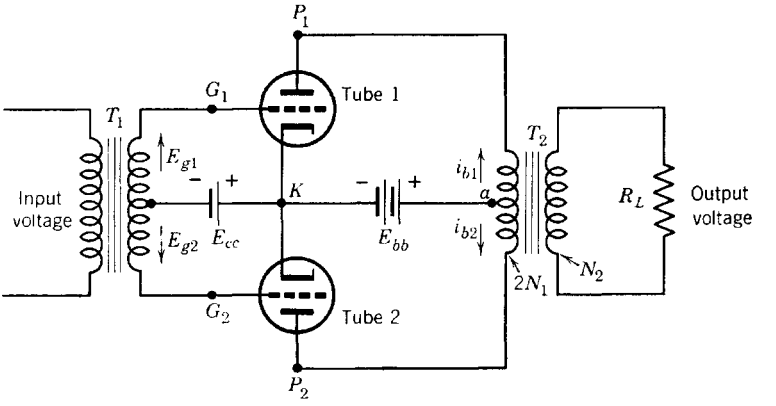

FIG. 3-19. Power stage, triodes in push–pull.

than twice the power output possible with a single tube, and no transformer core saturation. The reasons for these advantages will be given in the following discussion of the push–pull circuit.

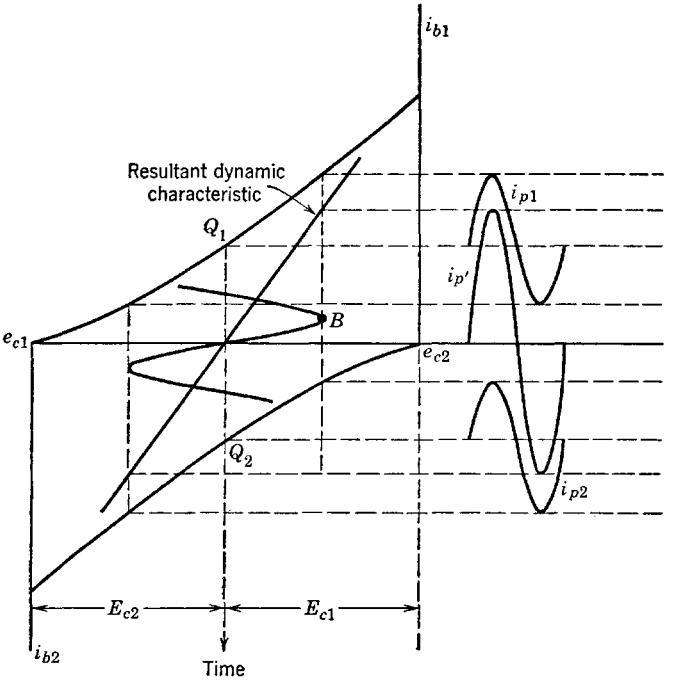

FIG. 3-20. Resultant or composite dynamic characteristic of a push–pull class-A amplifier.

The connection diagram of Fig. 3-19 shows that the grids of the two identical tubes driven by the input or coupling transformer T_1 will swing in the positive direction alternately, so that the grid-to-cathode voltage of G_1 will be 180° out of phase with that of G_2. If the grid bias and the excitation of each tube are such as to provide class-A operation, then the plate current of one tube will reach its maximum value at the same instant that the plate current of the other tube will be passing through its minimum value. This may be shown graphically by the use of two identical tube dynamic characteristics, one for each tube, arranged as shown in Fig. 3-20, in which the dynamic characteristic of tube 2 has been rotated 180° with respect to the characteristic of tube 1, with the operating points Q_1 and Q_2 in vertical alignment. It will be shown later that the resultant or composite dynamic characteristic of the two tubes is equivalent to the individual dynamic characteristics combined. It should be noticed that the individual plate currents i_{p1} and i_{p2} (Fig. 3-20) do not have identical positive and negative peak values, and are not sinusoids because of the curved individual dynamic characteristics, but the composite current wave form is symmetrical, and very closely sinusoidal. Also, the d-c zero signal components I_{b1} and I_{b2} are equal.

3-9. Harmonic Suppression with the Push–Pull Connection

It will be demonstrated in the present section that (1) no even harmonics of signal frequency exist in the output of a push–pull amplifier and (2) that no odd harmonics exist in the plate-supply connection.

It will be observed that the direct components of plate current I_{b1} and I_{b2} flow through the two halves of the primary winding of the output transformer T_2 of Fig. 3-19 in opposite directions. As a result, the d-c ampere-turns cancel and there is no magnetic core saturation. If there are N_1 turns on each half of the transformer primary coil and N_2 turns on the secondary, the instantaneous ampere turns of primary and secondary (for an ideal transformer) are related as follows:

$$N_1 i_{b1} - N_1 i_{b2} = N_2 i_2 \tag{3-47}$$

where i_2 is the secondary current. The instantaneous value of what may be called the composite primary current is expressed by the instantaneous difference of the total plate currents, or, with $I_{b1} = I_{b2}$,

$$i_{b1} - i_{b2} = (I_{b1} + i_{p1}) - (I_{b2} + i_{p2}) = i_{p1} - i_{p2} \tag{3-48}$$

For identical dynamic characteristics, the series representation of Eq. 2-11 may be used for each; then, for either i_{p1} or i_{p2}, referred to an origin through Q_1 or Q_2,

$$i_{p1,2} = C_1 e_g + C_2 e_g^2 + C_3 e_g^3 + \cdots + C_n e_g^n + \cdots$$

If $e_{g1} = \sqrt{2}\,E_g \cos \omega t$ is the equation for the input voltage between cathode and grid of tube 1, then $e_{g2} = -\sqrt{2}\,E_g \cos \omega t$ is the expression for the input voltage for tube 2. The alternating components of plate currents for the two tubes may then be obtained by substituting the respective excitation voltages in the expression for the dynamic characteristic and simplifying, as in Eq. 2-15. The results are

$$i_{p1} = B_0 + B_1 \cos \omega t + B_2 \cos 2\omega t + B_3 \cos 3\omega t + \cdots + \cdots \quad (3\text{-}49a)$$

$$i_{p2} = B_0 - B_1 \cos \omega t + B_2 \cos 2\omega t - B_3 \cos 3\omega t + \cdots + \cdots \quad (3\text{-}49b)$$

where B_1, B_2, B_3, etc. represent resulting harmonic amplitudes and B_0 is the change in the d-c component. The composite or equivalent instantaneous alternating current in the transformer primary winding, according to Eq. 3-48, is

$$i_p' = i_{p1} - i_{p2} = 2B_1 \cos \omega t + 2B_3 \cos 3\omega t + \cdots + \cdots \quad (3\text{-}50)$$

Equation 3-50 shows that even harmonics introduced by nonlinearity of the dynamic-tube characteristics are eliminated in the transformer primary and secondary windings by the push–pull connection. Because of elimination of the second-harmonic distortion, a wider range of the tube characteristic may be used, so that an output power more than twice that available from a single tube can be obtained.

If the individual tube plate currents represented by the individual tube dynamic characteristics of Fig. 3-20 are combined by algebraic addition of ordinates according to Eq. 3-48, the individual dynamic characteristics may be combined into a single composite dynamic characteristic for both tubes. As shown in Fig. 3-20, the composite dynamic characteristic is a straight line. The sinusoidal grid excitation voltage has been drawn in the usual way with its time axis through Q_1 and Q_2. The composite plate current i_p' may be obtained directly from the composite characteristic, or the individual plate currents may be obtained first from the individual dynamic characteristics and then combined algebraically according to Eq. 3-48. As previously mentioned, it should be observed that the individual currents i_{p1} and i_{p2} have unequal positive and negative amplitudes, but that the composite current i_p' is quite symmetrical and free from even harmonics. The composite current is obtained graphically by adding ordinates of i_{p1} and i_{p2} on Fig. 3-20.

The composite characteristic of two identical tubes in push–pull is more easily obtained than the individual tube dynamic characteristics. Since the two plates of the amplifier tubes in push–pull are connected together through a transformer, a change in the voltage of either plate will affect the voltage of the other plate. The result is that the individual

tube load lines and dynamic characteristics are not independent and are not straight lines. This will be shown in the analysis [7] to follow in Section 3-12.

The current in the mid-branch connection through the plate-supply battery (of Fig. 3-19) is the sum of the separate tube currents, or, using Eq. 3-49,

$$i_{b1} + i_{b2} = 2(I_b + B_0 + B_2 \cos 2\omega t + B_4 \cos 4\omega t + \cdots + \cdots) \quad (3\text{-}51)$$

According to Eq. 3-51, the fundamental and odd-harmonic a-c components of plate current add to zero in this part of the circuit. This fact has significance because of implications as to the use of a by-pass condenser across a biasing resistor inserted in the plate return, and because of a simplification of the equivalent a-c circuit. With regard to biasing, since the principal use of a by-pass condenser is to by-pass the fundamental signal frequency around the biasing resistor, the condenser may be omitted from the class-A push–pull amplifier circuit. Application to the equivalent a-c circuit will be discussed in Section 3-10.

3-10. Push–Pull Equivalent Circuits

The a-c equivalent anode circuit has been drawn only for linear operation, and its use is justified only for negligible harmonic distortion. If the harmonic distortion is negligible, as for class-A operation, then,

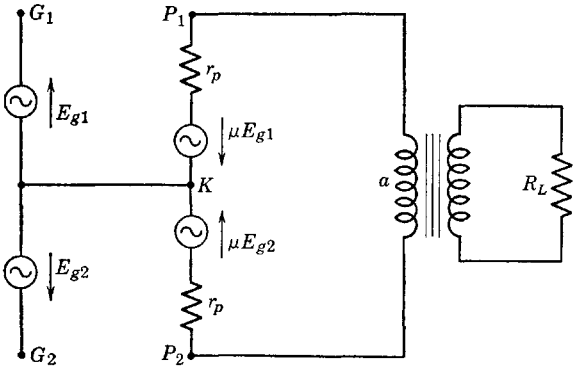

FIG. 3-21. Equivalent a-c circuit of a push-pull class-A amplifier.

since according to Eq. 3-51 the fundamental does not exist in the connection K to a (Fig. 3-19), this connection may be omitted from the equivalent a-c circuit of Fig. 3-21. A further simplification of the circuit is possible by using the relation between E_{g1} and E_{g2}. Since

[7] B. J. Thompson, Graphical Determination of Performance of Push–Pull Audio Amplifier, *Proc. IRE*, **21**, 591 (1933).

$E_{g1} = E_g$, and $E_{g2} = E_g\underline{/180°}$, the two equivalent generators will be in phase with voltage adding in the plate circuit and may be represented as one generator as shown in Fig. 3-22. The load resistance R_L when referred to the primary circuit becomes $(2N_1/N_2)^2R_L$, where $2N_1/N_2$ is the primary-to-secondary turns ratio, plate to plate. Since the tubes are identical, the two plate resistances have been lumped as $2r_p$.

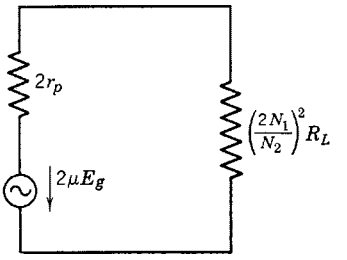

FIG. 3-22. Simplified a-c equivalent plate circuit of Fig. 3-21.

A note on the composite current is appropriate at this point. According to Eq. 3-50, the composite current in the absence of harmonic distortion is given by

$$i_p' = 2B_1 \cos \omega t = 2i_p \qquad (3\text{-}52)$$

where $i_p = B_1 \cos \omega t$ is the fundamental a-c component for one tube alone. The quantity i_p' defined by Eq. 3-50 as the composite current is equal to twice the instantaneous a-c component for a single tube of a pair in push–pull operating with negligible harmonic distortion. The composite current may be defined as the current flowing in an equivalent single-tube circuit. The desirable equivalent circuit for purposes of analysis is that which yields the composite current. For effective values and according to Eq. 3-47,

$$N_1 I_p' = N_2 I_2$$

or

$$N_1(2I_p) = N_2 I_2 \qquad (3\text{-}53)$$

where I_p is the effective value of the a-c component of plate current for a single tube of the push–pull pair.

Now the power delivered to R_L may be expressed in two ways, as follows:

(*a*) According to Eq. 3-53, for an ideal output transformer (zero primary and secondary resistances, unity coefficient of coupling) the power output is

$$P_o = I_2^2 R_L = (N_1 I_p'/N_2)^2 R_L \qquad (3\text{-}54)$$

where I_2 is the rms value of the current i_2 and I_p' the rms value of composite current i_p'.

(*b*) According to the equivalent circuit (Fig. 3-22),

$$P_o = \left[\frac{2\mu E_g}{2r_p + (2N_1/N_2)^2 R_L}\right]^2 4\left(\frac{N_1}{N_2}\right)^2 R_L$$

or

$$P_o = \left[\frac{\mu E_g}{r_p/2 + (N_1/N_2)^2 R_L}\right]^2 \left(\frac{N_1}{N_2}\right)^2 R_L \qquad (3\text{-}55)$$

For an ideal output transformer, both Eqs. 3-54 and 3-55 represent the power output. Therefore, by equating the two expressions for P_o, the composite current I_p' may be expressed in terms of the constants of a new equivalent circuit. Evidently

$$I_p' = \frac{\mu E_g}{r_p/2 + (N_1/N_2)^2 R_L} \tag{3-56}$$

so that the composite single-tube equivalent a-c circuit involves an equivalent generator of voltage μE_g and internal resistance $r_p/2$ connected to a resistance $(N_1/N_2)^2 R_L$. Equation 3-56 shows that the two tubes are in parallel so far as the composite current is concerned. The resistance $(N_1/N_2)^2 R_L$ is the resistance as seen between plate and mid-tap, a. The equivalent circuit shown in Fig. 3-23 is the desired one, since it gives the composite current and the correct value of the output current I_2.

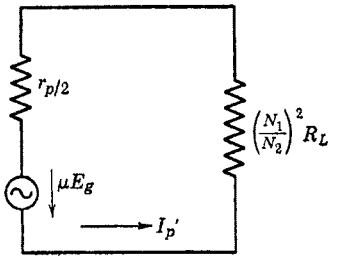

FIG. 3-23. Composite equivalent circuit.

3-11. Push–Pull Amplifier Input Circuits

The input voltage to a push–pull amplifier stage may be supplied by any of the usual coupling methods. Figure 3-24 shows an amplifier in which transformer coupling to the push–pull power stage is used. The d-c components of both plate currents flow through resistor R_{c2} providing bias. As shown by Eq. 3-51, the fundamental and all odd har-

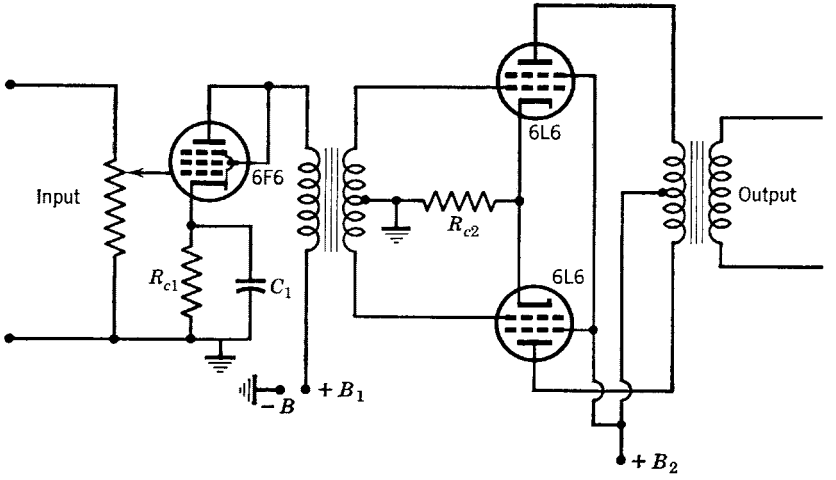

FIG. 3-24. Two-stage amplifier using transformer coupling.

monics are missing in this part of the circuit, so that no reduction of voltage will occur (as in the single-sided amplifier) if the by-pass condenser is omitted.

If R–C coupling is used, special means must be employed to provide the 180° phase relation between the input grid voltages of the two push–pull tubes. A method frequently used for this purpose is shown in Fig. 3-25 in which an amplifier tube and a phase-inverter tube together provide the first stage of amplification and the input to the push–pull stage. The output voltage of the first-stage amplifier tube is the voltage

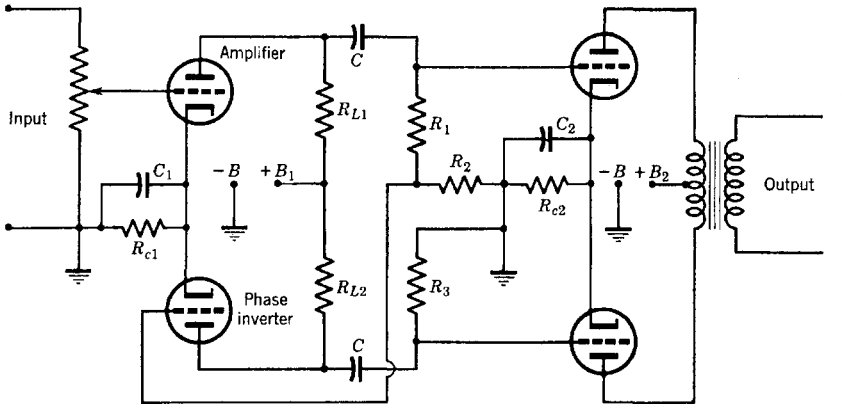

FIG. 3-25. Two-stage R–C-coupled amplifier using a phase inverter.

across R_1 and R_2 in series; the input voltage of the phase inverter is the voltage across R_2; the amplified output voltage of the phase inverter appears across R_3 and is the input voltage to the lower tube of the push–pull stage. If the resistors R_1, R_2, and R_3 are properly chosen, the voltage across R_1 and R_2 in series will be equal in magnitude and 180° out of phase with the voltage across R_3. Both tubes of the first stage may conveniently be built in the same glass envelope and use a common cathode. Examples of this type of dual-purpose tube are the twin triodes 6N7 and 12SC7.

3-12. Composite Characteristics

Because of the transformer primary winding which connects the plates of two tubes operating push–pull, an increase in the voltage at the plate of one tube will be accompanied by an equal decrease in the plate voltage of the other tube, just as for the grid-to-cathode voltages at the input. These relations may be stated as follows: At any instant, with a common bias voltage E_c, and an instantaneous grid voltage e_g, referred

to ground, the instantaneous total grid and plate voltages for tubes 1 and 2 are given by

$$\begin{aligned} e_{c1} &= E_c + e_g \\ e_{c2} &= E_c - e_g \\ e_{b1} &= E_b + e_p \\ e_{b2} &= E_b - e_p \end{aligned} \tag{3-57}$$

Equations 3-48 and 3-57 are sufficient to obtain the composite current corresponding to any value of the instantaneous grid excitation voltage e_g if the plate characteristics of the tube are available. For example, if a value of e_g is specified for a push–pull amplifier operating with a given grid bias E_c and plate voltage E_b, the individual plate characteristics involved are those corresponding to the values of e_{c1} and e_{c2} (Eq. 3-57). The composite current is $i_p' = i_{b1} - i_{b2}$. The e_{c1} characteristic relates corresponding values of i_{b1} and e_{b1}; the e_{c2} characteristic relates

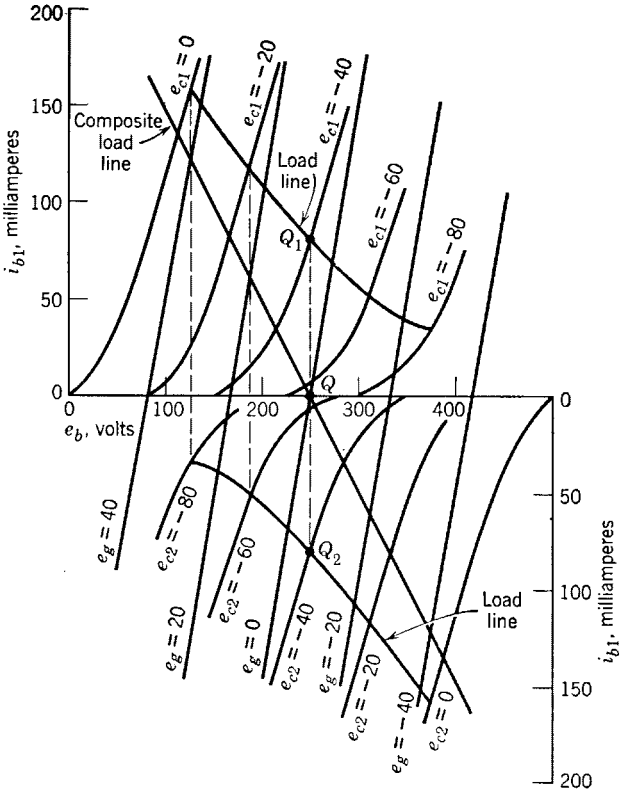

FIG. 3-26. Individual and composite static characteristics and load lines for type-2A3 tubes in push–pull class-A operation.

corresponding values of i_{b2} and e_{b2}; the composite current is the difference of the ordinates of the two characteristics. If two identical graph sheets of the plate characteristics are arranged as shown in Fig. 3-26 with the operating points Q_1 and Q_2 in vertical alignment, the ordinates of the e_{c1} and e_{c2} characteristics corresponding to a given grid excitation voltage e_g may easily be combined graphically with the aid of dividers.

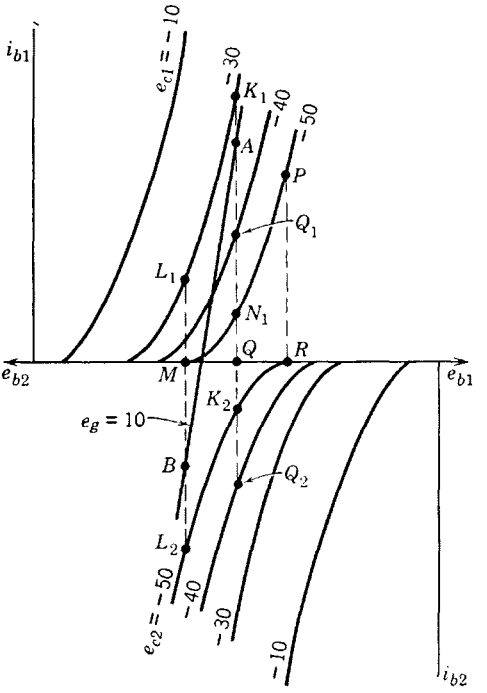

FIG. 3-27. Method of determining the composite static characteristic for tubes connected in push–pull.

For example, in Fig. 3-26, $E_c = -40$ volts; if $e_g = +40$ volts, $e_{c1} = E_c + e_g = 0$, $e_{c2} = E_c - e_g = -80$ volts. Ordinates of the $e_{c1} = 0$ characteristic of tube 1 are then combined with ordinates of the $e_{c2} = -80$ characteristic of tube 2. The resulting or composite characteristic is nearly a straight line which relates the values of the composite current to the plate voltages of the tubes. For triodes operating class A, the push–pull composite characteristics are found to be uniformly spaced, nearly parallel and straight lines.

The method of obtaining points for drawing the composite characteristic is shown more clearly in Fig. 3-27. For $e_g = 10$ volts, $e_{c1} = -40 + 10 = -30$ volts, and $e_{c2} = -40 - 10 = -50$ volts. The point A is

obtained by subtracting the distance QK_2 from QK_1; also, for point B,

$$MB = ML_2 - ML_1$$

If $e_g = 0$, the two $e_c = -40$ characteristics are combined, and the resulting composite characteristic passes through the composite operating point Q.

It should be noted that point B of Fig. 3-27 may be obtained without the use of the second or inverted sheet of plate characteristics. The $e_{c1} = -50$ characteristic already on the tube-1 characteristics may be used. For example, if $QR = QM$, then $RP = ML_2$, and

$$MB = RP - ML_1$$

This corresponds to the third and fourth equations of 3-57. Reference again to Fig. 3-27 shows that the voltage E_b corresponds to distance OQ or to $O'Q$; distance QM corresponds to a negative numerical value of e_p, for which $e_{b1} = QM$ and $E_{b2} = O'M$.

If one refers again to the push–pull amplifier circuit of Fig. 3-19, the voltage across N_1 turns of the transformer primary winding is seen to be

$$v = i_p'(N_1/N_2)^2 R_L \tag{3-58}$$

If i_p', the composite plate current, is increasing in tube 1, v is a voltage drop, and

$$e_{b1} = E_b - v, \qquad e_{b2} = E_b + v$$

These relations correspond exactly to the third and fourth equations of 3-57 where

$$e_p = -v = -i_p'(N_1/N_2)^2 R_L$$

Then,

$$e_{b1} = E_b - i_p'(N_1/N_2)^2 R_L \tag{3-59}$$

is the equation of the composite load line referred to the origin of coordinates e_{b1} and i_{b1} (or i_p'). The slope of the composite load line is

$$\frac{di_p'}{de_{b1}} = -\frac{1}{(N_1/N_2)^2 R_L} \tag{3-60}$$

The composite load line is drawn through the composite operating point Q (Fig. 3-26) with the slope given by Eq. 3-60. The intersections of the composite load line with the composite static characteristics may be transferred to the mutual diagram in the usual way to give the corresponding composite dynamic characteristic.

The individual tube-circuit load lines have been obtained from the composite load line and are shown on the diagram (Fig. 3-26). Points for the individual load lines are located by projecting vertically from intersections of the composite load line with composite characteristics

to corresponding points on the individual tube characteristics. The individual load lines are of value for computing harmonic components and output power in class-B operation, as shown in Chapter 4.

A numerical example will illustrate the agreement between values of the composite current obtained from the equivalent circuit of Fig. 3-23 and from the graphical solution. Assume that the tubes of Fig. 3-19 are 2A3's biased to operate at $E_c = -40$ volts, with $E_b = 250$ volts. Let $(2N_1/N_2)^2R_L = 4000$ ohms, the plate-to-plate resistance, and the signal voltage e_g (grid to cathode) $= 20 \sin \omega t$. Then at a time (ωt) when $e_g = +20$ volts, the instantaneous total grid voltage of tube 1 is $e_{c1} = -40 + 20 = -20$ volts; of tube 2, $e_{c2} = -40 - 20 = -60$ volts. The composite characteristic for $e_g = +20$ has been drawn in Fig. 3-26, and the composite load line has a slope corresponding to $(N_1/N_2)^2R_L = 1000$ ohms. From the intersection of load line and characteristic, $i_p' = 60$ ma. From the equivalent circuit (Fig. 3-23) using $\mu = 4.2$, $r_p = 800$ ohms,

$$i_p' = 4.2(20)/(400 + 1000) = 84/1400 = 0.06 \text{ amp}$$

or 60 ma. The corresponding values of e_{b1} and e_{b2} are: $e_{b1} = 187$ (graph) and $e_{b1} = 250 - 0.06(1000) = 190$ using Eq. 3-59; $e_{b2} = 313$ (graph) and $e_{b2} = 250 + 60 = 310$ using Eq. 3-59.

Triodes, pentodes, and beam-power tubes are also operated push–pull in class AB or class B. The composite static characteristics for triodes operated class AB are almost straight lines. The dynamic characteristics for typical class-B operation of triodes are shown in Fig. 3-28.

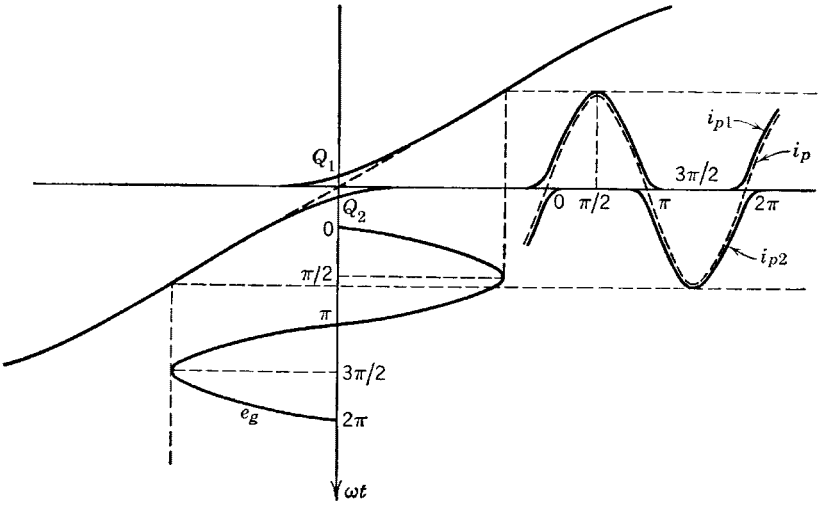

FIG. 3-28. Dynamic characteristics and tube currents, class-B push–pull amplifier.

The graphical method of determining the composite static characteristics and the load line applies also to push–pull tubes operated in class AB or in class B. Push–pull amplifiers using beam-power tubes frequently are operated class AB with low distortion. A further discussion of these matters will be given after power relations and efficiency in amplifiers have been examined.

3-13. The Use of Inverse Feedback in Voltage Amplifiers

As used in relation to amplifier circuits the term "feedback" may be defined as the insertion, in series with the input signal voltage of any

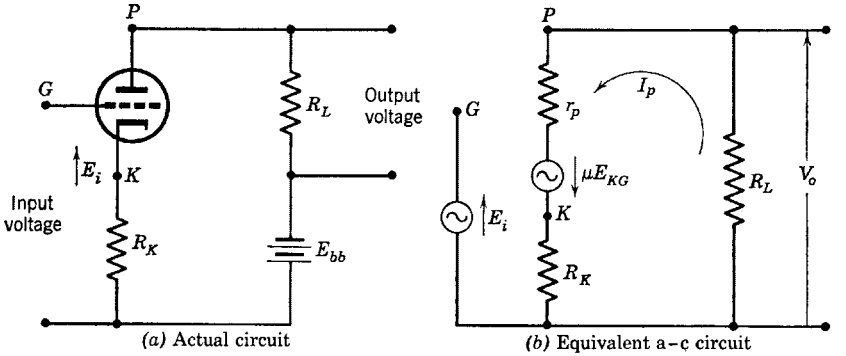

FIG. 3-29. Inverse-feedback single-stage amplifier.

stage, of a portion of the output voltage of that stage or of a later stage of amplification. If the voltage fed back is less than 90° out of phase with the signal voltage, the resulting input voltage will be increased and the feedback is said to be regenerative, direct, or positive. If the voltage fed back is more than 90° out of phase with the signal voltage, the feedback is said to be degenerative, inverse, or negative, and the resultant input voltage will be decreased. If the feedback is regenerative or direct, the amplifier output voltage may increase intil the amplifier becomes an oscillator. If the feedback is inverse, however, a number of effects upon the operating behavior of the amplifier result, as follows:

(*a*) The gain is reduced.

(*b*) The harmonic, frequency, and phase distortions are reduced.

(*c*) The stability of the amplifier is improved.

(*d*) The effective output impedance of the amplifier may be controlled.

A short discussion of the effect of inverse feedback on gain, distortion, and stability will be given by analyzing simple examples. In Fig. 3-29, a triode amplifier is shown with a connection providing both inverse feedback and cathode bias. The input signal voltage E_i is in series with

the voltage across resistor R_K. The voltage fed back expressed as a fraction of the output voltage is given by

$$I_pR_K/I_pR_L = V_f/V_o \tag{3-61}$$

and is dependent upon the relative magnitudes of R_K and R_L. The voltage rise from the cathode to the grid is

$$E_{KG} = E_i - I_pR_K$$

The plate current is then obtained from

$$I_p = \frac{\mu(E_i - I_pR_K)}{r_p + R_K + R_L}$$

whence

$$I_p = \frac{\mu E_i}{r_p + (\mu + 1)R_K + R_L} \tag{3-62}$$

It should be noted in Eq. 3-62 that one effect of this type of feedback is to increase the effective plate resistance of the amplifier. The output voltage drop V_o is

$$V_o = I_pR_L$$

The gain, with feedback, is

$$A_f = \frac{V_o}{-E_i} = -\frac{\mu R_L}{r_p + (\mu + 1)R_K + R_L} \tag{3-63}$$

If the grid (through voltage source E_i) were connected directly to K (suitable fixed bias being provided), there would be no feedback, and the gain would be

$$A = I_pR_L/-E_{KG} = -\mu R_L/(r_p + R_K + R_L) \tag{3-64}$$

The relation between A_f and A may now be obtained by dividing numerator and denominator of the right side of Eq. 3-63 by $r_p + R_K + R_L$. The result is

$$A_f = \frac{-\mu R_L/(r_p + R_L + R_K)}{1 + \mu R_K/(r_p + R_K + R_L)}$$

The quantity $\mu R_K/(r_p + R_K + R_L)$ may be written as

$$\frac{\mu R_L R_K}{(r_p + R_K + R_L)R_L} = -A\frac{R_K}{R_L}$$

using Eq. 3-64, so that, finally,

$$A_f = \frac{A}{1 - AR_K/R_L} \tag{3-65}$$

If for example the tube in Fig. 3-29 has $r_p = 10{,}000$, $\mu = 20$, then, if $R_L = 35{,}000$ ohms and $R_K = 5000$ ohms,

$$A = -20(35{,}000)/50{,}000 = -14$$

$$R_K/R_L = 5000/35{,}000 = \tfrac{1}{7}$$

then

$$A_f = \frac{-14}{1 - (-14)\frac{1}{7}} = -\frac{14}{3} = -4.66$$

The percentage decrease in gain due to feedback of this example is then $(9.34/14) \cdot 100$ or 66.6 per cent. Such a decrease is not desirable, but a

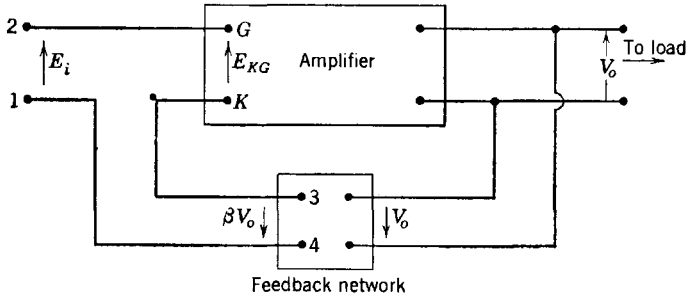

FIG. 3-30. Inverse feedback, generalized.

resulting improvement in freedom from distortion and in stability serves to compensate for the reduction of gain. In actual practice it may be desirable to provide for more gain than may be required and then discard the unnecessary gain by the use of inverse feedback to utilize the desirable features of the latter.[8]

Before discussing the reduction of distortion by the use of inverse feedback, one additional statement concerning Eq. 3-65 should be made. If a fraction β, called the feedback fraction, is defined as the ratio of the voltage fed back to the output voltage, then, for the circuit of Fig. 3-29, $\beta = R_K/R_L$, and Eq. 3-65 becomes

$$A_f = A/(1 - \beta A) \tag{3-66}$$

Equation 3-66 is a general relationship, applicable to any feedback arrangement, as may be shown by considering Fig. 3-30. The phase relation of the output voltage drop V_o to the input voltage rise E_i depends upon the number of amplifier stages and the phase shift in each

[8] H. S. Black, Stabilized Feedback Amplifiers, *Electrical Engineering*, **53**, 114 (1934).

stage. However, if the feedback is to be inverse or negative, the gain must be decreased so that the actual amplifier input voltage rise E_{KG} must be less than E_i, requiring that the voltage fed back be out of phase with E_i by more than 90°. It is the function of the feedback network to provide the proper magnitude and phase of the voltage fed back. The feedback network is in effect a potential divider to provide a fraction of the output voltage in series but more than 90° out of phase with E_i. From Fig. 3-30, applying Kirchhoff's voltage law, and the double-subscript notation,

$$E_{12} = V_{GK} + V_{34}$$

or

$$E_i = E_{KG} + \beta V_o$$

Thus,

$$E_{KG} = E_i - \beta V_o \tag{3-67}$$

If the gain of the amplifier without feedback is A, then, if one assumes steady-state conditions,

$$V_o = -AE_{KG} = -A(E_i - \beta V_o)$$

or

$$V_o = -AE_i/(1 - \beta A)$$

The gain of the amplifier with feedback is, by definition,

$$A_f = V_o/-E_i = A/(1 - \beta A) \tag{3-68}$$

which is identical with Eq. 3-66 and applies to any feedback amplifier.

In general, both β and A are frequency-dependent vector quantities. For a single-triode stage of amplification, the vector nature and frequency dependence of A was shown by the relation 3-16 as

$$A_H = \frac{g_m R_{eq}/(180° - \theta_H)}{\sqrt{1 + (f/f_H)^2}}$$

Since both magnitude and phase shift are involved in the product βA, it is difficult to interpret Eq. 3-68 over a wide frequency range, particularly with regard to the question of stability. For β obtained as a frequency-independent fraction of the output voltage, inverse feedback is achieved for a single-amplifier stage if $A\beta$ is negative, for then A_f is a fraction of A. However, if $A\beta$ is positive, as is possible with a single stage of transformer-coupled amplifier at the high-frequency end of the frequency range, the feedback may become regenerative with resulting increased gain. If the feedback is regenerative and large enough to replace the signal voltage E_i, the latter may be removed, and the amplifier becomes an oscillator. It must be remembered in the use of Eq. 3-66 that, in general, A, β, and A_f are complex or vector quantities.

To consider the effect of inverse feedback upon harmonic distortion, again refer to Fig. 3-30. In general,

$$V_o = -AE_{KG} = -A(E_i - \beta V_o)$$

With, for example, a second-harmonic distortion voltage of V_d volts without feedback, let the total output voltage be V_o', the total input voltage E_{KG}'. Then, the vector voltage relation applying is, since the distortion voltage is introduced by the amplifier itself,

$$V_o' = -AE_{KG}' + V_d = -A(E_i - \beta V_o') + V_d \qquad (3\text{-}69)$$

If Eq. 3-69 is solved for V_o', the result is

$$V_o' = -\frac{AE_i}{1 - A\beta} + \frac{V_d}{1 - A\beta} = -A_f E_i + \frac{V_d}{1 - A\beta} \qquad (3\text{-}70)$$

Equation 3-70 shows that the distortion voltage V_d will be reduced as a result of inverse feedback in the same proportion as is the gain. For example, refer to the circuit previously used where $A = -14$, $A_f = -4.66$, $\beta = 1/7$, $1 - A\beta = 3$; if the voltage E_i is adjusted so that the fundamental output voltage with feedback is the same as without feedback, then the value of signal required in each case can be determined from the relation

$$V_o = -AE_{i1} = -A_f E_{i2} \qquad (3\text{-}71)$$

Assume an input voltage E_{i1} (no feedback) of 0.5 volt; V_o (no feedback) will then be $14(0.5) = 7$ volts. With feedback and the same fundamental output voltage, $E_{i2} = 7/4.66 = 1.5$ volts, the required input. If the second-harmonic distortion is 10 per cent, the distortion voltage would be 0.7 volt without feedback, and the output voltage $V_o = 7$ volts (fundamental), with 0.7 volt (second harmonic). With feedback, the output voltage, according to Eq. 3-70 will be

$$V_o' = -A_f E_{i2} + V_d/(1 - A\beta)$$

where $(-A_f E_{i2}) = 4.66(1.5) = 7$ volts (fundamental), and $V_d/(1 - A\beta) = 0.70/3 = 0.233$ volt (second harmonic).* The per cent second-har-

* The total output voltage is not 7.233 volts. If the rms fundamental voltage is equal to 7, and the rms second-harmonic voltage is equal to 0.233, the rms output voltage is $\sqrt{7^2 + (0.233)^2}$.

monic distortion has then been reduced by feedback from 10 per cent to 23.3/7 = 3.33 per cent. A similar reduction of noise or hum voltages generated in the output circuit results from the use of inverse feedback.

In considering the effect of inverse feedback upon frequency and phase distortion, the easiest point of view may be based upon a rearrangement of Eq. 3-66. If both numerator and denominator of Eq. 3-66 are divided by $-\beta A$, the result is

$$A_f = \frac{-1/\beta}{1 - 1/\beta A} \tag{3-72}$$

It is generally true that the feedback fraction β can be made independent of frequency over a wide range by using pure resistance circuit elements. If then $|\beta A|$ is large so that $\left|\frac{1}{\beta A}\right| \ll 1$, the gain approaches $\left(-\frac{1}{\beta}\right)$ which does not depend upon frequency so that both frequency and phase distortions are eliminated. Although the large value of βA required involves a very great sacrifice in gain, the increase in effective bandwidth and the possibility of eliminating the dependence of amplifier properties upon the individual tube characteristics frequently justify the use of a large value of βA.

Although it is difficult except for specific circuits to show the reduction of frequency distortion by inverse feedback, experimental gain-frequency curves show it very clearly. Terman [9] has published experimental characteristics of an amplifier for which the gain-frequency curve without feedback was flat from about 400 to 2000 cps. With feedback, the gain-frequency curve of the same amplifier operating with the same plate voltage was flat through a frequency range extending from 30 to 30,000 cps.

The reduction of phase distortion as a result of the use of inverse feedback is shown by the vector diagram of Fig. 3-31, for a typical R–C-coupled amplifier. In this amplifier a fraction of the output voltage has been fed back in series with the input signal voltage E_i. The accompanying vector diagram has been drawn for a low frequency such that the reactance of the coupling capacitor C is 50,000 ohms. If the output voltage were maintained constant, and there were no feedback, the required value of input voltage E_i would be equal to and coincide with the voltage E_{KG}. The phase-shift angle would then be θ_L, and the phase shift between input and output voltages would be $(180° + \theta_L)$.

[9] F. E. Terman, Feedback Amplifiers, *Electronics*, **10**, 15 (Jan. 1937).

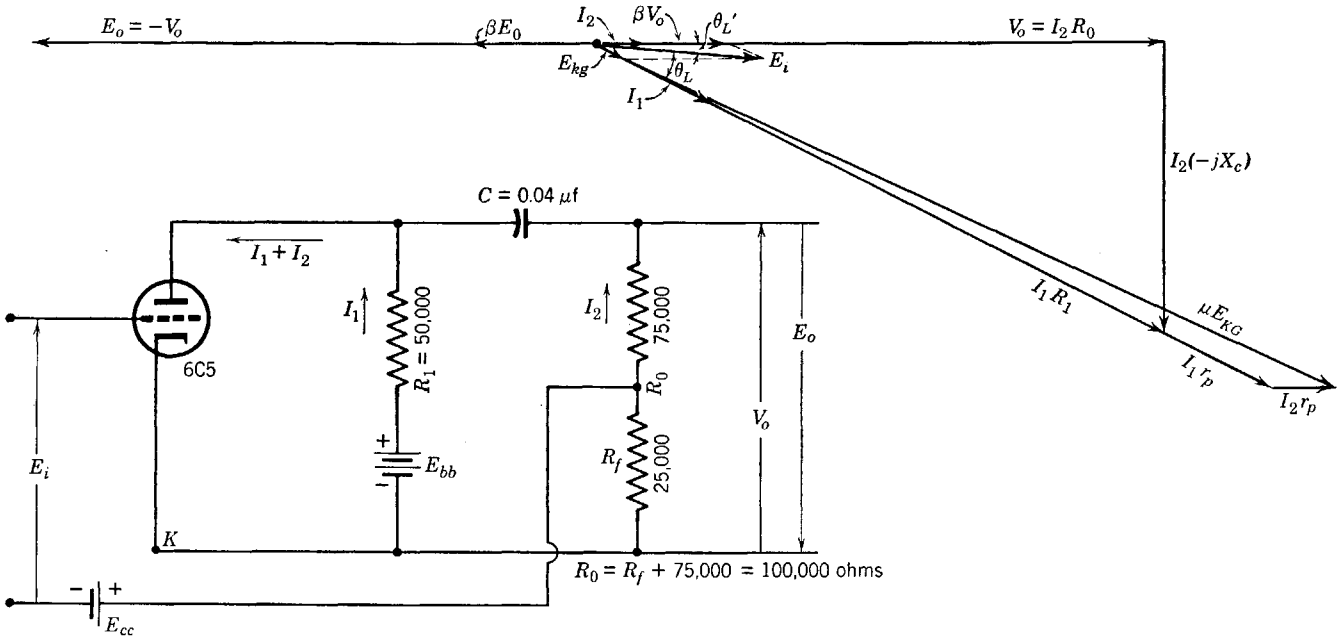

FIG. 3-31. Feedback amplifier circuit and vector diagram.

With feedback as shown in Fig. 3-31, however, the phase-shift angle is reduced to θ_L', and the phase shift differs by about 5° from the 180° desired. Because of the decrease in gain due to inverse feedback, it would be necessary to increase E_i greatly in order to obtain the same output voltage with feedback as without, as the vector diagram shows.

Example Problem. In connection with Fig. 3-31, the following problem solution will illustrate the principles involved in the use of inverse feedback. Let it be required to determine the gain of the amplifier of Fig. 3-31 with and without feedback, using

(*a*) Ordinary circuit theory.

(*b*) The general feedback theory.

In addition, the complete vector diagram of the amplifier is required. Let the frequency be 79.6 cps ($\omega = 500$).

Solution. (The equivalent circuit is shown in Fig. 3-32.)

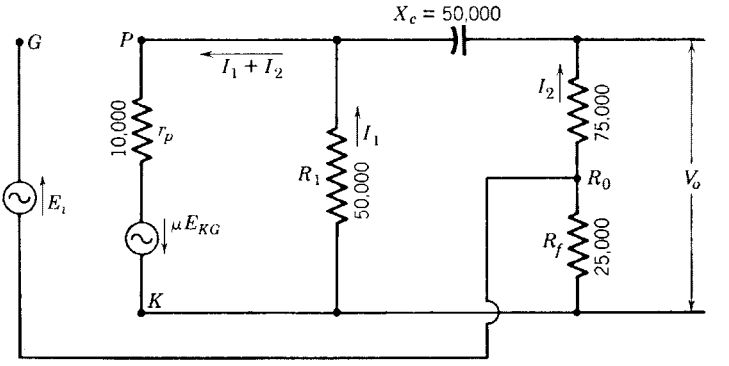

FIG. 3-32. Equivalent circuit of Fig. 3-31.

(*a*) For convenience, arbitrarily choose $I_2 = 1$ ma and the output voltage drop as the reference vector. Then,

$$V_o = I_2 R_0 = 10^{-3}(100{,}000) = \underline{100/0°} \text{ volts}$$

$$V_c = I_2(-jX_c) = 10^{-3}(-j50{,}000) = -j50 \text{ volts}$$

The sum of V_o and V_c is equal to the voltage across R_1. Then,

$$I_1 = \frac{100 - j50}{50{,}000} = (2 - j1)\cdot 10^{-3} \text{ amp} = \underline{2.24/-26.6} \text{ ma}$$

$$I_1 R_1 = I_2(R_0 - jX_c) = \underline{112/-26.6°} \text{ volts}$$

By Kirchhoff's voltage law,

$$\begin{aligned}\mu E_{KG} &= I_1R_1 + (I_1 + I_2)r_p \\ &= I_1(R_1 + r_p) + I_2r_p \\ &= 2.24\cdot10^{-3}\underline{/-26.6}(60{,}000) + 1\cdot10^{-3}(10{,}000) \\ &= 134.4\underline{/-26.6} + 10 = 120 - j60.2 + 10 = 130 - j60.2 \\ &= 143\underline{/-24.8^\circ}\end{aligned}$$

Then $$E_{KG} = \tfrac{143}{20}\underline{/-24.8}$$

$$= 7.15\underline{/-24.8} = 6.5 - j3.0 \text{ volts}$$

This is the actual resultant input voltage. To find the applied input voltage E_i, note that the voltage rise from K to G is

$$E_{KG} = -I_2R_f + E_i$$

whence

$$\begin{aligned}E_i &= E_{KG} + I_2R_f \\ &= 6.5 - j3.0 + 1\cdot10^{-3}(25{,}000) \\ &= 31.5 - j3.0 = 31.8\underline{/-5.46^\circ}\end{aligned}$$

These values have been plotted approximately to scale on the vector diagram of Fig. 3-31. The vector gain is

$$A_f = V_o/-E_i = -100\underline{/0^\circ}/31.5\underline{/-5.46} = -3.17\underline{/5.46^\circ}$$

Without feedback,

$$A = V_o/-E_{KG} = -100\underline{/0^\circ}/7.15\underline{/-24.8} = -14\underline{/24.8}$$

(*b*) Using the relation

$$A_f = A/(1 - A\beta), \qquad \beta = I_2R_f/I_2R_0 = \tfrac{1}{4}$$

$$A_f = \frac{-14\underline{/24.8}}{1 + 14\underline{/24.8}(0.25\underline{/0})}$$

$$= -\frac{14\underline{/24.8}}{1 + 3.18 + j1.47} = -\frac{14\underline{/24.8}}{4.42\underline{/19.3}}$$

$$= -3.17\underline{/5.5^\circ}$$

The gain-frequency curve for the amplifier of Fig. 3-31 is flat within 1.57 per cent from 50 to 100,000 cps, with phase-shift angles varying

from +8.7 to −8.5°. Without feedback, however, the gain-frequency curve is flat only in the range 400 to 13,800 cps. The phase-shift angle for the amplifier without feedback is (+36.4°) at 50 cycles and (−36°) at 100,000 cycles.

3-14. Inverse Feedback and Uniformity of Amplifier Operation

It has already been mentioned in relation to Eq. 3-72 that, for $|\beta A|$ large and $1/|\beta A| \ll 1$, the amplifier gain becomes dependent only on the feedback circuit. For this condition it may then be concluded that the amplifier behavior will not change because of small changes in tube characteristics, or in power-supply voltages. This is one of the most important advantages of inverse feedback because it provides assurance that the behavior of the amplifier will remain uniform over long periods of time. For vacuum-tube voltmeter circuits employing inverse-feedback amplifiers, it has meant the possibility of maintaining accurate instrument calibration unaffected by tube changes or replacements.

Even though βA is not large enough so that $A_f \cong -1/\beta$, large changes in A result only in small changes in A_f. For example, a change ΔA in A produces a change ΔA_f in A_f. Application of differential calculus to Eq. 3-72 shows that the fractional change in A_f is

$$\frac{dA_f}{A_f} = \frac{dA/A}{(1 - A\beta)} \tag{3-73}$$

If A changes by 10 per cent as a result of change in tube characteristics, voltage variations, and so on, then $dA/A = 0.1$. For the circuit of Fig. 3-31 in the mid-frequency range, $|A| = -15.4$, $\beta = \frac{1}{4}$, $1 - A\beta = 1 + 3.85 = 4.85$. Then,

$$dA_f/A_f = 0.01/4.85 = 0.0206$$

or 2.06 per cent change in gain resulting from a change of 10 per cent in the gain of the amplifier itself.

3-15. Inverse Feedback and Stability

As already mentioned in the discussion of Eq. 3-66, feedback is degenerative or inverse if $A\beta < 0$, regenerative if $A\beta > 0$. In the latter case the gain with feedback is increased with respect to the gain without feedback, so that there may be a tendency for the amplifier to become unstable. It is important to examine the complex quantity $(1 - A\beta)$ throughout the frequency range of the amplifier to see if there are any frequencies for which $(1 - A\beta)$ has a numerical value less than unity, for in such a frequency range the feedback would be

regenerative and the amplifier might behave as an oscillator. Since the complex gain A and corresponding angle θ_L or θ_H are available from universal amplification curves or from gain equations of the type given in Sections 3-5 and 3-7 for R–C- and transformer-coupled amplifiers, it is an easy matter to plot $A\beta$ in polar form for either of these amplifiers if β is independent of frequency. The resultant graph will then show immediately the range of frequencies, if any, for which the feedback is regenerative. For example, referring to the R–C-coupled amplifier of Fig. 3-31, $\beta = \frac{1}{4}$. In the mid-frequency range, $A_I = -15.4\underline{/0°}$. The values of $\left|\frac{A_L}{A_I}\right|$ and $\left|\frac{A_H}{A_I}\right|$, and the corresponding phase-shift angles are given in tabular form in Section 3-5, and graphically in Fig. 3-12. From the tabulation on page 91 and the computation of $f_L = 36.8$ and $f_H = 138{,}000$ for this amplifier (see page 91), the following values of $A\beta$ are computed:

f	$A\beta$
3.68	$0.383\underline{/180 + 84.3}$
7.36	$0.755\underline{/180 + 78.7}$
18.4	$1.72\ \underline{/180 + 53.4}$
36.8	$2.72\ \underline{/180 + 45}$
73.6	$3.44\ \underline{/180 + 26.6}$
184	$3.77\ \underline{/180 + 11.3}$
368	$3.83\ \underline{/180 + 5.8}$
Mid-frequency range	$3.85\ \underline{/180°}$
13,800	$3.83\ \underline{/180 - 5.8}$
27,600	$3.77\ \underline{/180 - 11.3}$
69,000	$3.44\ \underline{/180 - 26.6}$
138,000	$2.72\ \underline{/180 - 45}$
276,000	$1.72\ \underline{/180 - 63.4}$
690,000	$0.755\underline{/180 - 78.7}$
1,380,000	$0.383\underline{/180 - 84.3}$

The computed values of $A\beta$ are plotted, using polar-coordinate paper, on Fig. 3-33; the resulting curve is a circle. The vector $1\underline{/0}$ is drawn so that the vector difference $(1 - A\beta)$ may be shown graphically. A circle of unit radius is drawn around the point $(1 + j0)$. Since the vector $(1 - A\beta)$ is drawn from any point on the locus of the vector $A\beta$ to the end of the unit vector $1\underline{/0°}$, the numercial value of $(1 - A\beta)$ can never be less than unity unless the polar plot of $A\beta$ crosses inside the circle of unit radius with center at $(1 + j0)$. From Fig. 3-33 it may then be concluded

that the feedback amplifier of Fig. 3-31 has degenerative feedback at all frequencies and does not oscillate.

If a fraction β of the output voltage of a single-stage transformer-coupled amplifier is fed back into the input, the polar plot of the amplifier

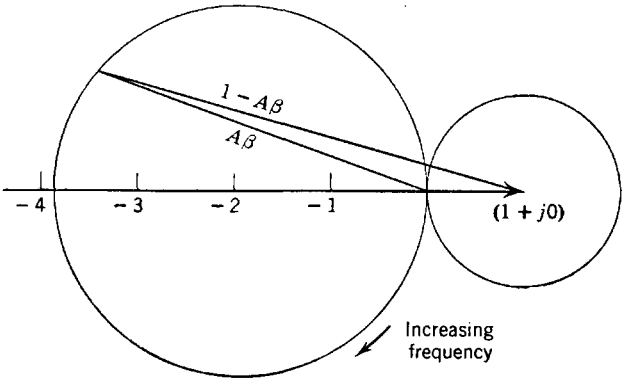

FIG. 3-33. Polar plot of $A\beta$ for an R–C amplifier.

may be obtained from the gain equations or from the gain-frequency curves of Section 3-7 (Fig. 3-17). Such a polar plot for a transformer-coupled stage has been drawn in Fig. 3-34, for $Q_0 = 1.25$. At low frequencies, the gain approaches zero and the phase-shift angle approaches $-90°$. As the frequency increases, the phase-shift angle becomes less and the gain greater, approaching zero phase-shift angle and uniform gain in the mid-frequency range. In the high-frequency range the phase shift and gain both increase because of resonance effects, and at still higher frequencies but with small gain the curve of $A\beta$ crosses over into the unit circle, so that for values of $A\beta$ within the unit circle the feedback is regenerative. If the curve of $A\beta$ passes around the point (1 + j0), the circuit is unstable and the amplifier becomes an oscillator. Nyquist [10] has developed a general criterion of

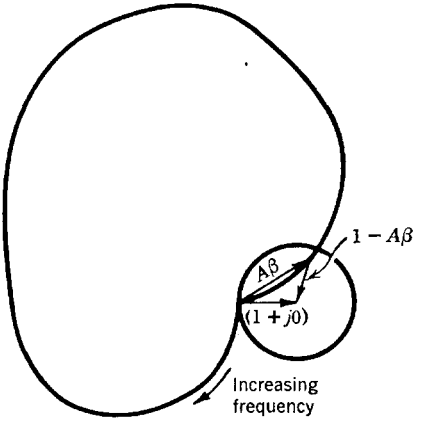

FIG. 3-34. Polar plot of $A\beta$ for a transformer-coupled amplifier.

[10] H. Nyquist, Regeneration Theory, *BSTJ*, **11**, 126–147 (1932).

feedback amplifier stability which may be stated as follows: If the polar plot of $A\beta$ includes the point $(1 + j0)$, the amplifier will oscillate, otherwise not. In order not to include the point $(1 + j0)$, the numerical value of $A\beta$ must be very much reduced where the phase shift is large so that $|A\beta| < 1$. Bode [11] has shown that for amplifier stability the gain must be controlled, i.e., reduced beyond danger of oscillation, over a frequency range many times greater than the useful range.

3-16. Output Impedance and Inverse Feedback

It was mentioned in Section 3-13 that the effective terminal impedance at the output terminals of an amplifier may be controlled by the use of inverse feedback. In this connection, it is important to note that there are two distinct types of inverse feedback and that the two examples of inverse-feedback circuits thus far discussed are examples of the two kinds of feedback. In the first example given, the circuit of Fig. 3-29, the voltage fed back is proportional to the current flowing in the plate circuit of the amplifier. If the load impedance R_L (or, more generally, Z_L) increases, the plate current I_p decreases, and the feedback voltage I_pR_K decreases, but this means that the gain of the amplifier increases which will tend to increase I_p and so will tend to maintain I_p constant. This is known as current feedback, and has the effect of causing the amplifier to approach the behavior of a constant-current source if the input voltage E_i remains constant. As shown in Eq. 3-62, the effective plate resistance or internal impedance of the amplifier is increased by current feedback, and this is generally true. If the load resistance R_L of Fig. 3-29 is replaced by a generator of voltage E, and the input voltage source E_i is replaced by a short circuit, solution of the equivalent circuit for the impedance Z_o, looking back into the amplifier at the terminals of the generator E shows that $Z_o = r_p + R_K(1 + \mu)$, which may be described as the output terminal impedance of the amplifier with the input short-circuited.

In Fig. 3-31 the feedback voltage depends upon the output voltage and is a fraction of it. If the load impedance is assumed to be an impedance Z_L in parallel with R_0, then the output voltage and also the feedback voltage would tend to increase or decrease with Z_L, but an increasing feedback voltage results in decreased gain, so that the effect of this type of feedback is to maintain the output voltage constant. This is known as voltage feedback, and amplifiers so equipped approach the behavior of a constant-voltage source for constant input voltage.

[11] H. W. Bode, Relations between Attenuation and Phase in Feedback-Amplifier Design, *BSTJ*, **19**, 421–454 (1940).

The resistance R_0 of Fig. 3-31 and Fig. 3-32 may be thought of as the feedback network. As such, it is merely a potentiometer connected across the load impedance, Z_L (Z_L is not shown in Fig. 3-31 or Fig. 3-32). If a generator of voltage E is connected across R_0 in the equivalent circuit (Fig. 3-32), the effective terminal impedance Z_o may be found by solving for the current I_1 which would be supplied by the generator E. The circuit has been redrawn in Fig. 3-35. For convenience, the reactance of the coupling capacitor has been neglected, and the input voltage source has been replaced by a short circuit. The impedance

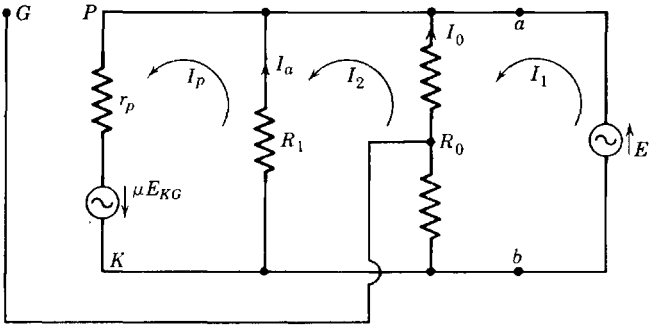

FIG. 3-35. Equivalent circuit of a voltage-feedback amplifier in which a generator E replaces the load.

$Z_o = E/I_1$. In the intermediate-frequency range and without feedback (grid connected directly to K) the impedance Z_o' as seen at the terminals a–b is given by

$$Z_o' = \frac{1}{1/R_o + 1/R_1 + 1/r_p}$$

With feedback, solution for I_1 gives

$$Z_o = \frac{E}{I_1} = \frac{1}{\beta g_m + 1/Z_o'} = \frac{Z_o'}{1 + \beta g_m Z_o'} \tag{3-74}$$

From Eq. 3-10, $A = -g_m Z_o'$, so that

$$Z_o = Z_o'/(1 - \beta A) \tag{3-75}$$

where $\beta = R_f/R_0$. It has been shown [12] that the relation of Eq. 3-75 is generally true for voltage feedback. The effective terminal impedance of the amplifier is therefore reduced by inverse voltage feedback. By

[12] H. F. Mayer, Control of the Effective Internal Impedance of Amplifiers by Means of Feedback, *Proc. IRE*, **27**, 213–217 (1939).

using combinations of current and voltage feedback, the amplifier may be made to present almost any desired impedance to the load.[12]

3-17. Other Inverse-Feedback Circuits

Only two feedback circuits have thus far been discussed. These circuits are quite basic and illustrate the general principles and properties of inverse current and voltage feedback. However, because many of the beneficial results derived from the use of inverse feedback increase with the gain A, it is desirable to increase A rather than β, and to use not only high-gain stages but several stages of amplification. Triodes have

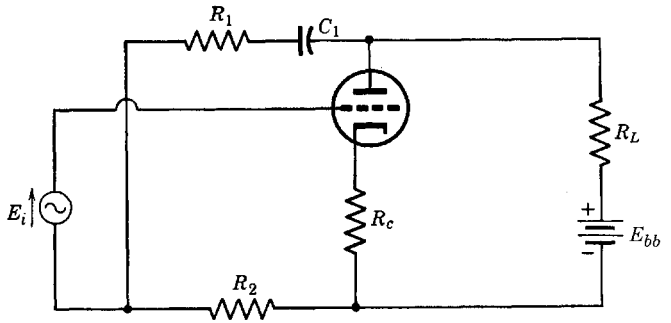

FIG. 3-36. Inverse-feedback amplifier.

been used in the feedback circuits already discussed, but tetrodes and pentodes are preferable because high intrinsic gain is desirable. The same principles apply to triodes, tetrodes, or pentodes. Many practical circuits have been described in the literature.[13,14] A few other examples of typical one- and two-stage circuits will be given here.

A single-stage circuit is shown in Fig. 3-36 in which both inverse current and voltage feedback are employed. Resistances R_1 and R_2, and R_c constitute the feedback network. Condenser C_1 is a blocking condenser and should have negligible reactance in the frequency range of the amplifier.

A feedback arrangement for the push–pull connection is shown in Fig. 3-37, and the inverse voltage-feedback network is seen to be identical with that of Fig. 3-36. No current feedback is utilized because of the fact that the fundamental and odd harmonics are not present in that part of the circuit for the push–pull connection, as shown in Section 3-9. The blocking condenser C_1 may be omitted if the connection

[13] F. E. Terman, Feedback Amplifier Design, *Electronics*, **10**, 13 (Jan. 1937).

[14] J. R. Day and J. B. Russell, Practical Feedback Amplifiers, *Electronics*, **10**, 16 (Apr. 1937).

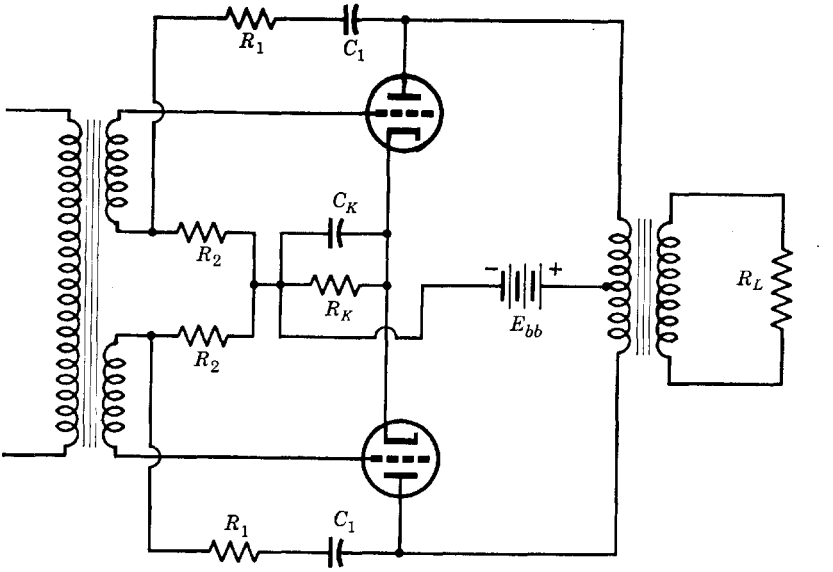

FIG. 3-37. Voltage inverse feedback for a push–pull amplifier stage.

through R_1 is made to the load side of the output transformer. As a result of the output voltage stabilizing property of inverse voltage feedback, the tendency of the gain to fall off at low frequencies because of low transformer primary reactance is partially counteracted.

A two-stage feedback-amplifier arrangement is shown in Fig. 3-38. The first stage is R–C-coupled to the second stage; R_d is a dropping resistor to provide the proper screen grid voltage for the pentode. The

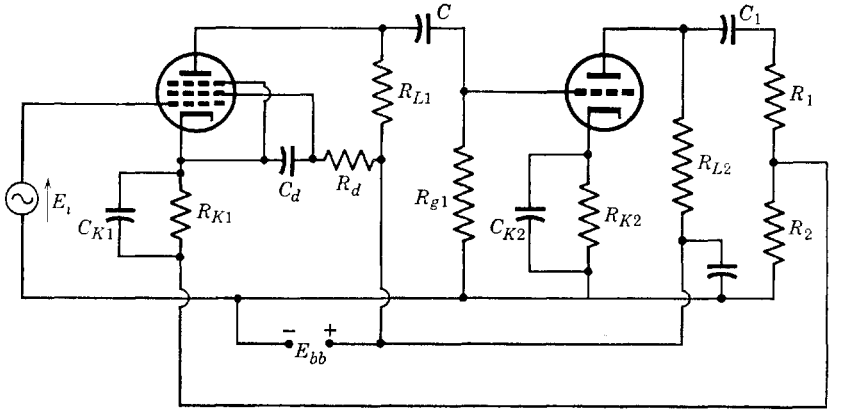

FIG. 3-38. Two-stage inverse voltage feedback.

biasing resistors R_{K1} and R_{K2} are well by-passed. The load impedance is R_{L2}, and C_1 is, as in Fig. 3-36, a blocking condenser. Resistors R_1 and R_2 have the same voltage-dividing function as in the circuit of Fig. 3-36. Differences in the feedback connections of Figs. 3-38 and 3-31 should be examined and explained. Feedback from the second to the first stage of transformer-coupled amplifiers is derived according to principles identical with those illustrated in Fig. 3-31.

It has been shown that the phase-shift angles of individual R–C-coupled amplifier stages approach 90° at low or at high frequencies. For three-stage amplifiers, the over-all phase-shift angle may then approach 270° at the frequency extremes. This means that the polar plot of $A\beta$ will cross into the unit circle, so that, to avoid oscillation, the gain-phase characteristic must be carefully adjusted at the high and low frequencies if oscillation is to be avoided. For transformer-coupled stages, the phase shift at high frequencies may approach 180° for a single stage (see Fig. 3-17), so that great care must be exercised in the design of multistage transformer-coupled amplifiers.

3-18. The Cathode Follower Stage

The amplifier circuit of Fig. 3-39 will be recognized as a feedback amplifier in which the feedback and the output voltages are identical.

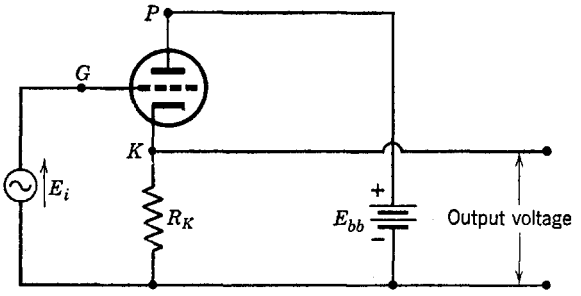

FIG. 3-39. A cathode follower or grounded plate amplifier.

This circuit has found many inportant applications which depend upon the utilization of one or more of the following list of properties:

1. Gain A_f, approximately equal but always less than unity.
2. Higher effective input impedance than that of an ordinary amplifier stage.
3. Low-output terminal impedance which may be made a pure resistance, over a large frequency range, of value less than 200 ohms.

Analysis of the equivalent circuit of the cathode follower is straightforward and has been left to the problems. The equivalent a-c circuit

including the interelectrode capacitances has been drawn in Fig. 3-40. Points 1 and P are at the same a-c potential (grounded plate), and, as a result, the input signal voltage applied between terminals G and 1 is shunted by the grid-plate capacitance. The input and output voltage drops may both conveniently be referred to the ground terminal, 1. The voltage gain then may be expressed as (see Figs. 3-39 and 3-40)

$$A_f = V_{1K}/V_{1G} = -I_6R_K/-E_i \tag{3-76}$$

It should be noted that the output voltage of the cathode follower

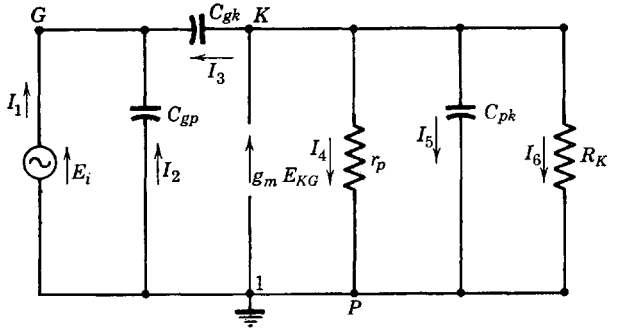

FIG. 3-40. Equivalent a-c circuit of the cathode follower of Fig. 3-39.

amplifier is in phase with the signal voltage. Analysis of the circuit of Fig. 3-40 shows that the voltage gain of Eq. 3-76 is given by

$$A_f = \frac{g_m + j\omega C_{gk}}{g_m + 1/r_p + 1/R_K + j\omega(C_{pk} + C_{gk})} \tag{3-77}$$

which, at low enough frequency, reduces to

$$A_f = \frac{\mu R_K}{r_p + (\mu + 1)R_K} \tag{3-78}$$

Examination of Eq. 3-78 shows that A_f is less than unity. For example, with $\mu = 20$, $r_p = 10{,}000$ ohms, $R_K = 8000$ ohms, $A_f = 20(8000)/178{,}000 = 160{,}000/178{,}000 = 0.9$.

The input admittance of the cathode follower may be derived from Fig. 3-40 by determining the ratio of I_1 to E_i. The result is

$$Y_{11} = I_1/E_i = j\omega[C_{gp} + (1 - A_f)C_{gk}] \tag{3-79}$$

in which it should be noticed that, with A_f positive and real, the input

admittance is a capacitance of value slightly greater than C_{gp}. For $A_f = 0.9$, as in the example already used,

$$Y_{11} = j\omega(C_{gp} + 0.1C_{gk})$$

The input impedance, $1/Y_{11}$, is evidently much higher than for an ordinary triode amplifier stage.

The effective output admittance with input short-circuited may be found, also, from analysis of Fig. 3-40. The method of approach is to connect an alternating voltage source at the output terminals 1–K, at the same time replacing the voltage source, E_i at G–1 by a short circuit. If the applied voltage source is E, and the current delivered at terminals 1–K is I, then the output admittance with input short-circuited is

$$Y_o = I/E = (\mu + 1)/r_p + 1/R_K + j\omega(C_{gk} + C_{pk}) \qquad (3\text{-}80)$$

In the frequency range where C_{gk} and C_{pk} may be neglected,

$$Z_o = \frac{1}{Y_o} = \frac{r_p}{(\mu + 1) + r_p/R_K} \qquad (3\text{-}81)$$

If R_K is made very much greater than r_p, and if $\mu \gg 1$,

$$Z_o \cong r_p/\mu = 1/g_m \qquad (3\text{-}82)$$

The effective output impedance with input short is therefore very small and may be in the range 200 to 1000 ohms.

These properties of the cathode follower have given it a number of interesting applications. It is frequently used as the first stage of a multistage amplifier where high input impedance is essential over a wide frequency range and where the first stage must handle a wide range in values of input voltage and not be overloaded. Such an application is the amplifier for the vertical plates of a cathode-ray oscillograph. The cathode follower is used also to reduce frequency and phase distortions by placing it between two high-gain amplifier stages. Still another application is that of impedance matching where it may be used instead of a transformer to match a high-impedance circuit to a much lower one.

3-19. Broad-Band Amplifiers

Television circuits employ many rectangular wave forms. The adequate amplification of these wave forms requires an extremely wide bandwidth characteristic. For example, the frame-scanning rate is 30 complete scans per second, and the amplifier used with the circuit must have a flat gain-frequency curve down to 30 cps, and, for adequate resolution (satisfactory images), the gain-frequency curve must remain

flat up to 3 or 4 Mc per sec. A similar requirement is necessary for cathode-ray tube amplifiers. This requirement may be met by the proper design of amplifier tubes and by circuit artifices which involve compensating for those circuit elements whose characteristics allow the gain to decrease at low or at high frequencies. The compensation is applied to the R–C-coupled circuit.

It was shown in Section 3-5 that the gain of an R–C-coupled amplifier stage in the high-frequency region of the gain-frequency curve is given by

$$A_H = -g_m R_{eq}/(1 + j\omega C_0 R_{eq}) \tag{3-83}$$

The frequency f_H is that frequency for which the reactance of the shunting capacitance C_0 is equal to the equivalent resistance R_{eq}, or for which $\omega C_0 R_{eq} = 1$. Therefore

$$f_H = 1/2\pi C_0 R_{eq} \tag{3-84}$$

and the product of mid-frequency gain magnitude and f_H is

$$g_m R_{eq} f_H = g_m/2\pi C_0 \tag{3-85}$$

The capacitance C_0 is determined by the output capacitance of the amplifier stage and by the input capacitance of the following stage. Thus the product in Eq. 3-85 is determined by properties of both the

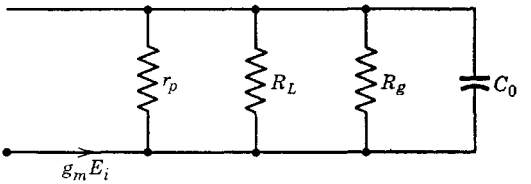

FIG. 3-41. High-frequency equivalent circuit of one stage of an R–C-coupled amplifier.

tube and the circuit used for the video or wide-band amplifier. For a high mid-frequency gain, with a given g_m, R_{eq} must be high. However, a large value of R_{eq} results in a low value of f_H, according to Eq. 3-84. As a compromise, small values of R_{eq} are used for video amplifiers, and special tubes of very large g_m are designed in order to increase the product $g_m R_{eq}$. Pentodes are always used for wide-band amplifiers. The familiar equivalent circuit of an R–C-coupled amplifier stage at high frequencies is shown in Fig. 3-41. In order to obtain the low value of R_{eq} needed for large f_H, R_L is made very small, and is generally of the order of 3000 ohms. For pentodes with r_p about 1 megohm, and R_g 500,000 ohms, as used in R–C-coupled wide-band circuits, $R_{eq} \cong R_L$.

3-20. High-Frequency Compensation

A widely used and very effective method of circuit compensation for broad-band R–C-coupled amplifiers involves the addition of an inductance in series with R_L. At low or mid-frequencies, the reactance of the inductance L is negligible, but, in the high-frequency region, its reactance, combined in parallel with that of C_0, results in increasing the circuit impedance, compensating for the tendency of the capacitive reactance to reduce the circuit impedance. The circuit is very simple, if $R_{eq} \cong R_L$ and is shown in Fig. 3-42. A discussion of the effect of inductance L upon the amplifier gain is simplified by a choice of parameters involving frequency ratios. As it is desirable to increase the actual half-power frequency f_H perhaps by some multiple of the uncompensated value, one parameter will be the uncompensated half-power or 3 db down frequency. Let this frequency be f_2. Its value is given by f_H in Eq. 3-84. Therefore,

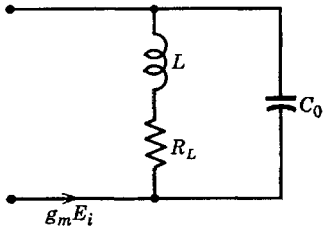

FIG. 3-42. Shunt compensation of an R–C-stage, wide-band amplifier.

$$2\pi f_2 = \omega_2 = 1/R_L C_0 \tag{3-86}$$

Now the angular frequency at which L and C_0 would be antiresonant, if connected separately and in parallel, is

$$\omega_0 = 1/\sqrt{LC_0} \tag{3-87}$$

The ratio of ω_0 to ω_2 is

$$\frac{\omega_0}{\omega_2} = \frac{1/\sqrt{LC_0}}{1/R_L C_0} = \frac{R_L}{\sqrt{L/C_0}} \tag{3-88}$$

Since, at angular frequency ω_0 the effective Q of R_L and L in series is

$$Q_0 = \frac{\omega_0 L}{R_L} = \frac{L}{R_L}\frac{1}{\sqrt{LC_0}} = \frac{\sqrt{L/C_0}}{R_L} \tag{3-89}$$

then

$$\omega_0/\omega_2 = 1/Q_0 \tag{3-90}$$

The quantity Q_0 may be used as the second parameter, or a different Q defined as

$$Q = \frac{\omega_2 L}{R_L} = \frac{\omega_0 L}{R_L} Q_0 = {Q_0}^2 \tag{3-90a}$$

may be used. Since the two Q's are related as indicated, either may be chosen. The final equations are given using Q_0. The quantity Q (or Q_0) is the second parameter, and the third is R_L. The circuit reactances then may be expressed in terms of ω_2, Q_0, and R_L as follows:

$$\omega L = \frac{\omega}{\omega_2}\omega_2 L = \frac{f}{f_2} R_L Q = \frac{f}{f_2} R_L Q_0^2 \tag{3-91}$$

Also,
$$\frac{1}{\omega C_0} = \frac{\omega_2}{\omega}\left(\frac{1}{\omega_2 C_0}\right) = \frac{f_2}{f} R_L \tag{3-92}$$

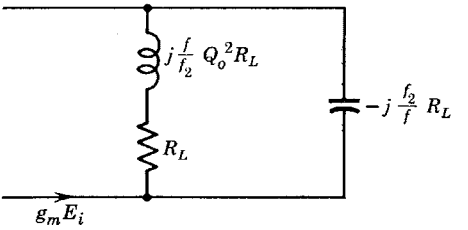

FIG. 3-43. Circuit of Fig. 3-42 with elements specified in terms of design parameters R_L, f_2, and Q_0.

The circuit with elements designated in terms of f_2, Q_0, and R_L is shown in Fig. 3-43. The gain is

$$A_H = -g_m Z_{eq} = -g_m \frac{R_L^2\left(1 + j\frac{f}{f_2}Q_0^2\right)\left(-j\frac{f_2}{f}\right)}{R_L\left[1 + j\left(\frac{f}{f_2}Q_0^2 - \frac{f_2}{f}\right)\right]} \tag{3-93}$$

The normalized gain is the gain per unit mid-frequency gain. This becomes

$$\frac{A_H}{(-g_m R_L)} = \frac{(-jf_2/f)(1 + jQ_0^2 f/f_2)}{(-jf_2/f)(1 - Q_0^2 f^2/f_2^2 + jf/f_2)}$$

or, finally,
$$\frac{A_H}{(-g_m R_L)} = \frac{1 + jQ_0^2 f/f_2}{1 - Q_0^2 f^2/f_2^2 + jf/f_2} \tag{3-94}$$

The magnitude of the ratio in Eq. 3-94 is

$$\frac{|A_H|}{g_m R_L} = \frac{\sqrt{1 + Q_0^4 (f/f_2)^2}}{\sqrt{(1 - Q_0^2 f^2/f_2^2)^2 + (f/f_2)^2}} \tag{3-95}$$

the ratio is a vector quantity of magnitude given by Eq. 3-95 and angle of phase lag

$$-\theta = \tan^{-1} Q_0^2 \frac{f}{f_2} - \tan^{-1} \frac{f/f_2}{1 - Q_0^2 f^2/f_2^2} \tag{3-96}$$

Curves of the magnitude $\left| \frac{A_H}{g_m R_L} \right|$ are sketched roughly in Fig. 3-44 for various values of the parameter Q_0.

It is evident that a considerable extension of the flat portion of the gain-frequency curve can be achieved by choosing values of inductance

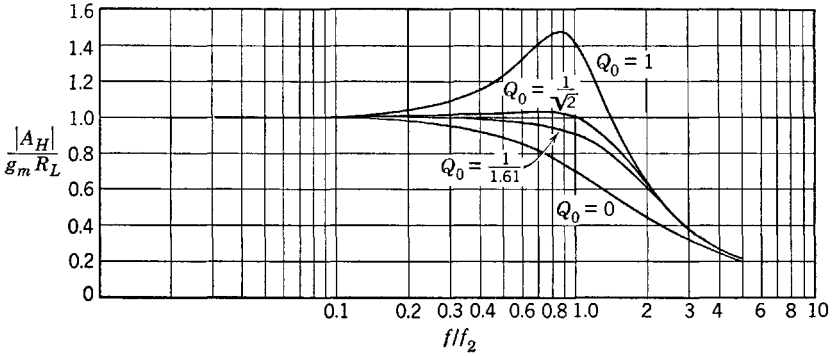

FIG. 3-44. Universal gain curves for a shunt-compensated amplifier.

and of R_L for which $Q_0 = 0.707$. The values of R_L and of L required may be obtained from Eqs. 3-86 and 3-90*a*. From Eq. 3-86,

$$R_L = 1/\omega_2 C_0 \tag{3-97}$$

and, from Eq. 3-90*a*, $$\omega_2 L = Q_0^2 R_L \tag{3-98}$$

Therefore, for $Q_0 = 1/\sqrt{2}$, $$L = R_L/2\omega_2 \tag{3-99}$$

where it is to be remembered that ω_2 is the uncompensated half-power angular frequency. The value of ω_2 may be chosen arbitrarily. If then it is required that the gain remain virtually flat up to $\omega = \omega_2$, the necessary value of R_L may be computed from Eq. 3-97 and the required inductance from Eq. 3-99.

In addition to the requirement of a flat gain-frequency curve, the wide-band amplifier must, particularly if used for television service, be free from phase distortion. This requirement may be met if the amplifier circuit is so designed that the phase shift is directly proportional to frequency. The last statement is more easily understood if stated in terms of time delay of circuit response than in terms of frequency.

Perhaps the best example is a long telephone line. If the signal input at the sending end contains many harmonic frequencies as for example in the transmission of music, the signal output at the receiving end should have the same wave shape as the input signal. However, it is known that the velocity of travel of waves on a transmission line depends upon the wave frequency and in fact is proportional to frequency. Therefore, it may be expected that the higher frequencies in the signal, traveling faster on the line than the lower frequencies, arrive sooner. The lower signal frequencies are longer delayed by the line. Therefore, the line will introduce phase shifts, and the output wave form will not be identical with the input wave form. Suppose, however, that the phase shift per mile of line is β rad. The number of miles of line required to shift the phase by 2π rad is defined as the wavelength λ of the traveling wave. Thus $\lambda = 2\pi/\beta$, and, since the velocity is given by $v = f\lambda$, then

$$v = 2\pi f/\beta = \omega/\beta$$

Now, however, if the line can be so designed that the phase shift per mile β is proportional to frequency, say, $\beta = k\omega$, then the velocity

$$v = 1/k$$

is independent of frequency, and the wave form is preserved. A line for which the phase shift is proportional to frequency is then referred to as a distortionless line.

From the point of view of time delays suppose that the time delay, or signal transit time along the line, is 1/1000 sec for all frequencies from 50 to 10,000 cps. Table 3-3 in which the time delay is expressed as a

TABLE 3-3

Frequency, f, cps	Fractional Time Delay, t_d/T	Phase Shift, $\theta = \omega t_d = (2\pi/T)t_d$	$\theta/f = k$
50	$0.001/0.02 = \frac{1}{20}$	$2\pi/20 = 18°$	$\frac{18}{50} = 0.36$
100	$\frac{1}{10}$	36°	0.36
1,000	1	360°	0.36
10,000	10	3600°	0.36

fraction of the period T will show that the phase shift of the line is then proportional to frequency.

Now a measurable time delay in the response of any circuit occurs if the circuit contains reactances. An amplifier, as a four-terminal network, then introduces a phase shift which is proportional to its time delay for a given frequency. A wide-band amplifier, therefore, like a

long line, must have, in addition to a flat gain-frequency curve, a time delay independent of frequency or a phase shift proportional to frequency in order to reproduce the input wave shape at the output terminals. This consideration is of prime importance for television or video applications.

In order to show the effect of choice of parameter Q_0 on the time delay and hence on the phase distortion introduced by a wide-band

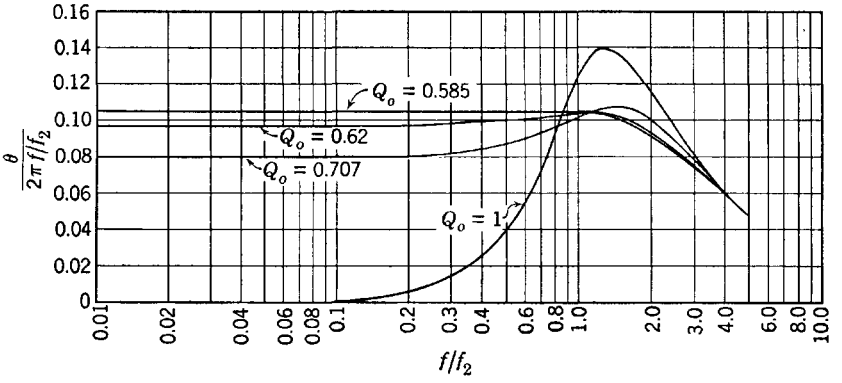

FIG. 3-45. Universal phase-shift curves for a shunt-compensated amplifier.

compensated amplifier, one may plot θ/ω as a function of f/f_2. If all frequencies have the same time delay, then θ/ω is constant. Now Eq. 3-95 may be written as follows:

$$A_H = A_I \angle 180° \frac{\sqrt{1 + Q_0^4(f/f_2)^2}\angle\theta_1}{\sqrt{(1 - Q_0^2 f^2/f_2^2)^2 + (f/f_2)^2}\angle\theta_2}$$

Evidently, the phase shift at high frequencies is $[180° - (\theta_2 - \theta_1)] = 180° - \theta$, where the shift of 180° is produced by the tube and the shift of $\theta = \theta_2 - \theta_1$, by the circuit. Values of θ may be computed for arbitrarily assigned values of f/f_2 from Eq. 3-96. In Fig. 3-45 the quantity $\left[\frac{\theta}{2\pi(f/f_2)}\right]$ is plotted as ordinate on semilog paper with (f/f_2) as abscissa. Only four values of Q_0 have been chosen. The optimum value of $Q_0 = 0.585$ does not, unfortunately, coincide with the optimum value of $Q_0 = 0.707$ indicated by the curves of Fig. 3-44, for the gain-frequency requirement, so that a compromise must be made between these values. The value of L chosen for a single stage is not necessarily the optimum value where several stages are to be used. Another consideration which will not be discussed here is the transient response of the over-all ampli-

fier. For more complete design theory reference should be made to a very complete study by Bedford and Fredenhall.[15] Calculated values are given for a few points on the $Q_0 = 1$ curve (Fig. 3-45) in Table 3-4.

TABLE 3-4. VALUES FOR $Q = 1$ CURVE (FIG. 3-45)

f/f_2	$\theta = \theta_2 - \theta_1$, degrees	$\frac{\theta}{360(f/f_2)}$
0.2	0.47	0.00653
0.5	7.10	0.0394
0.8	27.10	0.094
1.0	45.00	0.125
1.4	70.00	0.139
1.8	79.3	0.122
2.0	82.9	0.115

3-21. Low-Frequency Compensation

In the low-frequency range of the video amplifier, the extension of the region of flatness of the gain-frequency curve toward lower frequencies may be accomplished by the use of the circuit of Fig. 3-46. The plate

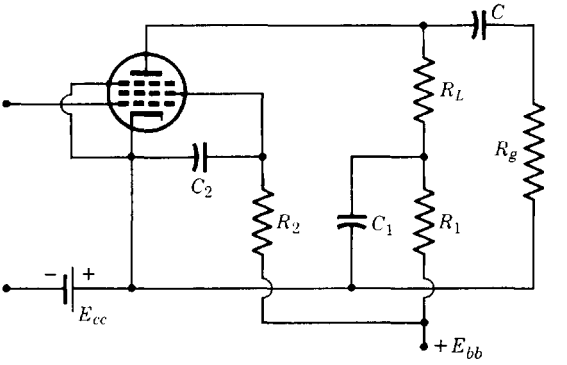

FIG. 3-46. Low-frequency compensation.

voltage is supplied through a high resistance R_1, necessitating a large power-supply voltage. The compensating capacitance C_1 is connected as shown. The high-frequency compensating inductance L in series with R_L has not been shown since its reactance is negligible in the low-frequency range. The screen-voltage dropping resistor R_2 and by-pass condenser C_2 also affect the low-frequency response, and, though they are shown in Fig. 3-46, their effects will be neglected in the following

[15] A. V. Bedford and G. L. Fredenhall, Transient Response of Video-frequency Amplifier, *Proc. IRE*, **27**, 277–284 (Apr. 1939).

analysis. The equivalent a-c circuit is shown in Fig. 3-47, in which the plate resistance of the pentode has been omitted.

In the circuit of Fig. 3-47, if R_g and C were interchanged, it might be reasoned that the impedance presented at terminals 1–2 is that of a bridge circuit. If so, and if the condition for bridge balance is met, then Z_{12}, although not independent of frequency, is a high impedance over a wide frequency range. The condition for bridge balance is

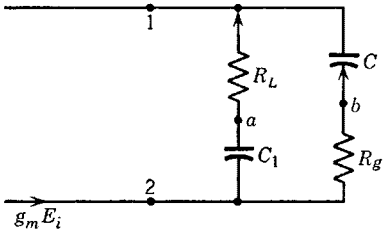

FIG. 3-47. Equivalent a-c circuit of Fig. 3-46.

$$\omega R_L C_1 = \omega R_g C$$

or

$$C_1 = R_g C / R_L \quad (3\text{-}100)$$

It is found that Eq. 3-100 provides a sufficiently accurate selection of the compensating capacitance C_1. It must be remembered, however, that resistance R_1 has been assumed infinite on Fig. 3-47. For practical purposes, compensation is found to be satisfactory if

$$R_1 \geqq 10(1/\omega C_1)$$

A more careful analysis of the circuit of Fig. 3-47 will now be presented very briefly.

The voltage gain of the low-frequency compensated circuit (Fig. 3-47) is given by

$$A_L = -g_m Z_1 R_g / (Z_1 + Z_g) \quad (3\text{-}101)$$

where $Z_1 = R_L - jX_{c1}, \qquad Z_g = R_g - jX_c$

Since $A_I \cong -g_m R_L R_g / (R_L + R_g)$, Eq. 3-101 may be written as

$$A_L = \frac{A_I(1 - jX_{c1}/R_L)}{1 - j(X_{c1} + X_c)/(R_g + R_L)} \quad (3\text{-}102)$$

From Eq. 3-102, $A_L = A_I$ if

$$X_{c1}/R_L = (X_{c1} + X_c)/(R_g + R_L) \quad (3\text{-}103)$$

$$C_1/C = (R_g/R_L) \quad (3\text{-}104)$$

or

$$A_L = \frac{|A_I| \angle 180° \sqrt{1 + (X_{c1}/R_L)^2} \angle -\theta_1}{\sqrt{1 + (X_{c1} + X_c)^2/(R_g + R_L)^2} \angle -\theta_2} \quad (3\text{-}105)$$

where $\theta_2 = \tan^{-1}[(X_{c1} + X_c)/(R_g + R_L)] \quad (3\text{-}106)$

and $\theta_1 = \tan^{-1}[X_{c1}/R_L] \quad (3\text{-}107)$

It is evident that the same condition 3-103 which ensures a flat gain-frequency curve in the low-frequency region provides the condition $\theta_2 = \theta_1$ required for zero phase shift.

3-22. Compensation for the Bias Impedance

If a bias resistance is used instead of the fixed bias of Fig. 3-46, both phase shift and gain attenuation will occur in the low-frequency range. In order to compensate for these effects, the resistance R_1 of Fig. 3-46 may be properly selected. The equivalent circuit (if screen impedance is neglected) is shown in Fig. 3-48. Again, the pentode plate resistance

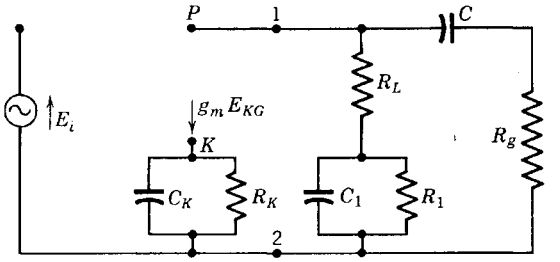

FIG. 3-48. Equivalent low-frequency circuit of a pentode wide-band compensated amplifier.

has been omitted from the constant-current generator circuit. Let $Y_K = (1/R_K) + j\omega C_K$ and $Y_1 = (1/R_1) + j\omega C_1$. The corresponding impedances are Z_K and Z_1. Then,

$$E_{KG} = E_i - g_m E_{KG} Z_K$$

whence

$$E_{KG} = E_i/(1 + g_m Z_K) \tag{3-108}$$

The voltage $V_{21} = g_m E_{KG} Z_{12}$, and the gain is

$$A_L = \left[\frac{V_{21}}{Z_g} R_g\right] \Big/ (-E_i) = -\frac{g_m R_g (Z_1 + R_L)}{(1 + g_m Z_K)(Z_g + Z_1 + R_L)} \tag{3-109}$$

where $Z_g = R_g - jX_c$. The quantity $Z_g + Z_1 + R_L$ or $R_g - jX_c + Z_1 + R_L$ differs very little from R_g. For example, if $C = 0.1$ μf, $R_g = 1$ megohm, $\omega = 500$, $R_L = 3000$, then $X_c = 20{,}000$ ohms and $C_1 \cong 0.01(10^6)/3000 = \frac{10}{3}$ μf and $X_{c1} = 600$ ohms. If R_1 be chosen as $10X_{c1}$ as recommended in Section 3-21, then $Z_1 \cong -j600$ ohms and $R_g - jX_c + Z_1 + R_L$ becomes $1{,}003{,}000 - j20{,}600$ ohms. Therefore, Eq. 3-109 may justifiably be written as

$$A_L \cong -\frac{g_m R_L R_g (1 + Z_1/R_L)}{(1 + g_m Z_K) R_g} = \frac{A_I (1 + Z_1/R_L)}{1 + g_m Z_K} \tag{3-110}$$

The magnitude of the ratio A_L/A_I becomes unity if

$$Z_1/R_L = g_m Z_K \tag{3-111}$$

or if

$$R_L Y_1 = Y_K/g_m \tag{3-112}$$

This requires that

$$R_L\left(\frac{1}{R_1} + j\omega C_1\right) = \frac{1}{g_m}\left(\frac{1}{R_K} + j\omega C_K\right)$$

whence

$$R_L/R_1 = 1/g_m R_K$$

and

$$R_L C_1 = C_K/g_m$$

Therefore, gain compensation for the bias impedance is achieved if

$$R_1 = g_m R_L R_K \tag{3-113}$$

and if

$$C_K = g_m R_L C_1 \tag{3-114}$$

For a type 6AC7, $g_m = 9000$ micromhos and $R_K \cong 160$ ohms. Thus, for the values already used as examples,

$$R_1 = 9000 \cdot 10^{-6}(3000) \cdot 160 = 27(160) = 4320 \text{ ohms}$$

(which is somewhat less than $10X_{c1}$), and

$$C_K = 27C_1 = 90\ \mu\text{f}$$

It appears from the foregoing discussion that it may not be possible to obtain perfect low-frequency compensation for both bias impedance and coupling capacitor in the same stage of amplification. It has been recommended [16] that phase shift and gain compensation be properly proportioned in fixed-bias stages in order to correct for imperfect compensation, including the effects of screen impedance, in self-biased stages. The general problem of video amplifier design is only briefly treated here, and careful reference to the literature is advised before the design of a complete wide-band amplifier is undertaken.

PROBLEMS

3-1. If T_1 in Fig. 3-6 is a 6J5 and T_2 is a 2A3, determine the resistors so that the tubes will have the following operating points:

6J5: $E_b = 200$ volts, $E_c = -6$ volts;
2A3: $E_b = 250$ volts, $E_c = -40$ volts.

Use $R_1 = 20{,}000$ ohms, $R_2 = 500$ ohms, and $R_5 = 1000$ ohms. Find the bleeder current I and the required power-supply voltage.

[16] Terman, *Handbook of Radio Engineering*, p. 417, McGraw-Hill Book Co.

3-2. Draw the equivalent a-c circuit of the two-stage amplifier of problem 3-1, assuming that R_c, R_3, R_4, and R_5 are all adequately by-passed by large-size condensers. Calculate the over-all voltage gain. If the signal voltage $E_g = 0.1$ volt, compute the effective value of the load current (a-c) in R_2. Draw a complete vector diagram for the circuit, and determine the phase relation between input voltage drop $(-E_g)$ and the output voltage drop in R_2.

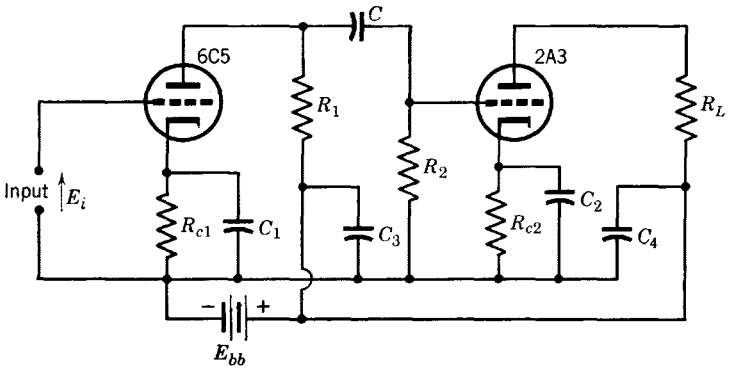

FIG. P3-3.

3-3. Given $R_1 = 50{,}000$ ohms
$R_2 = 250{,}000$ ohms
$C = 0.2$ μf
$E_{bb} = 400$ volts
$C_1 = C_2 = 10$ μf
$R_L = 2500$ ohms
$C_3 = C_4 = 1$ μf

(*a*) Determine R_{c1} and also R_{c2} so that the 6C5 will be biased at −8 volts, and the 2A3 at −43.5 volts.

(*b*) Determine the frequencies at which the gain of the first stage will fall to 70.7 per cent of the intermediate-frequency gain.

(*c*) If the amplitude distortion of the first stage is neglected, what is the maximum input voltage E_i for a second-harmonic distortion of 5 per cent in the second stage? (A cut-and-try method is required here.)

3-4. A 6K7 pentode operating at $E_b = 250$ volts, $E_{c1} = -3$ volts, $E_{c2} = 100$ volts, is *R–C*-coupled to a 6F6 power pentode (Fig. 2-8) operating at $E_b = 250$ volts, $E_{c1} = -16.5$ volts, $E_{c2} = 250$ volts. The coupling resistors are $R_1 = 50{,}000$ ohms, $R_2 = 250{,}000$ ohms, and $C = 0.2$ μf. The 6F6 is transformer coupled to a 2000-ohm load. The output transformer has negligible leakage reactance and d-c resistance, and a primary-to-secondary turns ratio of 2 to 1.

(*a*) Determine the plate-supply voltage required for each tube. Draw the amplifier circuit, using cathode biasing and screen dropping resistors so that a single power supply may be used. Compute required values of all resistors.

(*b*) Draw the a-c equivalent circuit, and determine the amplifier gain at $f = 796$ cps. What circuit elements may be expected to limit the region of uniform gain at high frequencies?

(*c*) Find the load current (a-c) if the input signal voltage is 0.2 volt rms.

3-5. A resistance–capacitance-coupled class-A voltage amplifier of two stages uses a 6J7 (pentode) in the first stage and a 6C5 in the second stage. The load resistance for the 6J7 is 250,000 ohms, and the grid leak is 1 megohm. Output resistance for the 6C5 is 20,000 ohms. Fixed bias is used.

(*a*) Draw the equivalent a-c circuit for the complete amplifier. Neglect inter-electrode capacitances.

(*b*) What should be the size of the coupling capacitor C such that the gain frequency curve will have 0.707 of its mid-frequency value at $f = 20$ cps?

(*c*) If $C = 0.005$ μf, what is the over-all gain of the amplifier in the mid-frequency range?

3-6. Derive gain-frequency relations for an L–C-coupled amplifier analogous to those derived for the R–C case.

3-7. Given $n = N_2/N_1 = 3$, $L_1 = 100$ henrys, $L_2 = 900$ henrys, $R_1 = 100$ ohms, $R_2 = 1000$ ohms, $E_{bb1} = 250$ volts, $E_{bb2} = 400$ volts. If the coefficient of coupling

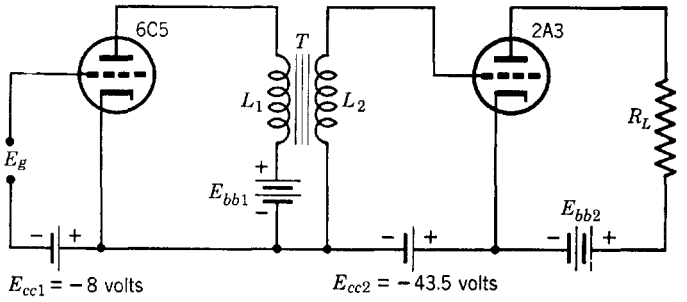

FIG. P3-7.

K is 0.988, and $R_L = 2500$ ohms, compute a gain-frequency curve for the range 20 cycles to 40 kc per sec, for the first stage. Assume that the total capacitance C_0 of Fig. 3-16 is 50 $\mu\mu$f.

3-8. Two 6L6 tubes are connected in push–pull and operated class A_1 with $E_b = 250$ volts, $E_{c1} = -15$ volts, $E_{c2} = 250$ volts. Obtain the composite plate and dynamic characteristics of the two tubes if the effective plate-to-plate load resistance is 5000 ohms. Find the fundamental a-c component of plate current flowing in the transformer primary by graphical means and by use of the equivalent circuit. Use an input voltage of $e_g = 15 \cos \omega t$.

3-9. (*a*) What is the equivalent plate-to-plate load resistance of two tubes connected in push–pull and operated class A if the output transformer has a turns ratio, primary- (plate side)to-secondary, of 3 to 1 and $R_L = 4000$ ohms?

(*b*) If each tube is said to be "working" into the equivalent external resistance between its plate and point a of Fig. 3-19, compute this resistance for conditions as in part a.

3-10. Two 2A3 tubes are operated in push–pull class AB_1 with $E_{c1} = -60$ volts, $E_b = 300$ volts. Determine graphically the fundamental component of plate current, if the effective plate-to-plate load resistance is 3000 ohms. Prepare a set of composite plate characteristics.

3-11. (*a*) Draw the a-c equivalent circuit of Fig. 3-25 for the mid-frequency range.

(*b*) If the amplifier and phase-inverter tubes of Fig. 3-25, first stage, are identical

and $\mu = 20$, $r_p = 10{,}000$ for each, compute R_2 (if $R_{L1} = R_{L2} = 50{,}000$, $R_3 = 200{,}000$ ohms) so that the input voltages to the push–pull stage will be equal.

3-12. Analyze the circuit of Fig. 3-29 for the effect of inverse feedback on frequency and phase distortions if R_L is replaced by an inductive load $Z_L = R_L + jX_L$ where $R_L = 30{,}000$ ohms, and $X_L = 2500$ ohms at $f = 5000$ cps, and $R_f = 5000$ ohms. Note that β is no longer independent of frequency. For the tube, use a type 6C5.

3-13. Derive the mid-frequency gain formula for the amplifier of Fig. 3-31 with and without the use of the feedback equation.

3-14. Plot the curve of gain versus frequency for the inverse feedback amplifier of Fig. 3-31, and compare with the curve obtained without feedback. How much has inverse feedback extended the region of flatness of the gain-frequency curve?

3-15. Derive Eq. 3-75 from Fig. 3-35.

3-16. Obtain an expression for the voltage gain of the amplifier of Fig. 3-36 in the intermediate-frequency range.

3-17. Write an expression for the input voltage of each grid of the push–pull amplifier of Fig. 3-37, if the secondary voltage of the top half of the input transformer is E_g volts.

3-18. Referring to the amplifier of Fig. 3-38, determine the over-all amplifier gain in the intermediate-frequency range if: the pentode is a 6J7 with operating values $E_b = 250$ volts, $E_{c1} = -3$ volts, $E_{c2} = 100$ volts, $I_b = 2$ ma, $I_{c2} = 0.5$ ma; the triode is a 6C5 with $E_b = 250$ volts, $E_c = -8$, $I_b = 8$ ma; $R_{L1} = 100{,}000$ ohms, $R_g = 250{,}000$ ohms, $R_{L2} = 25{,}000$ ohms, $C = 0.04$ μf, $C_{k1} = 10$ μf, $C_{k2} = 2.5$ μf, $C_1 = 0.4$ μf, $C_d = 0.1$ μf, $R_1 = R_2 = 50{,}000$ ohms. In addition,

(*a*) Find suitable values of R_{k1}, R_{k2}, and E_{bb}.

(*b*) Draw the complete intermediate-frequency equivalent circuit.

(*c*) If the total capacity shunting R_{g1} is 80 $\mu\mu$f, compute and plot a gain-frequency curve over the range 40 to 40,000 cycles.

(*d*) Compute a gain-frequency curve over the same range if $R_2 = 0$, $R_1 = 100{,}000$ ohms.

3-19. A two-stage R–C-coupled amplifier circuit is connected as shown in the circuit of problem 3-3. Feedback may be provided by means of a resistor R_3 connected directly from plate to plate (between P_1 and P_2) of the two triodes. Neglecting the reactance of the coupling capacitor C, draw the complete a-c equivalent circuit of the amplifier, and show that the gain of the second stage will be zero for $R_3 = 1/g_{m2}$, where g_{m2} is the grid-plate transconductance of the second tube. Derive the following expression for the over-all gain of the amplifier:

$$A = -A_2 g_{m1}/(Y_0 - A_2 Y_3)$$

where A_2 is the gain of the second stage, g_{m1} is the transconductance of the first tube, and

$$Y_0 = 1/r_{p1} + 1/R_1 + 1/R_2 + 1/R_3$$

with $Y_3 = 1/R_3$.

3-20. Compute the d-c and effective a-c components of current in resistor $R_3 = 50{,}000$ ohms of problem 3-19 using the circuit values given in problem 3-3. Neglect all condenser reactances, and compute the mid-frequency gain of the amplifier.

3-21. Compute the gain and input impedance of the cathode follower amplifier of Fig. 3-39 at $f = 79.6$, 796, 79,600, 796,000, and 1,593,000 cps if the tube is a 6C5 for which $r_p = 10{,}000$ ohms, $\mu = 20$, and $R_K = 10{,}000$ ohms.

3-22. Draw the equivalent circuit of the cathode follower (Fig. 3-39), and connect a generator of voltage E across the output terminals. Assuming the voltage E_g to be zero, derive Eq. 3-80.

3-23. Determine R_K (Fig. 3-39) so that the cathode follower output impedance (with input short) will be 400 ohms at 1000 cycles. Assume that the tube is a 6C5, $\mu = 20$, $r_p = 10{,}000$ ohms.

3-24. The voltage V applied to the circuit shown is the rms value of an applied sinusoidal voltage of variable frequency. Sketch a curve of V_c/V as a function of

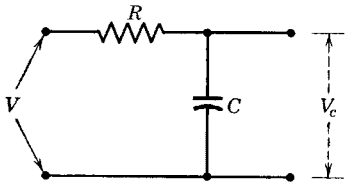

FIG. P3-24.

frequency and derive an expression for the upper "half-power" frequency; V_c is the rms voltage across C.

3-25. Derive the expression called for in problem 3-24 by applying four-pole theory and determining the four-pole admittances of the circuit.

3-26. A type 6AB7 is used in one stage of a video (wide-band) amplifier. Assume that the total output capacitance C_0 is 25 $\mu\mu$f; $R_g = 1$ megohm. Two requirements are to be met: (*a*) The gain must be constant (within ± 1 db) up to 4 mc; (*b*) at low frequencies, the gain must remain above 0.707 of the mid-band value for all frequencies above 10 cps. Design the stage, and sketch its predicted phase-frequency characteristic as in Fig. 3-45.

CHAPTER 4

THE AUDIO-AMPLIFIER POWER STAGE

THE WORK OF THE PRECEDING CHAPTERS HAS BEEN CONCERNED PRIMARILY with the increase of the voltage level in amplification. The present chapter will discuss the problems encountered in the design of the output or power stage of an audio-frequency amplifier. The power stage is required to provide, as nearly as possible, the optimum coupling to the load so that the requisite power will be delivered to the load with minimum distortion and at as high an efficiency as possible.

4-1. Power Relations in Amplifiers

Power may conceivably be delivered to an amplifier from two possible sources, namely, the source of grid excitation, and the voltage sources which supply the cathode heating, the screen- and control grid-bias voltages, and the plate voltage. In class-A amplifiers where linear operation is desired, the grid does not swing positive, grid current is very small, and the grid input power is negligible in the audio range. Grid- and screen-bias and plate voltages are usually supplied from a common power source usually derived from alternating current through a rectifier and filter system. Cathode heater or filament power may be derived from a low-voltage winding on the power transformer supplying the rectifier. The principal source of power is the plate-supply voltage.

Power is delivered by an amplifier to its load resistance, and the useful power output of the amplifier results usually from the a-c component. In an intermediate stage of a voltage amplifier, the power output of the stage might be defined as the a-c power developed in the resistor or equivalent resistor in which the input voltage for the succeeding stage is developed. For example, the useful output power of an *R–C*-coupled stage of a voltage amplifier would, by definition, be developed in the grid-leak resistor. Since the power so developed serves merely to heat the resistor and does not contribute to the power input of the succeeding stage, it is evident that intermediate-stage power output for *R–C*-coupled voltage amplifiers has no real significance as power

output. Amplifiers, however, generally terminate in what may be called a power stage; this supplies both voltage and power to an equivalent load resistor, which may be, for example, a relay or a loudspeaker. For maximum power transfer, such load resistances usually require matching networks or output transformers to match the power tube to its load. Optimum values of load resistance will be considered in a later section.

The following analysis of a power amplifier with a resistance load serves the purpose of illustrating fundamental definitions. The circuit

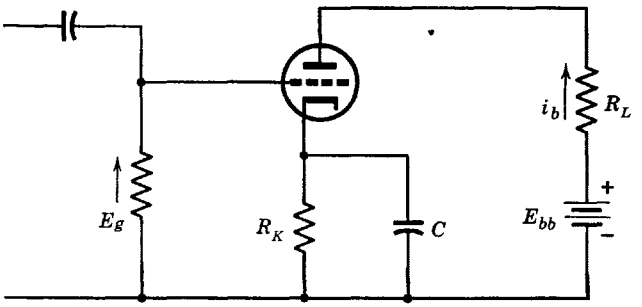

FIG. 4-1. Series-fed power amplifier.

of the amplifier is shown in Fig. 4-1. Linear class-A_1 operation is assumed. The power input is entirely from the plate supply if grid input power may be neglected. The power input, then, is

$$P_i = E_{bb}I_b \text{ watts}$$

where I_b = the average (or quiescent) value of plate current. The losses supplied by the plate battery are as follows: the d-c heat loss in the load resistor $I_b^2R_L$ and in the bias resistor $I_b^2R_K$ and the loss in heat at the anode of the tube. The energy dissipation at the anode is called the *plate dissipation.* It is the result of the conversion into heat of the kinetic energy of the incoming electrons. The temperature of the anode rises until it is able to radiate and conduct the heat of electron bombardment away as fast as it is generated. If the plate dissipation in watts is P_a, and the power output in watts is P_o, then the law of the conservation of energy requires that

$$P_i = \text{output} + \text{losses} = P_o + P_a + I_b^2(R_L + R_K) \qquad (4\text{-}1)$$

If the effective a-c component of plate current is I_p, then

$$P_o = I_p^2R_L \text{ watts}$$

The plate dissipation may then be obtained by solving Eq. 4-1; that is,

$$P_a = E_{bb}I_b - I_b^2(R_L + R_K) - I_p^2R_L \tag{4-2}$$

It is instructive to obtain P_a by another method. If e_b and i_b have their usual meanings, then the average power at the plate is given fundamentally by

$$P_a = \frac{1}{T}\int_0^T e_b i_b \, dt \tag{4-3}$$

where T is the period at the fundamental a-c component of plate current. Now

$$e_b = E_{bb} - I_b(R_L + R_K) - i_pR_L$$

as obtained by applying superposition of d-c and a-c values. Also, in Eq. 4-3,

$$i_b = I_b + i_p$$

Then, for $i_p = \sqrt{2}\, I_p \sin \omega t$, the integral of Eq. 4-3 results in Eq. 4-2, which shows that the maximum plate dissipation occurs when the power output is zero. If power is not delivered to the load or biasing resistors, it must be dissipated at the plate. The tube should therefore be operated with its plate dissipation at quiescence equal to the rated value.

Equivalent expressions for the power output may be obtained graphically from the plate diagram. Three typical triode plate characteristics and a load line are shown in Fig. 4-2. Assuming linear operation, bias

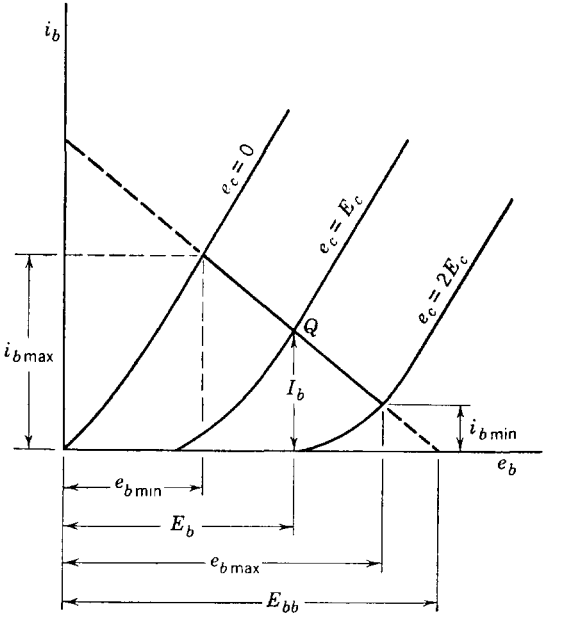

FIG. 4-2. Load line and plate diagram for a class-A power amplifier.

at $e_c = E_c$ volts (negative), and a grid swing of $e_{g\,\max} = |E_c|$ volts, then, by definition,

$$E_p = \frac{e_{b\,\max} - e_{b\,\min}}{2\sqrt{2}} \tag{4-4}$$

and

$$I_p = \frac{i_{b\,\max} - i_{b\,\min}}{2\sqrt{2}} \tag{4-5}$$

For a resistance load, the power output is

$$P_o = E_p I_p = \frac{(e_{b\,\max} - e_{b\,\min})(i_{b\,\max} - i_{b\,\min})}{8} \tag{4-6}$$

The function of the power amplifier is to convert d-c to a-c power, controlled by the alternating voltage and resulting electric field between grid and cathode. The *conversion efficiency* of the amplifier is measured by what is called its *plate-circuit efficiency*, defined as the useful plate output power divided by the plate input power. If η_p is the plate-circuit efficiency, then

$$\eta_p = \frac{E_p I_p}{E_{bb} I_b} \tag{4-7}$$

For the circuit of Fig. 4-2, and from Eq. 4-2,

$$\eta_p = \frac{E_{bb} I_b - I_b^2(R_L + R_K) - P_a}{E_{bb} I_b}$$

Evidently, the plate-circuit efficiency could be considerably increased by using parallel feed to eliminate the loss $I_b^2 R_L$.

4-2. Load-Coupling Circuits

Series feed as in Fig. 4-1 is wasteful of both power and battery voltage. Parallel feed using a choke and condenser as shown in Fig. 4-3, or trans-

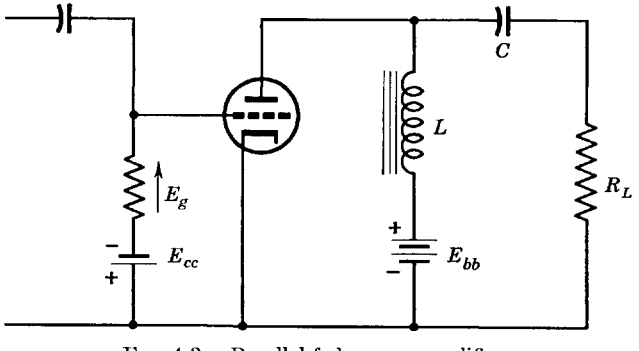

FIG. 4-3. Parallel-fed power amplifier.

former coupling as shown in Fig. 4-4, has the advantage of greater plate-circuit efficiency and the additional advantage that no d-c component flows in the load resistance. Because of the large value of the quiescent or average component of plate current in power amplifiers, the output

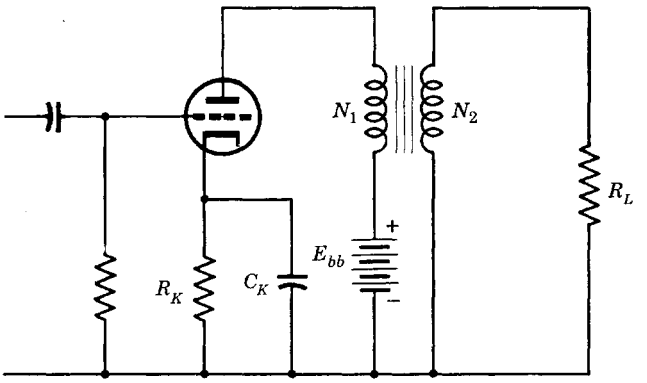

FIG. 4-4. Power amplifier with output transformer.

transformer primary inductance may be reduced as a result of iron saturation. For this reason, a choke and a condenser may be desirable in coupling the tube to the output transformer. As usual, the magnitude of choke inductance and condenser capacitance are desirably such that

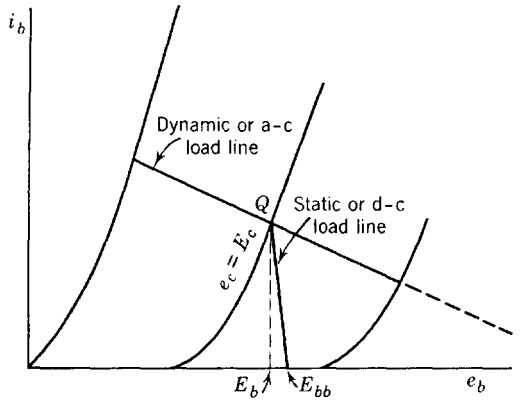

FIG. 4-5. Static and dynamic load lines for parallel feed.

the reactances of neither of them need be shown in the equivalent a-c circuit.

The location of the operating point on the plate diagrams for the circuits of Fig. 4-3 and Fig. 4-4 requires the construction of what may be called the *d-c load line.* This is a load line drawn in the usual way from

the point on the voltage axis corresponding to E_{bb} and with a slope determined by the d-c resistance of the choke or of the transformer primary plus the resistance of the biasing resistor. These resistances will be small compared with the effective load resistance for a power stage. If these resistances were neglected, the d-c load line would be vertical. The operating point is then determined by the intersection of the d-c load line and the plate characteristic corresponding to the grid bias as shown in Fig. 4-5. The *a-c load line* is then drawn through the operating point with a slope corresponding to the a-c resistance of R_L in Fig. 4-3 or to $(N_1/N_2)^2 R_L$ in Fig. 4-4. The required plate-supply voltage is approximately the operating voltage E_b. It is assumed that the biasing resistors are adequately by-passed, but this is difficult where the value of R_K is in the range 150 to 750 ohms. Fixed bias may be preferred.

4-3. Optimum Value of Triode Load Resistance

For triodes the maximum power output for specified conditions of operation is determined by the load resistance. Two cases are usually considered. In the first, a small excitation voltage of fixed effective value E_g is specified; E_g is numerically less than the grid bias so that operation may be considered as linear, class A_1. The equivalent circuit

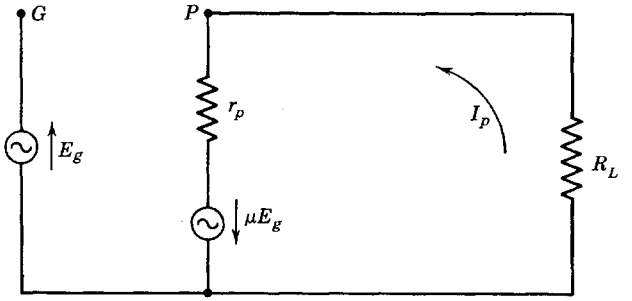

FIG. 4-6. Equivalent circuit of Fig. 4-3.

of Fig. 4-3, for example, could then be used and is shown in Fig. 4-6. Then

$$P_o = I_p^2 R_L = \left(\frac{\mu E_g}{r_p + R_L}\right)^2 R_L \tag{4-8}$$

Since the excitation is small, μ and r_p may be assumed constant, so that P_o and R_L are the variables. As predicted by the maximum power-transfer theorem, the maximum value of power output will be realized, at fixed excitation, for $R_L = r_p$.

The conditions of the second case are more frequently encountered in the use of single-tube power amplifiers. The only restriction upon the grid voltage is imposed by the amount of harmonic distortion that can be tolerated. This means that the grid should not swing positive or below the "knee" of the dynamic characteristic. It is then required to determine R_L for *maximum undistorted power* output, given a fixed value of the quiescent plate voltage E_b. To avoid distortion, the minimum

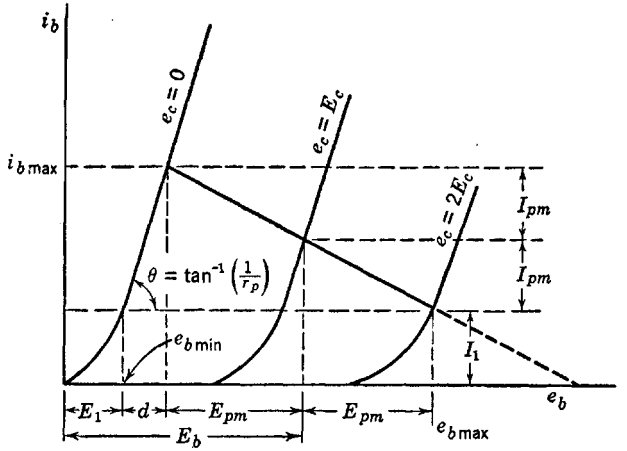

FIG. 4-7. Power-amplifier operation with maximum undistorted power output.

value of the plate current must never be less than some arbitrary constant I_1 (Fig. 4-7) determined by the curvature of the plate characteristics. The magnitude of I_1 is determined by the tolerable harmonic distortion. Summarizing, the conditions for maximum undistorted power output are:

(1) $(\sqrt{2}\,E_g) = E_{gm} = |\,E_c\,|$
(2) $i_{b\,\min} = I_1$
(3) E_b is fixed.

This requirement is met practically by requiring zero d-c impedance in the plate-supply circuit, as provided by parallel feed. Now for an arbitrary selected value of bias voltage E_c the operating point Q is determined. The maximum and minimum values of plate current and of plate voltage, and hence also the value of the power output depend upon the resistance of the effective plate load R_L, which determines the slope of the a-c or dynamic load line. The magnitude of $i_{b\,\min} = I_1$ may be selected arbitrarily. If then an optimum load resistance is determined by analysis, the resulting harmonic distortion may be checked,

and, if a decrease in $i_{b\,\min}$ is permissible, a new value of I_1 may be employed. The load resistance involved is optimum in the sense that it provides maximum power output for the assumed value of I_1 and for the fixed values of E_b, E_c, and E_{gm}. The problem of analysis, therefore, is to determine the best value of R_L to use with the given tube for the specified conditions.

The analysis is quite straightforward and proceeds as follows: The line $i_b = I_1$ intersects characteristic $e_c = 0$ at $e_b = E_1$. Let $\sqrt{2}\,E_p = E_{pm}$, and $\sqrt{2}\,I_p = I_{pm}$. If it is assumed that the characteristics are linear and evenly spaced, the values of E_{pm} and I_{pm} are as shown in Fig. 4-7. The distance d may be expressed as

$$d = 2I_{pm} \cot \theta = 2I_{pm}r_p$$

Then, Eq. 4-6 yields $$P_o = \frac{E_{pm}I_{pm}}{2} \tag{4-9}$$

But $$E_{pm} = E_b - 2I_{pm}r_p - E_1 \tag{4-10}$$

so that, substituting in Eq. 4-9, one obtains

$$P_o = \tfrac{1}{2}(E_bI_{pm} - 2I_{pm}{}^2r_p - E_1I_{pm}) \tag{4-11}$$

In Eq. 4-11, E_b, r_p, and E_1 are constants, and P_o depends upon I_{pm}. The existence of a maximum value of P_o may be determined by obtaining the derivative of P_o with respect to I_{pm}. Thus,

$$dP_o/dI_{pm} = \tfrac{1}{2}(E_b - 4I_{pm}r_p - E_1) = 0$$

or $$I_{pm} = (E_b - E_1)/4r_p \tag{4-12}$$

From Eq. 4-10,

$$E_b - E_1 = E_{pm} + 2I_{pm}r_p$$

Since numerically $$E_{pm} = I_{pm}R_L$$

$$E_b - E_1 = I_{pm}(R_L + 2r_p)$$

Substituting in Eq. 4-12 and simplifying, one obtains

$$R_L = 2r_p \tag{4-13}$$

Maximum undistorted power output in a triode amplifier will then be realized, according to the conditions assumed, if the load resistance is made equal to twice the tube plate resistance. It is assumed, however, that the rated plate dissipation will not be exceeded at zero excitation, so that it must be determined in practice if the operating point corresponding to the assumed value of E_b can be used without exceeding

allowable plate dissipation. If the maximum plate dissipation is specified, and no restrictions are placed on plate voltage, Nottingham [1] has shown that the optimum plate load for undistorted power output is in the range 15 to 20 times the plate resistance.

To determine the proper value of grid bias, Eq. 4-12 may be written as

$$E_{pm}/R_L = (E_b - E_1)/4r_p$$

For $$R_L = 2r_p, \qquad E_{pm} = (E_b - E_1)/2 \tag{4-14}$$

From the equivalent circuit, and $E_{gm} = -E_c$,

$$I_{pm} = -\mu E_c/(r_p + R_L) \tag{4-15}$$

Since $E_{pm} = I_{pm}R_L$ (neglecting phase), Eqs. 4-14 and 4-15 may be solved for E_c. The result is

$$E_c = -\tfrac{3}{4}(E_b - E_1)/\mu \tag{4-16}$$

Experience with power triodes shows that E_1 is approximately $0.1E_b$, so that it is sufficiently accurate for a first approximation to use

$$E_c = -0.675E_b/\mu \cong -0.7E_b/\mu \tag{4-16a}$$

The optimum or maximum power output corresponding to $R_L = 2r_p$ is usefully expressed in terms of E_b and r_p. From Eq. 4-15, at optimum operation,

$$I_{pm} = -\mu E_c/3r_p$$

and $$P_{o\,\max} = \tfrac{1}{2}I_{pm}{}^2 \cdot 2r_p = \mu^2 E_c{}^2/9r_p \tag{4-17}$$

Use of the approximate relation of Eq. 4-16a for E_c yields

$$P_{o\,\max} = 0.054E_b{}^2/r_p \text{ watts} \tag{4-17a}$$

the maximum power output that may be expected from a tube of resistance r_p operating at a plate voltage of E_b. Actually, because of the approximations necessary in its derivation, Eq. 4-17a should be considered as an optimistic approximation of the maximum power output.

4-4. Theoretical Efficiency

If triode plate characteristics were perfectly straight lines, then I_1 in Fig. 4-7 would be zero, and I_{pm} would be equal to I_b. This would be the ideal situation, and, although the conditions are theoretical, the plate-circuit efficiency determined by assuming straight-line characteristics is of value because it provides information as to the maximum possible

[1] Wayne B. Nottingham, Optimum Conditions for Maximum Power in Class A Amplifiers, *Proc. IRE*, **29**, 620 (1941).

theoretical efficiency of a triode power amplifier. Reference to Fig. 4-7 shows that the efficiency is (for $I_1 = 0$, straight-line characteristics)

$$\eta_p = E_{pm}I_{pm}/2E_{bb}I_b \tag{4-18}$$

according to Eq. 4-7. For series feed, the d-c loss in the load resistor must be considered, so that $E_{bb} = E_b + I_bR_L$. Since $I_b = I_{pm}$ for $I_1 = 0$, then $I_bR_L = E_{pm}$, and

$$\eta_p = E_{pm}/2(E_b + E_{pm}) \tag{4-19}$$

If the plate characteristics are all straight lines, then that for which $e_c = 0$ would be expected to pass through the origin so that $E_1 = 0$. Equation 4-10 may then be written as

$$E_b = E_{pm} + 2I_br_p$$

so that the efficiency may be expressed as

$$\eta_p = E_{pm}/2(2E_{pm} + 2I_br_p)$$

which may be simplified by dividing numerator and denominator by E_{pm}. Finally for the series-fed amplifier, the theoretical plate-circuit efficiency becomes

$$\eta_p = \frac{1}{4(1 + r_p/R_L)} \tag{4-20}$$

The maximum possible plate-circuit efficiency of the series-fed amplifier is, according to Eq. 4-20, 0.25, or 25 per cent. For the optimum power output with fixed E_b, $r_p = R_L$, and the upper limit of the plate-circuit efficiency is 12.5 per cent. Actual plate-circuit efficiencies are usually less than 10 per cent.

A considerable improvement in plate-circuit efficiency may be realized by using parallel feed, thereby practically eliminating the d-c loss due to the quiescent or average value of plate current. For parallel feed, $E_{bb} = E_b$, and Eq. 4-18 becomes, with $I_b = I_{pm}$,

$$\eta_p = E_{pm}/2E_b$$

Again using Eq. 4-10, with $E_1 = 0$,

$$\eta_p = \frac{E_{pm}}{2(E_{pm} + 2I_br_p)} = \frac{1}{2(1 + 2r_p/R_L)} \tag{4-21}$$

For parallel feed, the maximum possible theoretical plate-circuit efficiency is, from Eq. 4-21, 50 per cent. For the optimum conditions of maximum undistorted power output, $R_L = 2r_p$, the value of η_p drops to 25 per cent. It should be noted that the maximum value of theoretical

plate-circuit efficiency corresponds to infinite load resistance and therefore to zero output power. Actual values of plate-circuit efficiency at optimum conditions are around 20 per cent.

4-5. Optimum Operation of Power Pentodes and Beam Tubes

As shown in Chapter 2, the amplification factor is much higher for pentodes than for triodes whereas the grid-plate transconductance g_m is of the same order of magnitude. The shape of the static characteristics of pentodes is such that a much greater range of alternating plate voltage swing is available, so that both the power output and the plate-circuit efficiency are greater for pentodes than for triodes. Pentodes, however, introduce greater harmonic distortion than triodes, and, since the minimum distortion is comparatively high, it is harmonic distortion rather than maximum power output that determines the optimum load resistance for pentode power amplifiers. It is important to note that the definition of optimum operation for a triode cannot be used for either beam or pentode power amplifiers because of the change in shape of the plate characteristics. In fact, R_L is usually a small fraction of r_p for best operation.

It was shown in Chapter 2, Section 2-11, that the second-harmonic amplitude B_2 in pentode amplifiers can be reduced to zero by a proper choice of load resistance. This value of load resistance is a first approximation to the optimum value for a single tube but does not yield maximum power output. Since minimum distortion is the determining factor, the optimum load resistance is approximately that for which $B_2 = 0$. The best value of R_L is most easily determined experimentally. If determined by computation, the approach is a method of successive approximations beginning with the assumption of a value of $i_{b\,\max}$ near the knee of the $e_c = 0$ pentode plate characteristic. The allowable plate dissipation then determines a trial value of E_b since $P_a \cong E_b(i_{b\,\max}/2)$. A value of grid bias E_c is then chosen, and a trial R_L is determined by the operating point and the value of $i_{b\,\max}$ on the $e_c = 0$ characteristic. If the value of I_b at the operating point differs appreciably from $i_{b\,\max}/2$, the process is repeated. For each trial R_L, the harmonic distortion and the value of P_o are computed, and curves are plotted to show the best combination of values. Unfortunately, maximum P_o does not coincide with minimum harmonic distortion.

The variation of P_o with R_L is easily understood if the power output equation

$$P_o = \frac{(e_{b\,\max} - e_{b\,\min})(i_{b\,\max} - i_{b\,\min})}{8}$$

is interpreted with the help of a set of pentode plate characteristics and

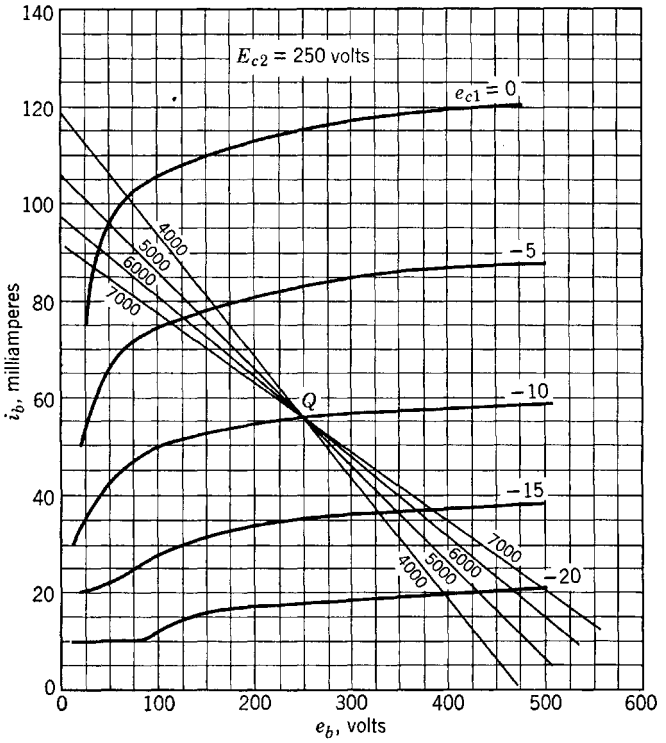

FIG. 4-8. Typical power-pentode static characteristics and load lines.

a load line, as shown in Fig. 4-8. The slope of the load line corresponds to $R_L \cong 4000$ ohms. The second-harmonic plate-current amplitude, assuming an operating point of $E_b = 250$ volts, $E_c = -10$ volts, and a grid swing of 10 volts, is approximately

$$B_2 = \frac{102 + 20 - 2(56)}{4} = \frac{10}{4} = 2.5 \text{ ma}$$

and

$$B_1 = \tfrac{1}{3}(i_{b\,\max} + i_{b(\frac{1}{2})} - i_{b(-\frac{1}{2})} - i_{b\,\min})$$

$$= \tfrac{1}{3}(102 + 79 - 37 - 20) = \tfrac{124}{3} = 41.6 \text{ ma}$$

The per cent second-harmonic distortion is $(B_2/B_1) \times 100$ or 6 per cent. Since

$$\frac{e_{b\,\max} - e_{b\,\min}}{2} = \frac{396 - 68}{2} = \frac{328}{2} = 164 \text{ volts}$$

$$P_o = \frac{164(41.6 \times 10^{-3})}{2} = 3.4 \text{ watts}$$

If now R_L is increased to 6000 ohms, $i_{b\,\min} \cong 20$ ma remains constant, but $i_{b\,\max}$ decreases to 91 ma. The plate swing increases, however, so that the power output is increased to approximately 3.8 watts, but the per cent second-harmonic distortion is now <1 per cent. If R_L is increased to 7000 ohms, P_o is slightly increased, but the second-harmonic distortion is about 3.6 per cent. Evidently, $R_L = 6000$ ohms is reasonably close to the optimum value.

In connection with Fig. 4-8, it is important to notice that the value of $e_{b\,\min}$ becomes quite small as R_L increases. It will be remembered from Chapter 2 that the *screen grid current is high for very low plate voltages, so that there is danger of exceeding the rated screen dissipation by using high values of load resistance.* It is important to remember that for pentodes or tetrodes the plate voltage must never be suddenly removed or greatly reduced unless the screen voltage is first removed because the flow of electrons to the screen may destroy the tube.

The same considerations as to optimum operation apply to beam-power amplifier tubes as to pentodes. The beam-power tubes have more nearly linear characteristics over a wider region of the plate diagram than pentodes and so are capable of delivering larger power output with less distortion than pentodes of equivalent size. Both pentodes and beam-power tubes are frequently operated in push–pull to reduce harmonic distortion. Choice of load resistance is then influenced by the requirement of minimum third-harmonic distortion.

4-6. Class-AB Power Amplifiers

Because serious distortion would otherwise result, class-AB audio-frequency amplifiers are always operated push–pull. The composite characteristics of triodes in push–pull class-A operation are nearly straight, parallel, evenly spaced lines, as shown in Fig. 3-26. Composite characteristics for the same tubes operating class AB have been drawn in Fig. 4-9, and, although the curves have been drawn as straight lines, some points obtained by the graphical method described in Section 3-12 fall slightly off the lines. However, operation is almost linear and the distortion is small, since even harmonics are eliminated by the push–pull connection. Because of the symmetry of the composite characteristics, the maximum instantaneous value of the composite current is equal to the negative of the minimum value, or $i_{b\,\max} = -i_{b\,\min}$; $i_{b(\frac{1}{2})} = -i_{b(-\frac{1}{2})}$, and, since $I_b = 0$, the harmonic-amplitude equations of Section 2-10 become, for the composite current,

$$\begin{aligned} B_0 &= B_2 = B_4 = 0 \\ B_1 &= \tfrac{2}{3}(i_{b\,\max} + i_{b(\frac{1}{2})}) \\ B_3 &= \tfrac{1}{3}(i_{b\,\max} - 2i_{b(\frac{1}{2})}) \end{aligned} \tag{4-22}$$

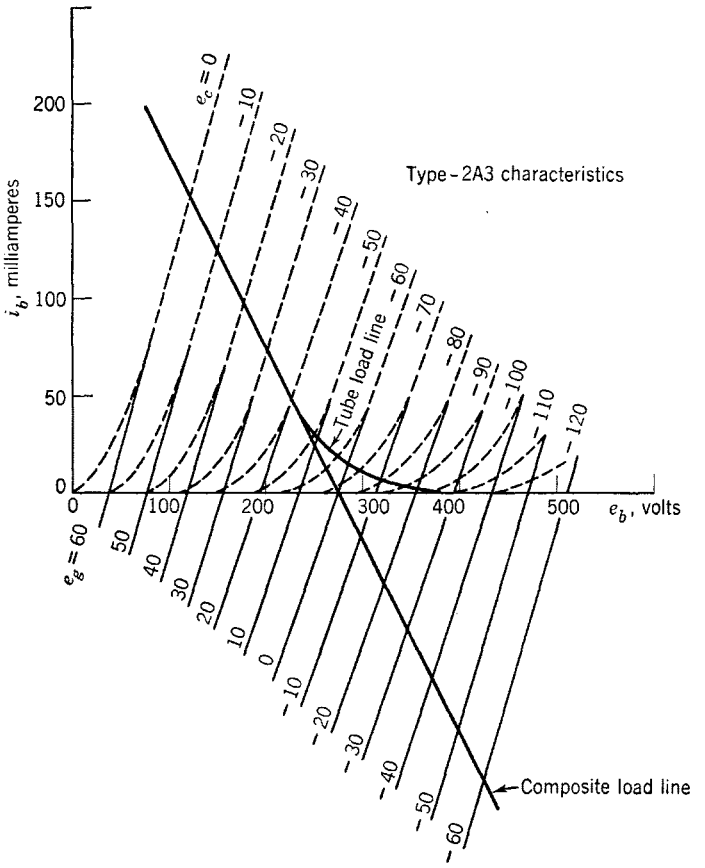

FIG. 4-9. Composite triode characteristics for push–pull operation, class AB. $E_c = -60$ volts, $E_b = 275$ volts; $(N_1/N_2)^2 R_L = 1000$ ohms.

Application of these relations to Fig. 4-9 shows that the third-harmonic distortion is very small.

Composite characteristics for positive grid swings have been drawn for two 6L6 beam-power amplifier tubes in push–pull, class-AB operation, and are shown in Fig. 4-10. Although not straight lines, the composite characteristics are more evenly spaced than the individual characteristics, and the distortion is small. The composite characteristic for $e_g = 20$ volts differs very little from the individual $E_{c1} = 0$ characteristic. Although the composite quiescent plate current I_b is zero, the individual quiescent plate currents are not zero. It was shown that the even harmonics are present in the mid-tap-to-cathode return, a–K, of Fig. 3-19. In case a biasing resistor is used in class-AB operation, a by-

pass condenser must be used, if feedback effects are to be avoided, although no condenser is necessary in class-A_1 push–pull operation. In the biasing resistor of the class-AB-operated push–pull amplifier, the biasing current is $I_{b\,avg} = I_{b1} + B_0$ at maximum excitation, where B_0 is the d-c component resulting from distortion. The grid bias, therefore, increases at high values of signal voltage, so that the distortion also in-

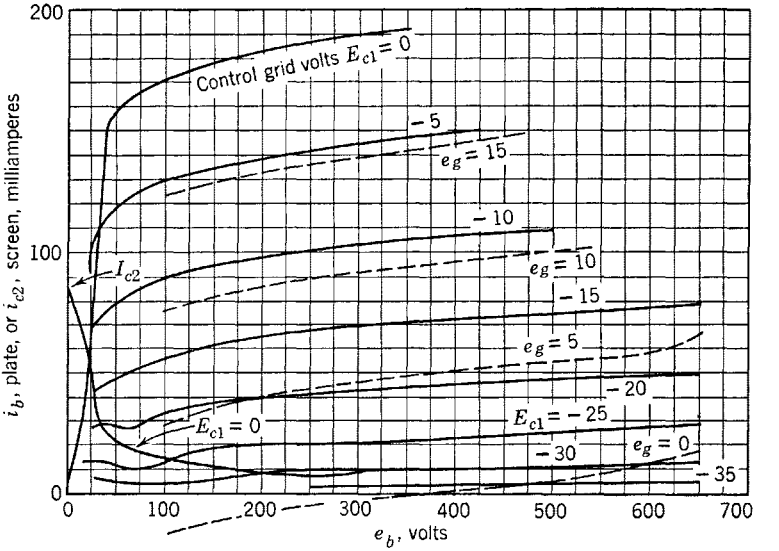

FIG. 4-10. Individual and composite static characteristics for two type-6L6 beam tetrodes in push–pull operation. $E_{c1} = -20$ volts, $E_b = 375$ volts.

creases with the excitation, requiring that the bias resistor must be selected approximately as though the operation were to be limiting class A.*

Because of the greater grid bias of class-AB operation, the operating plate current is smaller, and the operating plate voltage may be increased without exceeding the limiting plate dissipation. The result is a greater power output at higher efficiency. The power supplied to the tube increases with the signal voltage E_g for fixed E_{bb}, and, since the power to the load also increases, the plate dissipation (which is the difference between the input to the tube and the output) may either increase or decrease. In class-AB operation, P_a generally increases with E_g. It will be remembered that the reverse is true for class-A operation.

* By limiting class-A operation is meant that $i_b = 0$ for the most negative value of instantaneous grid voltage.

4-7. Optimum Class-A_1 and AB_1 Push-Pull Operation

For push-pull operation in either class A_1 or AB_1 for triodes where the composite plate characteristics are equally spaced parallel straight lines, Fig. 4-11 applies. Since the distortion is justifiably neglected, and the output transformer is assumed to be ideal, the power output is given by $P_o = \frac{1}{2}E_{pm}I_{pm}$, and the grid swing may have any value from zero to

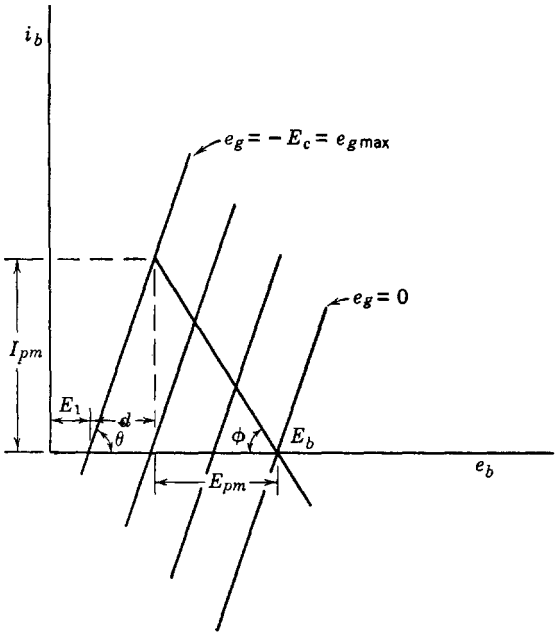

FIG. 4-11. Composite static plate characteristics and load line for a push-pull triode amplifier.

the magnitude of the grid bias. Then, from Fig. 4-11,

$$d = I_{pm} \cot \theta = I_{pm}R_{cp}$$

where R_{cp} is the reciprocal of the slope of the composite characteristics, and is usually obtained from the slope of the $e_g = 0$ characteristic. The maximum plate swing from quiescence is then

$$E_{pm} = (E_b - E_1 - I_{pm}R_{cp}) \tag{4-23}$$

so that

$$P_o = \tfrac{1}{2}(E_b - E_1 - I_{pm}R_{cp})I_{pm} \tag{4-24}$$

It is evident from Eq. 4-24 and Fig. 4-11 that P_o depends upon I_{pm} and

therefore upon the slope of the load line. For maximum P_o,

$$dP_o/dI_{pm} = \tfrac{1}{2}(E_b - E_1 - 2I_{pm}R_{cp}) = 0$$

or

$$I_{pm} = \frac{E_b - E_1}{2R_{cp}} \tag{4-25}$$

If the effective load resistance is R_L', then $E_{pm} = I_{pm}R_L'$, and, from Eq. 4-23,

$$E_b - E_1 = I_{pm}(R_L' + R_{cp}) \tag{4-26}$$

If Eq. 4-26 is substituted in Eq. 4-25, the result is

$$R_L' = R_{cp} \tag{4-27}$$

Therefore, for either class-A_1 or AB_1 push–pull operation of triodes the optimum operating load resistor is that for which the slope of the composite load line is equal numerically to the slope of the composite static characteristics, or

$$(N_1/N_2)^2R_L = R_{cp} \tag{4-28}$$

where R_L is the actual secondary load resistance.

In push–pull amplifiers using power pentodes or beam tetrodes, the optimum load resistance is determined by distortion in about the same way as for the single-tube power amplifier. The effective resistance should be such that the composite load line intersects the composite characteristic for maximum grid swing in the vicinity of the knee of the curve.

PROBLEMS

4-1. A type-10 power-amplifier triode is used in a circuit like that of Fig. 4-1 except that fixed bias is used. The tube and circuit constants are: $r_p = 5000$ ohms, $\mu = 8$, $R_L = 10{,}000$ ohms, $E_{bb} = 630$ volts, $E_c = -30$ volts.

(*a*) Locate the operating point (E_b, I_b), assuming fixed bias.

(*b*) For a grid swing of $E_{gm} = 30$ volts, determine the per cent second-harmonic distortion and the output voltage and power.

(*c*) Compute the plate dissipation and the plate-circuit efficiency.

(*d*) If parallel feed is used as in Fig. 4-3, find the new value of E_{bb} so that the same operating point and load line may be used as in parts *a* and *b*. Assume an ideal choke and condenser.

(*e*) Compute the power output, plate dissipation, and plate-circuit efficiency for the shunt-feed system.

4-2. The power stage of a voltage amplifier uses a 2A3 triode operating at $E_b = 250$ volts, $E_c = -45$ volts. If $E_{gm} = 45$ volts, compute the second-harmonic dis-

tortion, the power output, and the average or direct plate current for the following values of load resistance:

(*a*) $R_L = 400$ ohms
(*b*) $R_L = 800$ ohms
(*c*) $R_L = 1600$ ohms
(*d*) $R_L = 3200$ ohms

4-3. Given: T_1, a type 6C5, $\mu = 20$, $r_p = 10{,}000$, $R_{L1} = 50{,}000$, $R_1 + R_2 = 100{,}000$, $R_2 = 5000$. Reactances of all condensers negligible. T_2, a type 45, $\mu =$

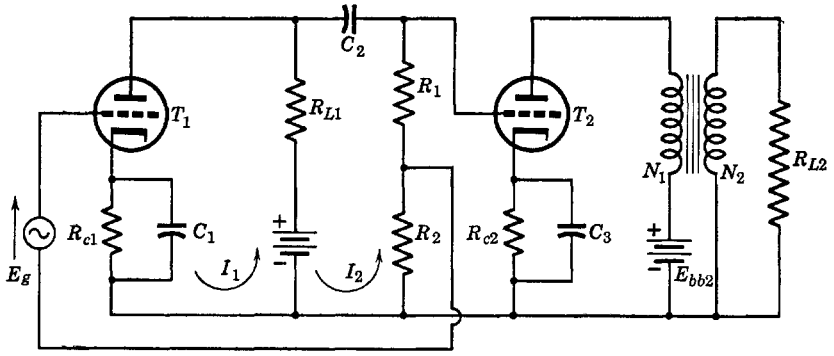

FIG. P4-3.

3.5, $r_p = 1600$, $N_1/N_2 = 2$, $R_{L2} = 800$ ohms. For the transformer, ωL_1 and ωL_2 are much greater than the winding resistances.

(*a*) If T_1 operates at $E_c = -8$ volts, $I_b = 4$ ma, and T_2 operates at $E_c = -50$ volts, $I_b = 34$ ma, $E_b = 250$ volts, find: R_{c1}, R_{c2}; E_{bb1}, E_{bb2}.

(*b*) Draw the equivalent a-c circuit.

(*c*) For $E_g = 5$ volts, find the input voltage to the second stage and the gain of the first stage. Do not neglect the feedback in finding the gain.

4-4. In the circuit of problem 4-3, compute the output power of the final stage, the plate-circuit efficiency of each tube, and the plate dissipation of each tube. Assume that distributed capacitance in the transformer may be neglected.

4-5. A power-amplifier stage consists of a 25A6 power pentode with an effective load resistance of 4000 ohms operating with $E_b = 135$ volts, $E_{c1} = -20$ volts, $E_{c2} = 135$ volts; $r_p = 36{,}000$ ohms, $g_m = 2450$ micromhos. Determine the output power, plate dissipation, and plate-circuit efficiency if the tube is transformer-coupled to the load resistance through an ideal transformer, and E_{gm} (sinusoidal) is 20 volts.

4-6. Determine the best value of load resistance to be used with the amplifier of problem 4-5 by computing power output, d-c components and total harmonic distortions up to the third, and plate-circuit efficiencies for the following effective values of load resistance: 2000, 4000, 6000, 8000, 10,000, and 12,000 ohms. Tabulate and plot the results.

4-7. Determine the proper value of load resistance to be used with a power-amplifier stage in which the tube is a 6L6 operating with a fixed bias of $E_{c1} = -15$ volts, $E_b = 250$ volts, $E_{c2} = 250$ volts. The load is coupled to the tube through an ideal transformer of turns ratio 2 to 1 stepdown (tube to load). It is desired that the load resistance be chosen so that the second-harmonic amplitude B_2 will be zero.

For this value of load resistance and with $E_{gm} = 15$ volts, compute: (*a*) the fundamental and third-harmonic amplitudes, (*b*) the d-c component of plate current, (*c*) the fundamental and total power outputs, (*d*) the plate dissipation and plate-circuit efficiency.

4-8. Two 6F6 power pentodes are connected in push–pull and operated class AB_2. The plate-supply voltage is 400 volts, $E_{c1} = -25$ volts, $E_{c2} = 250$ volts, and the peak value of the sinusoidal input voltage, grid to cathode is 35 volts. The transformer is assumed to be ideal and has a turns ratio, tube to load, of 2 to 1.

(*a*) Prepare a set of composite plate characteristics.

(*b*) Obtain a composite dynamic characteristic for each of three values of effective plate-to-plate load resistance as follows: 5000 ohms, 10,000 ohms, and 20,000 ohms.

(*c*) For each load resistance of part *b* compute the per cent third-harmonic distortion, the d-c supply current, and the power output.

4-9. Two 2A3 triodes are connected in push–pull and operated class AB_1, at $E_b = 300$ volts, $E_c = -60$ volts. What should be the value of load resistance for maximum undistorted power output if the ideal output transformer has a stepdown turns ratio of 3 to 1.

4-10. Design an audio-frequency amplifier to deliver a minimum of 5 watts to a 250-ohm load if the maximum input signal voltage is 0.2 volt. Draw the complete circuit, and compute all circuit constants. Discuss the expected behavior of your amplifier as to efficiency and distortion.

4-11. Two 6F6 pentodes are connected in push–pull and operated class AB from a 350-volt power supply. The grid bias is -25 volts, screen voltage 250 volts.

(*a*) Draw the composite static characteristics.

(*b*) Calculate output power, plate dissipation, and plate-circuit efficiency for a plate-to-plate load resistance of 10,000 ohms, peak signal voltage, grid to ground of 40 volts.

CHAPTER 5

GAS-FILLED TUBES AS CIRCUIT ELEMENTS

THE ELECTRON TUBES DESCRIBED IN THE CIRCUIT APPLICATIONS OF preceding chapters have been high-vacuum tubes. The vacuum in a high-vacuum tube is desirably as high as possible, although it is probable that many high-vacuum tubes of the receiving type operate quite satisfactorily at pressures of the order of 10^{-5} millimeter of mercury. The residual gas pressure for high-vacuum tubes should be less than 10^{-6} mm of mercury.

It is the objective of the present chapter to present the gas-filled electron tube as a circuit element. The extremely interesting and highly important internal physics of the gas-filled tube will be ignored—as was done in the case of the high-vacuum tube—until the behavior of the tube has been described in terms of simple current and voltage measurements made at the available external tube terminals. Then, after having achieved at least a degree of familiarity with the circuit behavior of both vacuum and gas-filled tubes, the student should find that a more extended analysis into the internal physical behavior of electron tubes in general will serve to answer a number of important questions which will have occurred to him and will enable him to use and to select tubes for specific applications with considerable assurance.

5-1. Effect of Gas upon the Diode Characteristic

Essentially the addition of certain gases to the envelope of a high-vacuum electron tube converts the tube from a variable resistance to a switch. Relatively few gases are satisfactory for the purpose, and the gases commonly used are mercury vapor, and the inert gases helium, argon, neon, krypton, and zenon. Hydrogen has been used for some applications. Many gases cannot be used because they "poison" the oxide-coated cathodes used in most tubes, reducing the available emission current. Gas pressures used in gas-filled tubes are roughly in the range 0.003 to 0.2 mm of mercury.

The fact that low-pressure gas added to the envelope of a high-vacuum

diode gives to the tube the properties of a switch may be very briefly explained. The diode characteristic shown in Chapter 1 (Fig. 1-2) is typical of the high-vacuum diode, and of the triode for a constant grid voltage. If the anode voltage (Fig. 1-2) is increased sufficiently to draw to the anode all of the available emission current from the cathode, the diode characteristic curve would flatten horizontally at this voltage and would remain flat at higher voltages since additional current is not available. This behavior is illustrated in Fig. 5-1, where the current is shown as emission limited at a voltage e_b'. The cathode of the tube operates at a fixed heater voltage, and therefore just as much current is available at anode voltages, less than e_b'' as at voltages greater than e_b'. As previously stated the anode current is a definite function of the anode voltage for values of $e_b < e_b''$. It suffices for present purposes to state that electrons emitted from the hot cathode at low anode voltages do not all proceed to the anode because the electrons already on their way to the anode exert large repulsive forces on electrons very near the cathode, forcing many of them to return to the cathode. This effect is described by saying that the current is limited by space charge. Thus, in Fig. 5-1, the anode current is limited by space charge for voltages less than e_b'', and by the ability of the cathode to emit electrons at its operating temperature for voltages greater than e_b'. The region between e_b' and e_b'' is a transition region between the two conditions.

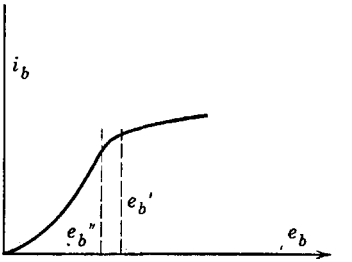

FIG. 5-1. Emission limitation of anode-current, high-vacuum diode.

If now mercury vapor is added to the high-vacuum tube, enough mercury atoms are ionized by electron collision to provide the positive ions which neutralize the electron space charge. Such neutralization is possible because the positive ions move very slowly compared with the electrons and move toward the negative cathode. The restraining effect of electron space charge upon electron flow from the cathode is removed at very low voltages, of the order of 10 to 20 volts for mercury, and the full emission current is made available at 10 or 20 volts instead of 400 volts. As soon as the anode voltage is increased enough to provide the necessary positive ions, the full cathode emission current suddenly becomes available. Thus the diode behaves as a switch, open for anode voltage less than the critical value, closed for anode voltages equal to or greater than the critical value.

5-2. Volt-Ampere Characteristics of the Gas-Filled Diode

Two or three general classifications of gas-filled diodes are in general use, depending upon the mechanism of electron release at the cathode. For present use, the tubes will be classified as cold-cathode or as hot-cathode tubes. The characteristic of a typical cold-cathode gas-filled diode is shown in Fig. 5-2. The tube begins to conduct at around 120 volts, but, after the tube "fires," the operating range of plate current extends from 5 to 30 or 35 ma at an anode voltage of 105 volts. The flow of current in the tube is accompanied by a luminous discharge of

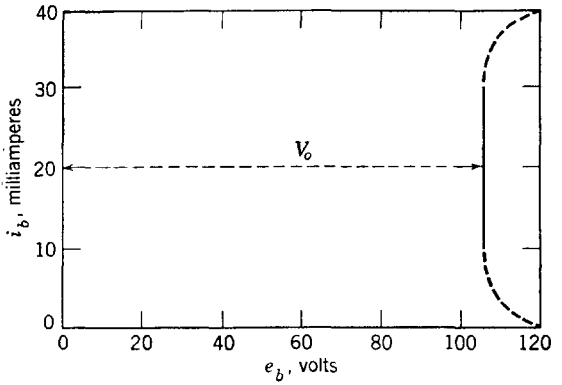

FIG. 5-2. Plate-current–plate-voltage characteristic of the VR-105 cold-cathode tube.

color depending upon the nature of the gas used. The particular value of current after discharge is initiated depends not at all upon the tube but upon the external circuit. It is therefore necessary to include sufficient circuit impedance in series with the tube to limit the current to values within its rating.

The constant voltage drop V_o across the gas tube during conduction is 105 volts for the cold-cathode tube of Fig. 5-2. The particular value of V_o for a given tube depends upon the tube design and the nature of the gas used. The thermionic or hot-cathode gas tube differs from the cold-cathode tube particularly in the magnitude of V_o and the respective current ratings. A typical mercury-vapor diode characteristic for a hot-cathode tube is shown in Fig. 5-3. The tube drop V_o is 15 volts over the entire operating range of plate current.

Cold-cathode tubes are also referred to as glow-discharge tubes. The discharge in hot-cathode tubes is known as an arc discharge. The mechanism of electron release at the cathode accounts for the differences in V_o between glow and arc tubes.

Cold-cathode glow-discharge tubes are quite rugged and are being

designed for switching operations in communication applications to have an operating life of 10 to 20 years. The hot-cathode arc-discharge tube is not so durable because of its heated cathode. The cathode coating used for hot-cathode tubes is nearly always a barium or strontium or mixed barium and strontium oxide coating. It is found experimentally that oxide coatings can withstand ionic bombardment from mercury ions without damage if V_o remains below about 22 volts. If sufficient electron emission from a heated cathode is available before the

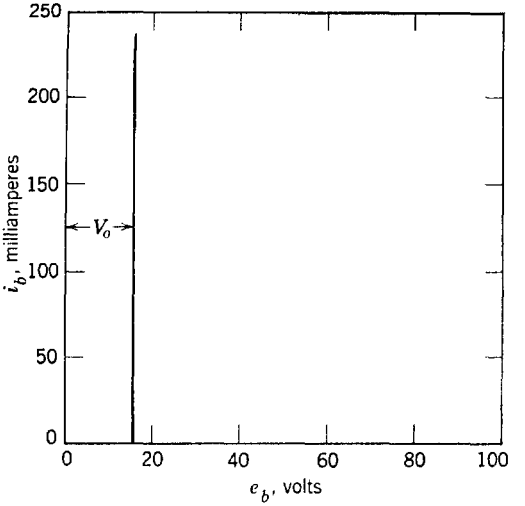

FIG. 5-3. Characteristic of a hot-cathode mercury-vapor diode.

application of plate voltage, the tube drop quickly falls to 10 or 15 volts when anode voltage is applied. However, if the cathode has not been given sufficient time to reach the rated emission temperature, the available current may not be sufficient to provide the arc discharge when anode voltage is applied, and, since the characteristic V_o for a glow discharge is considerably in excess of the safe value of 22 volts, the cathode may be destroyed. Therefore, the manufacturer always specifies a preliminary heating time for hot-cathode gas tubes to ensure adequate emission before the application of plate voltage.

5-3. Rating of Gas-Filled Diodes

Gas-filled diodes are designed primarily for rectifier service. The circuit of a half-wave rectifier is shown in Fig. 5-4, in which R_L is the load resistor, and the inductance L and capacitor C are used to filter the d-c output across the load. The dot near the cathode indicates that the

tube is gas-filled. The tube conducts only when the anode is positive and must be designed to hold the circuit open against the inverse peak voltage of the transformer secondary winding when the anode is negative. Such tubes are given the following ratings by the manufacturers:

1. Filament or heater current and voltage and filament heating time before the application of anode voltage.

2. Tube voltage drop, or the voltage across the tube, anode to cathode, when conducting. The exact value of this voltage cannot be specified since it is found to vary with the age of the tube. For a mercury-vapor tube, it is usually between 10 and 20 volts, and may be assumed to be 15 volts in computation of circuit behavior.

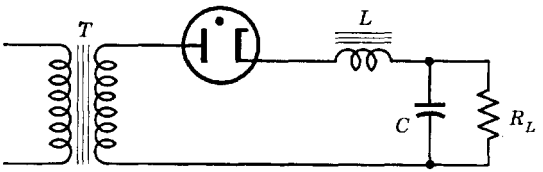

FIG. 5-4. Circuit of a half-wave rectifier, with filter.

3. The maximum instantaneous anode current is specified, and is usually about four or more times the maximum average anode current. A direct current equal to the maximum average anode current may be continuously delivered by the tube without injury provided that the maximum values of the peaks of the current wave during the conducting period are not in excess of the maximum instantaneous anode current rating. The maximum time of averaging the anode current is specified by the manufacturer. For example, the 323A Western Electric mercury-vapor-and-argon-filled tube is rated 1.5 amp maximum average anode current with time of averaging 5 sec or less. The maximum instantaneous anode current is 6.0 amp. If 2.5 amp flow for 3 sec and no current flows for 2 sec of the 5, the average current will be $(3 \cdot 2.5)/5 = 1.5$ amp over the 5 sec; if 5 amp flow for 1.5 sec of each 5 sec, $I_{avg} = (5 \cdot 1.5)/5 = 1.5$ amp. However, if 6 amp flow for 5 sec, and the current is zero for 15 sec, and this cycle of operations is repeated, the average current is $(5 \cdot 6)/20 = 1.5$ amp over the 20-sec period of the cycle, but the tube rating is greatly exceeded, since during the maximum time of averaging the anode current (5 sec) the average anode current is $(5 \cdot 6)/5 = 6$ amp. Fundamentally, the rating of tubes like other electrical apparatus, depends upon the ability of the tube to rid itself of the heat generated at anode or grid. In the example quoted, the approximate rated tube voltage drop is 15 volts. If the tube operates on the 5-amp 1.5-sec, 0-amp 3.5-sec cycle, the number of joules or

watt-seconds of energy dissipation at the anode in 20 sec would be $5(15)(1.5)(4) = 450$ watt-seconds. For the 6-amp 5-sec, 0-amp 15-sec cycle, the plate energy dissipation in 20 sec is $6(15)(5)\cdot 1 = 450$ joules. The total energy involved is the same in each case, but the maximum rate at which heat energy may be radiated, conducted, or convected away from the anode of this tube is $(1.5)(15) = 22.5$ joules per second, according to its rating. For the 5–1.5, 0–3.5 cycle, the average rate is not exceeded over the 5-, or over the 20-sec interval, but in the 6–5, 0–15 cycle, the average dissipation rate is $6\cdot 15 = 90$ joules per second over the first 5 sec. As the anode may be expected to get rid of only 22.5 joules per second during this interval, heat accumulates and the probable result would be the cracking of the glass envelope around the base, and the loss of the tube.

4. The maximum inverse peak voltage is the maximum instantaneous voltage that the tube may be expected to withstand without breakdown when the anode is negative. For the 323A previously mentioned, this rating is 500 volts.

5. Deionization time is the time required for recombination of ions with electrons after the anode voltage becomes negative. For the Western Electric 323A, the nominal deionization time is 1000 μsec. If the anode voltage applied to a 323A connected as in Fig. 5-4 is $220\sqrt{2}\sin 377t$, the inverse voltage at $t = t_1 + 10^{-3}$ is (for $377t_1 = \pi$ rad)

$$e = 220\sqrt{2}\sin(\pi + 0.377)$$

$$= -220\sqrt{2}\sin 0.377 = -115 \text{ volts}$$

This voltage might be sufficiently high to initiate a glow discharge in the reverse direction if sufficient ions remained in the tube. It is obvious that the deionization time will limit the frequency at which the tube will operate successfully as a rectifier.

5-4. Three-Electrode Gas-Filled Tubes

Two types of gas-filled triodes are in common use. The grid-glow tube operates with a cold cathode and a glow discharge, the thyratron with a heated cathode and an arc discharge. Grid control is, in each case, limited to the selection of the particular value of anode voltage at which glow or arc will be initiated between cathode and anode. After ignition or breakdown occurs, the grid becomes surrounded by a sheath of positive ions so that its field does not extend beyond the sheath, and the grid has no control over anode current. It merely controls the voltage at which current begins to flow and serves as the "trigger" that "fires" the tube. The same statement applies somewhat less emphati-

cally to grid-glow tubes. For both grid-glow tubes and thyratrons an additional rating is necessary—the maximum instantaneous forward voltage, which is the maximum positive anode voltage for which the grid can prevent the ignition of glow or arc.

The structure of a typical thyratron is illustrated by the sketches of Fig. 5-5. The cathode shown in *b* is of the inward-radiating type, open only at the top, and heated indirectly by a heater element in the inner

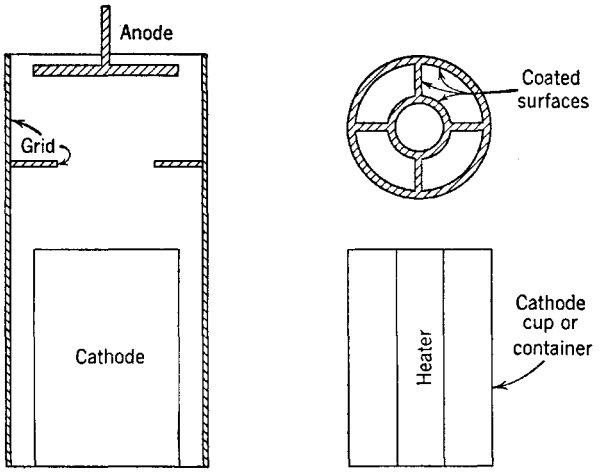

(a) Assembly, with grid and anode sectioned

(b) Cathode structure

FIG. 5-5. Typical electrode arrangement in a thyratron.

cylinder. The outside of the inner cylinder, the vanes, and the inside of the outer cylinder are coated with a highly emissive oxide layer. The assembly of anode, grid, and cathode given in Fig. 5-5*a* shows that the grid almost completely shields the cathode and is a hollow cylinder with a baffle between anode and cathode. For decreasing the deionization time, thyratron grids frequently are made with regularly spaced lattice-work openings in the grid to allow ion recombination in the cooler regions as quickly as possible after arc extinction.

5-5. Glow Tubes and Applications

Construction and ratings of glow tubes are so very different for the various applications that few general statements can be made. Such tubes are used as light sources, voltage regulators, rectifiers, relaxation oscillators, and as circuit-protective devices. The neon-sign tube is a glow tube used as a light source, as are the glow tubes of the strobotac.

A very important application of glow tubes is voltage regulation. The d-c supply voltage of Fig. 5-6 may be slightly variable as a result of line or source regulation. A series resistor and voltage-regulator tube

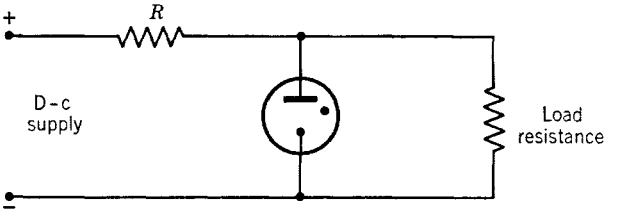

FIG. 5-6. Glow tube used as a voltage regulator.

are connected as shown. The regulation characteristic of the tube is shown in Fig. 5-2. Since the anode voltage remains practically constant for a wide range of current, the voltage across the load resistor will remain constant. If, for example, there is a small increase of the supply voltage, the increase in current will flow through the tube, the voltage across the load resistor remaining fixed.

The electrode arrangement of the glow tube of Fig. 5-2, the type-VR-105, is shown in Fig. 5-7. The starting voltage in these tubes may be greatly reduced by providing a projection extending from the cathode almost to the anode. As current increases, progressively larger areas of the cathode (outer cylinder) become covered with glow.

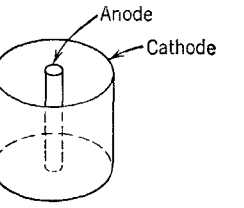

FIG. 5-7. Typical electrode arrangement in a glow tube.

A glow tube connected in parallel with a circuit element serves to protect that element from voltages higher than its voltage rating. The breakdown voltage of the glow tube should be approximately the upper limit of the voltage rating of the device to be protected, and the normal voltage across the tube should be too low to maintain the glow discharge.

In the circuit of Fig. 5-8, a glow tube is shown connected as a relaxation oscillator. When the switch S is first closed, the capacitor C begins to charge through resistance R, and the voltage e_c across tube and capacitor rises until the ignition potential of the tube is reached. At this voltage the tube breaks down, the capacitor discharges through the tube until the voltage e_c falls to a value insufficient to maintain the discharge; at this instant the glow disappears, and the voltage e_c begins to rise again. This behavior is shown in Fig. 5-9, in which the voltage across the capacitor is plotted against time. Since the voltage e_c is a transient voltage at

the terminals of a charging or discharging capacitor, it is not difficult to obtain an approximate formula for the frequency of oscillation. The

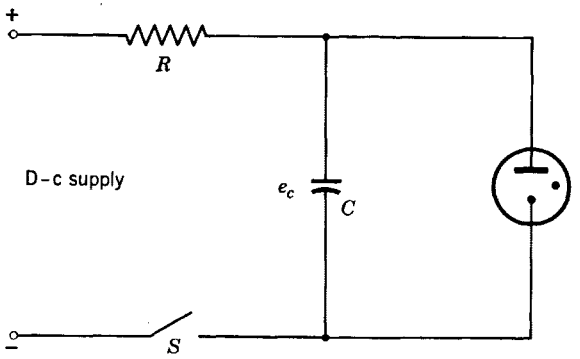

FIG. 5-8. Relaxation oscillator circuit.

charging current may be expressed as

$$i = dq/dt = C\, de_c/dt$$

and, if E = the d-c supply voltage, then

$$E = RC\, de_c/dt + e_c \tag{5-1}$$

The solution of Eq. 5-1, with zero initial capacitor voltage, is

$$e_c = E(1 - \epsilon^{-t/RC}) \tag{5-2}$$

If the discharge time is neglected, the frequency of the oscillation ob-

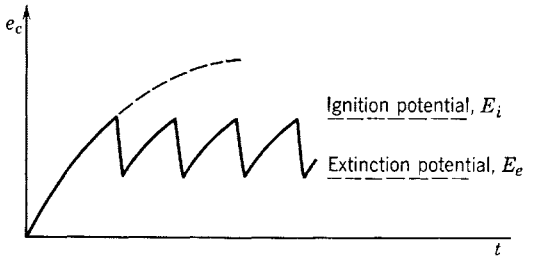

FIG. 5-9. Saw-tooth wave form of a relaxation oscillator.

tained from Eq. 5-2 and from Fig. 5-9 is

$$f = \frac{1}{RC \ln \dfrac{E - E_e}{E - E_i}} \tag{5-3}$$

where E_i and E_e are, respectively, the ignition and extinction potentials of the tube.

It is important that the charging rate of the R–C circuit of Fig. 5-8 be slow enough relative to the discharge rate of the capacitor through the tube that the voltage e_c will quickly fall below the value required to maintain the glow. Otherwise, the voltage of the capacitor may reach a steady value intermediate between E_e and E_i, while the current through R is conducted continuously through the tube. In such a case the capacitor is said to "block" the oscillation. Blocking is avoided by choosing R large enough that the available continuous current through the tube when conducting is not large enough to maintain the discharge.

Frequency of the oscillation is controllable, according to Eq. 5-3, by adjusting the product RC. The oscillation frequency can be made extremely small, as low as a fraction of a cycle per minute, or high enough to be in the upper audio range where deionization time imposes an upper limit on the frequency.

The wave shape of the relaxation oscillator is controllable by adjusting the voltage of the supply circuit. If a linear rise of potential before breakdown is desired, a high potential is used so that breakdown occurs relatively low down on the e_c vs. t curve.*

5-6. Arc Tubes and Applications

In tubes designed to carry relatively high currents—several amperes—at low tube voltages, arcs rather than glows are required. Arc discharges are obtainable by providing, as previously mentioned, a source of electrons at the cathode. Two types of electron source are in common use. These are the thermionic, oxide-coated cathode, and the mercury-pool cathode. Thermionic cathodes are used for rectifier and special control tubes carrying currents ranging from a few milliamperes to several amperes. The mercury-pool tube is a very rugged device capable of supplying hundreds of amperes but requiring special arc-initiating devices, all of which are designed to initiate or maintain what is called a cathode spot upon the surface of the mercury. Although an adequate and universally accepted explanation of the mechanism of electron emission from a cathode spot is still to be found, it is known that such a spot is capable of delivering almost unlimited currents. In the large metal-tank, mercury-arc power rectifiers used in supplying large amounts of d-c power in electric traction, elevator, and other similar applications, a special auxiliary anode is required to operate continuously to maintain the cathode spot. A number of anodes, one or

* A linear rise of condenser voltage may also be obtained by using a pentode instead of resistance R. This is referred to in the problems.

more for each phase of a three-phase system, are commonly operated from the same pool. It is the function of the auxiliary anode or "keep-alive" circuit to maintain the cathode spot at all times. The operating characteristics of this type of rectifier will be described further in Chapter 7.

The efficiency of a tube depends upon its energy dissipation. With their almost completely enclosed and inward-radiating cathodes and their low tube drop, the mercury-vapor arc tubes are the most efficient of the gas-discharge tubes.

Applications of the arc tubes are extremely numerous, and only a few fundamental applications will be selected for discussion. These include rectifiers, control applications, and inverters.

5-7. Tungar Rectifiers

The tungar rectifier is a two-electrode, gas-filled tube using a thermionic cathode and differing from other rectifiers in one important feature —the use of a relatively high-pressure gas, usually argon, or argon–mercury vapor. The gas pressure is usually between 1 and 5 mm of mercury. The cathode is a very heavy filament of thoriated or oxide-coated tungsten, operated at high temperature to provide the large currents—6 to 8 amp—required in battery charging, which is the principal application of these tubes. It is the function of the high-pressure gas in the tube to retard the evaporation of the coating of the filament, as well as to supply the ions required for removing the limitation due to space charge.

5-8. Thyratron Characteristics and D-C Control

The grid of the thyratron has only "trigger" control over anode current. The adjustment of grid bias serves to select a particular value of anode voltage at which the tube fires. When direct anode voltages are used, the grid may be biased to hold the anode circuit open, and a separate circuit may be employed to control the bias such that the tube fires as the result of some event actuating the grid-control circuit. Before giving circuit diagrams and specific examples, it is necessary to examine the grid-control characteristics of typical thyratrons. In Fig. 5-10 are the grid-control curves for a typical negative-grid thyratron, the Westinghouse WL-631. Similar characteristics for a positive-grid thyratron, the General Electric FG-33 are shown in Fig. 5-11. In the latter tube, shielding of the anode by the grid is complete enough that positive grid voltage is required to fire the tube. A tube in which the type of grid-control characteristic, positive or negative, may be selected

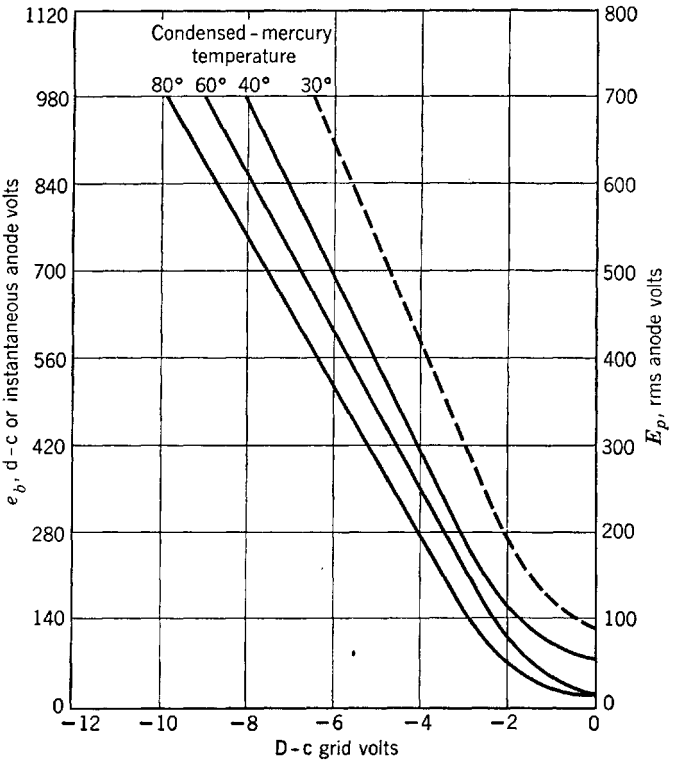

FIG. 5-10. Average control characteristics of a WL-631. (Courtesy Westinghouse Electric Corporation)

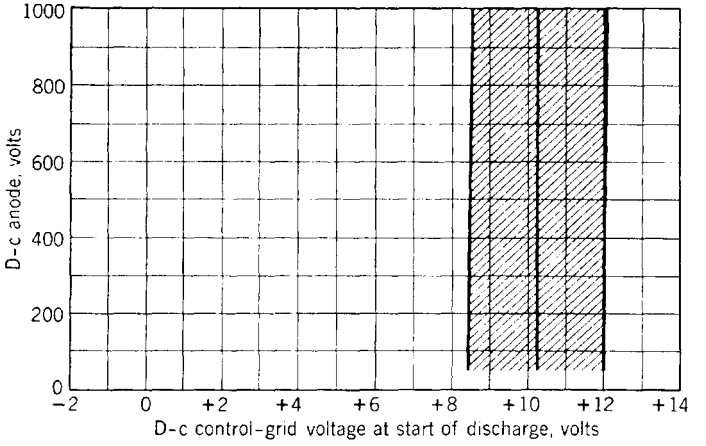

FIG. 5-11. Grid-control characteristics of the FG-33 thyratron. (Courtesy General Electric Company)

is illustrated in Fig. 5-12. This is a four-electrode gas tube known as a shield-grid thyratron. The sketch was drawn from a Westinghouse WL-632 tube. A few control characteristics for this tube are shown in Fig. 5-13.

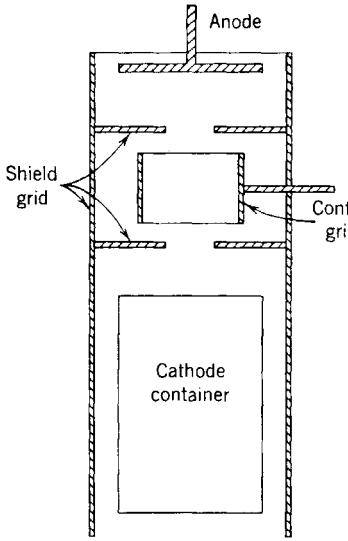

FIG. 5-12. Electrode arrangement of a shield-grid thyratron.

When direct voltages are used on thyratron anodes, the grid loses control after triggering the tube, and, if the anode current is to be reduced to zero, the anode circuit must be opened either by a switch or by electrical means. Means of d-c control vary in the methods used to interrupt the anode current, but most of these methods employ the voltage of a capacitor to apply a momentary positive voltage at the cathode with respect to the anode, preventing electrons from leaving the cathode long enough for deionization to take place, and for the grid to regain control. One such circuit is that of Fig. 5-14. When switch S_1 closes, the grid voltage becomes zero, and the tube fires. The current through R_1 is given by

$$i_1 = (E - V_o)/R_1 \tag{5-4}$$

where V_o is the tube drop when conducting. The current through R_2 can be obtained by solving the circuit equation

$$E = R_2 i_2 + e_c + V_o \tag{5-5}$$

since $i_2 = C\, de_c/dt$, where e_c is the instantaneous potential across the capacitor terminals. The resulting value of i_2 is given by

$$i_2 = \frac{E - V_o}{R_2}\, \epsilon^{-t/R_2C} \tag{5-6}$$

The charging current i_2 flows through the tube in the forward direction from anode to cathode, and the ultimate voltage across the capacitor will be just that across R_1, or $E - V_o$. If switch S_2 closes after the capacitor charging current has become approximately zero, the full voltage of the capacitor, $(E - V_o)$, is impressed across the tube, but,

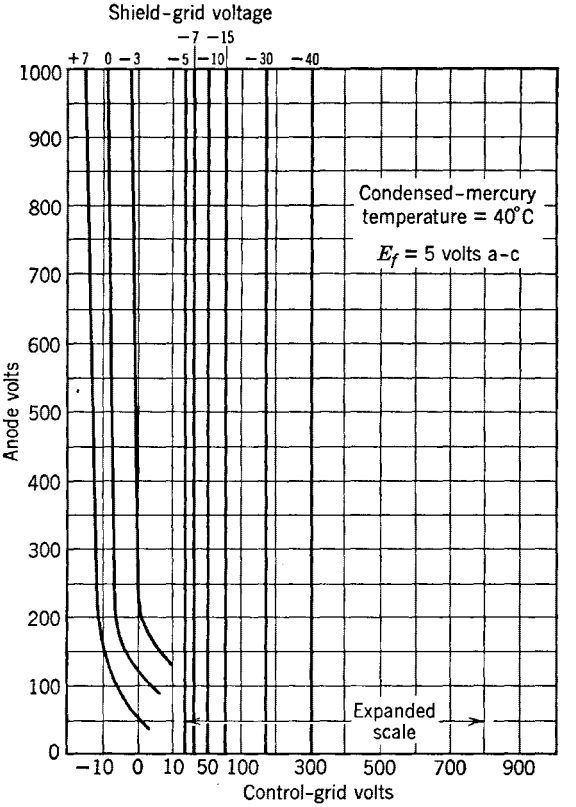

FIG. 5-13. Average control characteristics of a WL-632. (Courtesy Westinghouse Electric Corporation)

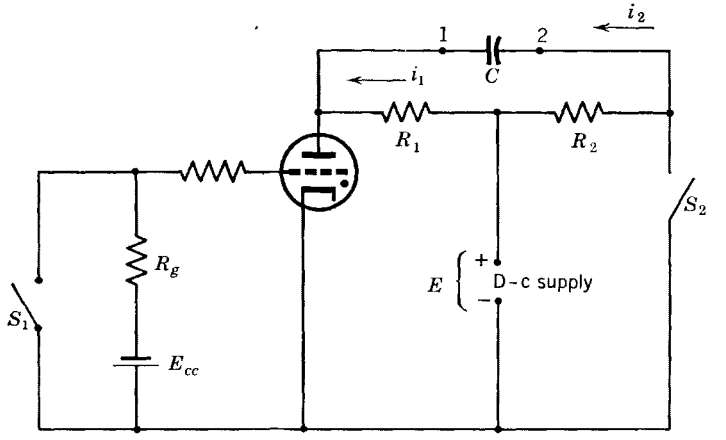

FIG. 5-14. Parallel control of thyratron anode current.

since terminal 2 is positive, terminal 1 negative, the anode becomes negative with respect to the cathode; the cathode emission current is held at the positive cathode, deionization occurs, and the anode current is interrupted. Meanwhile, if S_1 has been opened, the grid regains control, provided that the anode voltage does not reach the reignition value

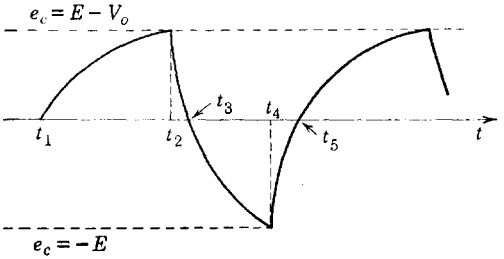

FIG. 5-15. Capacitor voltage versus time curve for the circuit of Fig. 5-14.

before sufficient deionization has occurred. With S_2 closed and the tube not conducting, the capacitor begins to charge in the opposite direction through S_2 and ultimately would reach the supply potential E, with terminal 1 positive. A graph of capacitor voltage versus time for the sequence of events just described is shown in Fig. 5-15. The original

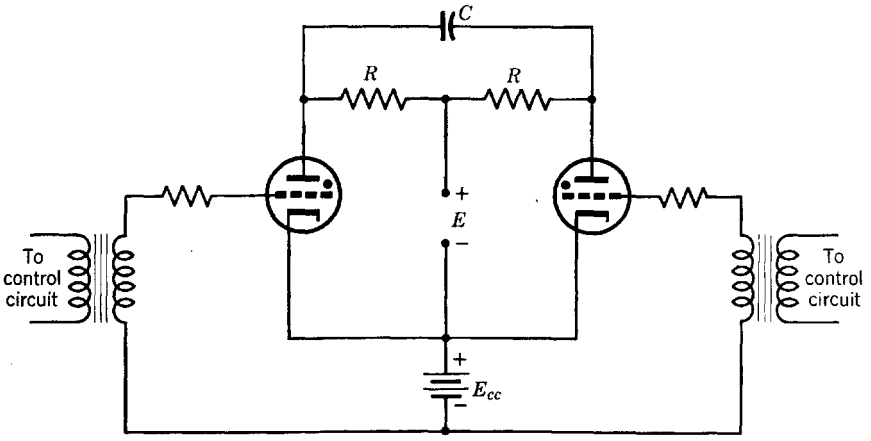

FIG. 5-16. Basic counter or inverter circuit.

direction of capacitor voltage, with the potential of terminal 2 greater than that of terminal 1 by $(E - V_o)$ volts, is shown as a positive voltage, and the reverse, with terminal 1 at a higher potential than 2, is shown as negative on the graph. At time t_1, switch S_1 closes, the tube fires and the capacitor begins to charge. At t_2 switch S_2 closes, S_1 opens,

and the capacitor begins to discharge. At t_3 the capacitor discharge is complete, and the capacitor begins to charge in the opposite direction. If, at t_4, switch S_1 closes (S_2 opens), the tube fires and the capacitor again discharges. At t_5 the entire sequence of events begins to repeat.

In applications of the basic circuit of Fig. 5-14, switch S_1 may be controlled, as a relay, by a phototube or high-vacuum-tube circuit or both. If S_2 is replaced by another thyratron, the circuit is that of Fig. 5-16. The graph of Fig. 5-15 applies to the circuit of Fig. 5-16 except that the lower extreme value of voltage is $e_c = -(E - V_o)$ instead of $-E$, since the thyratron acts as an imperfect switch requiring a volt-

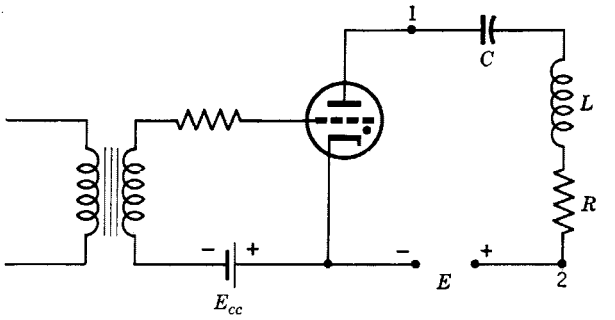

FIG. 5-17. Basic series control circuit.

age of V_o volts to keep it closed. The circuit of Fig. 5-16 is the fundamental circuit for the parallel inverter, to be described later, and has been used for high-speed counting.

Another method of d-c control is that illustrated by the circuit of Fig. 5-17, in which the capacitor C is in series with the inductive load and the supply voltage. The anode current is the charging current $C\,de_c/dt$ of the capacitor. Before firing, the tube itself acts as a condenser of small capacitance, plate to cathode, in series with C. Since the induced charges on the two series capacitors will be equal, the greater voltage q/C_{pk}, will exist across the tube. When the tube fires as a result of a positive grid impulse from the control circuit, the following relation is an expression of Kirchhoff's voltage law for the plate circuit:

$$E = RC\,de_c/dt + LC\,d^2e_c/dt^2 + e_c + V_o \qquad (5\text{-}7)$$

Since current can flow only while the capacitor is charging, the anode circuit will be open when the capacitor becomes fully charged. The solution of Eq. 5-7 for the condition $R^2/4L^2 < 1/LC$ is

$$e_c = \epsilon^{-at}(A \cos bt + B \sin bt) + (E - V_o)$$

where $a = R/2L, \qquad b = \sqrt{1/LC - R^2/4L^2}$

If $C \gg C_{pk}$, then $q_0/C \ll q_0/C_{pk}$, where q_0 = the initial capacitor charge before the tube fires. Neglecting the initial value of e_c before the tube fires, the following boundary conditions may be used:

(1) $e_c = 0$ at $t = 0$
(2) $i = 0$ at $t = 0$

From these,

$$A = -(E - V_o)$$

$$B = -\frac{a}{b}(E - V_o)$$

and
$$e_c = (E - V_o)\left[1 - \epsilon^{-at}\left(\frac{b \cos bt + a \sin bt}{b}\right)\right] \qquad (5\text{-}8)$$

The solution in Eq. 5-8 does not take into account the fact that the voltage across the tube will change suddenly from V_o to a much larger

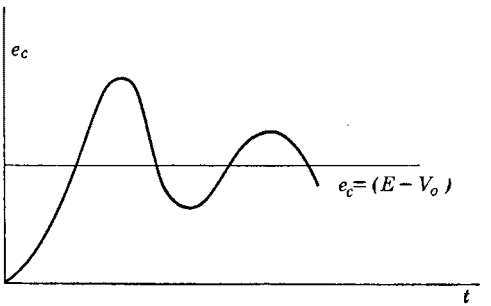

FIG. 5-18. Sketch of the graph of Equation 5-8 for small resistance R.

value when the current i becomes too small and deionization occurs. However, the equation does show that the capacitor voltage oscillates about the value $(E - V_o)$ and would ultimately approach that value if the tube continued to conduct and the tube drop remained constant at V_o. By differentiation of Eq. 5-8 the maximum value of e_c may be shown to approximate $2(E - V_o)$ for R small. The graph of Fig. 5-18 shows the theoretical variation of e_c with time after the tube fires.* For R large, the circuit is not oscillatory, and the maximum value of e_c is the limiting value, $(E - V_o)$.

In order for the tube to fire again, the capacitor must be discharged. This may be accomplished by the use of another thyratron. If the second thyratron is connected with its cathode to terminal 1 and its anode to terminal 2 (Fig. 5-17), the capacitor would discharge through tube 2

* Assuming that the tube continues to conduct as a switch.

and load impedance, but, if tube 1 were still conducting, the d-c supply would be short-circuited. In order to avoid this, the circuit of Fig. 5-19 may be used.

In Fig. 5-19, if tube 1 is conducting when tube 2 fires, but, if at that time the capacitor is nearly charged, then the capacitor discharge current flows in the direction i_{32} through the inductance L_1. The induced voltage in L_1, opposing this current is such as to make terminal 1, and therefore the anode of tube 1 negative, so that the arc is extinguished in tube 1. If L is the primary of a transformer, the circuit becomes that

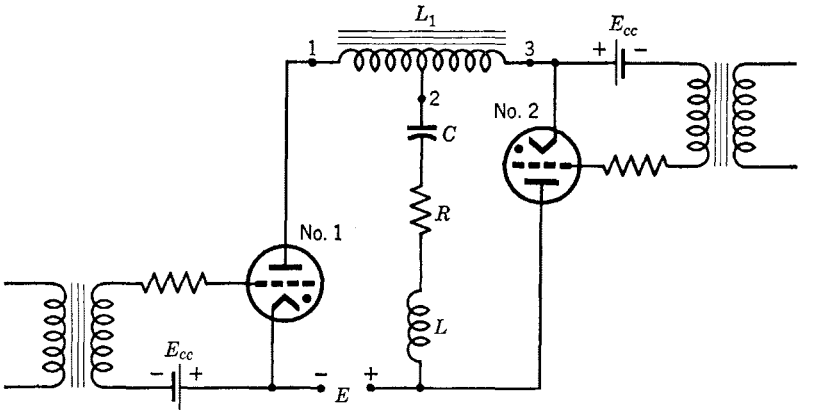

FIG. 5-19. Series control or series inverter using two tubes.

of a series inverter in which an a-c output is available at the secondary of the transformer. The grid-control circuits may be controlled either from a separate a-c source or from the proper selection of constants to provide an oscillating, self-excited circuit. In the former case, the frequency of the a-c output is controlled by the frequency of the grid supply; in the self-excited circuit, it is controlled by the circuit constants.

The circuit of Fig. 5-20 is that of a parallel inverter. An inverter is a circuit providing a-c power from a d-c source. The behavior of the circuit has been briefly explained in the discussion of Fig. 5-16. Inverters have been developed that technically would make possible long-distance d-c power transmission, and this may eventually become an important electronic application in the power field. Power would be generated as alternating current, perhaps at some remote waterfall, such as Victoria Falls in Africa. The voltage would then be raised by high-voltage stepup transformers to 300 kv, or more. This would be rectified and then transmitted by means of a d-c transmission line. Because of the capacitance and inductance of long transmission lines, it is impossible to transmit

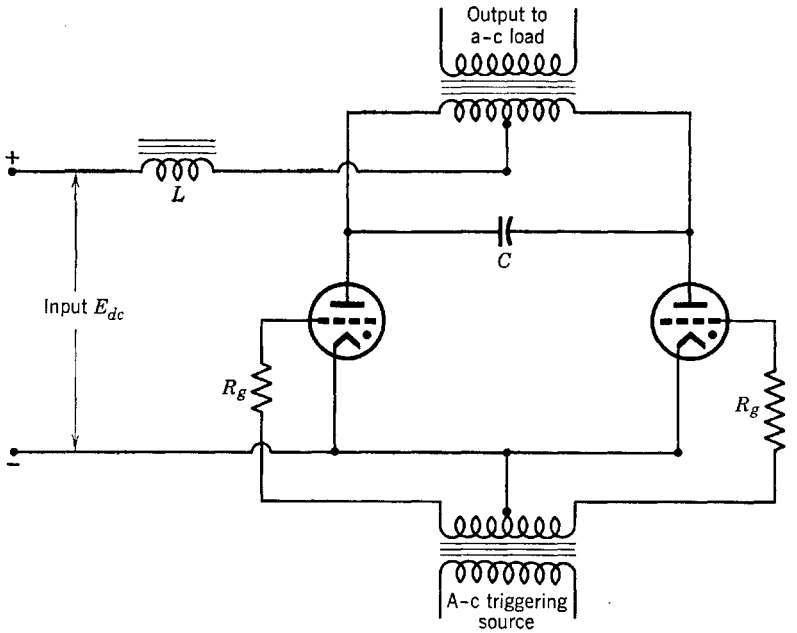

FIG. 5-20. Parallel inverter.

even commercial power frequencies a distance of 900 miles, approximately the distance of Victoria Falls from the nearest industrial center. But, with d-c transmission, power could be transmitted at high voltage much longer distances. To be used at the receiving end, however, the high voltage must be reduced. The first step in this process is efficient inversion to alternating current and then transformation downward to the 2300, 440, 220, or 110 volts alternating current used for distribution and utilization. As has been stated, such a process is entirely feasible, technically. It has not as yet become justified, economically.

PROBLEMS

5-1. An RCA VR-105 tube is used as a voltage regulator in the circuit of Fig. 5-6. If the load current varies from a minimum of 40 to a maximum of 65 ma, what value of resistance R should be used? (Note: the operating range, Fig. 5-2.) D-c supply voltage = 125 volts.

5-2. Using the value of R determined in problem 5-1, how much supply voltage fluctuation is possible without changing the output voltage, if the load current remains fixed at 50 ma?

5-3. Derive completely Eq. 5-3.

5-4. A thyratron is used in the relaxation circuit of Fig. 5-8. The tube is a WL-631 (Fig. 5-10), operating at a condensed mercury temperature of 40° C. A 50-ohm re-

sistor is used in the anode circuit of the thyratron, R of Fig. 5-8 is 200,000 ohms, $C = 0.02$ μf. It is desired that the tube fire at 400 volts. Draw a circuit diagram showing all circuit elements. Assume a tube voltage drop of 15 volts when conducting and that $E = 2000$ volts. The tube circuit opens at an anode current of 15 ma. Find (*a*) grid-bias voltage required, (*b*) frequency of the saw-tooth wave, (*c*) the time required, approximately, for the capacitor to discharge when the tube fires.

5-5. In the circuit of Fig. 5-16, $C = 2$ μf, $R = 1000$ ohms, tube drop is 15 volts, $E = 250$ volts direct current.

(*a*) When tube 1 fires and steady conditions have been reached, what are the currents through the resistors and the voltages, relative to cathode, of the anodes?

(*b*) Tube 2 fires. Draw an equivalent circuit, and find how long a time is required for the capacitor voltage to pass through zero.

(*c*) Sketch the voltage across the capacitor, assuming that each tube fires when capacitor voltage reaches 215 volts. Approximate the frequency of the capacitor voltage wave.

5-6. If the charging current of the capacitor in Fig. 5-8 is constant and equal to I, show that (neglecting capacitor discharge time) the frequency of oscillation of the resulting saw-tooth wave is

$$f = 1/C(E_i - E_e)$$

and is therefore independent of the magnitude of the supply voltage.

5-7. Draw a wiring diagram showing how a pentode might be used instead of R in Fig. 5-8 to provide a constant charging current. If the pentode used is a 6J7 operated at $E_{c1} = -3$ volts, $E_{c2} = 100$ volts, compute the oscillation frequency if $E_i = 110$ volts, $E_e = 10$ volts, $C = 2$ μf.

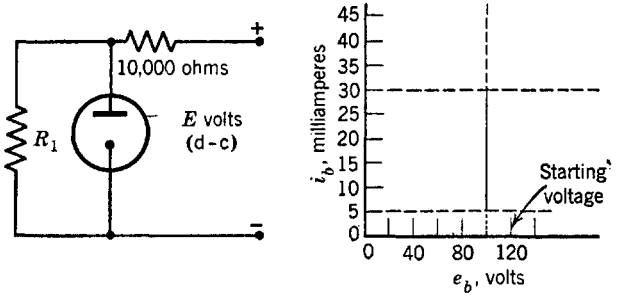

FIG. P5-8.

5-8. The characteristic for the glow-discharge tube T is given by the i_b–e_b graph.

(*a*) If $R_1 = 10{,}000$ and $E = 300$ volts, find the voltage across R_1, the current in each resistor, and the tube current, if the tube is conducting.

(*b*) What are the maximum and minimum values of E such that the voltage across R_1 remains constant and the tube current does not go above 30 nor below 5 ma?

CHAPTER 6

SINGLE-PHASE RECTIFIERS AND POWER SUPPLIES

ELECTRIC POWER IS GENERATED AS ALTERNATING CURRENT. WHEN d-c power is required, conversion from alternating to direct current is accomplished by use of a commutator on the shaft of the generator, or by the use of rectifiers. By definition:[1] "A rectifier is a device which converts alternating current into unidirectional current by virtue of a characteristic permitting appreciable flow of current in only one direction."

Oxides of copper and of selenium have rectifying properties and are widely used for low-voltage applications. A vacuum tube conducts only when its anode is positive with respect to its cathode and, as shown for the diode of Chapter 1, may be used as a rectifier. The discussion of this chapter will be confined to thermionic high-vacuum-tube rectifiers and to gas-filled thermionic and mercury-pool cathode-tube rectifiers in single-phase circuits. Such equipment may be used to supply d-c power in many applications, particularly to vacuum-tube plate circuits.

6-1. The Half-Wave Rectifier Circuit

The tube of Fig. 6-1 will conduct current only during that portion of the transformer secondary a-c cycle during which the tube anode is positive with respect to its cathode. The positive half-cycle is shown in Fig. 6-1*c*. If the tube is a high-vacuum diode, the anode current will begin to flow when the anode becomes positive, as indicated in Fig. 6-1*c*. If the tube is a gas-filled diode, current will not flow until the anode-to-cathode voltage has reached the breakdown value. This occurs when $e = E_i$, $\omega t = \alpha_i$, as shown in Figs. 6-1*b* and *e*. The idealized tube characteristics are shown in Figs. 6-1*d* and *f*. It is assumed in the drawings that the breakdown voltage is equal to the tube drop.

The current through the load resistance R of Fig. 6-1*a* is unidirectional but pulsating. From the point of view of Fourier analysis of the wave

[1] *American Standard Definitions of Electrical Terms*, p. 79, published by AIEE.

form, the current i has a d-c or average value and many a-c harmonic components. An important measure of rectifier circuit performance is the ripple voltage, which is defined as the alternating component of the unidirectional voltage. The per cent ripple is defined as the ratio of the effective or root-mean-square value of the ripple voltage to the average or d-c value of the total voltage, expressed in per cent. Other criteria

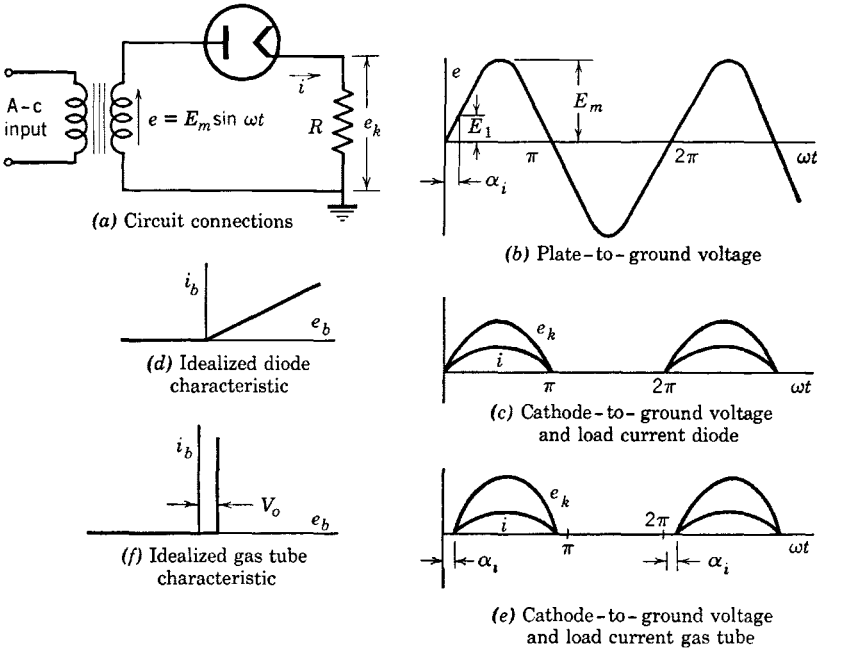

FIG. 6-1. Half-wave rectifier circuit and wave forms.

of rectifier circuits used as power supplies are voltage regulation, power output, and efficiency. The definitions of these quantities are the same as for any other electrical equipment to which they may apply.

6-2. The Half-Wave-Rectifier High-Vacuum Tube Circuit

An ideal rectifier would have the properties of a perfect switch, closing when the voltage is in the forward or conducting direction, and opening when the voltage reverses. The idealized tube characteristic of Fig. 6-1*d* is the characteristic of an ideal rectifier in series with a resistance R_b of value determined by the slope of the tube i_b–e_b characteristic. An expression for the current i, approximate because R_b is not a constant,

may then be written as follows:

$$0 < \omega t < \pi, \qquad i = \frac{e}{R + R_b} = \frac{E_m}{R + R_b} \sin \omega t \tag{6-1}$$

$$\pi < \omega t < 2\pi, \qquad i = 0$$

The maximum value of the output voltage e_k is then $\frac{E_m}{R + R_b} R$. The average or direct current is defined by the relation

$$I_{dc} = \frac{1}{2\pi} \int_0^{2\pi} i \, d(\omega t) = \frac{1}{2\pi} \int_0^{\pi} I_m \sin \omega t \, d(\omega t) \tag{6-2}$$

where $$I_m = E_m/(R + R_b)$$

From Eq. 6-2,

$$I_{dc} = \frac{1}{\pi} I_m = \frac{E_m}{\pi(R + R_b)} \tag{6-3}$$

and $$E_{dc} = I_{dc}R = \frac{E_m R}{\pi(R + R_b)} = \frac{1}{\pi}\left(\frac{E_m}{1 + R_b/R}\right) \tag{6-4}$$

If the origin for the load current is chosen as in Fig. 6-2, the Fourier analysis of the wave may be carried out in the usual way [2] by evaluating

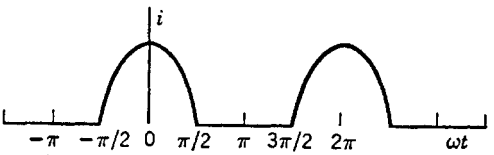

FIG. 6-2. Load-current wave form.

only the cosine coefficients. Because of the choice of origin, no sine terms will be obtained. Then

$$B_n = \frac{1}{\pi} \int_{-\pi}^{\pi} i \cos n(\omega t) \, d(\omega t) \tag{6-5}$$

Equation 6-5 applied to Fig. 6-2 yields the expression

$$B_n = \frac{I_m}{\pi}\left(\frac{-2}{n^2 - 1}\right) \cos \frac{n\pi}{2}, \qquad n \neq 1 \tag{6-6}$$

[2] K. Y. Tang, *Alternating Current Circuits*, Chap. 17, 2d Ed., International Textbook Co.

For $n = 1$, Eq. 6-5 shows that

$$B_1 = I_m/2$$

The Fourier series for the current i is then as follows:

$$i = \frac{I_m}{\pi}\left(1 + \frac{\pi}{2}\cos \omega t + \frac{2}{3}\cos 2\omega t - \frac{2}{15}\cos 4\omega t + \frac{2}{35}\cos 6\omega t - \frac{2}{63}\cos 8\omega t \cdots -\right) \quad (6\text{-}7)$$

$$-\pi/2 < \omega t < \pi/2, \qquad i = I_m \cos \omega t$$

$$-\pi < \omega t < -\pi/2 \quad \text{or} \quad \pi/2 < \omega t < \pi, \qquad i = 0$$

The current is shown, by Eq. 6-7, to contain the fundamental and all the even harmonics of the supply frequency. If the effective value of the voltage e_k is required, it may be obtained from the current series by multiplying by R and applying the fundamental relation [2] that the effective value E of the voltage of any nonsinusoidal wave is given by the square root of the sum of the squares of the average and of the effective values of the harmonic components. Thus, if E_1, E_2, E_4, E_6, E_8, etc. are the effective values of the respective harmonic components in the wave $e_k = iR$, then

$$E = \sqrt{E_{dc}^2 + E_1^2 + E_2^2 + E_4^2 + \cdots + E_n^2} \quad (6\text{-}8)$$

In the same way, the effective value of the a-c portion of the voltage wave is expressed as

$$E_{ac} = \sqrt{E_1^2 + E_2^2 + E_4^2 + \cdots + E_n^2} \quad (6\text{-}9)$$

From Eqs. 6-8 and 6-9,

$$E_{ac} = \sqrt{E^2 - E_{dc}^2} \quad (6\text{-}10)$$

The ripple factor, by definition, is expressed as the ratio

$$r = \frac{E_{ac}}{E_{dc}} = \frac{\sqrt{E^2 - E_{dc}^2}}{E_{dc}} = \frac{\sqrt{I^2 - I_{dc}^2}}{I_{dc}} = \sqrt{\frac{E^2}{E_{dc}^2} - 1} \quad (6\text{-}11)$$

where I represents the effective current of the nonsinusoidal wave. For the half-wave vacuum-tube rectifier, the effective voltage is obtained by definition from the relation

$$E = RI = R\sqrt{\frac{1}{2\pi}\int_{-\pi}^{\pi} i^2\, d(\omega t)}$$

The current i is expressed as in Fig. 6-2. The result is

$$E = R[I_m/2] \tag{6-12}$$

From Eqs. 6-4 and 6-12

$$E_{dc} = (I_m/\pi)R \quad \text{and} \quad E/E_{dc} = \pi/2$$

Then,
$$r = \sqrt{\pi^2/4 - 1} = 1.21 \tag{6-13}$$

and the per cent ripple is 121 per cent.

Examination of Eq. 6-4 shows that the circuit load voltage may be expected to vary considerably with variation of R unless R is always much larger than R_b. Equation 6-4 may also be rearranged as follows:

$$I_{dc}(R + R_b) = E_m/\pi \tag{6-4a}$$

$$I_{dc}R = E_{dc} = E_m/\pi - I_{dc}R_b \tag{6-14}$$

Equation 6-14 shows that the no-load direct voltage is equal to E_m/π but that the voltage decreases linearly with current at a rate dependent upon the magnitude of R_b. An expression for the voltage regulation in terms of the load current may be obtained from Eq. 6-14.

The d-c power output of the rectifier is expressed as the product of the d-c components of current and voltage, or, from Eqs. 6-3 and 6-4,

$$P_o = E_{dc}I_{dc} = E_m{}^2R/\pi^2(R + R_b)^2 \tag{6-15}$$

The power supplied by the secondary of the transformer delivering effective current I may be expressed as

$$P_{\text{in}} = I^2(R + R_b)$$

where, from Eq. 6-12, $I = E/R = I_m/2 = E_m/2(R + R_b)$

Then,
$$P_{\text{in}} = E_m{}^2/4(R + R_b)$$

and the efficiency of rectification is given by

$$\eta = \frac{P_o}{P_{\text{in}}} = \frac{4R}{\pi^2(R + R_b)} = \frac{0.406}{1 + R_b/R} \tag{6-16}$$

The theoretical maximum efficiency of the half-wave vacuum rectifier is evidently 40.6 per cent. It may easily be shown from Eq. 6-15 that the maximum power output occurs for $R = R_b$. For this value of load resistance the efficiency of rectification is only 20.3 per cent. The dependence of the efficiency of rectification upon the load current is

conveniently shown by rearranging Eq. 6-16 with the aid of Eqs. 6-4*a* and 6-14. The result is

$$\eta = 0.406\left(1 - \frac{\pi}{E_m} I_{dc} R_b\right) \tag{6-17}$$

Example problem. The plate resistance of a certain rectifier tube is obtained from its plate characteristic by assuming the characteristic to be a straight line passing through the origin and one point on the characteristic. If $R_b = 500$ ohms, and the tube is connected as a half-wave rectifier with a load resistance of 5000 ohms, find the output current and voltage (direct), the power output, and the rectifier efficiency if the transformer secondary voltage is 350 volts (rms).

Solution.

$$E_m = 350\sqrt{2} = 495 \text{ volts} \quad \text{from Fig. 6-1}a$$

$$I_m = E_m/(R + R_b) = 495/5500 = 0.09 \text{ amp} = 90 \text{ ma}$$

$$I_{dc} = I_m/\pi = 28.6 \text{ ma}$$

$$E_{dc} = RI_{dc} = 143.0 \text{ volts}$$

$$P_o = E_{dc}I_{dc} = 4.1 \text{ watts}$$

The effective current in the transformer secondary winding is

$$I = I_m/2 = 45 \text{ ma}$$

$$P_{\text{in}} = (45)^2 \cdot 10^{-6}(5500) = 11.13 \text{ watts}$$

$$\eta = 4.1/11.13 = 0.368 \quad \text{or } 36.8 \text{ per cent}$$

or

$$\eta = \frac{0.406}{1 + 500/5000} = \frac{0.406}{1.1} = 0.368$$

6-3. The Full-Wave Vacuum-Tube-Rectifier Circuit

The negative half-cycle of the applied voltage wave of Fig. 6-1 may also be utilized if applied to the anode of another tube, or to a second anode in the same tube, connected as shown in Fig. 6-3*a* to the center-tapped secondary winding of a transformer. When anode 1 is negative, anode 2 is positive, and current continues to flow through R in the direction shown. If the potential difference between the two ends of the secondary winding at any instant is 20 volts, with, for example, anode 2 positive, then anode 2 is 10 volts higher in potential than the

ground or mid-tap connection, and anode 1 is 10 volts lower than ground. At every instant, the voltages of anodes 1 and 2 with respect to ground are equal but opposite. This may be expressed mathematically by the relations

$$e_1 = E_m \sin \omega t \tag{6-18}$$

$$e_2 = -E_m \sin \omega t = E_m \sin (\omega t + 180°)$$

The secondary voltage rise may be expressed as

$$e_{21} = -e_2 + e_1 = 2E_m \sin \omega t$$

The voltage wave forms of Eq. 6-18 are shown in Fig. 6-3*b*, and the load

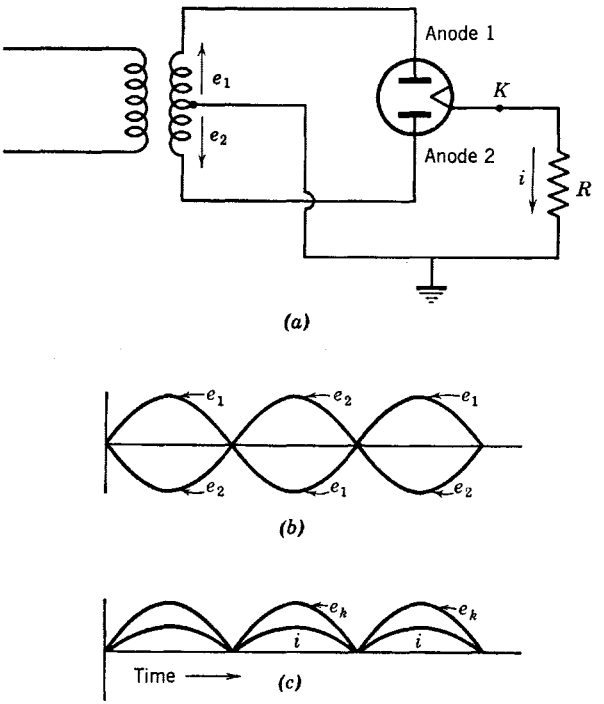

FIG. 6-3. Full-wave rectifier circuit—high-vacuum tube. (*a*) Full-wave circuit. (*b*) Applied anode-to-ground voltage. (*c*) Load voltage and current.

current and voltage, cathode to ground, in Fig. 6-3*c*. As shown in Fig. 6-3*b*, anode 1 conducts during the half-cycle in which it is positive; then the current shifts to anode 2 as the voltage of anode 1 falls below zero and that of anode 2 becomes positive. The currents i_1 and i_2 of anodes 1 and 2 are identical in form, but i_2 is displaced 180° along the

time axis from i_1. If an origin is chosen as shown for Fig. 6-2, the Fourier series for i_1 is (from Eq. 6-7)

$$i_1(\omega t) = \frac{I_m}{\pi}\left(1 + \frac{\pi}{2}\cos \omega t + \frac{2}{3}\cos 2\omega t - \frac{2}{15}\cos 4\omega t + \frac{2}{35}\cos 6\omega t - \cdots\right) \tag{6-7}$$

while

$$i_2 = i_1(\omega t + \pi)$$

$$= \frac{I_m}{\pi}\left(1 - \frac{\pi}{2}\cos \omega t + \frac{2}{3}\cos 2\omega t - \frac{2}{15}\cos 4\omega t + \frac{2}{35}\cos 6\omega t - \cdots\right) \tag{6-7a}$$

The current i through the load may be obtained as the sum of $i_1 + i_2$ or

$$i = \frac{2}{\pi} I_m\left(1 + \frac{2}{3}\cos 2\omega t - \frac{2}{15}\cos 4\omega t + \frac{2}{35}\cos 6\omega t + \cdots -\right) \tag{6-19}$$

Since the load current does not contain the fundamental, smoothing or filtering the output is easier than for the half-wave circuit. The d-c components of the tube currents flow through the secondary winding in opposite directions, and as a result d-c magnetization of the core is avoided, and the necessary a-c magnetizing component is smaller than that required by the half-wave circuit. The secondary instantaneous ampere turns may be expressed as $N_2(i_1 - i_2)$, where N_2 is the total secondary turns. The primary ampere turns for a primary load current of i_0 would be $i_0 N_1$. Then, $i_0 N_1 = N_2(I_m \cos \omega t)$, obtained by subtracting i_2 (Eq. 6-7a) from i_1 (Eq. 6-7). Since the primary load current is sinusoidal, transformer efficiency is higher, and inductive interference with telephone and other communication circuits is much less than in the case of the half-wave circuit. In Fig. 6-3 with the origin as in c the load current and voltage, a-c and d-c components may be expressed as follows:

$$-\frac{\pi}{2} < \omega t < \frac{\pi}{2}, \qquad i = \frac{E_m}{R_b + R}\cos \omega t, \qquad e_1 = E_m \cos \omega t$$

$$\frac{\pi}{2} < \omega t < 3\frac{\pi}{2}, \qquad i = -\frac{E_m}{R_b + R}\cos \omega t, \qquad e_2 = -E_m \cos \omega t \tag{6-20}$$

The peak value of the rectified current wave is

$$I_m = E_m/(R_b + R) \tag{6-21}$$

and the effective value of the rectified current is

$$I = \sqrt{\frac{1}{2\pi}\int_{-\pi}^{\pi} i^2\, d(\omega t)} = \frac{I_m}{\sqrt{2}} \tag{6-22}$$

The effective a-c value of the rectified voltage wave is

$$E = RI = RI_m/\sqrt{2} \tag{6-23}$$

and the average or direct load current is

$$I_{dc} = (2/\pi)I_m \tag{6-24}$$

The direct load voltage is

$$E_{dc} = RI_{dc} = \frac{2}{\pi} I_m R = \frac{2}{\pi}\frac{E_m}{1 + R_b/R} = \frac{2}{\pi}E_m - R_b I_{dc} \tag{6-25}$$

The ripple factor is

$$r = E_{ac}/E_{dc} = \sqrt{E^2 - {E_{dc}}^2}/E_{dc}$$

Since

$$\frac{E}{E_{dc}} = \frac{RI_m/\sqrt{2}}{(2/\pi)RI_m} = \frac{\pi}{2\sqrt{2}}$$

$$r = \sqrt{\frac{\pi^2}{8} - 1} = 0.48 \tag{6-26}$$

The power output, power input to the rectifier and the efficiency are obtained as for the half-wave case.

$$P_o = E_{dc}I_{dc} = (4/\pi^2){I_m}^2 R \tag{6-27}$$

$$P_{\text{in}} = I^2(R + R_b) = ({I_m}^2/2)(R + R_b) \tag{6-28}$$

$$\eta = \frac{P_o}{P_{\text{in}}} = \frac{8}{\pi^2}\left(\frac{1}{1 + R_b/R}\right)$$

$$= \frac{0.812}{1 + R_b/R} = 0.812\left(1 - \frac{\pi}{2E_m}R_b I_{dc}\right) \tag{6-29}$$

The theoretical maximum efficiency of the full-wave rectifier is then just twice that of the half-wave rectifier, and the per cent ripple has been reduced from 121 to 48.

6-4. The Full-Wave-Rectifier Circuit with Gas-Filled Tubes

The conduction period during the positive half-cycle of a gas-filled diode rectifier is somewhat less than 180° because the tube does not begin to conduct until the anode voltage exceeds the critical value E_i of Fig. 6-1*a* and ceases to conduct when the anode voltage falls below this value. The ignition voltage E_i is equal, practically, to the operating tube drop V_o. The wave forms of transformer secondary voltage e_1 and e_2 and of output voltage and current are shown in Fig. 6-4 for a gas-filled tube in a circuit identical with that of Fig. 6-3*a*. The con-

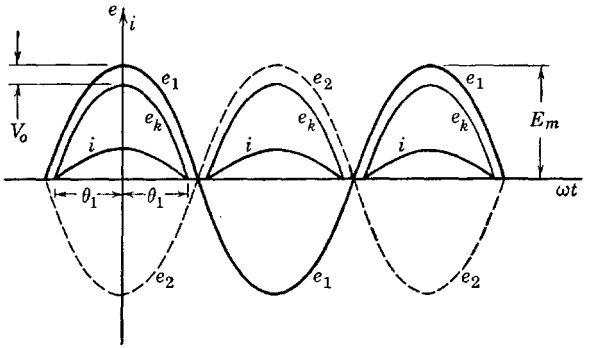

FIG. 6-4. Wave forms of input and output voltage and output current of a full-wave rectifier using gas-filled tubes.

duction period extends over an interval of 2θ rad in each anode's positive half-cycle. For anode 1, i_1 becomes zero when $e_1 = V_o$, or

$$\cos\theta = V_o/E_m \tag{6-30}$$

For mercury-vapor tubes, V_o is usually between 10 and 20 volts. If $E_m = 500$ volts, $V_o = 15$ volts, $\theta \cong 88.3°$. In this case, little error would result if tube drop were neglected.

During the conduction period for anode 1, the expression for current i may be obtained by applying Kirchhoff's voltage law,

$$i = \frac{E_m \cos\omega t - V_o}{R}, \qquad -\theta < \omega t < \theta \tag{6-31}$$

The load voltage e_k is

$$e_k = iR = E_m \cos\omega t - V_o \tag{6-32}$$

The curves for these equations have been plotted in Fig. 6-4, in which the ratio V_o/E_m has been made large enough that curves for e_k and e_1

are easily distinguishable. The average output voltage E_{dc} as obtained from Eq. 6-32 is as follows:

$$E_{dc} = \frac{1}{\pi}\int_{-\theta}^{\theta}(E_m \cos \omega t - V_o)\, d(\omega t)$$

$$= \frac{2}{\pi}E_m\left(\sin\theta - \frac{V_o}{E_m}\theta\right) \tag{6-33}$$

The average output current is

$$I_{dc} = \frac{E_{dc}}{R} = \frac{2}{\pi R}E_m\left(\sin\theta - \frac{V_o}{E_m}\theta\right) \tag{6-34}$$

The d-c power output is

$$P_{dc} = E_{dc}I_{dc} = \frac{4E_m^2}{\pi^2 R}\left(\sin\theta - \frac{V_o}{E_m}\theta\right)^2 \tag{6-35}$$

The average power input to the rectifier is given by

$$P_{\text{in}} = \frac{1}{\pi}\int_{-\pi/2}^{\pi/2} e_1 i\, d(\omega t) = \frac{2}{\pi}\int_0^{\theta} E_m \cos\omega t\left(\frac{E_m \cos\omega t - V_o}{R}\right) d(\omega t)$$

$$= \frac{E_m^2}{\pi R}\left(\theta - \frac{V_o}{E_m}\sin\theta\right) \tag{6-36}$$

Finally, the rectifier efficiency is expressed as

$$\eta = \frac{P_{dc}}{P_{\text{in}}} = \frac{4}{\pi}\left[\frac{(\sin\theta - V_o/E_m\theta)^2}{(\theta - V_o/E_m \sin\theta)}\right] \tag{6-37}$$

If V_o/E_m is small enough that θ is approximately $\pi/2$, $\sin\theta = 1$; then the expression for efficiency becomes

$$\eta = \frac{8}{\pi^2}\left[\frac{(1 - \pi V_o/2E_m)^2}{1 - 2V_o/\pi E_m}\right] \tag{6-38}$$

The maximum theoretical efficiency would be obtained if $V_o = 0$. From Eq. 6-38 for $V_o = 0$, $\eta = 0.812$, which is the same as the maximum theoretical efficiency of the high-vacuum-tube full-wave circuit. However, the efficiency is independent of the load, which is a rather important gas-tube rectifier property, not possessed by the high-vacuum tube circuit.

If tube drop is neglected, the ripple factor for the full-wave rectifier using vapor tubes is the same as for the high-vacuum-tube full-wave circuit, but is greater with decreasing values of conduction angle 2θ.

6-5. Filters

Circuit elements which store energy, e.g. capacitors and inductors, may be used to reduce the ripple in the rectifier output. Combinations of capacitances and inductances used to reduce ripple in a rectifier output are known as filters. The action of the filter is to store energy when the rectifier voltage is high and to discharge energy to the load when the rectifier voltage drops. The behavior of single filter elements will be considered first, and combinations of capacitive and inductive elements will then be discussed.

6-6. The Capacitance Filter

A full-wave circuit with capacitance filter and gas-filled tubes is shown in Fig. 6-5*a*. It will be shown in the discussion to follow that such a filter should not be used with vapor-type tubes, but may be used with

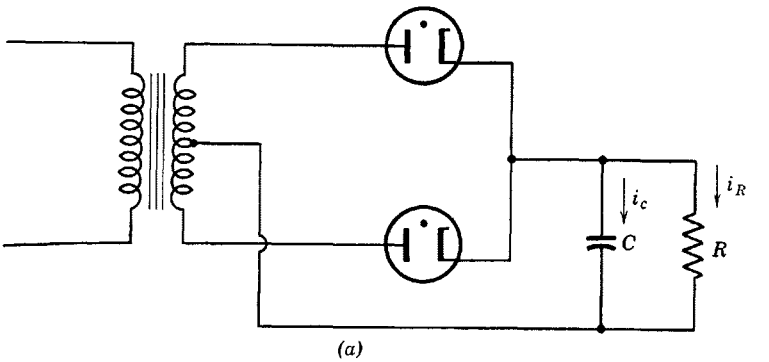

(*a*)

FIG. 6-5*a*. Full-wave rectifier with capacitance filter.

high-vacuum tubes. In Fig. 6-5, the positive half-cycles of voltage are shown for each tube. The current i_c through the capacitor is determined by the time rate of change of the voltage across the capacitor. If e_c is this voltage,

$$i_c = C\, de_c/dt \tag{6-39}$$

The voltage across the resistor is always the same as that across the capacitor, since they are in parallel. The current i_R in the resistor is then

$$i_R = e_c/R \tag{6-40}$$

and the tube current i is the sum

$$i = i_c + i_R = C\, de_c/dt + e_c/R \tag{6-41}$$

The current is limited by the restriction that it can never become negative since the tubes conduct only in the positive direction. If at any instant i becomes zero, then the load current i_R will be determined entirely by the discharge of the capacitor, for the tubes will deionize, and the circuit from transformer to load will be open.

In the analysis of the circuit of Fig. 6-5*a*, $t = 0$ will be chosen at the instant when the applied voltage e_1 has reached its positive maximum, or

$$e_1 = E_m \cos \omega t \tag{6-42}$$

If the tube drop is V_o volts when conducting,

$$e_c = e_1 - V_o = E_m \cos \omega t - V_o \tag{6-43}$$

and, at $t = 0$, $de_c/dt = 0$, and the capacitor current is zero. Tube 1 will be conducting, and the tube current will be

$$i = i_c + i_R = C \frac{d}{dt}(E_m \cos - V_o) + \frac{E_m \cos \omega t - V_o}{R}$$

$$= -\omega C E_m \sin \omega t + \frac{E_m \cos \omega t - V_o}{R} \tag{6-44}$$

Equation 6-44 will hold as long as the current is positive, that is, until $i = 0$. If $\omega t_1 = \theta_1$ when $i = 0$, then, if tube drop is neglected,

$$E_m/R \cos \theta_1 = \omega C E_m \sin \theta_1$$

or

$$\tan \theta_1 = 1/\omega CR \tag{6-45}$$

The angle θ_1 may be referred to as the "cutout" angle. After i becomes zero, Eq. 6-41 may be solved for e_c. Thus,

$$0 = C\, de_c/dt' + e_c/R \tag{6-46a}$$

and

$$e_c = A\epsilon^{-t'/RC} \tag{6-46b}$$

where t' is measured from that time at which $i = 0$. Then, referred to the original time axis,

$$t' = t - t_1$$

or

$$\omega t' = \omega t - \theta_1 \tag{6-47}$$

Equation 6-46 now becomes

$$e_c = A\epsilon^{-(\omega t - \theta_1)/\omega CR} \tag{6-48a}$$

and, since $e_c = E_m \cos \theta_1$ (neglecting tube drop) when $\omega t = \theta_1$, then

$$A = E_m \cos \theta_1$$

and

$$e_c = (E_m \cos \theta_1)\epsilon^{-(\omega t - \theta_1)/\omega CR} \tag{6-48b}$$

Equation 6-48*b* will hold for values of ωt between θ_1 and the value $\omega t_2 = \theta_2$ at which tube 2 fires. With C charged to a potential e_c, the voltage across tube 2 will not actually become positive, and the tube cannot fire, until e_2 exceeds e_c by the amount of the voltage V_o. Again neglecting tube drop, tube 2 fires when the rising voltage e_2 equals the exponentially decreasing voltage e_c as given by equation 6-48*b*. Then, when tube 2 fires,

$$E_m \cos \theta_1 \epsilon^{-(\theta_2 - \theta_1)/\omega CR} = -E_m \cos \theta_2$$

or

$$\epsilon^{\theta_1/\omega CR} \cos \theta_1 \epsilon^{-\theta_2/\omega CR} = -\cos \theta_2 \tag{6-49}$$

Equation 6-49 is most conveniently solved for θ_2 by plotting the curves

$$y_1 = k_1 \epsilon^{-(\theta_2/\omega CR)} \quad \text{where} \quad k_1 = \epsilon^{\theta_1/\omega CR} \cos \theta_1$$

and

$$y_2 = -\cos \theta_2$$

with θ_2 as abscissa. The angle θ_2 may be called the "cut-in" angle.

The curves of Fig. 6-5 show the effect of the capacitor upon the output voltage. During the interval $\theta_1 < \omega t < \theta_2$, the load voltage is prevented from dropping to zero by the capacitor. Filtering would be perfect if the load current were zero, since then the capacitor could not discharge, and e_c would remain at the peak value E_m. Effective filtering also depends upon the magnitude of the capacitance of the capacitor. As indicated by Eq. 6-45, cutout occurs earlier in the cycle, θ_1 approaches zero, as C increases. Also, the larger the value of C, the smaller the rate of discharge or decay of capacitor voltage, as shown by Eq. 6-46*a*. However, it must be remembered that a capacitor does not pass direct current. The average value of the current i_c of Fig. 6-5 must therefore be zero, requiring that the cross-hatched areas above and below the ωt axis be equal. Then, as C increases, it is evident from Fig. 6-5 that the interval $(\theta_2 - \theta_1)$ increases since θ_1 approaches zero and θ_2 increases toward π; at the same time, interval ϕ decreases. Since the requirement of equal areas must be met, the capacitor current becomes more and more peaked. The surge of current i at cut-in may greatly exceed the rating of a gas-filled rectifier tube even though the average current is well below the average rated value. For this reason, capacitor input

filters are not used with vapor tubes, but may be used with high-vacuum tubes since the current at cut-in is limited by the tube plate resistance.

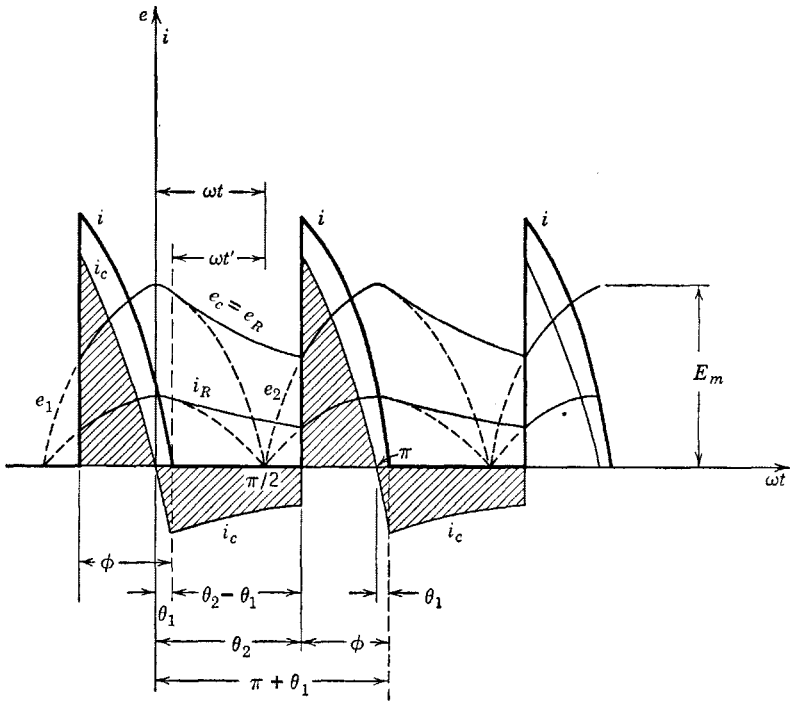

FIG. 6-5. Tube current, capacitor current, and load voltage for a full-wave rectifier with capacitor filter.

The output-voltage wave form of the rectifier with capacitor filter may be approximated by drawing straight-line segments as shown in Fig. 6-6. The average of such a triangular-topped wave is

$$E_{dc} = E_m - E_r/2 \tag{6-50}$$

where E_r is the maximum change in voltage during discharge of the capacitor. Since the capacitor has been assumed to be discharging at a

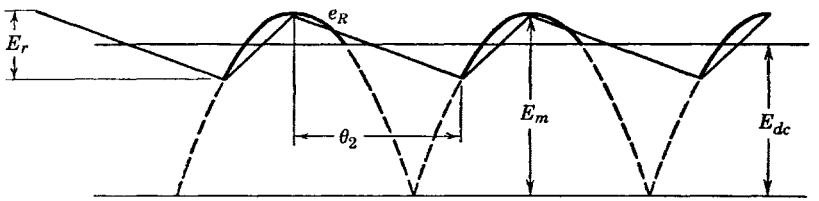

FIG. 6-6. Use of straight-line segments to approximate output voltage of Fig. 6-5.

constant rate, the current delivered by the capacitor to resistance R during this interval will be constant. Then the magnitude of the slope of the line segment over the interval θ_2 may be obtained as follows:

Since $$e_c = q/C$$

$$-\frac{de_c}{dt} = \frac{1}{C}\frac{dq}{dt} = \frac{I_{dc}}{C}$$

or $$-de_c/d(\omega t) = I_{dc}/\omega C \tag{6-51}$$

during the interval θ_2. From Fig. 6-6, over the interval θ_2, $e_c = e_R$, and

$$-de_c/d(\omega t) = -de_R/d(\omega t) = E_r/\theta_2$$

so that $$E_r = I_{dc}\theta_2/\omega C \tag{6-52}$$

It is easily shown that the effective (rms) voltage of the ripple portion of the wave of Fig. 6-6 is independent of the slopes of the line segments and depends only upon the peak value of the voltage. If the time axis were made to coincide with E_{dc} in Fig. 6-6, the root-mean-square value of the ripple voltage obtained in the usual way is

$$E_{ac} = E_r/2\sqrt{3} \tag{6-53}$$

The ripple fraction for the rectifier is then, by definition,

$$r = \frac{E_{ac}}{E_{dc}} = \frac{E_r}{2\sqrt{3}\,E_{dc}} = \frac{I_{dc}\theta_2}{(2\sqrt{3})\omega CRI_{dc}} = \frac{\theta_2}{4\sqrt{3}\,\pi fCR} \tag{6-54}$$

The value of θ_2, in radians, is required before the ripple fraction may be found. Equation 6-54 is somewhat misleading since, apparently, r increases with increasing θ_2. Inspection of the graph of Fig. 6-6 shows, however, that an increasing θ_2 is accompanied by a decreasing value of E_r since the point of intersection of the line segment with the rising cosine curve will move upward along the curve. A commonly used method of approximation of the ripple fraction in this case is to assume that the capacitor discharges for one-half cycle. This corresponds to $\theta_2 = \pi$, and results in a less exact but more convenient expression for r.

From the foregoing analysis, it should be evident that the capacitor is an effective filter at light load, that is, for R large and I_{dc} small. Also, filter action improves with increasing C, and the output voltage is high, but the tube currents are peaked, and gas tubes should not be used. The voltage regulation is also very poor.

6-7. The Voltage Doubler

A practical application of the principles discussed in the preceding section is found in the circuit of the voltage doubler (Fig. 6-7). The circuit is similar to that of a full-wave rectifier, with two filter capacitors in series shunting the load resistance. The voltage e_R across the load is at any instant equal to the sum of the two capacitor voltages, $e_{c1} + e_{c2}$. Capacitor C_1 charges when tube 1 is conducting, a-c supply terminal a

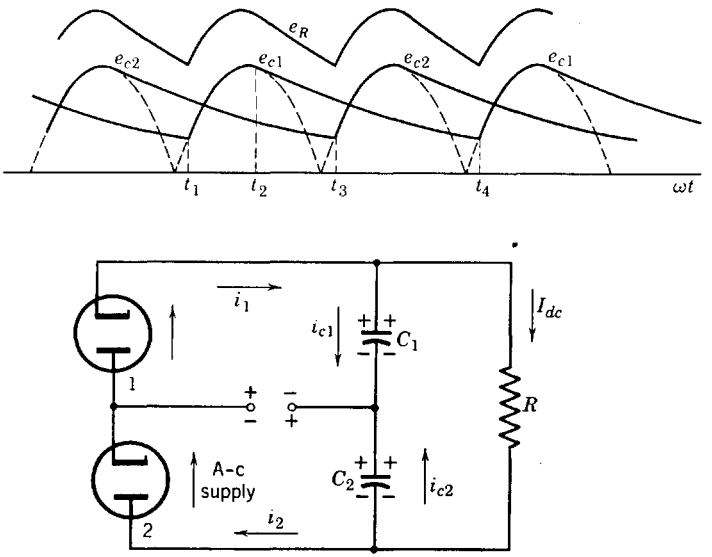

FIG. 6-7. Voltage doubler circuit and capacitor voltage wave forms.

positive. Capacitor C_2 charges during the next half-cycle, when tube 2 conducts and terminal b is positive. When steady-state conditions are reached, the capacitors charge and discharge as shown by the graphs of Fig. 6-7. The anode of tube 1 becomes positive with respect to its cathode at time t_1; tube 1 conducts until time t_2, delivering current to the load and charging C_1. At t_2, the tube current i_1 becomes zero and would reverse except that the tube will not pass inverse current. The circuit to the a-c supply is then open, and C_1 supplies current to R, aided by C_2 in series, until tube 1 again conducts at time t_4. Meanwhile the a-c supply is again connected to the load through C_1 at t_3 when tube 2 begins to conduct. Between t_3 and t_4 the charge on C_2 is replenished. The voltage e_R has been obtained by adding ordinates of the e_{c1} and e_{c2} curves. For light loads, the voltage e_R is approximately twice the peak voltages of the supply, neglecting tube drop. The circuit has been used as a power supply for loads requiring small current and has the

advantage of requiring no transformer. The average load voltage E_{dc} is twice the average voltage of either capacitor, and the ripple magnitude is the same as that of e_{c1} or e_{c2}. The ripple frequency of e_R is twice the ripple frequency of e_{c1} or e_{c2}. The ripple factor may be obtained by the same procedure as that used in Section 6-6.

6-8. The Inductance Filter

A single inductance used as a filter in a full-wave circuit is connected in series with the load as shown in Fig. 6-8. Essentially, the filter action of the inductance is to oppose any change in the current through it and

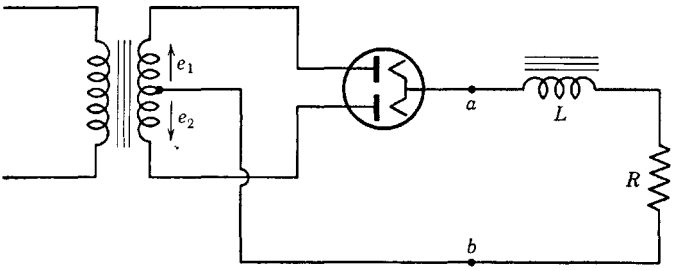

FIG. 6-8. Full-wave circuit with inductance filter.

to add its voltage to that of the rectifier. It is desirable that the iron of the inductance should not saturate with load current. If it may be assumed that there is no cutout or cut-in of tube current, as was the case for the capacitor filter, the open-circuited voltage at the terminals a–b of Fig. 6-8 will be a rectified sine loop voltage as in Fig. 6-3*b*. The Fourier series expression for the sine loop voltage is identical with the series for current (Eq. 6-19) except that E_m replaces I_m, where E_m is the peak value of the transformer secondary voltage between anode and mid-tap. The tube drop or tube resistance will be neglected in the analysis to follow: Transformer secondary leakage reactance and resistance, and also the resistance of the choke will be neglected in the preliminary analysis. The voltage applied at terminals a–b is given by

$$e_{ab} = \frac{2E_m}{\pi}\left(1 + \frac{2}{3}\cos 2\omega t - \frac{2}{15}\cos 4\omega t + \frac{2}{35}\cos 6\omega t - \cdots +\right) \quad (6\text{-}55)$$

In applying the superposition theorem, e_{ab} may be thought of as representing the voltages in series of one d-c generator and many a-c generators of frequencies $2\omega/2\pi$, $4\omega/2\pi$, $6\omega/2\pi$, etc. Currents in the load circuit resulting from the application of the several generators may be obtained one at a time, by superposition, by using one generator at a

time. For example, the peak value of the second-harmonic component of load current is

$$I_{2m} = \frac{4E_m}{3\pi\sqrt{R^2 + (2\omega L)^2}} \tag{6-56}$$

The fourth-harmonic amplitude is

$$I_{4m} = \frac{4E_m}{15\pi\sqrt{R^2 + (4\omega L)^2}} \tag{6-57}$$

Now for effective filtering, $2\omega L$ is large compared with R. Then, approximately,

$$I_{4m}/I_{2m} \cong \tfrac{1}{10}$$

and the higher harmonics are progressively smaller fractions of I_{2m}. It is therefore justifiable, as a useful approximation, to replace the circuit

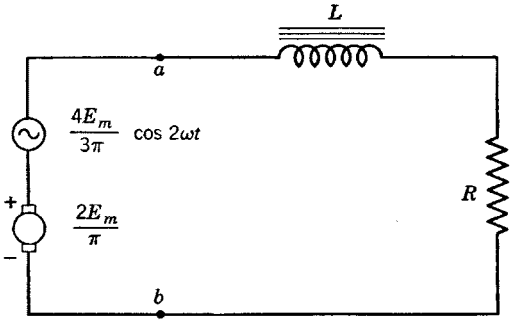

FIG. 6-9. Approximate equivalent to the circuit of Fig. 6-8.

to the left of terminals a–b in Fig. 6-8 by an equivalent circuit consisting of a d-c generator and an a-c second-harmonic generator in series, as shown in Fig. 6-9. The currents in the load are then as follows:

$$I_{dc} = 2E_m/\pi R \tag{6-58}$$

and

$$i_2 = \frac{4E_m}{3\pi\sqrt{R^2 + (2\omega L)^2}} \cos(2\omega t - \theta) \tag{6-59}$$

where

$$\theta = \tan^{-1}(2\omega L/R)$$

The ripple is produced by the second harmonic of load current. The ripple fraction is, by definition,

$$r = \frac{I_{2m}/\sqrt{2}}{I_{dc}} = \frac{\sqrt{2}}{3\sqrt{1 + 4\omega^2 L^2/R^2}} \tag{6-60}$$

Equation 6-60 shows that, for a given choke, the effectiveness of the filter is greater, the smaller the value of the load resistance R, and therefore increases with increasing load current. This contrasts with the capacitance filter which, as has been noted, was most effective for small load current.

If, in Eq. 6-60, $4\omega^2L^2/R^2$ is large compared with unity,

$$r = \sqrt{2}\,R/6\omega L \tag{6-61}$$

so that, with a given load resistance, the ripple fraction decreases with increasing L. Since the capacitor is most effective for small load currents and the choke for large currents, it may be surmised that the use of series choke and shunt capacitor together will provide effective filter action over most of the load range of a power supply.

6-9. The L-Section Filter

The circuit of a full-wave rectifier power supply with combined choke–capacitor or L-section filter is shown in Fig. 6-10. The resistance R_B is known as a "bleeder" resistance and is permanently connected across

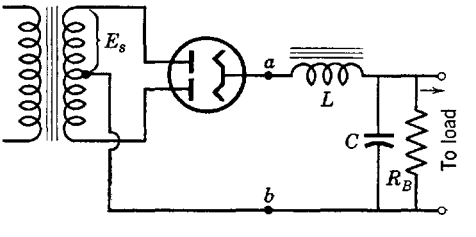

FIG. 6-10. Full-wave rectifier with L-section filter and bleeder resistance.

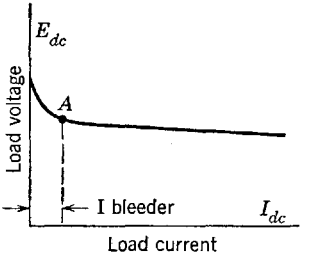

FIG. 6-11. Load voltage curve for a full-wave rectifier.

the load terminals of the rectifier. The required value of R_B will be found in the analysis of the circuit. Experimentally, the load voltage as a function of load current follows a curve similar to that shown in Fig. 6-11. A large voltage drop occurs for a small increase of current from the no-load value. After point A is passed, the voltage decrease with load is at a very much smaller rate. It is therefore desirable for improved voltage regulation to operate the rectifier only for values of current to the right of point A on the curve. A bleeder resistor is therefore chosen so that with the load completely removed the rectifier will operate at point A. The reason for the large change of voltage to the left of point A is that the tube anodes are not conducting for their full half-cycles, but cutout and cut-in are occurring.

Typical filter-circuit values require an inductance around 20 henrys, and a capacitor of 4 to 8 μf. With such values, and a 60-cycle power source, $2\omega L \cong 15{,}000$ ohms; $X_c = 1/2\omega C \cong 300$ ohms. For practical purposes, the reactance of the capacitor should be small compared to the effective load and bleeder resistances. In the absence of cutout and cut-in, the equivalent applied voltage at terminals *a–b* of Fig. 6-10 is the same as that used in the approximate analysis of the inductance filter. For R = the effective load resistance (actual load in parallel with R_B), and $X_c \ll R$,

$$R(-jX_c)/(R - jX_c) \cong -jX_c$$

Then, the second-harmonic current amplitude in the capacitor is given, approximately, by

$$I_{2m} = \frac{4E_m/(3\pi)}{(2\omega L - 1/2\omega C)} \tag{6-62}$$

The peak ripple voltage across the capacitor, and also across the load, is $I_{2m}(-jX_c) = E_{rm}$ which, in magnitude, is

$$|E_{rm}| = \frac{4E_m/(3\pi)}{(4\omega^2 LC - 1)} \tag{6-63}$$

The ripple fraction is

$$r = \frac{(1/\sqrt{2})|E_{rm}|}{E_{dc}} = \frac{\sqrt{2}\,E_m}{3\pi(4\omega^2 LC - 1)^2(E_m/\pi)}$$

$$= \frac{\sqrt{2}}{3(4\omega^2 LC - 1)} \tag{6-64}$$

A sketch of the ripple current is given in Fig. 6-12, where the second-harmonic ripple current is shown superimposed upon the direct component. If the load resistance increases, the value of I_{dc} decreases, but, since the peak value of the ripple current is independent of R, according to Eq. 6-64, a critical value of R is reached as shown in Fig. 6-12*b*. If the current I_{dc} were further decreased beyond the value shown in Fig. 6-12*b*, the ripple component would try to become negative. Since the rectifier tube does not pass inverse current, cutout occurs. The critical load resistance corresponding to tangency of the ripple current with the time axis is the required value of the bleeder resistance. From Fig. 6-12*b*,

$$I_{2m} = I_{dc}$$

or, since $2\omega L \gg 1/2\omega C$,

$$4E_m/3\pi(2\omega L) = 2E_m/\pi R_B \tag{6-65}$$

The required value of R_B may then be expressed, for a 60-cycle supply, as

$$R_B = 1131L \tag{6-66}$$

It has been shown experimentally by Dellenbaugh and Quinby [3] that point A of Fig. 6-11 corresponds to a value of $R_B = 1000L$. In view of the approximations used in the derivation of Eq. 6-66, the confirmation is satisfactory. Dellenbaugh and Quinby also showed that improved

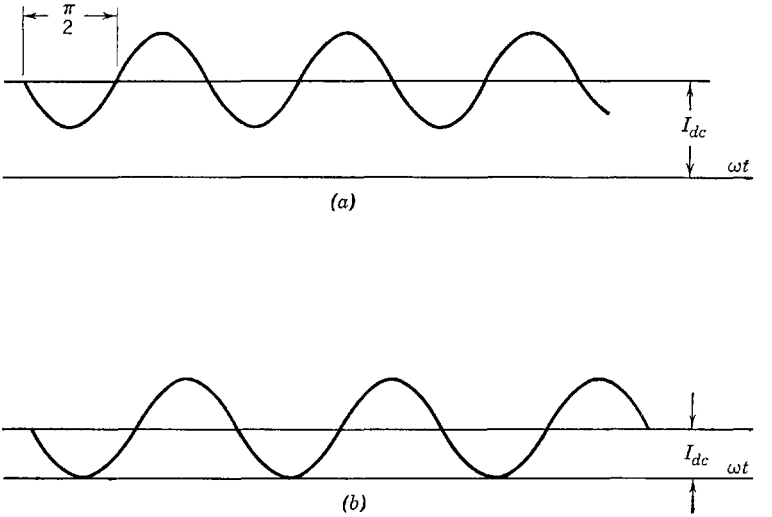

FIG. 6-12. Second-harmonic ripple current.

operation results if $R_B = 500L$. The latter value of R_B is recommended, particularly for gas tubes, in order to decrease the ratio of the peak alternating current to the direct current.

Equation 6-66 has been interpreted as giving the critical value of R_B for a given L. It may also be used as the recommended relation of Dellenbaugh and Quinby to give a minimum value of inductance for a given load resistance R. Thus,

$$L_0 = R/500 \tag{6-67}$$

At full load, the value of R is least, and also the required value of L. Since the iron core of an inductor tends toward saturation with in-

[3] *QST*, **16** (Feb., Mar., Apr. 1932).

creasing load current, it is possible to provide sufficient inductance at both full load and no load, even though L decreases, by proper design of an air gap in the iron core of the inductance. Such an inductance is called a "swinging choke" and may be designed to provide a value of L which though variable with load, always exceeds the critical value specified by Eq. 6-67.

In the design of a power supply, the permissible ripple fraction r is usually specified. By solving Eq. 6-64, the necessary value of LC may be expressed as follows:

$$LC = \frac{1}{4\omega^2}\left(1 + \frac{0.471}{r}\right) \tag{6-68}$$

Usually more than one filter section is used. If n identical L sections are used in tandem, it may easily be shown that the value of r is given approximately by

$$r = \sqrt{2}/3(4\omega^2 LC - 1)^n \tag{6-69}$$

From Eq. 6-69, with $\omega = 377$,

$$LC = 1.76[1 + (0.471/r)^{1/n}] \tag{6-70}$$

where C is in microfarads.

6-10. The Capacitor-Input Filter

The addition of a capacitor between terminals a and b of Fig. 6-10 considerably complicates the analytical determination of filter constants

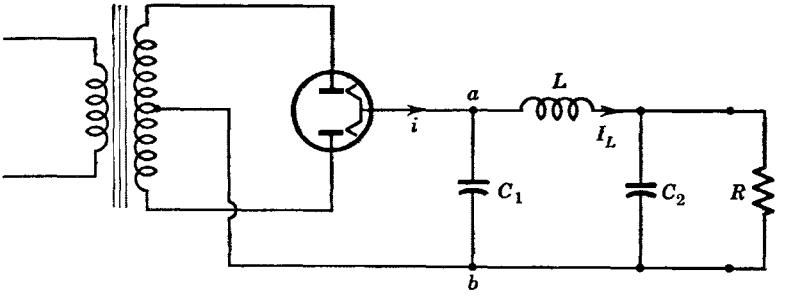

FIG. 6-13. Capacitor-input, π-section smoothing filter.

required to provide a given value of ripple fraction. The full wave rectifier circuit using such a π-section low-pass filter is shown in Fig. 6-13.

Because of energy storage in the filter elements, the wave form of the voltage at filter input terminals a–b is similar to that shown in Fig. 6-6. A simple analysis of the circuit to obtain an expression for the ripple

fraction may be based upon the results of Section 6-6, where it was shown that the transformer secondary winding is connected through the rectifier tube to the filter input during only a portion ϕ/π of the period of the half-cycle transformer secondary voltage, as indicated in Fig. 6-5. If the capacitance C_1 is of the order of magnitude normally required for adequate filter action, and if the tube resistance is relatively small, C_1 charges quickly to a voltage which differs very little from the peak value of the transformer secondary voltage. The time required for such

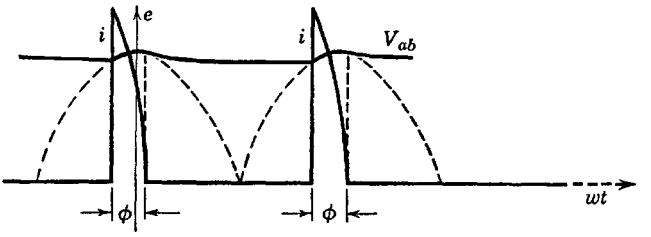

FIG. 6-14. Approximate wave forms of tube current i and input voltage at a–b, Fig. 6-13.

restoration of the voltage of C_1 is represented by angle ϕ in Fig. 6-5 and also in Fig. 6-14. The peaks of current under conditions shown in Fig. 6-14 are sharp and of relatively large magnitude. It has already been mentioned in Section 6-6 that gas-filled tubes are likely to be damaged by current overload during conduction periods if used with a capacitance input filter.

It will be observed that the peaks of current occur during the angular time interval near the voltage maxima of the transformer secondary voltage. Let it be assumed that the average value of this current flows through choke and load. Then,

$$I_{dc} = \frac{1}{2\pi}\int_{-\pi}^{\pi} i\, d(\omega t) \tag{6-71}$$

also, the second-harmonic voltage component, peak value, is given by

$$I_{2m} = \frac{1}{\pi}\int_{-\pi}^{\pi} i \cos 2\omega t\, d(\omega t) \tag{6-72}$$

It is assumed that during the duration of the current pulse $\cos 2\omega t \cong 1$. Then,

$$I_{2m} \cong \frac{1}{\pi}\int_{-\pi}^{\pi} i\, d(\omega t) = 2I_{dc} \tag{6-73}$$

and the effective value of the second-harmonic component of tube current is

$$I_2 = I_{2m}/\sqrt{2} = \sqrt{2}\, I_{dc} \tag{6-74}$$

Several additional assumptions may be made in obtaining a simple approximation for the ripple fraction. These include:

1. That all of I_2 flows in C_1.
2. That $2\omega L \gg 1/2\omega C_1$ and that

$$1/2\omega C_2 \ll R$$

Then, if the effects of higher-harmonic components are neglected, the ripple voltage across C_1 is

$$V_{c1} = I_2(1/2\omega C_1) = \sqrt{2}\, I_{dc}/2\omega C_1 \tag{6-75}$$

It is further assumed that all the voltage V_{c1} exists across inductance L, requiring a current of magnitude

$$I_L = V_{c1}/2\omega L = I_{dc}/2\sqrt{2}\,\omega^2 LC_1 \tag{6-76}$$

in the inductance.

If all the current I_L flows through C_2, the output ripple voltage is

$$V_{c2} = I_L(1/2\omega C_2) = I_{dc}/4\sqrt{2}\,\omega^3 LC_1C_2 \tag{6-77}$$

and from this result, the ripple fraction is

$$r = V_{c2}/V_{dc} = 1/4\sqrt{2}\,\omega^3 LC_1C_2R \tag{6-78}$$

Equation 6-78 provides a reasonably good practical expression for the ripple fraction. Usually, $C_1 = C_2$, and L may be chosen arbitrarily from available commercial chokes. The resulting filter has somewhat inferior characteristics (including voltage regulation) compared with the choke input type but requires a lower transformer secondary voltage for a given required output voltage.

6-11. Grid-Controlled Rectifiers

When gaseous rectifiers with grids are used in rectifier circuits, the function of the grid is to delay the initiation of tube conduction until a definite, calculable time in the a-c cycle of positive anode voltage. After conduction begins, the field of the grid does not extend beyond its ion sheath and it exerts no further control upon the anode current. With an alternating voltage applied to the anode, however, the anode voltage falls below the value necessary to maintain the arc as the positive

half-cycle approaches completion, so that conduction ceases, and the grid regains control during the negative half-cycle. There are many different circuits used in controlling the time of initiation of arc discharge in thyratrons, but the methods may be classified as d-c, a-c, or combinations of the two, depending upon the nature of the grid voltage. With these various grid control circuits, it is possible to control the magnitude of the rectified direct load voltage or current continuously or with a fixed magnitude to specify whether the load current flows or does not flow. The latter method is referred to as on-off control. The general principles of such control methods will be analyzed briefly in the following paragraphs.

6-12. Critical Control Curves

The grid-control characteristics of three typical thyratrons were shown in Figs. 5-10, 5-11, and 5-13 of Chapter 5. In rectifier applications, the anode voltage is a function of time, and it is desirable to be able to specify the critical firing control-grid voltage also as a function

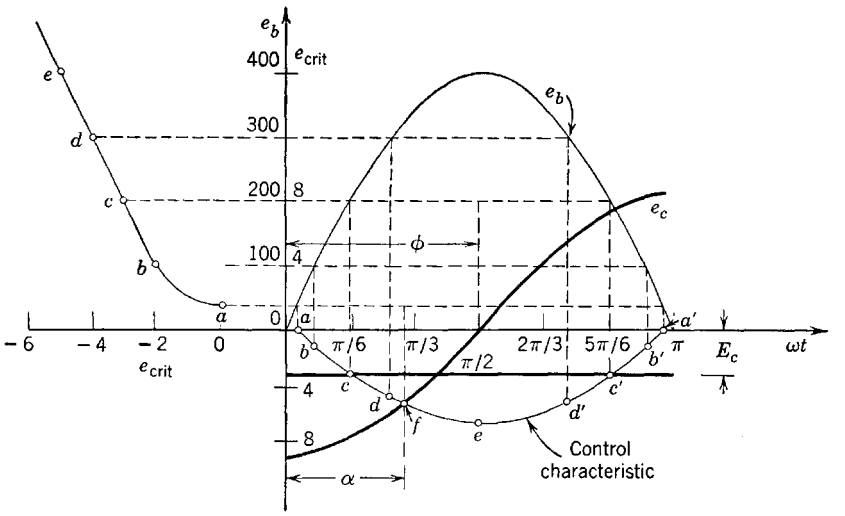

FIG. 6-15. Critical control characteristic for a thyratron.

of time. Since the anode and critical firing voltages are related experimentally as shown, for example, by Fig. 5-10, it is easy to obtain a critical firing voltage curve as a function of time. The process is illustrated in Fig. 6-15, in which points from a control characteristic have been transferred to a graph of the time-varying positive half-cycle of the anode voltage. Points *a*, *b*, *c*, *d*, and *e* on the critical control character-

istic transfer to points a, a', b, b', c, c', d, d', and e during the positive half-cycle. If the grid voltage is also a function of time, the tube begins to conduct at that instant in the positive half-cycle at which the actual grid voltage crosses the critical firing curve from below. Two actual grid voltages are shown in heavy black ink. The horizontal line at -3 volts corresponds to a fixed d-c grid bias. The intersection of this line with the critical firing curve shows that conduction would begin at a time corresponding to point c or at $\omega t = \pi/6$ in the cycle. If an alternating voltage of peak value 8 volts and phase lag 90° (referred to the anode voltage) is applied to the grid, the firing point corresponds to the intersection at point f. Evidently, the ignition angle α may be varied from approximately zero to approximately π rad by varying the angle of phase lag ϕ of the alternating grid voltage behind the anode voltage, but α can be varied only between approximately 0 and $\pi/2$ rad by varying only the amount of d-c bias grid voltage. If both an a-c and a d-c component of voltage are simultaneously applied to the grid, and if the a-c component lags the anode voltage in phase by $\pi/2$ rad, then considerable variation in α may be achieved by varying the d-c component alone. These three methods of varying α are known as d-c bias, phase-shift, and bias-phase control. Circuits for accomplishing the required variations in α are described in later sections.

6-13. Load-Current Analysis, Resistance Load

The resistance R in the circuit of Fig. 6-16 is the load resistance in which it is desired to control the magnitude of the rectified direct current by adjustments in the grid control circuit of the thyratron T. If the

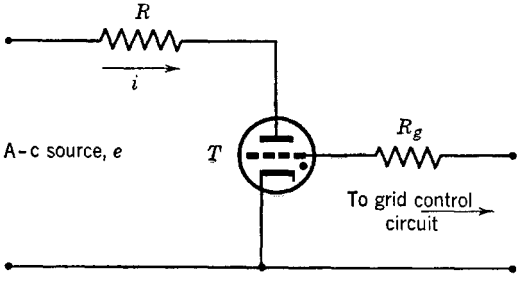

FIG. 6-16. Single-phase, grid-controlled rectifier.

grid control circuit is adjusted so that the ignition angle is α (Fig. 6-17), then the tube conducts during the interval $\alpha < \omega t < (\pi - \delta)$ during the positive half-cycles. The angle δ depends upon the tube drop, since conduction ceases when the anode voltage falls below the value necessary

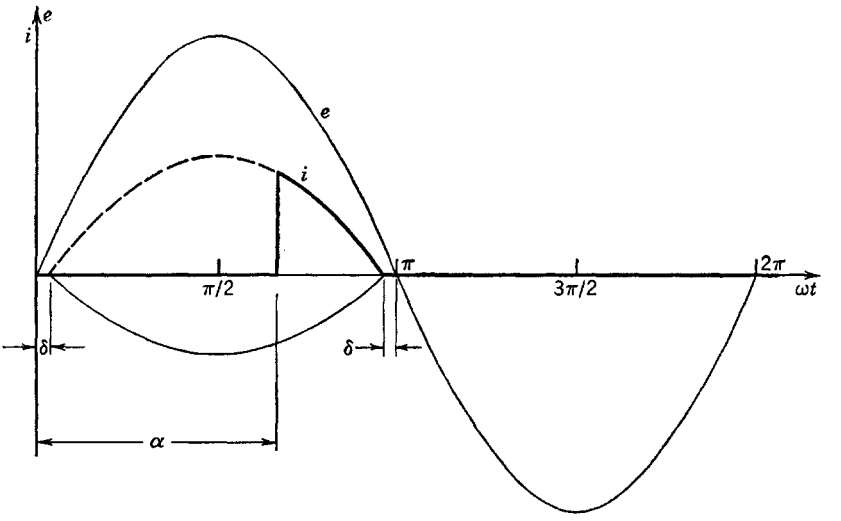

FIG. 6-17. Current wave form, half-wave, grid-controlled rectifier.

to maintain the arc and cannot begin until the applied anode voltage exceeds this value.

If the applied voltage e is a sinusoid given by

$$e = E_m \sin \omega t$$

then the instantaneous anode current during a complete a-c cycle is expressed as follows:

$$i = \frac{E_m \sin \omega t - V_o}{R} \quad \text{for} \quad \alpha < \omega t < \pi - \delta$$

$$i = 0 \quad \text{for} \quad 0 < \omega t < \delta \tag{6-79}$$

and $$i = 0 \quad \text{for} \quad \pi - \delta < \omega t < 2\pi$$

The direct current in the load resistance R is then given by

$$I_{dc} = \frac{1}{2\pi} \int_{\alpha}^{\pi-\delta} \left(\frac{E_m \sin \omega t - V_o}{R} \right) d(\omega t) \tag{6-80}$$

In cases where the tube drop is small compared with the peak value of the applied a-c anode voltage, δ is a very small correction on π and may

be neglected. In such cases,

$$I_{dc} = \frac{1}{2\pi R}[E_m(1 + \cos\alpha) - V_o(\pi - \alpha)] \tag{6-81}$$

and

$$E_{dc} = RI_{dc} \tag{6-82}$$

If tube drop is neglected completely, the load direct current may be varied from a minimum of zero, for $\alpha = \pi$, to a maximum of

$$I_{dc} = \frac{1}{\pi}\frac{E_m}{R} \quad \text{for} \quad \alpha = 0$$

This control of large values of current may be achieved quite economically by controlling the ignition angle through the use of low-voltage low-current control grid circuits.

6-14. Bias Control

A circuit for bias control involves any arrangement by means of which a variable direct voltage may be applied to the grid. Such an arrangement is shown in Fig. 6-18. Instead of the potentiometer, a voltage

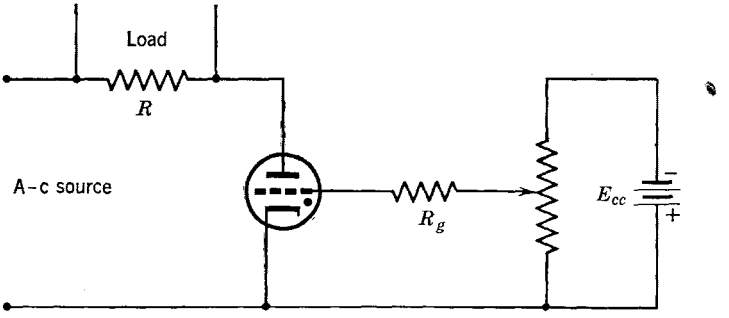

FIG. 6-18. Bias-control circuit.

divider consisting of a fixed resistor in series with a phototube may be used, thus providing a control voltage dependent upon light intensity.

6-15. On–Off Control

An on–off circuit in which the main load current is interrupted or permitted to flow by switching in the grid circuit is shown by Fig. 6-19. If the switch S is open, the load current is zero, since the tube is biased below the critical control voltage. If switch S is closed, the grid voltage

is made equal to that of the anode, and the tube conducts with a conduction period of $\delta < \omega t < (\pi - \delta)$ in the positive half-cycle. Other

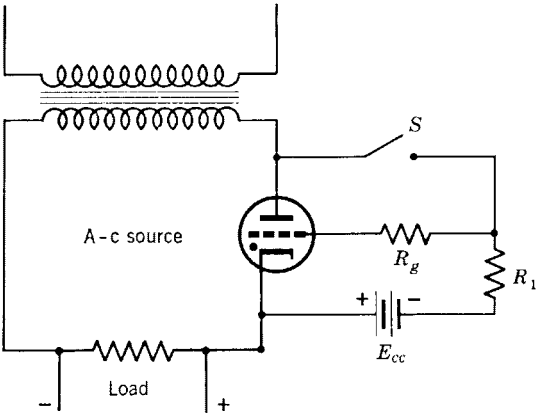

FIG. 6-19. On-off control circuit.

positions of the switch and of R_1 are possible and should suggest themselves to the student.

6-16. Phase-Shift Control

The control of average current in a thyratron circuit by shifting the phase of the alternating grid voltage with respect to the anode voltage is the method best adapted to most thyratron control applications and

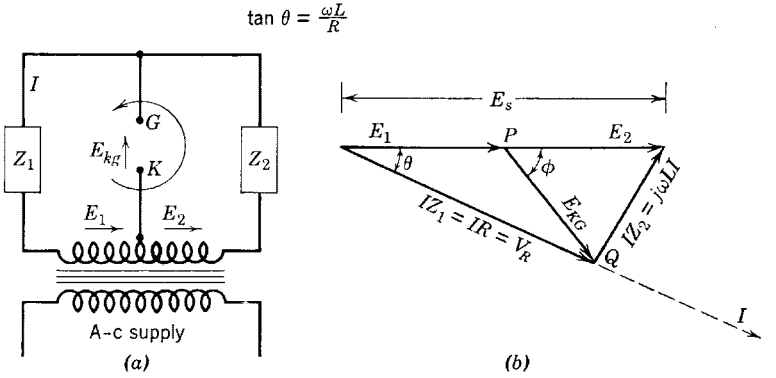

FIG. 6-20. Circuit and vector diagram for thyratron phase shift.

is often used where automatic control or servomechanisms are employed. The control of the firing angle α of Fig. 6-15 may be accomplished by use of the general circuit of Fig. 6-20*a*. The vector diagram for the circuit

is shown in Fig. 6-20*b* where the impedance Z_1 is a pure resistance, and Z_2 is a pure inductive reactance. Thus the current I lags the voltage by angle θ, where

$$\tan \theta = \omega L/R$$

From Kirchhoff's voltage law, $E_s = E_1 + E_2 = I(Z_1 + Z_2)$. Also,

$$E_1 = V_{KG} + IZ_1 \tag{6-83}$$

where E_1 is the voltage rise across the indicated half of the supply transformer secondary winding and V_{KG} is the voltage drop between terminals K and G. If the voltage rise between these two terminals is specified, Eq. 6-83 becomes

$$E_1 + E_{KG} = IZ_1 = IR \tag{6-84}$$

and

$$E_2 = IZ_2 + E_{KG} = j\omega LI + E_{KG} \tag{6-85}$$

as shown on the vector diagram (Fig. 6-20*b*). Now, if R is varied and L remains fixed, θ can be made to change from approximately zero for very large R to approximately 90° for very small R. The resulting locus of the end of the vector V_R may most easily be determined from the vector diagram,

$$V_R = (E_1 + E_2) \cos \theta = E_s \cos \theta \tag{6-86}$$

Since E_s, the voltage of the secondary of the transformer, is constant, Eq. 6-86 is the polar form of the equation of a circle, with center at $(E_s/2, 0°)$ or $(E_1, 0°)$, that is, at point P.* The radius of the circle is $E_s/2$ (see footnote)

so that

$$|E_{KG}| = E_s/2 \tag{6-87}$$

For the physical case in question, the point Q moves in a semicircle, and, if Eq. 6-87 is used, $\phi = 2\theta$. Therefore, as θ varies from 0 to 90°, ϕ varies from 0 to 180°. If the phase-shifting circuit is then connected so that E_{KG} is the voltage rise between cathode and grid of the thyratron before ignition, the circuit will provide continuous control of the magnitude of the average anode current, provided the applied anode voltage is in phase with E_s. This latter condition can easily be obtained, as shown in the circuit of Fig. 6-21.

* Consider the equivalent equation in polar coordinates $\rho = a \cos \theta$. By transformation to rectangular coordinates $\rho = \sqrt{x^2 + y^2}$, $\cos \theta = x/\sqrt{x^2 + y^2}$, $\sqrt{x^2 + y^2} = ax/\sqrt{x^2 + y^2}$ or $x^2 + y^2 - ax + a^2/4 = a^2/4$, and, finally, $(x - a/2)^2 + y^2 = (a/2)^2$, the equation of a circle, center at $(a/2, 0)$, radius $a/2$.

It is assumed in the circuit of Fig. 6-21 that the phase-shifting transformer secondary voltage $E_s = E_1 + E_2$ is in phase with the anode supply voltage E. If so, an increase of R will cause a decrease in angle θ and twice as much decrease in angle ϕ. Before the tube fires, the circuit

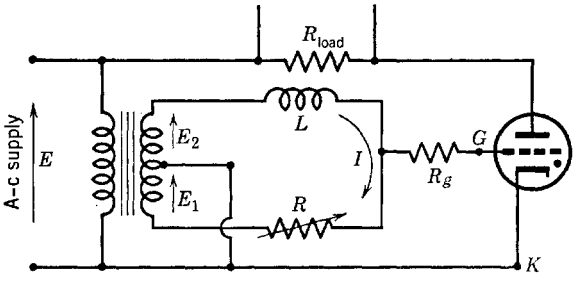

FIG. 6-21. Phase-shifting circuit for thyratron control.

K to G is assumed to be open; also grid-limiting resistor R_g is large compared with circuit impedance in the phase-shifting circuit, and so current I is very closely the same as in Fig. 6-20a where the terminals K to G are open. Since, then, an increasing R is accompanied by a decreasing phase lag ϕ, the average current will increase with increase of R.

The wave forms of the tube current and of the voltage across the tube are shown in Fig. 6-22 for the circuit of Fig. 6-21 with a pure resistance

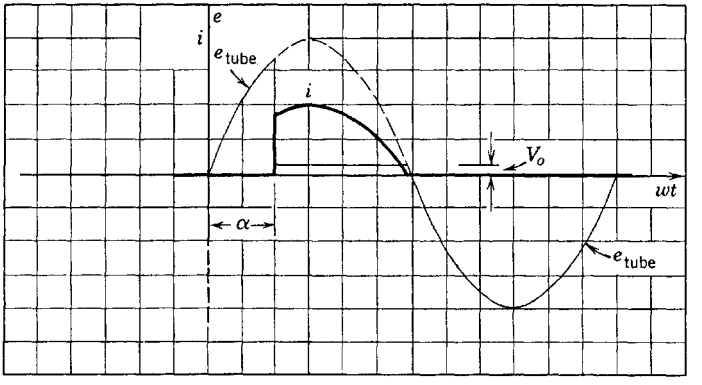

FIG. 6-22. Tube voltage and current wave forms. Thyratron with resistance load.

load. The voltage across the tube is the applied alternating voltage until the tube fires. At $\omega t = \alpha$, the ignition angle, the tube voltage falls to a value equal to the conduction tube drop V_o and remains at this voltage until the current decreases to zero. This occurs approximately

at the instant in the applied a-c cycle when the applied voltage equals V_o (toward the end of the positive half-cycle). At this instant, the applied voltage is just sufficient to maintain the arc so that the voltage across the resistance is zero. The conduction current becomes zero and the tube voltage for the remainder of the cycle is equal to the applied voltage.

If R and L (Fig. 6-20) are interchanged in position in the circuit, the result is a shift of 180° in the phase of voltage E_{KG}. The new position

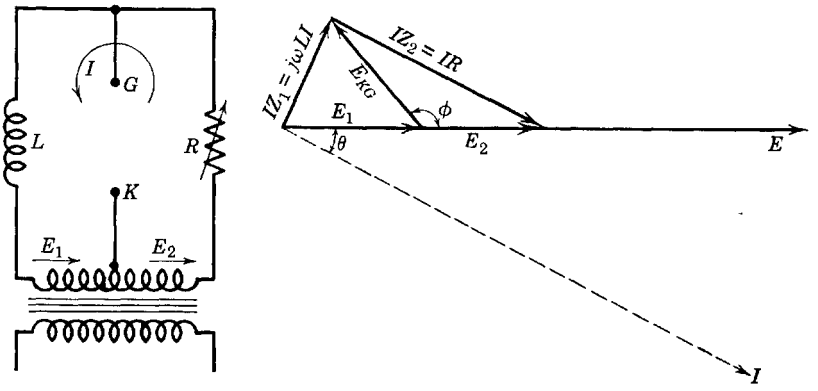

FIG. 6-23. Phase-shift circuit with no control.

of E_{KG} is shown by the vector diagram of Fig. 6-23. From the circuit and vector diagrams,

$$E_1 = V_{KG} + I(j\omega L) = -E_{KG} + I(j\omega L)$$

or $$E_1 + E_{KG} = Ij\omega L$$

and $$E_2 = IR + V_{GK} = IR + E_{KG}$$

The grid voltage E_{KG} now leads the applied anode voltage E, which is assumed to be in phase with $E_s = (E_1 + E_2)$. The tube will fire as early as possible in the anode positive half-cycle, and a change in phase angle ϕ will have no effect upon the average current. In other words, there is no control. In case a phase-shift control circuit is incorrectly connected and exerts no control over the average current, control may be obtained either (*a*) by interchanging the positions of R and L in the circuit, or (*b*) by reversing the phase of the phase-shifting transformer secondary voltage.

Phase-shift control may be provided by using an R–C instead of an R–L circuit. In this case the current will lead the voltage E_s, and control will be obtained if R and C are connected in the proper positions with respect to the terminals of the phase-shifting transformer in exactly the

same way as explained for the R–L circuit. It should be noted that θ must always be an angle of lag of the grid voltage E_{KG} behind the applied anode voltage E in order to obtain control.

6-17. The Use of Saturable Reactors in Phase-Shift Control

Saturable iron-core reactors have been used in phase-shift control circuits because of the wide range of reactance variation controllable by means of a few milliamperes of direct current. The direct current

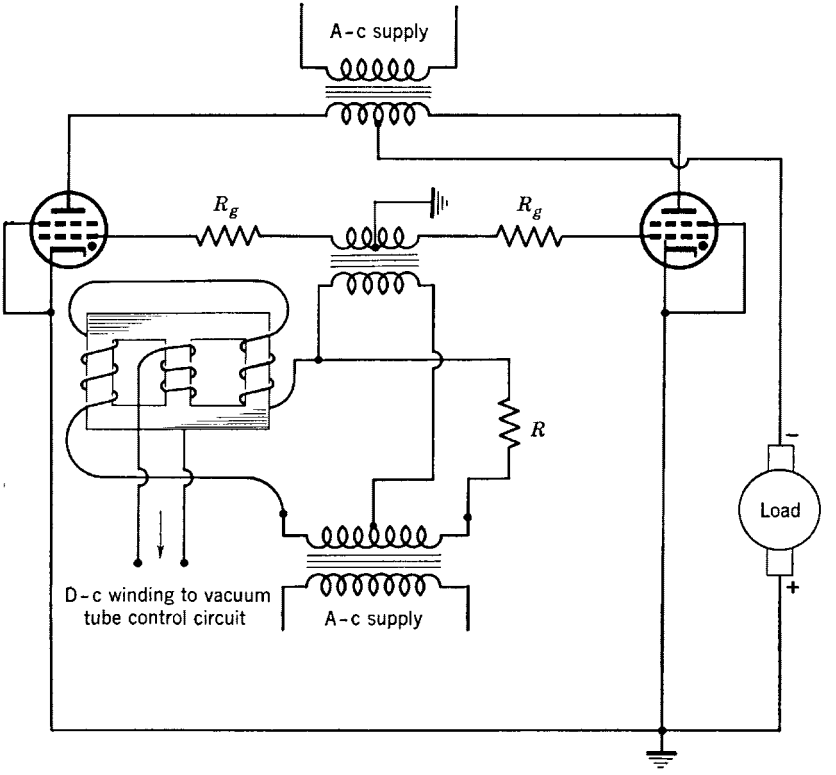

FIG. 6-24. Phase-shift control circuit using saturable reactor.

may be supplied from a small, receiving-type high-vacuum triode. The grid voltage of the triode may then be used to control the direct voltage of the output circuit. It is possible by this means to control the armature and field currents of a d-c motor supplied from an a-c source, and thus to control the speed of the motor through the variations of the grid voltage of a small triode. A typical phase-shift control circuit using a saturable reactor is shown in Fig. 6-24. Two thyratrons are used in a

full-wave rectifier circuit. The a-c windings of the saturable reactor are wound in such a way that their fluxes cancel in the d-c winding. The d-c winding has many more turns than the a-c winding. High-permeability iron is used. In a typical reactor with a 3300-ohm d-c winding, 2.5 ma of current will saturate the reactor. A typical saturation curve is shown in Fig. 6-25, in which the d-c flux is plotted against the control

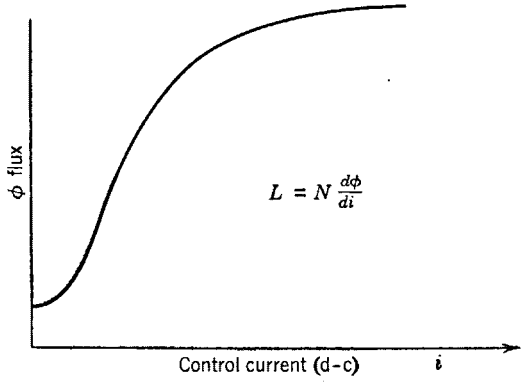

FIG. 6-25. Typical saturation curve.

direct current. As the current i increases beyond the knee of the saturation curve, the inductance L decreases rapidly, which means that the angle ϕ of phase lag decreases, since

$$\phi = 2 \text{ arc tan } \omega L/R$$

The tubes therefore conduct longer, and the load voltage is increased. This method of control has been applied to d-c motor speed control in applications where extremely accurate and extensive speed control is necessary. A circuit similar to Fig. 6-24 is used for the field excitation, and another separate circuit for the armature supply. A standard reference voltage is provided from a small full-wave rectifier circuit using cold-cathode voltage-regulator tubes. A portion of this fixed voltage is compared with a voltage proportional to armature speed. If the speed is not as specified, the difference or error voltage actuates the grid of a vacuum triode in which the plate current in turn controls the grid voltage of a second triode. The plate current of the second triode is the d-c control current of the saturable reactor. Thus control can be made automatic, and the motor may be driven at any predetermined fixed speed, even with variable load, where the necessary vacuum-tube control circuits are utilized.[4]

[4] E. E. Moyer, Electronic Control of D-C Motors, *Electronics*, **16** (May, June, July, Sept., Oct. 1943).

PROBLEMS

6-1. Compute the ripple factor for the wave shown.

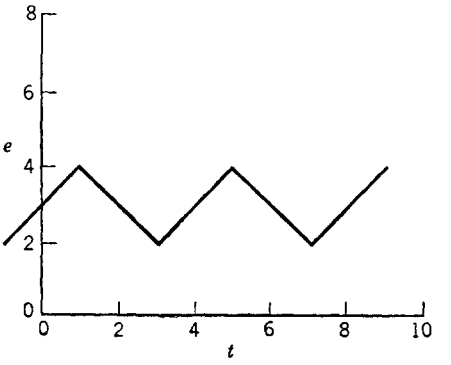

FIG. P6-1.

6-2. A type-5Z4 diode full-wave rectifier is connected as shown in Fig. 6-3*a*. The plate characteristic (for one plate only) may be plotted from the following (e_b, i_b) values: (10 volts, 45 ma); (17.5, 100); (22.5, 150); (27.5, 200); (40, 355).

(*a*) Plot the diode plate characteristic.

(*b*) For R (Fig. 6-3*a*) = 5000 ohms, obtain the composite characteristic.

(*c*) If $e_1 = 200 \cos \omega t$, where $\omega = 377$ rad per sec, obtain data for and sketch a complete cycle of the voltage between anode 1 and the cathode. What is the maximum inverse peak voltage?

6-3. Apply circuit analysis to the circuit of Fig. 6-3*a*, and compute I_m, I_{dc}, P_o, E_{dc}, P_{in}, and the efficiency for a load resistance of $R = 5000$ ohms. Use the tube of problem 6-2.

6-4. The rectifier circuit shown uses copper oxide rectifiers for battery charging. The voltage E, to center tap, is 8.48 volts, rms. Resistance and reactance of the transformer are negligible. The battery voltage is 6 volts, its internal resistance 0.1 ohm. The rectifier resistance is 0.5 ohm in the conduction direction.

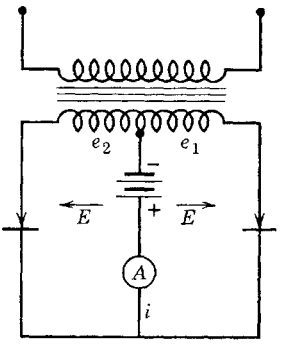

FIG. P6-4.

(*a*) Sketch the voltage and current wave forms, and write the equations for the instantaneous voltages e_1, e_2, and the current i.

(*b*) If the ammeter is a d-c meter, compute its reading.

(*c*) If the ammeter is an a-c meter reading rms current, compute its reading.

6-5. For problem 6-4, compute: (*a*) power delivered by the transformer, (*b*) power in rectifier and battery resistances, (*c*) total losses and power delivered to the battery.

6-6. A gas diode is used in a half-wave circuit to supply a 500-ohm resistance load from 220 volt a-c mains. The breakdown and maintaining voltages are constant at 10 volts. Calculate the readings of the following instruments: (*a*) a d-c ammeter in series with the load, (*b*) an a-c ammeter in series with the load, (*c*) a d-c voltmeter

placed across the tube, (*d*) an a-c voltmeter placed across the tube, (*e*) a wattmeter connected with its current coil in series with the load and its voltage coil across the input.

6-7. In the circuit shown, the transformer secondary voltage, plate to plate, is 500 volts rms (center-tapped). For $C = 4$ μf, $R = 1000$ ohms, find the angles, as measured on the time axis, at which cutout and cut-in occur; obtain equations for and plot i_C, i_R, i_0, and e_R for cut-in and cutout periods. Neglect tube drop.

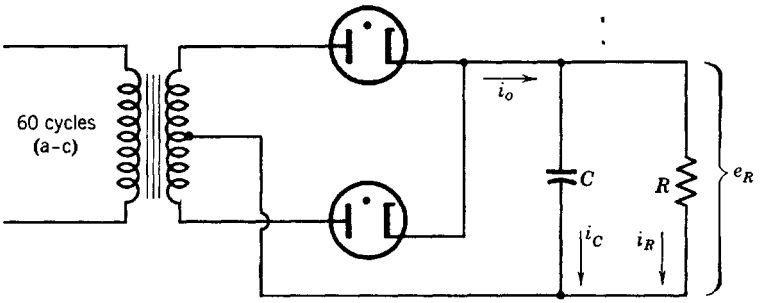

FIG. P6-7.

6-8. Derive Eq. 6-53 from Fig. 6-6.

6-9. Compute the ripple fraction for the circuit of problem 6-7. What is the d-c output voltage?

6-10. A full-wave rectifier circuit uses a type-82 full-wave mercury-vapor tube and an L-section filter consisting of a 20-henry inductance and a 20-μf capacitor. The transformer secondary voltage is 500 volts rms (250 volts to center tap). The load resistance is 500 ohms. Assume that $\omega = 400$ rad per sec, and neglect tube drop.

(*a*) Sketch the rectifier circuit diagram.

(*b*) Sketch the approximate equivalent circuit, and write the equations for (1) the instantaneous current in the capacitor, (2) the total voltage—d-c and superimposed a-c—across the load.

(*c*) Compute the ripple fraction.

(*d*) Compute the inverse peak voltage across the tube.

6-11. Specifications for a full-wave single-phase power supply to operate from 115 volt 60-cycle mains are as follows:

(*a*) Output 250 ma at 1500 volts.

(*b*) Ripple fraction not to exceed 0.001.

The tubes to be used are type-866-A mercury-vapor rectifiers, rated 15 volts arc drop, inverse peak voltage 7500, maximum average current 250 ma.

Specify filter elements and power-transformer secondary voltage, assuming choke resistance of 75 ohms and bleeder resistance of 50,000 ohms. Assume that the full-load choke inductance may be only one-half the inductance at no load.

Compute (1) the expected full-load to no-load voltage regulation of the power supply, (2) the peak inverse voltage on the tube anodes, (3) the expected per cent ripple.

6-12. Derive Eqs. 6-69 and 6-70.

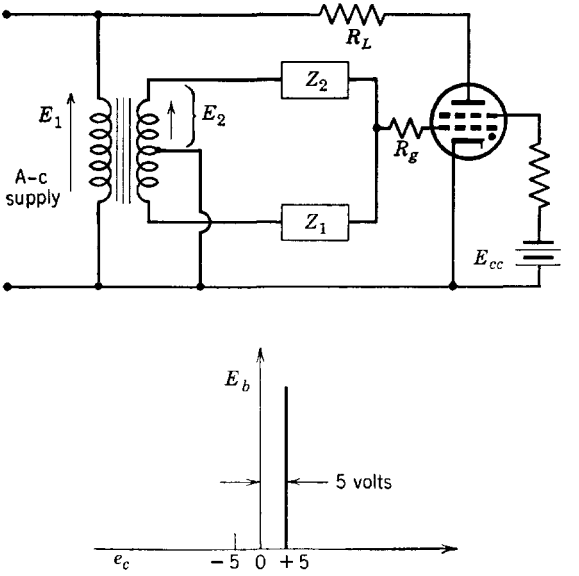

FIG. P6-13.

6-13. A thyratron rectifier is connected as shown:

$E_1 = 220$ volts rms
$E_2 = 10$ volts rms
$R_g = 50{,}000$ ohms
$Z_1 = R = 1732$ ohms
$Z_2 = j\omega L = j1000$ ohms
$R_L = 50$ ohms
$V_o = 15$ volts when conducting

Assume sinusoidal voltages, and that E_2 is in phase with E_1. If the control characteristic of the thyratron is as shown on the accompanying sketch, determine the following: (*a*) the ignition angle α, (*b*) the direct load voltage across R_L, (*c*) the wave form of the conduction current for one cycle and of the anode-to-cathode voltage.

6-14. For the assumed positive sense of voltage rise in problem 6-13, what should be the values of Z_1 and Z_2 if an R–C phase-shift circuit is used and $R = 2000$ ohms, if it is specified that a 90° phase lag is required for E_{KG}, behind E_1. For this circuit, compute the ignition angle, with the thyratron biased as in problem 6-13.

CHAPTER 7

POLYPHASE RECTIFIERS

7-1. Polyphase Rectifiers in General

Single-phase rectifier circuits were described in Chapter 6. The ripple factor was shown to be large, even for the full-wave case, in the absence of filtering. By the use of filtering with the L-section filter, for example, it was shown that the ripple fraction can be reduced to very small values. Direct-current power supplies for small power applications are usually designed for single-phase operation with filters. Where the power requirements are large, however, and where d-c power requirements in kilowatts must be met with small ripple fraction, the single-phase filter becomes uneconomical, and polyphase rectification is used for reasons to be brought out in the following paragraphs. Radio transmitters as well as electric railway motors may be supplied with d-c power from polyphase rectifiers.

Practically all large electric-power systems in the United States generate and distribute three-phase power. Where d-c power requirements are to be met, power conversion from alternating to direct current is practicable through the use of motor-generator sets, rotary convertors, or mercury-arc rectifiers, and, of these methods of conversion, the mercury-arc rectifier has the highest efficiency and in addition has no moving parts. It has therefore been very extensively used either in the form of multianode, single-tank rectifiers, or as single-anode, sealed-off ignitrons. In the power applications to be dealt with in the present chapter, either all the anodes of the rectifier operate from a common cathode such as the mercury pool in a tank rectifier, or else the cathodes of separate tubes or ignitrons are connected together externally, so that the circuit applications are the same in either case. Several of the more commonly used polyphase circuits will be described in order to present the fundamental principles of polyphase rectifier operation. The analysis to be given is purposely made very brief since many excellent books provide detailed analysis of polyphase power-rectifier circuits. The student will find that the sketching of current and voltage wave forms will often serve as a key to problem solutions.

7-2. The Three-Phase Half-Wave Circuit

Practically all polyphase rectifier circuits used for power rectification in the United States employ the delta connection for transformer primary windings. In drawing circuit diagrams, such as Fig. 7-1, it is convenient to sketch corresponding primary and secondary windings parallel to each other though separated by some distance on the wiring

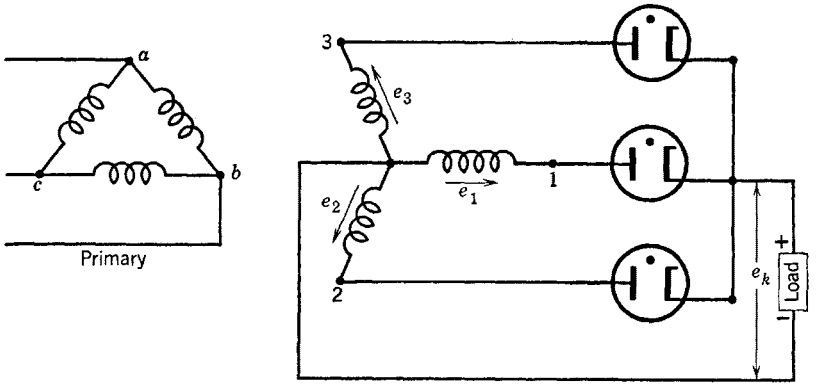

FIG. 7-1. Three-phase, delta-wye rectifier circuit.

sketch. For example, primary winding a–b corresponds to secondary winding 0–3. The ends of the secondary windings are connected to the anodes of three rectifier tubes whose cathodes are connected together. The cathode return from the d-c load circuit requires a neutral connection

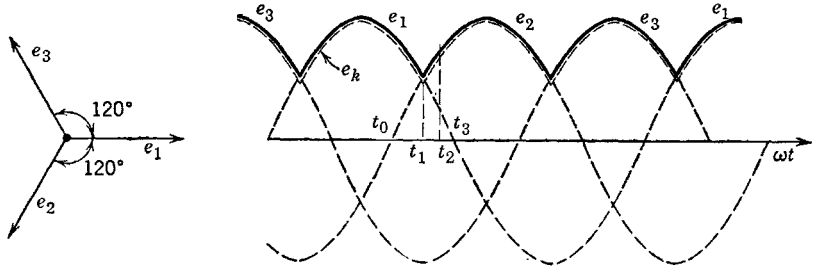

FIG. 7-2. Wave form of secondary and rectified load voltages for the circuit of Fig. 7-1 with resistance load.

in the secondary circuit, which is conveniently supplied by the use of a wye-connected secondary.

The positive sense of voltage rise in the secondary circuit is shown by the arrows and the three secondary voltages are represented by e_1, e_2, and e_3. The vector relation and the wave form of these voltages are

shown by Fig. 7-2, in which sinusoidal secondary transformer voltages are assumed. As shown in Fig. 7-2, the anodes conduct in consecutive order 1, 2, 3, 1, 2, 3, etc. The voltage of the cathodes e_k is always less than that of the conducting anode by the amount of the tube drop, which is assumed to be constant during conduction, as in Chapters 5 and 6. The conduction current shifts or commutates from anode to anode, and the reason for this shift may be seen from an application of Kirchhoff's voltage law to the circuit. Suppose, for example, that anode 1 is conducting and the interval of time t_0 to t_3 is considered during which both anode 1 and anode 2 are positive. For any time between t_0 and t_1, with anode 1 conducting, and with tube voltage drop V_o,

$$e_1 = V_o + V_{k2} + e_2 \tag{7-1}$$

where V_{k2} is the assumed voltage drop between cathode and anode of tube 2. The anode-to-cathode voltage drop of tube 2 is $V_{2k} = -V_{k2}$. Then,

$$V_{2k} = (e_2 - e_1) + V_o \tag{7-2}$$

According to Eq. 7-2 and the wave forms of Fig. 7-2, $e_2 < e_1$ for $t_0 < t < t_1$, and $(e_2 - e_1)$ is negative. Tube 2 cannot conduct until $V_{2k} \geqq V_o$; at $t = t_1$, $e_2 = e_1$, and $V_{2k} = V_o$. At this instant, the voltage of anode 2 is, for the first time in the interval $t_0 < t < t_1$, sufficiently positive with respect to its cathode for the tube to conduct. As soon, therefore, as e_2 is equal to and ready to exceed e_1, $V_{2k} \geqq V_o$, and tube 2 conducts. Conversely, between t_1 and t_3, with tube 2 conducting,

$$e_2 = V_o - V_{1k} + e_1 \tag{7-3}$$

so that $V_{1k} = (e_1 - e_2) + V_o$, and, since $e_2 > e_1$ for $t_1 < t < t_3$, $V_{1k} < V_o$, and anode 1 cannot conduct. To summarize, the following relations have been stated as applying in the time interval during which anodes 1 and 2 are both positive:

$$t_0 < t < t_1, \qquad (e_2 - e_1) < 0$$

$$t_1 < t < t_3, \qquad (e_2 - e_1) > 0$$

As soon as $(e_2 - e_1)$ becomes positive, the arc is commutated from anode 1 to anode 2. The voltage $(e_2 - e_1)$ is called the commutating voltage.

Some general conclusions may be drawn from Figs. 7-1 and 7-2. If a polyphase rectifier has p anodes and one of the p anodes is conducting at all times during the a-c cycle of the supply voltage, and all anodes conduct for equal intervals of time, then the conduction angle of any one anode is $2\pi/p$ rad.

The rectified voltage e_k differs from the secondary voltage of the conducting anode by the amount of the constant tube drop. If tube drop is neglected, the analysis of the output circuit is greatly simplified. Let e_d = the instantaneous value of the rectified voltage, which is actually e_k but approximately e_1, or e_2, or e_3 during the respective conducting periods of these anodes. This rectified voltage is shown for the general

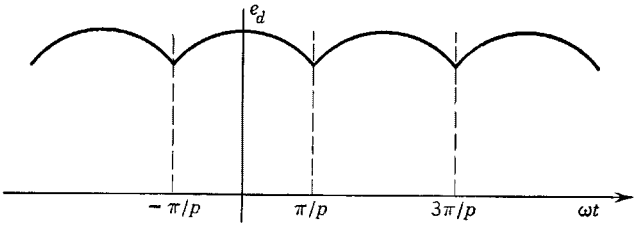

FIG. 7-3. Rectified-voltage wave form of a p-anode rectifier.

case of a p-anode rectifier in Fig. 7-3. The vertical axis has been chosen so that the Fourier analysis of the voltage e_d will be simplified. In the interval

$$-\pi/p < \omega t < \pi/p, \qquad e_d = E_m \cos \omega t \tag{7-4}$$

where E_m is the peak voltage to neutral of the transformer secondary. Also, for

$$\pi/p < \omega t < 3\pi/p$$

$$e_d = E_m \cos (\omega t - 2\pi/p) \tag{7-5}$$

Let E_d be the average value of the rectified voltage. Then,

$$E_d = \frac{p}{2\pi} \int_{-\pi/p}^{\pi/p} E_m \cos \omega t \, d(\omega t) = \frac{p}{\pi} E_m \sin \frac{\pi}{p} \tag{7-6}$$

If $E_m = \sqrt{2}\, E_s$, where E_s is the rms value of the secondary voltage to neutral, then

$$E_d/E_s = \sqrt{2}\, p/\pi \sin \pi/p \tag{7-7}$$

The ratios of E_d to E_s as computed from Eq. 7-7 are tabulated according to number of anodes as follows:

p	2	3	6	12	24	∞
$E_{d/Es}$	0.90	1.17	1.35	1.40	1.41	$\sqrt{2}$

7-3. Harmonic Analysis, p-Anode Rectifier

The amplitude of any harmonic in the general wave form of Fig. 7-3 may be obtained by applying the Fourier analysis to the wave form. The symmetry of the wave form of Fig. 7-3 about the vertical axis (even function) indicates that only cosine terms are needed in the Fourier representation. Then,

$$e_d(\omega t) = E_d + \sum_{k=1}^{\infty} E_{km} \cos k\omega t \tag{7-8}$$

where E_{km} is the amplitude or peak value of the kth harmonic of voltage. The wave form of Fig. 7-3 is repetitive at intervals of $2\pi/p$ rad. Therefore,

$$e_d\left(\omega t + \frac{2\pi}{p}\right) = E_d + \sum_{k=1}^{\infty} E_{km} \cos\left(k\omega t + k\frac{2\pi}{p}\right)$$

must be identical with $e_d(\omega t)$. This requirement will be met provided that

$$k2\pi/p = 2\pi n$$

where n is any integer. Therefore,

$$k = np \tag{7-9}$$

and only those harmonics are involved that are multiples of p. For $p = 3$, only the third, sixth, ninth, etc. harmonics are to be expected. For $p = 6$, the fundamental frequency component is the sixth.

In accordance with the methods of Fourier analysis,

$$E_{km} = \frac{1}{\pi}\int_{-\pi}^{\pi} e_d \cos k\omega t \, d(\omega t) \tag{7-10}$$

Because of symmetry of the wave form of Fig. 7-3, Eq. 7-10 reduces to

$$\begin{aligned} E_{km} &= \frac{p}{\pi}\int_{-\pi/p}^{\pi/p} e_d \cos k\omega t \, d(\omega t) \\ &= \frac{2p}{\pi}\int_{0}^{\pi/p} E_m \cos \omega t \cos k\omega t \, d(\omega t) \\ &= \left(-\frac{2p}{\pi} E_m \sin\frac{\pi}{p}\right)\frac{\cos k\pi/p}{k^2 - 1} \end{aligned} \tag{7-11}$$

Also, Eq. 7-8 becomes

$$e_d = \frac{p}{\pi} E_m \sin\frac{\pi}{p}\left[1 + \sum_{n=1}^{\infty}\left(\frac{-2\cos n\pi}{n^2p^2 - 1}\right)\cos np\omega t\right] \tag{7-11a}$$

If k is replaced by np, the nth-harmonic ripple fraction may be expressed as follows:

$$r_n = \frac{E_{npm}}{\sqrt{2}\,E_d} = \frac{\sqrt{2}}{[(np)^2 - 1]} \tag{7-12}$$

For $p = 3$, $n = 1$, the fundamental ripple fraction is

$$r_1 = \sqrt{2}/8 = 0.177$$

For $p = 6$, $n = 1$,

$$r_1 = \sqrt{2}/35 = 0.0401$$

7-4. Load Current

The use of a high-current smoothing inductive reactor in series with the load of Fig. 7-1 permits the assumption of a constant load current as shown by Fig. 7-4. The load current for any anode conducting for

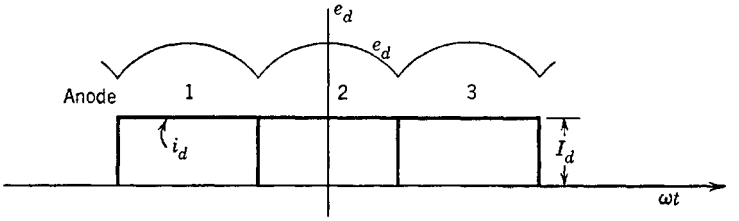

FIG. 7-4. Load current with heavily inductive load circuit.

$2\pi/p$ rad of each cycle is I_d amp; the rms value of the secondary current is given by

$$I_s = \sqrt{\frac{1}{2\pi}\int_{-\pi/p}^{\pi/p} I_d^2\, d(\omega t)} = \frac{I_d}{\sqrt{p}} \tag{7-13}$$

The secondary volt-ampere requirement for a load current of I_d amp is then pE_sI_s. A quantity known as the secondary utilization factor $(UF)_s$ is defined as the ratio of the d-c power output of the rectifier to the volt-amperes supplied in the secondary. Thus, using Eqs. 7-13 and 7-7, one has

$$(UF)_s = \frac{E_dI_d}{pE_sI_s} = \frac{E_d}{\sqrt{p}\,E_s} = \frac{\sqrt{2p}\sin \pi/p}{\pi} \tag{7-14}$$

It can be shown that $(UF)_s$ has a maximum value of 0.675 for $p = 2.69$. A tabulation of values of $(UF)_s$ indicates that $p = 3$ is the best practical

choice as far as the highest secondary utilization factor is concerned. The decrease in $(UF)_s$ with increasing number of anodes or phases in-

p	2	3	6	12
$(UF)_s$	0.637	0.674	0.55	0.40

dicates that a higher secondary kilovolt-ampere rating is required for a given d-c power output as the number of phases increases. This is one of the principal disadvantages of polyphase rectifiers, but special secondary winding connections to be described later permit the reduction of ripple fraction through the use of six anodes while securing effectively the secondary utilization factor of the three-phase star arrangement.

7-5. Six-Phase Star or Three-Phase Full-Wave Circuit

Six-phase rectifier operation may be achieved by the use of center taps on each of the three secondary windings of Fig. 7-1. The center taps are all connected together as the neutral, as shown in Fig. 7-5. The voltages, with respect to neutral of the two ends of each center-tapped

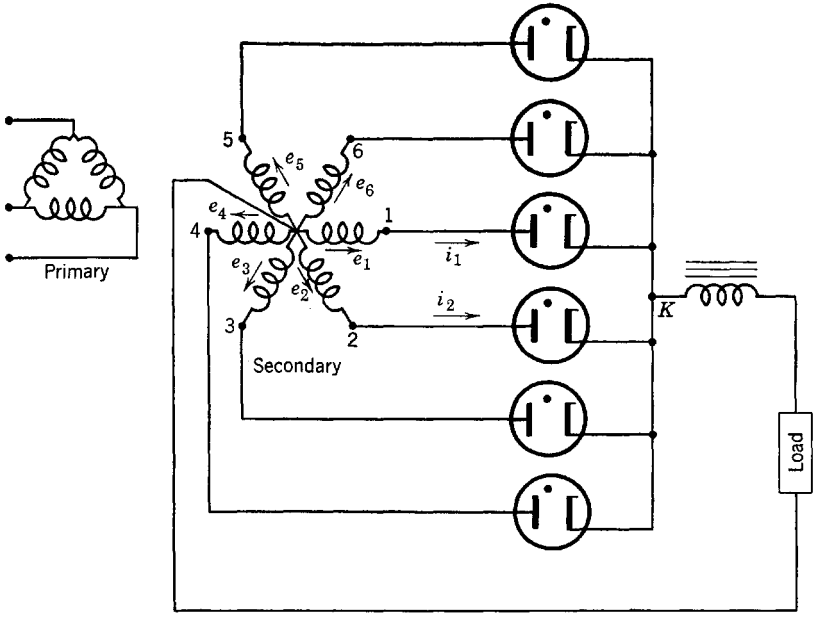

FIG. 7-5. Six-phase star or three-phase full-wave rectifier connection.

winding, are 180° out of phase, exactly as in the single-phase full-wave case. The resulting phase relations between the respective anode voltages are then as shown by the vector diagram of Fig. 7-6. The rectified voltage wave form consists only of the caps of the sine waves. Assuming perfect commutation, each anode conducts for $\pi/3$ rad of each cycle. The conduction-current wave forms are shown in Fig. 7-6 for anodes 6, 1, and 2.

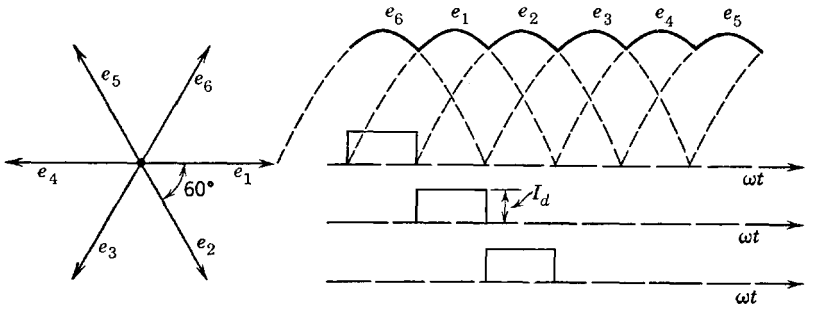

FIG. 7-6. Vector diagram of six-phase star rectifier, with rectified-voltage wave form.

An advantage of the six-phase star circuit over the three-phase half-wave is the fact that the d-c components cancel in the secondary windings of the six-phase star, thus avoiding any tendency toward core saturation. This is the usual advantage possessed by any full-wave circuit over the half-wave circuit. Occasion will be found to refer to this advantage in circuits to be described in later paragraphs.

7-6. Overlap; the Effect of Transformer Leakage Reactance

It has been assumed that commutation from one conducting anode to the next is instantaneous. Actually, as a result of the presence of leakage inductance in the transformer secondary windings, there is a period of overlap during which the current of the outgoing anode decreases toward zero while the current of the incoming anode rises toward its maximum value. The inductance involved includes not only the leakage inductance of the transformer secondary windings, but also inductances, including leakage inductances, reflected into the secondary from the primary circuit. A portion of the rectified wave form of Fig. 7-6 has been reproduced in Fig. 7-7, with the vertical axis coinciding with the intersection of the voltage waves e_1 and e_2. Tube drop has been neglected.

Let L = the leakage inductance per phase, referred to the secondary winding. With the origin of coordinates chosen as in Fig. 7-7, the

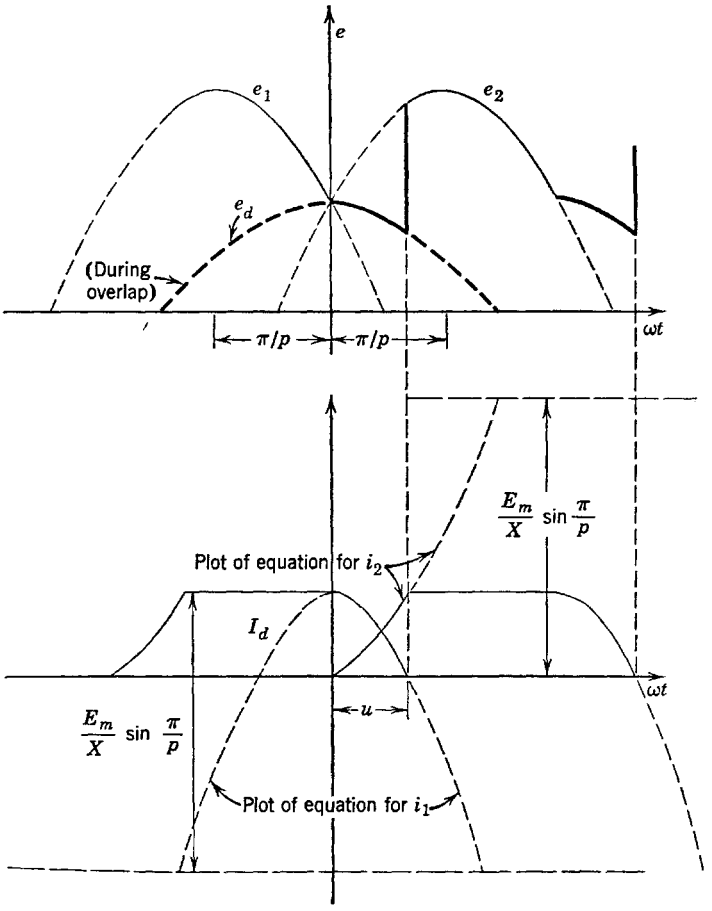

FIG. 7-7. Overlap of conducting anodes.

equations of the overlapping voltage waves e_1 and e_2 are

$$e_1 = E_m \cos(\omega t + \pi/p)$$
$$e_2 = E_m \cos(\omega t - \pi/p) \tag{7-15}$$

If anode 1 continues to conduct after e_2 exceeds e_1, the following relation is obtained by applying Kirchhoff's voltage law around the circuit 0-1-K-2-0, Fig. 7-5;

$$e_1 - L\,di_1/dt + L\,di_2/dt - e_2 = 0$$

or

$$e_1 - e_2 = L(di_1/dt - di_2/dt) \tag{7-16}$$

Also, the sum of the instantaneous anode currents during overlap is equal to the constant load current I_d, or

$$i_1 + i_2 = I_d \tag{7-17}$$

From Eq. 7-17,

$$\frac{di_1}{dt} + \frac{di_2}{dt} = 0 \tag{7-18}$$

Now Eq. 7-16 may be written as follows, if tube drop is neglected:

$$e_1 - L\,di_1/dt = e_2 - L\,di_2/dt = e_d \tag{7-19}$$

whence

$$e_d = (e_1 + e_2)/2 \tag{7-20}$$

From Eqs. 7-16 and 7-18,

$$e_1 - e_2 = 2L\,di_1/dt \tag{7-21}$$

or

$$E_m[\cos(\omega t + \pi/p) - \cos(\omega t - \pi/p)] = -2E_m \sin \omega t \sin \pi/p = 2L\,di_1/dt \tag{7-22}$$

From Eq. 7-21,

$$i_1 = -\frac{E_m}{\omega L} \sin \frac{\pi}{p} \int \sin \omega t\, \omega dt$$

$$= \frac{E_m}{\omega L} \sin \frac{\pi}{p} \cos \omega t + C_1$$

where C_1 is a constant of integration. At time $t = 0$ (Fig. 7-7) the current in phase 1 is equal to the load current I_d, and the current in phase 2, anode 2, is zero, with anode 2 beginning to conduct. Therefore,

$$C_1 = I_d - \frac{E_m}{\omega L} \sin \frac{\pi}{p}$$

and, after $t = 0$, the expression for current i_1 is given by

$$i_1 = I_d - \frac{E_m}{\omega L} \sin \frac{\pi}{p} (1 - \cos \omega t) \tag{7-23}$$

From Eq. 7-17, and with $\omega L = X$,

$$i_2 = I_d - i_1 = \frac{E_m}{X} \sin \frac{\pi}{p} (1 - \cos \omega t) \tag{7-24}$$

According to Eq. 7-20, the voltage e_d during overlap is

$$e_d = \tfrac{1}{2}E_m[\cos(\omega t + \pi/p) + \cos(\omega t - \pi/p)]$$

$$= E_m \cos \omega t \cos \pi/p \tag{7-25}$$

At $\omega t = u$, the angle of overlap as shown on Fig. 7-7,

$$i_1 = 0 = I_d - \frac{E_m}{X} \sin \frac{\pi}{p} (1 - \cos u)$$

so that

$$\cos u = 1 - \frac{I_d X}{E_m \sin \pi/p} \tag{7-26}$$

Computation of the angle of overlap is possible from Eq. 7-26 if the reactance X is known. The rectified voltage equation during overlap (Eq. 7-25) has been sketched in heavy black ink with $p = 3$, on Fig. 7-7. The actual output voltage, beginning with $\omega t = 0$, follows the solid black portion of the cosine curve, Eq. 7-25, for $0 < \omega t < u$. At the end of this interval, the current i_2 reaches the d-c value I_d. In the interval $u < \omega t < 2\pi/p$, $di_2/dt = 0$, and $e_d = e_2$ (see Eq. 7-19). The effect of the leakage inductance and resulting overlap is shown, in Fig. 7-7, to cause a distortion of the output-direct-voltage wave form. The new value of the average output voltage E_d is given by

$$E_d = \frac{p}{2\pi} \left[\int_0^u E_m \cos \omega t \cos \frac{\pi}{p} d(\omega t) + \int_u^{2\pi/p} E_m \cos \left(\omega t - \frac{\pi}{p} \right) d(\omega t) \right]$$

$$= \frac{pE_m}{\pi} \sin \frac{\pi}{p} - \frac{pXI_d}{2\pi} = \frac{p}{\pi} \left(E_m \sin \frac{\pi}{p} - \frac{I_d X}{2} \right) \tag{7-27}$$

which indicates that the output voltage decreases linearly with load current I_d. Since, from Eq. 7-26,

$$I_d X = E_m \sin \frac{\pi}{p} (1 - \cos u)$$

$$E_d = \frac{p}{\pi} E_m \sin \frac{\pi}{p} \left[1 - \frac{(1 - \cos u)}{2} \right]$$

$$= \frac{p}{\pi} E_m \sin \frac{\pi}{p} \left(1 - \sin^2 \frac{u}{2} \right)$$

$$= E_{do} - E_{do} \sin^2 \frac{u}{2} \tag{7-28}$$

where now E_{do} is the direct output voltage found before (Eq. 7-6) by neglecting the leakage inductance. The quantity $E_{do} \sin^2 u/2$ is evidently a decrease in direct output voltage due to leakage reactance.

Expressions for the currents i_1 and i_2 may be obtained in terms of the angle of overlap u by use of Eq. 7-26 in the form

$$\frac{E_m \sin \pi/p}{I_d X} = \frac{1}{1 - \cos u}$$

Thus,
$$i_1 = I_d\left(1 - \frac{1 - \cos \omega t}{1 - \cos u}\right) \tag{7-29}$$

and
$$i_2 = I_d\left(\frac{1 - \cos \omega t}{1 - \cos u}\right) \tag{7-30}$$

The rms value of the secondary current I_s was computed in Eq. 7-13 for the condition of zero overlap. The dependence of I_s upon the angle of overlap may be obtained from Eqs. 7-29 and 7-30 and Fig. 7-7. During the indicated intervals along the ωt axis, the respective currents in phase 2 are given by the following:

$$0 < \omega t < u, \qquad i_2 \text{ given by Eq. 7-30}$$

$$u < \omega t < \left(\frac{2\pi}{p}\right), \qquad I_d \text{ constant}$$

$$\left(\frac{2\pi}{p}\right) < \omega t < \frac{2\pi}{p} + u, \qquad i_1 \text{ given by Eq. 7-29}$$

for the interval $0 < \omega t < u$ in which the current is identically the same at the end of the conduction period of anode 1 as at the end of the conduction period of anode 2. Then, the rms phase current is

$$I_s^2 = \frac{1}{2\pi}\left[\int_0^u i_2^2\, d(\omega t) + \int_u^{(2\pi/p)} I_d^2\, d(\omega t) + \int_0^u i_1^2\, d(\omega t)\right]$$

$$= \frac{I_d^2}{p}\left\{1 - \frac{p}{2\pi}\left[\frac{\sin u(2 + \cos u) - u(1 + 2\cos u)}{(1 - \cos u)^2}\right]\right\} \tag{7-31}$$

The expression for I_s may be simplified by the substitution

$$2\pi\psi(u) = \frac{\sin u(2 + \cos u) - u(1 + 2\cos u)}{(1 - \cos u)^2} \tag{7-32}$$

A series for $\psi(u)$ may be convenient for computation, and is given by

$$\psi(u) = \frac{2u}{15\pi}\left(1 + \frac{u^2}{84} + \cdots\right) \tag{7-33}$$

The function $\psi(u)$ determines the correction to be made in the expression previously developed for I_s; thus, Eq. 7-31 becomes

$$I_s = \frac{I_d}{\sqrt{p}} \sqrt{1 - p\psi(u)} \tag{7-34}$$

The effects of overlap upon rectifier performance may be shown graphically. Curves are available in various references [1,2] and will not be repeated here.

7-7. The Three-Phase Bridge Circuit

A three-phase circuit which achieves an output wave form equivalent to that of the six-phase star is known as a three-phase bridge circuit and is shown in Fig. 7-8. The secondary line-to-line voltages E_{CB}, E_{BA}, and

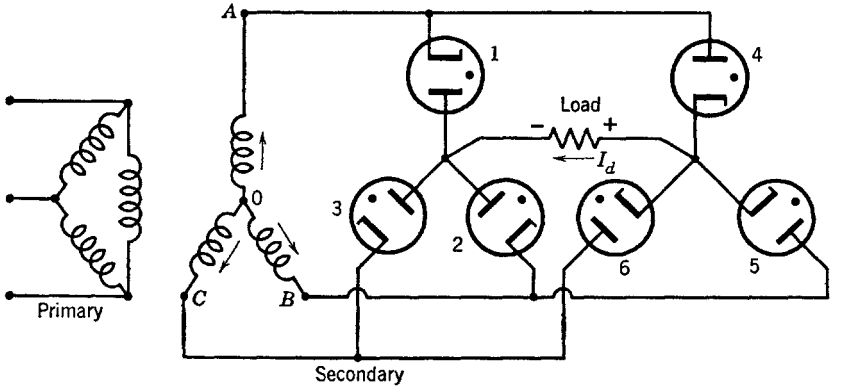

FIG. 7-8. Three-phase bridge.

E_{AC} are applied to the load through two tubes in series. For example, E_{CB} is applied through tubes 5 and 3 when B is positive with respect to C; E_{BA} is applied through tubes 4 and 2 when A is positive with respect to B. Later by π rad in the a-c cycle, these voltages have reversed polarity. Thus, for example, when C is positive and B negative, E_{BC} is applied through tubes 6 and 2. In each cycle, each tube conducts for two 60° intervals, overlap being neglected. An advantage of the three-phase bridge circuit is that it combines the desirable secondary utilization factor of the three-phase circuit with the wave form of the six-phase star. Further, current flows in both directions in the transformer

[1] Marti and Winograd, *Mercury Arc Rectifiers—Theory and Practice*, McGraw-Hill Book Co.

[2] Millman and Seely, *Electronics*, McGraw-Hill Book Co.; MIT Staff, *Applied Electronics*, John Wiley & Sons.

secondary winding, eliminating the tendency toward core saturation. An analysis of this circuit has been called for in the problems.

7-8. The Three-Phase Double-Wye Circuit

One of the most frequently used polyphase rectifier circuits is the three-phase double-wye shown in Fig. 7-9. The delta-connected primary

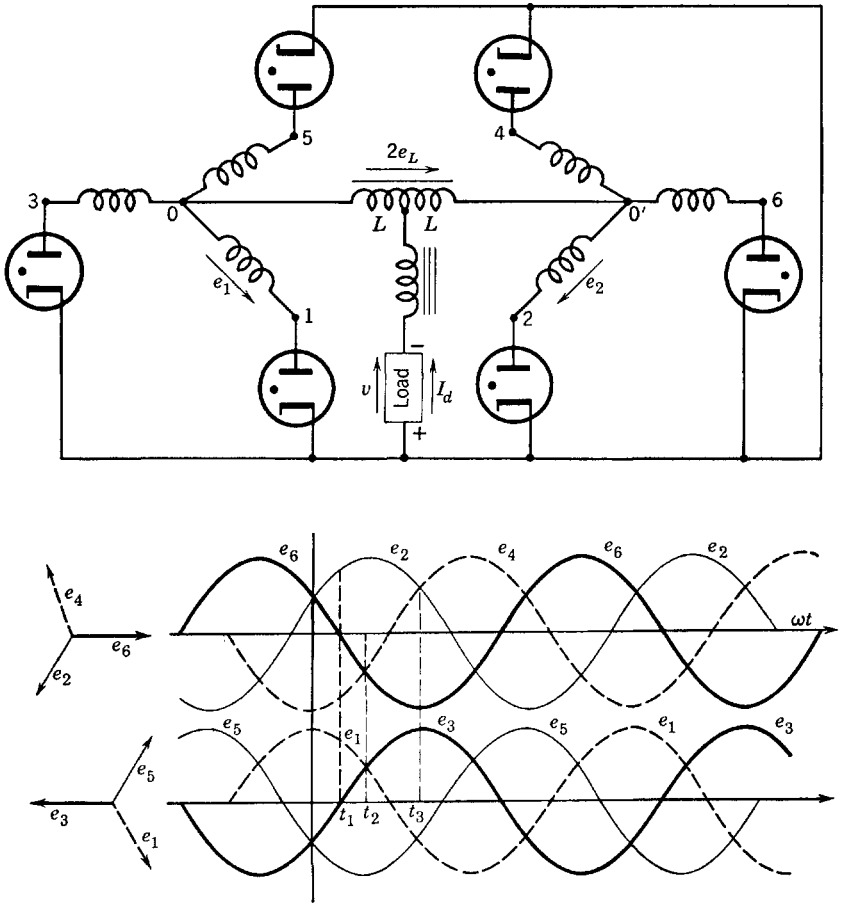

FIG. 7-9. Circuit and secondary-voltage wave forms of a three-phase double-wye rectifier.

is not shown. The circuit consists essentially of two wye-connected secondaries with neutrals connected together through a center-tapped inductor known as an interphase reactor or transformer. Secondary windings 0–1 and 0′–4 are fed by the same primary winding and have

voltages 180° out of phase. The same relation exists between windings 0–3 and 0′–6 and between 0–5 and 0′–2. The vector diagrams of the respective secondary-phase voltages are shown in the lower parts of Fig. 7-9, along with the wave forms. At a time such as t_1, anodes 1 and 2 are both conducting; voltages e_6 and e_3 are zero, and e_5 and e_4 are negative. At t_2, there is commutation of conduction current from 1 to 3. Meanwhile, anode 2 continues to conduct until t_3 when anode 4 takes over. Two anodes, one from the odd-numbered group and one from the even-numbered group, conduct simultaneously, and the two groups of anodes are enabled to behave independently of each other as a result of the presence of the interphase reactor. Overlap resulting from transformer leakage reactance has been neglected in the foregoing.

In the following analysis tube drop will be neglected. The voltage across the interphase reactor is shown in assumed positive sense by the arrow (Fig. 7-9), and the voltage between mid-tap and either end of the interphase reactor is represented by e_L. Kirchhoff's voltage law will now be written for time t_1, first for a loop involving the two conducting anodes and the interphase reactor, and second for a loop including one conducting anode and the load. For this purpose, the voltage across the smoothing choke will be neglected. The equations, with v = the voltage drop across the load, are:

$$e_1 - e_2 - 2e_L = 0 \tag{7-35}$$

$$e_1 - e_L = v \tag{7-36}$$

$$e_2 + e_L = v \tag{7-37}$$

From Eq. 7-35, and the sum of Eqs. 7-36 and 7-37,

$$e_L = (e_1 - e_2)/2 \tag{7-38}$$

and

$$v = (e_1 + e_2)/2 \tag{7-39}$$

One of the important differences between the six-phase star and the three-phase double wye is the load wave form. For the six-phase star, the load wave form is identical with the secondary voltage of the conducting anode during its period of conduction, if tube drop and overlap are neglected. For the three-phase double-wye circuit, however, the load voltage wave form is the average of the voltages of the two windings supplying the simultaneously conducting anodes, as shown by

Eq. 7-39. The sketch of v given on Fig. 7-10 was obtained from Eq. 7-39 where

$$e_1 = E_m \cos \omega t$$

and

$$e_2 = E_m \cos (\omega t - \pi/3)$$

with the origin of coordinates taken as shown on Fig. 7-9. Then,

$$v = \frac{\sqrt{3}}{2} E_m \cos \left(\omega t - \frac{\pi}{6} \right) \tag{7-40}$$

for the interval during which anodes 1 and 2 conduct simultaneously. Then, at $t = t_2$, the current shifts from 1 to 3, and shortly thereafter,

$$v = \frac{e_2 + e_3}{2} = \frac{\sqrt{3}}{2} E_m \sin \omega t \tag{7-41}$$

The caps of the two waves for which the equations are given by Eqs. 7-40 and 7-41 are portions of the output voltage waves from their intersec-

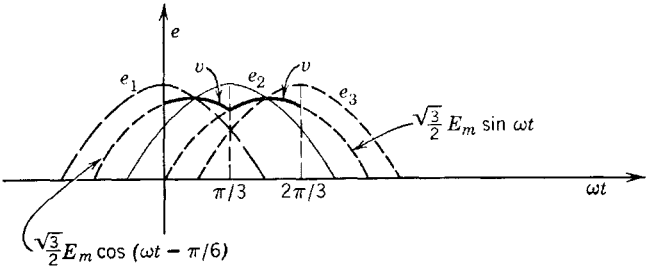

FIG. 7-10. Load-voltage wave form, resistance load, for three-phase, double-wye circuit.

tions to the right and to the left (Fig. 7-10) until similar intersections with other average voltages v are encountered. The complete output-voltage wave form may be plotted from equations obtained from the individual secondary-winding voltages combined two at a time as in Eqs. 7-40 and 7-41.

Another method of analysis avoids writing the individual equations for the separate portions of the various anode voltages by using the Fourier series to represent the wave tops between intersections of the positive portions of the waves of Fig. 7-9. Two Fourier series are needed, one for the odd-, the other for the even-numbered group of voltages, under the condition of zero load. Let $e_{d1}(\omega t)$ represent the no-load

voltage of the odd-numbered group of windings, lower part of Fig. 7-9, and $e_{d2}(\omega t)$ the even-numbered voltage wave form. Equations 7-8 and 7-11 provide the relations from which the series may be written. For $p = 3$,

$$E_{3nm} = -\frac{3\sqrt{3}}{\pi} E_m \frac{\cos n\pi}{(3n)^2 - 1}$$

and

$$e_{d1}(\omega t) = \frac{3\sqrt{3}}{2\pi} E_m \left[1 + \sum_{n=1} \frac{-2\cos n\pi}{(3n)^2 - 1} \cos 3n\omega t\right]$$

$$= \frac{3\sqrt{3}}{2\pi} E_m \left(1 + \frac{1}{4}\cos 3\omega t - \frac{2}{35}\cos 6\omega t + \frac{2}{80}\cos 9\omega t - \cdots + \right) \tag{7-42}$$

The even-numbered voltages lag the odd voltages by $\pi/3$ rad but are otherwise identical. Therefore,

$$e_{d2}(\omega t) = e_{d1}(\omega t - 60°)$$

$$= \frac{3\sqrt{3}}{2\pi} E_m \left(1 - \frac{1}{4}\cos 3\omega t - \frac{2}{35}\cos 6\omega t - \frac{2}{80}\cos 9\omega t - \cdots - \right) \tag{7-43}$$

The load voltage v as expressed by Eqs. 7-39 and 7-41 involves specific sine-wave caps. For the general case, using the series,

$$v = \frac{e_{d1} + e_{d2}}{2} = \frac{3\sqrt{3}\, E_m}{2\pi} \left(1 - \frac{2}{35}\cos 6\omega t - \cdots\right) \tag{7-44}$$

and the fundamental frequency is the sixth harmonic, as for the six-phase star. The interphase reactor voltage e_L as given by Eq. 7-38 becomes

$$e_L = \frac{e_{d1} - e_{d2}}{2} = \frac{3\sqrt{3}\, E_m}{2\pi} \left(\frac{1}{4}\cos 3\omega t + \frac{1}{40}\cos 9\omega t + \cdots\right)$$

$$= \frac{3\sqrt{3}\, E_m}{8\pi} \left(\cos 3\omega t + \frac{1}{10}\cos 9\omega t + \cdots + \cdots\right) \tag{7-45}$$

The analysis for the current in load and secondary is facilitated by the use of Eq. 7-45. Since two anodes overlap at all times, each contributes half of the direct current I_d. The wave form is complicated, however, by the current in the interphase reactor. The voltage e_L in each half of the interphase reactor produces a current i_L lagging the

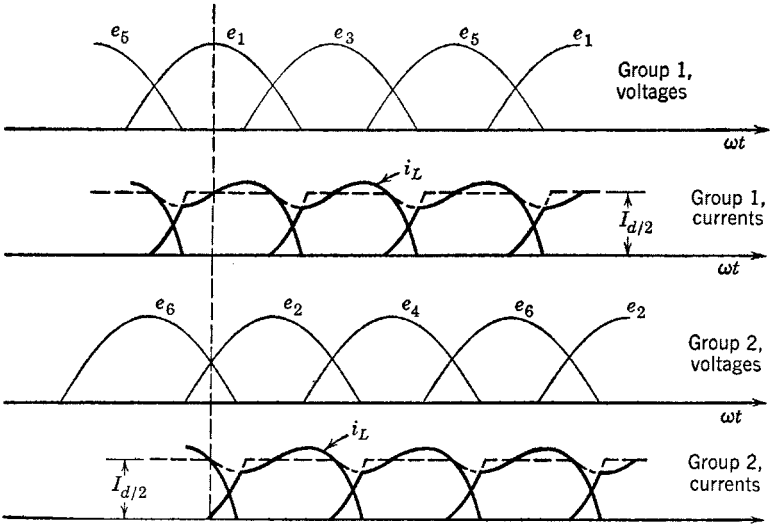

FIG. 7-11. Anode voltages and currents, three-phase double-wye.

voltage. If the resistance of the interphase reactor is neglected, and if e_L be represented by the first term only of Eq. 7-45, then

$$i_L = \frac{3\sqrt{3}\,E_m}{8\pi(3\omega L)} \cos(3\omega t - 90°) = \frac{\sqrt{3}\,E_m}{8\pi\omega L} \sin 3\omega t \qquad (7\text{-}46)$$

This current i_L flows through the two windings, one of group 1 and the other of group 2, which are operating in parallel, and is therefore superimposed upon their normal load currents. This superposition is shown by the heavy-line curve in Fig. 7-11. The amplitude of i_L must of necessity be less than $\frac{1}{2}I_d$ in order for the anodes to pass current always in the forward direction. For the maximum value of i_L to flow, the load current must be such that

$$i_{L\,\max} = I_{d/2} = e_{L\,\max}/3\omega L \qquad (7\text{-}47)$$

Let $X = 2(3\omega L)$, the entire reactance of the interphase reactor at the

third-harmonic frequency. Then Eq. 7-47 may be written as

$$I_d' = \frac{2(3\sqrt{3}\,E_m)}{8\pi X/2} = \frac{3\sqrt{3}\,E_m}{2\pi X} = \frac{1.17E_s}{X} \tag{7-48}$$

where I_d' may be referred to as the transition or critical load current, and an abrupt change in output voltage may be expected as the load current is increased from zero and as it passes through the transition value. For values of load current less than I_d', the relations previously derived do not hold, for the rectifier does not pass reverse current. At zero load current, the current i_L must become zero, since conduction in the inverse direction through one of the overlapping anodes would be required for its existence. Therefore, at no load, there is no voltage across the interphase reactor and the neutrals of the two wye-connected secondary windings are at the same potential. The rectifier then behaves, for zero load, as a six-phase star connected rectifier, and the no-load voltage is

$$E_d = \frac{6}{\pi} E_m \sin\frac{\pi}{6} = \frac{3\sqrt{2}}{\pi} E_s = 1.35E_s \tag{7-49}$$

At transition, $$E_d = 3\sqrt{3}\,E_m/2\pi = 1.17E_s \tag{7-50}$$

Thus, the per cent regulation between zero load and the load corresponding to transition is

$$100(1.35 - 1.17)E_s/1.17E_s = 15.4 \text{ per cent}$$

Between zero load and critical load current, the drop in voltage depends

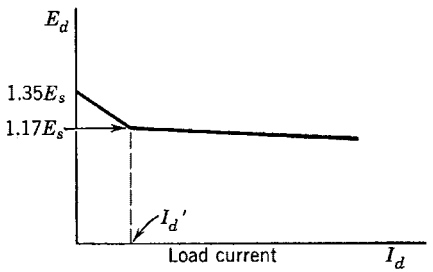

FIG. 7-12. Voltage regulation of double-wye rectifier.

upon the interphase reactor, but, for loads greater than I_d', the drop in voltage depends upon the leakage reactance of the transformer. The curve of Fig. 7-12 shows a typical variation of output voltage with increasing load current.

The angle of overlap between consecutively conducting anodes for load currents exceeding I_d' may be found by applying Eq. 7-26. Let X' be the leakage reactance per phase referred to the secondary. Then,

$$\cos u = 1 - \frac{I_d/2X'}{E_m \sin \pi/3} \tag{7-51}$$

or

$$\frac{I_d X'}{2} = E_m \sin \frac{\pi}{3} (1 - \cos u) \tag{7-52}$$

From Eq. 7-27,

$$E_d = \frac{3E_m}{2\pi}\left(2 \sin \frac{\pi}{3} - \frac{I_d X'}{2E_m}\right) \tag{7-53}$$

where $I_d/2$ for the three-phase double-wye case replaces the I_d in the general case of Eq. 7-27. From Eqs. 7-52 and 7-53,

$$E_d = \frac{3E_m}{\pi} \sin \frac{\pi}{3}\left(1 - \sin^2 \frac{u}{2}\right)$$

$$= 1.17E_s \cos^2 \frac{u}{2} \tag{7-54}$$

The secondary utilization factor of the three-phase double-wye circuit is exactly the same as that of the three-phase half-wave circuit, but the primary utilization factor is very good and exactly the same as that of the three-phase bridge circuit. Both primary and secondary utilization factors are better for the three-phase double-wye than for the six-phase star. The comparative values are as follows:

	$(UF)_p$	$(UF)_s$
Double wye	0.955	0.675
Six-phase star	0.78	0.551

PROBLEMS

7-1. Assuming a one-to-one primary-to-secondary turns ratio, sketch the primary current wave form for a three-phase half-wave rectifier circuit. Assume that all harmonics existing in the secondary wave form (except of course the d-c term) are reflected in the primary current. Compute the primary and secondary utilization factors. Neglect overlap.

7-2. Compute the primary utilization factor for the six-phase star rectifier circuit, with assumptions as in problem 7-1.

7-3. Compute $(UF)_s$ and $(UF)_p$ for the three-phase double-wye circuit. Sketch primary-current wave forms as in problem 7-1, but neglect the third-harmonic component of current in computing $(UF)_p$.

7-4. A certain double-wye rectifier is required to deliver 1000 kw at a full-load output voltage of 625 volts. It is specified that the transition current be 2 per cent of full-load current. The allowable voltage regulation from critical to full load is 4 per cent. Compute (*a*) inductance of the interphase reactor, (*b*) maximum permissible transformer leakage reactance.

7-5. A three-phase double-wye rectifier circuit is rated to supply 600 kw at 600 volts. The tube drop is 20 volts. The output current is assumed constant, and overlap is neglected. Compute (*a*) the transformer secondary voltage per phase, (*b*) the ratio of d-c power delivered to the load to the power delivered at transformer secondary, (*c*) the direct current supplied by each anode, (*d*) the rms value of secondary-winding current to each anode, (*e*) the required kva ratings of primary and secondary.

7-6. The equation for the rectified voltage of a p-anode rectifier, if tube drop is neglected, is

$$e_d = \frac{p}{\pi} E_m \sin\frac{\pi}{p}\left[1 + \sum_{n=1}\left(\frac{-2\cos n\pi}{n^2p^2 - 1}\right)\cos np\omega t\right]$$

(*a*) Obtain an expression for the ripple factor for a three-phase half-wave rectifier for a resistance load with no filter.

(*b*) Derive an expression for the ripple factor if an L-section filter of series inductance and shunt capacitance is connected between rectifier and load. In each case, approximations are suggested.

7-7. Derive an expression for the efficiency of rectification of a p-anode rectifier with pure resistance load R_L, tube drop V_o, peak secondary voltage to neutral E_m.

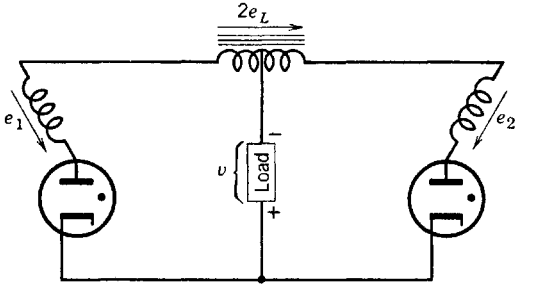

FIG. P7-8.

7-8. Two simultaneously conducting anodes of a three-phase double-wye rectifier are shown in the sketch. Voltages e_1, e_2, and e_L are voltage rises in the indicated positive sense; v is the instantaneous load voltage drop. Take $e_1 = E_m \cos \omega t$ as reference voltage. Neglect tube drop.

(*a*) Obtain expressions for the instantaneous values of e_L and of v from the given data, and sketch v on the same diagram with e_1 and e_2.

(*b*) By the use of the proper limits, namely, $0 < \omega t < \pi/3$, for v in part *a*, show that the rectified direct load voltage is $E_d = 1.17E_s$, where $E_s = E_m/\sqrt{2}$.

7-9. The primary-secondary transformer winding relations for the three-phase double-wye circuit above are shown partially by the sketch below. Sketch the block current diagrams for (*a*) the two secondary windings and (*b*) the primary winding.

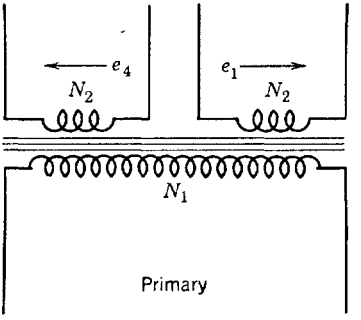

FIG. P7-9.

Show proper phase relations. (*c*) Derive the following over-all (all-winding) volt-ampere relations:

(1) $(\text{va})_p = 1.225E_sI_d$

(2) $(\text{va})_s = \sqrt{3}\,E_sI_d$

(I_d is the direct load current.)

7-10. A three-phase, double-wye rectifier delivers 100 kw at 500 volts direct current and operates delta to double wye from a 2300-volt line. Tube drop is 20 volts when conducting. Do not neglect it. Find (*a*) the required transformer turns ratio, (*b*) the input kva rating required.

7-11. The secondary-winding voltage of a six-phase star-connected rectifier transformer is 550 volts rms. Tube drop is 20 volts when conducting. The transformer is rated 2 kva. Compute the maximum d-c power and direct load current which may be delivered to a resistance load without exceeding the transformer rating.

7-12. Derive the following relations for a three-phase double-wye rectifier:

(*a*) $\cos u = 1 - 0.408I_dX'/E_s$

(*b*) $E_d = 1.17E_s - 0.239I_dX'$

where the symbols have their usual meanings and X' is the leakage reactance of each secondary individual winding.

7-13. A delta-to-double-wye rectifier transformer is delivering 200 kw at 250 volts direct current. Arc drop is 20 volts and must not be neglected. The transformer is fed from a 13,000-volt three-phase system.

(*a*) Determine the secondary voltage to neutral, rms.

(*b*) Assuming the usual block currents, sketch the current wave forms in correct phase relation for the two secondary windings, fed from a single primary winding.

(*c*) Sketch the primary-winding wave form.

(*d*) Sketch the line-current wave form.

(*e*) Compute the maximum values of primary and of line currents.

7-14. It is desired to use three transformers with center-tapped secondary windings in a six-phase star rectifier. The rectifier is to supply 500 kw at 500 volts. The rectifier is to operate from a 440-volt line. Neglect overlap and tube drop. Find (*a*) E_{rms} of secondary winding, (*b*) volt-ampere rating of secondary winding,

(*c*) volt-ampere rating of primary winding, (*d*) ripple factor, (*e*) wave form of line current to primary winding if primary coils are connected in delta.

7-15. It is required to provide d-c power of 220 kw at 550 volts. An a-c power system will supply power at 2300 volts line to line, three phase. Specify primary and secondary transformer ratings, including kva and rms voltage if (*a*) a delta to six-phase star connection is used, (*b*) a delta to three-phase double-wye connection is used. Neglect leakage reactance and arc drop.

7-16. Assume that the leakage reactance (per primary winding) of the three-phase double-wye transformer used to supply the load in problem 7-15 is 6 per cent as given by $X_p = 0.06E_p/I_p$, where E_p and I_p are the rms primary voltage and current.

(*a*) Compute the necessary inductance of the interphase reactor if it is required that transition from six-phase star to double-three-phase operation occur at 20 amp load current.

(*b*) Compute the voltage regulation of the rectifier between full load and transition.

7-17. Including the effects of leakage reactance (problem 7-16):

(*a*) Compute the actual full-load voltage with the transformer used, three phase double wye, and sketch $e_d(\omega t)$.

(*b*) Make any indicated corrections in transformer turns ratio (problem 7-15*b*) to overcome the effects of overlap.

7-18. Analyze the delta-wye three-phase bridge circuit of Fig. 7-8 as follows:

(*a*) Sketch the load-voltage wave form, neglecting tube drop.

(*b*) Sketch the anode current block wave forms, identifying with specified anodes and secondary voltages.

(*c*) Show that $E_s = KE_d$, neglecting tube drop and overlap, and find K.

7-19. (*a*) Specify transformer primary and secondary ratings for a three-phase bridge rectifier supplying 10 kw d-c power at 5000 volts. Neglect overlap.

(*b*) Analyze for overlap and specify the nature of the needed corrections if transformer leakage reactances are 7 per cent per primary winding.

CHAPTER 8

TUNED RADIO-FREQUENCY AND BAND-PASS AMPLIFIERS

THE CIRCUIT THEORY AND BEHAVIOR OF ELECTRON TUBES HAS BEEN illustrated in earlier chapters by providing first-order linear analysis of behavior of high-vacuum tubes as used in audio-frequency voltage and power amplifiers. The present chapter is concerned with a brief analysis of the tuned radio-frequency and of the intermediate-frequency band-pass amplifier. In each of these tube applications, the circuit theory is somewhat more complex than for the audio-frequency range, and it is advisable to begin the study by presenting, in the first sections, the necessary review of circuit theory.

8-1. Tuned Circuits

If the current flowing in a series circuit of R, L, and C is plotted against frequency, the result is illustrated by the curve of Fig. 8-1. It is assumed that the current is supplied by a constant-voltage generator of variable frequency and negligible internal impedance. The sharpness of resonance of the circuit, which is a measure of its frequency-selective property or selectivity, is usually expressed by the frequency interval $f_2 - f_1 = \Delta f$, the bandwidth of the circuit. The frequencies f_1 and f_2 are defined by the reactances

$$X_1 = 1/\omega_1 C - \omega_1 L = R \tag{8-1}$$

and

$$X_2 = \omega_2 L - 1/\omega_2 C = R \tag{8-2}$$

from which the bandwidth is

$$\Delta f = R/2\pi L \tag{8-3}$$

At resonance $X_r = \omega_r L - 1/\omega_r C = 0$ and $I_r = E/R$. At either frequency, f_1 or f_2, $| I | = E/\sqrt{2R^2} = 1/\sqrt{2}\, I_r$, and the power delivered

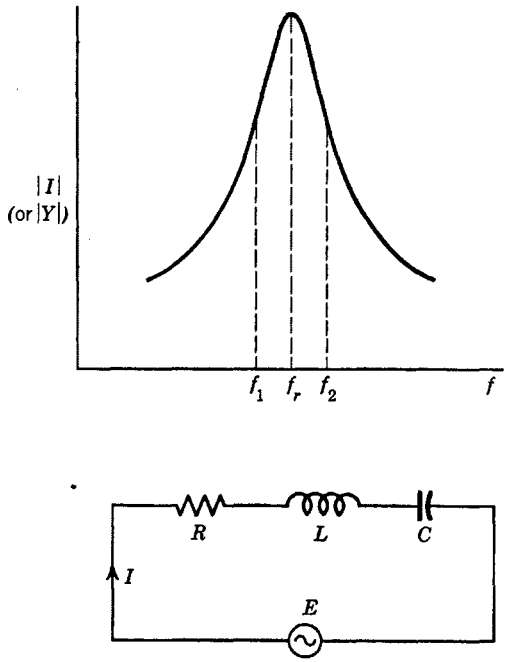

FIG. 8-1. Resonance curve for series R, L, C circuit.

to the circuit is one-half that delivered at the resonant frequency. The ratio

$$\Delta f/f_r = R/\omega_r L = 1/Q_s \tag{8-4}$$

is the fractional frequency discrimination of the circuit. Here, $Q_s = \omega_r L/R$.

In a parallel circuit of R_{ar}, L, and C, the magnitude of the impedance depends upon frequency as shown in Fig. 8-2, where it is assumed that both reactive elements have negligible losses, and that the current is

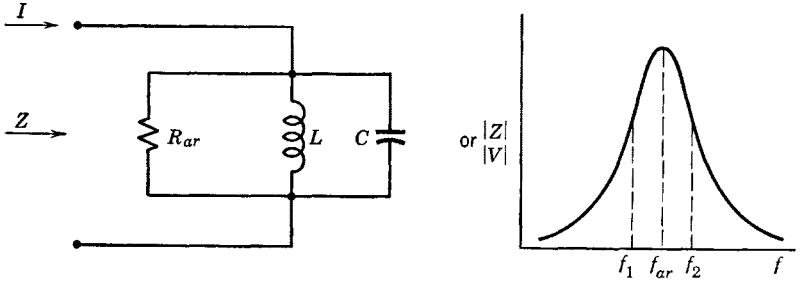

FIG. 8-2. Resonance curve for a parallel R, L, C circuit.

supplied by a constant-current generator of variable frequency and very high internal resistance. Again, the angular frequencies ω_1 and ω_2 are defined by the susceptances

$$1/\omega_1 L - \omega_1 C = 1/R_{ar} \tag{8-5}$$

and

$$\omega_2 C - 1/\omega_2 L = 1/R_{ar} \tag{8-6}$$

The bandwidth is

$$f_2 - f_1 = \Delta f = 1/2\pi R_{ar} C \tag{8-7}$$

and the fractional frequency discrimination is

$$\frac{\Delta f}{f_{ar}} = \frac{1}{2\pi f_{ar} R_{ar} C} = \frac{1}{Q_p} \tag{8-8}$$

where

$$Q_p = \frac{R_{ar}}{(1/\omega_{ar} C)} = \omega_{ar} C R_{ar} \tag{8-9}$$

The admittance of the circuit is Y, the impedance Z. The impedance is given by

$$1/Z = 1/R_{ar} + j(\omega C - 1/\omega L) \tag{8-10}$$

At the frequency of antiresonance, the total susceptance becomes zero, or

$$\omega_{ar} C = 1/\omega_{ar} L \tag{8-11}$$

and $Z = R_{ar}$.

Equation 8-10 may be expressed in terms of Q_p as follows:

$$\frac{R_{ar}}{Z} = 1 + j\omega_{ar} C R_{ar} \left(\frac{\omega}{\omega_{ar}} - \frac{1}{\omega_{ar} \omega LC} \right)$$

$$= 1 + jQ_p(f/f_{ar} - f_{ar}/f) \tag{8-12}$$

From Eq. 8-12,

$$Z = \frac{R_{ar}}{1 + jQ_p(f/f_{ar} - f_{ar}/f)} \tag{8-13}$$

from which may be obtained a normalized resonance curve of $|Z|/R_{ar}$ plotted against $Q_p(f/f_{ar} - f_{ar}/f)$, Fig. 8-3.

The normalized resonance curve is frequently presented in terms of the frequency off-resonance expressed in fractional form. A quantity that may be referred to as the fractional frequency deviation from resonance is defined as

$$\delta = (f - f_{ar})/f_{ar} \tag{8-14}$$

so that

$$f/f_{ar} = 1 + \delta \tag{8-15}$$

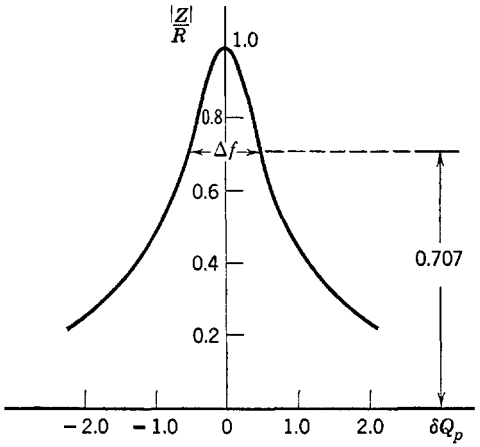

FIG. 8-3. Universal resonance curve for the circuit of Fig. 8-2.

In terms of the parameters Q_p and δ, Eq. 8-13 becomes

$$\frac{Z}{R_{ar}} = \frac{1}{1 + jQ_p\delta(2 + \delta)/(1 + \delta)} \tag{8-16}$$

If the circuit is sufficiently selective, $\delta \ll 1$, and Eq. 8-16 becomes

$$\frac{Z}{R_{ar}} \cong \frac{1}{1 + j2Q_p\delta} \tag{8-17}$$

The bandwidth, from Eq. 8-17, may be obtained from the requirement that

$$2Q_p\delta_1 = 1 \tag{8-18}$$

or

$$2\delta_1 = 2(f_1 - f_{ar})/f_{ar} = \Delta f/f_{ar} = 1/Q_p$$

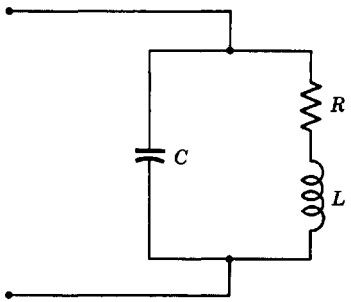

FIG. 8-4. Another form of the parallel-resonant circuit.

If the circuit of Fig. 8-2 is represented as shown in Fig. 8-4, Eq. 8-17 still applies, with $Q_p = \omega_{ar}L/R$.

A useful interpretation of Q_p (or of Q_s) may be obtained as follows. Assume that the voltage across the circuit of Fig. 8-2 is sinusoidal. Then, the maximum energy stored in the capacitor in a cycle is

$$\tfrac{1}{2}CV_m^2$$

where V_m is the peak value of the voltage. The energy dissipated in the resistance per cycle is

$$\int_0^T \frac{V_m^2 \sin^2 \omega t}{R_{ar}} dt = \frac{V_m^2}{2R_{ar}} T$$

The ratio

$$\frac{\text{Maximum energy stored in a cycle}}{\text{Energy dissipated per cycle}} = \frac{\frac{1}{2}CV_m^2}{\frac{1}{2}(V_m^2/R_{ar})T}$$

$$= fR_{ar}C = 2\pi fR_{ar}C/2\pi = Q_p/2\pi$$

Therefore, a more general definition of Q may be stated as 2π times the ratio of energy stored to energy dissipated per frequency cycle. In this form, the parameter Q is usefully applied to circuits having distributed constants. Examples of such circuit elements are sections of transmission lines, wave guides, and cavity resonators.

8-2. Tuned Coupled Circuits

If R_1, R_2, L_1, L_2, C_2 are, respectively, the primary- and secondary-circuit constants of the magnetically coupled circuit in Fig. 8-5, then,

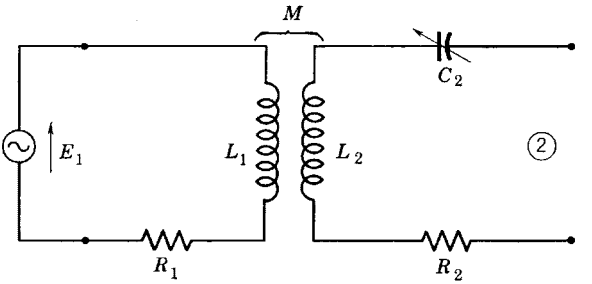

FIG. 8-5. Tuned secondary coupled circuit.

with $X_p = \omega L_1$, $X_s = \omega L_2 - 1/\omega C_2$, $X_m = \omega M$, the driving-point impedance as seen at the secondary terminals 2 is

$$Z_{22}' = R_2 + jX_s + X_m^2/(R_1 + jX_p)$$

$$= R_2 + \frac{X_m^2}{R_1^2 + X_p^2} R_1 + j\left(X_s - \frac{X_m^2}{R_1^2 + X_p^2} X_p\right) \quad (8\text{-}19)$$

If the secondary reactance X_s is adjustable, the secondary current will be maximum (resonance) when the circuit is closed at 2 if

$$X_s = \frac{X_m^2}{R_1^2 + X_p^2} X_p \quad (8\text{-}20)$$

The circuit impedance as seen at terminals 2 becomes a pure resistance, R_{22}' or

$$R_{22}' = R_2 + \frac{X_s}{X_p} R_1 \tag{8-21}$$

In case the primary reactance only is adjustable, as in Fig. 8-6, since at

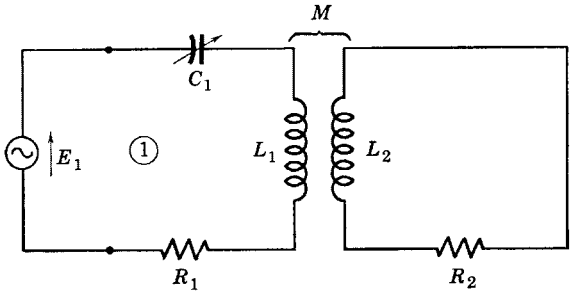

FIG. 8-6. Coupled circuit with primary tuning.

terminals 1 the driving-point impedance is

$$\begin{aligned} Z_{11}' &= R_1 + jX_p + X_m^2/(R_2 + jX_s) \\ &= R_1 + \frac{X_m^2}{R_2^2 + X_s^2} R_2 + j\left(X_p - \frac{X_m^2}{R_2^2 + X_2^2} X_s\right) \end{aligned} \tag{8-22}$$

then the primary current will be maximum, the power delivered to the secondary will be maximum, and thus also the secondary current will be a maximum if X_p is tuned such that

$$X_p = \frac{X_m^2}{R_2^2 + X_s^2} X_s \tag{8-23}$$

The driving-point impedance at 1 is then a pure resistance of value

$$R_{11}' = R_1 + (X_p/X_s)R_2 \tag{8-24}$$

The secondary-current response as a function of frequency has a resonant peak, similar to that of Fig. 8-1, at the resonant frequency, regardless of whether the tuning is done in the primary or in the secondary. For the case of two tuning adjustments, one in the primary and one in the secondary, as in Fig. 8-7, the response current has, in general, two resonant peaks. The optimum tuning adjustment is that for which the driving-point impedances at 1 and at 2 are both pure resistances.

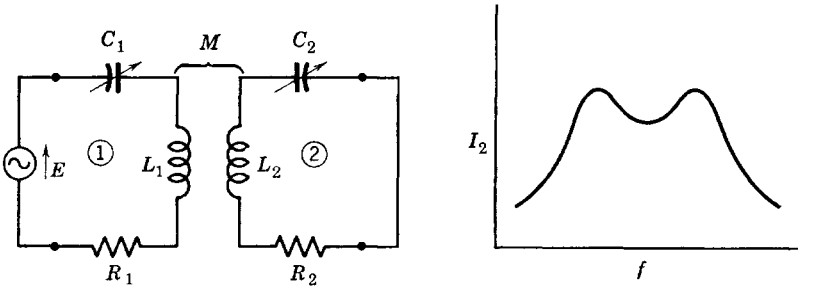

FIG. 8-7. Coupled circuit with both primary and secondary tuning.

The requirements are those of Eqs. 8-20 and 8-23 occurring simultaneously. The result obtained by eliminating X_m^2 from Eqs. 8-20 and 8-23 is that

$$X_p/X_s = R_p/R_s \tag{8-25}$$

where R_p and R_s include all the resistances of the respective meshes, including those of the generator and of the load. The driving-point impedances become

$$Z_{11}' = R_p + (X_p/X_s)R_s$$

$$= R_p + (R_p/R_s)R_s = R_p + R_p \tag{8-26}$$

and

$$Z_{22}' = R_s + (R_s/R_p)R_p = R_s + R_s \tag{8-27}$$

Therefore, the simultaneous adjustment, at a given frequency of primary and secondary reactances according to Eqs. 8-20 and 8-23 results in an impedance match with maximum power transfer in both primary and secondary meshes. The corresponding expression for X_m is

$$X_m = \sqrt{R_pR_s + X_pX_s} \tag{8-28}$$

The response curve of secondary current (Fig. 8-7) depends upon the amount of coupling between primary and secondary circuits. Thus, if X_m is less than $\sqrt{R_pR_s}$, the coupling is said to be insufficient, and a single resonant peak of secondary current occurs at the resonant frequency. If both primary and secondary meshes are tuned according to Eqs. 8-20 and 8-23 at the same frequency of resonance, then a series of

curves similar to those shown in Fig. 8-8 may be obtained as the value of k, the coefficient of coupling, is varied. Curve 1 has insufficient coupling, and curve 2 has critical coupling for which

$$X_m = \sqrt{R_p R_s} \tag{8-29}$$

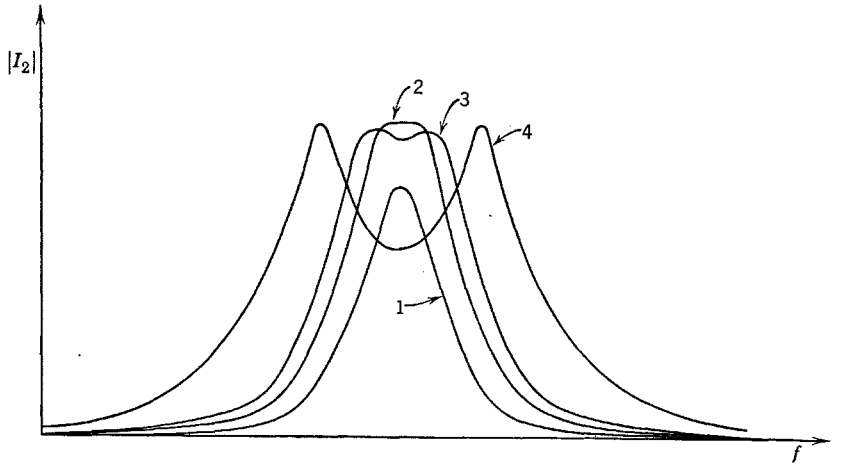

FIG. 8-8. Secondary resonance curves, 1 to 4, with respectively increasing k.

The secondary response curve of the double-tuned circuit can be made to approximate a band-pass filter characteristic, as illustrated in Fig. 8-9, by properly coupling the circuits together. This is the fundamental problem of design of a band-pass amplifier.

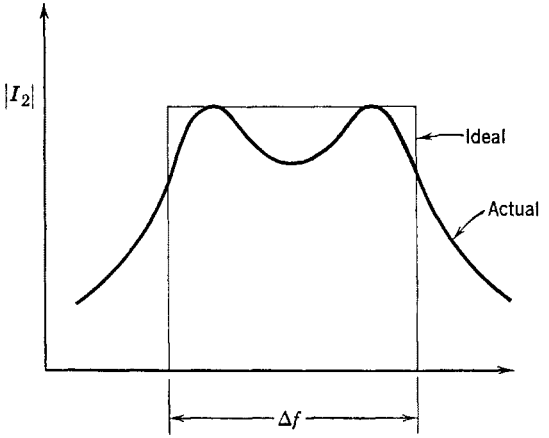

FIG. 8-9. Ideal and actual frequency characteristics of a band-pass amplifier.

8-3. Analysis of the Tuned Coupled Circuit

Before beginning the study of the tuned amplifier, it seems desirable to present a more complete analysis of the tuned coupled circuit than was given in Section 8-2. In particular, it is important to know the conditions under which two resonant peaks occur in the secondary response curve, the location of the peaks, and the bandwidth of the secondary response when two peaks occur. This information is desirably presented in terms of circuit Q, the critical coefficient of coupling, and the resonant

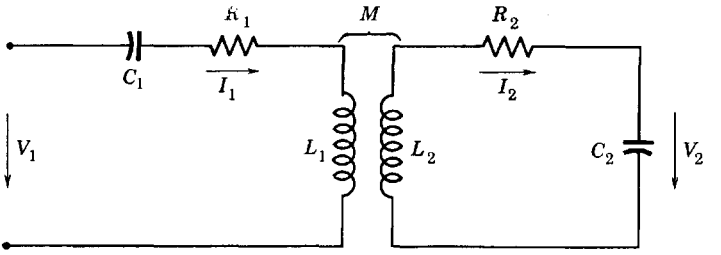

FIG. 8-10. Coupled circuit, with tuning capacitors so adjusted that both primary and secondary are tuned individually to series resonance at $\omega = \omega_0$.

frequency. The objective of the present section is to present such a general analysis. This analysis will later be used for the study of the tuned radio-frequency and tuned band-pass amplifiers.

The commonly used, inductively coupled circuit is shown in Fig. 8-10. The mesh equations for the circuit are

$$\begin{aligned} V_1 &= I_1 Z_{11} + I_2 Z_{12} \\ 0 &= I_1 Z_{12} + I_2 Z_{22} \end{aligned} \tag{8-30}$$

where

$$\begin{aligned} Z_{11} &= R_1 + jX_{11} = R_1 + j(\omega L_1 - 1/\omega C_1) \\ Z_{22} &= R_2 + jX_{22} = R_2 + j(\omega L_2 - 1/\omega C_2) \\ Z_{12} &= -j\omega M \end{aligned} \tag{8-31}$$

The secondary current I_2 is then given by

$$I_2 = \frac{-V_1 Z_{12}}{Z_{11} Z_{22} - Z_{12}^2}$$

and the voltage across C_2 by

$$V_2 = I_2 \left(\frac{1}{j\omega C_2} \right) = \frac{V_1 M}{[(R_1 + jX_{11})(R_2 + jX_{22}) + \omega^2 M^2] C_2} \tag{8-32}$$

Now $k = M/\sqrt{L_1L_2}$, the coefficient of coupling; it is assumed that the primary and secondary are individually tuned to series resonance at $\omega = \omega_0$ and that the two circuits are then coupled together magnetically. Then,

$$\omega_0^2 = 1/L_1C_1 = 1/L_2C_2 \tag{8-33}$$

the primary and secondary circuit Q's are, respectively,

$$\begin{aligned} Q_1 &= \omega L_1/R_1 \\ \text{and} \qquad Q_2 &= \omega L_2/R_2 \end{aligned} \tag{8-34}$$

where ω is any frequency near resonance. The first and second equations of 8-31 may then be revised so as to involve the Q's, ω_0, and k so that

$$Z_{11} = R_1 + j\omega L_1(1 - \omega_0^2/\omega^2) = \omega L_1[1/Q_1 + j(1 - 1/F^2)]$$

$$Z_{22} = \omega L_2[1/Q_2 + j(1 - 1/F^2)]$$

where F is a frequency ratio,

$$F = \omega/\omega_0 = f/f_0 = 1 + \delta \tag{8-35}$$

Also, in Eq. 8-32, $M = k\sqrt{L_1L_2}$. Thus, Eq. 8-32 expressed as a voltage ratio becomes, with some algebraic simplification,

$$\frac{V_2}{V_1} = \frac{k\sqrt{L_2/L_1}}{F^2\left[k^2 + \dfrac{1}{Q_1Q_2} - \left(1 - \dfrac{1}{F^2}\right)^2 + j\left(\dfrac{Q_1 + Q_2}{Q_1Q_2}\right)\left(1 - \dfrac{1}{F^2}\right)\right]} \tag{8-36}$$

Equation 8-32 is the fundamental equation from which nearly all the following equations and interpretations are to be derived. No approximations have been used in the derivation of Eq. 8-36.

In case Q_1 and Q_2 are very large (negligible R_1 and R_2), Eq. 8-36 becomes

$$\frac{V_2}{V_1} = \frac{k\sqrt{L_2/L_1}}{F^2[k^2 - (1 - 1/F^2)^2]} \tag{8-37}$$

At resonance, $F = 1$, and

$$\frac{V_2}{V_1} = \frac{1}{k}\sqrt{\frac{L_2}{L_1}} \tag{8-38}$$

At resonance, but with R_1 and R_2 not neglected,

$$\frac{V_2}{V_1} = \frac{k\sqrt{L_2/L_1}}{k^2 + 1/Q_1Q_2} \tag{8-39}$$

The voltage ratio V_2/V_1 becomes maximum at a critical value of $k = k_c$, which, from Eq. 8-39 is (by maximizing V_2/V_1)

$$k_c = 1/\sqrt{Q_1Q_2} \tag{8-40}$$

the critical coupling. Since

$$k_c = M/\sqrt{L_1L_2} = \sqrt{R_1R_2}/\omega\sqrt{L_1L_2}$$

the corresponding value of ωM is

$$\omega M = \sqrt{R_1R_2} \tag{8-41}$$

The resistance coupled into the primary at resonance with critical coupling is

$$\omega^2M^2/R_2 = R_1R_2/R_2 = R_1$$

Thus at resonance, with $k = k_c$, the secondary current reaches the maximum possible value, and the maximum possible voltage ratio V_2/V_1 is then

$$\left(\frac{V_2}{V_1}\right)_{\max} = \frac{k_c\sqrt{L_2/L_1}}{2k_c^2} = \frac{1}{2}\sqrt{Q_1Q_2}\sqrt{\frac{L_2}{L_1}} \tag{8-42}$$

8-4. Condition for Double Peaks

The coupling necessary to produce two peaks of the given curve, V_2/V_1 vs. f/f_0, may be obtained to a very good approximation from Eq. 8-36 by noting that the frequency ratio $F = f/f_0$ remains reasonably constant, and not too different from unity, in the range of frequency of interest, while the quantity $(1 - 1/F^2)$ varies rapidly with very small changes in F. Therefore, it is justified that the factor F in the denominator of Eq. 8-36 be considered constant in the vicinity of a peak of the curve (V_2/V_1), but that the frequency-dependent variable be designated as

$$a = (1 - 1/F^2) \tag{8-43}$$

With Eq. 8-36 written as

$$\left|\frac{V_2}{V_1}\right| = \frac{k\sqrt{L_2/L_1}}{F^2\sqrt{(k^2 + k_c^2 - a^2)^2 + \left(\frac{Q_1 + Q_2}{Q_1Q_2}\right)^2 a^2}} \tag{8-44}$$

the derivative of $|V_2/V_1|$ with respect to a^2 becomes zero for

$$2(k^2 + k_c^2 - a^2) = \left(\frac{Q_1 + Q_2}{Q_1 Q_2}\right)^2 \tag{8-45}$$

Therefore, a critical value of the frequency-varying quantity a^2 may be found from Eq. 8-45 as

$$a^2 = k_c^2 \left[\frac{k^2}{k_c^2} + 1 - \frac{1}{2k_c^2}\left(\frac{Q_1 + Q_2}{Q_1 Q_2}\right)^2\right] \tag{8-46}$$

A corresponding critical value of $a = (1 - 1/F^2)$ then requires that

$$\frac{k^2}{k_c^2} + 1 \geqq \frac{1}{2k_c^2}\left(\frac{Q_1 + Q_2}{Q_1 Q_2}\right)^2$$

or

$$\left(\frac{k}{k_c}\right)^2 \geqq -1 + \frac{(Q_1 + Q_2)^2}{2(Q_1 Q_2)}$$

which becomes

$$\frac{k}{k_c} \geqq \sqrt{\frac{1}{2}\left(\frac{Q_2}{Q_1} + \frac{Q_1}{Q_2}\right)} \tag{8-47}$$

Thus, if the actual-to-critical coupling ratio exceeds the value given by Eq. 8-47, two peaks of the secondary response curve occur. The fact that the critical values of $a = (1 - 1/F^2)$ represent frequencies at which the ratio $|V_2/V_1|$ is maximum rather than minimum may be shown by sketching the gain curve or by locating the minimum which occurs between the two maxima.

It should be observed from Eq. 8-47 that for identical coils, that is, for $Q_1 = Q_2$, the condition for double peaks becomes simply

$$k \geqq k_c \tag{8-48}$$

The frequencies at which the peaks occur may be found closely enough for practical purposes by use of Eq. 8-46, from which

$$a = 1 - \frac{1}{F^2} = \pm k\sqrt{1 - \left(\frac{k_c}{k}\right)^2\left[-1 + \frac{(Q_1 + Q_2)^2}{2Q_1^2 Q_2^2 k_c^2}\right]}$$

and

$$F_p = \frac{\omega_{1,2}'}{\omega_0} = \frac{1}{\sqrt{1 \pm k\left[1 - \frac{k_c^2}{2k^2}\left(\frac{Q_1}{Q_2} + \frac{Q_2}{Q_1}\right)\right]^{1/2}}} \tag{8-49}$$

where ω_1' is the lower, ω_2' the upper angular frequency at which the peaks, corresponding to the + or − sign in Eq. 8-49, occur. For spe-

cific values of the Q's and the coefficient of coupling, the frequency interval $f_2' - f_1'$ between peaks may easily be computed from Eq. 8-49.

In the particular case for which $Q_1 = Q_2$, and provided $k \gg k_c$,

$$F_p \cong 1/\sqrt{1 \pm k} \tag{8-50}$$

If, in addition, k is small compared to unity, which is frequently the case, the binomial theorem applied to Eq. 8-50 yields

$$F_p \cong 1 \pm k/2 \tag{8-51}$$

which shows that, for the approximations used,

$$\omega_1' = \omega_0(1 - k/2)$$

and

$$\omega_2' = \omega_0(1 + k/2) \tag{8-52}$$

Then,

$$\omega_2' - \omega_1' = k\omega_0$$

or

$$\Delta f' = f_2' - f_1' = kf_0 \tag{8-53}$$

Aiken [1] has shown that the bandwidth over which $\left| V_2/V_1 \right| \geqq$ the gain at resonance is equal to $\sqrt{2}\,\Delta f'$, where $\Delta f'$ is the frequency interval between peaks.

The magnitude of the ratio V_2/V_1 at the two peaks may be found by substituting into Eq. 8-44 the values of F_p from Eq. 8-49. Substitution shows that the peaks are not quite equal in magnitude, but, since $F_p = \omega'/\omega_0$ is so nearly equal to unity, the difference is small and is ordinarily neglected.

8-5. Bandwidth for Narrow-Band Circuits Critically Coupled

The case for which identical coils are used is a practical one and if, in addition, critical coupling is used, a considerable simplification in design formulas may be realized. Equation 8-44 with $Q_1 = Q_2$ and $k = k_c$ becomes

$$A = \frac{V_2}{V_1} = \frac{k_c\sqrt{L_2/L_1}}{F^2\sqrt{(2k_c^2 - a^2)^2 + (2k_c a)^2}}$$

$$= \frac{k_c\sqrt{L_2/L_1}}{F^2\sqrt{4k_c^4 + a^4}} \tag{8-54}$$

[1] C. B. Aiken, Two-Mesh Tuned Coupled Circuit Filters, *Proc. IRE*, **25**, 230 (Feb.) 672 (June 1937).

At the resonant frequency, $F = 1$ and $a = 0$ so that

$$A_{\text{res}} = \frac{\sqrt{L_2/L_1}}{2k_c} \tag{8-55}$$

Then

$$\frac{A}{A_{\text{res}}} = \frac{2k_c^2}{F^2\sqrt{4k_c^2 + a^4}} = \frac{1}{F^2\sqrt{1 + (a^2/2k_c^2)^2}} \tag{8-56}$$

The bandwidth for this important case as applied to narrow-band circuits is obtainable from Eq. 8-56. Since F is so nearly unity between half-power points, the condition for which $A/A_{\text{res}} = 1/\sqrt{2}$ is

$$a^2/2k_c^2 = 1 \tag{8-57}$$

or

$$\frac{a}{\sqrt{2}\,k_c} = 1 = \frac{f^2 - f_0^2}{\sqrt{2}f^2}Q \tag{8-58}$$

Now $\Delta f = 2(f - f_0)$, where f is the frequency of the upper half-power point on the gain ratio curve. Then, with $f = f_0 + \Delta f/2$, Eq. 8-58 becomes

$$\frac{\Delta f/2(2f_0)(1 + \Delta f/4f_0)}{f_0^2(1 + \Delta f/2f_0)^2} = \frac{\sqrt{2}}{Q} \tag{8-59}$$

The quantity $\Delta f/f_0 \ll 1$ for the broadcast receiver. Thus, for such an application Eq. 8-59 reduces essentially to

$$\Delta f = \sqrt{2}\,\frac{f_0}{Q} \tag{8-60}$$

which gives a convenient expression for the effective bandwidth of identical coils each tuned to resonance at $f = f_0$ and critically coupled. Since the coupling is critical, there is only one peak of the resonance curve.

8-6. Calculation for Two Resonant Coupled Circuits, $k > k_c$

It will be assumed that $Q_1 = Q_2$ is known and that each circuit is individually tuned to resonance at $f = f_0$. Since $k > k_c$, there will be two peaks. If the two coils are identical and if $L_1 = L_2$ and k are known, then the circuit behavior is determined and may be predicted. The gain at resonance V_2/V_1 may be computed from Eq. 8-39, critical coupling from Eq. 8-40. The frequencies at which the peaks of the gain-frequency curve occur may be obtained from Eq. 8-49, and the gain at the peaks from Eq. 8-44. The frequencies above and below resonance at which the gain falls to the value at resonance may be simply obtained from the fact,

mentioned before, that the frequency interval between these frequencies is $\sqrt{2}$ times the frequency interval between peaks. Additional points on the gain curve may be computed from Eq. 8-36 or from Eq. 8-44, if required.

8-7. The Tuned Voltage Amplifier

Requirements of radio receivers usually involve amplification of the modulated carrier frequency voltage induced in the receiving antenna by the received radio wave. The necessary amplifier must, in general,

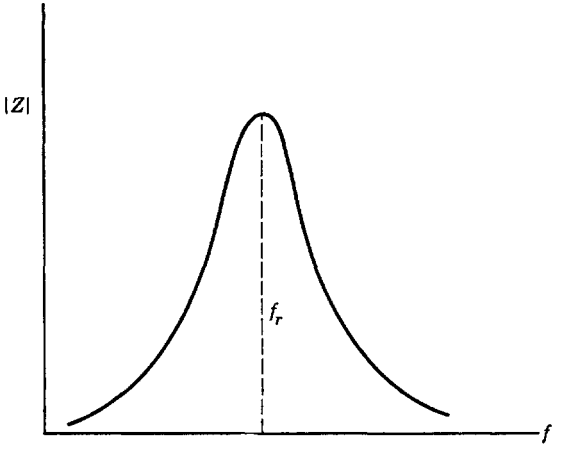

FIG. 8-11. Impedance-frequency characteristic.

meet the following three requirements: (1) It must provide the maximum gain available from a single stage, and is therefore operated as a class-A amplifier; (2) it is required to amplify over a relatively narrow bandwidth which is a small percentage of the center frequency in the band; (3) it is expected to provide voltage gain of such small value for frequencies outside the specified band that such frequencies are in effect rejected by the amplifier.

Power levels of such a tuned amplifier are low, and power efficiency is not an important consideration. In order to satisfy the requirements specified, a tuned circuit is usually employed involving a parallel combination of inductance and capacitance. At the resonant frequency and over a small range of frequencies centered about the resonant frequency, as shown by Fig. 8-11, the impedance of the circuit is maximum and is effectively a pure resistance. Thus, it is possible to design the resonant circuit as a load impedance such that an impedance match is achieved between the high impedance of the tube and the impedance of the load

over a limited range of frequencies. Frequencies outside this limited range over which amplification is desired are attenuated by the tuned circuit and may be neglected in the amplifier output.

Circuits employed as load impedances for tuned radio-frequency amplifiers cannot utilize iron cores because of excessive iron losses at radio frequencies. In addition, distributed capacitances of iron-core transformers are such that the reactance of the transformer primary may actually decrease with frequency at high enough frequencies. Pentodes

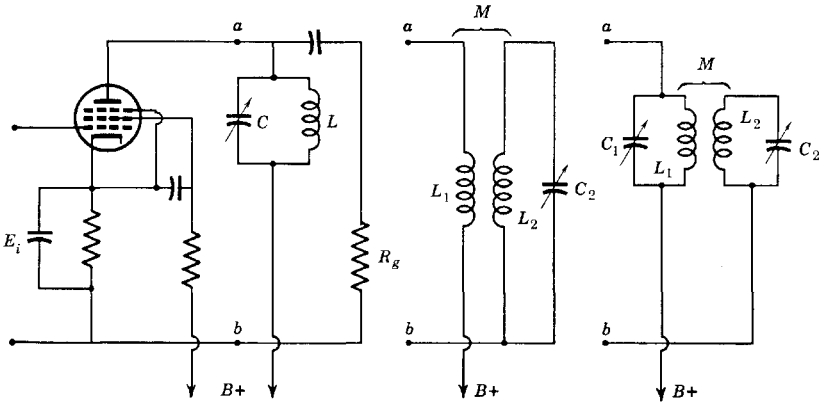

FIG. 8-12. Typical circuits of tuned voltage amplifiers.

are used to provide high gain and also because of their negligible grid-plate interelectrode capacitance. Triodes, if used because they are less noisy than pentodes, require special circuit arrangements to neutralize the effects of currents flowing in the grid-plate capacitance. Triodes may be used without neutralization if connected with the grid at ground potential. The grounded-grid method of operation and neutralizing circuits will be discussed in a later section.

Typical tuned voltage amplifier circuits are shown in Fig. 8-12. Power supply connections are indicated and only the load or coupling circuits are shown in Figs. 8-12*b* and 8-12*c*. The response characteristics of Figs. 8-12*a* and *b* are similar to that shown in Fig. 8-11. The response characteristic of Fig. 8-12*c* is described as a band-pass characteristic as shown by Fig. 8-9.

For the single-tuned case, the transformer coupling Fig. 8-12*b* is preferred to the so-called direct coupling because fewer circuit elements are required for d-c isolation.

The tuned radio-frequency amplifier circuits of Fig. 8-12 operate class A and may be analyzed from their equivalent a-c circuits. The equivalent a-c circuit of Fig. 8-12*a* is shown in Fig. 8-13. The coil re-

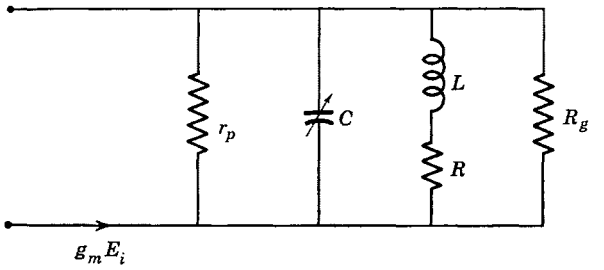

FIG. 8-13. Equivalent a-c circuit of Fig. 8-12*a*.

sistance is shown as R. The admittance of the parallel L–C combination alone is given by

$$Y_{LC} = \frac{R}{R^2 + (\omega L)^2} + j\left(\omega C - \frac{\omega L}{R^2 + (\omega L)^2}\right)$$

$$= \frac{1}{R(1 + Q^2)} + j\left[\omega C - \frac{1}{\omega L(1 + 1/Q^2)}\right] \tag{8-61}$$

Now the coil $Q = \omega_0 L/R$ is assumed to remain reasonably constant in the vicinity of the resonant angular frequency ω_0. For values of $Q \geqq 10$, $Q^2 \gg 1$, and $1/Q^2 \ll 1$, so that a very good approximation for Y_{LC} is available and is written as follows:

$$Y_{LC} = 1/RQ^2 + j(\omega C - 1/\omega L) \tag{8-62}$$

At resonance the circuit impedance is $(Z_{eq})_0$; with RQ^2 replaced by $\omega_0 LQ$, and $\omega_0 C = 1/\omega_0 L$, the gain of the amplifier is given by $A_0 = -g_m(Z_{eq})_0 = -g_m/(Y_{eq})_0$ which becomes

$$A_0 = -\frac{g_m}{1/r_p + 1/R_g + 1/\omega_0 LQ}$$

$$= -\frac{g_m \omega_0 LQ}{1 + \omega_0 LQ(1/r_p + 1/R_g)} \tag{8-63}$$

The gain at any frequency near resonance is

$$A = -\frac{g_m}{Y_{eq}} = -\frac{g_m}{g_p + G_g + 1/RQ^2 + j(\omega C - 1/\omega L)} \tag{8-64}$$

where $g_p = 1/r_p, \qquad G_g = 1/R_g$

As previously shown in the discussion of Section 8-1, introduction of $\delta = (\omega - \omega_0)/\omega_0$ into the expression for an impedance or admittance of a narrow-band circuit may simplify the expression. The circuit admittance takes the form

$$Y_{eq} = g_p + G_g + 1/RQ^2 + j\omega_0 C(\omega/\omega_0 - \omega_0/\omega) \tag{8-65}$$

Since $\omega/\omega_0 = \delta + 1$ and $\omega_0/\omega = 1/(\delta + 1) \cong 1 - \delta$ for $\delta \ll 1$ (which is true for ω near ω_0), then

$$Y_{eq} = g_p + G_g + 1/RQ^2 + j\omega_0 C(2\delta) \tag{8-66}$$

Since $\omega_0 C = 1/RQ$, the ratio of the gain at frequencies near resonance to the gain at resonance becomes

$$\frac{A}{A_0} = \frac{1}{1 + j\dfrac{(2\delta/RQ)}{g_p + G_g + 1/RQ^2}} \tag{8-67}$$

From Eq. 8-67, the bandwidth is obtained from the value of δ for which $A/A_0 = 1/(1 \pm j)$. If the upper frequency for which the gain is 3 db down is ω_2, then $\delta_2 = (\omega_2 - \omega_0)/\omega_0$

$$\frac{2\delta_2}{RQ(g_p + G_g) + \dfrac{1}{Q}} = 1 \quad \text{and} \quad \left|\frac{A}{A_0}\right| = \frac{1}{\sqrt{2}}$$

Then, $$\Delta\omega/\omega_0 = \Delta f/f_0 = 2\delta_2 = \omega_0 L(g_p + G_g) + 1/Q \tag{8-68}$$

Thus, the bandwidth of the parallel L–C circuit alone is $(\Delta f)_{LC} = f_0/Q$, but the bandwidth of the tuned amplifier is

$$\Delta f = f_0[\omega_0 L(g_p + G_g) + 1/Q] \tag{8-69}$$

The ratio of the bandwidth of the tuned L–C combination to the bandwidth of the amplification curve has been defined [2] as the ratio of the effective Q of the amplification curve to the actual Q of the tuned circuit and is

$$\frac{(\Delta f)_{LC}}{\Delta f} = \frac{1}{\omega_0 LQ(g_p + G_g) + 1} \tag{8-70}$$

[2] Terman, *Radio Engineer's Handbook*, p. 435.

8-8. Single-Tuned, Direct-Coupled, Broad-Band Amplifier

In television circuits as contrasted with radio-receiver applications, much greater bandwidths are required. It has already been mentioned in Chapter 3 in connection with compensated broad-band amplifiers that bandwidths in excess of 4 Mc are required in the video output sections of a television receiver. Television channel allocations are 6 Mc wide. For instance, channel 2 employs frequencies in the range 54 to 60 Mc, and channel 10 covers the range 192 to 198 Mc. At such frequencies, the ratio $\delta = (f - f_0)/f_0$ is of the order of $3/57 \cong 0.053$ or $3/195 = 0.0154$; thus the approximations requiring $\delta \ll 1$ are met as before. However, the bandwidth requirement of 4 to 6 Mc is such that the effective shunting resistance for a coupling circuit such as that of Fig. 8-2 is of the order of 4000 ohms. The total shunt capacitance C (Fig. 8-2 or 8-13) is the tube output plus the stray wiring plus the following stage input capacitance and is not adjustable. The required inductance L is that required to resonate with C, which is generally in the range 6 to 10 $\mu\mu$f. If C is taken as 10 $\mu\mu$f, $f_0 = 57$ Mc, $L = 0.78$ microhenry. Since $\Delta f/f_0 = 4/57 = 1/Q$, $\omega_0 C R_{ar} = Q = 14.2$, and $R_{ar} = 3980$ ohms. Because of the low value of the required shunt resistance, it is possible practically to ignore the pentode plate resistance which, in general, is in excess of 500,000 ohms. Therefore, the gain equation as obtained from Fig. 8-13 with L, C, and R in parallel and R_g and r_p removed, is

$$A = -\frac{g_m}{Y} = -\frac{g_m R}{1 + jR(\omega C - 1/\omega L)}$$

$$= \frac{g_m R}{1 + jQ[f/f_0 - f_0/f]} = \frac{g_m R}{1 + j2\delta Q} \tag{8-71}$$

Here $Q = \omega_0 CR$, and R is the effective shunting resistance including the input resistance (Miller effect) of the following stage. The bandwidth $\Delta f = 1/(2\pi RC)$.

8-9. The Single-Tuned, Transformer-Coupled, Radio-Frequency Amplifier

The equivalent circuit of Fig. 8-12*b* has been drawn in Fig. 8-14. It may be assumed that the input to a second stage of amplification is shunted across C_2. Certain justifiable approximations and assumptions at broadcast frequencies in the range 500 to 1600 kc may be used. These are: (1) the input conductance of the second, negatively biased, stage is negligible; (2) the input capacitance of the second stage and stray wiring capacitances are small corrections on the required value of C_2 and

are included in C_2; (3) the tube plate resistance is very large compared with either the winding resistance R_1 or the reactance $X_1 = \omega L_1$; if for example L_1 is of the order of 100 microhenrys, and $f = 1000$ kc, then

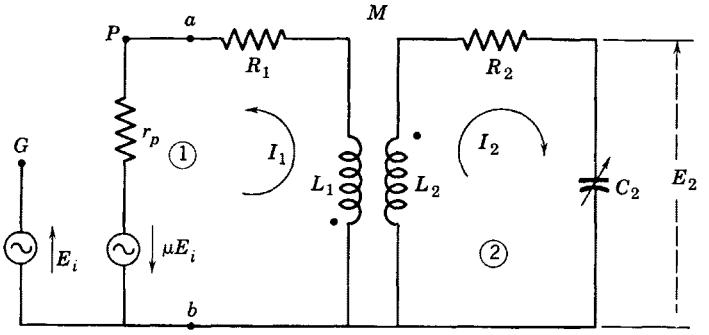

FIG. 8-14. Equivalent a-c circuit of Fig. 8-12*b*.

$X_1 = 628$ ohms, which is small compared with the plate resistance of a pentode or high-mu triode.

The voltage gain of the amplifier may be obtained from Fig. 8-14 and is

$$A = \frac{I_2(1/j\omega C_2)}{E_i}$$

Since

$$I_2 = \frac{-\mu E_i Z_{12}}{Z_{11}Z_{22} - Z_{12}^2}$$

where $Z_{12} = -j\omega M$, $\quad Z_{11} \cong r_p + j\omega L_1$, $\quad Z_{22} = R_2 + jX_{22}$

$$X_{22} = \omega L_2 - 1/\omega C_2$$

then

$$A = \frac{\mu\omega M/(\omega C_2)}{(r_p + j\omega L_1)(R_2 + jX_{22}) + \omega^2 M^2} \tag{8-72}$$

Now the tuning adjustment C_2 will provide a maximum gain at a specified frequency, and the proper design choice of M will ensure that an optimum value of the maximum gain will result at this frequency. At this point a distinction should be made between mutual coupling requirements needed for pentodes as compared with triodes in the tuned amplifier. The distinction is easily stated. Pentodes have intrinsically higher gains than triodes and are generally operated in circuits having much less than critical coupling. The use of a small value of M, much less than optimum, is recommended for the pentode amplifier in order to reduce the possibility of oscillations which may occur with close coupling in spite of the small capacitance between control grid and plate. With

optimum coupling, the plate load impedance of a pentode may be comparable with the reactance $1/(\omega C_{g1p})$; in the case of a triode, neutralizing circuits are used, and the tube plate resistance is smaller, so that optimum coupling may be used.

The gain at resonance of a pentode tuned radio-frequency amplifier may then be obtained very easily from Eq. 8-72. Tuning is such that, approximately, at the specified resonant frequency ω_0,

$$X_{22} = \omega_0 L_2 - 1/\omega_0 C_2 = 0 \tag{8-73}$$

Then,
$$A_0 = \frac{\mu\omega_0 M/\omega_0 C_2}{r_p R_2(1 + j\omega_0 L_1/r_p) + \omega^2 M^2}$$

and with $\omega_0 L_1/r_p \ll 1$, the gain becomes

$$A_0 = \frac{g_m\omega_0 M(\omega_0 L_2/R_2)}{1 + \omega_0{}^2 M^2/r_p R_2} = \frac{g_m\omega_0 M Q_2}{1 + \omega_0{}^2 M^2/r_p R_2} \tag{8-74}$$

and is approximately, for $(\omega_0 M)^2/r_p R_2 \ll 1$

$$A_0 \cong g_m\omega_0 M Q_2 \tag{8-75}$$

This voltage gain (Eq. 8-74 or 8-75) is not the maximum voltage gain which may be obtained with simultaneous adjustment of C_2 and design or adjustment of M. Nor can the value of A_0 be increased indefinitely as M increases, as may erroneously be concluded by using Eq. 8-75 alone, for, with increasing M, the approximation used to obtain Eq. 8-75 no longer holds. An optimum value of M for maximum A_0 exists and may be obtained from Eq. 8-74 by differentiation, or from the requirement for an impedance match in the secondary circuit, mesh 2. The impedance in mesh 2 at any angular frequency ω is

$$Z_{22}' = R_2 + \frac{\omega^2 M^2}{r_p{}^2 + (\omega L_1)^2} r_p + j\left(X_{22} - \frac{\omega^2 M^2}{r_p{}^2 + (\omega L_1)^2}\omega L_1\right) \tag{8-76}$$

For optimum resonance, tuning should be such that, at $\omega = \omega_0$,

$$X_{22}\Big]_{\omega_0} = \omega_0 L_2 - \frac{1}{\omega_0 C_2} = \frac{\omega_0{}^2 M^2}{r_p{}^2 + (\omega_0 L_1)^2}(\omega_0 L_1) \tag{8-77}$$

and coupling should be such that

$$\frac{\omega_0{}^2 M^2}{r_p{}^2 + (\omega_0 L_1)^2} r_p = R_2 \tag{8-78}$$

From Eqs. 8-77 and 8-78,

$$\left.\frac{X_{22}}{X_1}\right]_{\omega_0} = \frac{R_2}{r_p} = \frac{\omega_0^2 M^2}{r_p^2 + (\omega_0 L_1)^2} = \frac{\omega_0^2 M^2}{r_p^2[1 + (\omega_0 L_1/r_p)^2]} \tag{8-79}$$

If $\omega_0 L_1/r_p \ll 1$,

then
$$\left.\frac{X_{22}}{X_1}\right]_{\omega_0} = \frac{R_2}{r_p} \cong \frac{\omega_0^2 M^2}{r_p^2}$$

whence
$$\omega_0^2 M^2 = R_2 r_p \tag{8-80}$$

and
$$\omega_0 L_2 - \frac{1}{\omega_0 C_2} = \frac{R_2}{r_p}(\omega_0 L_1) \tag{8-81}$$

It is shown, then, that for optimum tuning, the capacitance C_2 is adjusted according to Eq. 8-81 rather than Eq. 8-73. However, with $\omega_0 L_1/r_p \ll 1$, $(\omega_0 L_1/r_p)R_2$ is small so that Eq. 8-73 is a reasonable approximation. Also, the optimum value of M may be obtained from Eq. 8-80. With optimum tuning and coupling, the total mesh impedance of mesh 2 is $2R_2$, which provides a perfect impedance match and maximum power in mesh 2.

The gain at resonance with optimum tuning and coupling may then be obtained from Eqs. 8-74 and 8-80 and is

$$A_{00} = g_m Q_2 \sqrt{r_p R_2}/2 = (\mu Q_2/2)\sqrt{R_2/r_p} \tag{8-82}$$

a form particularly useful for triodes.

The bandwidth of the single-tuned transformer-coupled circuit may be determined from Eq. 8-72. At any angular frequency ω near resonance,

$$A = \frac{g_m M/R_2 C_2}{[1 + jQ_2(\omega/\omega_0 - \omega_0/\omega) + \omega^2 M^2/r_p R_2]} \tag{8-83}$$

The same substitution of $\omega/\omega_0 = \delta + 1$ may be used as in Eqs. 8-65 and 8-66. The value of C_2 used is that required for resonance at ω_0; $M/R_2 C_2 = \omega_0 M/\omega_0 R_2 C_2 = Q_2 \omega_0 M$. Then, with some algebraic rearrangement, Eq. 8-83 becomes

$$A = \frac{g_m \omega_0 M Q_2}{1 + \omega^2 M^2/r_p R_2 + j2\delta Q_2} \tag{8-84}$$

and
$$A_0 = \frac{g_m \omega_0 M Q_2}{1 + \omega_0^2 M^2/r_p R_2} \tag{8-74}$$

Thus,
$$\frac{A}{A_0} = \frac{1}{\dfrac{1 + \omega^2 M^2/r_p R_2}{1 + \omega_0{}^2 M^2/r_p R_2} + j\dfrac{2\delta Q_2}{1 + \omega_0{}^2 M^2/r_p R_2}}$$

and since $\left(\dfrac{1 + \omega^2 M^2/r_p R_2}{1 + \omega_0{}^2 M^2/r_p R_2}\right)$ differs very little from unity,

$$\frac{A}{A_0} \cong \frac{1}{1 + j\dfrac{2\delta Q_2}{1 + \omega_0{}^2 M^2/r_p R_2}} \tag{8-85}$$

and $| A/A_0 | = 1/\sqrt{2}$ for

$$2\delta = \frac{\Delta f}{f_0} = \frac{1}{Q_2}\left(1 + \frac{\omega_0{}^2 M^2}{r_p R_2}\right) \tag{8-86}$$

If reference is made to Eqs. 8-17, 8-67, and 8-70, it may be seen that the effective Q of the circuit is the coefficient of 2δ when the ratio of the gain at any frequency to the gain at resonance is expressed in the form of Eq. 8-85. If the effective Q is Q_e, then,

$$\frac{Q_e}{Q_2} = \frac{(\Delta f)_{LC}}{\Delta f} = \frac{1}{1 + \omega_0{}^2 M^2/r_p R_2} \tag{8-87}$$

Equation 8-87 applies, subject to the approximations used in its derivation, to transformer-coupled single-tuned circuits using either triodes or pentodes. Triodes may be chosen in an effort to reduce noise, and, with the triode amplifier, optimum coupling may be used, and, from Eqs. 8-80 and 8-87, the bandwidth is seen to be twice the bandwidth of the tuned secondary circuit ($Q_e = \frac{1}{2}Q_2$). This may require using less than optimum coupling to decrease the bandwidth where necessary for the required selectivity. For the pentode case, however, the coupling is very much less than optimum, so that the bandwidth of the amplifier approaches that of the tuned circuit.

Optimum coupling and design for optimum coupling are indicated where a transformer-coupled single-tuned circuit is used to couple an antenna to the grid of a vacuum tube. In this case the design procedure may be made to yield unique design values, provided critical coupling is used. Design procedures for single-tuned, transformer-coupled interstage circuits may require arbitrary selection of one or more parameters so that the factors of engineering experience and judgment may enter. Such matters belong more properly in a text on communication circuits.

8-10. The "Band-Pass" Amplifier. Theory

A reasonably general analysis of two circuits tuned to the same frequency and coupled together magnetically was given in Sections 8-3 and 8-4, where it was shown that double peaks of the response curve of the circuit will occur if the coupling is made to exceed a specified value given

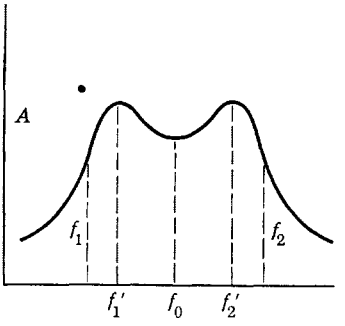

FIG. 8-15. Gain-frequency curve for band-pass amplifier.

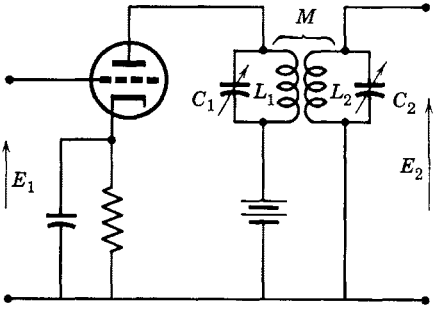

FIG. 8-16. Amplifier with band-pass coupling.

by Eq. 8-47. The gain-frequency characteristic of such a circuit is shown in Fig. 8-15, and the circuit as used for an amplifier coupling or load is shown in Fig. 8-16. The effective bandwidth of the amplifier is approximately $f_2 - f_1$; input frequencies well outside this interval are amplified in voltage very little at the output. Amplification is provided only for a band of frequencies centered about f_0. This type of amplifier

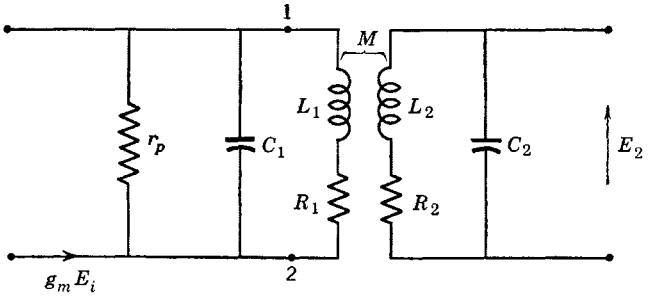

FIG. 8-17. Equivalent a-c circuit of Fig. 8-16.

is particularly useful as an intermediate-frequency amplifier in a superheterodyne receiver, in which the center frequency and the pass band can remain fixed. The amplifier operates class A.

The equivalent a-c circuit of Fig. 8-16 is shown in Fig. 8-17. The theory developed in Sections 8-3 and 8-4 may be shown to be applicable to the circuit of Fig. 8-17. Since pentodes are generally used, r_p is high

and may be omitted. Also, identical coils are often used for L_1 and L_2. The new and simplified equivalent circuit is shown in Fig. 8-18. For television applications, the capacitances C are determined by the total of residual capacitances of the circuits, assumed to be the same. For broadcast radio-receiver applications, the capacitances C are small, fixed

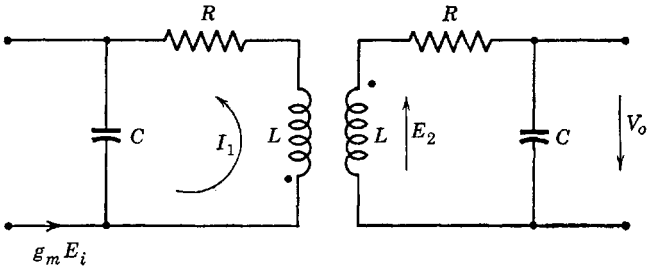

FIG. 8-18. Simplified equivalent circuit of a double-tuned pentode amplifier.

capacitors. If resistances R_s exist in shunt with the inductances, and if, for such resistances,

$$R_s \gg \omega L$$

then it may easily be shown that the impedance equivalent to R_s and L in parallel is $R + j\omega_0 L$ where

$$R = \omega_0^2 L^2 / R_s \tag{8-88}$$

Then
$$Q = \omega_0 L / R = R_s / \omega_0 L \tag{8-89}$$

The mesh impedance of the secondary is

$$Z_s = R + j(\omega L - 1/\omega C)$$

The impedance reflected into the primary from the secondary is

$$Z_r = (\omega M)^2 / Z_s \tag{8-90}$$

The current $g_m E_i$ divides between C and the primary such that the current I_1 is

$$I_1 = \left[\frac{-j(1/\omega C)}{-j(1/\omega C) + R + j\omega L + (X_m^2/Z_s)} \right] g_m E_i \tag{8-91}$$

The voltage E_2 (Fig. 8-18) is then

$$E_2 = -j\omega M I_1,$$

and the voltage V_o is given by

$$V_o = \frac{E_2}{R + j(\omega L - 1/\omega C)}[-j(1/\omega C)]$$

$$= \frac{-j\omega M(1/\omega C)^2 g_m E_i}{[R + j(\omega L - 1/\omega C)]^2 + (\omega M)^2} \tag{8-92}$$

The voltage V_o becomes maximum at a frequency $\omega = \omega_0$ for which

$$\omega_0 L = 1/\omega_0 C$$

provided that the coupling is critical. Critical coupling, as previously defined, requires an impedance match in the primary (or secondary) which is achieved if the reflected impedance at $\omega = \omega_0$ is

$$Z_r = (\omega_0 M_c)^2/R = R$$

or

$$(\omega_0 M_c) = R \tag{8-93}$$

For these conditions, then,

$$V_{o\,\max} = -j\frac{g_m E_i}{2R\omega_0{}^2 C^2} = -j\frac{g_m E_i L}{2RC} \tag{8-94}$$

The maximum amplifier gain is

$$A_{o\,\max} = \frac{V_{o\,\max}}{-E_i} = j\frac{g_m}{2R\omega_0{}^2 C^2} \tag{8-95}$$

and the gain at any angular frequency ω and for any coupling is

$$A = \frac{jg_m\omega M(1/\omega^2 C^2)}{[R + j(\omega L - 1/\omega C)]^2 + \omega^2 M^2} \tag{8-96}$$

It is proposed to express the relative gain $A/A_{o\,\max}$ in terms of the dimensionless parameters Q, $F = f/f_0$, and $\gamma = k/k_c$. The parameter γ is the ratio of the actual to the critical coefficient of coupling. Substitutions may be made as follows:

Thus

$$\left.\begin{aligned} M &= k\sqrt{L^2} = kL \\ M_c &= k_c L \\ \omega M &= \frac{\omega}{\omega_0}(\omega_0 M_c)\left(\frac{M}{M_c}\right) = FR\gamma \\ \omega L &= \frac{\omega}{\omega_0}(\omega_0 L) = FRQ \\ \frac{1}{\omega C} &= \frac{\omega_0}{\omega}\left(\frac{1}{\omega_0 C}\right) = \frac{1}{F}(\omega_0 L) = \frac{RQ}{F} \end{aligned}\right\} \tag{8-97}$$

Then,
$$\frac{A}{A_o} = \frac{\omega M(2R)\omega_0^2/\omega^2}{[R + j(\omega L - 1/\omega C)]^2 + \omega^2 M^2} \tag{8-98}$$

becomes
$$\frac{A}{A_o} = \frac{2\gamma/F}{[1 + jQ(F - 1/F)]^2 + (\gamma F)^2} \tag{8-99}$$

which may be used to plot relative gain-versus-frequency curves (referred to gain at the peaks) for identical coils tuned to resonance at $f = f_0$ and coupled together.

It can be shown that the center of symmetry of the relative gain-frequency curve is not a vertical line, although the gain-frequency curve is very closely symmetrical about a vertical line at the frequency f_0 for all frequencies not too far removed from f_0. A useful parameter is the width Δf of the relative gain-frequency curve between two frequencies for which the relative gain has the same magnitude. Let the relative gain be $A_r = A/A_0$. Then the quantity $(F - 1/F)$ has two values for which the relative gain is a given value of A_r. If the upper and lower of these two frequencies, which are above and below f_0, are designated, respectively, by f_a and f_b, then the width of the curve between them is given by

$$\Delta f = f_a - f_b \tag{8-100}$$

It is easily shown in the case of the tuned circuit of R, L, and C in parallel that the resonant frequency is the geometric mean between frequencies f_1 and f_2 as defined in Section 8-1. That is, $f_0 = \sqrt{f_1 f_2}$. Similarly here it is true that

$$f_0^2 = f_a f_b \tag{8-100}$$

so that the quantity $(F - 1/F)$ becomes

$$\left(\frac{f_a}{f_0} - \frac{f_0}{f_a}\right) = \frac{f_a^2 - f_a f_b}{f_a f_0} = \frac{f_a - f_b}{f_0} = \frac{\Delta f}{f_0} = \frac{f_b}{f_0} - \frac{f_0}{f_b} \tag{8-101}$$

where Δf is the width of the relative gain curve between any two frequencies above and below resonance for which the relative gain is A_r. The quantity $\Delta f/f_0$ may also be expressed as $\Delta f/f_0 = (f_a - f_0)/f_0 + (f_0 - f_b)/f_0$ which is equivalent to 2δ as previously defined.

In terms of Δf and the frequency ratios, Eq. 8-99 then becomes

$$A_r = \frac{2\gamma/F}{(1 + jQ\,\Delta f/f_0)^2 + (F\gamma)^2} \tag{8-102}$$

However, $F = f/f_0$ differs very little from unity over the useful bandwidth. Therefore, approximately,

$$A_r = \frac{2\gamma}{(1 + jQ\,\Delta f/f_0)^2 + \gamma^2} \tag{8-103}$$

and, in magnitude,

$$|A_r| = \frac{2\gamma}{\sqrt{[1 + \gamma^2 - (Q\,\Delta f/f_0)^2]^2 + 4(Q\,\Delta f/f_0)^2}} \tag{8-104}$$

Peaks of the relative gain curve will correspond to values of Δf for which the denominator of Eq. 8-104 becomes minimum. It may be shown by differentiation of this denominator as a function of Δf that the minimum value is obtained for

$$(\Delta f)_p = \frac{f_0}{Q}\sqrt{\gamma^2 - 1} \tag{8-105}$$

which is the frequency interval between peaks.

It is of interest to solve Eq. 8-104 for Δf as a function of γ, Q, f_0, and relative gain A_r. After both sides of Eq. 8-104 are squared, the result may be obtained by solving a biquadratic equation and is

$$\Delta f = \frac{f_0}{Q}\sqrt{\gamma^2 - 1 + 2\gamma\sqrt{\frac{1}{A_r^2} - 1}} \tag{8-106}$$

The bandwidth 3 db down then follows immediately from Eq. 8-106 by placing $A_r = 1/\sqrt{2}$ and is

$$(\Delta f)_{BW} = \frac{f_0}{Q}\sqrt{\gamma^2 + 2\gamma - 1} \tag{8-107}$$

If the inductances are critically coupled, $\gamma = 1$, and the bandwidth is

$$(\Delta f)_{BW} = \sqrt{2}\,f_0/Q \tag{8-108}$$

Now the gain at the peaks for $\gamma > 1$ is the same as the maximum gain at resonance with $\gamma = 1$. From Eqs. 8-95 and 8-88,

$$|A_{o\,\max}| = g_m\omega_0^2L^2/2R = g_mR_s/2 \tag{8-109}$$

Also, from Eq. 8-89,

$$Q = R_s\omega_0C$$

so that Eq. 8-107 may be written as

$$(\Delta f)_{BW} = \frac{f_0}{\omega_0R_sC}\sqrt{\gamma^2 + 2\gamma - 1} \tag{8-110}$$

For a specified coupling ratio γ, a specified bandwidth $(\Delta f)_{BW}$, and a known shunt capacitance C, the required value, for design, of the shunting resistance R_s is then obtained from Eq. 8-110.

As an example of a double-tuned amplifier computation, suppose an interstage is required between two pentodes for which $g_m = 5000$ micromhos, $r_p = 1$ megohm. The output plus stray capacitance of the first tube is taken as 10 $\mu\mu$f which is equal to the input plus stray capacitance of the second stage. Thus $C = 10$ $\mu\mu$f. If the amplifier stage is to operate as an intermediate-frequency amplifier of a television receiver, the center frequency of the response (gain-frequency) curve may be chosen as $f_0 = 22.25$ Mc, or $\omega_0 = 140 \cdot 10^6$. Thus, $\omega_0 C = 1400 \cdot 10^{-6}$ and

$$\omega_0 L = 10^6/1400 = 714 \text{ ohms}$$

The required inductance is

$$L = \frac{714}{140 \cdot 10^6} = 5.1 \cdot 10^{-6} \text{ henry}$$

If the bandwidth is specified as 4.35 Mc, a convenient value of coupling ratio γ may be chosen arbitrarily, or it may be fixed by a requirement on the variation of gain between peak and minimum values. For present purposes, if γ is selected as 3, then, from Eq. 8-110,

$$R_s = \frac{22.25 \cdot 10^6 \sqrt{14}}{140 \cdot 10^6 (10 \cdot 10^{-12})(4.35 \cdot 10^6)} = 13{,}700 \text{ ohms}$$

The required Q is

$$Q = \omega_0 C R_s = (1400 \cdot 10^{-6}) 13{,}700 = 19.2$$

Since, for critical coupling,

$$\omega_0 M_c = \omega_0 k_c L = R$$

$$k_c = R/\omega_0 L = 1/Q$$

Thus,

$$\gamma = k/k_c = kQ$$

so that the required coefficient of coupling is

$$k = \gamma/Q = 3/19.2 = 0.156$$

which is easily obtained. The relative gain at resonance may be obtained from Eq. 8-104. Thus

$$| A_r |_{\Delta f = 0} = 2\gamma/(1 + \gamma^2) = 0.6$$

so that $|A|_{\omega=\omega_0} = 0.6$ [gain at the peaks]. The gain at the peaks, from Eq. 8-109, is

$$|A_{0\ \max}| = \frac{g_m R_s}{2} = \frac{5000 \cdot 10^{-6}(13{,}700)}{2} = 34.2$$

and

$$|A|_{\omega=\omega_0} = 20.5$$

The frequency interval between peaks is, from Eq. 8-105,

$$\Delta f = \frac{22.25 \cdot 10^6 \sqrt{8}}{19.2} = 3.28 \text{ Mc}$$

Since $(\Delta f)_{BW} = 4.35$ Mc, a rough sketch of the response curve can be drawn easily from the data that have been computed. The circuit is shown as an equivalent a-c circuit in Fig. 8-19.

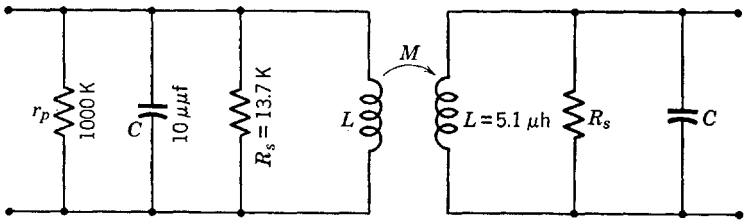

FIG. 8-19. Equivalent a-c circuit of an intermediate-frequency amplifier with bandwidth of 4.35 Mc, $k = 0.156$, $f_0 = 22.25$ Mc.

8-11. Gain-Bandwidth Products

It has been shown by Wheeler [3,4] and others that there are definite limitations to the amount of amplifier gain that can be realized over a certain bandwidth. Conversely, the maximum bandwidth that can be achieved with a specified gain is definitely limited by the constants of tubes and circuits comprising the amplifier. These facts have been dealt with in the literature. For present purposes, the gain-bandwidth products of the tuned voltage amplifiers just discussed will be examined.

The capacitance-coupled (direct-coupled) circuit of Fig. 8-12*a* has a gain at resonance given by Eq. 8-63 in magnitude as

$$A_0 = g_m \omega_0 L Q_e \tag{8-111}$$

where

$$Q_e = \frac{Q}{1 + \omega_0 L Q (1/r_p + 1/R_g)} \tag{8-112}$$

[3] H. A. Wheeler, *Proc. IRE*, **27**, 429 (July 1939).
[4] J. A. Morton and R. M. Ryder, *BSTJ*, **29**, 496 (Oct. 1950).

The bandwidth is given by Eq. 8-69 and may be written as

$$\Delta f = f_0/Q_e \tag{8-113}$$

Thus, for this amplifier, the gain-bandwidth product is

$$A_0(\Delta f) = g_m\omega_0 L f_0 = \frac{g_m}{2\pi}\omega_0^2 L = \frac{g_m}{2\pi C} \tag{8-114}$$

since $\omega_0^2 = 1/LC$. An inspection of Fig. 8-13 shows that C includes the output capacitance of the amplifier stage itself plus the input capacitance of the following stage, if any. The gain-bandwidth product is limited, therefore, by the magnitude of the transconductance of the tube g_m and the capacitances associated with the coupling circuit and with the tube. So far as the tube alone is concerned, an important merit figure known as the gain-band figure of merit for amplifier use is the product in Eq. 8-114 in which C is the sum of the input and output capacitances of the tube alone.

The gain-bandwidth product for the single-tuned, transformer-coupled circuit of Fig 8-12*b* may be obtained from the resonant gain of Eq. 8-74, equivalent Q of Eq. 8-87, and bandwidth of Eq. 8-86. The result is

$$A_0(\Delta f) = (g_m\omega_0 M Q_e)(f_0/Q_e) = g_m\omega_0^2 M/(2\pi) \tag{8-115}$$

For $\omega_0^2 = 1/L_2C_2$,

$$A_0(\Delta f) = g_m M/2\pi(L_2C_2) \tag{8-116}$$

for the general case of either pentodes or triodes.

For the case of the double-tuned circuit, the gain-bandwidth product may be computed easily for critically coupled circuits having equal Q's. The gain, as obtained from Eqs. 8-96 and 8-97 is

$$\begin{aligned} A &= \frac{jg_m\gamma RQ^2/F}{[1 + jQ\ \Delta f/f_0]^2 + (\gamma F)^2} \\ &\cong \frac{jg_m\gamma RQ^2}{[1 + \gamma^2 - (Q\ \Delta f/f_0)^2] + j2Q\ \Delta f/f_0} \end{aligned} \tag{8-117}$$

for which the magnitude is

$$|A| = \frac{g_m\gamma RQ^2}{\sqrt{[1 + \gamma^2 - (Q\ \Delta f/f_0)^2]^2 + 4(Q\ \Delta f/f_0)^2}} \tag{8-118}$$

Thus, for critical coupling, $\gamma = 1$, and, at $f = f_0$, $\Delta f = 0$, $A = A_{0\,\max}$. Then,

$$|A_{0\,\max}| = g_m RQ^2/2 \tag{8-119}$$

The corresponding bandwidth is given by Eq. 8-108. The gain-bandwidth product is

$$|A_{0\,\max}|(\Delta f)_{BW} = g_m RQf_0/\sqrt{2}$$

$$= \frac{g_m R f_0}{\sqrt{2}}\left(\frac{1}{R\omega_0 C}\right) = \frac{g_m}{\sqrt{2}\,(2\pi C)} \qquad (8\text{-}120)$$

If the C's (Fig. 8-19) are not equal, it can be shown that Eq. 8-120 becomes, for shunt capacitances C_i and C_0,

$$|A_{0\,\max}|(\Delta f)_{BW} = g_m/\sqrt{2}\,(2\pi)\sqrt{C_i C_0} \qquad (8\text{-}121)$$

The gain-bandwidth tube merit figures may now be computed for the single-tuned, direct-coupled case for comparison with the double-tuned, transformer-coupled case. For the single-tuned case, from Eq. 8-114, with $C = C_i + C_0$,

$$(A_0\,\Delta f)_1 = g_m/2\pi(C_i + C_0)$$

and, from Eq. 8-121 for the double-tuned case (subscripts max and BW omitted),

$$(A_0\,\Delta f)_2 = g_m/\sqrt{2}\,(2\pi)\sqrt{C_i C_0}$$

If the same tube is used, the ratio of the gain-bandwidth products is

$$(A_0\,\Delta f)_2/(A_0\,\Delta f)_1 = (C_i + C_0)/\sqrt{2}\,\sqrt{C_i C_0} \qquad (8\text{-}122)$$

For a comparison of relative magnitudes, assume that $C_i = C_0$; then,

$$(A_0\,\Delta f)_2/(A_0\,\Delta f)_1 = \sqrt{2} \qquad (8\text{-}123)$$

The gain-band tube merit figure is therefore larger by a factor of $\sqrt{2}$ for the double-tuned circuit, for the same tube. Also, the double-tuned circuit response characteristic has steeper sides, more nearly approximating the ideal band-pass characteristic.

Tube design has taken into account the need, in certain applications, for high gain-band products. Examples are: (1) the 6AB7 television amplifier pentode, with $g_m = 5000$ micromhos, $C_i = 8$, $C_0 = 5$ $\mu\mu$f, $(A_0\,\Delta f)_1 \cong 61$ Mc per sec, $(A_0\,\Delta f)_2 = 89$ Mc per sec; (2) the 6AK5 miniature pentode amplifier, with $g_m = 5000$ micromhos, $C_i = 4$, $C_0 = 2.8$ $\mu\mu$f, $(A_0\,\Delta f)_1 = 117$ Mc per sec, $(A_0\,\Delta f)_2 = 168$ Mc per sec.

8-12. Bandwidth of Cascaded, Tuned Amplifiers

The over-all gain requirement of an amplifier is frequently such that several stages connected in cascade are necessary. The over-all gain of the complete amplifier is then the product of the gains of separate stages.

The response characteristic of the tuned amplifier has sloping sides, as has been shown. The product of two such characteristics results in a characteristic having a somewhat different bandwidth than either component. This effect of stage-gain multiplication upon bandwidth may rather easily be analyzed in the case of the single-tuned circuits of Fig. 8-12 by expressing the voltage gain at any frequency near resonance in terms of the gain at resonance, or, preferably, by using the ratio of these two gains. For the circuit of Fig. 8-12*a*, the gain ratio is given by Eq. 8-67. Since $RQ^2 = \omega_0 LQ$, the gain ratio may be expressed in terms of the equivalent Q_e of Eq. 8-112 as

$$A/A_0 = 1/(1 + j2\delta Q_e) \tag{8-124}$$

Similarly, for the circuit of Fig. 8-12*b*, the gain ratio in terms of Q_e of Eq. 8-87 is identical in form with that of Eq. 8-124. The bandwidth of n identical single-tuned amplifier stages (all tuned to the same resonant frequency) may then be obtained from the over-all gain-ratio expression for the n stages, since

$$\left| \frac{A}{A_0} \right|^n = \frac{1}{[\sqrt{1 + (2\delta Q_e)^2}]^n} \tag{8-125}$$

becomes equal to $1/\sqrt{2}$ for

$$[\sqrt{1 + (2\delta Q_e)^2}]^n = 2^{1/2} \tag{8-126}$$

Thus,
$$2\delta = (\Delta f)_n/f_0 = (2^{1/n} - 1)^{1/2}/Q_e \tag{8-127}$$

and, since the bandwidth for a single stage is f_0/Q_e, the over-all bandwidth is a fraction, $(2^{1/n} - 1)^{1/2}$, of the single-stage bandwidth. For two stages, $(\sqrt{2} - 1)^{1/2} = \sqrt{0.414} = 0.644$; for three stages, $(2^{1/3} - 1)^{1/2} = \sqrt{0.26} = 0.510$. The quantity $(2^{1/n} - 1)^{1/2}$ may be called the bandwidth reduction factor.

The bandwidth reduction factor for cascaded double-tuned stages is more difficult to compute in general terms. The gain at any frequency off resonance is given, in magnitude, by Eq. 8-118. The relative gain, as previously used, is then referred to the gain at the peaks. From Eqs. 8-119 and 8-118,

$$|A_r| = \left| \frac{A}{A_{0\,\max}} \right| = \frac{2\gamma}{\sqrt{[1 + \gamma^2 - (Q\,\Delta f/f_0)^2]^2 + 4(Q\,\Delta f/f_0)^2}} \tag{8-128}$$

and, for critical coupling, $\gamma = 1$, the relative gain reduces to

$$|A_r| = \frac{1}{\sqrt{1 + \frac{1}{4}(Q\,\Delta f/f_0)^4}} \tag{8-129}$$

Then, for n identical stages critically coupled,

$$\left| \frac{A}{A_{0\,\max}} \right|^n = \frac{1}{[1 + \frac{1}{4}(Q\,\Delta f/f_0)^4]^{n/2}} \tag{8-130}$$

and the bandwidth 3 db down is that value of Δf for which

$$1 + \tfrac{1}{4}(Q\,\Delta f/f_0)^4 = 2^{1/n} \tag{8-131}$$

Thus, the over-all bandwidth of the n-stage amplifier is

$$(\Delta f)_n = (2^{1/n} - 1)^{1/4}\sqrt{2}\, f_0/Q \tag{8-132}$$

The bandwidth reduction factor here is then equal to the square root of that (Eq. 8-127) encountered for the single-tuned cases previously considered. It is to be expected that the bandwidth reduction would be smaller for the double-tuned circuit since its response characteristic has more nearly vertical sides, approximating the ideal band-pass filter response characteristic.

8-13. Staggered Tuning, Response Characteristic

Single-tuned circuits are more easily adjusted and aligned than those with two tuning capacitors. The advantage of the double-tuned circuit in providing a band-pass response is responsible for its usefulness in receivers. However, an equivalent or improved response characteristic can be obtained by using two single-tuned stages in cascade, each tuned to a frequency slightly displaced on either side of the center of the desired transmission band. This effect may be easily understood with the aid of the gain-ratio equation for the single-tuned circuit (Eq. 8-124). The quantity $2\delta Q_e$ may be considered the independent variable in a graph of $|A/A_0|$ as a function of frequency off-resonance. Let

$$x = 2\delta Q_e \tag{8-133}$$

so that

$$\left| \frac{A}{A_0} \right| = \frac{1}{|1 + jx|} = \frac{1}{\sqrt{1 + x^2}} \tag{8-134}$$

The graph of Eq. 8-134 is identical with that of Fig. 8-3. It has been shown that a desirable over-all characteristic results from stagger-tuning two stages such that

$$\left| \frac{A}{A_0} \right|_1 = \frac{1}{\sqrt{1 + (x + 1)^2}} \tag{8-135}$$

for the first, and

$$\left| \frac{A}{A_0} \right|_2 = \frac{1}{\sqrt{1 + (x - 1)^2}} \tag{8-136}$$

for the second. The over-all gain-ratio is

$$\left|\frac{A}{A_0}\right|_{1,2} = \frac{1}{\sqrt{[1 + (x + 1)^2][1 + (x - 1)^2]}} \tag{8-137}$$

which has been shown graphically in Fig. 8-20, in addition to the response characteristics of the component stages. The resultant response curve has also been normalized (each ordinate has been divided by the ordinate of maximum gain) to permit easier comparison with the components.

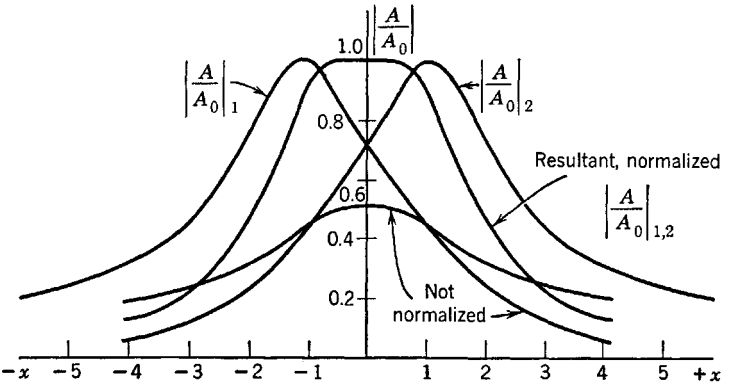

FIG. 8-20. Response characteristics of individual components and of resultant amplifier, stagger-tuned.

The resultant has a reasonably good band-pass characteristic, steeper sides, and a bandwidth that is greater than that of either component. In terms of units of x, the bandwidth of each component is 2. The gain-ratio equation for the resultant reduces to

$$\left|\frac{A}{A_0}\right|_{1,2} = \frac{0.5}{\sqrt{1 + x^4/4}} \tag{8-138}$$

the maximum gain occurs at $x = 0$ where the gain ratio is equal to 0.5. The gain ratio falls to 0.707 of its maximum value at $x = \pm \sqrt{2}$. Thus, the bandwidth of the resultant response in units of x is $2\sqrt{2}$, or $\sqrt{2}$ times that of either component.

8-14. The Grounded-Grid, or Cathode Input, Amplifier

The desirable linearity of triodes in addition to their better noise properties as compared with pentodes leads to choice of them in many amplifier applications. At radiobroadcast frequencies, the interelectrode capacitances cause trouble, as has previously been discussed in

Chapter 1. Certain methods of connecting the driving generator or signal source and also the load permit special advantages in terms of input impedance, gain, and useful frequency range with no additional added circuit elements. In previous chapters, two connection methods have been described and analyzed. These are the grounded cathode described in Chapter 1, and the grounded plate or cathode follower in Chapter 3. A third possibility, the grounded grid connection, has not been described and has several interesting properties which will be discussed in the following paragraphs.

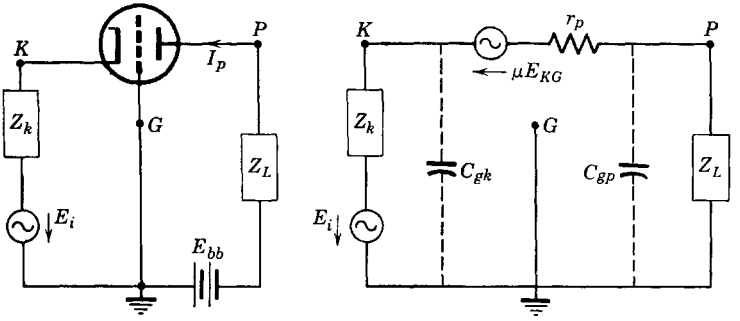

FIG. 8-21. Grounded-grid amplifier and equivalent a-c circuit.

The circuit connections for a grounded-grid triode amplifier are shown in Fig. 8-21, where a sinusoidal signal source of rms voltage E_i and internal impedance Z_k is driving the amplifier, and a load impedance Z_L is connected between plate and ground. The interelectrode capacitances C_{gk} and C_{gp} are in parallel with signal source and load, respectively. The shielding between plate and cathode of tubes designed for grounded-grid operation is good enough so that C_{pk} may be omitted from the equivalent circuit. This is analogous to the reduction of C_{gp} in tetrodes or pentodes with grounded screen grids.

Analysis of the equivalent circuit of Fig. 8-21, neglecting C_{gk} and C_{gp} which may be combined with Z_k and Z_L, and neglecting grid current, provides the following pertinent relations: The gain of the amplifier is

$$A = \frac{(\mu + 1)Z_L}{r_p + Z_L + (\mu + 1)Z_k} \tag{8-139}$$

the input impedance at the terminals of the constant-voltage signal generator is

$$Z_{11} = Z_k + \frac{r_p + Z_L}{\mu + 1} \tag{8-140}$$

the tube input impedance is

$$Z_{kg} = \frac{r_p + Z_L}{\mu + 1} \tag{8-141}$$

The analysis shows that: (1) There is no 180° phase shift introduced by the tube; if Z_g and Z_L are pure resistances, input and output voltages will be in phase; (2) for Z_k small, the gain approximates that of the grounded-cathode amplifier; (3) the input impedance at terminals K–G is small; for example, the 6C5 with a load impedance of 20,000 ohms,

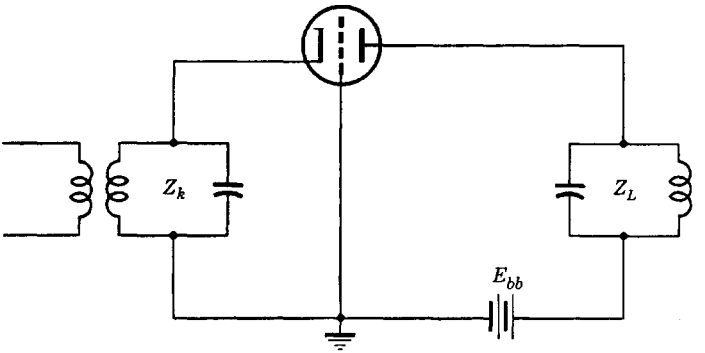

FIG. 8-22. Grounded-grid circuit with tuned input and output.

$\mu = 20$, $r_p = 10{,}000$ ohms, would present an impedance $Z_{kg} = 30{,}000/21 = 1430$ ohms. The impedance at the terminals of the load impedance looking back into the tube circuit is

$$Z_{pg} = r_p + (\mu + 1)Z_k \tag{8-142}$$

which for the 6C5 with negligible Z_k would be approximately 10,000 ohms. Thus the amplifier behaves as an impedance transformer useful for coupling low input impedances to high-impedance loads. It is evident that the frequency may reach fairly high values before the shunting reactance of C_{gk} becomes small enough to be comparable with the tube input impedance.

Tuned circuits are often used with grounded-grid operation. A typical circuit is shown in Fig. 8-22. Grounded-grid operation is indicated where triodes are required or preferred, or where neutralization of C_{gp} is difficult, and in specific applications where it is necessary to operate the grid at ground potential. The close-spaced triodes such as the General Electric 2C-40, 2C-43 and the Western Electric 416-A are designed primarily for grounded-grid operation and employ coaxial or wave-guide input and output connections.

PROBLEMS

8-1. The circuits shown are identical at a certain frequency f_r. Prove that $Q_s = \omega_r L_1/R_1$ and $Q_p = R_2/\omega_r L_2$ are equivalent.

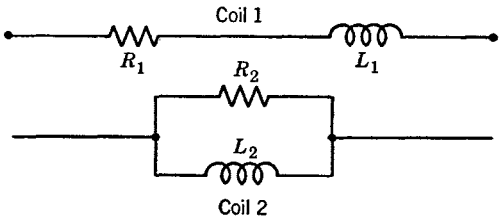

FIG. P8-1.

8-2. If the Q_s of coil 1 in problem 8-1 is equal to or greater than 10, and a variable capacitor C_1 is added in series with L_1 and is adjusted for resonance at f_r, obtain an approximate expression for the magnitude of a capacitor C_2 in parallel with L_2 such that coil 2 will be in antiresonance at f_r. Compare the impedances of the two circuits at f_r.

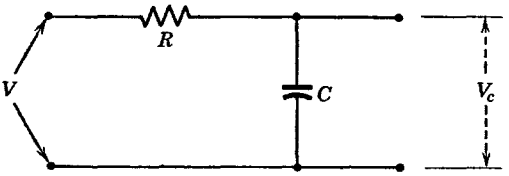

FIG. P8-3.

8-3. The voltage V applied to the circuit shown is the rms value of an applied sinusoidal voltage of variable frequency. Sketch a curve of V_c/V as a function of frequency, and derive an expression for the upper "half-power" frequency; V_c is the rms voltage across C.

8-4. Derive the expression called for in problem 8-3 by applying four-pole theory and determining the four-pole admittances of the circuit.

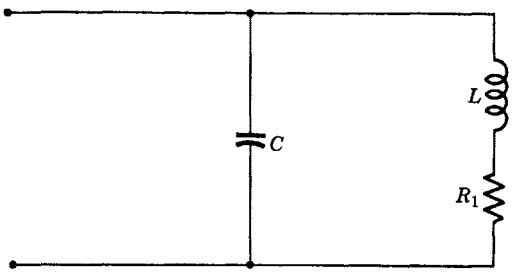

FIG. P8-5.

8-5. The circuit shown is to be used as the load of a tuned radio-frequency amplifier.

(*a*) Show that the impedance of the circuit at the antiresonant frequency is Q^2R_1 where $Q \geqq 10$.

(*b*) By comparing with the circuit of Fig. 8-2, show that Eq. 8-10 may be applied to the circuit of this problem provided that R_{ar} in Eq. 8-10 is L/CR_1.

8-6. An antiresonant matching network is required at $f_{ar} = 4 \cdot 10^6$ cps to match a generator of 100,000 ohms impedance and to have a bandwidth of 50 kc. Determine all circuit constants necessary.

8-7. A radio-frequency coil has an inductance of 50 microhenrys, and $Q = 20$. It is to be used in a parallel-resonant circuit, with $f_{ar} = 4$ Mc. Find (*a*) the required tuning capacitance in micromicrofarads, (*b*) the bandwidth.

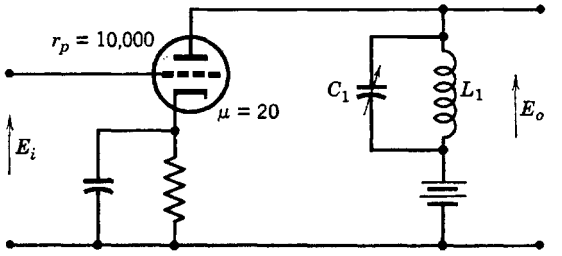

FIG. P8-8.

8-8. Given $Q_1 = \omega L_1/R_1 = 100$, $L_1 = 50$ microhenrys, determine the maximum gain at 800 kc and the bandwidth.

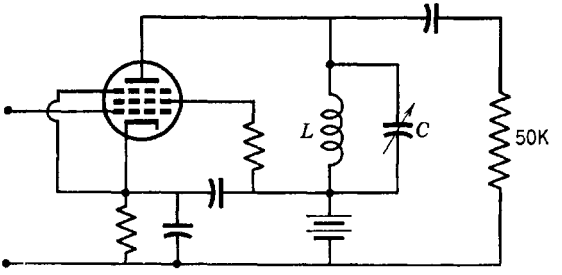

FIG. P8-9.

8-9. A pentode amplifier tube of $r_p = 10^6$ ohms, $g_m = 2000$ micromhos is coupled to a 50,000-ohm load as shown; coil inductance $L = 0.5$ millihenry, and $Q = 60$. If the condenser is tuned to antiresonance at $f_0 = 10^6$ cps, find (*a*) the gain of the amplifier at $f = f_0$, (*b*) the bandwidth.

8-10. For the 6AK5, $r_p = 250{,}000$ ohms; output capacitance = 3 $\mu\mu$f. For the single-tuned coupled circuit, as shown, it is required to couple the plate of the 6AK5 to the 100-ohm line (input impedance = R_0) at a carrier frequency of 1.59 Mc per sec. The required bandwidth is 53 kc per sec. The stray wiring capacity in the plate circuit of the tube is 5 $\mu\mu$f; the minimum capacity of the tuning condenser is 10 $\mu\mu$f. It may be assumed that $\omega_0 L_2 = R_0$, $k = 0.2$, and the coil Q's are each 100

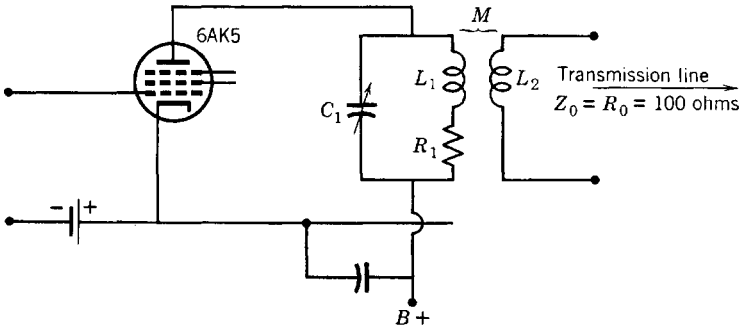

FIG. P8-10.

(coils alone). Determine L_2, L_1, and the setting of C_1 for maximum power transfer at $f_0 = 1.59$ Mc per sec.

8-11. Design a single-tuned, transformer-coupled circuit to match a 100-ohm line to the grid of a 6K7 pentode at 1050 kc and to meet the following additional requirements: (1) to have a bandwidth of 9.55 kc at 1050 kc; (2) to tune over the range 556 to 1590 kc. Additional data are: Input capacitance of the 6K7 = 7 $\mu\mu$f; maximum value of tuning, condenser, 350 $\mu\mu$f; resistance of primary coil may be neglected; coupling between primary and secondary to be kept at the minimum possible value.

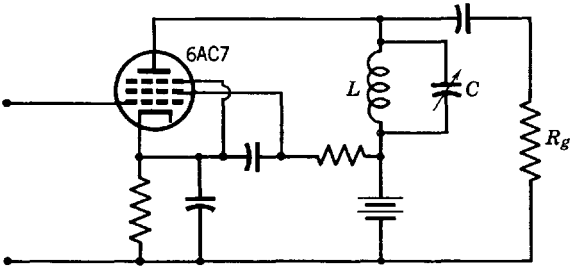

FIG. P8-12.

8-12. For the pentode amplifier shown, class-A operation is assumed. The bandwidth desired is 10 kc at a C setting of 100 $\mu\mu$f. The inductance $L = 100$ microhenrys. A lossless inductance is assumed.

(*a*) Compute the maximum gain of the amplifier.

(*b*) At what frequency does the maximum gain occur if $C = 100$ $\mu\mu$f?

(*c*) Compute the maximum gain, the frequency at which it occurs, and the bandwidth if $C = 350$ $\mu\mu$f.

8-13. The primary and secondary circuits of a band-pass transformer are identical. The transformer is used with a 6D6 amplifier tube and is designed to transmit 450 kc with a bandwidth of 20 kc. The resonant peaks are selected at 7.5 kc above and below the center frequency, 450 kc. Compute k and the coil Q's for (*a*) an allowable gain variation in the pass band of 1 db, (*b*) an allowable gain variation in the pass band of 0.5 db.

8-14. $C_1 = 10\ \mu\mu f$, $R_1 = 13{,}700$ ohms, $L_2 = 6.4\ \mu h$, $R_2 = 5000$
$L_1 = 5.1\ \mu h$, $g_m = 5000 \cdot 10^{-6}$ mho, $C_2 = 8\ \mu\mu f$, $g_m = 5000 \cdot 10^{-6}$ mho
$k = 0.156$, $r_p = 10^6$ ohms, $r_p = 10^6$ ohms

Given: $e_i = 0.0172 \cos (151 \cdot 10^6 t)$ the input voltage to the intermediate-frequency amplifier. Find $e_{out}(t)$. Sketch the over-all response curve of the amplifier. Specify its bandwidth and gain.

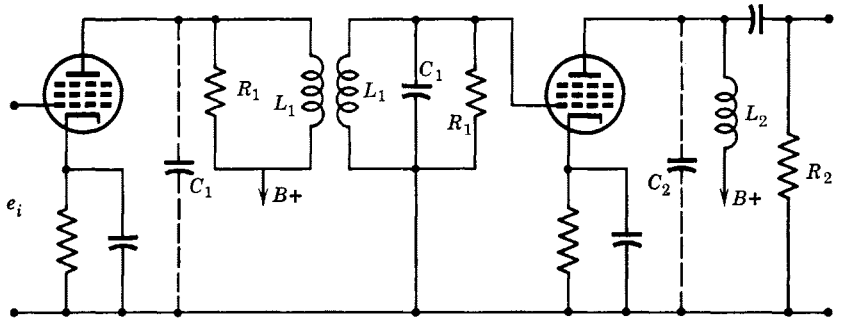

FIG. P8-14.

CHAPTER 9

RADIO-FREQUENCY POWER AMPLIFIERS

THE RADIO-FREQUENCY AMPLIFIERS DISCUSSED IN CHAPTER 8 ARE essentially voltage amplifiers; they are used in radio receivers where power levels are low, particularly in the radio-frequency components of the system. For purposes of generation and transmission of radio-frequency (r-f) power, it is necessary to operate tubes at or near the maximum rated power level, and to design circuits for high-power efficiencies.

It is frequently shown in elementary circuit texts that a circuit consisting of a lossless charged capacitor C connected to the terminals of a lossless inductor L would provide, across the common terminals of C and L, a sinusoidally varying voltage. The expression for this voltage is

$$v_{LC} = V_o \cos\left(\frac{1}{\sqrt{LC}}t\right)$$

where V_o is the voltage to which the capacitor was charged before its connection to the inductor. The point of this discussion is that a physically realizable parallel combination of L and C may be used as a source of sinusoidal oscillations if a means is provided for supplying the energy required for load and for circuit losses. For example, if a battery could be connected in such a way as to provide short-duration regularly repeated pulses of current to the tuned L–C circuit, both the losses and the load power requirements would be supplied and the circuit would provide an a-c output from a d-c source. The battery switching circuit necessary might be called a synchronous switch, and, for best results, the switching frequency should be the same as the output frequency which would require an increment of energy to the L–C storage or "tank" circuit once each cycle.

The vacuum tube, properly biased, provides the synchronous switch required. Synchronism or timing is provided by a signal voltage in the grid circuit of the tube, which is biased either at cutoff, class B, or beyond

cutoff, class C. Such synchronous switches are called class-B or C amplifiers, and each has important applications in radio-frequency transmitter use.

The circuit of a class-B or C amplifier (Fig. 9-1) is capable of a much higher operating efficiency than the class-A circuits of Chapter 8. The

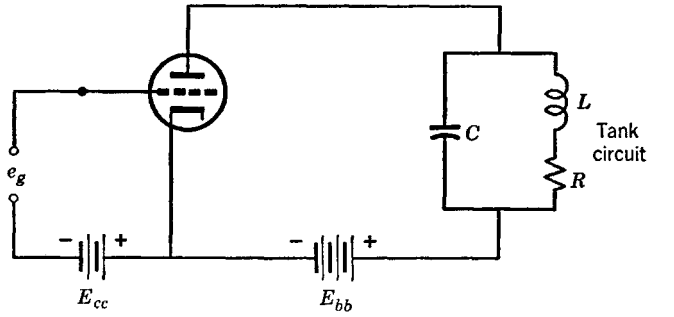

FIG. 9-1. Class-*B* or *C* amplifier circuit.

reason for this increased efficiency is that current flows in the plate circuit of the tube only during the portion of the plate-voltage cycle during which the plate voltage is minimum. If the tank circuit is

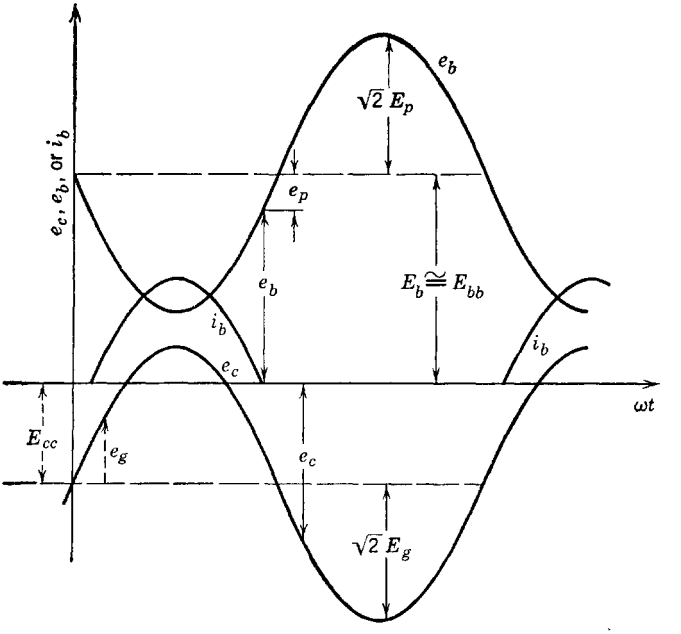

FIG. 9-2. Phase relations, class-*C* amplifier.

resonant at the frequency of the signal voltage, e_g, assumed to be sinusoidal, then at this frequency the tank circuit impedance is a pure resistance, R_{ar}. The phase relations between grid and plate voltages and plate current are then as shown by Fig. 9-2. The phase relations are the same as for the class-A case with resistance load, but plate current flows only during the portion of the signal voltage cycle that e_c is above cutoff.

Tuned class-B and C radio-frequency amplifiers are used to build up the power level at a specified frequency or over a band of frequencies as required in a radio transmitter. Such amplifiers are inherently nonlinear, and large-amplitude harmonics are generated and appear in the plate current. Although the amplitude of some of these harmonics may be comparable with the amplitude of the fundamental, the use of a tuned circuit with effective Q of 10 or more is sufficient to reduce the harmonic output to negligible values.

9-1. External Characteristics of Class-B and C Power Amplifiers

The analysis of operation of class-B and C power amplifiers is involved because of the discontinuous intermittent character of the plate-current pulses. It is therefore desirable to interpret the experimentally obtained characteristics of the over-all amplifier before considering the necessarily approximate analysis or graphical determination of operating behavior.

The independent variables involved in class-C operation are shown in Fig. 9-2 and are, in standard IRE symbols, E_c, E_g, E_b, and E_p (or R_{ar}). The dependent variables are the currents i_b and i_c and their components, the alternating current in the tank circuit, and the derived quantities of power output, power input, and efficiency. Although the large number of variables necessitate a tremendous number of measurements for a complete description, typical measured values are available [1] and are very helpful as an aid to the understanding of class-B and C amplifier operating behavior.

Typical examples * of external characteristics are shown in Figs. 9-3 and 9-4. Measurement of the tank current may be obtained by inserting an a-c ammeter in series with the capacitance C of Fig. 9-1. The measured value of the tank current is, for high Q circuits, very closely the rms value of the current component at frequency f_0, the antiresonant frequency to which the tank circuit is tuned.

The important properties of the curves of Figs. 9-3 and 9-4 are the following:

1. For $E_b = 700$ volts (Fig. 9-3) the tank current, and hence also the output voltage, is linearly related to the driving grid voltage for all

[1] W. L. Everitt, *Communication Engineering*, pp. 531–544, McGraw-Hill Book Co.

* Taken from *Communication Engineering*, by W. L. Everitt, with permission.

values of $E_{gm} < 120$ volts. The plate operating voltage and the bias are adjusted for class-B operation, since, for the tube used ($\mu \cong 8$)

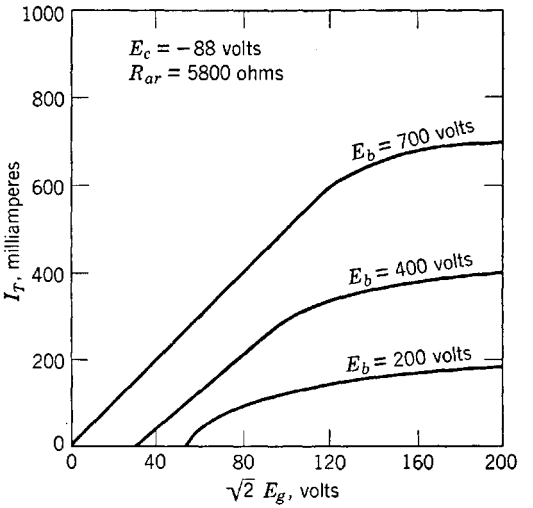

FIG. 9-3. Tank current as a function of E_g and E_b, E_c and R_{ar} constant.

$\mu E_c = 8(-88) = -704$ volts, and $E_b + \mu E_c \cong 0$, the tube is biased approximately at cutoff with zero signal. This arrangement is often

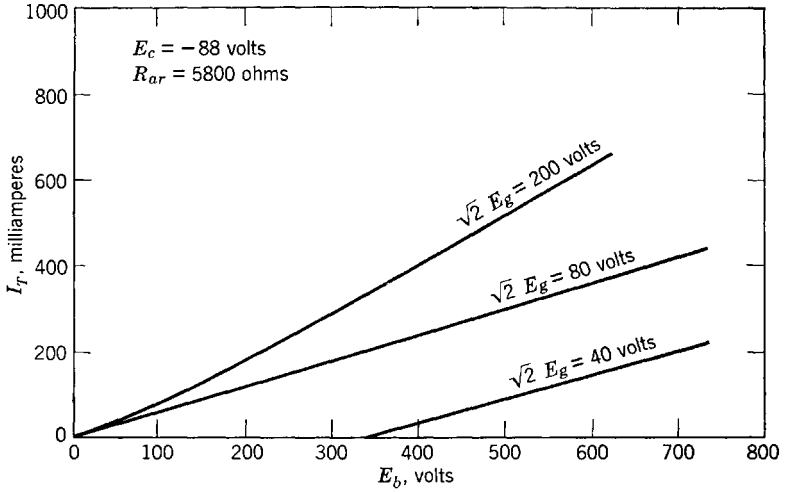

FIG. 9-4. Tank current as a function of E_b and E_g, E_c and R_{ar} constant.

referred to as a *linear amplifier*, and is used in the amplification of amplitude-modulated voltages applied in the grid circuit. In the case

shown, the variations in amplitude of the input grid voltage should not exceed 120 volts.

2. Saturation effects are shown in Fig. 9-3 and may be explained with the aid of Fig. 9-2, in which the plate and grid voltages are referred to the same zero voltage axis. With increasing amplitudes of e_g and e_b, the grid voltage at its positive peak may equal or exceed the plate voltage at its negative peak, and, since these peaks occur simultaneously, secondary electrons released at the plate will begin to be collected at the grid when

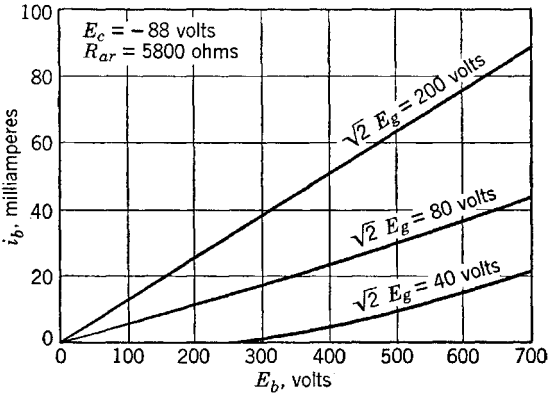

FIG. 9-5. Variation of total plate current with plate voltage, class-B or C amplifier.

$e_c > e_b$. For this condition the *tank current* curve begins to level off. In case of a secondary-emission yield ratio exceeding unity at the plate, an actual decrease in *plate current* (a dip in the top of the i_b vs. ωt curve, Fig. 9-2) will occur at the peaks of the grid swing.

3. The curves of $E_b = 200$, 400, or 700 volts are typical class-C characteristics for a large grid-voltage amplitude. The class-C characteristics are better illustrated in Fig. 9-4, which shows that the a-c response in the tuned circuit is linearly dependent on the d-c component of plate voltage except for very small values of E_b. Such characteristics as that for $\sqrt{2}\,E_g = 200$ volts have led to the use of the class-C amplifier as a modulator. For this purpose, a constant-amplitude grid voltage obtained from the output of a radio-frequency oscillator is applied in the grid circuit, and the plate circuit has a variable-amplitude audio-frequency voltage source in series with the fixed d-c supply voltage. Operation should be such that $\sqrt{2}\,E_g$ is sufficient to cause the tank current to level off, requiring usually a grid bias voltage approximately twice that required for zero-signal cutoff. Thus, according to Fig. 9-4, the voltage in the output will faithfully reproduce the variations of audio-frequency plate voltage, producing a modulated wave.

Another characteristic of interest is shown in Fig. 9-5. Here the dependence of total plate current upon the d-c component of plate voltage is shown for three different values of grid-voltage amplitude. The importance of linearity here is again related to the use of the class-C amplifier as a modulator. For a characteristic such as that for $\sqrt{2}\,E_g = 200$ volts, the load resistance presented by the class-C amplifier tube to the audio-frequency modulator is constant, an important requirement for distortionless representation of the audio-frequency wave form. The

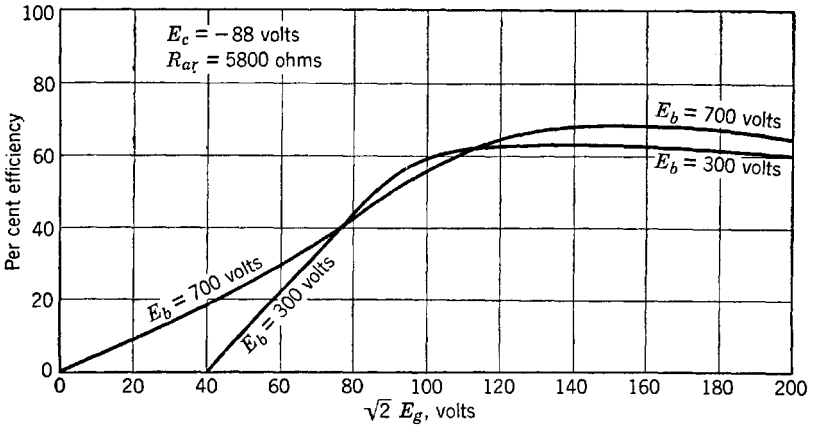

FIG. 9-6. Plate-conversion efficiency, class-B or C amplifier.

peak driving grid voltage must therefore be high enough to produce the tank current saturation shown by Fig. 9-3.

The power requirements of radio transmitters are sufficiently high that the conversion efficiency of the class-B or C amplifier is an important consideration. Losses in both grid and plate circuits must be reduced to a minimum. The grid drive must be adjusted for best operating efficiency. A typical curve of conversion efficiency is shown in Fig. 9-6, for the same tube and operating conditions that supplied the data for Figs. 9-3, 9-4, and 9-5. A comparison of Figs. 9-3 and 9-6 will show that very little is gained in efficiency by driving the grid voltage beyond the value required for tank current saturation. However, because grid current flows, losses in the grid circuit will increase with excessive grid drive, with no increase in efficiency. The efficiency plotted in Fig. 9-6 is the ratio of the a-c power output (proportional to the square of the tank current, I_T) to the d-c power input in the plate, $E_{bb}I_b$. Class-B operating efficiency is illustrated by the curve for $E_b = 700$ volts, class-C by the $E_b = 300$ volts curve. By reducing E_b to 350 volts, $2E_b/\mu \cong \frac{700}{8} = 87.5$ volts. The grid bias is $E_c = -88$ volts, so that the amplifier is biased

for recommended class-C operation at $E_b = 350$ volts. There is very little difference [2] in efficiency near saturation between curves for $E_b = 300$ and $E_b = 500$ volts.

9-2. The Problem of Analysis, Tuned Power Amplifiers

The observed operating characteristics of tuned power amplifiers have been described in preceding sections, and certain applications have been suggested by the measured characteristics. Ideally, a synchronous switch supplying power to the tuned circuit should connect the d-c power source to the circuit only during a very short or infinitesimal interval at the negative maximum of the fundamental, or selected harmonic, voltage across the capacitor. The current flowing through the switch during the short interval of connection must necessarily be very large in order to supply the power output as well as the losses of the amplifier. The vacuum tube, as a switch, cannot deliver unlimited pulses of current because of cathode emission limitations. The tube must supply current over the entire positive half-cycle of the driving grid voltage or over a large fraction of the half-cycle in order to supply power requirements. Thus, for class-B tuned power amplifiers, the operating angle of conduction is 180°, but for class-C operation the angle is less than 180°, and its best value for optimum operation is a design parameter which is not known in advance and which is difficult to specify in general.

It is the function of analysis to select the independent variables, the dependent variables, and the engineering criteria of efficient operation of a device or system, and then to attempt to obtain relations between the variables such that the desired criteria can be described in their quantitative dependence upon the variables involved. The final results lead to an intelligent choice of parameters and to a knowledge of the conditions for optimum operation. Usually simplifying assumptions are necessary in order to obtain usable analytical expressions. Experimental verification is always necessary to determine the accuracy of the analytical approximations.

In the case of the tuned power amplifier, analysis of the class-B case is possible with the aid of numerous simplifying assumptions, and the results are valuable as a guide to the understanding of operating behavior and to design. For the class-C case, however, semigraphical methods based on tube characteristics are usually resorted to, and such methods are inherently unsatisfying because they apply to individual tubes and circuits already selected and do not result in general principles which contribute to a final solution of the engineering problem. A brief discussion of the semigraphical method, applicable to both class-B and

[2] See *Communication Engineering, op. cit.*, p. 536.

class-C operation, will be given in a later section. A simple analysis of the class-B case following the approach first used by Everitt [2] is given in the following section.

9-3. The Class-B Tuned Power Amplifier

It has been observed that experimentally obtained class-B characteristics have led to the description of this amplifier as linear. Therefore, it may not be too surprising that linear methods of analysis provide usable results. It is assumed:

1. That the tuned circuit is tuned to parallel resonance at the frequency f_0 of the driving grid voltage.
2. That the grid voltage is sinusoidal.
3. That the Q of the tuned circuit is high enough so that its impedance Z_L is negligible at harmonics of f_0.
4. That the triode characteristics are linear.
5. That the bias is such that $i_b = 0$ for zero signal voltage.

The method of Chapter 1 may be used in obtaining a suitable expression for the triode plate characteristics. The functional dependence of plate current upon plate and grid voltage is expressed as

$$i_b = i_b(e_c, e_b) \tag{9-1}$$

A Taylor series may be used to represent the function in the vicinity of any set of values of e_c and e_b for which i_b is continuous and has continuous and finite derivatives. In Chapter 1 the expansion was obtained at the operating point where the origin of coordinates had been established. This may easily be seen from the general expansion, according to Taylor's series in two independent variables, as follows:

$$\begin{aligned} i_b = i_b(e_c, e_b) = {} & i_b(E_c, E_b) + (e_c - E_c)\frac{\partial}{\partial e_c}[i_b(E_c, E_b)] \\ & + (e_b - E_b)\frac{\partial}{\partial e_b}[i_b(E_c, E_b)] + \frac{1}{2!}\Bigg[(e_c - E_c)^2\frac{\partial^2}{\partial e_c{}^2} i_b(E_c, E_b) \\ & + 2(e_c - E_c)(e_b - E_b)\frac{\partial^2}{\partial e_c\,\partial e_b} i_b(E_c, E_b) \\ & + (e_b - E_b)^2\frac{\partial^2}{\partial e_b{}^2} i_b(E_c, E_b)\Bigg] + \text{higher-order terms} \end{aligned} \tag{9-2}$$

Now $i_b(E_c, E_b) = I_b$, the current at the operating point; $(\partial/\partial e_c) i_b(E_c, E_b) = g_m$ as measured at the operating point; $(\partial/\partial e_b) i_b(E_c, E_b) = g_p = 1/r_p$ as determined at the operating point. For the linear approxi-

mation, higher-order terms may be neglected. Thus,

$$i_b = I_b + i_p = I_b + g_m(e_c - E_c) + g_p(e_b - E_b) \tag{9-3}$$

Since $e_c = E_c + e_g$, $e_b = E_b + e_p$, the expression

$$i_p = g_m e_g + g_p e_p \tag{9-4}$$

used in Chapter 1 is obtained.

In class-B operation,

$$i_b(E_c, E_b) = I_b = 0 \tag{9-5}$$

because the tube is biased to cutoff with zero signal. Then, Eq. 9-3 becomes

$$i_b = g_m\left[\left(e_c + \frac{g_p}{g_m} e_b\right) - \left(E_c + \frac{g_p}{g_m} E_b\right)\right] \tag{9-6}$$

and with $g_p/g_m = 1/\mu$, and $E_c + E_b/\mu = 0$ as required for class-B bias, there is obtained the relation

$$i_b = g_m(e_c + e_b/\mu) \tag{9-7}$$

a linear approximation for the tube characteristics for $i_b \geqq 0$. The parameters g_m and μ are the familiar ones of class-A analysis. The tri-

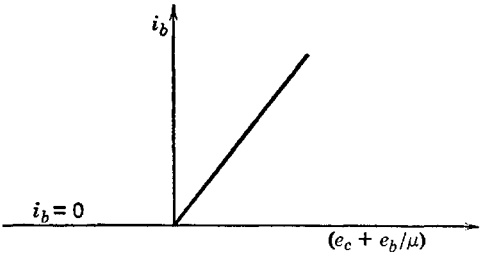

FIG. 9-7. Linear approximation for plate current of a triode.

ode characteristics in terms of the *equivalent diode* voltage $(e_c + e_b/\mu)$ are reduced to a single characteristic as shown in Fig. 9-7. The slope of the line is seen to be g_m.

The tuned circuit presents an impedance

$$Z_L = \frac{R_{ar}}{1 + j2Q_0\delta} \tag{9-8}$$

which is Eq. 8-17 of the preceding chapter. Here

$$Q_0 = \omega_0 L/R \tag{9-9}$$

and

$$\delta = (\omega - \omega_0)/\omega_0 \tag{9-10}$$

is the fractional frequency off-resonance. At $\omega = \omega_0$, the angular frequency of the sinusoidal grid input voltage, $\delta = 0$, and the tank impedance is a pure resistance

$$R_{ar} = L/RC \tag{9-11}$$

For this frequency, the voltage across the load impedance is sinusoidal and of angular frequency ω_0. Whatever the nature of the plate-current pulse wave form, a Fourier analysis of the plate current will provide the

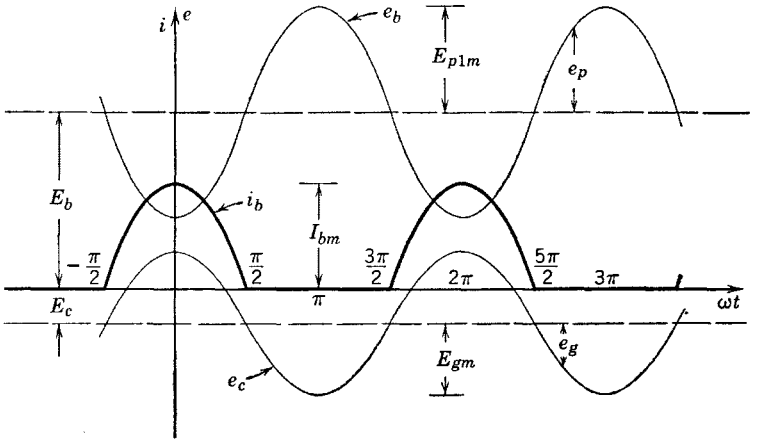

FIG. 9-8. Phase relations in the class-B amplifier.

various harmonic amplitudes. For Q_0 high, say, in the range 10 to 100 or more, it can easily be verified that the separate or combined harmonic voltages sustained across Z_L by the plate-current pulses are negligible in comparison with the voltage produced by the component of angular frequency ω_0. Therefore, the phase relations between the various voltages and currents are as shown by Fig. 9-8, in which all voltages and the current are referred to the same reference axes. Here E_{p1m} is the peak value of the fundamental frequency a-c component of voltage across Z_L.

The equations of the instantaneous values of grid and plate voltage as shown by Fig. 9-8 are the following:

$$e_c = E_c + E_{gm} \cos \omega_0 t \tag{9-12}$$

$$e_b = E_b - E_{p1m} \cos \omega_0 t \tag{9-13}$$

The plate current as given by Eq. 9-7 then becomes

$$i_b = g_m(E_c + E_{gm} \cos \omega_0 t + E_b/\mu - E_{p1m}/\mu \cos \omega_0 t), \qquad i_b \geq 0$$

which reduces, since $E_c + E_b/\mu = 0$, to

$$\begin{aligned} i_b &= g_m(E_{gm} - E_{p1m}/\mu)\cos\omega_0 t, \qquad (2n - \tfrac{1}{2})\pi \leqq \omega_0 t \leqq (2n + \tfrac{1}{2})\pi \\ &= I_{bm}\cos\omega_0 t \qquad (9\text{-}14) \\ i_b &= 0, \qquad (2n - \tfrac{3}{2})\pi \leqq \omega_0 t \leqq (2n - \tfrac{1}{2})\pi \end{aligned}$$

in accordance with the diagram (Fig. 9-8). Thus, the pulses of current are rectified half-cosine waves.

In terms of the peak value of total plate current, a Fourier analysis of the current pulses of Fig. 9-8 provides a necessary relation between the amplitude I_{p1m} of the fundamental-frequency current component and I_{bm}. Since the choice of origin has been such that the expression for current during the period of tube conduction is an even function, only cosine terms will be involved in the Fourier analysis. Then,

$$\begin{aligned} I_{p1m} &= \frac{1}{\pi}\int_{-\pi}^{\pi} i_b \cos\omega_0 t\, d(\omega_0 t) \\ &= \frac{2}{\pi}\int_0^{\pi/2} I_{bm}\cos^2\omega_0 t\, d(\omega_0 t) = \frac{1}{2}I_{bm} \qquad (9\text{-}15) \end{aligned}$$

Similarly,

$$I_{b\,\text{avg}} = \frac{1}{\pi}I_{bm} \qquad (9\text{-}16)$$

The amplitude of the current pulse in Eq. 9-14 has been expressed as

$$I_{bm} = g_m(E_{gm} - E_{p1m}/\mu) \qquad (9\text{-}17)$$

Then, from Eq. 9-15, and since $E_{p1m} = I_{p1m}R_{ar}$,

$$I_{p1m} = \tfrac{1}{2}g_m(E_{gm} - I_{p1m}R_{ar}/\mu) \qquad (9\text{-}18)$$

If Eq. 9-18 is solved for I_{p1m}, the result may be written as follows:

$$I_{p1m} = \mu E_{gm}/(2r_p + R_{ar}) \qquad (9\text{-}19)$$

The form of Eq. 9-19 suggests an equivalent a-c circuit for the fundamental component of the class-B linear amplifier. The circuit is shown in Fig. 9-9 and applies only to the calculation of the fundamental a-c component of plate current of angular frequency ω_0. The gain of the amplifier for resonant-frequency components is easily obtained from Fig. 9-9 and is

$$A_{f0} = \mu R_{ar}/(2r_p + R_{ar}) \qquad (9\text{-}20)$$

Equation 9-20 illustrates one of the important properties of the class-B amplifier, namely, that the gain at frequency f_0 is independent of voltage

amplitude. Thus an amplitude-modulated, radio-frequency voltage applied at the grid will be amplified without distortion. The external characteristics already discussed confirm this conclusion, provided that the proper adjustments in circuit operation are made.

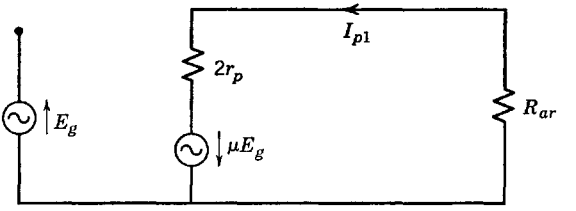

FIG. 9-9. Equivalent circuit of the class-B amplifier for the current component of resonant frequency f_0.

The average value of the plate current is given by Eq. 9-16 and, with the help of Eqs. 9-15 and 9-19, may be expressed in terms of E_g as

$$I_{b\,\text{avg}} = \frac{1}{\pi} 2\sqrt{2}\, I_{p1} = \frac{2\sqrt{2}}{\pi} \frac{\mu E_g}{2r_p + R_{ar}} \tag{9-21}$$

Therefore, as the external characteristics have already shown, both the average value of the plate current and the effective (or peak) value of the fundamental component of plate current are proportional to the driving grid voltage to the extent that r_p and μ are constants.

The power output, power input, plate dissipation, and efficiency are now very easily expressed in terms of the fundamental component of current or of load voltage. In particular, the efficiency of conversion in the plate circuit may be written (using Eq. 9-21) as

$$\eta_p = \frac{P_o}{P_i} = \frac{I_{p1}{}^2 R_{ar}}{E_{bb} I_{b\,\text{avg}}} = \frac{\pi}{2\sqrt{2}} \frac{I_{p1} R_{ar}}{E_{bb}} = \frac{\pi}{4} \frac{E_{p1m}}{E_{bb}} \tag{9-22}$$

The maximum theoretical efficiency is obtained if $E_{p1m} = E_b \cong E_{bb}$, and is 78.5 per cent. The actual operating efficiencies of a class-B amplifier as already indicated are usually in the range 55 to 65 per cent. If E_{gm} were increased sufficiently that $E_{p1m} = E_b$ (Fig. 9-8), then the maximum value of e_c might exceed the minimum value of e_b. Secondary electrons released at the plate would be collected by the grid, a dip in the top of the plate current pulse might result, and the linear relations assumed and desired would no longer hold. It is therefore necessary that $e_{c\,\text{max}}$ remain less than or at most equal to $e_{b\,\text{min}}$ for linear operation.

For the condition (see Fig. 9-8)

$$e_{c\,\max} = e_{b\,\min}$$

or
$$E_{gm} + E_c = E_b - E_{p1m} \tag{9-23}$$

(where it must be remembered that the value to be assigned to E_c is negative) then since $E_c = -E_b/\mu$, the necessary value of E_{gm} may be obtained from Eq. 9-23, from which

$$E_{gm} = E_b\left(1 + \frac{1}{\mu}\right) - I_{p1m}R_{ar} = E_b\left(1 + \frac{1}{\mu}\right) - \frac{\mu E_{gm}R_{ar}}{2r_p + R_{ar}}$$

Finally,
$$E_{gm} = E_b\left(1 + \frac{1}{\mu}\right)\left[\frac{2r_p + R_{ar}}{2r_p + (\mu + 1)R_{ar}}\right] \tag{9-24}$$

is the necessary value of grid driving peak voltage for optimum power output for a given plate supply and resonant load impedance R_{ar}. The corresponding values of fundamental a-c component and of average plate current are, respectively,

$$I_{p1} = \frac{1}{\sqrt{2}}\left[\frac{(\mu + 1)E_b}{2r_p + (\mu + 1)R_{ar}}\right] \tag{9-25}$$

and
$$I_{b\,\text{avg}} = \frac{2}{\pi}\frac{(\mu + 1)E_b}{2r_p + (\mu + 1)R_{ar}} \tag{9-26}$$

The efficiency corresponding to Eq. 9-23 then is

$$\eta_p = \frac{\pi}{4}\frac{I_{p1m}R_{ar}}{E_b} = \frac{\pi}{4}\frac{(\mu + 1)R_{ar}}{2r_p + (\mu + 1)R_{ar}} \tag{9-27}$$

The plate dissipation is

$$P_p = E_{bb}I_{b\,\text{avg}} - I_{p1}{}^2R_{ar} \tag{9-28}$$

and, since $E_{bb} \cong E_b$,

$$P_p = \frac{2}{\pi}\frac{(\mu + 1)E_b{}^2}{2r_p + (\mu + 1)R_{ar}} - \frac{(\mu + 1)^2E_b{}^2R_{ar}}{2[2r_p + (\mu + 1)R_{ar}]^2} \tag{9-29}$$

Equation 9-29 involves the tube parameters r_p and μ, the allowable plate dissipation, and the operating plate voltage (or plate-supply

voltage) in addition to the resonant load resistance R_{ar}. The necessary value of R_{ar} may be obtained from Eq. 9-29 for the condition of $e_{c\,\max} = e_{b\,\min}$ and for a given tube and plate supply. The result is best expressed as a quadratic in R_{ar} which may be solved after numercial values have been inserted. This relation is given in the following form:

$$R_{ar}^2 + \left[\frac{4r_p}{\mu + 1} + \frac{E_b^2}{P_p}\left(\frac{1}{2} - \frac{2}{\pi}\right)\right] R_{ar} + \left[\frac{4r_p^2}{(\mu + 1)^2} - \frac{4r_p E_b^2}{\pi(\mu + 1)P_p}\right] = 0 \tag{9-30}$$

In case a maximum safe value of e_b is specified by the tube manufacturer, it is evident from Fig. 9-8 that E_{bb} or E_b should not exceed one half of $e_{b\,\max}$. The plate dissipation is a limiting factor in tube operation. The value of P_p used in Eq. 9-30 was the plate dissipation existing when the amplifier is delivering its optimum power output. In case the load were suddenly disconnected without the plate supply being disconnected or in case of a loss of grid excitation, the full input power $E_{bb}I_{\text{avg}}$ must be dissipated at the plate. The rated plate dissipation may then be exceeded. The plate temperature will rise until the plate can radiate and conduct away energy at the same rate it is being supplied.

The foregoing linear algebraic analysis of the class-B tuned power amplifier is simple and straightforward and valuable as an aid to the understanding of amplifier operation. It should be remembered, however, that it is approximate and may be considerably in error if the linear range of operation is exceeded.

9-4. Graphical Solution, Class-B or C Tuned Power Amplifiers

The graphical solution to be presented in the following pages applies equally well to both class-B and class-C operation, but, since the class-C case requires the use of a graphical method in order to determine the operating angle of plate-current conduction, emphasis will be placed upon class-C operation. The use of a high-Q tuned circuit providing, as it does, a sinusoidal response at resonant frequency to a sinusoidal grid signal voltage of the same frequency, permits a particularly simple representation of what may be called the *path of operation*[3] on e_c–e_b coordinate axes. If both e_g and e_p are sinusoidal, have equal periods, and differ in phase by π rad, it may be shown that the path of operation is a straight line. On e_c–e_b axes, constant-current characteristics may be drawn, just as in Chapter 1 where the slopes of such curves were used to

[3] I. E. Mouromtseff and H. N. Kozenowski, Analysis of the Operation of Vacuum Tubes as Class C Amplifiers, *Proc. IRE*, **23**, 752–778 (1935).

illustrate the region of constancy of μ for the triode. The determination of two points on the path of operation is illustrated in Fig. 9-10. The quiescent point Q is determined by the choice of the plate-supply voltage E_{bb} and the grid bias voltage E_{cc}. One other point is needed, such as P, and is determined by an arbitrarily selected pair of values of $e_{b\,\min}$ and $e_{c\,\max}$. Thus the graphical method is cut-and-try. Points along the

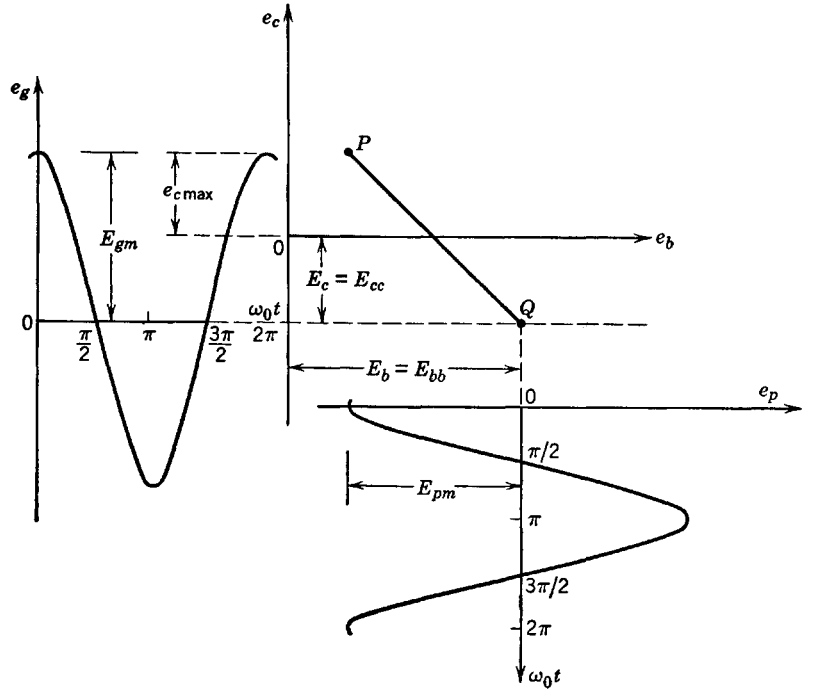

FIG. 9-10. Determination of the path of operation on the e_c–e_b diagram.

path of operation correspond to instantaneously occurring values of e_b and e_c, so that values of $\omega_0 t$ may be assigned to each point of the line.

The problem to be solved is that of obtaining values of plate and grid currents for enough values of $\omega_0 t$ to plot these current pulses as functions of time. Manufacturers of transmitter tubes usually supply a set of constant-current curves plotted on e_c–e_b axes for the purpose of graphical determination of class-C (or B) amplifier operation. The intersections of the plate or grid constant-current curves with the path of operation provide the data for a set of values of $i_b(\omega_0 t)$. In order to avoid interpolation between constant-current curves caused by the selection of arbitrary values of $\omega_0 t$, the intersections available may be

used and the corresponding values of e_c read directly from the vertical scale. Since $e_c = e_g + E_c$, the phase angles $\omega_0 t$ may be computed from the following relation:

$$\cos \omega_0 t = (e_c - E_c)/E_{gm} \tag{9-31}$$

A set of constant-current curves for the type-892 power triode is shown in Fig. 9-11. Calculations will be made from Fig. 9-11 for typical

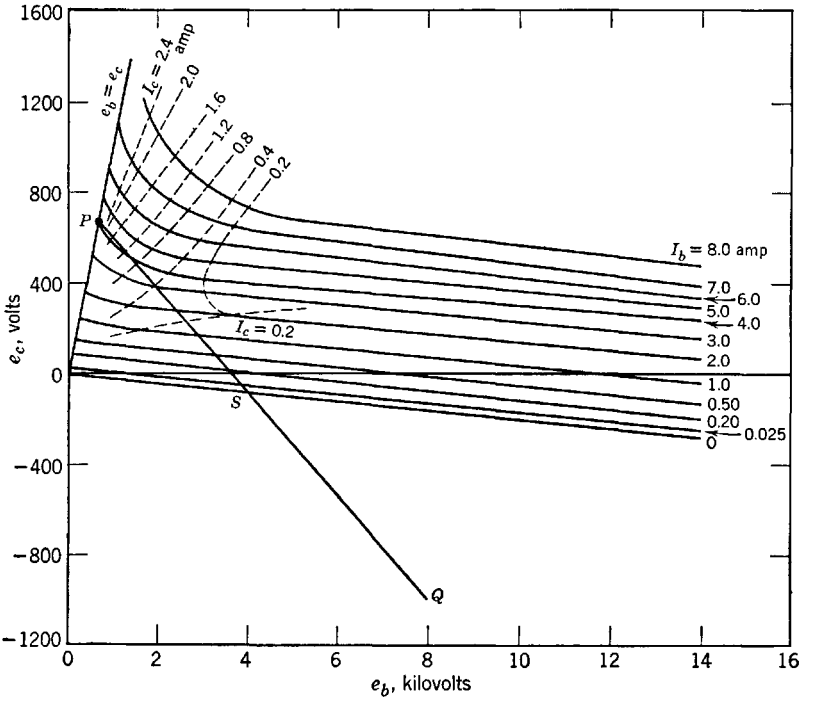

FIG. 9-11. Constant-current curves for the type-892 power triode. (Courtesy RCA)

operating values of $E_b = E_{bb} = 8000$ volts, $E_c = E_{cc} = -1000$ volts, $E_{gm} = 1700$ volts, and $e_{b\,\min}/e_{c\,\max} = 1$. Now

$$e_{c\,\max} = E_c + E_{gm} = -1000 + 1700 = 700 \text{ volts} = e_{b\,\min}$$

The coordinates of Q are $e_b = 8$ kv, $e_c = -1000$ volts; the coordinates of P are $e_b = e_{b\,\min} = 700$ volts, $e_c = 700$ volts. The operating line has been drawn and the coordinates of the intersections of the operating

line with the constant-current curves have been recorded, along with computed values of the corresponding phase angles, in Table 9-1.

TABLE 9-1

i_b	i_c	e_b	e_c	$e_c - E_c$	$\cos \omega_0 t$	$\omega_0 t$
0	0	4100	−80	920	0.540	57.3°
0.025	0	3950	−60	940	0.553	56.1
0.20	..	3600	+20	1020	0.600	53.1
0.50	..	3350	80	1080	0.635	50.5
1.0	..	3000	170	1170	0.688	46.5
..	0.20	2700	230	1230	0.724	43.6
2.0	..	2500	280	1280	0.753	41.1
3.0	..	2100	380	1380	0.811	35.7
	0.40	1950	410	1410	0.829	34.0
4.0	0.80	1600	500	1500	0.882	28.0
4.3	1.20	..	570	1570	0.924	22.4
4.4	1.60	..	630	1630	0.959	16.0
4.45	2.00		660	1660	0.975	12.7
4.5	2.40		670	1670	0.982	11.0

A sketch of the grid- and plate-current pulses (Fig. 9-12) shows that the wave forms differ considerably from partial cosine waves. Data for

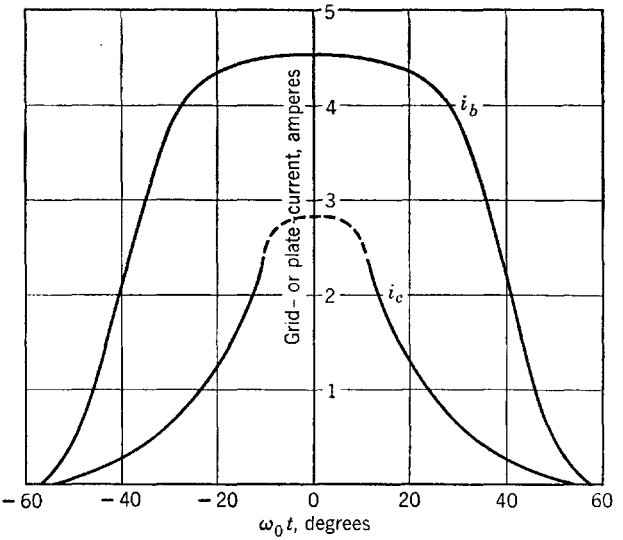

FIG. 9-12. Plate- and grid-current wave forms for class-C amplifier.

the grid-current curve were not available for $-10° < \omega_0 t < 10°$, and this part of the curve has been drawn in by guess. It is assumed that grid current begins to flow when the grid becomes positive with respect

to the cathode. According to Fig. 9-10, this occurs at $e_g = |E_{cc}|$, or

$$\cos \theta_c = |E_{cc}|/E_{gm} = 1000/1700$$

whence $\theta_c = \pm 54°$. Similarly, point S (Fig. 9-11) marks the beginning of plate-current flow, and the corresponding half-angle of conduction may be computed from either the e_c or the e_b coordinate of point S. Thus the graphically determined data for $i_b(\omega_0 t)$ and for $i_c(\omega_0 t)$ are obtained.

The needed values of the average grid current, the average value, and the amplitude of the fundamental a-c component of plate current may now be obtained from the values of $i_c(\omega_0 t)$ and $i_b(\omega_0 t)$ which are available. Graphical integration is indicated by the equations

$$I_{c\,\text{avg}} = \frac{1}{2\pi} \int_{-\pi}^{\pi} i_c(\omega_0 t)\, d(\omega_0 t) \tag{9-32}$$

$$I_{b\,\text{avg}} = \frac{1}{2\pi} \int_{-\pi}^{\pi} i_b(\omega_0 t)\, d(\omega_0 t) \tag{9-33}$$

and

$$I_{p1m} = \frac{1}{\pi} \int_{-\pi}^{\pi} i_b(\omega_0 t) \cos(\omega_0 t)\, d(\omega_0 t) \tag{9-34}$$

since the functions i_c and i_b are known graphically but not analytically. If the trapezoidal rule for graphical integration is used, and if the values of i_b and i_c are read at n equal intervals along the ωt axis between 0 and π, then the integrals Eqs. 9-33 and 9-34 may be expressed approximately as follows:

$$I_{b\,\text{avg}} = \frac{1}{n}\left[\frac{i_b(0)}{2} + \sum_{k=1}^{n} i_b\left(\frac{k\pi}{n}\right)\right] \tag{9-35}$$

$$I_{p1m} = \frac{2}{n}\left[\frac{i_b(0)}{2} + \sum_{k=1}^{n} i_b\left(\frac{k\pi}{n}\right) \cos\left(\frac{k\pi}{n}\right)\right] \tag{9-36}$$

Equations 9-35 and 9-36 indicate that the required values may be obtained by addition of ordinates at regular intervals along the $\omega_0 t$ axis, and without plotting $i_b(\omega_0 t)$ provided i_b has been obtained from Fig. 9-11 at the stated intervals. Interpolation must be resorted to in any event, and so it seems preferable to interpolate from a graph of i_b instead of guessing at the points along the operating line between constant-current curves. Readings taken from the i_b and i_c curves of Fig. 9-12 are recorded in Table 9-2 along with the corresponding values of $\omega_0 t$ and $\cos \omega_0 t$. Columns for the computed products and for the sums as in-

dicated in Eqs. 9-35 and 9-36 have been included. For 10° intervals, $n = 18$; $k\pi/n = k\pi/18$ rad, or $10k$ degrees.

TABLE 9-2

k	$\frac{k\pi}{n}$	$i_b\left(\frac{k\pi}{n}\right)$	$\cos\left(\frac{k\pi}{n}\right)$	$i_b\left(\frac{k\pi}{n}\right)\cos\left(\frac{k\pi}{n}\right)$	$i_c\left(\frac{k\pi}{n}\right)$	$E_{gm}\cos\left(\frac{k\pi}{n}\right)$	$e_c\frac{(k\pi)}{n}$	$i_c\left(\frac{k\pi}{n}\right)e_c\left(\frac{k\pi}{n}\right)$
1	$\frac{\pi}{18}$	4.1	0.985	4.04	2.5	1675	675	1690
2	$\frac{\pi}{9}$	4.1	0.940	3.86	1.3	1600	600	780
3	$\frac{\pi}{6}$	4.0	0.866	3.47	0.7	1473	473	331
4	$\frac{2\pi}{9}$	2.0	0.766	1.53	0.3	1302	302	90.6
5	$\frac{5\pi}{18}$	0.5	0.643	0.32	0.1	1092	92	9.2
Sums		14.7		13.22	4.9			2900.8
$\frac{i(0)}{2}$		2.05		2.05	1.4		$\frac{i_c(0)e_c(0)}{2} = \frac{2.8(700)}{2} = \frac{980}{3881}$	
		16.75		15.27	6.3			

From the values in the tabulation,

$$I_{b\,\text{avg}} = 16.75/18.00 = 0.93 \text{ amp}$$

$$I_{p1m} = 15.27/9 \cong 1.7 \text{ amp}$$

$$I_{c\,\text{avg}} = 6.3/18 = 0.35 \text{ amp}$$

The power output of the amplifier is then

$$P_o = E_{pm}I_{p1m}/2 = 7300(1.7)/2 = 6200 \text{ watts}$$

The power input to the plate circuit is

$$P_b = E_{bb}I_{b\,\text{avg}} = 8000(0.93) = 7450 \text{ watts}$$

The plate conversion efficiency is

$$\eta_b = 6200/7450 = 0.83$$

The required load resistance at antiresonance is

$$R_{ar} = E_{pm}/I_{p1m} = 7300/1.7 \cong 4300 \text{ ohms}$$

The plate dissipation is

$$P_p = P_b - P_o = 1250 \text{ watts}$$

The necessary grid driving power is given by the fundamental equation

$$P_c = \frac{1}{2\pi}\int_{-\pi}^{\pi} i_c e_c \, d(\omega_0 t) \tag{9-37}$$

and may be computed using the graphically obtained data from the corresponding summation, which is

$$P_c = \frac{1}{n}\left[\frac{i_c(0)e_c(0)}{2} + \sum_{k=1}^{n} i_c\left(\frac{k\pi}{n}\right) e_c\left(\frac{k\pi}{n}\right)\right] \tag{9-38}$$

The required values for the example of the type 892 have been recorded in the tabulation. From these,

$$P_c = 3881/18 = 215 \text{ watts}$$

the necessary grid driving power. The power P_c is necessary at the grid-cathode terminals to drive the tube. However, the flow of electrons to the grid constitutes a flow of current in such a direction in the bias supply circuit (Fig. 9-1) as to charge the bias battery or to deliver energy to the bias supply. This energy must be supplied by the excitation source, the grid-cathode circuit behaving as a rectifier with grid current flowing during that portion of the a-c cycle for which the grid is positive with respect to the cathode. The total amount of the grid driving power is then given by

$$P_g = P_c + |E_{cc}|I_{c\,\text{avg}} = \frac{1}{2\pi}\int_{-\pi}^{\pi} e_g(\omega_0 t) i_c(\omega_0 t) \, d(\omega_0 t) \tag{9-39}$$

This example solution of the class-C tuned power-amplifier problem shows a simple method of obtaining the required information as to plate and grid current wave forms and operating angle from which the average and fundamental components of the currents may be found. There remain the problems of optimum operation and of the design of the tuned circuit. Optimum operation may be determined by assuming $e_{b\,\min} = e_{c\,\max}$ as in the example, and trying several operating lines through the Q point recommended by the tube manufacturer. This procedure will enable the designer to select the best values of R_{ar}, E_{gm}, and E_c. The method is equally applicable to power pentodes. The problem of tuned circuit design is discussed in the following section.

9-5. Analysis of Load Coupling, Class-B or C Amplifiers

The tuned circuit of the class-B or C power amplifier will in general be much more complicated than the simple R, L, C combination of Fig. 9-1. In particular, the final stage preceding the radiating antenna

of a transmitter will involve antenna tuning and impedance matching sections necessary to present the proper load to the tube and to the transmission line leading to the antenna. However, the effective load circuit for such a case may be represented as shown in Fig. 9-13*a*, and this in turn may be reduced, at the frequency ω_0 only, to the familiar circuit of Fig. 9-13*b*. By means of tuning and proper design of the impedance matching and transmission circuits, the actual load impedance and also the impedance at terminals *a*–*b* will be made pure resistances at ω_0. Then, if C_2 is chosen such that the reactance of L_2

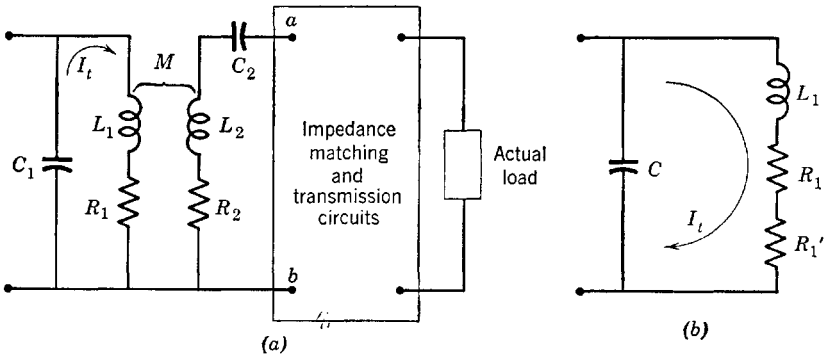

FIG. 9-13. Load circuit of a tuned power amplifier.

is canceled at ω_0, the impedance reflected into the tube plate circuit load will be a pure resistance in series with R_1 and L_1 and of magnitude

$$R_1' = \omega_0^2 M^2/(R_2 + R_{ab}) \tag{9-40}$$

Thus the effective resistance in the circuit of Fig. 9-13*b* at ω_0 is

$$R_e = R_1 + R_1' \tag{9-41}$$

and the effective or loaded Q of the tuned circuit at ω_0 is

$$Q_{e1} = \omega_0 L_1/R_e \tag{9-42}$$

The unloaded Q of the primary circuit of Fig. 9-13*a* is

$$Q_1 = \omega_0 L_1/R_1 \tag{9-43}$$

at the fundamental frequency. Some idea of the desired magnitudes of Q_1 and Q_{e1} may be obtained by considering the efficiency of transfer of power from the primary to the secondary circuit (Fig. 9-13). In terms of the tank current I_t, the power delivered to the primary circuit is

$I_t^2\ (R_1 + R_1')$ whereas that delivered to the secondary is $I_t^2 R_1'$. The efficiency is then given by the ratio

$$\eta = R_1'/(R_1 + R_1') \tag{9-44}$$

which may be expressed in terms of the loaded and unloaded Q's with the help of Eqs. 9-42 and 9-43. The result is that

$$\eta = 1 - Q_{e1}/Q_1 \tag{9-45}$$

from which it follows that Q_1 should be as large, Q_{e1} as small, as practicable. However, the entire analysis fails if Q_{e1} is so small that the voltage across the tuned circuit is not sinusoidal. The circuit loaded Q must necessarily be sufficiently large to ensure the required selectivity and to reduce the power at frequencies other than f_0 to negligible values. As previously stated, it becomes necessary to require that Q_{e1} be not less than 10, and desirably in the range between 10 and 15.

The values of L_1 and C_1 needed for design may be determined uniquely in terms of Q_{e1}, R_{ar}, and ω_0. At the frequency ω_0, for which the equivalent circuit of Fig. 9-13*b* is correct, the admittance at the terminals of C_1 is

$$Y = \frac{R_e}{R_e^2 + \omega_0^2 L_1^2} + j\left(\omega_0 C_1 - \frac{\omega_0 L_1}{R_e^2 + \omega_0^2 L_1^2}\right) \tag{9-46}$$

from which $$R_{ar} = R_e(1 + Q_{e1}^2) \tag{9-47}$$

and $$\omega_0 C_1 = Q_{e1}/R_e(1 + Q_{e1}^2) \tag{9-48}$$

If $Q_{e1} \geqq 10$,

$$R_{ar} \cong R_e Q_{e1}^2 = \omega_0 L_1 Q_{e1} \tag{9-49}$$

Then, $$L_1 = R_{ar}/\omega_0 Q_{e1} \tag{9-50}$$

and, from Eqs. 9-42, 9-48, and 9-50,

$$C_1 = \frac{Q_{e1}^2}{\omega_0^2 L_1(1 + Q_{e1}^2)} \cong \frac{1}{\omega_0^2 L_1} = \frac{Q_{e1}}{\omega_0 R_{ar}} \tag{9-51}$$

From Eq. 9-43, $$R_1 = \omega_0 L_1/Q_1 = R_{ar}/Q_1 Q_{e1} \tag{9-52}$$

and, from Eqs. 9-41, 9-42, and 9-52,

$$R_1' = \omega_0 L_1\left(\frac{1}{Q_{e1}} - \frac{1}{Q_1}\right) = \frac{R_{ar}}{Q_{e1}}\left(\frac{1}{Q_{e1}} - \frac{1}{Q_1}\right) \tag{9-53}$$

The secondary circuit parameters may likewise be computed from the resistance R_{ab} and secondary circuit Q's. If

$$Q_2 = \omega_0 L_2/R_2 \tag{9-54}$$

and

$$Q_{e2} = \omega_0 L_2/(R_2 + R_{ab}) \tag{9-55}$$

and

$$\omega_0 L_2 = 1/\omega_0 C_2 \tag{9-56}$$

then the desired relations may be easily derived in terms of the Q's, ω_0, and R_{ab}. The resistance R_{ab}, though not the actual load resistance, will be known from the design of the transmission and matching networks and may therefore logically be used in computing the remaining circuit constants. Since

$$Q_2/Q_{e2} = (R_2 + R_{ab})/R_2 = 1 + R_{ab}/R_2$$

then

$$R_2 = R_{ab}\left(\frac{Q_{e2}}{Q_2 - Q_{e2}}\right) \tag{9-57}$$

Also, from Eqs. 9-54 and 9-57,

$$L_2 = Q_2 Q_{e2} R_{ab}/\omega_0(Q_2 - Q_{e2}) \tag{9-58}$$

The remaining parameter M is given by Eq. 9-40 as

$$M^2 = R_1'(R_2 + R_{ab})/{\omega_0}^2$$

which becomes

$$M^2 = \frac{R_{ar}(Q_1 - Q_{e1})}{{\omega_0}^2 {Q_{e1}}^2 Q_1}\left(\frac{\omega_0 L_2}{Q_{e2}}\right) = \frac{R_{ar} R_{ab} Q_2 (Q_1 - Q_{e1})}{{\omega_0}^2 {Q_{e1}}^2 Q_1 (Q_2 - Q_{e2})} \tag{9-59}$$

Although relations have been readily obtained between the load circuit parameters, the required resistances and the various Q's, the real problem is the proper selection of the Q's to provide the required R_{ar}, a high tank circuit efficiency, and the necessary selectivity. As the required Q's depend upon the particular application involved, no definite specifications on their magnitudes can be stated until the requirements of the application are known. The unloaded Q magnitudes available depend upon size and power level. For low-power applications the coils are measured in dimensions of a few inches and have Q's ranging from 100 to 200. High-power level transmitters may use coils of a few feet in length having Q's in the range 500 to 800.

A worth-while analogy may be drawn between the operating principles of a class-C amplifier and a pendulum clock. The period, or the frequency of oscillation, of the pendulum depends upon its length. If the mass of the bob is large, considerable stored energy is converted from

potential to kinetic between the highest and lowest points of the swing of the pendulum. If energy sufficient to supply the losses is delivered by an escapement mechanism at the end of the swing, the pendulum will continue to oscillate with simple harmonic motion.

In the analogous class-C amplifier case, the electron tube provides the mechanism for supplying power at the minimum values of the plate swing. The stored energy transfers from L to C and back at a rate determined by the magnitudes of L and C, and will be zero in the inductance and maximum in the condenser, when the tank current is zero, maximum in the inductance and zero in the condenser when the tank current is maximum with time rate of change zero. If the energy storage is large compared with the rate of dissipation (high Q), the resulting oscillations will be very closely sinusoidal, that is, contain negligible harmonic frequencies.

9-6. The Class-C Frequency Multiplier

The class-C amplifier is often used as a frequency multiplier simply by tuning the load circuit to a multiple of—usually twice or three times—the frequency of the grid voltage. Energy is delivered on each positive grid swing but only once every n cycles of the load voltage where the

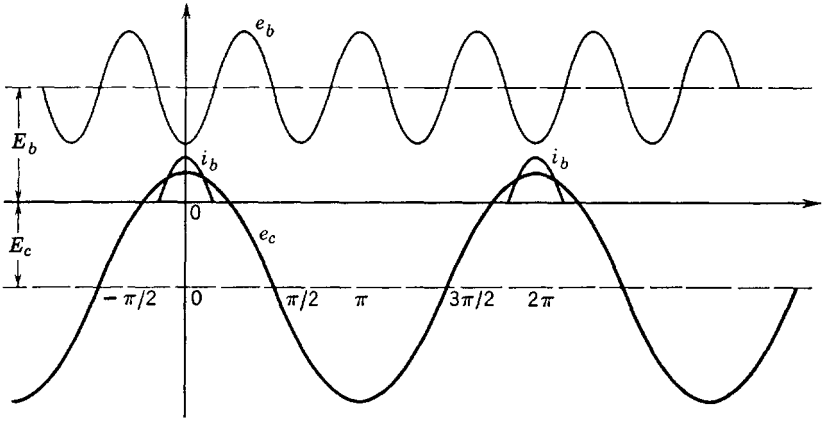

FIG. 9-14. Phase relations in a class-C frequency tripler.

output voltage is the nth harmonic of the grid signal frequency. A sketch of the desired phase relations among load voltage, grid voltage, and plate current shows that the duration of the plate-current pulse should not exceed one-half cycle of the load voltage. For a tripler, as shown in the sketch (Fig. 9-14), the angle $2\theta_b$ should not exceed 60°. It is evidently necessary to bias the grid very much farther below cutoff

than for amplification at the fundamental frequency, and the driving grid voltage must have a correspondingly large amplitude if triodes are used. Multipliers frequently use tetrodes or pentodes because of the smaller bias voltages required.

9-7. Neutralization of Triode Tuned Power Amplifiers

Triodes are used for high-power-level amplification in radiobroadcast transmitters partly because of the difficulty of cooling screen grids of pentodes at power levels of several hundreds or thousands of watts. The

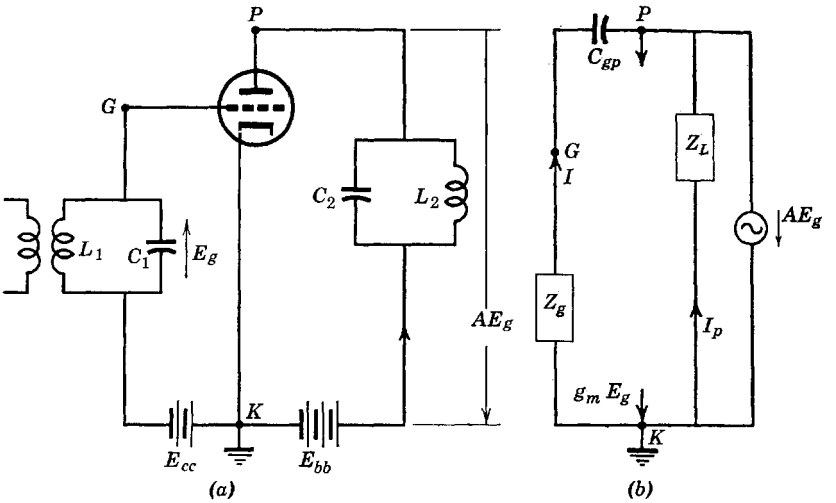

FIG. 9-15. Circuit and schematic of a class-C tuned amplifier showing the feedback path through C_{gp}.

grid-plate capacity of a triode used in the grounded-cathode circuit is a source of difficulty because it couples the output or load circuit to the input circuit. As previously discussed, both input and output circuits are tuned to the same frequency at which power amplification is desired. The power and voltage levels in the output circuit are much higher than in the input circuit. Conditions are therefore such that currents of appreciable magnitude will flow through the coupling capacitance C_{gp} from the output to the input. For example, the type-892 triode has a grid-plate capacitance of 30 $\mu\mu$f, which represents a reactance of about 5300 ohms at 1000 kc. The current at load- and source-resonant frequency f_0 produced in this reactance by the voltage across it will flow through the grid-to-cathode impedance of the input source and produce across this impedance a voltage of exactly the same frequency. If this voltage happens to be in phase with the input signal voltage, the output-

voltage amplitude will build up, as will the voltage due to feedback in the input. This unstable condition will terminate in a stable one in which the amplifier produces its own exciting voltage and becomes an oscillator. As shown in the following chapter, this behavior is deliberately provided for in an oscillator, but must be avoided in the amplifier. The feedback requirements for oscillation may be more easily understood by referring to Fig. 9-15. Here a class-C tuned amplifier circuit is shown in Fig. 9-15*a* with a signal of frequency f_0 and rms voltage E_g impressed at the grid, and a resulting output voltage AE_g across the output tank circuit. Here A is the amplifier gain at frequency f_0, and only the fundamental or f_0 component of output voltage is considered. The circuit of Fig. 9-15*b* is intended to represent a schematic equivalent a-c circuit at frequency f_0. Here the grid-cathode and plate-cathode capacitances have been included with the total grid and plate impedances to ground, respectively, Z_g and Z_L. Grid-plate capacitance C_{gp} is shown. It is assumed that a class-A equivalent circuit may be used to explain the effect of C_{gp}. It is also assumed that the feedback through C_{gp} provides a current in Z_g of the proper phase and magnitude necessary to produce E_g exactly. Therefore, the external source of E_g may be removed, as shown in Fig. 9-15*b*. The feedback requirement just stated may be formulated with the aid of Fig. 9-15*b* as follows: The positive voltage drop IZ_g must replace $-E_g$, or

$$\frac{(AE_g)Z_g}{Z_g + 1/j\omega C_{gp}} = -E_g \qquad (9\text{-}60)$$

from which a requirement is imposed upon Z_g, namely,

$$Z_g = \frac{j(1/\omega C_{gp})}{1 + A} \qquad (9\text{-}61)$$

The interpretation of Eq. 9-61 is merely that, for A a real positive number, Z_g must be an inductive reactance of fairly small magnitude. In general, both the L_1–C_1 and L_2–C_2 circuits become inductive at frequencies slightly below f_0; therefore, the condition for oscillation is present, and means must be taken to prevent the feedback. The vector diagram of Fig. 9-16 has been drawn with current I as reference for $|Z_g| < 1/\omega C_{gp}$, whence $V_g < V_{Cgp}$.

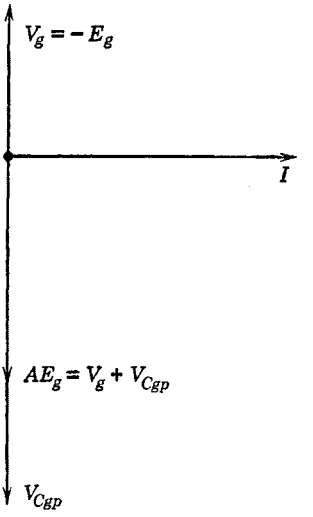

FIG. 9-16. Vector diagram for the circuit of Fig. 9-15*b*.

A knowledge of the nature of the positive feedback through C_{gp} leads easily to methods of preventing it. One method would be to connect an inductance of susceptance $1/\omega L_N = \omega C_{gp}$ in parallel with C_{gp}. The resulting tuned circuit would present such high impedance between P

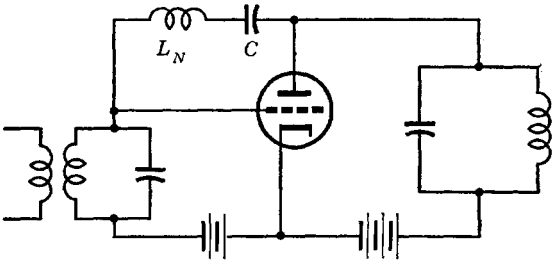

FIG. 9-17. Negative susceptance neutralization of C_{gp}.

and G (Fig. 9-15*b*) that the feedback current would be reduced to a negligible value. However, the tuned circuit would present a high impedance only at one frequency and would therefore be useful only in fixed-frequency applications, such as transmitters in which this neutralizing method has found extensive use. The arrangement is shown in Fig. 9-17, in which the capacitor C is a blocking condenser of negligible reactance.

The neutrodyne method of neutralization is illustrated by the circuits of Fig. 9-18. The principle involved is merely the cancelation at node G of equal currents 180° out of phase arriving through C_{gp} and through C_N. The additional coil L_2 closely coupled to L_1 provides a voltage equal to but 180° out of phase with the voltage across L_1. If the voltages

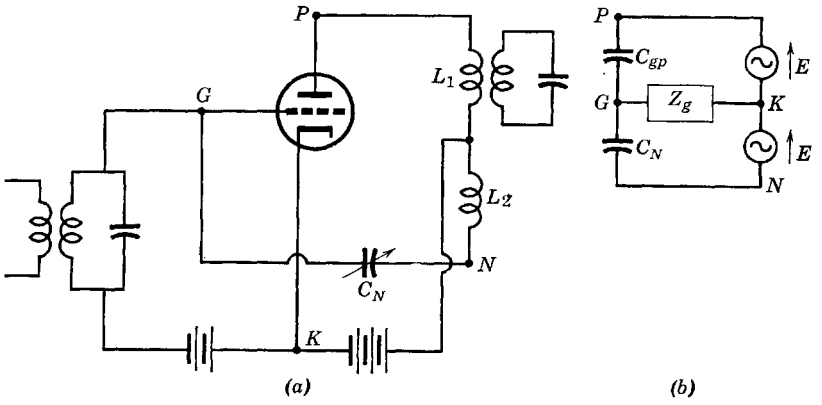

FIG. 9-18. Neutrodyne method of neutralization.

across L_1 and L_2 are each equal to E, the circuit may be represented schematically as in Fig. 9-18*b*. It is convenient to apply Norton's theorem at the terminals of the impedance Z_g. The resulting current-source circuit is shown in Fig. 9-19. Since current I is the difference between currents $j\omega C_{gp}E$ and $j\omega C_N E$ which would flow in a short circuit placed between G and K, the current-source current is zero for $C_N = C_{gp}$ at any frequency, and thus no voltage derived from the output will exist across Z_g if connected between G and K.

Tests for proper adjustment of C_N can be accomplished by applying excitation voltage to the grid circuit, disconnecting the plate supply, and

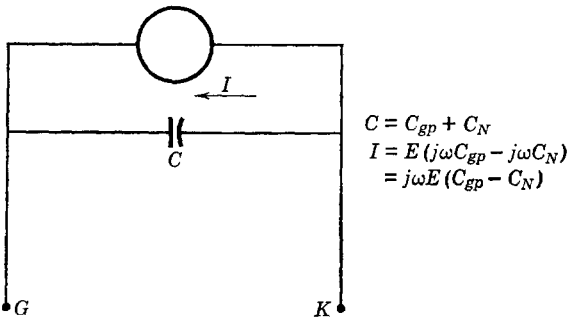

FIG. 9-19. Current source equivalent of Fig. 9-18*b*.

checking for energy in the plate coil by means of a small search coil connected to a sensitive detector. The variable C_N is then adjusted until the reading of the detector is zero or minimum.

Class-C amplifiers connected in push–pull are easily neutralized by the connection of two neutralizing condensers from the plate of each tube to the grid of the other. The balanced voltages of the output coil are already available without the use of an additional coil.

9-8. Power Supplies and Bias Sources for Tuned Power Amplifiers

Class-B and class-C amplifiers used in broadcast transmitters require high voltage and large amounts of d-c power and are usually supplied from polyphase rectifiers similar to those discussed in Chapter 7. Filters are necessary and are simplified by the use of polyphase rectification.

Bias voltage may be derived from the output of a rectifier and filter, or from resistors and resistor-capacitor combinations connected in cathode or grid circuits. A combination of power source providing bias to cutoff plus additional cathode or grid bias is preferred because of danger to self-biased tubes which would occur upon loss of grid excitation. Automatic safety cutouts are used with commercial transmitters

to remove plate voltage instantly in the event of the loss of grid signal voltage.

Since grid current flows in class-C or B tuned power amplifiers, the source and polarity of bias voltage in the circuits of Fig. 9-20 should be evident. Electrons flowing to the grid produce the external conventional

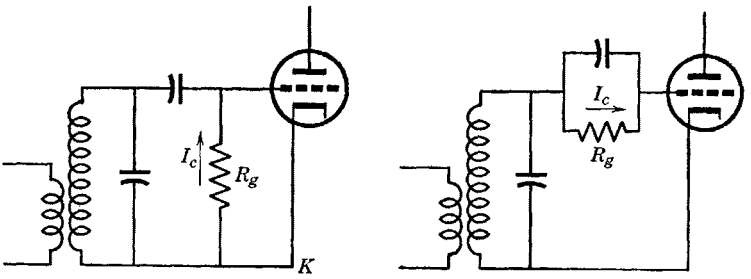

FIG. 9-20. Use of grid current in producing bias.

current in the indicated direction. The direct current I_c is the average of the grid-current pulses.

9-9. The Grounded-Grid Tuned Power Amplifier

Neutralization is unnecessary if the grounded-grid connection is used. This fact becomes particularly important at frequencies high enough that distributed circuit parameters make neutralization very difficult. The schematic circuit of Fig. 9-21 provides interesting information as to

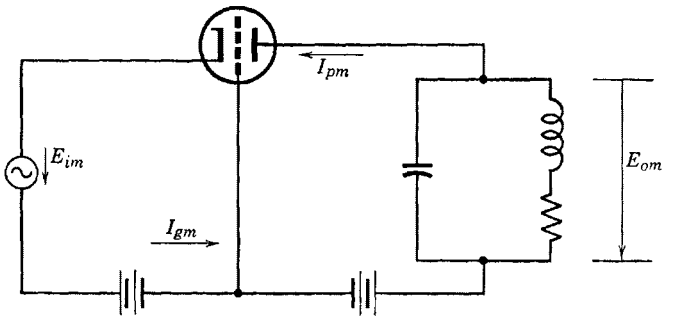

FIG. 9-21. Grounded-grid, tuned power amplifier.

power relations in the grounded-grid circuit. The currents and voltages shown on the diagram are the peak values of the fundamental a-c components. Since E_{im} and E_{om}, the peak input and output voltages at frequency f_0, are in phase, and since the peak plate current flows through

the signal generator, then the available output power is

$$P_o = (E_{im}I_{pm} + E_{om}I_{pm})/2 \tag{9-62}$$

The power input supplied by the driving or signal generator is

$$P_i = E_{im}(I_{gm} + I_{pm})/2 = P_g + E_{im}I_{pm}/2 \tag{9-63}$$

in which $P_g = E_{im}I_{gm}/2$ is grid dissipation, but the component of driving power $E_{im}I_{pm}/2$ is recognized as part of the output.

PROBLEMS

9-1. Positive pulses of current of rectangular wave shape are applied at a uniform rate of 796,000 per second to a circuit consisting of an inductance of 80 microhenrys in parallel with a capacitance of 500 $\mu\mu$f. The coil Q is 40. Pulse duration is 0.04π μsec, amplitude 0.5 amp.

(*a*) Compute the amplitudes of the fundamental and of third-harmonic components of impressed current.

(*b*) Compute the peak values of fundamental and of third-harmonic frequency voltages across the parallel circuit.

9-2. If the circuit of problem 9-1 were tuned to the third harmonic of the current wave, compute the voltage across the tuned circuit at third-harmonic frequency.

9-3. Assume that the current pulse of problem 9-1 consists of half sine waves of the same repetition rate but of amplitude 100 ma. If the tuned circuit consists of a coil of $Q = 50$, $L = 20$ microhenrys, and $C = 500$ $\mu\mu$f, determine the effective alternating voltage across C and the power delivered to the tuned circuit.

9-4. Refer to manufacturer's data on a type-806 power amplifier, and obtain the values of μ and r_p necessary for analysis of the tube as a class-B power amplifier operating at $E_b = 2000$ volts, $E_c = -150$ volts, $E_{gm} = 180$ volts. If the maximum allowable plate dissipation is 150 watts, compute the impedance of the tuned circuit at resonance, assume $e_{b\,\min} = e_{c\,\max}$.

9-5. Compute the power output and the plate-circuit efficiency for the amplifier of problem 9-4.

9-6. A class-B amplifier using a type-810 triode is to be operated at 30 Mc. Typical operating conditions are:

$$E_b = 1500 \text{ volts}$$

$$E_c = -50 \text{ volts}$$

$$E_{gm} = 110 \text{ volts}$$

$$P_p = 125 \text{ watts, maximum}$$

If $e_{b\,\min} = 2e_{c\,\max}$, compute for a plate supply of 1500 volts (*a*) power output, (*b*) plate efficiency, (*c*) operating plate dissipation, (*d*) L and C of tuned circuit if the loaded $Q = 15$.

9-7. A type-891 power triode operates as a class-C power amplifier at:

$$E_b = 8000 \text{ volts}$$
$$E_c = -1800 \text{ volts}$$
$$E_{gm} = 2400 \text{ volts}$$
$$I_b = 1.15 \text{ amp}$$
$$I_c = 0.09 \text{ amp}$$

If $e_{b\,\min} = e_{c\,\max}$, and $f_0 = 1.59$ Mc, compute (*a*) the average plate current (d-c), (*b*) the fundamental component of plate current I_{p1m}, (*c*) the power output, (*d*) the power input to the plate, (*e*) the plate conversion efficiency, (*f*) the required load resistance at antiresonance, (*g*) the plate dissipation, (*h*) the grid driving power, (*i*) the elements of the tank circuit if the loaded Q is 20.

CHAPTER 10

VACUUM-TUBE OSCILLATORS

THE POSSIBILITY THAT A VACUUM-TUBE AMPLIFIER MAY BECOME AN oscillator has been referred to in preceding chapters where precautions needed to prevent such an event have been discussed. The present chapter, however, will be concerned with the solution of the problem of producing a-c output power at constant frequency at the output terminals of a vacuum-tube amplifier which supplies its own input. It is basic in the vacuum-tube production of alternating voltage or power from a d-c source to provide a means whereby the kinetic energy of the electron stream may be converted into the alternating field energy at the output terminals. This general principle applies to any type of vacuum-tube oscillator; however, the material of the present chapter will be primarily concerned with the rather conventional vacuum-tube oscillators which provide single-frequency (sinusoidal) output voltage in the audio- and radio-frequency ranges up to a few megacycles. Such oscillators can provide a better frequency stability and a wave form more nearly sinusoidal than is possible by any other means.

10-1. Simplified General Theory of Oscillators

The conditions essential for producing a sinusoidal voltage across the terminals of a tuned L–C circuit were discussed briefly at the beginning of Chapter 9. It is instructive to examine the same circuit except that now it is assumed that the elements are not lossless, so that an equivalent circuit must involve a resistance. Suppose, for example, the switch in the circuit of Fig. 10-1 is closed suddenly at a time when no energy is stored in L or C. The current $g_m e_g$ shown as driving the equivalent a-c circuit is initially zero since e_g, the input signal voltage at the grid, is zero. It is interesting to write and solve the node equation at node P at the initial instant of closing the switch. Since a voltage cannot instantly be impressed upon a capacitance, initially the node voltage V at the plate will be zero. At any instant, the sum of the currents at node P must be zero, or

$$V\left(\frac{1}{r_p}+\frac{1}{R_L}\right)+C\frac{dV}{dt}+\frac{1}{L}\int_0^t V\,dt=0 \tag{10-1}$$

Let the combined resistance of r_p and R_L in parallel be R. It is then convenient to differentiate Eq. 10-1 with respect to time and to divide

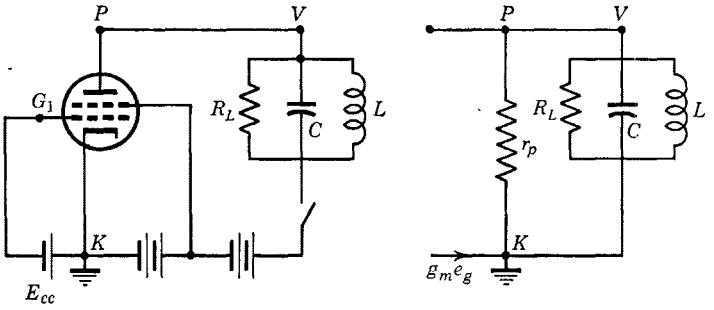

FIG. 10-1. Circuit of a dynatron oscillator.

through by C in order to obtain the differential equation

$$d^2V/dt^2+(1/RC)\,dV/dt+(1/LC)V=0 \tag{10-2}$$

which is in a form quite familiar to students of electric-circuit theory. The solution of Eq. 10-2 is easily obtained by the usual methods. If the constants of the circuit are such that

$$1/LC > 1/(2RC)^2$$

and with $\quad a=1/2RC, \qquad b=\sqrt{1/LC-1/(2RC)^2}$

then the solution is

$$V=\epsilon^{-at}(K_1\sin bt+K_2\cos bt) \tag{10-3}$$

The condition that $V=0$ at $t=0$ requires that integration constant $K_2=0$. Then the solution

$$V=K_1\epsilon^{-t/2RC}\sin\left(\sqrt{1/LC-1/(2RC)^2}\right)t \tag{10-4}$$

shows that a damped sinusoidal voltage exists across the tuned circuit for the conditions assumed.

Additional interesting interpretations of Eq. 10-4 are now possible and provide the reasons for the introduction of the differential equation

and its solution at this point. The expression for the quantity b may be revised as follows:

$$b = \omega = \frac{1}{\sqrt{LC}}\sqrt{1 - \frac{LC}{(2RC)^2}} = \omega_0\sqrt{1 - \frac{1}{2(R/\sqrt{L/C})^2}} \quad (10\text{-}5)$$

Here $\omega_0 = 1/\sqrt{LC}$, the resonant frequency of the parallel combination of L and C, and, since $\omega_0 L = \sqrt{L/C} = 1/\omega_0 C$, the effective circuit Q may be introduced as *

$$Q_e = \frac{R}{\omega_0 L} = \omega_0 RC = \frac{R}{\sqrt{L/C}} \quad (10\text{-}6)$$

Equation 10-4 now becomes

$$V = K_1\epsilon^{-t/2RC}\sin\omega_0(\sqrt{1 - 1/4Q_e^2})t \quad (10\text{-}7)$$

which shows that the voltage V is a damped sinusoid provided $Q_e > \frac{1}{2}$; also, the angular frequency approaches ω_0 if $1/4Q_e^2 \ll 1$. Thus, if $Q_e \geqq 5$, the angular frequency is practically that of the tuned circuit.

The question of damping as represented by the factor $\epsilon^{-t/2RC}$ is of equal interest. If by some means $R = r_p R_L/(r_p + R_L)$ could be made infinite, then the exponent $t/2RC$ would become zero, and the output voltage would be a pure sine wave with no damping. This could occur provided r_p is negative and equal in magnitude to R_L. The possibility of a negative r_p exists as shown by the plate characteristic of a tetrode at low plate voltage (Fig. 2-3). In fact, the dynatron oscillator depends upon just this negative slope region of the tetrode plate characteristic to eliminate damping. Another and more important possible interpretation, however, is that the resistance R_L represents the source of all losses in the tuned circuit. If by connection of the tube to the tuned circuit not only the losses but also the power output can be supplied, then R_L is effectively canceled. This is, again, the class-C synchronous switch interpretation of Chapter 9.

One further interpretation of Eq. 10-7 is the possibility that the tube provide in effect a negative resistance of magnitude such that R is negative but not zero. In such a case, the exponential $\epsilon^{-t/2RC}$ increases with time and the oscillation amplitude increases or builds up. This is, of course, the expected behavior as any generator begins to build up voltage, but in the case of the tube the important question of what ultimately limits the oscillation amplitude must be answered. The answer is that limitation is imposed by the properties of the tube itself.

* See Eq. 8-9, Chapter 8.

The plate resistance and transconductance can no longer be considered constants but are dependent upon the location of the operating point which shifts position, as the oscillation amplitude builds up, in the direction of current saturation in the nonlinear region of the tube characteristics. Thus, the operation is inherently nonlinear, and harmonics are introduced in the output unless special means external to the tube are provided to limit the amplitude of oscillation.

The possibility is inherent in the circuit of Fig. 10-1—and has perhaps been suggested by the discussion—that a properly designed coupling loop connected in the grid circuit could be used to provide a fraction of the voltage V to be used as grid excitation. In this case, the circuit becomes a feedback amplifier in which all the excitation is derived from the output in the form of regenerative feedback. This is a much more practical concept and type of oscillator than the dynatron. The analysis of such oscillators is given in the following section.

10-2. Conditions for Oscillation of an Amplifier

A vacuum-tube amplifier is capable of producing an a-c power gain through transfer of energy from the electron-stream kinetic energy to the energy of the a-c field in the output circuit. Because of this power gain, it is possible to feed back a fraction of the output power into the input in such a way that stable self-oscillations are produced. The remaining output power is available for a useful load. The design specifications of most interest for such oscillators are the following:

(*a*) The magnitude and stability of the output frequency.

(*b*) The magnitude of the output power.

(*c*) The efficiency of operation.

(*d*) The dependence of the frequency, power, and efficiency upon the load admittance.

Because of the positive feedback necessary to establish self-oscillation, it is inherently necessary that some part of the oscillator system provide a limiting action to establish a stable equilibrium and to prevent the amplitude from growing without limit. This limiting action generally arises from nonlinearity in the electron-stream portion of the device, unless amplitude-limiting circuits designed for that purpose are provided. Although in the absence of external amplitude-limiting circuits the nonlinearity would seem to rule out the use of the four-pole theory, in fact a considerable amount of qualitative and some quantitative information may be obtained by the use of the four-pole admittance concepts, or by other methods of linear circuit analysis.

It has frequently been possible in previous amplifier analysis to assume the feedback admittance y_{12} to be negligible. Actually, of

course, amplifiers are designed to make the feedback admittance negligible, whereas the feedback admittance is necessary for the tube transducer to operate as an oscillator. Because of the positive feedback, an oscillator is driven as an amplifier from its own output, and the necessary energy is provided by the d-c plate supply. A four-pole equivalent tube circuit with input and output terminations is shown in Fig. 10-2 and is

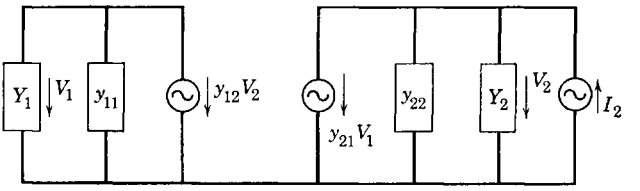

FIG. 10-2. Equivalent circuit of an amplifier, driven from the output.

assumed to be driven from a generator of current I_2 connected across the output.

The voltage V_2 in Fig. 10-2 is built up by the driving generator. The current I_2 is then given by the expression

$$I_2 = V_2(Y_2 + y_{22}) + y_{21}V_1 = V_2\left(Y_2 + y_{22} + \frac{V_1}{V_2}y_{21}\right) \quad (10\text{-}8)$$

The relation $$V_1/V_2 = -y_{12}/(y_{11} + Y_1) = A_b \quad (10\text{-}9)$$

was derived in Chapter 1 (Eq. 1-54) and is referred to as the backward voltage gain.

It is required that the tube circuit of Fig. 10-2 behave as an oscillator. As such, it will require no driving generator of current I_2. Let it be assumed that a certain steady amplitude of the voltage V_2 will be maintained by the circuit as an oscillator. Thus, as exciting current I_2 is reduced gradually to zero, voltage V_2 must approach a steady value if the circuit oscillates. The necessary condition for I_2 to approach zero and for V_2 to approach simultaneously some steady value not equal to zero is, from Eqs. 10-8 and 10-9, for the sum of the admittances to reduce correspondingly until in the limiting case for $I_2 \rightarrow 0$,

$$Y_2 + y_{22} + A_b y_{21} \rightarrow 0$$

Then, the condition for oscillation must be

$$Y_2 + y_{22} + A_b y_{21} = 0 \quad (10\text{-}10)$$

which may be written in the form

$$1 + A_b y_{21}/(y_{22} + Y_2) = 0$$

or

$$A_b A = +1 \tag{10-11}$$

since $A = -y_{21}/(y_{22} + Y_2)$ (derived in Chapter 1, Eq. 1-50) is the forward voltage gain of the circuit as an amplifier.

Admittance y_{22} may be separated into two parts: y_c which depends only upon the circuit, and y_e which depends only upon the electron stream. Since y_{21} depends upon the electron stream, let y_e be grouped with $A_b y_{21}$ so that in Eq. 10-10 a separation may be effected between circuit-dependent and electron-stream-dependent admittances. Thus, let

$$Y_e = y_e + A_b y_{21} \tag{10-12}$$

and since

$$y_{22} = y_c + y_e \tag{10-13}$$

then, Eq. 10-10 becomes

$$Y_2 + y_c + Y_e = 0 \tag{10-14}$$

Here the admittance Y_e is dependent upon both the voltage V_2 and the angular frequency ω and may be expressed functionally as $Y_e(V_2, \omega)$.

In terms of component conductances and susceptances, the conditions for oscillation voltage amplitude V_2 to exist at a fixed frequency are

$$G_2 + g_c + G_e(V_2) = 0 \tag{10-15}$$

and

$$B_2 + b_c + B_e(V_2) = 0 \tag{10-16}$$

If a simple antiresonance is assumed, then

$$B_2 + b_c = \omega C - 1/\omega L$$

where C and L are the equivalent net capacitance and inductance of the circuit portion. If further,

$$B_e(V_2) = \omega C_e(V_2) \tag{10-17}$$

then

$$\omega C - 1/\omega L + \omega C_e(V_2) = 0$$

or

$$\omega^2 = 1/L[C + C_e(V_2)] \tag{10-18}$$

and

$$-G_e(V_2) = G_2 + g_c \tag{10-19}$$

Equation 10-19 states that equilibrium will be established at that value of V_2 for which $-G_e(V_2)$ becomes equal to $G_2 + g_c$, and Eq. 10-18 provides information as to the dependence of ω upon $C_e(V_2)$ as well as the circuit constants. Thus, both the frequency and the power output $V_2^2 G_2$ are dependent upon the load admittance. Variations of the power

output and frequency with load admittance are often presented in a form known as a Riecke diagram.

The interpretations that have been obtained from the condition $AA_b = 1$ for the sustained oscillation of an amplifier are generally applicable to oscillators. The requirement that $AA_b = 1$ may be called a criterion for self-excitation. Another approach to the criterion for the self-excitation of a single tube amplifier or oscillator is available through the feedback theory of Chapter 3. This requirement for self-

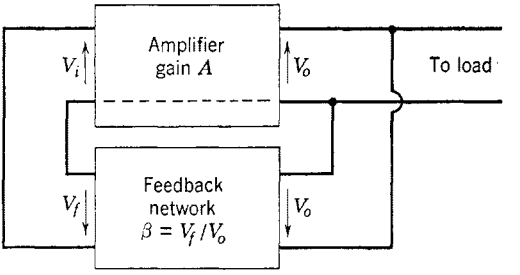

FIG. 10-3. Oscillator input supplied by feedback from its output.

excitation, known as the Barkhausen criterion, is very easily obtained from the diagram of Fig. 10-3. The voltage gain of the amplifier is

$$A = V_o/V_i \tag{10-20}$$

The output voltage is impressed across the feedback network which provides the voltage

$$V_f = \beta V_o \tag{10-21}$$

at its own output. The feedback network is required to provide the proper magnitude and phase of V_f such that it is identical with the voltage V_i. If $V_i \equiv V_f$, then Eq. 10-20 becomes

$$A = V_o/V_f = V_o/\beta V_o = 1/\beta \tag{10-22}$$

or

$$A\beta = 1 \tag{10-23}$$

which is the requirement for self-excitation and oscillation.

The application of Eq. 10-23 to a vacuum-tube amplifier of gain A, load impedance Z_L, results in a requirement on β. Thus,

$$A\beta = -\frac{\mu Z_L}{r_p + Z_L}\beta = 1$$

or

$$\beta = -\left(\frac{r_p + Z_L}{\mu Z_L}\right) = -\left(\frac{1}{\mu} + \frac{1}{g_m Z_L}\right) \tag{10-24}$$

which is known as the Barkhausen criterion for sustained oscillations. If Z_L is a pure resistance, the minus sign in Eq. 10-24 represents the 180° phase reversal necessary in the feedback network in order to provide the proper voltage phase at the input. If Z_L is complex, then an additional phase correction in the feedback network is necessary. The required feedback network gain β therefore depends upon both load and tube.

10-3. Application of Oscillation Criteria to the Tuned-Plate Oscillator

Certain interesting results may be obtained by an application of Eq. 10-11. If the separation into electronic and circuit parts of the admittances of Eq. 10-14 is possible, the same results may be obtained more easily by direct resort to Eq. 10-14 or to Eqs. 10-15 and 10-16.

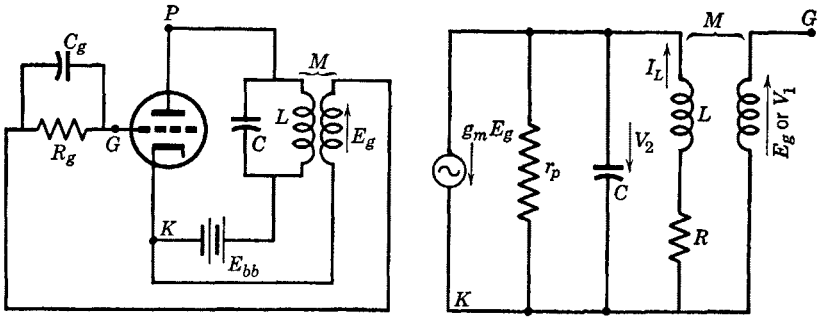

FIG. 10-4. Actual and equivalent circuits of a tuned-plate oscillator.

However, it is difficult to write down immediately the separation indicated in Eq. 10-14. Therefore, Eq. 10-11 will be applied directly to the case of the tuned-plate oscillator.

The circuit of the tuned-plate oscillator is shown in Fig. 10-4 and is the same as that shown in Fig. 10-1 except that feedback is provided. Resistance R_g is a biasing resistor, C_g a by-pass condenser. The equivalent a-c circuit is drawn under the assumption of linear operation. Resistance R is the effective value of the resistance of the load, as seen from the tank circuit and includes the coil resistance of the inductance L. It is assumed that the load is either directly in series with L or is coupled into the tank circuit.

An application of Kirchhoff's current or node equation to the equivalent circuit of Fig. 10-4 gives the following:

$$g_m V_1 = -V_2 \left(\frac{1}{r_p} + j\omega C + \frac{1}{R + j\omega L} \right)$$

or
$$A = \frac{V_2}{V_1} = -\frac{g_m}{1/r_p + j\omega C + 1/(R + j\omega L)} \tag{10-25}$$

Also, the voltage V_1 is given by

$$V_1 = j\omega M I_L = j\omega M\left(-\frac{V_2}{R + j\omega L}\right)$$

so that
$$A_b = V_1/V_2 = -j\omega M/(R + j\omega L) \tag{10-26}$$

The condition for self-sustained oscillation is given by Eq. 10-11. Thus,

$$\left(\frac{-j\omega M}{R + j\omega L}\right)\left[-\frac{g_m}{1/r_p + j\omega C + 1/(R + j\omega L)}\right] = +1$$

and
$$\frac{j\omega M}{R + j\omega L} = \frac{1/r_p + j\omega C + 1/(R + j\omega L)}{g_m}$$

$$= \frac{1}{\mu} + \frac{j\omega C(R + j\omega L) + 1}{g_m(R + j\omega L)} \tag{10-27}$$

Equation 10-27 may be simplified by multiplying through by $[(R + j\omega L)/j\omega C]$. The result, with some algebraic simplification, is

$$-\frac{M}{C} + \frac{R + j\omega L}{j\mu\omega C} + \frac{R}{g_m} + j\frac{1}{g_m}\left(\omega L - \frac{1}{\omega C}\right) = 0$$

whence, by rationalization,

$$\left(\frac{L}{\mu C} + \frac{R}{g_m} - \frac{M}{C}\right) + j\left[\frac{1}{g_m}\left(\omega L - \frac{1}{\omega C}\right) - \frac{R}{\mu\omega C}\right] = 0 \tag{10-28}$$

Thus, the following two equations result:

$$L/\mu C + R/g_m - M/C = 0 \tag{10-29}$$

and
$$(\omega L - 1/\omega C) - Rg_m/\mu\omega C = 0 \tag{10-30}$$

From Eq. 10-29
$$M = L(1/\mu + RC/Lg_m) \tag{10-31}$$

which specifies the value of M required for sustained oscillations. For M greater than the value given by Eq. 10-31, the oscillation amplitude will increase until the current is driven into nonlinear regions of the tube characteristics such that g_m and μ will satisfy Eq. 10-31. The quantity $L/RC = R_{ar}$, the impedance of the load at the resonant frequency. Thus, Eq. 10-31 written as

$$-M/L = -(1/\mu + 1/R_{ar}g_m)$$

will be recognized as the Barkhausen criterion of Eq. 10-24, with $-M/L$ proportional to β. From Eq. 10-30,

$$\omega^2 = \frac{1}{LC}\left(1 + \frac{R}{r_p}\right) \tag{10-32}$$

or with $$\omega_0{}^2 = 1/LC, \qquad \omega = \omega_0\sqrt{1 + R/r_p} \tag{10-33}$$

Now ω_0 is the natural angular frequency of the tuned circuit. Thus, Eq. 10-33 indicates that the oscillation frequency is slightly greater than the natural frequency of the tuned circuit, but that the difference is small if $r_p \gg R$.

Another interpretation of Eq. 10-29 is that, for a fixed M, the bias is such as to provide the necessary value of

$$g_m = \mu RC/(\mu M - L) \tag{10-34}$$

Oscillations in the tuned-plate oscillator are self-starting if the value of g_m at zero bias is greater than the critical value imposed by Eq. 10-34. The presence of the biasing resistor R_g causes a shift in operating point as oscillations begin and build up, and grid current begins to flow. The stable operating point is that for which the average value of g_m between extreme values of grid voltage is that specified by Eq. 10-34. The quantity μ is reasonably constant over the same range.

The analysis given herein for the tuned-plate oscillator applies reasonably well for frequencies such that lumped circuit values may be used. For higher frequencies where the circuits must be analyzed in terms of distributed constants, a different analytical method is utilized.

10-4. Vector Diagram of the Tuned-Plate Oscillator

The vector diagram of the tuned-plate oscillator is obtained from the equivalent circuit, and assumed linear operation. Although operation is not linear, the vector diagram is instructive and reasonably accurate. The steps taken in the preparation of the vector diagram of Fig. 10-5 are listed in their proper sequence as follows:

(1) Assume current I_L as reference vector; draw:
(2) RI_L
(3) $j\omega LI_L$
(4) $-V_2 = RI_L + j\omega LI_L$
(5) $I_c = j\omega C(-V_2)$
(6) $I_p = -V_2 g_p = -V_2/r_p$
(7) $g_m V_1 = I_c + I_p + I_L$ and must be perpendicular to I_L.
(8) $V_1 = E_g = g_m V_1/g_m$

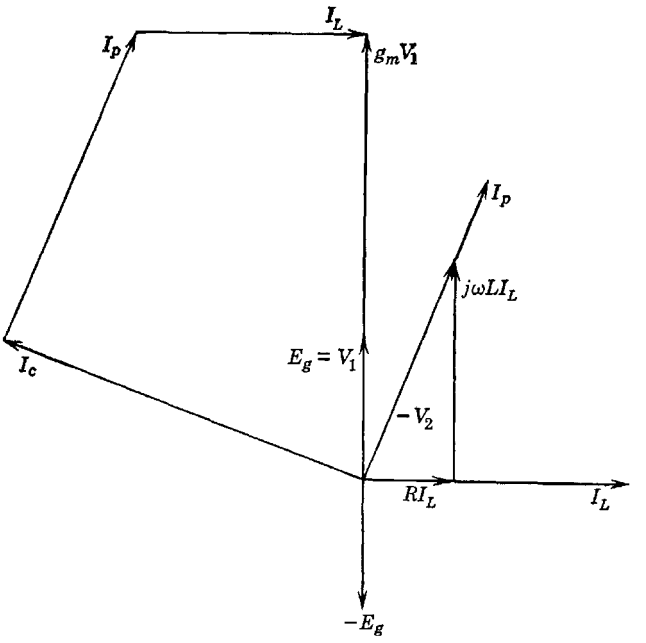

FIG. 10-5. Vector diagram of the tuned-plate oscillator.

In order for V_1 or E_g to lead I_L by 90°, $g_m V_1$ must lead $(-V_2)$. The tuned circuit then behaves as a capacitance, and the reactance curve of Fig. 10-6 indicates that the frequency at which the tank circuit presents a capacitive reactance is greater than f_{ar}.

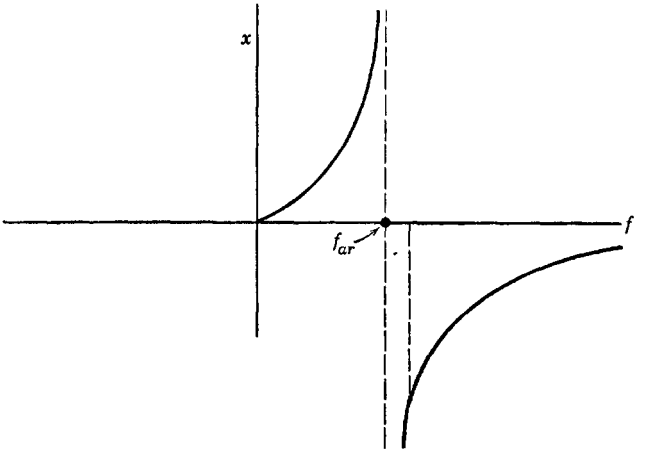

FIG. 10-6. Reactance curves for the tank circuit of a tuned-plate oscillator with negligible R.

10-5. Classification of Feedback Oscillator Circuits

Oscillator circuits have been classified as those that do and those that do not have external feedback networks. For the first group, those

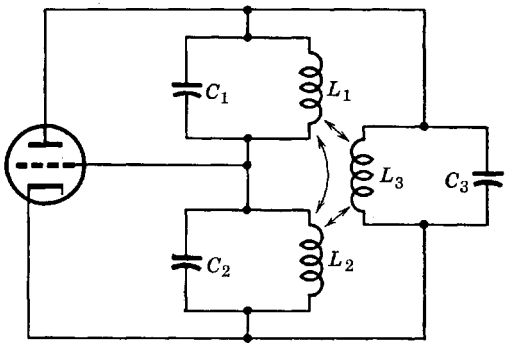

FIG. 10-7. Prototype oscillator circuit, plate supply not shown.

providing external feedback circuits, Jen [1] has shown that four basic circuits may be derived from a single prototype, shown in Fig. 10-7. Three are obtained by omitting one inductive element successively from

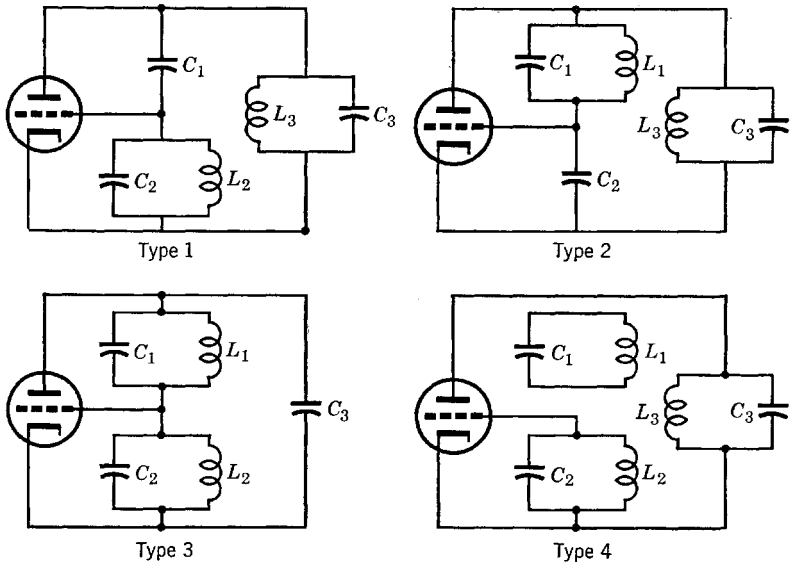

FIG. 10-8. Basic feedback oscillator circuit types derived from the prototype of Fig. 10-7.

[1] C. K. Jen, *Proc. IRE*, **19**, 2109 (Dec. 1931).

each of the three parallel tuned circuits, the fourth by making one of the resonant circuits conductively separate from the remaining portion. Inductive coupling may exist among all three coils.

The four derived circuits are shown in Fig. 10-8. This classification has been used by Thomas [2] to show that the commonly used oscillator circuits may be derived from the four types. The tuned-plate oscillator,

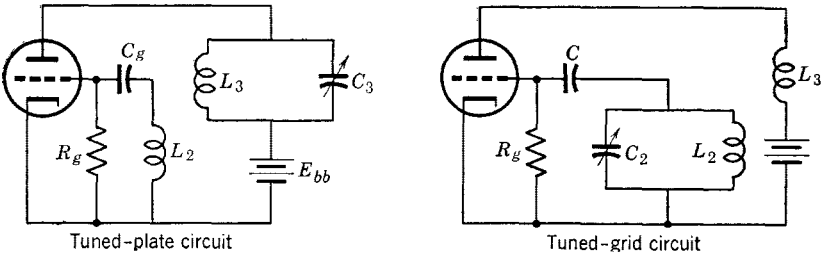

FIG. 10-9. Tuned-plate and tuned-grid practical type-1 circuit derivatives.

for example, is type 1 with C_1 and C_2 removed. A similar circuit, the tuned-grid oscillator, also may be derived from type 1 by removing C_1 and C_3. Practical arrangement of the tuned-plate and tuned-grid circuits are given in Fig. 10-9. The elements R_g and C_g are added to provide grid bias. A third and very frequently used circuit, the Hartley circuit,

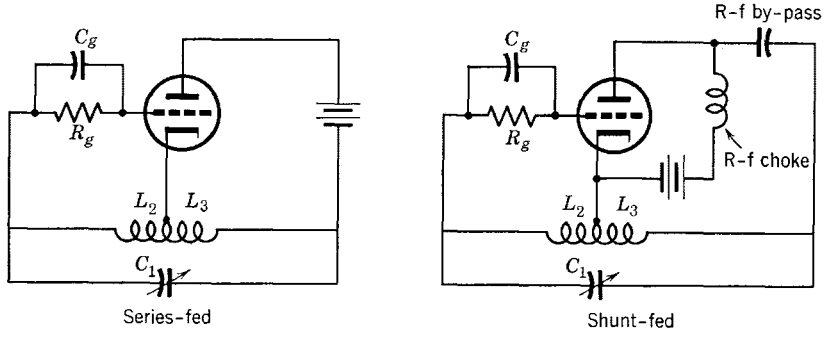

FIG. 10-10. Hartley oscillator circuits, type-1 derivatives.

may be derived from type 1 by omitting C_2 and C_3. Since the two coils have a common terminal, they may be represented as a single coil with a tap connection for the cathode as shown in the practical circuit of Fig. 10-10, which includes both series- and shunt-fed versions. The usefulness of the Hartley circuit depends largely upon the fact that a single

[2] H. A. Thomas, *Theory and Design of Value Oscillators*, Chapman & Hall, London.

tapped coil may be used, with the tap joint adjustable if desired. The series-fed circuit is usually avoided because of the shunting capacitance of the power source.

The type-1 circuit of Fig. 10-8 with all elements present except mutual coupling between L_2 and L_3 and with or without the capacitive

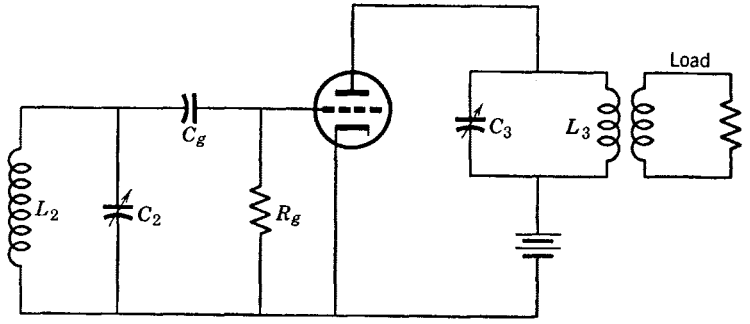

FIG. 10-11. Tuned-plate, tuned-grid type-1 derivative without external coupling C_1.

coupling C_1 between grid and plate circuits is called the tuned-plate, tuned-grid circuit. Where shielding is employed between plate and grid circuits, feedback depends upon the grid-plate capacitance $C_{gp} + C_1$ or C_{gp} alone. The oscillation frequency is determined by the grid-circuit tuning, since the loading of the plate circuit results in a lowering

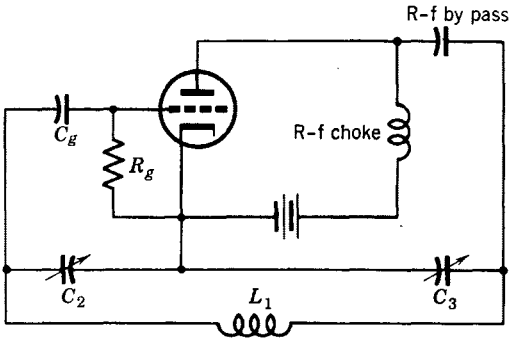

FIG. 10-12. The Colpitts oscillator, type-2 derivative.

of its effective Q. The plate-circuit tuning may then be used to adjust oscillator loading. A practical form of this circuit is shown in Fig. 10-11.

The type-2 circuit of Fig. 10-8 has one important derivative, the Colpitts oscillator of Fig. 10-12. This circuit may be derived from type 2 by omitting L_3 and C_1. The practical circuit of Fig. 10-12 uses shunt feed to the plate. Tuning capacitances C_1 and C_2 are ganged

(tuned with a single adjustment) once their proper capacitance ratio has been determined.

No practical circuits seem to have developed from the type-3 prototype, but the type 4 is represented by the Meissner circuit in which C_2 and C_3 and the coupling between L_2 and L_3 are omitted. This leaves the nonconductively coupled L_1–C_1 circuit as both tank circuit and feedback path between plate and grid. A practical form of this circuit may be arranged as shown in Fig. 10-13.

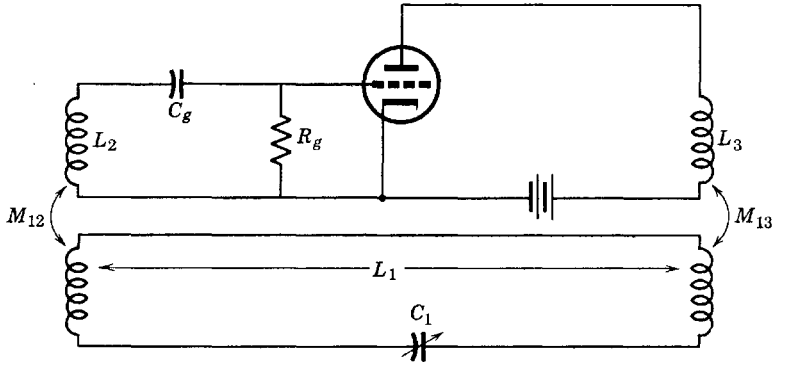

FIG. 10-13. Meissner oscillator, type 4.

10-6. Electron-Stream Feedback Coupling

A problem common to all the oscillator circuits thus far described is the change of frequency which tends to accompany a change in load impedance. Such frequency changes may be prevented or reduced by the proper circuit isolation of the oscillator tuned circuit from the load. One practical means of accomplishing this isolation is to connect a class-A amplifier, called a buffer amplifier, as the oscillator load, and to drive a class-C power amplifier from the output of the buffer amplifier which takes negligible grid current at its input terminals and thus provides a constant high-impedance load for the oscillator.

It should be kept in mind that oscillators, unless provided with external amplitude-limiting circuits, operate class C. Another means of accomplishing isolation of oscillator tuned circuit from load is provided in a single tetrode or pentode tube by using cathode, control grid, and screen as a triode oscillator and coupling in the load circuit as a class-C amplifier through the plate. The circuit is drawn in Fig. 10-14 as a Hartley circuit, but the method may be applied to any of the circuits that have been described. The screen acts as the anode in the triode oscillator section, but sufficient current passes through the screen to the anode of the pentode to provide the voltage and power output of the

load, just as described in Chapter 9 for the class-C amplifier. Since power coupling to the load is through the electron stream, the circuit is said to be "electron-coupled." It is an effective means of improving frequency stability.

It is experimentally observed that a small increase in screen voltage of the electron-coupled oscillator results in a small increase in frequency, but that a small increase in plate voltage causes a small decrease in frequency. These separate effects may be utilized to nullify each other by supplying the screen voltage at an experimentally adjusted tap on a potentiometer, as shown in Fig. 10-14.

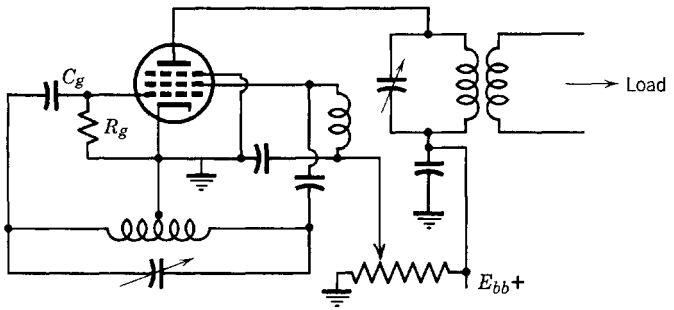

FIG. 10-14. Electron-coupled Hartley oscillator circuit.

10-7. Control of the Stability of the Output Frequency

The effect of load variations in causing changes in output frequency has been mentioned in Section 10-6, where isolation of the load by use of a class-A buffer amplifier stage or by use of the electron-coupled load has been suggested as a possible solution. The effect of load on frequency is often referred to as frequency pulling. In low-power circuits, the effect may be minimized by inserting sufficient attenuation or resistance between oscillator and load.

Oscillation frequency changes, however, result from a number of other causes. These include mechanical and thermal effects such as vibration, shock, and changes in temperature which affect frequency-critical physical properties such as dimensions and resistivity, resulting in changes of L, M, C, and R of the external network. They also include voltage variations which affect the magnitudes of plate and grid resistances, r_p and r_g, and the transconductance, g_m. These also vary with the amplitude of oscillation. Adequately regulated power supplies are essential for maintaining constant frequency of an oscillator but are not sufficient. Although tube amplification factor μ varies very little with E_{bb}, its variation may not be neglected where extreme frequency stability is necessary. Effects of plate resistance variation upon frequency

may be minimized by adding a high resistance to the plate circuit so that the percentage variation due to changes in r_p will be small. This is known as resistance stabilization.

Llewellyn [3] in 1931 analyzed the problem and obtained an interesting and useful practical solution by mathematical analysis. A brief account of this analysis and an example of its useful results should be of interest at this point. Principles rather than details are important and will be stressed. The analytical method depends upon the fundamental principle, already used in the foregoing, that, if an energy-storing circuit

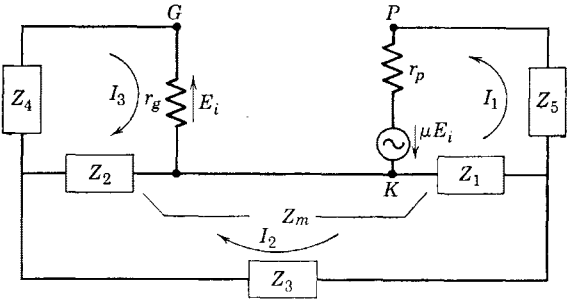

FIG. 10-15. Generalized feedback-oscillator equivalent circuit, with stabilizing impedances Z_4 and Z_5.

oscillates, or is in steady oscillation, no external exciting alternating voltage source is needed. To present this principle quantitatively, Llewellyn assumed a circuit of R, L, and C in series with a vacuum tube and an a-c source of sinusoidal excitation of rms voltage E. Although the vacuum-tube circuit is nonlinear, the alternating voltage at steady state across the tube may be expressed rigorously in terms of a Fourier series and represented at one frequency as $I(r + jX)$ in Kirchhoff's mesh equation for the tube circuit, Eq. 10-35, where I is the rms mesh current. Thus,

$$E = (R + j\omega L + 1/j\omega C + r + jX)I \tag{10-35}$$

From Eq. 10-35, if steady oscillations exist, then $E = 0$, but $I \neq 0$, so that the conditions for oscillation are:

$$R + r = 0 \tag{10-36}$$

and

$$\omega L - 1/\omega C + X = 0 \tag{10-37}$$

Now a number of the feedback oscillator circuits that have been discussed, including the Hartley, Colpitts, and Meissner circuits, may be represented by the same generalized equivalent circuit (Fig. 10-15). Impedances Z_4 and Z_5 have been inserted for the purpose of securing

[3] F. B. Llewellyn, Constant Frequency Oscillators, *Proc. IRE*, **19**, 2063 (1931).

the independence of frequency and applied voltage which is the desired end result of the analysis. The problem then is to determine the conditions imposed upon Z_4 and Z_5. Since $E_i = I_3 r_g$, the mesh equation for the plate mesh is

$$\mu I_3 r_g = I_1(Z_1 + Z_5 + r_p) + I_2(Z_1 + Z_m) - I_3 Z_m$$

or
$$0 = I_1(Z_1 + Z_5 + r_p) + I_2(Z_1 + Z_m) - I_3(\mu r_g + Z_m) \quad (10\text{-}38)$$

and for the other meshes

$$0 = I_1(Z_1 + Z_m) + I_2(Z_1 + Z_2 + Z_3 + 2Z_m) - I_3(Z_2 + Z_m) \quad (10\text{-}39)$$

$$0 = -I_1 Z_m - I_2(Z_2 + Z_m) + I_3(r_g + Z_2 + Z_4) \quad (10\text{-}40)$$

This set of three equations is in homogeneous form; that is, the variables with their coefficients are arranged on one side, but only zeros occur on the other side of each equation. In this form, a solution [4] exists provided that the determinant of the system is zero. If a solution exists, currents I_1, I_2, and I_3 of fixed frequency exist, and, since there is no external excitation, the system is behaving as an oscillator. Therefore, the condition for oscillation is that

$$\begin{vmatrix} Z_{11} & Z_{12} & Z_{13} \\ Z_{21} & Z_{22} & Z_{23} \\ Z_{31} & Z_{32} & Z_{33} \end{vmatrix} = 0 \quad (10\text{-}41a)$$

where

$$\left.\begin{aligned} Z_{11} &= Z_1 + Z_5 + r_p \\ Z_{12} &= Z_1 + Z_m = Z_{21} \\ Z_{13} &= -(\mu r_g + Z_m) \\ Z_{22} &= Z_1 + Z_2 + Z_3 + 2Z_m \\ Z_{23} &= -(Z_2 + Z_m) = Z_{32} \\ Z_{33} &= r_g + Z_2 + Z_4 \\ Z_{31} &= -Z_m \neq Z_{13} \end{aligned}\right\} \quad (10\text{-}42)$$

From Eq. 10-41a, and with two terms combined by factoring, one may obtain the condition for oscillation in the form

$$Z_{11}Z_{22}Z_{33} + Z_{12}Z_{23}(Z_{31} + Z_{13}) - Z_{12}^2 Z_{33} - Z_{23}^2 Z_{11} - Z_{13}Z_{31}Z_{22} = 0 \quad (10\text{-}41b)$$

which is merely the expansion of the determinant of Eq. 10-41a. If now

[4] See E. A. Guillemin, *The Mathematics of Circuit Analysis*, pp. 16–17, John Wiley & Sons.

it is assumed that circuits external to the tube have negligible losses, the impedances Z_1, Z_2, Z_3, Z_4, Z_5, and Z_m become pure reactances. Substitutions into Eq. 10-41*b* from Eq. 10-42 then provide the relation, with $X_{22} = X_1 + X_2 + X_3 + 2X_m$,

$$[r_p + j(X_1 + X_5)](jX_{22})[r_g + j(X_2 + X_4)]$$
$$+[j(X_1 + X_m)][-j(X_2 + X_m)][-(\mu r_g + j2X_m)]$$
$$-[j(X_1 + X_m)]^2[r_g + j(X_2 + X_4)] - [-j(X_2 + X_m)]^2[r_p + j(X_1 + X_5)]$$
$$-[-(\mu r_g + jX_m)](-jX_m)(jX_{22}) = 0$$

which reduces to the two equations:

$$-X_{22}[r_p(X_2 + X_4) + r_g(X_1 + X_5)] - (X_1 + X_m)(X_2 + X_m)\mu r_g$$
$$+(X_1 + X_m)^2 r_g + (X_2 + X_m)^2 r_p + X_{22}X_m\mu r_g = 0 \qquad (10\text{-}43)$$

$$X_{22}[r_p r_g - (X_1 + X_5)(X_2 + X_4) + X_m{}^2] - 2X_m(X_1 + X_m)(X_2 + X_m)$$
$$+(X_1 + X_m)^2(X_2 + X_4) + (X_2 + X_m)^2(X_1 + X_5) = 0 \qquad (10\text{-}44)$$

The second of these equations, 10-44, may be written as

$$X_{22} = \frac{\left\{\begin{array}{l} 2X_m(X_1 + X_m)(X_2 + X_m) - (X_1 + X_m)^2(X_2 + X_4) \\ \quad - (X_2 + X_m)^2(X_1 + X_5) \end{array}\right\}}{r_p r_g - (X_1 + X_5)(X_2 + X_4)} \qquad (10\text{-}45)$$

from which it may be seen that, if X_4 and X_5 have the proper values at the frequency of oscillation, which is the frequency at which the second mesh has zero reactance, then this reactance X_{22} will be zero at the resonant frequency whatever the values of r_p and r_g. The numerator of Eq. 10-45 is zero for values of X_4 and X_5 for which

$$2X_m(X_1 + X_m)(X_2 + X_m) = (X_1 + X_m)^2(X_2 + X_4)$$
$$+ (X_2 + X_m{}^2)(X_1 + X_5) \qquad (10\text{-}46)$$

It has been shown by Llewellyn that the requirement for frequency stabilization stated in Eq. 10-46 leads to physically realizable or possible values of r_p, r_g, and μ necessary to sustain oscillations. Also, stabilization is achieved with reasonable values of X_4 and X_5. It may also be

concluded from Eq. 10-46 that stabilization may be achieved by the use of only one reactance, either X_4 or X_5 but not both. Thus, if plate impedance stabilization alone is used, $X_4 = 0$, and

$$X_5 = \frac{2X_m(X_1 + X_m)}{(X_2 + X_m)} - \left(\frac{X_1 + X_m}{X_2 + X_m}\right)^2 X_2 - X_1 \qquad (10\text{-}47)$$

A similar relation may be obtained for X_4, grid stabilization, with $X_5 = 0$.

The Hartley circuit may now be chosen as a specific example. Reference to the circuit of Fig. 10-10 shows that $X_m = \omega_0 M$, $X_1 = \omega_0 L_3$, and $X_2 = \omega_0 L_2$. Then Eq. 10-47 becomes

$$X_5 = \frac{2\omega_0 M(L_3 + M)}{(L_2 + M)} - \omega_0 L_2 \left(\frac{L_3 + M}{L_2 + M}\right)^2 - \omega_0 L_3 \qquad (10\text{-}48)$$

which turns out to be a negative quantity. If a capacitive reactance is required, then

$$X_5 = -1/\omega_0 C_5$$

and

$$C_5 = \frac{1}{\omega_0^2 \left[L_3 + L_2\left(\frac{L_3 + M}{L_2 + M}\right)^2 - 2M\left(\frac{L_3 + M}{L_2 + M}\right)\right]}$$

But ω_0 is the resonant frequency for which

$$X_{22} = X_1 + X_2 + X_3 + 2X_m$$

$$= \omega_0 L_3 + \omega_0 L_2 - 1/\omega_0 C_3 + 2\omega_0 M = 0$$

whence

$$\omega_0^2 = 1/C_3(L_3 + L_2 + 2M) \qquad (10\text{-}49)$$

Finally, then, the necessary capacitance for plate stabilization is

$$C_5 = \frac{C_3(L_3 + L_2 + 2M)}{L_3 + L_2\left(\frac{L_3 + M}{L_2 + M}\right)^2 - 2M\left(\frac{L_3 + M}{L_2 + M}\right)} \qquad (10\text{-}50)$$

Actually, of course, a high-impedance choke in parallel with C_5 is required to by-pass the direct current to the plate. A corresponding expression may be derived for C_4 if grid stabilization alone is used, or stabilizing reactances may be used in both grid and plate leads simultaneously. For tunable oscillators, stabilization would require new values of capacitance at each frequency unless M were zero, and $L_3 = L_2$.

In this case, the value of the stabilizing capacitance would depend upon C_3 only, and tuning could be accomplished by simultaneous variation of L_3 and L_2 with fixed C_3 and C_5. For applications to other circuits and for experimental confirmation of the theory, reference should be made to the original paper by Llewellyn.

The problem of frequency stabilization of an oscillator has many aspects, and there are numerous methods of solution. This section has been concerned primarily with the means of minimizing the effects upon frequency of the changes in voltage-dependent tube parameters. The following section deals briefly with the use of crystals of quartz or tourmaline in the precise control of oscillator frequency.

10-8. The Piezoelectric Crystal-Controlled Oscillator

The important frequency-controlling properties of a properly prepared quartz or tourmaline crystal are dependent upon the piezoelectric effect which, simply stated, consists of the mechanical vibration in thickness, bending, or shear of the crystal in response to an alternating voltage

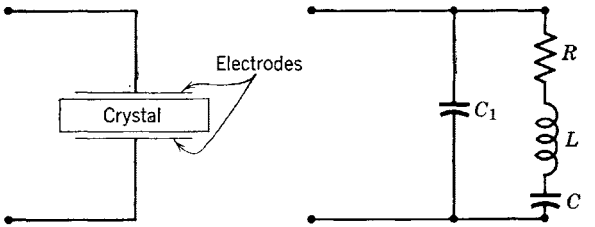

(a) Circuit arrangement *(b)* Equivalent electric circuit

FIG. 10-16. Electrode arrangement and equivalent electric circuit of a piezoelectric crystal.

properly impressed upon the crystal, and of the converse effect of the appearance of an alternating voltage between electrodes containing the crystal if mechanical vibrations are present. Electric energy may be stored in the crystal in the mechanical vibrational form and recovered with small loss of energy. The properly prepared crystal has a natural resonant vibration frequency of the value desired; the Q or energy storage-to-dissipation ratio is higher than may be obtained with ordinary tuned circuits with an order of magnitude of several to many thousands.

The crystal properties are ideal for use as the tuned circuit of an oscillator. A typical crystal designed for a resonant thickness vibration and electrical frequency of 430 kc is rectangular in shape with dimensions 3.33 cm long, 2.75 cm wide, and 0.63 cm thick. If such a crystal is mounted between capacitor plates, as shown in Fig. 10-16*a*, its equivalent

electric circuit [5] is shown by Fig. 10-16*b*. The capacitance C_1 is the capacitance between electrodes with the crystal inserted but not vibrating. The series circuit of R, L, and C represents, respectively, the electrical analogs and counterparts of the frictional losses, the vibrating mass, and the reciprocal elastic constant or compliance of the vibrating crystal. For the 430-kc crystal of dimensions as given, $R \cong 4500$ ohms, $L = 3.3$ henrys, $C = 0.042$ $\mu\mu$f, and $C_1 = 5.8$ $\mu\mu$f. The approximate Q of the crystal is about 2300. The equivalent circuit indicates the presence of two resonant frequencies, but in general the series-resonant frequency of L and C is desired.

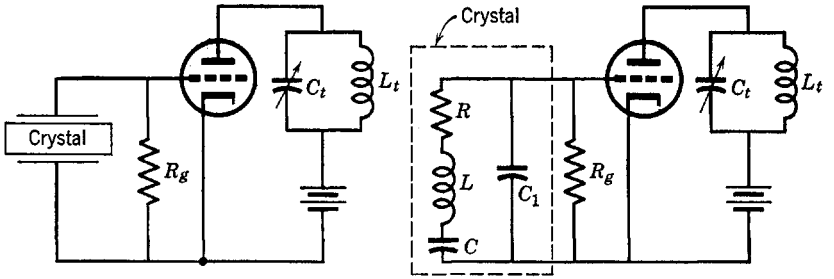

FIG. 10-17. Tuned-grid, tuned-plate crystal-controlled oscillator.

The most commonly used circuit arrangement of a crystal-controlled oscillator is probably the tuned-grid, tuned-plate circuit with the crystal used as the high-Q tuned-grid circuit which determines oscillation frequency. The arrangement and equivalent crystal circuit are shown by Fig. 10-17. Tuning of the plate tank circuit is such that the tank circuit presents an inductive reactance to the tube, and influences the frequency primarily through the input admittance in parallel with the crystal at the grid-cathode input. This effect on frequency, however, is usually so small as to be negligible, and the main effect of plate tuning is to control the amplitude of oscillation at the crystal-resonant frequency. Pentodes are often used in the circuit of Fig. 10-17, and require less grid drive and thus entail smaller crystal currents and heating for a given output than triodes, but may require the addition of a small capacitance grid-to-plate to supply the feedback available through C_{gp} in the triode.

Crystals permit the control of frequency to an accuracy of 1 to 10 cycles per megacycle over a range of frequencies roughly from a few thousand cycles to 10 or 15 Mc per sec. Power output varying from 5 to 15 watts is available from practical, crystal-controlled oscillators.

[5] K. S. Van Dyke, The Piezoelectric Resonator and Its Equivalent Network, *Proc. IRE*, **16**, 742 (1928).

Crystals are prepared by cutting the natural quartz crystalline form in specified directions and at the proper angles with the main crystal axis. The methods of preparation are too involved in technical detail to present much importance with respect to the objectives of this book and so are omitted. An interested reader is referred to the references.[6] A particularly interesting development[7] is the so-called GT-cut crystal which has practically zero temperature coefficient of frequency change in the temperature range 0° to 100° C.

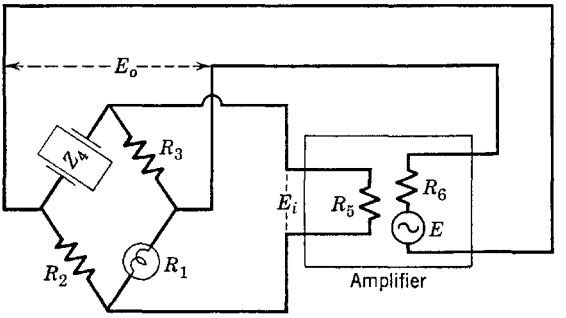

FIG. 10-18. Bridge-stabilized oscillator circuit.

10-9. Other Methods of Frequency Stabilization

The oscillation amplitudes of oscillator circuits which have been discussed in preceding sections have been limited by nonlinearity of tube characteristics. This limitation on amplitude results in harmonic distortion and consequent frequency variation. It would be desirable for an oscillator to operate only over the linear range of tube characteristics, and this is possible if means be provided to limit oscillation amplitude by circuits external to the tube. Two such circuits which permit class-A linear operation of the oscillator tube are of interest here. The first is the bridge-stabilized circuit of Meacham,[8] shown in Fig. 10-18. The output of the amplifier is connected across one diagonal of the bridge, the input across the other. The bridge is in a state of near but not complete balance. Impedance $Z_4 = R_4 + jX_4$ is a crystal operated at series resonance, so that $X_4 = 0$ at the desired frequency. Resistance R_1 is a tungsten-filament lamp of low wattage and of cold resistance such that initial oscillation buildup is permitted, but of gradually in-

[6] R. A. Heising, *Quartz Crystals for Electric Circuits—Their Design and Manufacture*, D. Van Nostrand Co. (1946).

[7] W. P. Mason, Low-Temperature Coefficient Quartz Crystals, *BSTJ*, **19**, 74 (1940).

[8] L. A. Meacham, The Bridge-Stabilized Oscillator, *Proc. IRE*, **26**, 1278 (1938).

creasing resistance as the oscillation amplitude builds up and the temperature of the tungsten filament increases. At the desired amplitude, the bridge is only slightly unbalanced, but is kept in as nearly exact balance as possible. A slight unbalance is necessary in order to supply sufficient feedback voltage E_i to sustain steady oscillation. Accordingly, at the desired operating amplitude and frequency the resistance of R_1 is

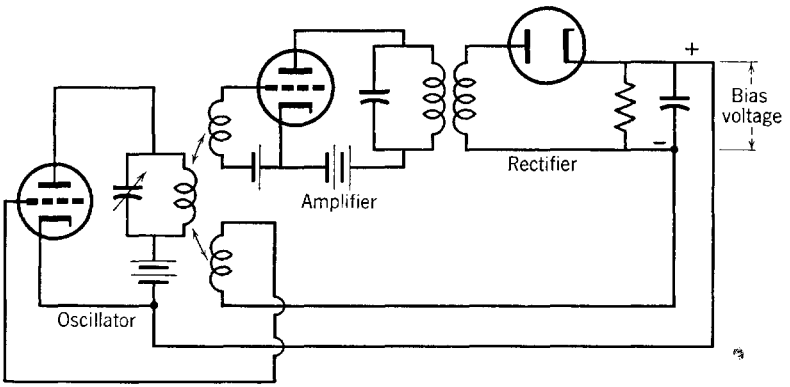

FIG. 10-19. Linear oscillator, with self-controlled bias.

made slightly smaller than the balance requirement R_2R_3/R_4. At this value of R_1 the attenuation through the bridge, which is

$$\beta = E_i/E_o \tag{10-51}$$

is just equal to the gain of the amplifier,

$$A = E_o/E_i \tag{10-52}$$

so that the oscillation criterion $A\beta = 1$ is met. Under these conditions, the amplifier operates on a strictly class-A basis with no frequency variations—over short intervals—of more than 2 parts in 10^8.

Another amplitude-limiting circuit permitting class-A operation is shown in Fig. 10-19. The circuit will be recognized as a tuned plate oscillator, with the grid feedback coil connected in series with a bias voltage of magnitude depending on the magnitude of the oscillation amplitude. The rectifier supplying bias is fed by an amplifier for which the input is proportional to the oscillator output voltage. If the oscillation amplitude increases, so does the negative grid bias. An equilibrium is reached at an amplitude for which the values of g_m and r_p as determined by the bias are such as to sustain oscillations, according to the Barkhausen criterion (Eq. 10-24).

10-10. Resistance-Capacitance Tuned Oscillators

An oscillator designed primarily for laboratory use and using an R–C-coupled, two-stage amplifier with positive feedback and no tank

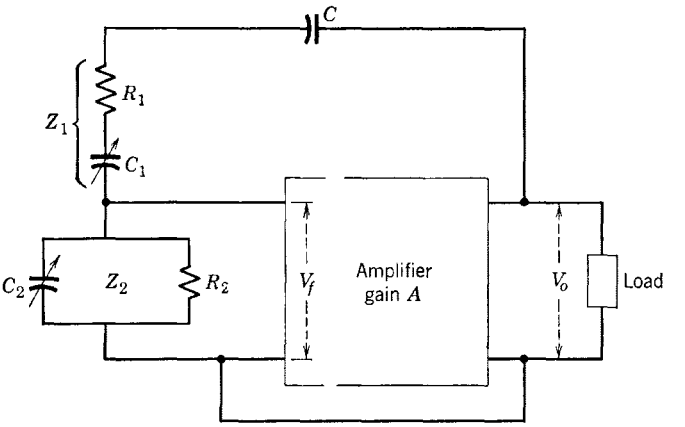

FIG. 10-20. R–C tuned amplifier.

circuit of L and C is shown schematically in Fig. 10-20. The feedback network consists of impedances

$$Z_1 = R_1 + 1/j\omega C_1 \tag{10-53}$$

and

$$Z_2 = \frac{R_2(1/j\omega C_2)}{R_2 + 1/j\omega C_2} \tag{10-54}$$

The capacitance C has negligible reactance at the oscillation frequency and is intended merely as a d-c blocking capacitor. The feedback fraction β is given by

$$\beta = Z_2/(Z_1 + Z_2) = V_f/V_o \tag{10-55}$$

Application of the requirement for oscillation,

$$A\beta = 1 = AZ_2/(Z_1 + Z_2) \tag{10-56}$$

leads to two necessary conditions to meet the magnitude and phase requirements for sustained oscillation. These are:

$$\omega^2 = 1/R_1R_2C_1C_2 \tag{10-57}$$

which specifies the frequency at which the feedback network provides the proper phase—the frequency of oscillation—and

$$A = C_2/C_1 + R_1/R_2 + 1 \tag{10-58}$$

which specifies the amplifier gain required for oscillation in terms of the constants of the feedback network. A simplified case is that for which $R_1 = R_2 = R$ and $C_1 = C_2 = C$. In this case,

$$\omega = 1/RC \tag{10-59}$$

and

$$A = 3 \tag{10-60}$$

In practice, the R–C tuned oscillator takes the form shown in Fig. 10-21. It has been shown [9] that, if $R_1C_1 = R_2C_2$, the curve of the voltage

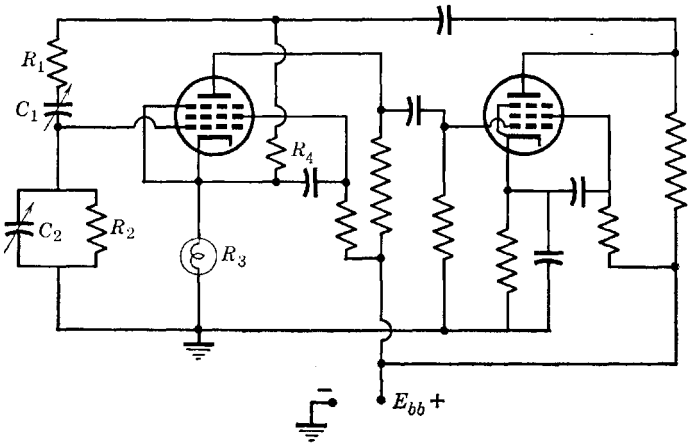

FIG. 10-21. Practical form of the R–C tuned oscillator.

ratio V_o/V_f has a maximum at the angular frequency given by Eq. 10-57 and is similar to a resonance curve. Negative feedback has also been included in R_3 and R_4. Resistance R_3 is a small incandescent lamp providing a temperature-sensitive variable resistance. An increased oscillation amplitude is accompanied by increasing current and higher resistance in R_3 and consequently of increased negative feedback, reduced gain, and reduced input. Thus, the oscillation amplitude is stabilized at values determined by the proper proportions of R_4 and R_3.

An important property of this oscillator is its wide tuning range. For the conditions applying to Eq. 10-59, the frequency is inversely proportional to C and not to the square root of C as is true of the L–C tuned oscillator. Therefore, tuning over a 10-to-1 frequency range is easily possible, and a change in frequency band with another 10-to-1 range is possible by tapping resistances R_1 and R_2. Ganged condenser and resistor control settings permit easy frequency and band selection.

[9] F. E. Terman, R. R. Buss, W. R. Hewlett, and F. C. Cahill, *Proc. IRE*, **27**, 649 (1939).

10-11. The Multivibrator

The multivibrator is an R–C-coupled amplifier feeding its own input. Although its circuit is similar to that of the R–C tuned oscillator of Section 10-10, its behavior and applications are very different. It belongs more properly to a class of electron-device circuits described as timing, triggering, pulse-forming, or wave-shaping circuits. It does oscillate, however, in the sense that it shifts quickly from one point of operation to another along a current-voltage characteristic which has a negative-resistance region. It can be analyzed in terms of this negative-

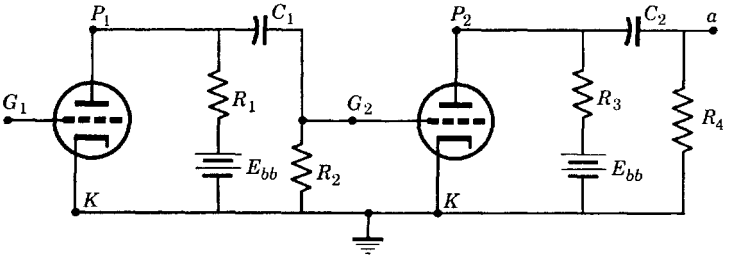

FIG. 10-22. An amplifier circuit which becomes a multivibrator if a is connected to G_1.

resistance characteristic or by considering the circuit as a regenerative-feedback amplifier. The latter approach is considered briefly in the following paragraphs.

The two-stage, R–C-coupled amplifier circuit of Fig. 10-22 will oscillate if terminal a is connected to grid G_1. No biasing sources are needed. A single plate-voltage source may be used, and the circuit diagram is usually arranged as shown in Fig. 10-23, known as a plate-coupled

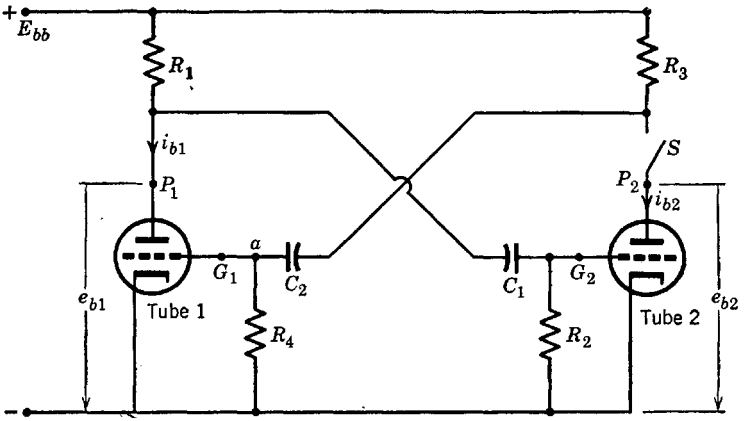

FIG. 10-23. Typical multivibrator circuit obtained from Fig. 10-22 with a connected to G_1 and with only one plate-voltage source.

circuit. The coupling capacitors are connected from the grid of one tube to the plate of the other, as shown.

A switch S has been included in the plate circuit of tube 2 (Fig. 10-23) in order to provide a starting point for a discussion of the behavior of the multivibrator. Tube 1 will conduct heavily if plate voltage is applied, since the bias of tube 1 is zero. The capacitors C_1 and C_2 both charge, C_1 reaching the potential e_{b1} of the plate of tube 1 and C_2 reaching the potential E_{bb} of the source. The voltage e_{b1} may be found from a load line determined by the voltage E_{bb} and the resistor R_1. With C_1 fully charged, the current in R_2 is zero, and the bias voltage of the grid of tube 2 is zero. Thus, if switch S is closed, tube 2 will immediately conduct. The voltage e_{b2} will drop from its previous value of E_{bb} because of the voltage drop in R_3 and will quickly approach an equilibrium value determined by R_3 and E_{bb} and analogous to the value e_{b1} reached by tube 1. The conduction of tube 2 provides a discharge path for C_2 through tube 2 and provides a negative voltage e_{c1} at G_1 which reduces the plate current of tube 1. Since the voltage across C_2, initially E_{bb}, cannot change suddenly, the bias voltage e_{c1} on tube 1 at the instant after S closes is

$$e_{c1} = -(E_{bb} - e_{b2}) \tag{10-61}$$

This is sufficient to bias tube 1 well below cutoff. Since i_{b1} is reduced to zero, e_{b1} rises to the supply voltage E_{bb}. The increased charging current through C_1 and R_2 biases tube 2 positively; i_{b2} is further increased and R_2 is shunted by a grid resistance R_{g2} resulting from grid conduction current. The grid resistance R_{g2} is small compared with R_2, and thus C_1 charges quickly, reducing the bias on tube 2 to zero.

The zero-bias conduction of tube 2, however, is not the end result but a condition persisting for a relatively long time period during which the voltage across C_2, which was responsible for the bias of tube 1 to cutoff, decreases as the charge on C_2 leaks off. The leakage path is through R_4 in series with $(R_3 r_{p2})/(R_3 + r_{p2})$, where r_{p2} is the plate resistance of tube 2. Let the leakage path resistance for C_2 be R_a; then,

$$R_a = R_4 + R_3 r_{p2}/(R_3 + r_{p2}) \cong R_4 \tag{10-62}$$

where $$R_4 \gg R_3 r_{p2}/(R_3 + r_{p2})$$

Then the voltage e_{c1} is given by

$$e_{c1} = -(E_{bb} - e_{b2})\epsilon^{-t/R_a C_2} \tag{10-63}$$

which shows that the bias on tube 1 ultimately is reduced to a value such

that tube 1 conducts again. But, as tube 1 conducts, the voltage e_{c2} of G_2 drops to a negative value

$$e_{c2} = -(E_{bb} - e_{b1}) \tag{10-64}$$

which biases tube 2 to cutoff. In addition, e_{b2} rises to E_{bb}, producing a suddenly increased positive bias on G_1 so that tube 1 conducts heavily. Tube 2 remains cutoff until the charge on C_1 is reduced sufficiently that the grid voltage

$$e_{c2} = -(E_{bb} - e_{b1})\epsilon^{-t/C_1R_b} \tag{10-65}$$

rises to the conduction value of tube 2. Here

$$R_b = R_2 + R_1r_{p1}/(R_1 + r_{p1}) \cong R_2$$

Thus, the operation is repeated. For the symmetrical multivibrator, the two halves of the circuit are identical, with $R_1 = R_3$, $R_2 = R_4$, and $C_1 = C_2$. The tubes are also identical so far as possible. Such a circuit is known as a free-running plate-coupled multivibrator.

10-12. Wave Forms of the Free-Running Multivibrator

The wave forms of the plate voltages and of the grid voltages of the tubes of a multivibrator are of particular interest. An attempt has been made in the following paragraphs to develop these wave forms in a step-by-step procedure. A specific circuit (Fig. 10-24) has been chosen for this purpose. It is assumed, initially, that tube 2 is not conducting and that its grid voltage is below cutoff but rising toward cutoff. The

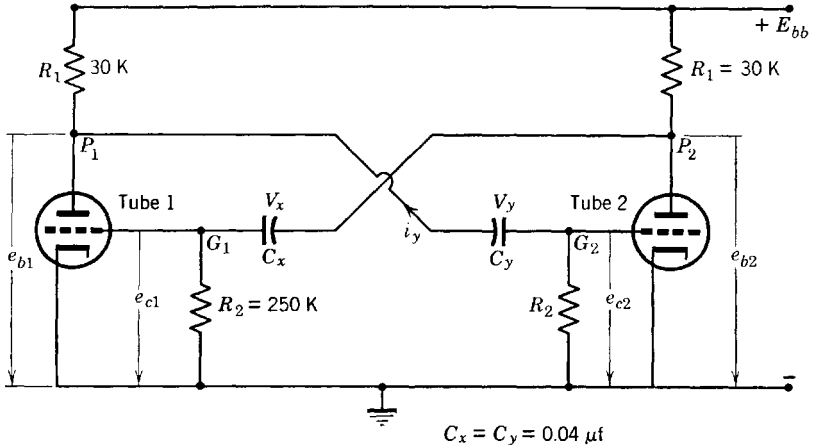

FIG. 10-24. Free-running, symmetrical multivibrator.

tubes are identical and have plate characteristics as shown by Fig. 10-25, on which the load line corresponding to $R_1 = 30{,}000$ ohms has been drawn. The intersection of the load line and the $e_c = 0$ characteristic shows that the plate voltage of either tube when conducting with zero bias is $e_{b1} = e_{b2} \cong 82$ volts.

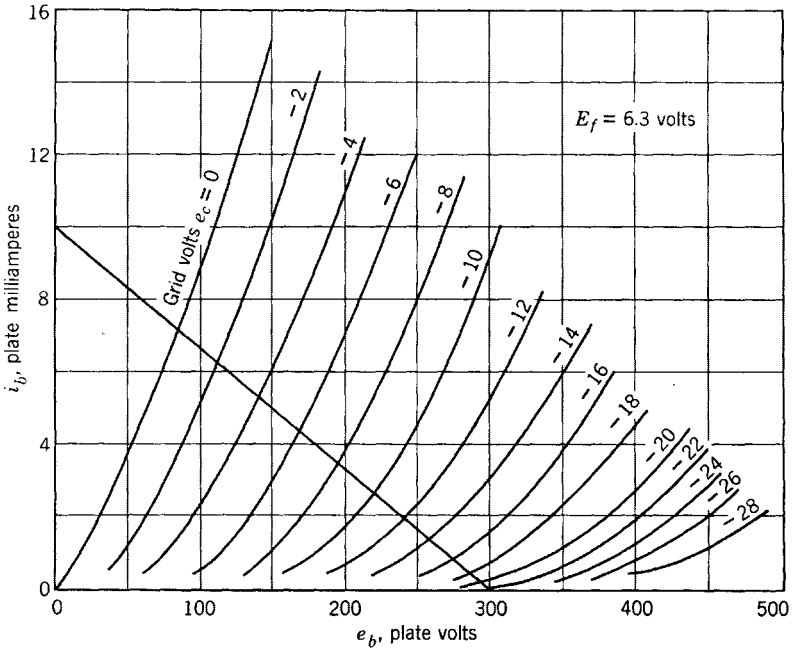

FIG. 10-25. Plate characteristics for the triodes of Fig. 10-24.

Capacitor C_y was responsible for the cutoff of tube 2 because, when tube 1 began to conduct, C_y was fully charged to $V_y = 300$ volts, and the conduction of tube 1 provided a discharge path for current i_y to flow through R_2 toward G_2. The discharge circuit is shown by Fig. 10-26. The voltage drops around the discharge path through the tube are given by

$$i_y R_2 - V_y + e_{b1} = 0 \tag{10-66}$$

Just before tube 1 began to conduct, i_y was zero and $V_y = 300$ volts. At conduction of tube 1, e_{b1} falls to 82 volts, but V_y cannot change instantly. Therefore, the initial value of i_y is given by

$$i_y = \frac{V_y - e_{b1}}{R_2 + r_p R_1/(r_p + R_1)} \cong \frac{V_y - e_{b1}}{R_2} \tag{10-67}$$

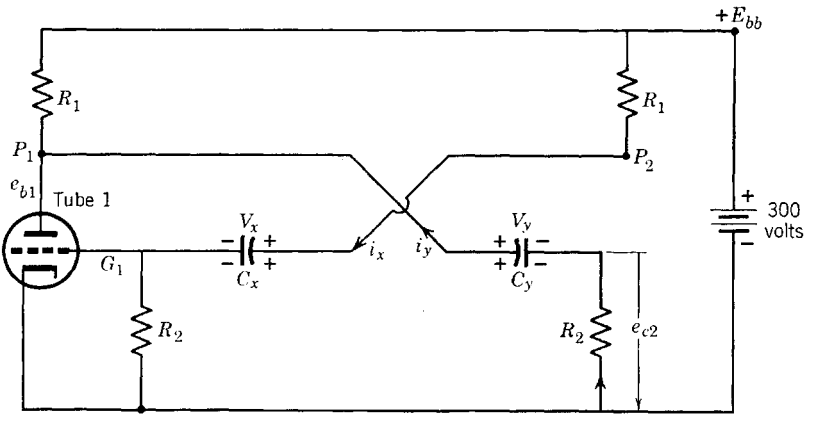

FIG. 10-26. Discharge of C_y and charge of C_x.

Thus, the initial negative bias on tube 2 was

$$e_{c2} = -i_y R_2 \cong -(V_y - e_{b1}) \tag{10-68}$$

For the circuit of Fig. 10-24, this bias is

$$e_{c2} = -(300 - 82) = -218 \text{ volts}$$

Then the equation for the instantaneous bias on tube 2 is, according to Eq. 10-65,

$$e_{c2} \cong -218\epsilon^{-t/R_2C_y}$$

$$= -218\epsilon^{-1000t} \tag{10-69}$$

where time t is measured from the beginning of conduction of tube 1. The grid-voltage wave form for tube 2 is shown in Fig. 10-27 along with the other wave forms of interest. Attention should be focused first over the time interval 0 to t_1 during which tube 2 does not conduct. During this interval the voltage e_{b2} is constant at 300 volts, e_{c1} is constant at zero, and e_{b1} is constant at 82 volts.

During the interval $0 < t < t_1$ the capacitor C_x (Fig. 10-26) had charged to a potential of $V_x = E_{bb} = 300$ volts. The charging current i_x had the direction shown so that e_{c1} had actually become positive for a short interval at the beginning of conduction of tube 1. The grid resistance shunting R_2 when e_{c1} is positive may be of the order of 500 to 1000 ohms. At $t = 0$, the voltage equation around the circuit through C_x (Fig. 10-26) is

$$E_{bb} = [R_1 + R_2R_g/(R_2 + R_g)]i_x + V_x \cong R_1 i_x + V_x \tag{10-70}$$

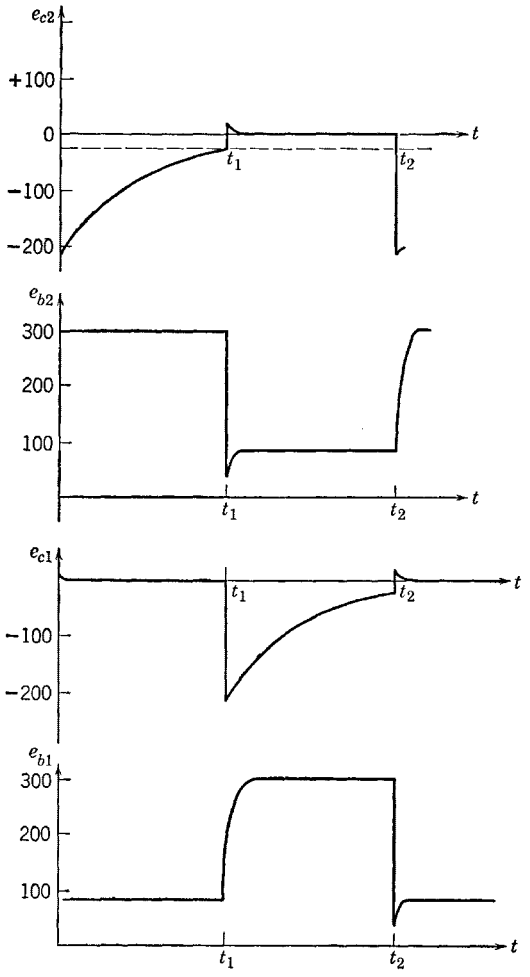

FIG. 10-27. Voltage wave forms for the multivibrator of Fig. 10-24.

Also, at $t = 0$, tube 1 had just begun to conduct so that the voltage of G_1 with respect to ground was the cutoff voltage (Fig. 10-25)

$$e_{c1} = -E_{c0} \cong -22 \text{ volts}$$

Since the voltage at P_2 just before tube 2 ceased to conduct had been

$$e_{b2} = 82 \text{ volts}$$

then the value of V_x at $t = 0$ was

$$V_x = 82 + 22 = 104 \text{ volts}$$

The initial value of the current i_x, as given by Eq. 10-70, is then, approximately,

$$i_x \cong (E_{bb} - V_x)/R_1 = (300 - 104)/30{,}000 \text{ amp} = 6.53 \text{ ma}$$

The positive bias resulting is then

$$e_{c1} = i_x \left(\frac{R_g R_2}{R_g + R_2} \right) \cong i_x R_g$$

For $R_g = 1000$ ohms, $e_{c1} = 6.53$ volts. This short-duration positive bias is shown at the beginning of the interval $0 < t < t_1$ of Fig. 10-27.

At time t_1 (Fig. 10-27) e_{c2} reaches the cutoff voltage $E_{c0} \cong -22$ volts. At this instant tube 2 begins to conduct, and the series of events already described for tube 1 now applies to tube 2. The discharge of C_x biases tube 1 to $e_{c1} = -218$ volts and reduces i_{b1} to zero; e_{b1} rises toward $E_{bb} = 300$ volts, and thus capacitor C_y charges so that e_{c2} becomes suddenly positive. Plate voltage e_{b2} is reduced to a value below 82 volts during the interval of positive grid voltage e_{c2}, but returns quickly to the stable value of 82 volts as e_{c2} reaches zero. Grid voltage e_{c1} rises exponentially until, at t_2, tube 1 conducts again, and the cycle is repeated.

The frequency of oscillation may be obtained approximately from Eq. 10-63, or, for the specific circuit discussed, from Eq. 10-69. The period of oscillation is

$$T = t_1 + t_2 \cong 2t_1$$

From Fig. 10-27 and Eq. 10-69,

$$\epsilon^{1000T/2} = 218/22 = 9.9$$

$$T = \ln 9.9/500$$

and

$$f = 500/2.29 = 218 \text{ cps}$$

PROBLEMS

10-1. Draw the linear equivalent circuit of a Hartley oscillator. Write the equations for currents and voltages as in Section 10-4, and draw the vector diagram. Is the frequency of oscillation greater or less than the resonant frequency of the tuned circuit?

10-2. Repeat problem 10-1 for the Colpitts circuit.

10-3. A tuned-plate oscillator uses a type-800 triode and is operated at 1.59 Mc with:

$$E_b = 750 \text{ volts}$$
$$E_c = -100 \text{ volts}$$
$$E_{gm} = 225 \text{ volts}$$
$$I_b = 70 \text{ ma}$$
$$I_c = 15 \text{ ma}$$

If $e_{b\,\min} = e_{c\,\max}$, and the tank circuit loaded Q is 15, tuning capacitance = 200 $\mu\mu$f, compute (*a*) the power output and efficiency, (*b*) the constants of the tank circuit. Use the class-C amplifier analysis of Chapter 9.

10-4. The tube of problem 10-3 is operated in a Hartley circuit. Again compute the power output, circuit constants of tank circuit (C = 200 $\mu\mu$f, Q_e = 15), and oscillator efficiency.

10-5. An oscillator operating under class-A conditions uses a triode with r_p = 8500 ohms, μ = 16 in a Colpitts circuit for which the inductance is 20 microhenrys and the capacitors are each 500 $\mu\mu$f. Determine the conditions required for oscillation and the oscillation frequency if the coil Q is 20.

10-6. Obtain a relation similar to Eq. 10-47 for the value of X_4 necessary for grid stabilization of an oscillator, with $X_5 = 0$.

10-7. Apply the relation obtained in problem 10-6 to the Colpitts oscillator, and obtain relations analogous to Eqs. 10-49 and 10-50.

10-8. Compute the grid-stabilizing element necessary for the oscillator of problem 10-5.

10-9. Design a resistance-capacitance tuned oscillator to operate in the audio-frequency range at 796 cps, and compute the expected output voltage. Work out a tuning arrangement to tune over the audio range.

10-10. Sketch wave forms for the voltages V_x and V_y and for the currents i_x and i_y of the multivibrator (Fig. 10-24).

10-11. Compute capacitances for a symmetrical, free-running multivibrator using type-6J5 tubes and designed to operate at 5000 cps if, in Fig. 10-24, $R_1 = 20K$, $R_2 = 400K$, and E_{bb} = 300 volts.

CHAPTER 11

MODULATION AND DEMODULATION

AN ELECTRON-TUBE-CIRCUIT FUNCTION, SUCH AS THAT OF THE AMPLIfier, rectifier, control device, or oscillator, has been introduced in previous chapters in connection with discussion or analysis of the tube as a circuit element. It becomes increasingly important with increasing knowledge of components for the student of electron tubes to understand the requirements imposed upon the tube as a circuit component by the system in which the tube is a vital part. Component development proceeds in a direction determined by system requirements. Communication system requirements involve tubes as modulators or demodulators (detectors). It will not be assumed that the terms modulation and demodulation are as familiar as, for example, are the terms amplification or rectification. It therefore becomes necessary, (1) to examine briefly the needs of a communication system which necessitate the processes known as modulation and detection, (2) to define the terms necessary in describing the processes of modulation and detection, and (3) to discuss briefly the circuit theory of the electron tubes involved in these processes.

Communication systems differ tremendously in complexity but they all exist for the same fundamental system function—the transmission of intelligence or information from one space location to another. Primitive man used modulation in the process of communicating by smoke signals. The amount of information that can be conveyed by a single, continuous column of smoke is very small compared to the possibilities available in the use of discrete puffs of smoke released at intervals according to a prearranged code.

Electric communication systems operate by virtue of the transmission of energy in wave form through space, either guided by conductors as in telephone or telegraph communication, or as radiated from antennas in radio and television broadcasting. The first question to be answered is: What is a wave? The Institute of Radio Engineers, Standards on Radio Propagation, 1948, provide the following definition: A wave is "a physical activity in a medium such that at any point in the medium

some of the associated quantities vary with time, while at any instant of time, they vary with position." In the case of a radio wave propagated through space, the associated quantities which vary with both time and distance are the electric and magnetic field intensities. The electric field intensity is measured in volts per meter at any given point. At such a point, a voltage is induced in a receiving antenna, and, if the voltage is sinusoidal and of peak value V_m, it may be represented by the equation

$$v = V_m \cos \omega t \tag{11-1}$$

which is not the equation of a wave but rather of the voltage at the antenna terminals which are fixed in space with respect to the earth. The equation of an unattenuated voltage wave traveling on a transmission line may take the form

$$v = V_m \cos (\omega t - \beta x) \tag{11-2}$$

At any fixed value of x, the voltage varies sinusoidally with time, while, at any instant, it also varies sinusoidally with distance from the origin x. Equation 11-1 is frequently referred to as the equation of a wave in discussions of modulation. It is a cosine wave and has sinusoidal wave form but is not a wave in the sense of the IRE definition. However, in defining modulation, it is desirable to consider only the wave forms of voltage and current at circuit terminals adjacent to the transmitting medium in order to avoid the additional complications of waves traveling in guided paths along wires or in space.

11-1. The Reasons for, and Nature of, Modulation

Just as a single smoke column may convey a minimum of information of the yes or no variety, so a single-frequency tone or note conveys very little information. Either it is there or it is not there; it may convey an answer, yes or no, but little else. It is possible to determine its frequency, or measure its amplitude, or to compare its phase with respect to a reference. However, amplitude, phase, and even frequency may be altered by the transmitting medium, so that the reliable information content of a single-frequency voltage or current is very small. If the single-frequency tone is intermittent so as to represent a code of dots and dashes separated by intervals of silence, the amount of information that can be transmitted is enormously increased. This process may be regarded as an elementary form of modulation and results in increasing the possible information content of a signal, one of the important reasons for modulation.

The simple example of modulation by interrupting a single-frequency tone has other implications which are of interest. According to the Fourier theorem, any transient voltage or current can be expressed as

a continuous band or spectrum of frequencies. In order for a single frequency to exist, it must always have been in existence, at constant amplitude. The use of a telegraph key in modulating a 1000-cps tone results in the introduction of a bandwidth requirement upon the transmitting equipment. A relation between information content and bandwidth of a signal was suggested in 1928 by Hartley in the following form: The amount of information that can be transmitted by a communication system is proportional to the product of the bandwidth of the system and the time available for transmission. Although qualitative, this principle is a useful concept and has proved to be the first step in a quantitative theory of information or of communication presently in a rapid process of development.[1]

The process of modulation consists in the alteration, according to a signal or intelligence to be transmitted, of the amplitude, frequency, or phase of a voltage wave which can be transmitted by the transmitting medium. Even if the original voltage wave is sinusoidal, alteration of amplitude, frequency, or phase imposes a bandwidth requirement of a severity depending upon the type of modulation used and the particular system involved. In other words, the bandwidth necessary depends upon the quality requirements on reproduction of the signal. The original, unmodulated voltage, is called the *carrier*. The carrier frequency must be selected so that efficient transmission is possible.

The Standards on Antennas, Modulation Systems, and Transmitters published in 1948 by The Institute of Radio Engineers provide definitions of terms, some of which are included in the following list. In each case, the wave referred to is a time-varying quantity, usually a voltage, at a fixed location, as already explained. Order and numbering have been selected for convenience.

1. *Carrier.* A wave suitable for modulation by a modulating wave. Note. Examples of carriers are a sine wave and a recurring series of pulses.

2. *Modulating wave.* A wave that causes a variation of some characteristic of the carrier.

3. *Modulated wave.* A wave, some characteristic of which varies in accordance with the value of a modulating wave.

4. *Modulation* (of a carrier):

(1) The process by which some characteristic of a carrier is varied in accordance with a modulating wave.

(2) The variation of some characteristic of a carrier.

5. *Modulator.* A device to effect the process of modulation.

[1] C. E. Shannon, A Mathematical Theory of Communication, *BSTJ*, 379 (July), 623 (Oct. 1948).

6. *Amplitude modulation* or AM. Modulation in which the amplitude of a wave is the characteristic subject to variation.

7. *Angle modulation.* Modulation in which the angle of a sine-wave carrier is the characteristic subject to variation. Note. Phase and frequency modulation are particular forms of angle modulation.

8. *Angle or phase of a sine wave.* The measure of the progression of the wave in time or space from a chosen instant or position. Note. In the expression for a sine wave the angle or phase is the value of the entire linear function. Note. In the representation of a sine wave by a rotating vector, the angle or phase is the angle through which the vector has progressed.

9. *Frequency modulation* or FM. Angle modulation in which the instantaneous frequency of a sine-wave carrier is caused to depart from the carrier frequency by an amount proportional to the instantaneous value of the modulating wave.

10. *Instantaneous frequency.* The time rate of change of the angle of a wave which is a function of time. Note. If the angle is measured in radians, the frequency in cycles (per second) is the time rate of change of the angle divided by 2π.

11. *Frequency swing.* In frequency modulation, the peak difference between the maximum and the minimum values of the instantaneous frequency.

12. *Phase modulation* or PM. Angle modulation in which the angle of a sine-wave carrier is caused to depart from the carrier angle by an amount proportional to the instantaneous value of the modulating wave.

13. *Phase deviation.* The peak difference between the instantaneous angle of the modulated wave and the angle of the carrier.

14. *Sidebands.* All the frequencies produced by modulation. Note. In a modulation system with a sine-wave carrier the upper sideband includes those frequencies that are higher than the carrier frequency; the lower sideband includes those frequencies that are lower than the carrier frequency.

15. *Transducer.* A device by means of which energy can flow from one or more transmission systems to one or more other transmission systems. Note. The energy transmitted by these systems may be of any form—for example, it may be electric, mechanical, or acoustical—and it may be of the same form or different forms in the various input and output systems.

16. *Limiter.* A transducer whose output is constant for all inputs above a critical value. Note. A limiter may be used to remove amplitude modulation and transmit angle modulation.

17. *Discriminator.* A device in which amplitude variations are derived in response to frequency variations.

18. *Deviation ratio.* In a frequency-modulation system, the ratio of the maximum frequency deviation to the maximum modulating frequency of the system.

19. *Detection.* The process by which a wave corresponding to the modulating wave is obtained in response to a modulated wave.

20. *Detector.* A device to effect the process of detection.

It is now possible with the aid of the foregoing list of definitions to discuss modulation and its usefulness more completely. Modulation is employed to shift or translate signal frequencies from a frequency range that is very difficult to transmit to another that may be easily transmitted. For example, radiobroadcast transmission of audio frequencies centered around a carrier of 10,000 cycles would require a transmitting antenna of dimensions of the order of 30,000 meters, the wavelength of a 10,000-cycle radio wave. A vertical radiator of one-eighth wavelength would be 3750 meters or about 12,300 feet high! As a further complication to this absurd requirement, only one audio-frequency program could be broadcast at one time because of interference. Modulation, then, not only permits the selection of a carrier frequency suitable for efficient and economical transmission, but, in addition, by frequency translation, a large number of carriers may be transmitted simultaneously, by wire or radio-communication systems; tuned circuits may be used to select a particular carrier, and the signal frequencies then may be recovered from the carrier by the process of detection.

Comments with respect to definitions 3 and 8 may be helpful. In 3, "value of a modulating wave" usually refers to its amplitude. With respect to the first note under definition 8, the angle or phase of a sine wave of voltage in the relation

$$v = V_m \cos (\omega t + \theta)$$

is the quantity

$$\phi(t) = (\omega t + \theta)$$

which is the entire linear function of time.

11-2. Mathematical Formulation of a Modulated Wave

The discussion of this section will be limited to amplitude and angle modulation. Many other systems exist, notably those using pulses, such as pulse-duration, pulse-position, and pulse-time modulation, all of which are defined by the IRE Standards already referred to.

In amplitude and angle modulation, the carrier is usually a sine wave

which may be described as a voltage by the equation

$$v_c = A \cos \phi(t) \tag{11-3}$$

in which A is the instantaneous amplitude of the carrier voltage and $\phi(t)$ is its instantaneous angle or phase. In amplitude modulation A is made dependent upon the signal voltage or modulating wave (definition 2) and becomes a function of time. In angle modulation $\phi(t)$, already a function of time, is made to vary in accordance with the modulating wave. The frequency of the carrier is (definition 10) given by

$$2\pi f_c = (d/dt)\phi(t) \tag{11-4}$$

In general, the modulating wave is not a sinusoid but may be represented in terms of sinusoidal-component frequencies by means of a Fourier series. The equation of any one frequency component of the modulating wave may then have the form of

$$v_m = A_m \cos \omega_m t \tag{11-5}$$

Then, amplitude modulation is obtained if A depends upon the modulating wave as given by

$$A = A_c + k_a v_m = (A_c + k_a A_m \cos \omega_m t) \tag{11-6}$$

where A_c is the amplitude of the unmodulated carrier and k_a is a constant of proportionality. The corresponding AM wave, according to Eqs. 11-3 and 11-6, then may be expressed as

$$v = A_c \left(1 + \frac{k_a A_m}{A_c} \cos \omega_m t\right) \cos \omega_c t \tag{11-7}$$

where $\phi(t) = \omega_c t$

and $\omega_c = 2\pi f_c = d\phi(t)/dt$ is the fixed angular frequency of the carrier.

Angle modulation, as shown by the definitions, may be either phase or frequency modulation, and it is important to distinguish carefully between the two.

Phase modulation requires that $\phi(t)$ depend upon the instantaneous values of the modulating wave. According to definition 12, the carrier angle is caused to depart or deviate from its unmodulated value by an amount proportional to the instantaneous value of the modulating wave. This definition, stated symbolically, then requires that

$$\phi(t) = \omega_c t + k_p A_m \cos \omega_m t \tag{11-8}$$

where k_p is a design constant of proportionality. The expression for the phase-modulated voltage wave then becomes

$$v = A_c \cos (\omega_c t + k_p A_m \cos \omega_m t) \tag{11-9}$$

It should be observed that the instantaneous angular frequency of the phase-modulated wave, which is

$$\omega(t) = d\phi(t)/dt = \omega_c - k_p A_m \omega_m \sin \omega_m t \tag{11-10}$$

has a maximum deviation from the carrier frequency proportional to the modulating frequency. However, the maximum deviation of angle or phase (Eq. 11-8) is independent of the modulating frequency and proportional to the amplitude of the modulating wave.

The definition of frequency modulation (definition 9) requires that

$$(d/dt)\phi(t) = \omega(t) = \omega_c + k_f A_m \cos \omega_m t \tag{11-11}$$

where again k_f is a design constant. The instantaneous angle $\phi(t)$ then may be found from Eq. 11-11 as

$$\phi(t) = \int_0^t (\omega_c + k_f A_m \cos \omega_m t)\, dt = \omega_c t + (k_f A_m/\omega_m) \sin \omega_m t \tag{11-12}$$

where $\phi(0)$ is assumed to be zero. Here it should be observed that, in frequency modulation (1) the maximum frequency deviation is independent of the modulating frequency and (2) the maximum angular deviation is inversely proportional to the modulating frequency. The fundamental differences between phase and frequency modulation are found in the quantities

$$\Delta\phi_p = k_p A_m \tag{11-13}$$

which is the amplitude of the phase deviation in phase modulation, and

$$\Delta\omega_f = k_f A_m \tag{11-14}$$

which is the amplitude of the angular-frequency deviation in frequency modulation. These quantities are each independent of the modulating frequencies and proportional to the amplitude of the modulating wave. Also, the amplitude of the angular-frequency deviation in phase modulation is

$$\Delta\omega_p = k_p A_m \omega_m \tag{11-15}$$

which is proportional to modulating frequency, whereas the amplitude of the phase deviation in frequency modulation,

$$\Delta\phi_f = k_f A_m/\omega_m \tag{11-16}$$

is inversely proportional to modulating frequency. The equation of the FM voltage wave is, using Eqs. 11-3 and 11-12,

$$v = A_c \cos (\omega_c t + k_f A_m/\omega_m \sin \omega_m t) \tag{11-17}$$

A discussion of amplitude and frequency modulation is given in following sections. Phase modulation is important primarily with respect to systems of frequency modulation and will not be considered further except in relation to frequency modulation.

11-3. Amplitude Modulation

The equations of carrier and of sinusoidally modulated AM voltages were given in Section 11-2. In Eq. 11-7, it is convenient to define

$$k_a A_m/A_c = m_a \tag{11-18}$$

as the modulation factor or degree of modulation. Sketches of carrier and of modulated wave are given in Fig. 11-1. The quantity $100m_a$ is called the per cent modulation. It is customary to restrict modulation

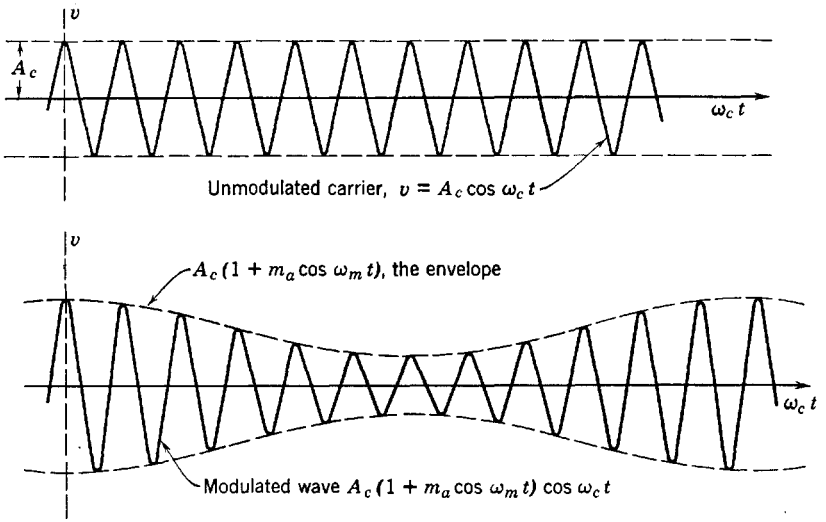

FIG. 11-1. A carrier, before and after amplitude modulation.

to 100 per cent, which results in doubling the carrier amplitude at the peak of the modulating wave and in reducing it to zero at the minimum of the modulating wave. For $m_a > 1$, periods of zero amplitude of the modulated wave would result.

The expression for the sinusoidally modulated wave (Eq. 11-7) may be transformed trigonometrically with the aid of the cosine product-to-sum transformation. The result is

$$\begin{aligned} v &= A_c(1 + m_a \cos \omega_m t) \cos \omega_c t \\ &= A_c \cos \omega_c t + m_a A_c/2 \cos (\omega_c + \omega_m)t \\ &\quad + m_a A_c/2 \cos (\omega_c - \omega_m)t \end{aligned} \tag{11-19}$$

which shows that three frequencies are present in the modulated wave. These three frequencies are: (1) the carrier, f_c, (2) the upper side frequency, $f_c + f_m$, (3) the lower side frequency, $f_c - f_m$. The distribution of these frequencies and the modulating frequency f_m with their relative amplitudes may be shown as a frequency spectrum as in Fig. 11-2. The modulating frequency is shown although it does not appear in Eq. 11-19, the equation of the modulated wave.

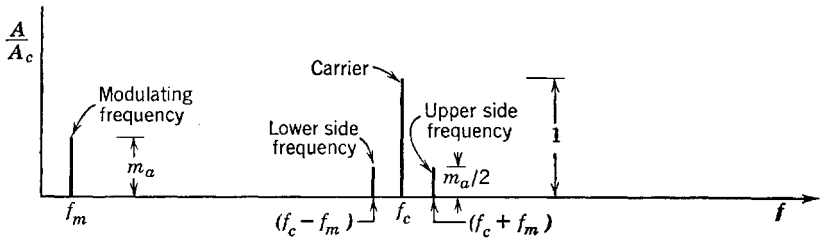

FIG. 11-2. Frequency spectrum, carrier-modulated by a single frequency.

In general, the modulating wave is not a sinusoid. For example, if speech or music is to be transmitted, frequencies covering most of the audible range are involved. Although the audible spectrum is generally considered to cover the range from 20 to 20,000 cps, a bandwidth of 3000 cycles is adequate for speech transmission, and 10,000 cycles for program broadcast by radio. In either case, the equation of the modulating wave may be written as a Fourier series, and, if it is so expressed, the product of each term of the series with the quantity $\cos \omega_c t$ may be replaced by two sinusoidal terms involving, respectively, the sum and the difference of carrier and modulating component frequency. The result is a translation of all the modulating frequencies f to bands $(f_c + f)$ and $(f_c - f)$ symmetrically disposed on either side of the carrier and referred to as the upper and lower sidebands. The component frequencies of the complex modulating wave have varying amplitudes A, and the translated sideband spectrum will have amplitudes $k_a A/2 = m_a A_c/2$. The bandwidth available for transmission must be sufficiently wide to permit, at

the receiver, the desired accuracy of reproduction of the modulating wave.

Another interesting interpretation of Eq. 11-19 is possible by the use of the familiar method of vector representation of sine waves. In Fig. 11-3, the carrier voltage is represented by a vector of length A_c rotating counterclockwise with angular velocity ω_c. Added to the carrier voltage are the two side frequencies, rotating with angular velocities $(\omega_c + \omega_m)$ and $(\omega_c - \omega_m)$. To an observer riding with the carrier and referring all motion to the carrier vector, ω_c is zero. Thus, to such an observer the carrier vector is stationary, the upper side frequency vector appears

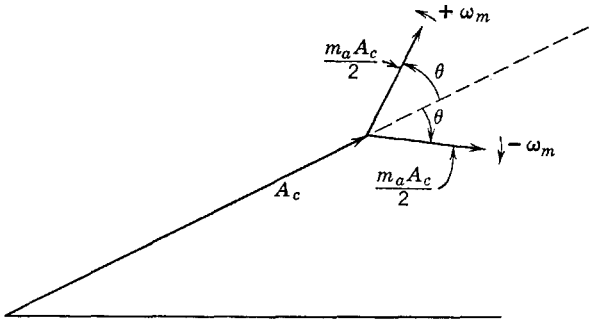

FIG. 11-3. Vector representation of an amplitude-modulated wave.

to have an angular velocity of $+\omega_m$, counterclockwise, while the lower side frequency vector appears to be rotating clockwise with angular velocity $-\omega_m$. Since the initial phase of the two side frequency components is the same for each, the resultant vector is always in line with A_c and either adds to or subtracts from its magnitude, because the components perpendicular to A_c cancel. The wave form of the modulated wave may now be obtained in the usual way by plotting the projection on the vertical axis of the resultant vector. The cancelation of the normal components shows that the resultant vector rotates with constant angular velocity ω_c, which shows that no frequency or phase modulation is present in the modulated wave. With either but not both of the normal components present, as is the case where one sideband is suppressed, the resultant vector varies in angular velocity with respect to the carrier, introducing angle modulation.

The distribution of power in an AM wave may be easily found since the power in a component frequency is proportional to the square of the amplitude of that component. Thus, for the carrier modulated by a sinusoidal frequency, the total power is

$$P = k[A_c^2/2 + \tfrac{1}{2}(m_a^2 A_c^2/4) + \tfrac{1}{2}(m_a^2 A_c^2/4)] \qquad (11\text{-}20)$$

of which the carrier power is

$$P_c = kA_c^2/2 \tag{11-21}$$

and the power associated with the sidebands is

$$P_{sb} = km_a^2A_c^2/4 \tag{11-22}$$

where k is a factor of proportionality. The ratio of power in sidebands to power in carrier is then

$$P_{sb}/P_c = m_a^2/2 \tag{11-23}$$

The factor ½ in Eq. 11-20 is necessary because A_c is the peak value of the amplitude. Thus, for sinusoidal 100 per cent modulation, the power in the sidebands is one-half that in the carrier. Since the sidebands contain all the intelligence, the power associated with the carrier is waste. The complete signal may be recovered if both the carrier and one sideband are suppressed and not transmitted, and this is done in very long-range radiotelephony and in carrier-current telephony, although by virtue of the additional equipment needed the method is not economical for other applications.

11-4. Methods of Producing Amplitude Modulation

Use of the nonlinear tube characteristics. One of the earliest methods of producing amplitude modulation was based upon the use of the nonlinear portion of a tube characteristic. If such a characteristic may be represented as a second degree curve (as in Chapter 2 in connection with distortion), then carrier plus modulating frequencies expressed as a sum and substituted in the second-degree term would result in *products* of the carrier with each modulating-frequency term. Such products, as already shown, may be replaced by single-frequency terms involving the sum and difference of carrier and modulating-frequency components. Unfortunately, there are also distortion terms present derived from the squares of separate components and from the products of modulating frequencies with each other. These must be eliminated by the tuned circuit. This process, known as square-law modulation, although not used in commercial broadcasting, does have its place in communication generally and has been thoroughly discussed in many textbooks.[2]

Use of a linear characteristic. Plate modulation. The external characteristics of a properly biased and driven class-C amplifier have led to its use as a modulator of approximately linear characteristics. This property was mentioned in Chapter 9 in the discussion of class-C amplifiers and is illustrated by Figs. 9-3, 9-4, and 9-5. These show: (1) that, if the

[2] See, for example, *Applied Electronics*, MIT Staff, John Wiley & Sons.

a-c grid excitation is sufficiently large to produce tank-current saturation the tank current and hence also the amplifier output voltage are linearly dependent upon the d-c component of plate voltage; (2) the load resistance presented at the plate terminals of the class-C amplifier tube to a modulator is constant, as shown by Fig. 9-5 for the characteristic labeled $\sqrt{2}\,E_g = 200$ volts. Thus, an a-c source of modulating voltage connected in series with the plate supply of the class-C amplifier, and of frequency small compared with the frequency of the carrier, will determine the amplitude of the carrier output during the a-c cycle of the

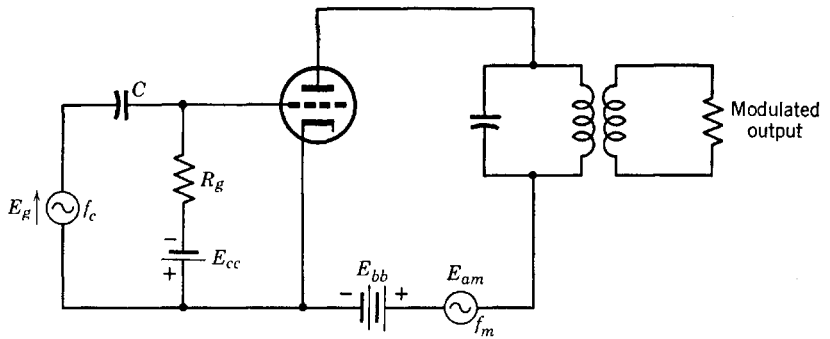

FIG. 11-4. Simplified circuit diagram of a plate-modulated class-*C* amplifier.

modulator. Amplitude modulation which can be made, with proper adjustment, a reasonably close approximation of that described by Eq. 11-19 is achieved by this method which is known as plate modulation of a class-C amplifier. The modulating source is, in general, a push–pull audio-frequency amplifier, operating class B. A simplified circuit is shown in Fig. 11-4. Voltage E_g is the carrier voltage and is derived originally from an oscillator. The audio or modulating frequencies are represented by the output of the audio oscillator of peak voltage E_{am} in the plate circuit. Neutralizing and radio-frequency by-passing capacitors and radio-frequency chokes have been omitted, but are necessary in a practical circuit. Bias is obtained by a combination of grid leak and fixed bias.

Plate modulation is used at high-power levels, utilizing the high efficiency of the class-C amplifier. A simple analysis of the power relations involved is essential in order to avoid exceeding the plate dissipation ratings of the tubes involved in both the modulator and the class-C amplifier. The d-c and audio-frequency components of plate voltage (Fig. 11-4) may be expressed as

$$E_b(t) = (E_{bb} + E_{am}\cos\omega_m t) = E_{bb}(1 + E_{am}/E_{bb}\cos\omega_m t) \quad (11\text{-}24)$$

It is assumed that the tank circuit presents a negligible impedance to the modulator at the modulating frequencies. The tube, as shown by Fig. 9-5, presents a resistance $R_b = E_b/I_b$ which is constant. Other components of the total plate current include the fundamental radio-frequency component of the carrier and its harmonics, and frequencies introduced by tube nonlinearities, but these are not matched in frequency by corresponding frequencies in the modulator input and thus do not contribute to modulator power. The d-c and slowly varying components of plate current which contribute to modulator power may then be expressed as

$$I_b(t) = \frac{E_b(t)}{R_b} = \frac{E_{bb} + E_{am}\cos\omega_m t}{R_b} = I_b\left(1 + \frac{E_{am}}{E_{bb}}\cos\omega_m t\right) \quad (11\text{-}25)$$

where

$$I_b = E_{bb}/R_b \quad (11\text{-}26)$$

Then the average power supplied in the plate circuit is

$$\begin{aligned} P_b &= \frac{1}{2\pi}\int_0^{2\pi} E_b(t)I_b(t)\, d(\omega_m t) \\ &= \frac{1}{2\pi}\int_0^{2\pi} E_{bb}I_b\left(1 + \frac{E_{am}}{E_{bb}}\cos\omega_m t\right)^2 d(\omega_m t) \\ &= E_{bb}I_b(1 + \tfrac{1}{2}E_{am}^2/E_{bb}^2) \end{aligned} \quad (11\text{-}27)$$

The interpretation of Eq. 11-27 is simplified by reference to Fig. 11-5, where a class-C linear characteristic is shown. This idealized characteristic is similar to the one already mentioned (Fig. 9-4) except that the radio-frequency peak output voltage at carrier frequency, $I_T X_c = E_{pm}$, is shown instead of I_T. The instantaneous values of carrier amplitudes are obtained from the characteristic as indicated. The quantity $E_{cm} = A_c$ is the unmodulated carrier amplitude. It is evident that, for 100 per cent modulation, $E_{am} = E_{bb}$. Since the modulation factor is E_{am}/E_{bb}, then Eq. 11-27 becomes

$$P_b = E_{bb}I_b(1 + m_a^2/2) \quad (11\text{-}28)$$

Since $E_{bb}I_b$ is the power delivered by the plate supply, then

$$P_m = (m_a^2/2)E_{bb}I_b \quad (11\text{-}29)$$

is the power supplied by the modulator. The power delivered by the audio-frequency modulator is then, for 100 per cent modulation, half the power delivered by the d-c plate supply.

If the plate-circuit conversion efficiency of the class-C amplifier is η_{pc}, the a-c power output supplied to the unmodulated carrier wave is

$$P_{oc} = \eta_{pc} E_{bb} I_b \tag{11-30}$$

(Actually, this power is supplied to the input terminals of an output transformer. The efficiency of this transformer is involved in determining

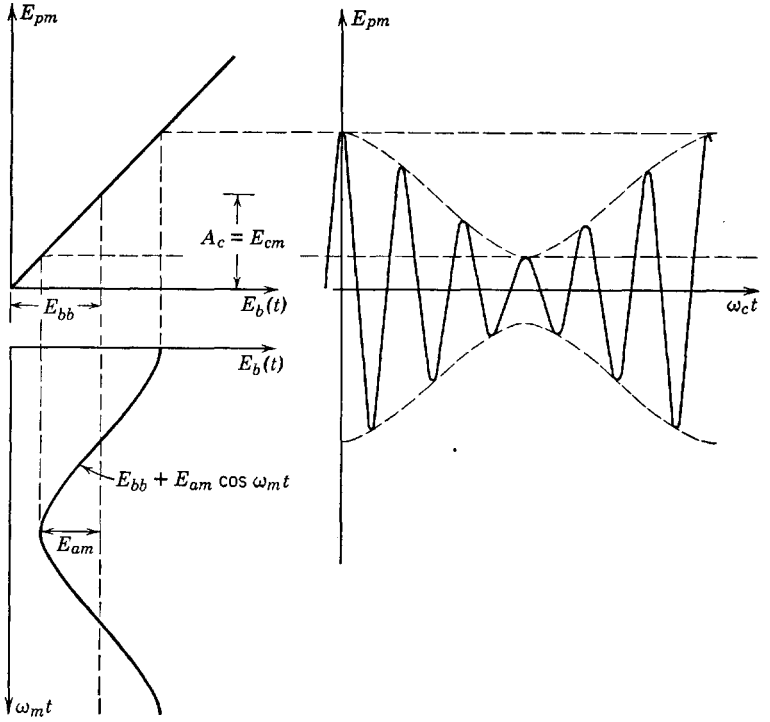

FIG. 11-5. Class-C linear-characteristic, plate-sinusoidal modulating wave, and modulated-output wave, linear-amplitude modulation.

the actual power output.) The power output of the class-C amplifier when plate-modulated by the sinusoidal voltage $E_{am} \cos \omega_m t$ is then obtained from the average plate input power (Eq. 11-28) and is

$$P_{ocm} = \eta_{pc} P_b = \eta_{pc} E_{bb} I_b (1 + m_a^2/2) \tag{11-31}$$

Here it is assumed that the class-C amplifier plate efficiency remains constant over the audio cycle. Thus, it may be observed that

$$P_{ocm} = P_{oc} + \eta_{pc} P_m \tag{11-32}$$

where, in terms of the earlier notation,

$$\eta_{pc}P_m = P_{sb} \tag{11-33}$$

the power supplied to the sidebands which is derived from the modulator.

The plate dissipations of amplifier and modulator tubes may now be determined. For the class-C amplifier tube, the plate dissipation with no modulation is

$$P_{pc} = E_{bb}I_b - P_{oc} = E_{bb}I_b(1 - \eta_{pc}) \tag{11-34}$$

With modulation, the class-C-amplifier tube-plate power dissipation is the power supplied in the plate circuit minus the output power, or

$$P_{pcm} = P_b - P_{ocm} \tag{11-35a}$$

which, with the aid of Eqs. 11-28 and 11-31, may be written as

$$P_{pcm} = E_{bb}I_b(1 + m_a^2/2)(1 - \eta_{pc}) \tag{11-35b}$$

A comparison of Eq. 11-35*b* with Eq. 11-34 will show that modulation *increases* the plate dissipation of the class-C amplifier tube by a factor of $1 + m_a^2/2$ or, at 100 per cent modulation, by 3/2. In other words, a 50 per cent increase in plate dissipation must be expected to accompany 100 per cent modulation. It is therefore necessary to operate this tube at two thirds of rated plate dissipation when unmodulated.

The plate dissipation P_{pm} of the modulator tubes may be expressed in terms of the power output of the modulator. Since the power output of the modulator is P_m, its power input is $(1/\eta_{pm})\,P_m$, where η_{pm} is the plate-conversion efficiency of the modulator. Then the plate dissipation of the modulator tubes is

$$P_{pm} = \frac{1}{\eta_{pm}}P_m - P_m = \frac{m_a^2}{2}E_{bb}I_b\left(\frac{1}{\eta_{pm}} - 1\right) \tag{11-36}$$

Specific values of efficiency are necessary in order to compare the necessary plate dissipation rating of the class-C amplifier tube with the modulator tubes. Efficiencies of $\eta_{pc} = 0.8$, $\eta_{pm} = 0.5$ are obtainable. For these values,

$$P_{pm} = (m_a^2/2)E_{bb}I_b$$

and

$$P_{pcm} = (1 + m_a^2/2)(0.2)E_{bb}I_b$$

If $m_a = 1$,

$$P_{pm}/P_{pcm} = 0.5/0.3 = 1.67$$

For the set of values chosen, the total plate dissipation required for the modulator tubes is considerably greater than for the amplifier. Results

given neglect modulating transformer efficiency. The ratio P_{pm}/P_{pcm} is much greater if a class-A modulator is used.

Plate modulation is more commonly used for transmitters than any other method. It has the advantage of linearity and low distortion. Its disadvantage is the fact that operation is required at high-power levels. Low-level modulation is used, but requires class-B radio-frequency power amplification to raise the power level to the desired value. Class-B radio-frequency amplifiers are inherently lower in efficiency than class C.

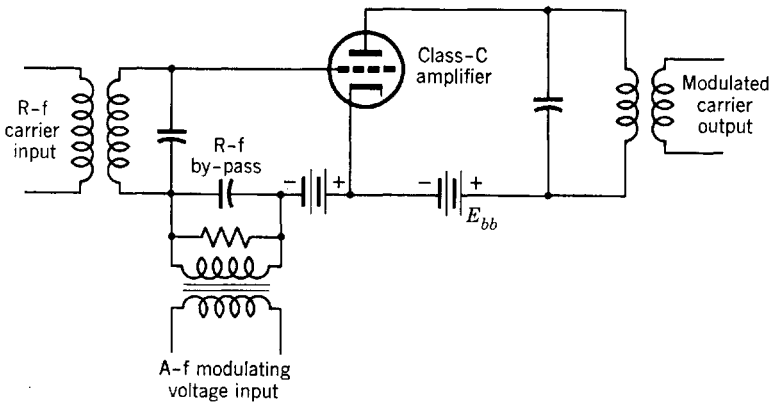

FIG. 11-6. Grid-bias-modulated class-*C* amplifier.

Grid-bias modulation of a class-C amplifier. Another method of amplitude modulation involves a variation of grid-bias voltage by the modulating source. Again, a class-C amplifier is used, but adjustments are made such that at the crest of the modulation cycle, when the grid is least negative, the grid excitation is not large enough to produce tank-current saturation. Thus, the grid-bias modulated class-C amplifier operates at much lower efficiency than with plate modulation. However, power requirements from the modulator are much smaller. Figure 11-6 is a simplified circuit diagram of a grid-bias-modulated class-C amplifier (neutralizing or by-pass circuit elements not shown). The radio-frequency carrier input is of constant amplitude. The audio- or modulating-frequency voltage, frequently obtained from a class-A push–pull amplifier, in series with the bias battery causes the bias to vary at a rate that is very slow compared with the rate of variation of the radio-frequency carrier voltage. The external characteristic of interest is a plot of the class-C-amplifier output voltage as a function of the instantaneous values of modulating plus bias voltage. Desirably this characteristic should be linear, but in general it varies somewhat from linearity

at high output voltages. Typical characteristics are supplied by the tube manufacturer.

Other methods of modulating the class-C amplifier. Other methods of approximately linear amplitude modulation are used and depend fundamentally upon the same principles that apply to the plate and grid-bias modulation methods. Control grid-bias modulation is used with tetrodes and pentodes; screen-grid modulation, similar to plate modulation, requires less modulating power, but tetrodes and pentodes do not provide the degree of linearity of characteristic available from triodes. Cathode modulation, in which the modulating voltage is applied between cathode and ground of the class-C amplifier, involves the modulating voltage in both grid and plate circuits, and combines some of the features of both grid and plate class-C modulation. Reference should be made to the literature and to texts on radio or communication engineering for details on linear amplitude modulation.

11-5. Frequency Modulation

It was shown in Section 11-2 that a voltage wave frequency modulated by a sinusoidal modulating wave may be represented by the equation

$$v = A_c \cos (\omega_c t + k_f A_m/\omega_m \sin \omega_m t) \tag{11-17}$$

The instantaneous frequency of the modulated wave as given by Eq. 11-11 is

$$f = \omega(t)/2\pi = f_c + k_f A_m/2\pi \cos \omega_m t \tag{11-37}$$

Thus the instantaneous frequency (definition 10) has a maximum value of

$$f_{\max} = f_c + k_f A_m/2\pi \quad \text{cps} \tag{11-38}$$

and a minimum value of

$$f_{\min} = f_c - k_f A_m/2\pi \quad \text{cps} \tag{11-39}$$

The frequency swing (definition 11) is

$$f_{\max} - f_{\min} = k_f A_m/\pi \tag{11-40}$$

The maximum frequency deviation from the carrier frequency is

$$\Delta\omega_f/2\pi = f_{\max} - f_c = f_c - f_{\min} = k_f A_m/2\pi \tag{11-41}$$

or one-half the frequency swing. The deviation ratio (definition 18) is

$$\delta = k_f A_m/2\pi f_m = k_f A_m/\omega_m = \Delta\omega_f/\omega_m \tag{11-42}$$

provided ω_m is the maximum modulating frequency of the system. In the following, the deviation ratio will be used with f_m defined as any

modulating frequency. Thus, δ is a variable which depends upon f_m and upon A_m.

An analysis of the FM wave (Eq. 11-17) for its frequency spectrum can be carried out by expanding the equation as follows:

$$v = A_c[\cos \omega_c t \cos (\delta \sin \omega_m t) - \sin \omega_c t \sin (\delta \sin \omega_m t)] \quad (11\text{-}43)$$

The quantities $\cos (\delta \sin \omega_m t)$ and $\sin (\delta \sin \omega_m t)$ have been expanded in a Fourier series. The coefficients of the sine and cosine terms of the series are themselves functions of δ which are very frequently encountered in engineering analysis—the Bessel functions of the first kind. Further information regarding the Fourier expansion and Bessel functions as used here is readily available in texts on advanced calculus and electric-circuit analyses.[3, 4, 5] The Bessel functions may be thought of as quite analogous to the trigonometric functions sine and cosine if the latter were defined only by their power series representation. The Bessel functions as represented graphically have some resemblance to damped sinusoids. Extensive tables of values of these functions are available.

The expansion of Eq. 11-43 into frequency components may be completed by the use of the relations

$$\cos (\delta \sin \omega_m t) = J_0(\delta) + 2[J_2(\delta) \cos 2\omega_m t + J_4(\delta) \cos 4\omega_m t + \cdots + J_{2n-2}(\delta) \cos (2n - 2)\omega_m t + \cdots \quad (11\text{-}44)$$

and

$$\sin (\delta \sin \omega_m t) = 2[J_1(\delta) \sin \omega_m t + J_3(\delta) \sin 3\omega_m t + \cdots + J_{2n-1}(\delta) \sin (2n - 1)\omega_m t + \cdots \quad (11\text{-}45)$$

where $J_{2n}(\delta)$ is a Bessel function of the first kind and of even order $2n$; the Bessel functions do not involve t. Reference to Eq. 11-43 will show that each term of the series in Eq. 11-44 will be multiplied by $\cos \omega_c t$, and each term in Eq. 11-45 will form products with $\sin \omega_c t$. As already shown in the section on amplitude modulation, each such product may be replaced by two terms involving, respectively, the sum and difference of carrier and modulating frequency or its multiple. The result as obtained from Eqs. 11-43, 11-44, and 11-45 with use of the trigonometric identities

$$\cos x \cos y = \tfrac{1}{2}[\cos (x + y) + \cos (x - y)]$$

and

$$\sin x \sin y = \tfrac{1}{2}[\cos (x - y) - \cos (x + y)]$$

[3] F. S. Woods, *Advanced Calculus*, 1926, Revised Ed., Ginn and Co., Boston.

[4] E. A. Guillemin, *The Mathematics of Circuit Analysis*, John Wiley & Sons (1949).

[5] L. B. Archimbau, *Vacuum-Tube Circuits*, John Wiley & Sons (1948).

is the following:

$$v = A_c[J_0(\delta)\cos\omega_c t + J_1(\delta)\cos(\omega_c + \omega_m)t - J_1(\delta)\cos(\omega_c - \omega_m)t + J_2(\delta)\cos(\omega_c + 2\omega_m)t + J_2(\delta)\cos(\omega_c - 2\omega_m)t + J_3(\delta)\cos(\omega_c + 3\omega_m)t - J_3(\delta)\cos(\omega_c - 3\omega_m)t] + \cdots + \cdots \quad (11\text{-}46)$$

The form of Eq. 11-46 is such that the frequency spectrum of the FM wave can easily be determined. It consists of the carrier, and of an infinite number of sidebands (where ω_m represents any frequency in the modulating wave) symmetrically distributed about the carrier. The amplitudes of these sideband frequencies and of the carrier depend upon the value of δ, which is determined by the frequency bandwidth allotted by statute, usually in terms of the maximum permissible frequency deviation from the carrier. An idea of the order of magnitude of the Bessel functions of δ is given by Table 11-1.

TABLE 11-1. SELECTED VALUES OF THE BESSEL FUNCTIONS

δ	$J_0(\delta)$	$J_1(\delta)$	$J_2(\delta)$	$J_3(\delta)$	$J_4(\delta)$
0	1.000	0.000	0.000	0.000	0.000
0.5	0.938	0.242	0.0306		
1.0	0.765	0.440	0.115	0.0196	0.0025
1.5	0.512	0.558			
2.0	0.224	0.577	0.353	0.129	0.034
2.5	−0.048	0.497			
3.0	−0.260	0.339	0.486	0.310	0.132
3.5	−0.380	0.137			
4.0	−0.397	−0.066	0.364	0.430	0.281
4.5	−0.321	−0.231			
5.0	−0.178	−0.328	0.0466	0.365	0.391
5.5	−0.007	−0.341			
6.0	0.151	−0.277	−0.243	0.115	0.358
7.0	0.300	−0.005	−0.301	−0.168	0.158
8.0	0.172	0.235	−0.113	−0.291	−0.105
9.0	−0.090	0.245	0.145	−0.181	−0.265
10.0	−0.246	0.045	0.255	−0.058	−0.220

It is evident from Eq. 11-46 that a large number of frequencies are included in the FM wave spectrum even though only one modulating frequency is present in the modulating wave. In order to examine an actual frequency spectrum of an FM wave, and to compare the relative amplitudes of the components, it is necessary to assign a numerical value to δ. The maximum frequency deviation from carrier permitted by Federal Communication Commission regulations is 75 kc above

or below the carrier. In Eq. 11-41, then, $\Delta\omega_f/2\pi = 75{,}000$. The value of $\delta = \Delta\omega_f/\omega_m$ (Eq. 11-42) then depends upon the particular frequency chosen in the modulating wave. If $f_m = 5000$ cps, $\delta = 75{,}000/5000 = 15$. It then becomes necessary to compute $J_n(15)$ as required by Eq. 11-46 for as many values of n as may be necessary be-

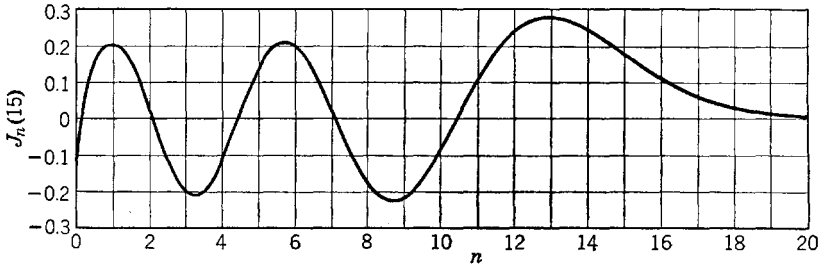

FIG. 11-7. Graph of the values of $J_n(15)$ for $0 < n < 20$.

fore the magnitude of $J_n(15)$ becomes negligible in comparison with amplitudes occurring earlier in the series. A curve of $J_n(15)$ plotted for values of n in the range $0 < n < 20$ (Fig. 11-7) shows that terms of the series beyond that corresponding to $n = 20$ have negligible amplitudes. The necessary frequency bandwidth, then, required to transmit the FM wave is $2(20f_m)$ or $40(5000) = 200{,}000$ cps or 200 kc. The relative

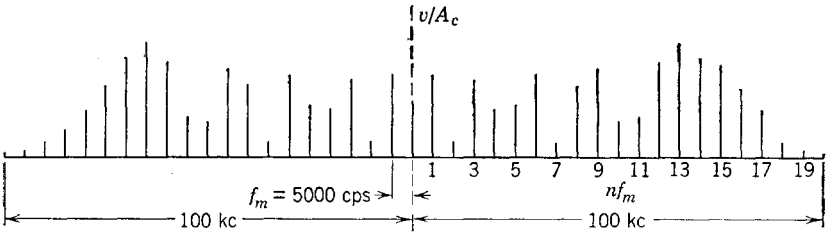

FIG. 11-8. FM frequency spectrum, $\Delta\omega_f/2\pi = 75$ kc, $\omega_m = 5$ kc, $\delta = 15$.

magnitudes of the various components of the FM frequency spectrum are easily determined by scaling the curve at integer values of n. The algebraic sign has been ignored in preparing the frequency spectrum of Fig. 11-8, which shows the distribution of frequencies around the carrier when the carrier voltage is frequency-modulated with a 5000-cycle voltage wave, with $\delta = 15$. The bandwidth of 200 kc required to transmit all frequency components corresponds exactly with the bandwidth allowed by the FCC.

It is of interest to compare with Fig. 11-8 the frequency spectrum necessary for a 3000-cps frequency. For $f_m = 3000$ cps, $\delta = \frac{75}{3} = 25$.

Values for $J_n(25)$ obtained from tables[6] have been used to construct the spectrum of Fig. 11-9. It should be observed that a slightly smaller bandwidth is necessary for transmission of the 3-kc modulating wave; although a larger number of frequency components are involved, they are more closely spaced.

The value of δ is determined by the selection of the quantities $\Delta\omega_f$ and ω_m. The required bandwidth then depends upon the number of terms of the series (Eq. 11-46) necessary to provide for all frequency components of appreciable amplitude. In practice, the maximum frequency deviation from carrier, $\Delta\omega_f$, is fixed by statute, as already mentioned. The required transmission bandwidth is then determined by the range

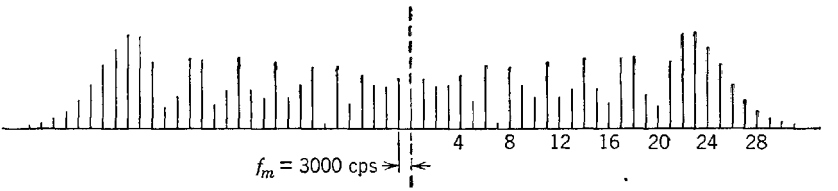

FIG. 11-9. FM frequency spectrum, $\Delta\omega_f/2\pi = 75$ kc, $\omega_m = 3$ kc, $\delta = 25$.

of modulating frequencies that it is necessary or desirable to reproduce at the receiver. The bandwidth problem is illustrated by Figs. 11-10 and 11-11. The effect on bandwidth of variations in δ with varying $\Delta\omega_f$ and fixed ω_m is shown in Fig. 11-10; the more realistic case with $\Delta\omega_f$ fixed and ω_m variable is shown in Fig. 11-11. Although values of $\Delta\omega_f$ and of ω_m used in these figures have been chosen so as to conform with available tabulations of Bessel functions, the bandwidth required for transmission of most of the side frequency components is seen to be equivalent to $2(\Delta\omega f/2\pi)$. The magnitude of the carrier varies also with δ because of the term $J_0(\delta)$. Since $J_0(2.4) = 0$, the carrier disappears for a frequency such that $\Delta\omega_f/\omega_m = 2.4$. This has been used to determine the frequency deviation $\Delta\omega_f$. Since $\Delta\omega_f$ is dependent upon the modulation frequency amplitude (Eq. 11-41), then two modulating signals of equal amplitudes but of different frequencies would produce the same frequency deviation but would require a different number of side-frequency components. Suppose, for example, that $\Delta\omega_f/2\pi =$ 75,000 cps as determined by the equal amplitudes of two audio components of frequency 15,000 and 3000 cps, respectively. For the 15,000-cps signal, $\delta = 5$, and Fig. 11-10 shows that approximately 7 side frequencies are required, or an over-all bandwidth of $2(7)(15{,}000) =$

[6] E. Jahncke and F. Emde, *Tables of Higher Functions*, 4th Revised Ed., B. G. Teubner, Leipzig (1948).

210,000 cps. In the case of the 3000-cps signal, $\delta = 25$, and Fig. 11-9 shows that 30 side frequencies are adequate. The corresponding bandwidth required for the 3-kc signal is 2(30)3000 = 180,000 cps. Since, in general, the amplitudes of the higher audio frequencies in speech or music are small, the corresponding frequency deviations are reduced, involving a smaller value of δ and consequently fewer side frequencies.

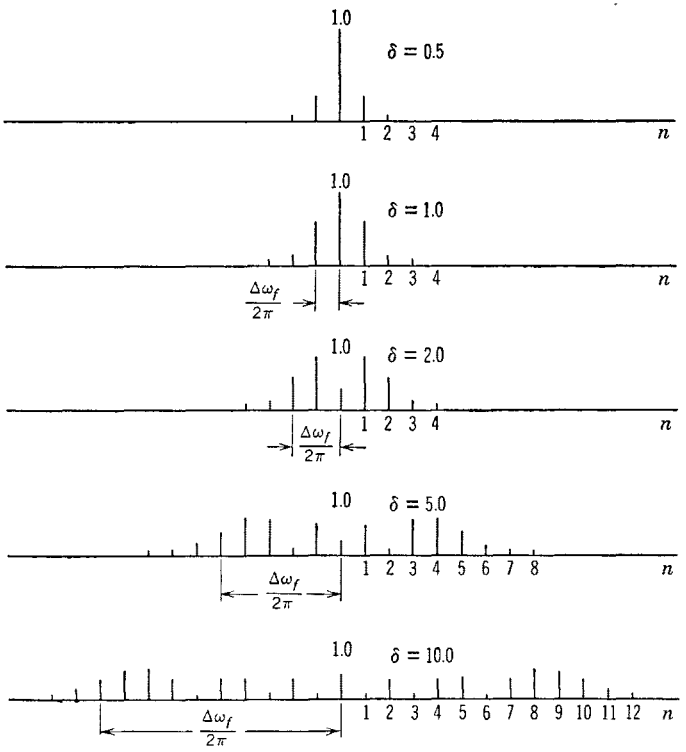

FIG. 11-10. FM frequency spectrum with variable-frequency deviation, $\Delta\omega_f/2\pi$, and constant $f_m = \omega_m/2\pi$.

Thus, a choice of 200 kc bandwidth is practical and adequate. Usually, the number of side frequencies required is of the order of magnitude and slightly larger than δ.

It will be remembered that, in amplitude modulation, the carrier power remains constant, and the power in the sidebands is supplied by the modulator. It has been remarked that, in frequency modulation, the carrier amplitude remains constant, but the FM spectra show that the effect of modulation is to cause a change in the amplitude of the carrier considered as one component in the frequency spectrum. Fre-

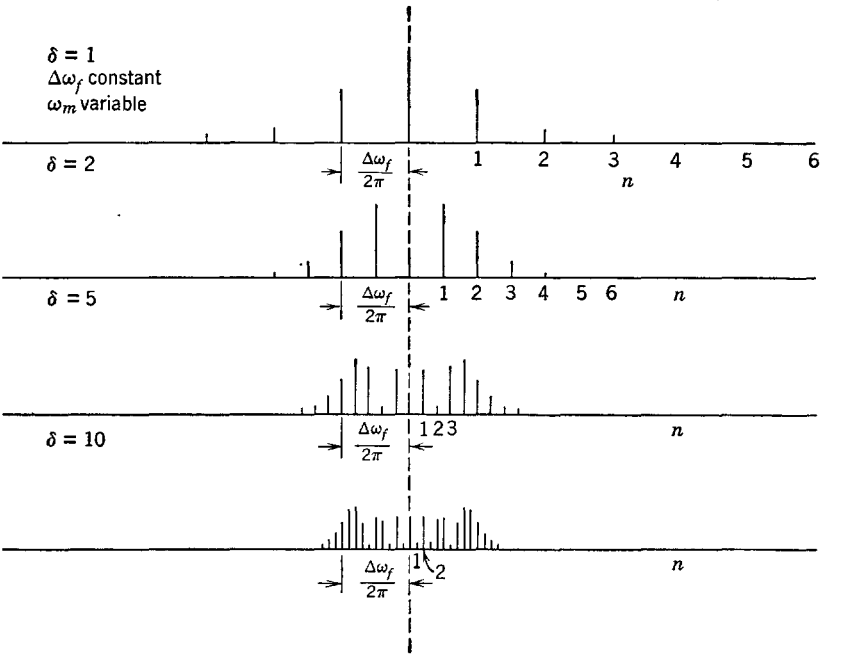

FIG. 11-11. FM frequency spectrum with variable ω_m and constant $\Delta\omega_f/2\pi$.

quency modulation results in a change in the *distribution* of power among the component frequencies of the spectrum with no change in the total power. In other words, the power in the side frequencies is derived from the carrier. This constancy of power may be shown with the aid of Eqs. 11-17 and 11-46. Before modulation, with $\delta = 0$, the carrier power is given by

$$P_c = GA_c^2 \tag{11-47}$$

where G is a constant of proportionality. After modulation, the power in the FM wave is

$$P_{cm} = GA_c^2[J_0^2(\delta) + 2\sum_{n=1}^{\infty} J_n^2(\delta)] \tag{11-48}$$

But it has been shown in the theory of Bessel functions that

$$J_0^2(\delta) + 2\sum_{n=1}^{\infty} J_n^2(\delta) = 1 \tag{11-49}$$

for all values of δ. Therefore $P_{cm} = P_c$, which shows that the power in the side frequencies is derived from the carrier.

11-6. Production of FM Wave

A discussion of FM transmitters is not appropriate to the purposes of this text. However, the circuit application of electron tubes is pertinent, and a few such applications will be discussed.

If either the inductance or the capacitance of the tank circuit of an oscillator could be varied in magnitude at any selected audio frequency, the output of the oscillator would be frequency-modulated. A means of

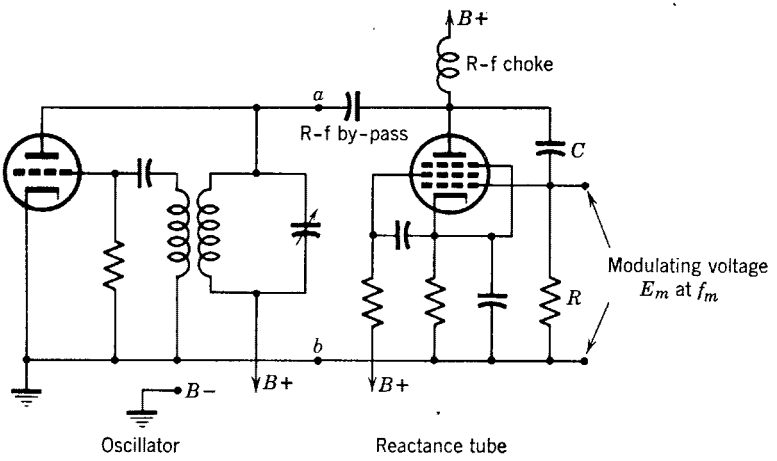

FIG. 11-12. Tuned-plate oscillator with reactance-tube modulator.

accomplishing this objective is found in the use of a vacuum tube with suitable external circuit shunted across the tank circuit of the oscillator. Proper choice of circuit and vacuum-tube constants will result in the alternating current to the tube circuit leading—or lagging—the a-c plate voltage by 90°, with the magnitude of the circuit current controlled by an audio-frequency modulating voltage applied to the grid. The tube thus applied is known as a reactance tube and is commonly used in frequency modulation. The circuit of Fig. 11-12 shows a reactance tube used as part of the tuned circuit of a tuned-plate oscillator. The terminals *a–b* connect the reactance tube, a pentode, across the oscillator tuning condenser. The class-A equivalent circuit of the reactance tube at *a–b* (Fig. 11-13) is to be analyzed for its input admittance. The modulating voltage across R may be regarded merely as a means of controlling or varying the tube transconductance g_m. For any value of g_m, it is required to determine the admittance Y. Let the oscillator radio-frequency output voltage be designated as V_p as referred to ground. Then the input current to the reactance tube is

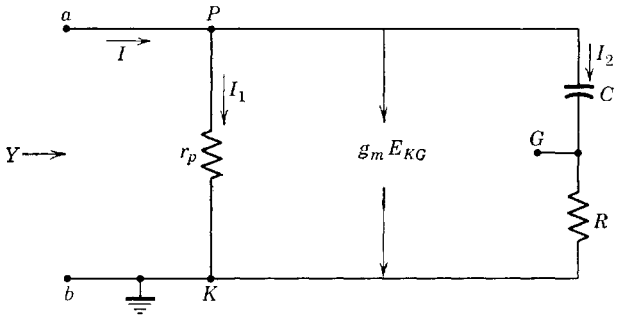

FIG. 11-13. Equivalent circuit of the reactance tube, Fig. 12-12, as seen at terminals *a–b*.

given by

$$I = I_1 + g_m E_{KG} + I_2 \tag{11-50}$$

Since $E_{KG} = I_2 R$

$$I = I_1 + I_2(g_m R + 1) \tag{11-51}$$

For a pentode, r_p is large enough that I_1 may be neglected in comparison with the other two current components. The current I becomes

$$I = V_p\left(\frac{1}{r_p} + \frac{g_m R + 1}{R + 1/j\omega C}\right) \cong V_p\left[\frac{g_m R + 1}{R - j(1/\omega C)}\right] \tag{11-52}$$

and the admittance Y is given by

$$Y = \frac{I}{V_p} = \frac{g_m R + 1}{R - j(1/\omega C)} \tag{11-53}$$

which, when rationalized, may be written in the form

$$Y = \frac{\omega^2 C^2 R(g_m R + 1)}{R^2\omega^2 C^2 + 1} + j\omega\frac{C(g_m R + 1)}{R^2\omega^2 C^2 + 1} \tag{11-54}$$

The problem of design of the reactance-tube circuit consists of the proper proportioning of C and of R such that, in the range of oscillator frequency deviation, R though large is small compared to $1/\omega C$, and Rg_m is large compared with unity. Since it is required that $R^2\omega^2 C^2 \ll 1$, and $g_m R \gg 1$, then

$$Y \cong \omega^2 C^2 R^2 g_m + j\omega g_m CR \tag{11-55}$$

The quantity $\omega^2 C^2 R^2 g_m$ is a small variable conductance in parallel with r_p and desirably negligible. The quantity

$$C_e = g_m CR \tag{11-56}$$

is a variable capacitance shunted across the tuning capacitor of the oscillator tank circuit and controllable in magnitude by variation of g_m. A curve of g_m as a function of control grid voltage for a type-7C7 pentode is shown in Fig. 11-14. The variation of g_m is linear over a large portion of the range. In order to establish the required orders of magnitude

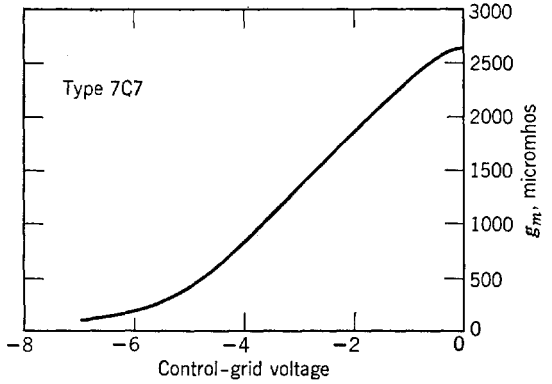

FIG. 11-14. Variation of g_m with control-grid voltage, type 7C7.

necessary for the approximations specified, it may be necessary to operate the oscillator at frequencies lower than the desired carrier frequency, then to pass the FM wave through a frequency multiplier and class-C amplifier before transmission from the transmitting antenna. In order to ensure that the center frequency remain stable within the specified range of ±2 kc, a sample of the output frequency may be

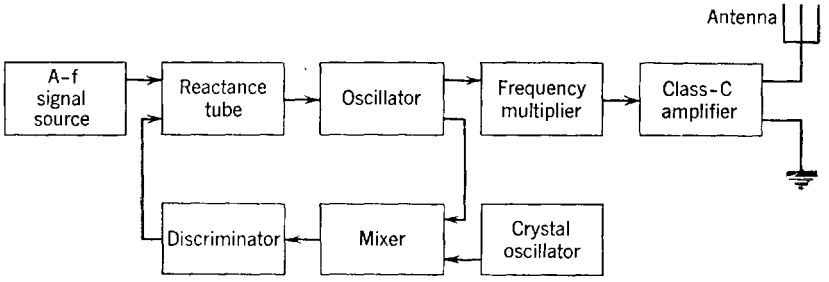

FIG. 11-15. Block diagram of an FM transmitter.

compared with a crystal oscillator frequency, and the difference frequency voltage is rectified and fed back to the reactance-tube-modulator control grid as a bias correction for any error. A circuit called a frequency discriminator may be used to provide the correcting bias as illustrated in the block diagram of Fig. 11-15.

The reactance-tube modulator of Fig. 11-12, as shown by the analysis, is a variable capacitance. A variable inductance is obtained from a properly designed circuit arranged as shown by Fig. 11-16. Other reactance-tube circuits have been included in the problems.

The frequency deviation produced by a reactance-tube modulator can be computed approximately by using a linear approximation for the g_m–e_c characteristic of Fig. 11-14. An idealized g_m–e_c characteristic, as shown in Fig. 11-17, may be expressed as the equation of a straight line. The transconductance may be expressed in terms of any known

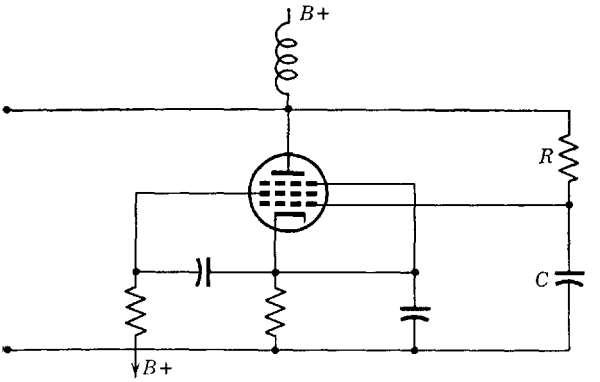

FIG. 11-16. L-type reactance tube.

point on the line, such as that determined by the bias voltage E_c, the value of $g_m = g_{m0}$ at this zero signal voltage, and the slope of the line. However, the intercept form of the equation of the line is more convenient. Thus, from Fig. 11-17,

$$g_m = g_{m2} + (g_{m2}/E_1)e_c \tag{11-57}$$

is the equation of the characteristic, where g_{m2} is the value of g_m at the vertical intercept and $-E_1$ is the total grid voltage at the horizontal intercept. If the instantaneous value of the modulating voltage shown in Fig. 11-17 is

$$e_m = E_m \cos \omega_m t \tag{11-58}$$

then, referred to the e_c axis, this voltage is given by

$$e_c = E_c + E_m \cos \omega_m t \tag{11-59}$$

where, as usual, E_c has a negative numerical value. The instantaneous

value of g_m as the modulating voltage varies as obtained from Eqs. 11-57 and 11-59 and is

$$g_m = g_{m2} + \frac{g_{m2}}{E_1} E_c + \frac{g_{m2}}{E_1} E_m \cos \omega_m t \tag{11-60}$$

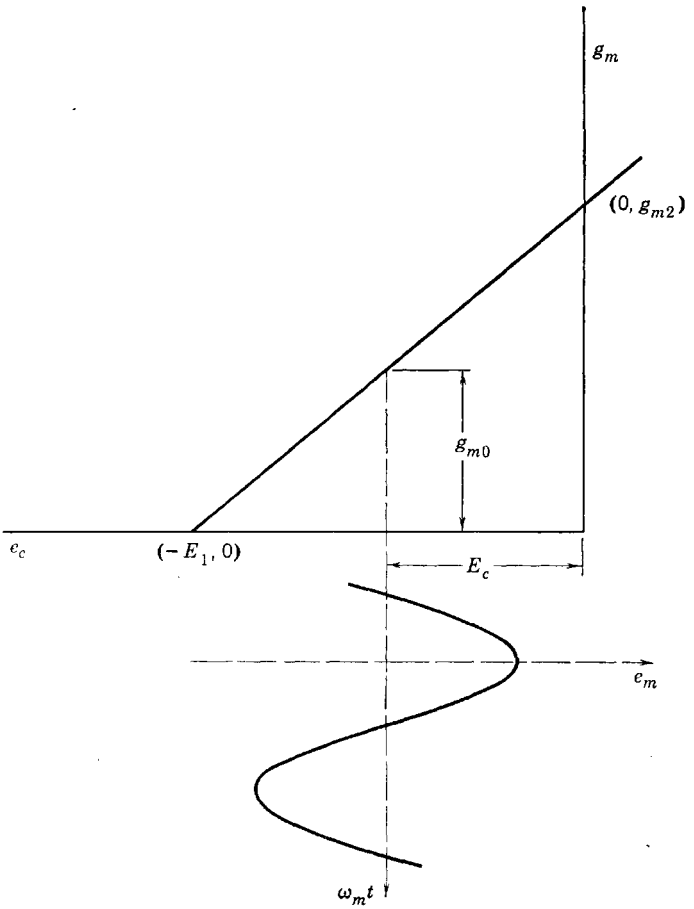

FIG. 11-17. Idealized g_m–e_c characteristic.

From Eqs. 11-56 and 11-60,

$$C_e = g_{m2}CR(1 + E_c/E_1 + E_m/E_1 \cos \omega_m t) \tag{11-61}$$

The oscillation frequency of the oscillator, if determined by the constants of the tank circuit, is given by

$$f = 1/2\pi\sqrt{L_t(C_t + C_e)} \tag{11-62}$$

where L_t is the inductance and C_t the capacitance of the tank circuit elements. An expression for the instantaneous frequency as obtained from Eqs. 11-62 and 11-61 is

$$f = \frac{1}{2\pi\sqrt{L_t[C_t + g_{m2}CR(1 + E_c/E_1 + E_m/E_1 \cos \omega_m t)]}} \tag{11-63}$$

and the carrier frequency f_c is the value of f in Eq. 11-63 when the modulating voltage $E_m \cos \omega_m t$ is zero. Therefore,

$$f_c = \frac{1}{2\pi\sqrt{L_t[C_t + g_{m2}CR(1 + E_c/E_1)]}} \tag{11-64}$$

and the ratio of f/f_c may be expressed in the form

$$\frac{f}{f_c} = \left\{1 + \left[\frac{g_{m2}CRE_m \cos \omega_m t}{C_t E_1 + g_{m2}CR(E_1 + E_c)}\right]\right\}^{-\frac{1}{2}} \tag{11-65}$$

If the value in the bracket (Eq. 11-65) is small compared with unity, the binomial expansion will result in an infinite series converging rapidly enough so that only the first two terms need be retained for a first approximation. In this way,

$$\frac{f}{f_c} = 1 - \frac{1}{2}\frac{g_{m2}CRE_m \cos \omega_m t}{C_t E_1 + g_{m2}CR(E_1 + E_c)} \tag{11-66}$$

If now the quantity k_f in Eq. 11-37 is sought in Eq. 11-66, it may be identified with the coefficient of $(E_m/2\pi) \cos \omega_m t$ in

$$f = f_c + \left[-\frac{\pi g_{m2}CRf_c}{C_t E_1 + g_{m2}CR(E_1 + E_c)}\right]\frac{E_m}{2\pi} \cos \omega_m t \tag{11-67}$$

or,

$$k_f = -\frac{\pi g_{m2}CRf_c}{C_t E_1 + g_{m2}CR(E_1 + E_c)} \tag{11-68}$$

The required relation for FM,

$$f = f_c + k_f E_m/2\pi \cos \omega_m t \tag{11-37}$$

is then realized, subject to the approximations made, since g_{m2}, C, R, f_c, C_t, E_1, and E_c are all constants.

Other systems of frequency modulation are used and are discussed in radio and communication engineering texts and in the literature.[7,8]

[7] See E. H. Armstrong, *Proc. IRE*, **24,** 689 (1936).

[8] J. F. Morrison, *Proc. IRE*, **28,** 444 (1940).

Only one other method will be described here, a more recent development involving a new electron tube, the General Electric phasitron.[9]

11-7. Frequency Modulation by Means of the Phasitron

Frequency modulation is derived from phase modulation in the phasitron. The tube has a cylindrical cathode consisting of a standard 6J5 assembly coated for 0.25 inch. Two cylindrical anodes coaxial with the cathode and operating at a positive potential with respect to the cathode are used to provide a flat disk of electron flow from the cathode. The active portion of the electron stream is limited by the edges of two focusing electrodes, which shape the flat disk so that it tapers to a thin outer edge before reaching the first anode. The thin-edged, tapered disk of electron flow passes between a so-called neutral plane and a set of 36 grid wires supported in a plane perpendicular to the cathode axis by radial slots in a ceramic core. The grid wires are connected such that every third wire is part of the same circuit operating at the same potential. There are thus three groups, of 12 radial wires each, distributed over the flat surface of the ceramic support. Each group of wires is connected to one leg of a three-phase, wye-connected, radio-frequency input circuit supplied by a crystal-controlled oscillator. The neutral of the wye-connected secondary winding is maintained at +80 volts direct current. The three-phase connection provides a rotating electric field between the grid wires (called deflectors) and the neutral plane. The effect of the rotating field upon the thin disk of flowing electron space charge—which flows between deflector grids and neutral plane—is to warp the disk into ruffles similar to those shown in the sketch of Fig. 11-18. The ruffles, not the electrons, rotate with the three-phase electric field and impinge upon the first anode in which openings are arranged to match the positions of the ruffles. As the ruffles rotate, the edge of the ruffled disk passes in successive order either through an opening in the anode or against the barrier between anode openings. The second anode collects the electrons which pass through the openings in the first. A push–pull tuned circuit connected between the anodes is driven by the alternate collections of electrons by the two anodes and supplies a radio-frequency voltage at the crystal oscillator frequency which is approximately 230 kc and must be multiplied to the required carrier value.

The tube as thus far described provides only a carrier frequency, but the rotating ruffles in the electron disk can easily be shifted in phase and in spatial position with respect to the first anode openings by the appli-

[9] F. M. Bailey and H. P. Thomas, Phasitron FM Transmitter, *Electronics*, **19**, 108 (Oct. 1946).

cation of a magnetic field parallel to the axis of the tube and perpendicular to the direction of electron flow. The magnetic field is controlled by an audio-frequency modulating coil surrounding the anodes. The magnetic field is concentrated by means of the second focusing electrode—which is constructed of magnetic material and serves the dual purposes of focusing and of supplying the magnetic flux for modulating the electron flow. The magnetic flux of the modulating field is confined to a

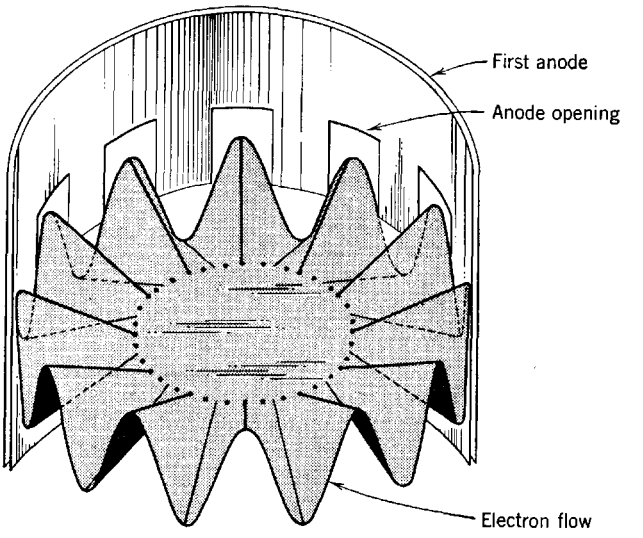

FIG. 11-18. Ruffled, rotating electron disk of a phasitron. (Courtesy General Electric Co.)

narrow region at the edge of the deflector or ruffle-producing grid. The magnetic field either advances or retards the phase of the rotating ruffles with respect to the anode openings by rotating the whole disk. The magnetic field thereby introduces a corresponding phase shift in the tuned circuit. The phase deviation of the output voltage is almost linearly dependent upon the magnetic field strength for values ranging from $+15$ to -15 gausses.

The conversion necessary from phase modulation to frequency modulation is accomplished by keeping a constant direct voltage across the modulating coil at all audio frequencies such that, with the coil behaving as practically a pure inductance L at all frequencies in the range from 50 to 15,000 cps, the alternating component of coil current $E_m/(\omega_m L)$ and also the resulting magnetic field are inversely proportional to modulating frequency f_m. Thus, the requirement of $k_f E_m/\omega_m$ for the deviation ratio is met.

The advantage claimed for the phasitron is that the necessary frequency multiplication is reduced by its use. For the range 88 to 108 Mc required carrier frequency, a multiplication in frequency of 432 is required at the phasitron output, as compared with 7000 in some other systems.

11-8. The Problem of Detection

The transmitted wave arriving at its destination requires demodulation in order to make available the information content which had originally been inserted on the carrier through the process of modulation. The process of demodulation or detection (definitions 19 and 20) depends of course upon the nature of the modulated wave, so that the detection of AM waves is a process completely different from that required for FM waves. An ideal detector will exactly reproduce at the receiver the wave form of the original modulating wave. In effect, the process involves the frequency translation back from the band represented by the carrier and its sidebands to the original frequency band.

11-9. Detection of AM Waves

Principles rather than methods are primarily of interest in introducing the subject of detection of AM waves. However, the principles involved are so intimately related to the detectors themselves that an

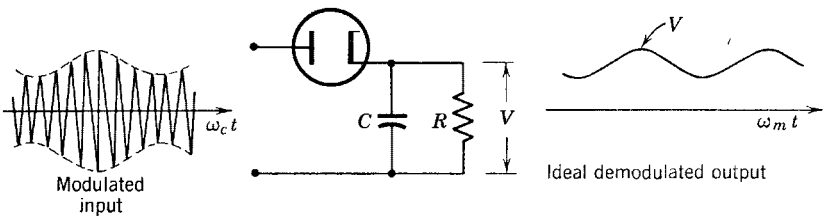

FIG. 11-19. Ideal demodulated output.

attempt will be made to integrate a discussion of both principles and methods in the present section.

The demodulation of AM waves is accomplished in radio receivers generally by the use of linear detection. This method involves a diode rectifier which conducts only during the positive half-cycles of the radio-frequency carrier. The principle of operation is to be found in the requirement that the voltage across the R–C output circuit (Fig. 11-19) follow the envelope of the AM wave. An ideal demodulated output as shown by Fig. 11-19 is not achieved. Actually, as reference to Chapter 6 will show, the circuit is the same as the half-wave rectifier with capacitance filter when conduction occurs only as long as a positive voltage

exists between anode and cathode. The voltage across the tube reaches zero and then becomes negative at a time immediately following the peak of the positive radio-frequency half-cycle because this voltage is the difference between the instantaneous applied voltage and the voltage V across the capacitance C. The diagram of Fig. 11-20, although much exaggerated, shows the wave forms of the applied radio-frequency voltage positive half-cycles, of the detector output voltage V, and of the

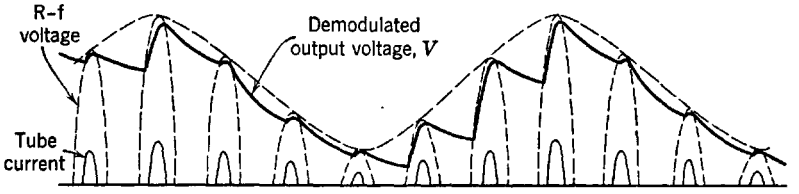

FIG. 11-20. Wave forms of voltage v, Fig. 12-19, and of tube current for diode detector.

pulses of plate current. The diagram is similar to that of Fig. 6-5, and the principles involved are identically the same. The only difference is that the peak voltages of the detector input wave vary in amplitude according to the modulating wave. It may be concluded that the demodulated output voltage V in Fig. 11-20 is a very poor approximation of the envelope of the modulated wave, but actually the difference in frequencies between carrier and modulation components is so much

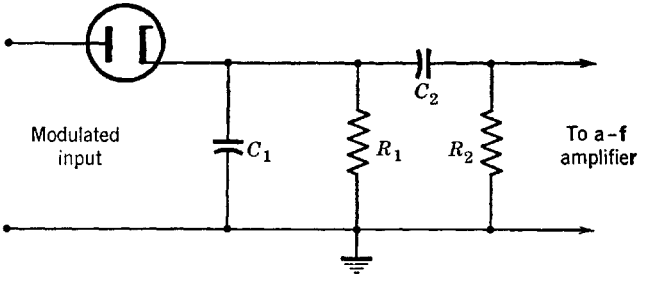

FIG. 11-21. Linear detector and R_2–C_2-coupling circuit.

greater than that shown in Fig. 11-20 that a very good approximation of the envelope can be achieved with the proper design of the load circuit, R and C. The linear detector circuit of Fig. 11-19 is followed by an audio amplifier in the receiver. Either R–C or transformer coupling to the input of the audio amplifier may be used in order to eliminate the d-c component of the detector output voltage. The R–C circuit is shown in Fig. 11-21; the requirements to be met by C_2 and R_2 are

identical with those required in audio-amplifier R–C-coupling circuits as discussed in Chapter 3. A rough idea of the magnitudes required of C_1 and C_2 is to be found in the requirements that the reactance of C_1 should be negligible compared with R_1 at radio (or carrier) frequencies, and that of C_2 negligible with respect to R_2 at audio—or modulation—frequencies. Capacitance C_1 then becomes a radio-frequency by-pass to ground; resistance $R = R_1R_2/(R_1 + R_2)$ then becomes approxi-

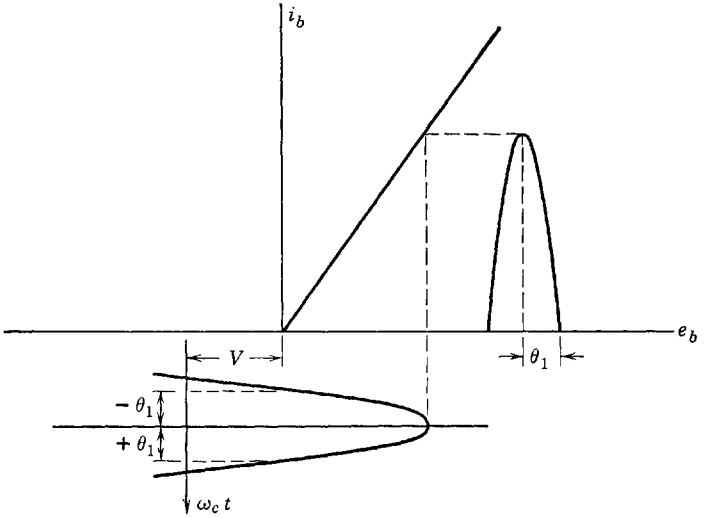

FIG. 11-22. Linear diode-detector characteristic, with one r-f half-cycle, varying bias voltage v, and pulse of diode current.

mately the audio-frequency output impedance, provided the reactance of C_1 at audio frequencies is large compared with R_1. Under such conditions, the effective, slowly varying (a-f) bias of the diode is determined by the voltage drop in resistance R produced by the audio or modulation component of current in the output. This component may be thought of as the average of the pulses of plate current (Fig. 11-20). Such an explanation is only approximate but has the merit of simplicity. It is further illustrated by Fig. 11-22, which shows the tube characteristic as linear and the slowly varying output voltage V as a cathode bias. The variation of V is the result of the amplitude variations of the carrier voltage; V is the product of the d-c component of the diode plate current (which is the average of the pulses of current shown in Figs. 11-20 and 11-22) and the load resistance of the diode. At the input terminals (Fig. 11-21) the modulated voltage is given by Eq. 11-19 as

$$v = A_c(1 + m_a \cos \omega_m t) \cos \omega_c t$$

The current pulse during the conduction period is then given by

$$i = \frac{A_c}{r_p + R}(1 + m_a \cos \omega_m t) \cos \omega_c t, \qquad -\theta_1 < \omega_c t < \theta_1 \quad (11\text{-}69)$$

Since the pulse duration is $2\theta_1$ (Fig. 11-22), the average current over a period of the radio-frequency cycle is

$$i_a = \frac{1}{2\pi}\int_{-\pi}^{\pi} i \, d(\omega_c t)$$

$$= \frac{1}{2\pi}\int_{-\theta_1}^{\theta_1} \frac{A_c}{r_p + R}(1 + m_a \cos \omega_m t) \cos \omega_c t \, d(\omega_c t) \quad (11\text{-}70)$$

If $\cos \omega_m t$ is assumed to be constant over the period $2\theta_1$ of duration of i, then

$$i_a = \frac{A_c}{\pi(r_p + R)}(1 + m_a \cos \omega_m t)(\sin \theta_1)$$

$$= \frac{A_c \sin \theta_1}{\pi(r_p + R)} + \frac{m_a A_c \sin \theta_1}{\pi(r_p + R)} \cos \omega_m t \quad (11\text{-}71)$$

The output voltage of the detector is $i_a R$; thus, the output voltage contains only the modulating-frequency components and no distortion terms, and the detection is linear.

It may be observed from the foregoing discussion that the variables of importance in the operation of a linear diode detector are the voltage amplitudes of the carrier, the average plate current of the tube, and the direct voltage across the detector load. The amplitude of the carrier voltage, the direct component of plate current, and the direct voltage across the load all vary at an audio- or modulating-frequency rate. These three related variables are frequently presented graphically, either

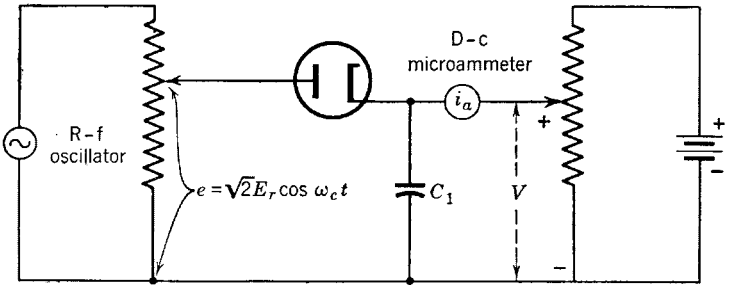

FIG. 11-23. Circuit arrangement for measurement of rectification or detector characteristics.

by the tube manufacturer or by measurements made on the diode detector circuit as shown in Fig. 11-23. Families of curves derived from measurements of E_r, i_a, and V are usually presented as shown in Fig. 11-24

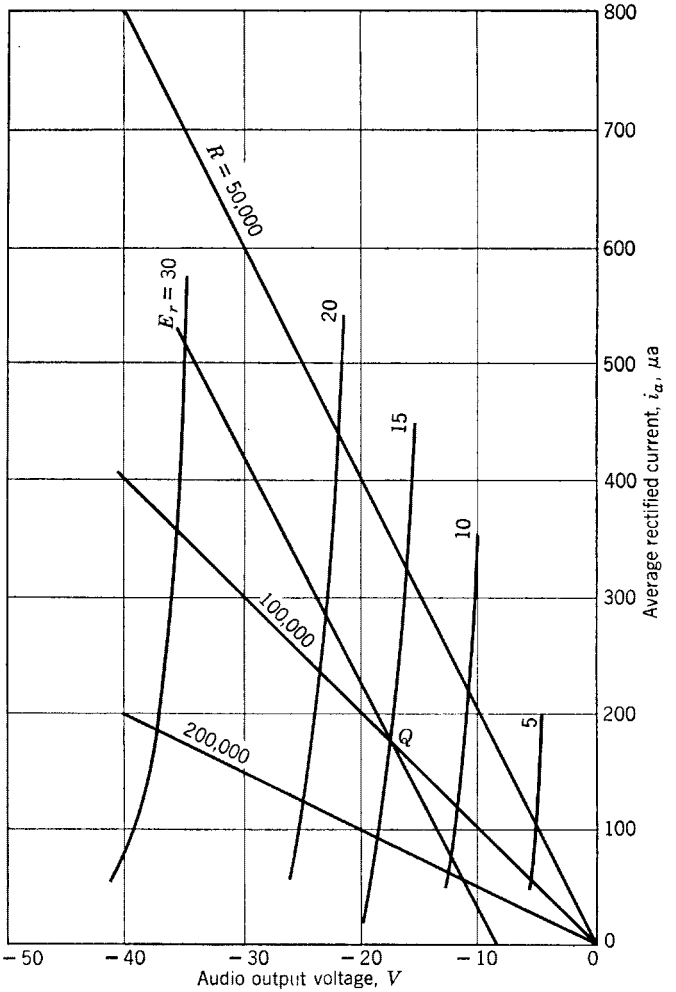

FIG. 11-24. Rectification characteristics for a linear diode detector and several load characteristics.

for a type-6H6 diode. Curves of average rectified current i_a are plotted against output voltage V, which is plotted on the negative side of the axis because it provides, in effect, a negative bias for the diode. A curve is drawn for each selected value of the rms voltage of the radio-frequency

oscillator, and the family of curves so obtained constitute the rectification characteristics of the tube.

In the case of a single load resistor, as in Fig. 11-19, the load resistance characteristic may be plotted on Fig. 11-24 just as the load line is drawn on the plate characteristic diagram of a triode amplifier. Several load resistance characteristics are shown. Physically realizable combinations of average rectified current and direct voltage V across the load resistance are represented by the intersections of a load line with the curves of constant rms carrier voltage. For example, if the rms value of unmodulated carrier voltage is 15 volts, and the load resistance R (Fig. 11-19) is 100,000 ohms, then the average rectified current is about 175 μamp, and the output voltage is 17.5 volts. If the carrier is amplitude-modulated 33⅓ per cent, the maximum rms voltage will be 20 volts, the minimum 10 volts. Variations in i_a will be in the range 230 to 120 μamp, and V will vary from a maximum of 23 to a minimum of 12 volts. The operating locus will be along the load resistance characteristic. Point Q (Fig. 11-24) is the operating point.

If the detector output is R–C-coupled to the input of an audio amplifier, as in Fig. 11-21, then a load line determined by the value of R_1 may be drawn as in Fig. 11-24 to locate Q; the operating dynamic load line may then be drawn through point Q with a slope determined by $R = R_1R_2/(R_1 + R_2)$, if the reactance of C_2 is negligible at the modulation frequency. For values of $R_1 = R_2 = 100{,}000$, the dynamic load line corresponds to $R = 50{,}000$ ohms and has been drawn on Fig. 11-24. The operating locus is therefore limited to the range of values along the dynamic load line extending from the intersection of the line with the V axis and thence upward through Q to a maximum determined by the allowable modulation. The allowable modulation possible without distortion may be determined from the value of E_r corresponding to the rectification characteristic which intersects the load line at the horizontal axis. If R (Fig. 11-19) were infinite, the load line through the origin would coincide with the horizontal axis, and V would equal the peak value of the radio-frequency carrier voltage since the condenser would charge to this value and remain charged. Therefore, the values of V at the intersections of the rectification characteristics with the V axis are the peak voltage amplitudes of the unmodulated carrier. The allowable modulation factor for the case $R_1 = R_2 = 100{,}000$ (Fig. 11-21) may be determined from the intersection of the dynamic load line with the V axis, which occurs at approximately $V = -9$ volts. The rectification characteristic which, if drawn on the graph, would intersect the V axis at -9 volts would have $E_r = 9/\sqrt{2} = 6.35$ volts. Accord-

ing to Eq. 11-19, the minimum carrier amplitude is

$$A_c(1 - m_a) = \sqrt{2}\, E_r(1 - m_a)$$

Since $E_r = 15$ volts, and the minimum magnitude of V is 9 volts, then

$$\sqrt{2}\,(15)(1 - m_a) = 6.35\sqrt{2}$$

whence $$m_a = 1 - 6.35/15 = 1 - 0.423 = 0.577$$

is the maximum allowable value of the modulation factor for the circuit if linear operation is desired.

11-10. Circuit Requirements for Linear Detection

Two requirements must be met by the diode detector circuits of Figs. 11-19 or 11-21 in order to secure the high-quality distortionless operation of which the diode detector is capable.

The first requirement may be understood by reference to Fig. 11-20. During the period of zero tube current, the capacitor discharge through resistance R (Fig. 11-19) should reduce the voltage V at a rate equal to that at which the modulation or envelope voltage is decreasing in order that the variations in V should reproduce the modulation voltage. Although the actual envelope of the AM carrier varies sinusoidally only

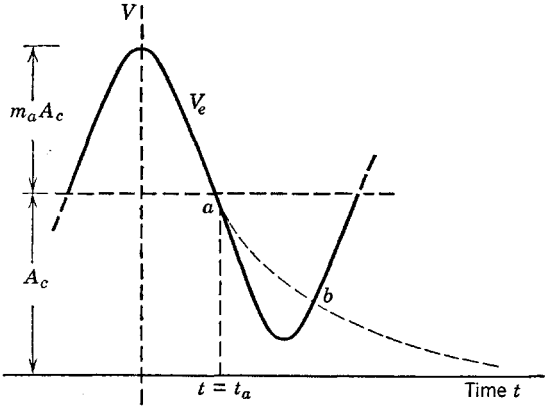

FIG. 11-25. Sketch of the top portion of the carrier envelope, $V_e = A_c(1 + m_a \cos \omega_m t)$.

in the case of a single, sinusoidal modulating frequency, a satisfactory design value of the RC product obtained at the highest component audio or modulating frequency is also satisfactory for lower component frequencies. The rate of decrease of output voltage V necessary for the sinusoidal modulating angular frequency ω_m of Eq. 11-19 is then the same

as that of the envelope V_e (Fig. 11-25) or

$$\frac{dV}{dt} = \frac{dV_e}{dt} = \frac{d}{dt} A_c(1 + m_a \cos \omega_m t) = -\omega_m A_c m_a \sin \omega_m t \quad (11\text{-}72)$$

The magnitude of the necessary rate of decrease of V will depend upon time during the modulating-frequency cycle (Fig. 11-25). Peaks of carrier voltage touch the envelope many times during the period of decrease of the audio cycle. At any one of these times, it is necessary that the voltage across C decrease at least as rapidly as the envelope in order to avoid the condition represented by the dotted exponential decay curve of Fig. 11-25 and known as diagonal clipping. Since the capacitor voltage exceeds the peak carrier voltages occurring during the time interval between points a and b (Fig. 11-25), the tube does not conduct, and the output voltage does not reproduce the modulating wave form so that distortion results. If at some time during the period of decrease of the voltage $V_e = A_c(1 + m_a \cos \omega_m t)$ when the tube current becomes zero the voltage across capacitance C is V_a, then before conduction is resumed near the peak of the next positive radio-frequency half-cycle, the output voltage V is given by

$$V = V_a \epsilon^{-t'/RC} \quad (11\text{-}73)$$

where

$$t' = t - t_a \quad (11\text{-}74)$$

Since

$$dV/dt = -(1/RC) V_a \epsilon^{-t'/RC} \quad (11\text{-}75)$$

and since it is required that

$$V_a \epsilon^{-(t-t_a)/RC} = A_c(1 + m_a \cos \omega_m t) \quad (11\text{-}76)$$

for $t > t_a$ in order to reproduce the envelope, then

$$dV/dt = -A_c(1 + m_a \cos \omega_m t)/RC \quad (11\text{-}77)$$

follows from Eq. 11-76 substituted in Eq. 11-75. From Eqs. 11-72 and 11-77, the rate of fall of envelope and capacitor voltage will be the same if

$$\omega_m A_c m_a \sin \omega_m t = A_c(1 + m_a \cos \omega_m t)/RC$$

from which

$$\omega_m RC = \frac{1 + m_a \cos \omega_m t}{m_a \sin \omega_m t} \quad (11\text{-}78)$$

Equation 11-78 may be regarded as affording a maximum value of the

product RC, since, the larger the product RC, the slower the rate of capacitor discharge. The expression on the right side of Eq. 11-78 has a maximum value for t such that $\omega_m t = \theta$, or

$$\cos \theta = -m_a$$

which, from Fig. 11-25, requires that θ lie in the range 90 to 180°. Thus

$$\sin \theta = +\sqrt{1 - m_a^2} \tag{11-79}$$

and

$$\omega_m RC = \frac{1 - m_a^2}{m_a\sqrt{1 - m_a^2}} = \sqrt{\frac{1}{m_a^2} - 1} \tag{11-80}$$

It would appear from Eq. 11-80 that the diode detector cannot cope with a signal for which $m_a = 1$. However, for the frequently used values of $C = 100\ \mu\text{f}$ and $R = 250{,}000$ ohms, and at $f_m = 5000$ cps, $m_a = 0.786$. At $f_m = 796$ cps, $m_a = 0.994$. Thus, this combination of values might be satisfactory for frequencies less than 5000 cps.

The second circuit requirement is that the impedance of the detector load circuit at modulating frequencies should differ as little as possible from its resistance to direct current. The impedance at modulating frequency of the load circuit of Fig. 11-21 is approximately $R' = R_1R_2/(R_1 + R_2)$, provided the reactances of C_1 and C_2 are such that these elements may be neglected. The impedance at d-c is R_1. The average direct voltage across the load, as obtained from Fig. 11-25, has a magnitude equal to A_c. The peak variation from average of the modulation voltage is m_aA_c. The peak variation from average of the sinusoidal modulating voltage cannot exceed the average without introducing distortion, because the negative peaks would dip below the axis, and clipping would result since the tube does not conduct current in the inverse direction. Again, there is imposed a restriction on m_a since, to avoid distortion due to clipping,

$$m_aA_c/R' \leqq A_c/R_1$$

or

$$m_a \leqq \frac{R'}{R_1} = \frac{R_2}{R_1 + R_2} = \frac{1}{1 + (R_1/R_2)} \tag{11-81}$$

The requirement $R_1 \ll R_2$ is difficult to meet since R_2 is limited by requirements at the grid of the amplifier and R_1 cannot be greatly reduced without lowering the output voltage of the detector. A compromise is

indicated, and may be secured by use of the circuit of Fig. 11-26 where an additional resistance R_3 is introduced in series with R_1. The max-

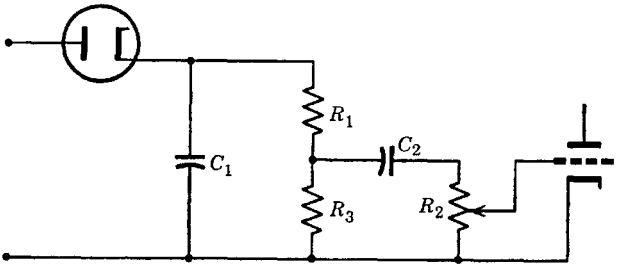

FIG. 11-26. Detector load and coupling circuit for reducing distortion.

imum value of m_a (which, according to Eq. 11-81, is the ratio of modulating a-c impedance to d-c resistance) now becomes

$$m_a \leqq \frac{R_1 + R_2R_3/(R_2 + R_3)}{R_1 + R_3} \tag{11-82}$$

and may be written as

$$m_a \leqq \frac{1}{1 + R_3^2/(R_1R_2 + R_1R_3 + R_2R_3)} \tag{11-83}$$

It is possible for m_a to approach unity if R_3 is small and R_1 large, and thus the d-c resistance of the load is kept large.

A completely mathematical analysis of the linear diode detector based upon an assumed linear diode characteristic has been developed [10] and should be of interest to students who wish to pursue the subject further.

11-11. Receivers for AM Waves

The problem of tuning AM receivers and of providing the necessary over-all radio-frequency gain has led to the almost universal use of the superheterodyne system. The tuning problem involves the simultaneous adjustment of the tuned circuits of one or more stages of radio-frequency amplification which precede the detector in addition to detector input circuit tuning. The 9-to-1 variation in tuning capacitance C necessary to produce the 3-to-1 variation of resonant frequency in the range 550 to 1650 kc greatly affects the bandwidth unless the equivalent shunt conductance G_{eq} is varied such that G_{eq}/C remains constant. But, if G_{eq} varies, so does the gain at resonance. These difficulties have been

[10] See, for example, W. L. Everitt, *Communication Engineering*, pp. 427–433, McGraw-Hill Book Co. (1937).

avoided by the almost universal use of the heterodyne principle, which involves the generation by the receiver itself of a radio frequency which may be tuned or adjusted as desired. The local oscillator which supplies the locally generated radio frequency is tuned to a frequency f_x such that the difference between f_x and the carrier frequency f_c is always the same, whatever the value of f_c. The difference frequency, $f_x - f_c$, is known as the intermediate frequency (or i-f) and may be designated f_i. The usually chosen value of f_i in the commercial broadcast band is 465 kc. Thus, the required frequency variation of the local oscillator is from 1015 to 2115 kc in order to supply a constant difference of 465 kc when combined with any signal or carrier frequency in the range 550 to 1650

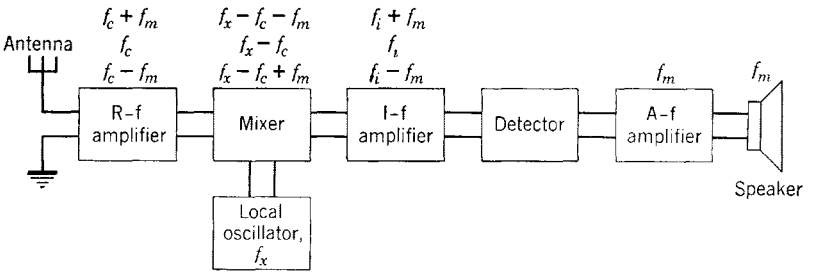

FIG. 11-27. Block diagram of a superheterodyne receiver.

kc. The same difference could be achieved if the local oscillator worked over the range 85 to 1185 kc, but the percentage change in frequency would be much greater, involving a tremendously larger over-all tuning capacitor variation.

The operation of a superheterodyne receiver is illustrated by the use of the component-block diagram of Fig. 11-27. All carriers and their sidebands exist as induced voltages in the antenna. The radio-frequency amplifier and the antenna circuits are tuned to a selected carrier, and the same adjustment simultaneously tunes the local oscillator to a frequency 465 kc above that of the selected carrier. The mixer is a component, thus far not discussed, which combines the frequencies f_x, f_c, $f_c + f_m$, and $f_c - f_m$ and produces the difference frequencies $f_x - f_c$, $f_x - (f_c + f_m)$ and $f_x - (f_c - f_m)$ at the mixer output. The input to the intermediate-frequency amplifier is then a band of frequencies $f_i + f_m$, $f_i - f_m$ centered around the same intermediate frequency, f_i, whatever the signal. Thus the intermediate-frequency amplifier may be designed with fixed tuning and for high gain and fixed bandwidth. Doubly tuned circuits are used to provide the band-pass characteristic discussed in Chapter 8. The intermediate-frequency amplifier provides voltage of the proper magnitude for the detector, usually of the linear

diode type. The detector, as already shown, again translates the frequency to the audio- or modulating-frequency range and eliminates the carrier, providing only modulating frequencies f_m at its output for audio amplification.

Components of the receiver of Fig. 11-27 have been considered in previous chapters. The audio-frequency amplifier was discussed in Chapters 3 and 4, the radio-frequency amplifier in Chapter 8, the oscillator in Chapter 10, and the linear AM detector in the present chapter. The frequency-shifting device as a modulator has also been discussed in the present chapter, but frequency changing as usually accomplished in a mixer or frequency converter requires additional discussion.

11-12. The Heterodyne Oscillator

The adjective "heterodyne" has been defined by Webster as "pertaining to the production of a difference frequency between two radio frequencies." The heterodyne oscillator is a generator of audio- or of radio-frequency voltage obtained as the difference between two frequencies. It is perhaps better known as a beat-frequency oscillator.

The beat-frequency or heterodyne oscillator was not discussed in Chapter 10 because it depends functionally upon the process of modulation or of demodulation. It may appropriately be included here as an introduction to the use of difference frequencies in the superheterodyne receiver.

If two alternating sinusoidal voltages of slightly different frequencies are added together, the resulting wave form, although somewhat resembling the wave form of a modulated wave, does not contain a new frequency. The frequencies present in the additively synthesized wave are merely those of the two components. However, if the synthesized wave is applied to a nonlinear device for which the response current is related to the applied voltage by a power series such as

$$i_p = C_1 e_g + C_2 e_g^2 + C_3 e_g^3 + \cdots + C_n e_g^n + \cdots \qquad (11\text{-}84)$$

then, as shown in Chapter 2, new frequencies result from the terms involving products. A modulator or detector characteristic (of response current as a function of applied voltage) which can be approximated by the first two terms of Eq. 11-84 is called a square law characteristic.

The heterodyne principle is illustrated in the circuit of the beat-frequency oscillator (Fig. 11-28). The complete oscillator circuit would involve two oscillators of outputs $e_1 = E_{m1} \cos \omega_1 t$ and $e_2 = E_{m2} \cos \omega_2 t$, a demodulator (or modulator), and an amplifier at the output of the

demodulator. The demodulator portion is shown in Fig. 11-28 and consists of a pentode operating in the nonlinear region of its characteristic. The load circuit consists of a parallel combination of R and C of such magnitudes that the output voltage at the difference frequency $\omega_1 - \omega_2$ far exceeds that at the sum of $(\omega_1 + \omega_2)$, for which C provides a low-impedance by-pass.

The frequencies of interest at the output (Fig. 11-28) are obtained from the second-degree term of Eq. 11-84. However, it may be worth

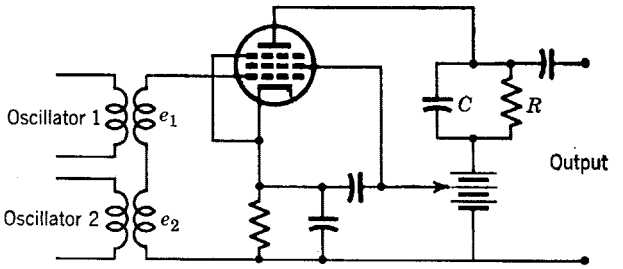

FIG. 11-28. Demodulator portion of a heterodyne or beat-frequency oscillator.

while to examine the frequencies that result from other terms as well. In Fig. 11-28, the a-c component of grid voltage is given by

$$e_g = e_1 + e_2 = E_{m1} \cos \omega_1 t + E_{m2} \cos \omega_2 t \tag{11-85}$$

From Eq. 11-84, the corresponding plate current as obtained from the first three terms only is

$$\begin{aligned} i_p = {} & (\tfrac{1}{2}C_1{E_{m1}}^2 + \tfrac{1}{2}C_2{E_{m2}}^2) + (C_1E_{m1} \\ & + \tfrac{3}{4}C_3{E_{m1}}^3 + \tfrac{3}{2}C_3E_{m1}{E_{m2}}^2) \cos \omega_1 t \\ & + (C_2E_{m2} + \tfrac{3}{4}C_3{E_{m2}}^3 + \tfrac{3}{2}C_3{E_{m1}}^2E_{m2}) \cos \omega_2 t \\ & + \tfrac{1}{2}C_2{E_{m1}}^2 \cos 2\omega_1 t + \tfrac{1}{2}C_2{E_{m2}}^2 \cos 2\omega_2 t \\ & + \tfrac{1}{4}C_3{E_{m1}}^3 \cos 3\omega_1 t + \tfrac{1}{4}C_3{E_{m2}}^3 \cos 3\omega_2 t \\ & + C_2E_{m1}E_{m2} \cos (\omega_1 + \omega_2)t + C_2E_{m1}E_{m2} \cos (\omega_1 - \omega_2)t \\ & + \tfrac{3}{4}C_3{E_{m1}}^2E_{m2} \cos (2\omega_1 + \omega_2)t \\ & + \tfrac{3}{4}C_3{E_{m1}}^2E_{m2} \cos (2\omega_1 - \omega_2)t \\ & + \tfrac{3}{4}C_3E_{m1}{E_{m2}}^2 \cos (2\omega_2 + \omega_1)t \\ & + \tfrac{3}{4}C_3E_{m1}{E_{m2}}^2 \cos (2\omega_2 - \omega_1)t \end{aligned} \tag{11-86}$$

It should be observed that the nonlinearity of the tube-response char-

acteristic has introduced the following frequencies not present in the original oscillator input voltages:

$$2\omega_1,\ 2\omega_2,\ 3\omega_1,\ 3\omega_2,\ \omega_1 + \omega_2,\ \omega_1 - \omega_2,\ 2\omega_1 + \omega_2$$

$$2\omega_1 - \omega_2,\ 2\omega_2 + \omega_1,\ 2\omega_2 - \omega_1$$

For the case of a beat-frequency audio oscillator, ω_1 and ω_2 are both radio frequencies, and so are every other one of the frequencies in the foregoing list except $(\omega_1 - \omega_2)$. Therefore, the condenser C by-passes all but the difference frequency $(\omega_1 - \omega_2)$, and the output voltage amplitude at $(\omega_1 - \omega_2)$ is the only appreciable output.

11-13. Mixers and Frequency Converters

The Institute of Radio Engineers Standards on Electron Tubes, 1950, provides the following pertinent definitions of terms useful in the discussion of the mixers and frequency converters as used in superheterodyne receivers:

1. *Conversion Transducer.* An electric transducer in which the input and output frequencies are different. Note. If the frequency-changing property of a conversion transducer depends upon a generator of frequency different from that of the input or output frequencies, the frequency and voltage or power of this generator are parameters of the conversion transducer.

2. *Heterodyne Conversion Transducer* (converter). A conversion transducer in which the output frequency is the sum or difference of the input frequency and an integral multiple of a local oscillator frequency. Note. The frequency and voltage or power of the local oscillator are parameters of the conversion transducer. Ordinarily, the output signal amplitude is a linear function of the input signal amplitude over its useful operating range.

3. *Mixer Tube.* An electron tube that performs only the frequency-conversion function of a heterodyne conversion transducer when it is supplied with voltage or power from an external oscillator.

4. *Converter Tube.* An electron tube that combines the mixer and local-oscillator functions of a heterodyne conversion transducer.

5. *Conversion Transconductance* (of a heterodyne conversion transducer). The quotient of the magnitude of the desired output-frequency component of current by the magnitude of the input-frequency (signal) component of voltage when the impedance of the output external termination is negligible for all of the (other) frequencies which may affect the result.

To the foregoing definitions, there may be added the statement that the combination of signal and local oscillator frequencies in order to

produce an intermediate frequency may be thought of as modulation, has been referred to frequently as detection (the first detector), but is now known as frequency conversion. The theory of frequency conversion has been dealt with in the literature by numerous writers. It has been shown [11] that the general principles of modulation or frequency conversion by applying signal and local oscillator voltages on the same or different grids of the conversion transducer are the same for all types of tubes. The determination of the conversion transconductance may be accomplished by use of a curve of signal electrode transconductance as a function of local oscillator voltage. Such a curve is analogous to the curve of Fig. 11-14 except that the transconductance is represented as a function of time and is then analyzed from the experimental characteristic by Fourier analysis for the nth-harmonic component at local oscillator frequency as expressed in the relations [11]

$$g_m = a_o + \sum_{n=1}^{\infty} a_n \cos n\omega_0 t \tag{11-87}$$

$$\begin{aligned} i_p &= g_m E_{ms} \cos \omega_s t \\ &= a_o E_{ms} \cos \omega_s t + \tfrac{1}{2} E_{ms} \sum_{n=1}^{\infty} a_n \cos (n\omega_0 + \omega_s)t \\ &\quad + \tfrac{1}{2} E_{ms} \sum_{n=1}^{\infty} a_n \cos (n\omega_0 - \omega_s)t \end{aligned} \tag{11-88}$$

$$\begin{aligned} g_{cn} &= I_{m(n\omega_0 - \omega_s)}/E_{ms} = \tfrac{1}{2} a_n \\ &= \frac{1}{2}\left[\frac{1}{\pi}\int_{-\pi}^{\pi} g_m \cos n\omega_0 t \, d(\omega_0 t)\right] \end{aligned} \tag{11-89}$$

It is assumed in this analysis that the signal voltage is very small compared with the local oscillator voltage. The signal voltage is $e_s = E_m \cos \omega_s t$; the local oscillator angular frequency is $n\omega_0$. The conversion transconductance at intermediate angular frequency $\omega_i = (n\omega_0 - \omega_s)$ is given by Eq. 11-89.

Mixing and conversion circuits have been described, using diodes, triodes, tetrodes, pentodes, hexodes, heptodes, and octodes. Modern superheterodyne receivers use the heptode or pentagrid converter, but early superheterodynes used tetrodes and pentodes. A circuit in which the local oscillator voltage is derived from a separate oscillator is shown

[11] E. W. Herold, The Operation of Frequency Converters and Mixers for Superheterodyne Reception, *Proc. IRE*, **30**, 84 (Feb. 1942).

in Fig. 11-29. The tube, type 6SA7, is a pentagrid converter with grids 2 and 4 serving as screen grids, grid 5 as a suppressor. The signal voltage e_s is applied between grid 3 and cathode; the local oscillator voltage $e_{n\omega_0}$ is applied between grid 1 and cathode and modulates the electron stream. Grids 3, 4, and 5 and the plate constitute a pentode for which the electron source is the modulated space-charge cloud of electrons

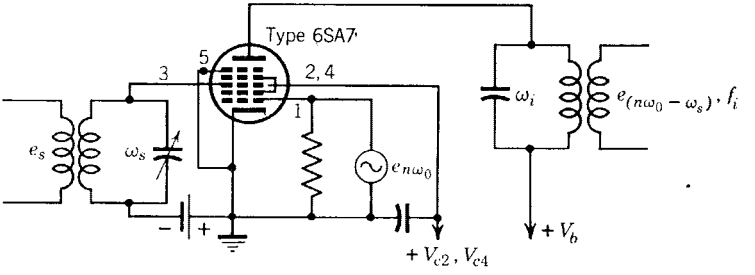

FIG. 11-29. A pentagrid mixer circuit using a separate, external local oscillator.

which have passed grid 2. Screen grid 2 located between grid 1 (the modulator grid) and grid 3 (the input grid) accelerates electron flow and also prevents coupling between the modulator and input grids. The same tube may be used in a self-oscillating circuit as shown in Fig. 11-30. Here the frequency-converter tube can itself supply the local oscillator frequency and mix it with the radio input frequency to provide the

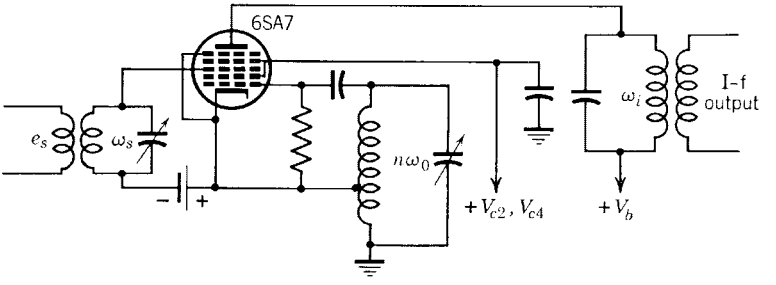

FIG. 11-30. Mixer and local oscillator functions combined in heterodyne conversion transducer.

desired intermediate frequency. The oscillator will be recognized as the Hartley circuit.

Another, somewhat different heterodyne conversion transducer circuit which uses a pentagrid converter is shown in Fig. 11-31. Grids 1 and 2 with the cathode are connected in a tuned-grid triode-oscillator circuit, with grid 2 supplying a positive voltage. The triode-oscillator

circuit supplies to the region of grid 4 through screen grid 3 an electron stream varying at oscillator frequency. An additional signal is imposed

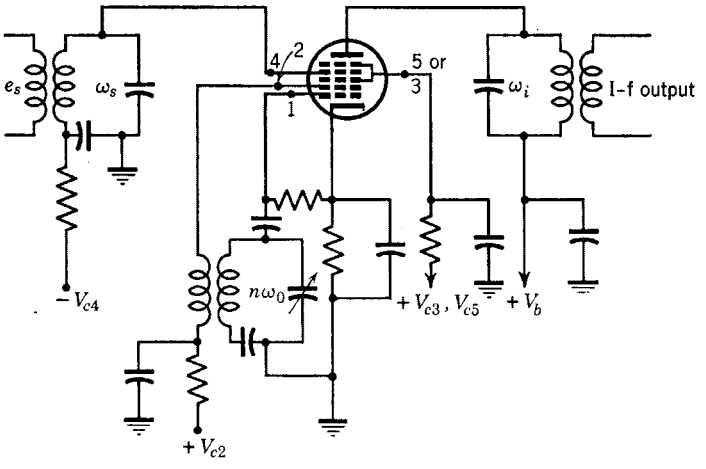

FIG. 11-31. Pentagrid converter.

upon the electron stream by the input radio-frequency signal voltage on grid 4, so that the plate-current variations are the result of the combination of oscillator and signal frequencies. Grids 3 and 5 accelerate the electron stream and, in addition, shield the signal grid, 4, from the other electrodes.

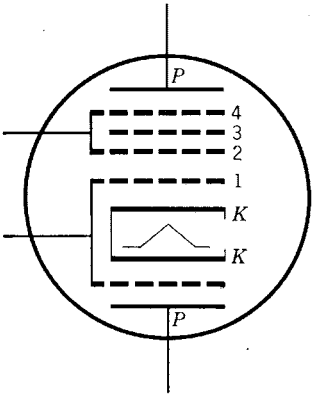

FIG. 11-32. Electrode arrangement of the triode-hexode converter, 6K8.

The pentagrid mixer tube and circuit of Fig. 11-29 and the converter circuit of Fig. 11-30 will operate effectively at higher frequencies than is possible with the pentagrid converter circuit of Fig. 11-31 because of better isolation of signal and oscillation sections of the tube. A combination of triode-hexode, for example, the 6K8 shown schematically in Fig. 11-32, can be used to cover an extremely wide range of frequencies and is used in all-wave receivers. Isolation of oscillator from mixer section is achieved by using two electron streams derived from the two sides of a cathode sleeve. The grid of the triode oscillator section at the bottom (Fig. 11-32) is connected internally to the grid of the hexode mixer section. The hexode unit uses two screen grids, 2 and 4, connected together, and the radio-frequency signal

is applied between hexode grid 3 and the cathode. The oscillator frequency from the triode section is transferred to the hexode mixer section through hexode grid 1.

11-14. Detection of FM Waves

Receivers for FM waves are similar to those for AM in respect to radio-frequency amplifier, local oscillator and frequency converter (two converters may be used to produce a final intermediate frequency in

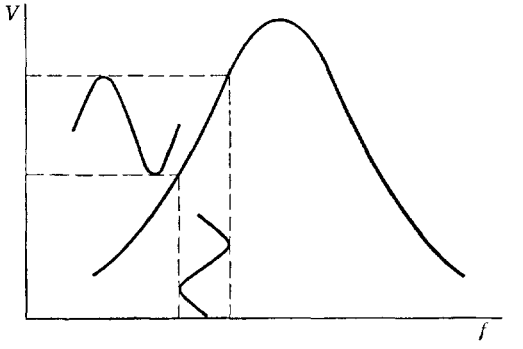

FIG. 11-33. Use of a resonance, characteristic of a tuned circuit as a discriminator.

two stages), and intermediate-frequency amplifier. The stages following the intermediate-frequency amplifier, however, must convert a frequency-varying wave of constant amplitude to an amplitude-varying wave at audio or signal frequency as input to an audio-amplifier stage. Such a requirement results in one or more component stages which are peculiar to the FM receiver.

Noise, including static and interference from other electric equipment, modifies or amplitude-modulates an AM wave and is received and converted into audio output along with the signal in an AM receiver. The noise-free advantages of frequency modulation are achieved partly by virtue of complete freedom from amplitude variations of the radio-frequency carrier. In order to eliminate any amplitude variations that may exist, a device known as a limiter is used in many FM receivers immediately following the intermediate-frequency amplifier. The limiter consists merely of a tube circuit which, by virtue of a dynamic characteristic that is flat on each end, passes only a given amplitude. Another FM feature is the fact that any frequency or frequency variation of amplitude less than half the desired signal frequency amplitude will not produce interference at the receiver output. For these reasons, much greater gain may be used in FM receivers without excessive noise being produced in the output.

The conversion from frequency to amplitude modulation and frequency translation to the audio or signal range is accomplished by a unit known as a discriminator. One method of converting from frequency to amplitude variations involves the use of a portion of a resonance curve, as shown by Fig. 11-33, where a sinusoidal variation of frequency is shown converted by the voltage resonance characteristic of a tuned circuit into voltage or amplitude variations. This method is not too useful because of the nonlinearity of the tuned-circuit characteristic. Two frequently used practical discriminator circuits are discussed in the following section.

11-15. FM Discriminator Circuits

The FM discriminator combines the functions of conversion to amplitude modulation with detection. Two types of FM detectors are to be described. The first, shown in Fig. 11-34, involves a pentode double-

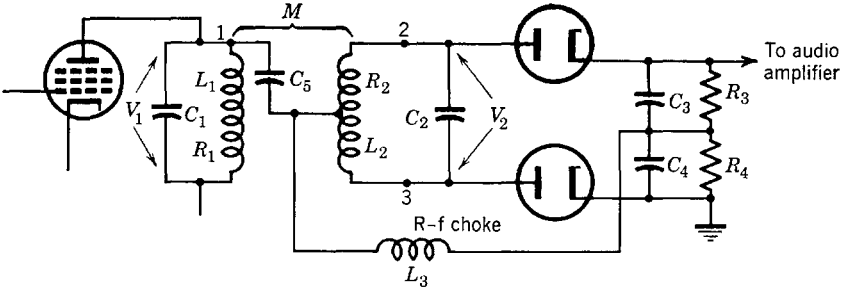

FIG. 11-34. A practical discriminator circuit.

tuned transformer-coupled amplifier circuit and two diodes used as detectors. Capacitors C_1 and C_2 are tuning condensers; at the center frequency, f_0, $\omega_0 L_1 = 1/\omega_0 C_1$; $\omega_0 L_2 = 1/\omega_0 C_2$; C_5 is a by-pass of negligible reactance for intermediate frequency; C_3 and C_4 are also adequate by-passes for intermediate frequency. Inductance L_3 is a radio-frequency choke. Tube connections are omitted, but class-A operation of the pentode is assumed. The equivalent a-c circuit is given by Fig. 11-35. The various voltages are shown on the circuit diagram: V_1 is the input voltage with respect to ground and appears across the radio-frequency choke if the reactance of C_4 is negligible; V_{12} and V_{13} are the voltages across the two halves of the transformer secondary; V_3 and V_4 are direct voltages across resistors R_3 and R_4, and $R_3 = R_4$; $V_3 = I_2 R_3$; $V_4 = I_3 R_4$; the output voltage $V_o = V_3 - V_4$. A qualitative explanation of the circuit behavior may be given in terms of the parameters of the circuit with the help of a vector diagram.

The voltage E_i is the input voltage at the grid of the pentode. The frequency of the voltage E_i is centered about the intermediate-frequency center frequency but varies on either side of this frequency f_0 by the

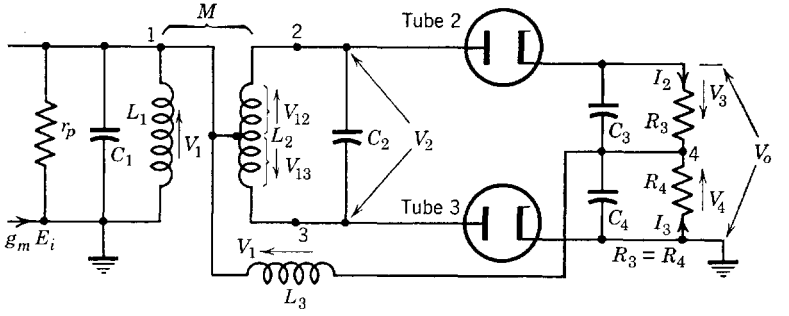

FIG. 11-35. Equivalent a-c circuit of the discriminator of Fig. 12-34.

half bandwidth necessary to contain all the signal frequency spectrum. At f_0, both primary and secondary transformer circuits are resonant as already specified. It will be shown that, to a good approximation, voltage V_1 and V_2 are in phase quadrature at $f = f_0$; since $V_2 = V_{13} - V_{12}$, the phase relations are as shown by the vector diagram of Fig. 11-36*a*.

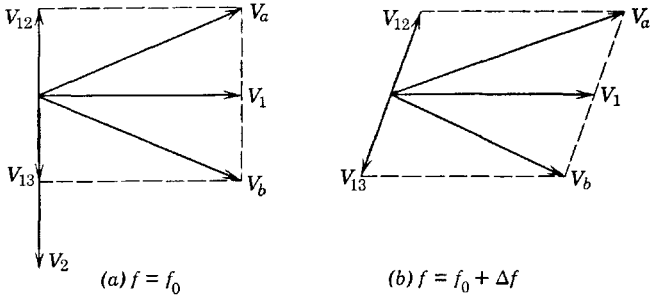

FIG. 11-36. Vector diagrams showing the phase relations of voltages on the r-f side of the detector of Fig. 12-35.

The voltages producing current in the diode detectors as obtained by inspection of the circuit (Fig. 11-35) are $V_a = V_1 + V_{12}$ across points 2 and 4, including tube 2, and $V_b = V_1 + V_{13}$ across 3 and 4, including tube 3. These voltages are shown for $f = f_0$ in Fig. 11-36*a*, and are equal since the magnitudes of V_{12} and V_{13} are equal. Therefore, for identical diodes, the output voltages V_3 and V_4 are equal, and $V_o = V_3 - V_4 = 0$ at $f = f_0$, since on the d-c side of the rectifier V_3 and V_4 are direct voltages and phase is not involved.

At frequencies off resonance, V_2 is no longer in phase quadrature with V_1. The angular deviation from phase quadrature is dependent upon the frequency deviation from resonance. Therefore, as shown by Fig. 11-36*b*, for a frequency on one side of resonance, V_a becomes greater in magnitude than V_b; therefore, $V_3 > V_4$ and $V_3 - V_4$ is a positive voltage. For a frequency on the other side of resonance, the reverse

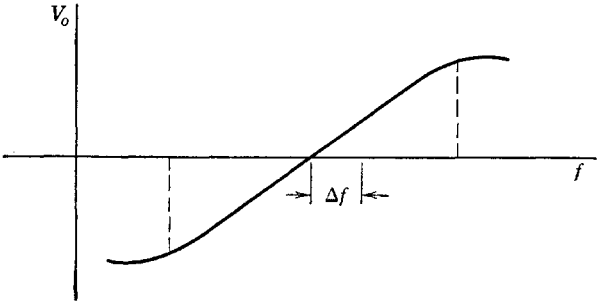

FIG. 11-37. Discriminator or FM-detector output characteristic.

condition is true so that $|V_b| > |V_a|$, $V_3 < V_4$, and $V_3 - V_4$ is a negative voltage. As the frequency varies above and below resonance, the magnitude and polarity of the voltage V_o will also vary, translating frequency variations into output voltage variations as shown approximately by the curve of Fig. 11-37. The discriminator characteristic of Fig. 11-37 is linear over a certain range of frequency. If this range is

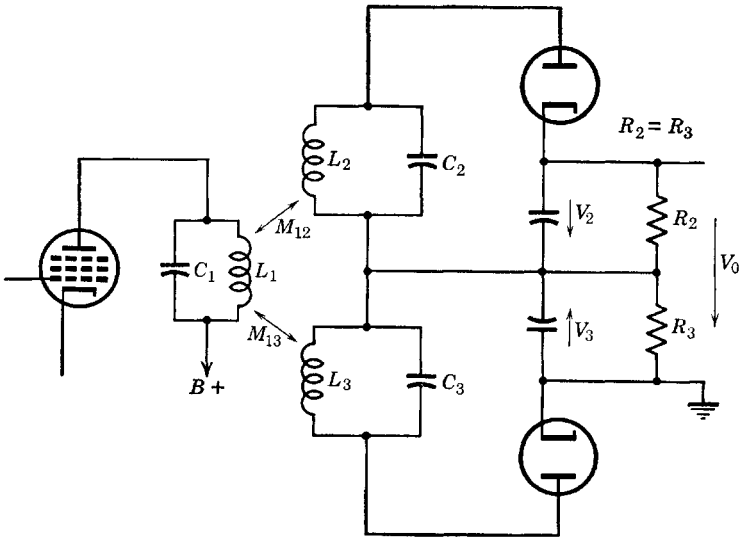

FIG. 11-38. FM discriminator using two stagger-tuned circuits.

sufficient to include the FM frequency spectrum, the output voltage will be a faithful replica of the signal voltage.

A second practical method of FM detection is illustrated by the circuit of Fig. 11-38, which involves three tuned circuits. The input circuit, L_1–C_1, is tuned to the center intermediate frequency f_0; the L_2–C_2

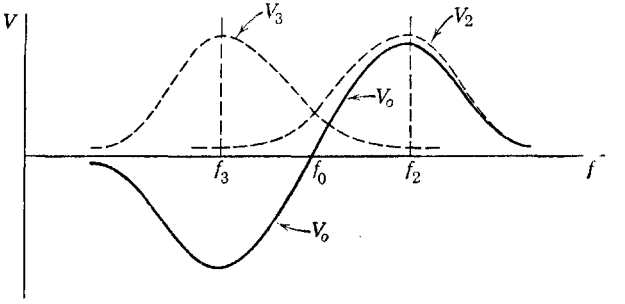

FIG. 11-39. Response characteristics of the diodes of Fig. 11-38 and their difference, V_0

circuit is tuned to a frequency somewhat higher, the L_3–C_3 circuit is tuned to a frequency somewhat lower than f_0. The result is that the diodes produce outputs across their respective load resistors R_2 and R_3 which have maximum values at different frequencies, as shown by the dotted curves of Fig. 11-39. The voltage V_0 is the difference, $V_2 - V_3$, of the diode outputs, and is shown by the full-line curve of Fig. 11-39. It has been shown experimentally [12] that, if the Q's of the secondary circuits are each twice the Q's of the primary, which in turn should be equal to the ratio of carrier frequency to $3\Delta f$, where Δf is the deviation from the mean frequency, then the detector response (Fig. 11-39) will be linear over most of the frequency deviation between f_2 and f_3.

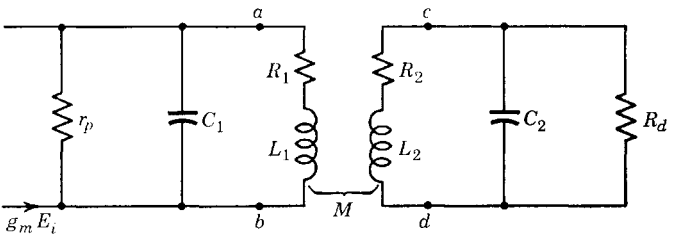

FIG. 11-40. Equivalent a-c circuit of Fig. 11-34 without L_3

11-16. Analysis of an FM Discriminator Circuit

The equivalent circuit of the discriminator of Figs. 11-34 and 11-35 has been redrawn in Fig. 11-40, with the inductance L_3 omitted. The re-

[12] M. G. Crosby, *RCA Review*, **5**, 89 (July 1940).

sistance R_d replaces the diode circuit and its loading. Coil resistances R_1 and R_2 are shown in the equivalent circuit of Fig. 11-40 but with high Q coils assumed, R_1 and R_2 will be neglected in the circuit analysis to follow.

The circuit to the left of terminals a–b may be simplified for analysis by the use of Thevenin's theorem. The impedance looking to the left at a–b is $Z_g = (r_p - jr_p{}^2\omega C_1)/(\omega^2 C_1{}^2 r_p{}^2 + 1)$, which reduces to

$$Z_g = 1/\omega_c{}^2 C_1{}^2 r_p - j(1/\omega C_1) \tag{11-90}$$

if $\omega C_1 r_p \gg 1$; since a pentode is used, $r_p \gg (1/\omega C_1)$ so that the approximation is justified. Similarly the impedance Z_{cd} looking toward the diode load at terminals c–d is given by

$$Z_{cd} = 1/\omega^2 C_2{}^2 R_d - j(1/\omega C_2) \tag{11-91}$$

provided $\qquad R_d \gg 1/\omega C_2 \quad \text{or} \quad \omega C_2 R_d \gg 1$

The revised and somewhat simplified approximate equivalent circuit

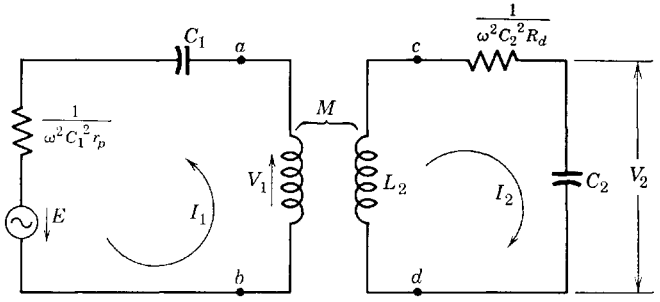

FIG. 11-41. Approximate equivalent of the circuit of Fig. 11-40.

has been drawn in Fig. 11-41. The voltage E of the equivalent Thevenin generator is given by the expression

$$E = \left[\frac{r_p(g_m E_i)}{r_p + 1/j\omega C_1}\right]\left(\frac{1}{j\omega C_1}\right)$$

$$= \frac{g_m E_i}{1 + 1/j\omega C_1 r_p}\left(\frac{1}{j\omega C_1}\right) \cong \frac{g_m E_i}{j\omega C_1} \tag{11-92}$$

where again use is made of the fact that $1/\omega C_1 r_p$ is negligible compared with unity.

It is convenient to use the fractional frequency deviation from resonance as previously defined, namely:

$$\delta = (\omega - \omega_0)/\omega_0 \quad \text{or} \quad \omega/\omega_0 = 1 + \delta \tag{11-93}$$

The impedance of the primary mesh than may be expressed as

$$\begin{aligned} Z_{11} &= R_{11} + j(\omega L_1 - 1/\omega C_1) \\ &= R_{11} + j\omega_0 L_1(\omega/\omega_0 - \omega_0/\omega) \\ &= R_{11} + j\omega_0 L_1\left(1 + \delta - \frac{1}{1+\delta}\right) \end{aligned} \tag{11-94}$$

Since $1/(1+\delta) \cong 1 - \delta$ for $\delta \ll 1$, then

$$Z_{11} = R_{11}(1 + j2\delta Q_1) \tag{11-95}$$

where
$$Q_1 = \omega_0 L_1/R_{11} \tag{11-96}$$

and
$$R_{11} = 1/\omega_0^2 C_1^2 r_p \tag{11-97}$$

Similarly, the impedance of the secondary mesh is

$$Z_{22} = R_{22}(1 + j2\delta Q_2) \tag{11-98}$$

where
$$Q_2 = \omega_0 L_2/R_{22} \tag{11-99}$$

and
$$R_{22} = 1/\omega_0^2 C_2^2 R_d \tag{11-100}$$

The mutual impedance is

$$\begin{aligned} Z_{12} &= -j\omega M = -j(\omega_0 + \Delta\omega)M \\ &= -j\omega_0(1+\delta)M \end{aligned} \tag{11-101}$$

The driving-point impedance at the terminals of the Thevenin generator is

$$\begin{aligned} Z_{11}' &= Z_{11} - Z_{12}^2/Z_{22} \\ &= R_{11}(1 + j2\delta Q_1) + \frac{\omega_0^2 M^2(1+\delta)^2}{R_{22}(1 + j2\delta Q_2)} \\ &= \frac{\omega_0 L_1}{Q_1}(1 + j2\delta Q_1) + \frac{\omega_0^2 k^2 L_1 L_2(1+2\delta)}{(\omega_0 L_2/Q_2)(1 + j2\delta Q_2)} \end{aligned} \tag{11-102}$$

where the second-order term δ^2 has been neglected. The product δk^2 is also very small since the coupling is small. Equation 11-102 may first be expressed as

$$Z_{11}' = \frac{\omega_0 L_1}{Q_1}\left[1 + j2\delta Q_1 + \frac{Q_1 Q_2(k^2 + 2\delta k^2)}{1 + j2\delta Q_2}\right]$$

and, since $2\delta k^2 \ll k^2$, a further simplification is possible so that

$$Z_{11}' = \frac{\omega_0 L_1}{Q_1}\left[1 + j2\delta Q_1 + \frac{k^2 Q_1 Q_2}{1 + j2\delta Q_2}\right] \tag{11-103}$$

The current I_1 is then easily expressed as

$$I_1 = E/Z_{11}'$$

and the voltage V_1 across terminals a–b is

$$V_1 = I_1 Z_{ab} = EZ_{ab}/Z_{11}' \tag{11-104}$$

The impedance Z_{ab} looking to the right (Fig. 11-41) is given by

$$\begin{aligned} Z_{ab} &= j\omega L_1 - Z_{12}^2/Z_{22} \\ &= j\omega_0 L_1(1 + \delta) + \frac{\omega_0^2 M^2(1 + \delta)^2 Q_2}{\omega_0 L_2(1 + j2\delta Q_2)} \\ &= j\omega_0 L_1\left[1 + \delta + \frac{k^2(1 + \delta)^2 Q_2}{j(1 + j2\delta Q_2)}\right] \end{aligned} \tag{11-105}$$

Again, neglect of second-order terms involving δ^2 and $k^2\delta$ results in simplification. Equation 11-105 after algebraic revision may be written as

$$Z_{ab} = j\omega_0 L_1\left(\frac{1 + \delta + j2\delta Q_2 - jk^2 Q_2}{1 + j2\delta Q_2}\right) \tag{11-106}$$

The equations needed for the analysis of the discriminator circuit must provide expressions for the voltages V_1 and V_2. These may be obtained more easily if equal coil Q's are assumed. Thus, with $Q_1 = Q_2 = Q$,

$$\frac{Z_{ab}}{Z_{11}'} = \frac{j(1 + \delta + j2\delta Q - jk^2 Q)Q}{(1 + j2\delta Q)^2 + k^2 Q^2} \tag{11-107}$$

so that, from Eqs. 11-104, 11-107, and 11-92,

$$V_1 = \frac{jQ(1 + \delta + j2\delta Q - jk^2 Q)g_m E_i}{[(1 + j2\delta Q)^2 + k^2 Q^2]j\omega_0 C_1(1 + \delta)}$$

and, if $k^2 Q$ is neglected,

$$V_1 \cong \frac{g_m E_i Q\omega_0 L_1(1 + j2\delta Q)}{(1 + j2\delta Q)^2 + k^2 Q^2} \tag{11-108}$$

which is the first required equation.

The expression for V_2 is next to be found. Since

$$I_2 = -\frac{I_1 Z_{12}}{Z_{22}} = \frac{V_1 j\omega_0 M(1+\delta)Q}{Z_{ab}\omega_0 L_2(1+j2\delta Q)} \tag{11-109}$$

then $$V_2 = I_2(1/j\omega C_2) = I_2/j\omega C_2(1+\delta) \tag{11-110}$$

Thus, $$V_2 = -j\left[\frac{g_m E_i Q^2 \omega_0 M}{(1+j2\delta Q)^2 + k^2Q^2}\right] \tag{11-111}$$

The phase of voltages V_1 and V_2 may be compared for any value of δ. Thus, at $f = f_0$, $\delta = 0$, and, from Eq. 11-108,

$$V_1 = g_m E_i Q \omega_0 L_1/(1+k^2Q^2) \tag{11-112}$$

and $$V_2 = -jg_m E_i Q^2 \omega_0 M/(1+k^2Q^2) \tag{11-113}$$

From Eqs. 11-112 and 11-113, it is observed that, at $f = f_0$, V_2 lags V_1 by 90° as shown by Fig. 11-36*a*. The ratio of V_2 to V_1 is

$$\frac{V_2}{V_1} = -j\frac{Q(M/L_1)}{1+j2\delta Q}$$

or $$V_2 = \frac{\left(\frac{QM}{L_1}V_1\right)\angle -90°}{1+j2\delta Q} \tag{11-114}$$

If $\delta = (f - f_0)/f_0$ is positive, $f > f_0$ and $\theta = \tan^{-1} 2\delta Q$ is a positive angle, so that the phase angle of V_2 with respect to V_1 is $(-90° - \theta)$. Thus, for $f > f_0$, V_2 lags V_1 by more than 90°, as shown in Fig. 11-36*b*. However, for frequencies below resonance, $f < f_0$ and δ is negative, so that $\theta = \tan^{-1} 2\delta Q$ is a negative angle. Let $\theta = -\phi$, where $\phi > 0$. Then the phase of V_2 becomes $(-90° + \phi)$, and V_2 lags less than 90° behind V_1.

PROBLEMS

11-1. The equation of a nonlinear triode dynamic characteristic may be expressed in power series form as

$$i_p = C_1 e_g + C_2 e_g^2 + C_3 e_g^3 + \cdots + C_n e_g^n + \cdots$$

Two alternating-voltage sources are connected in series in the grid circuit. Their voltages are, respectively:

$$e_1 = A_1 \cos \omega_c t \quad \text{and} \quad e_2 = A_2 \cos \omega_m t$$

where $\omega_c = 2\pi \cdot 10^6$ rad per sec, $\omega_m = 2\pi \cdot 10^3$ rad per sec. Using only the first three terms of the power series, obtain answers to the following:

(*a*) What terms of the series produce modulation of the output current?

(*b*) What are the frequencies present in the plate current?

(*c*) Identify carrier, upper and lower side frequencies, and distortion (undesired) components.

(*d*) Design a load circuit that would provide the necessary bandwidth, and obtain relative amplitudes referred to carrier of the component frequencies in the output load voltage.

11-2. Typical operation of a type-805 triode as a class-C amplifier is given by the manufacturer as follows:

D-c plate voltage 1250 volts
D-c grid voltage −100 volts
Peak r-f grid voltage 230 volts
Direct plate current 200 ma
Direct grid current 40 ma
Grid driving power 8.5 watts
Power output 170 watts

For the conditions given, compute (*a*) the plate dissipation rating, (*b*) the plate-circuit conversion efficiency.

11-3. The type 805 of problem 11-2 is to be 100 per cent plate-modulated by an audio source. The plate dissipation under plate modulation is not to exceed that when the tube is used as an unmodulated class-C amplifier. Compute (*a*) the impedance of the 805 plate circuit presented to the audio modulator, (*b*) the maximum allowable audio power input, with 170 watts power output.

11-4. Plate dissipation rating of a type-892-R power triode used as a class-C radio-frequency power amplifier at 800 kc and typical operating characteristics are summarized as follows: Maximum plate dissipation is 4000 watts. Typical operation is:

E_b = 10,000 volts
E_c = −1300 volts
E_{gm} = 2150 volts (peak r-f grid voltage)
I_b = 1.40 amp
I_c = 0.24 amp
Grid driving power 495 watts
Power output 10,000 watts

(*a*) If this amplifier is to be 100 per cent plate-modulated, what should be the new plate dissipation rating?

(*b*) If the output transformer is 90 per cent efficient, compute the power output.

(*c*) What should be the value of I_b as E_b is reduced to 8000 volts?

11-5. Two type-891-R tubes in push–pull operate class B and supply audio-modulating power to the class-C amplifier of problem 11-4. Typical operating values for two tubes are:

E_b = 8000 volts
E_c = −860 volts
I_b = 0.5 amp (zero signal)
I_b = 2.1 amp (maximum signal)
Peak a-f grid-to-grid voltage 2260 volts
Effective load resistance, plate-to-plate, 8000 ohms
Maximum signal driving power 50 watts
Maximum signal power output 10,000 watts

(*a*) Find the turns ratio of the output transformer of the modulator.

(*b*) Find the plate dissipation of the modulator tubes.

11-6. Assuming that average plate current and tank current are linearly related to instantaneous grid voltage for a grid-modulated amplifier, analyze the amplifier,

and obtain expressions for tank voltage, input plate power, power output, efficiency, and plate dissipation. Define all symbols.

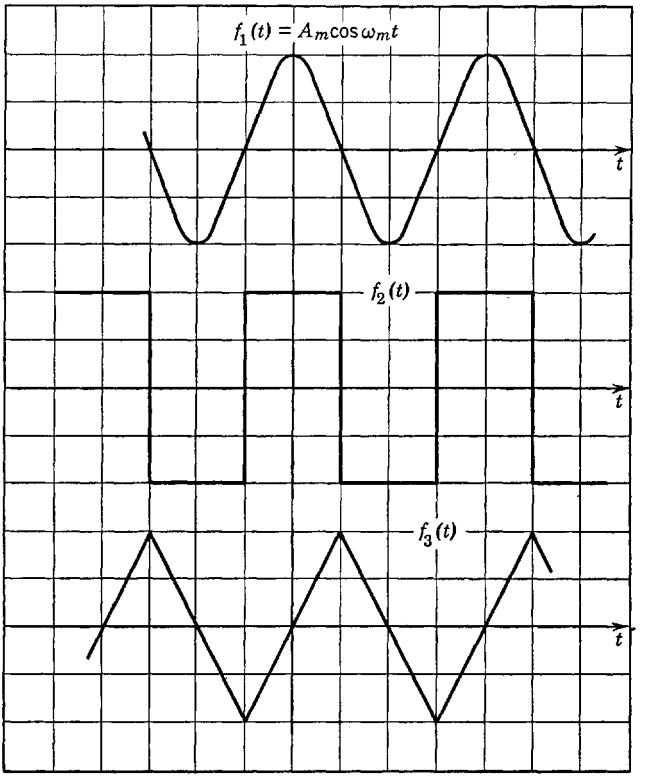

FIG. P11-7.

11-7. The sketch shows three time-varying functions, $f(t)$. Each is to be taken as a modulating wave in (*a*) phase modulation, (*b*) frequency modulation. For each case, sketch wave forms showing (1) phase deviation from $\omega_c t$, (2) frequency deviation from ω_c.

11-8. An 80-Mc carrier of unmodulated amplitude 20 volts is frequency modulated ± 75 kc by a 15-kc sinusoidal voltage of amplitude 10 volts.

(*a*) Write the equation of the instantaneous carrier voltage.

(*b*) Plot the frequency spectrum, and calculate the necessary bandwidth.

11-9. For a deviation ratio of $\delta = 5$, what percentage of the total energy of an FM wave is contained in side frequencies beyond the seventh? See Eq. 11-80.

11-10. Analyze the circuit of Fig. 11-16, and obtain an expression for the input impedance. State the requirements for a variable inductive input.

11-11. A reactance-tube circuit is shown in the accompanying diagram. Derive expressions for the resistance and for the reactance or susceptance at the input ter-

minals a–b if (a) Z_1 is a resistance R and Z_2 is an inductance L, (b) Z_1 is an inductance L and Z_2 is a resistance R.

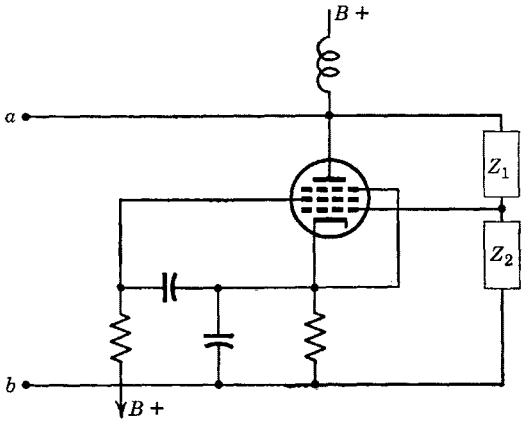

FIG. P11-11.

11-12. (a) Obtain an equivalent circuit for the reactance tube modulator involving only elements in parallel with C_t.

(b) If the g_m–e_c characteristic of the reactance-tube modulator is the same as that given by Fig. 11-14, and with $E_c = -3$ volts, $e_g = e_m = 3 \cos \omega_m t$, $f = 15{,}900$ cps, $2\pi fCR = 0.1$, design the reactance-tube circuit such that a frequency deviation of 5 per cent is possible.

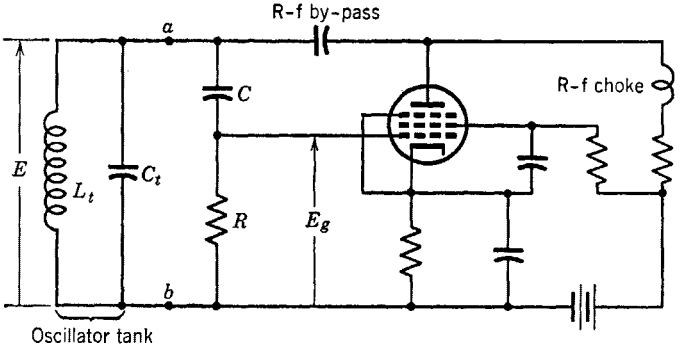

FIG. P11-12.

11-13. Obtain an expression for the instantaneous frequency of the oscillator of problem 11-12.

11-14. The output of a linear 6H6 diode detector is R–C-coupled to the input of an audio amplifier. The rms value of the unmodulated carrier voltage is 10 volts, applied at the input of the diode; R_1 (Fig. 11-21) is 200,000 ohms, and the grid-leak resistance of the amplifier input is also 200,000 ohms. The carrier is 75 per cent modulated by an audio frequency of 7960 cps.

(a) What should be the maximum value of C_1 for no distortion (Fig. 11-21)?

(b) Compute the allowable percentage modulation for no-negative peak clipping.

CHAPTER 12

CIRCUIT THEORY OF TRANSISTORS

THE TRANSISTOR, AT THE TIME THIS IS BEING WRITTEN, IS SOME THREE years old and is just at the beginning of its applicational development. It is already invading the field of the vacuum tube in low-current, low-power applications and promises to replace receiving-type vacuum tubes in scores of important applications within the next few years. This chapter will be devoted to the circuit theory of the transistor but will not completely neglect the fascinating physical theory of transistor action. In fact the chapter will begin with some of the fundamental physical concepts.

12-1. Conductors, Insulators, and Semiconductors

A brief account of the electron theory of metals serves as a convenient starting point in a presentation of the elementary physical theory of transistor behavior. Since transistors as presently constructed are tiny pieces of solid germanium with three properly connected circuit terminal wires, it may reasonably be enquired how the conducting mechanism of the solid state can perform functions that permit the transistor to amplify as does the three-electrode vacuum tube. In order to provide a satisfactory answer to such a question, it is desirable in the beginning to compare solid-state conductors, insulators, and semiconductors on the basis of energy-level diagrams.

An energy-level diagram of a metal (Fig. 12-1) is a graphical representation of energy states or levels which may be occupied by the valence or conduction electrons of the metal. At absolute zero of temperature, all valence-electron kinetic energies in a metal are represented by horizontal lines below the Fermi level. Each line corresponds to a specific level of electron kinetic energy measured in joules or in electron-volts * plotted on a vertical energy scale with its zero level as shown. The energy states available to electrons are characteristic of the

* An electron-volt is the amount of energy possessed by an electron that has been accelerated from rest by a difference of potential of one volt. It is therefore equivalent to $1.6 \cdot 10^{-19}$ joule.

crystal structure in the solid state just as the line spectrum of a luminous gas is characteristic of the gas. At zero degrees absolute, all energy levels of a metal below the Fermi level are filled. At temperatures greater than absolute zero, electrons in metals may occupy levels above the Fermi level between V_N and V_G electron volts. At sufficiently high temperatures for electrons to have kinetic energies in excess of V_G electron volts, electrons may escape from the metal. This is the mechanism of emission of electrons from heated cathodes.

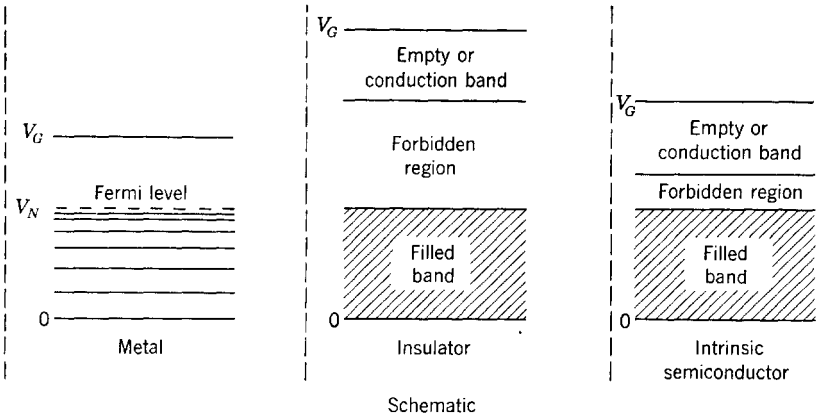

FIG. 12-1. Schematic energy-level diagrams for a metal conductor, an insulator, and a semiconductor, not to scale and not to the same scale.

The energy-level diagrams of Fig. 12-1 illustrate the differences in a metallic conductor, an insulator, and a semiconductor. There is no filled energy band in the case of the conductor. Electrons are easily displaced above the Fermi level by thermal or field energy and are free to exchange energy with applied electric fields as is necessary in electric conduction.

The number of valence electrons of an insulator is the exact value needed to fill all energy levels of the filled band completely. Also, the electron configurations are such that no energy levels are possible in a band of several electron-volts in width located just above the filled band. Therefore, it is extremely difficult to displace an electron from the filled band to the conduction band which remains empty even at fairly elevated temperatures.

The semiconductor is similar to the insulator except in the width of the forbidden region which, instead of several electron volts as for the insulator, is only about 1 electron volt wide. At absolute zero, the semiconductor is an insulator, but at sufficiently elevated temperatures

electrons from the filled band may be displaced to the conduction band. In such an event, electrons can move around in the filled band since vacancies exist there, and the electrons that have been displaced to the conduction band are free to exchange energy with the electric field so that both mechanisms contribute to conduction. In the case of the filled band, the motion of electrons in progressively filling vacancies is equivalent to a motion in the opposite direction of the vacancies that the electrons leave behind in the material. This situation leads to the concept of "hole" current which will be an important concept in transistor

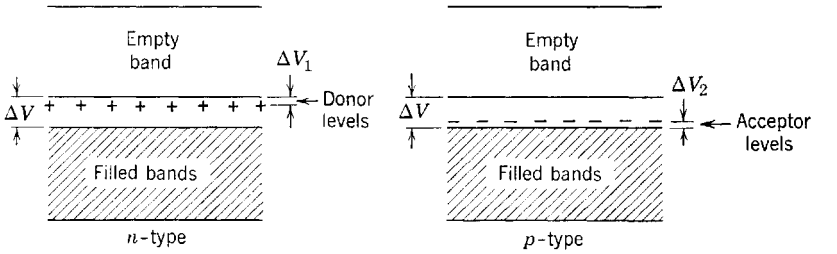

FIG. 12-2. Extrinsic semiconductors.

action. The semiconductor described by the energy-level diagram of Fig. 12-1 is referred to as intrinsic. Intrinsic semiconductors are not important as transistors.

Extrinsic semiconductors are illustrated by the diagrams of Fig. 12-2. Extrinsic semiconductors were of very great technical importance as silicon or germanium crystal diode rectifiers or detectors long before the advent of transistors. The properties of the extrinsic semiconductor depend upon the presence of small quantities of impurities within the crystal structure of the semiconductor. Wilson [1] has listed four types of such semiconductors of which two are shown in Fig. 12-2.

It will be observed that the extrinsic semiconductor has the same band structure as the intrinsic. The difference is that impurity atoms present in small numbers in the crystal lattice provide extra energy levels which lie in the normally forbidden region between a filled band and an empty band. These extra energy levels lie either very close (~ 0.1 e v) to the empty band or to the filled band. If the extra energy levels are filled at 0° K with electrons, they act as *donors* of electrons to the empty band at higher temperatures. Conduction is the result of electron motion in the empty band and is termed "*n*-type" for negative-charge carrier. The donor levels, if filled, are electrically neutral; if empty, as at normal room temperatures, each has a single charge of $+e = 1.6 \cdot 10^{-19}$ coulomb.

[1] A. H. Wilson, *Semiconduction and Metals*, pp. 45–46, Cambridge University Press, Macmillan.

The other type of extrinsic semiconductor shown in Fig. 12-2 has extra energy levels (due to impurity atoms) lying close to the filled band in the forbidden region. These levels, normally empty at 0° K, act as *acceptors* of electrons from the filled band at higher temperatures leaving empty levels or holes in that band. Conduction is now possible in the filled band because an electron may be transferred by field action into a vacant level. As an electron moves into a vacancy from left to right, the vacancy moves the same distance from right to left, and is equivalent to a positive-charge carrier moving from right to left. The conduction is said to be p-type, and holes are the carriers. A filled acceptor level has a negative charge of e coulombs but is electrically neutral when empty.[2]

It is possible by use of two different types of impurity atoms to have both donor and acceptor levels existing simultaneously in the same material. In this case conduction is both n- and p-type. Finally, it may be stated that a semiconductor that conducts by electrons in a nearly empty band is n-type; a semiconductor that conducts by hole motion in a nearly filled band is p-type. Thus the impurities provide electrons in the otherwise empty band or holes in the otherwise filled band and thus control the conductivity.

12-2. Some Quantitative Physical Data on Semiconductors

Quantitative data and orders of magnitude of physical constants of electronic semiconductors of the type discussed in Section 12-1 may be of interest at this point. Electrical resistivities of electronic semiconductors at or near room temperature fall in the range 10^2 to 10^{-6} ohm cm; at the same temperature, metals have resistivities around 10^{-5} ohm cm, and insulators vary in resistivity from 10^6 to 10^{15} ohm cm or higher.[3] One of the distinguishing differences between metal conductors and semiconductors is the dependence of resistivity on purity. The resistivity of a metal is decreased by purification, whereas the resistivity of a semiconductor is decreased by the addition of impurities.

The width of the forbidden region may vary from 0 electron volts for a conducting metal to 10 electron volts for an insulator. For silicon, a semiconductor, it is 1.2 electron volts. Pearson [3] states that the addition of 3 boron atoms for every 10,000 silicon atoms to a sample of as pure silicon as is possible to prepare reduced the resistivity by a factor of 500. The width ΔV of the forbidden region is related to the semi-

[2] Torry and Whitmer, *Crystal Rectifiers*, pp. 45–49, Radiation Laboratories Series, McGraw-Hill Book Co.

[3] G. L. Pearson, The Physics of Electronic Semiconductors, *Trans. AIEE*, **66**, 209–214 (1947).

conductor resistivity by the equation

$$\rho = A\epsilon^{\Delta V/2kT} \tag{12-1a}$$

derived by Wilson,[1] where A is a quantity varying very slowly with temperature, ρ is the resistivity in ohm centimeters, T is the temperature in degrees Kelvin, and k is Boltzmann's constant which is $8.69 \cdot 10^{-5}$ electron volts per degree. The value of ΔV may be determined from a plot of $\ln \rho$ against $1/T$ which, at sufficiently high temperatures in which conduction is intrinsic, is a straight line of slope $\Delta V/2k$. Values of ΔV given in Table 12-1 have been obtained in this manner.

TABLE 12-1

From G. L. Pearson [3]

Material	ΔV, electron volts
Diamond	7
Boron	2
Cu_2O	1.4
Silicon	1.2
Germanium	0.76

The energy differences ΔV_1 and ΔV_2 for the n- and p-type extrinsic semiconductors of Fig. 12-2 depend upon both the kinds and the amount of impurity present in the crystal structure. These differences are found to vary from 0.001 to 0.3 electron volts.

It has been shown [4] that the conductivity of a semiconductor containing holes and electrons is given by the relation

$$\gamma = e(N_e g_e + N_h g_h) \tag{12-1b}$$

where γ is the conductivity in mhos per centimeter, e is the electronic charge in coulombs, N_e and N_h are, respectively, the electron and hole concentrations per cubic centimeter, and g_e and g_h are, respectively, the electron and hole mobilities in centimeters per second per volt per centimeter.

The Hall effect has been of very great importance in the measurement of constants such as those occurring in Eq. 12-1b. If a magnetic field is applied in a direction perpendicular to the direction of flow of current in a long thin semiconductor (or conductor), the charge carriers, both electrons and holes, are crowded toward the same side of the semiconductor, and, as a result, a measurable voltage appears across the transverse dimension of the semiconductor. By measuring n- or p-type

[4] W. Shockley, *Electrons and Holes in Semiconductors*, Chaps. 1 and 8, D. Van Nostrand Co. (1950).

semiconductors at such temperatures that only one carrier type is involved, Eq. 12-1*b* for an *n*-type semiconductor becomes

$$\gamma = eN_e g_e \tag{12-1c}$$

A similar equation results for *p*-type. Such equations, combined with Hall-effect measurements and experimental determination of γ, permit the evaluation of both carrier concentration and mobility. Mobilities determined by use of the Hall effect for germanium and for silicon are as shown in Table 12-2.

TABLE 12-2

Semiconductor Material	Mobility, cm/sec per volt/cm	
	g_e	g_h
Germanium	2600 (Hall mobility)	1700
	3600 (Drift mobility)	1700
Silicon	300	100

12-3. Illustrations of the Effect of Added Impurities

Studies of the crystal formation of germanium show that the atoms are arranged [5] somewhat as shown by Fig. 12-3. Since the valence of Ge

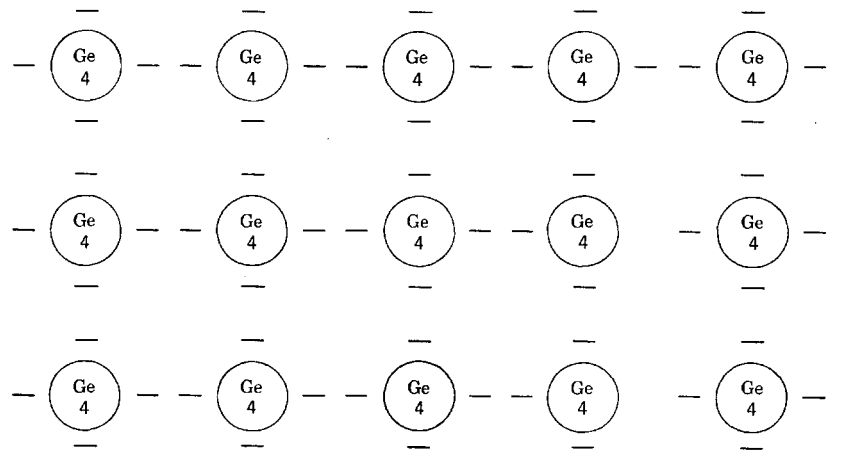

FIG. 12-3. Arrangement of atoms and electron-pair bonds in a crystal of pure germanium.

is 4, each atom has a charge of +4 and is surrounded by 4 neighbors, arranged like the bases on a baseball diamond. The bonds between neighbors are electron-pair bonds, since each Ge atom contributes 4

[5] William Shockley, Holes and Electrons, *Physics Today*, **3**, 16–24 (Oct. 1950).

electrons. This configuration is a stable one. All possible energy states are occupied, and conduction is impossible unless the valence-bond structure is altered. This may occur, either as a result of an increase of temperature or by the absorption by an electron of a photon of energy. In the case of pure Ge, an intrinsic semiconductor, this would require a wavelength of

$$\lambda = 12{,}400/0.76 = 16{,}300 \text{ A}$$

or shorter. For example, visible light of wavelength $\lambda = 6000$ A would provide an energy of

$$V_{ph} = 12{,}400/6000 = 2.06 \text{ electron-volts}$$

which is more than adequate to transfer an electron across the forbidden region and into the empty conduction band. In such an event, a hole-

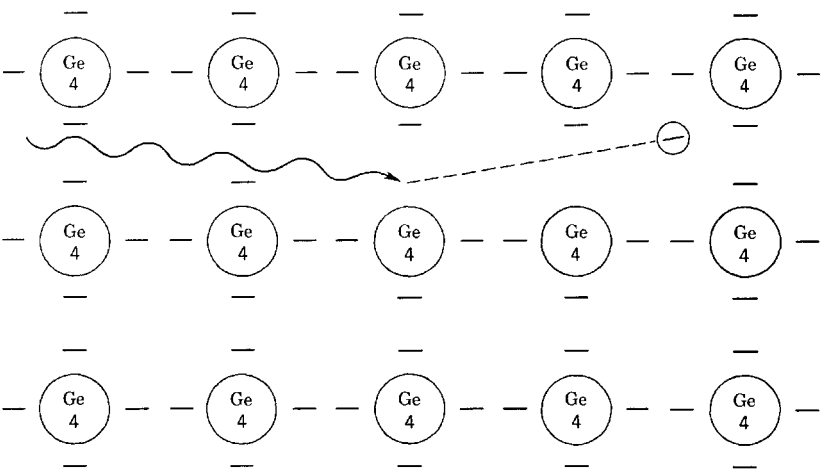

FIG. 12-4. Production of a hole-electron pair by absorption of a photon by an electron of the middle atom of the array.

electron pair is created, with a hole in the filled band and an electron in the empty band. This situation is illustrated by Fig. 12-4. The freed electron is now free to move about through the crystal. Another electron may be displaced from its position in the bonded structure and may move into the hole left by the first electron. One hole still remains, and one free electron, but both have moved. There is accordingly a net displacement of the hole, which carries a charge of $+e$. The freed electron tends to drift in a direction opposite to the direction of an applied field. Similarly, a hole tends to drift in the direction of the field, because a hole is a localized disturbance of the valence electrons. The

motion of holes and electrons have been directly observed [5] in experiments on transistor action. Thermal agitation of the crystal lattice serves continually to break up electron-pair bonds with the formation of hole-electron pairs, but the reverse process is equally rapid so that, at room temperature, a balance is reached such that the concentration of holes and electrons is sufficient to provide, for germanium, a resistivity [5] of 60 ohm cm. This is the phenomenon of hole-electron conduction in equal concentrations characteristic of intrinsic semiconductors.

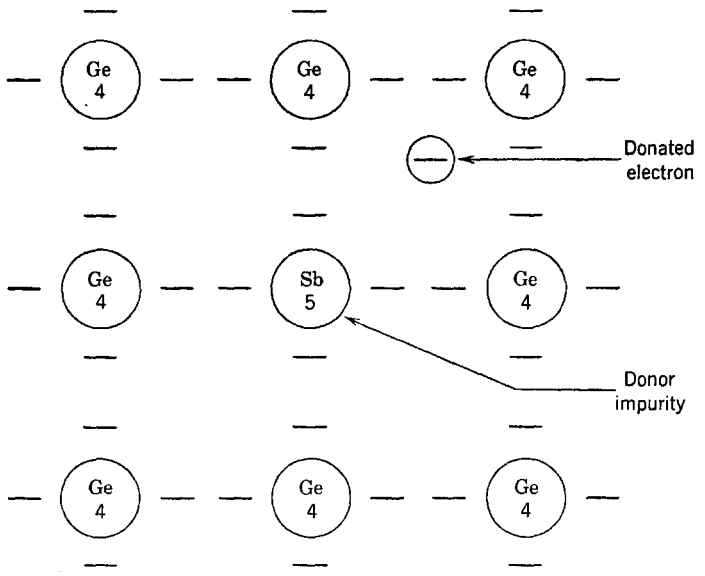

FIG. 12-5. Production of an n-type Ge semiconductor by the addition of a donor impurity of valence 5.

The extrinsic semiconductor may be similarly explained. For example, if the middle germanium atom in the array of Fig. 12-3 is replaced by an impurity atom of valence 5, for example antimony, the semiconductor becomes n-type, since the extra valence electron brought in by the antimony has no place to go and at temperatures above 0° K wanders around the crystal in the conduction band ready for acceleration by an electric field. This state of affairs is illustrated by Fig. 12-5. Similarly, if the middle germanium atom of Fig. 12-3 is replaced by a gallium atom of valence 3, p-type germanium results. The gallium atom accepts an electron in addition to its own three and becomes a negative ion at the expense of an electron from the electron-pair bond of a Ge atom. The result is a hole, as illustrated by Fig. 12-6.

It is interesting to note that, if donors and acceptors are installed in the Ge crystal lattice in equal numbers, the resulting conductivity is the same approximately as though neither were present. The explanation is that the electrons supplied by the donors combine with the holes produced by the acceptors such that the equilibrium concentration of holes and electrons is the same as that occurring as a result of thermal agitation in pure Ge.

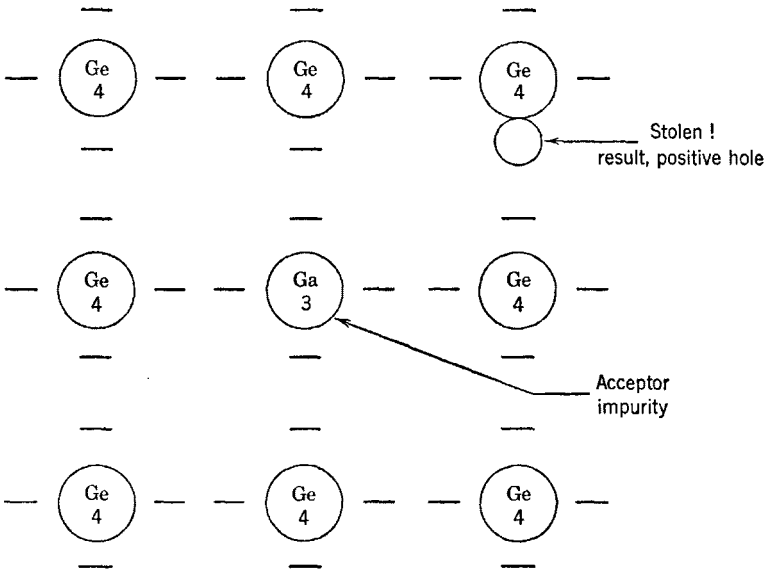

FIG. 12-6. Production of a p-type Ge semiconductor by the addition of an acceptor impurity of valence 3.

12-4. Boundary-Layer Effects in Semiconductors

The experimental fact that a metal in contact with a semiconductor can be used as a rectifier has had great commercial importance in supplying crystal rectifiers and detectors in many communication applications. The theory of point contact rectification as presently developed [6] requires the presence of a barrier layer of space charge in the semiconductor adjacent to the metal contact. The space-charge layer in n-type germanium is believed to result from positively ionized donor atoms bound in the surface layers from which the released electrons have been drained away, leaving the positive charge unneutralized. Donor ion space charge is neutralized by conduction electron space charge in the interior

[6] J. Bardeen and W. H. Brattain, Physical Principles Involved in Transistor Action, *BSTJ*, **28**, 239 (Apr. 1949).

of the material where the concentrations are equal. There is evidence that the barrier layer occurs at the surface in both silicon and germanium and that it is independent of the metal contact. A potential-energy-level diagram for a metal-semiconductor contact is curved at the boundary, as shown in Fig. 12-7, because of the space-charge layer. The height of the conduction band rises with respect to the Fermi level as the

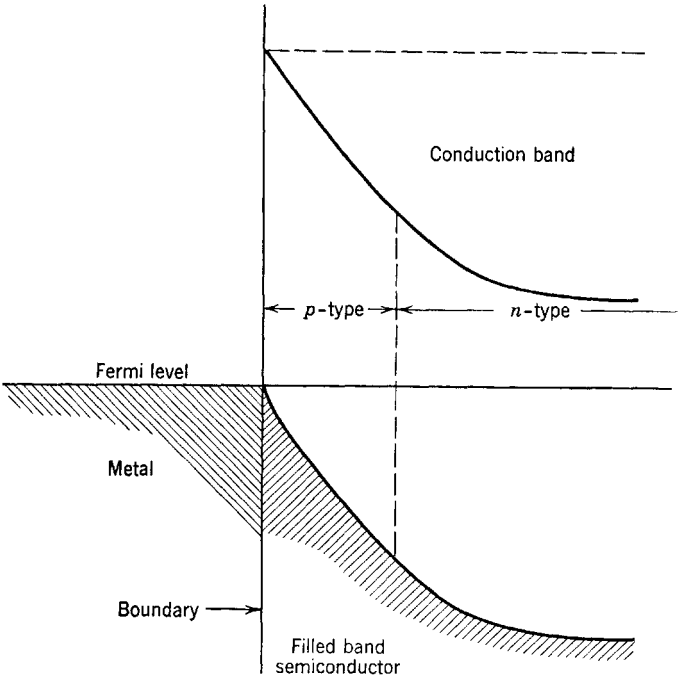

FIG. 12-7. Energy-level diagram at a contact surface between a metal and a semiconductor.

surface is approached, and there is an indicated inversion from n- to p-type. It is believed that electrons trapped in surface states on the semiconductor compensate the surface-charge layer. The theory indicates that the barrier layer is about 10^{-4} cm in thickness.

For n-type germanium, a forward voltage is such that the germanium is negative, the metal point contact positive. Such a voltage reduces the thickness of the barrier layer and produces relatively large current flow across the metal-semiconductor contact. A reverse voltage increases the thickness of the barrier layer, so that current flow is reduced and rectifying action results. A typical diode characteristic for high-back-voltage n-type germanium is shown in Fig. 12-8. The battery polarities

corresponding to the forward and backward directions are also indicated.

A frequently given explanation of the rectification at a metal-semiconductor contact is based upon the raising or lowering of energy levels in the semiconductor by the applied voltage. For n-type germanium, the levels are raised by a voltage in the forward direction in which the germanium is negative with respect to the metal point contact. The

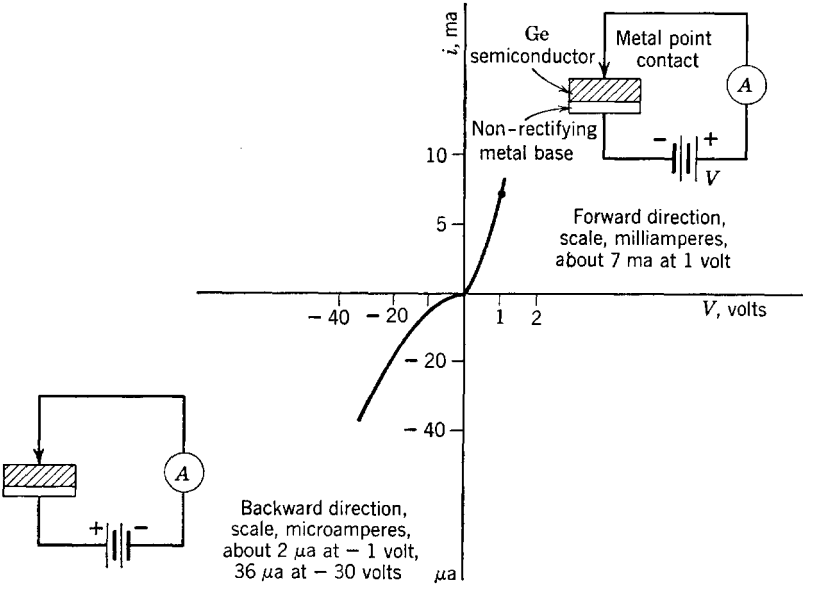

FIG. 12-8. Diode characteristic for high-back-voltage n-type germanium.

barrier to electron flow from germanium to metal is thereby reduced, while the barrier from metal to germanium remains the same. In the backward direction with the germanium positive, the levels of energy in the semiconductor are lowered, which raises the barrier and reduces the electron flow from semiconductor to metal.

12-5. The Transistor [6]

In its earliest form, the transistor consisted of a point-contact rectifier similar to those shown in Fig. 12-8 except that two metal point contacts instead of one were used. One of the point contacts, called the emitter, is biased slightly in the forward or highly conducting direction. The other, called the collector, is biased heavily in the backward or low-conducting direction. The third electrode is a large, nonrectifying contact to a large surface of the semiconductor and is called the base.

The arrangement of the type-A transistor is shown in Fig. 12-9 as a four-terminal network with emitter base as input terminals and collector base as output terminals. If the current source a-c signal generator and load are connected as indicated in Fig. 12-9, the transistor can be used as an amplifier.

The germanium semiconductor used in the type-A transistor is n-type. Its resistivity is of the order of 10 ohm cm, and its material is the same as that used in high-back-voltage germanium rectifiers. The contacts are made from phosphor bronze, are wedge-shaped, and cover an area of approximately 10^{-6} cm^2 each. The point contacts are located with separations varying from 0.005 to 0.025 cm.

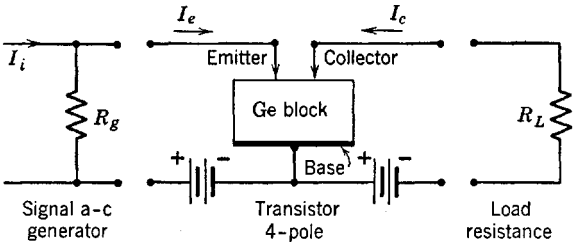

FIG. 12-9. The type-A transistor.

Transistor action consists of the control of the magnitude of collector current by controlling the magnitude of the emitter current. The emitter current consists of holes flowing into the semiconductor, and the collector current of electrons flowing out of the semiconductor. The collector-current change resulting from a change in emitter current may be larger than the change in emitter current.

12-6. Performance Data Comparison, Transistors and Vacuum Tubes

The transistor, as a system component, compares favorably in many respects with vacuum tubes and is superior with regard to low operating temperature (no heater power), space requirements, resistance to shock and vibration. Limitations on transistor application are due to low power and temperature ratings and low upper-frequency limits. The upper-temperature limit at this writing is about 80° C. The comparison[7] in Table 12-3 between vacuum tube and transistor affords an indication of the tremendous possibilities inherent in the use of transistors for CW transmission application. The best transistors available in October 1951 are used in the comparison.

[7] Data obtained from oral presentation by J. A. Morton to a joint meeting of Columbus sections of IRE and AIEE, Oct. 30, 1951, and available in *The Transistor*, a compilation of selected reference material prepared by the Bell Telephone Labs.

TABLE 12-3. DATA COMPARISON, TUBES AND TRANSISTORS

Figure of Merit	Vacuum Tube	Transistor
Amplification		
Gain per stage	20–40 db	20–40 db
Noise figure	0–30 db	10–50 db at 1 kc
Operating frequency range	0–60,000 Mc	0–30 Mc
Power output	0 to kilowatts	0–2 watts
Class-A efficiency	35%	35–49%
Class-B efficiency	79%	>80%
Generation		
Frequency range	0–60,000 Mc	0–300 Mc
Efficiency	60–70%	>70%
Power output	0–100 kw	0–10 watts
Other ratings		
Heater power	25 mw–1 watt	0
Plate dissipation	25 mw–1 watt	—
Total power dissipation	50 mw–2 watts	Type A, 4–50 mw Junction, 1–100 μw
Space required	0.125–1.0 cu in.	0.0005–0.02 cu in.
Developmental age	40 years	3 years
Upper temperature limit	>200° C	80° C

12-7. Static Characteristics of the Type-A Transistor [8]

In beginning the circuit theory of the transistor, it seems desirable to utilize as far as possible the techniques that have been found useful in vacuum-tube circuit theory. It is soon found to be impossible, however, to depend upon one-to-one comparisons or analogies. For example, the vacuum tube requires fixed-voltage supplies which desirably are regulated and which present negligible internal impedance. The vacuum tube is short-circuit stable, whereas just the reverse is true of type-A transistors, which need current sources of high impedance as power supplies. In the case of vacuum tubes, the fundamental functional relations are written for currents with voltages as independent variables as

$$i_c = F_c(e_c, e_b) \tag{12-2}$$

$$i_b = F_b(e_c, e_b) \tag{12-3}$$

which may be represented by the several well-known sets of static characteristics. The transistor, however, is a current-controlled device, and its static characteristics are better expressed by the relations

$$v_e = F_1(i_e, i_c) \tag{12-4}$$

$$v_c = F_2(i_e, i_c) \tag{12-5}$$

where the independent variables i_e and i_c are, respectively, the total

[8] R. M. Ryder, The Type A Transistor, *Bell Laboratories Record* (Mar. 1949).

values of emitter and collector current, and v_e and v_c are the corresponding values of emitter and collector voltages measured relative to the base. There are, then, six possible sets of curves depicting the voltage-current

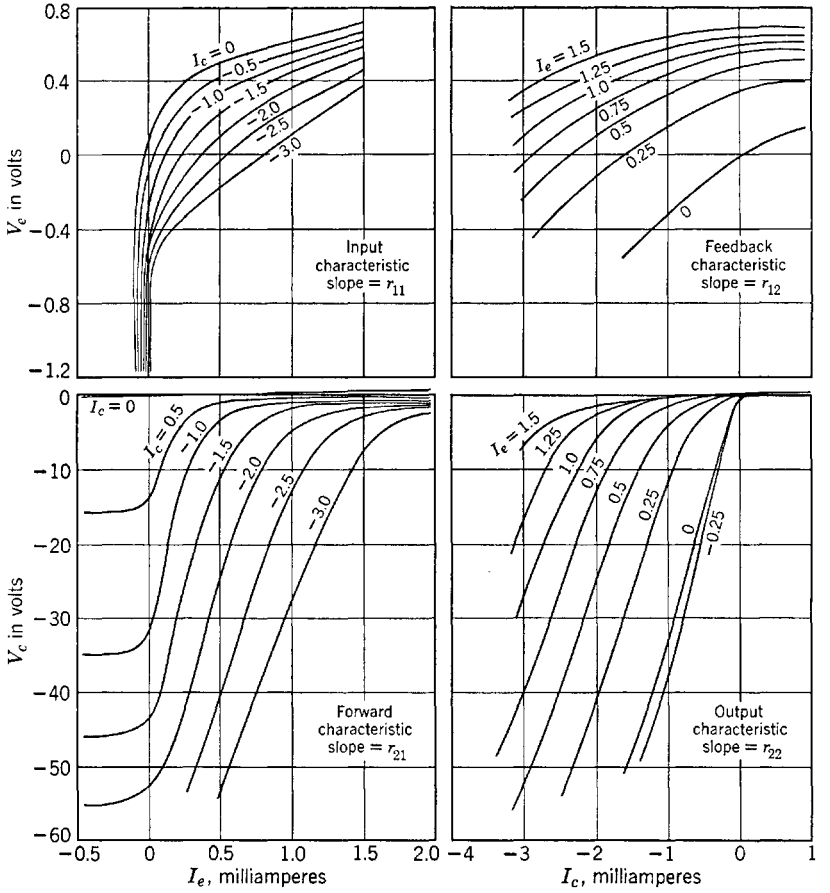

FIG. 12-10. Four sets of static characteristics for the type-*A* transistor. (Reproduced from *Bell Laboratories Record*, with permission)

relationships of the transistor. Four of these have been shown in Fig. 12-10. They have been designated as follows:

$$v_e = f_1(i_e),\ i_c \text{ constant, the input characteristics}$$

$$v_e = f_2(i_c),\ i_e \text{ constant, the feedback characteristics}$$

$$v_c = f_3(i_e),\ i_c \text{ constant, the forward characteristics}$$

$$v_c = f_4(i_c),\ i_e \text{ constant, the output characteristics}$$

12-8. Equivalent Circuits of the Grounded-Base Transistor

The transistor, considered as a four-pole, may be accurately described circuitwise by the following linear approximations, provided the variations of the currents from values at quiescence are small:

$$\Delta v_e = \frac{\partial v_e}{\partial i_e}\Delta i_e + \frac{\partial v_e}{\partial i_c}\Delta i_c \tag{12-6}$$

$$\Delta v_c = \frac{\partial v_c}{\partial i_e}\Delta i_e + \frac{\partial v_c}{\partial i_c}\Delta i_c \tag{12-7}$$

The terms involved in Eqs. 12-6 and 12-7 may be defined in a manner entirely analogous to that used for vacuum tubes in Chapter 1. The resistances

$$r_{11} = \frac{\partial v_e}{\partial i_e}, \quad r_{12} = \frac{\partial v_e}{\partial i_c}, \quad r_{21} = \frac{\partial v_c}{\partial i_e}, \quad r_{22} = \frac{\partial v_c}{\partial i_c} \tag{12-8}$$

are the slopes of the appropriate static characteristics in the vicinity of an operating point. The differences

$$\Delta v_e, \quad \Delta v_c, \quad \Delta i_e, \quad \Delta i_c \tag{12-9}$$

may be defined as instantaneous a-c values of the respective voltages and currents. A convenient set of equations applicable for small signals in any frequency range and for any linear network apply very well to the transistor. These are

$$V_1 = I_1 z_{11} + I_2 z_{12} \tag{12-10}$$

$$V_2 = I_1 z_{21} + I_2 z_{22} \tag{12-11}$$

in which subscript 1 refers to the input terminals, subscript 2 to the output terminals of the four-pole. The currents and voltages are effective sinusoidal components and the z's are the open-circuit driving-point

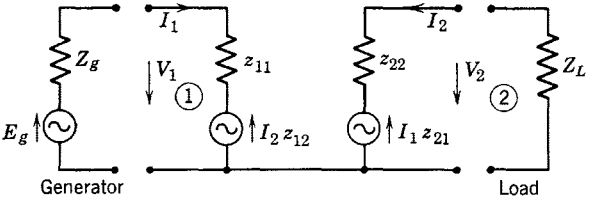

FIG. 12-11. Equivalent a-c circuit of a transistor according to Eqs. 12-10 and 12-11.

input, feedback, transfer, and output impedances at the specified frequency.

An equivalent circuit for the transistor may be obtained from Eqs. 12-10 and 12-11 and is shown in Fig. 12-11. In relation to the circuit

of Fig. 12-9, which may be described as the grounded base circuit, I_1 is equivalent to I_e, I_2 to I_c; at low enough frequencies, $z_{11} = r_{11}$, $z_{12} = r_{12}$, $z_{21} = r_{21}$, and $z_{22} = r_{22}$, as already defined from the slope of the static characteristics.

With the load connected, the input impedance of the circuit of Fig. 12-11 as obtained from Eq. 12-10 is

$$Z_{11} = V_1/I_1 = z_{11} + (I_2/I_1)z_{12} \tag{12-12}$$

From Fig. 12-11, $V_2 = -I_2Z_L$, and from Eq. 12-11,

$$I_2/I_1 = -z_{21}/(z_{22} + Z_L) \tag{12-13}$$

Therefore,

$$Z_{11} = z_{11} - z_{12}z_{21}/(z_{22} + Z_L) \tag{12-14}$$

In a similar manner, the impedance at the output terminals of Fig. 12-11 with the generator impedance Z_g connected across the input terminals is

$$Z_{22} = z_{22} - z_{12}z_{21}/(z_{11} + Z_g) \tag{12-15}$$

An equivalent circuit with only one voltage generator instead of the two shown in Fig. 12-11 may be obtained by algebraic manipulation of Eqs. 12-10 and 12-11 and reinterpretation of the result. Thus, Eq. 12-10 may be written as

$$V_1 = I_1(z_{11} - z_{12}) + (I_1 + I_2)z_{12}$$

and Eq. 12-11 as

$$V_2 = I_1(z_{21} - z_{12}) + I_2(z_{22} - z_{12}) + (I_1 + I_2)z_{12}$$

which reduce identically to Eqs. 12-10 and 12-11. However, if

$$z_{11} - z_{12} = Z_e \tag{12-16}$$

$$z_{12} = Z_b \tag{12-17}$$

$$z_{21} - z_{12} = Z_m \tag{12-18}$$

and

$$z_{22} - z_{12} = Z_c \tag{12-19}$$

then

$$V_1 = I_1Z_e + (I_1 + I_2)Z_b \tag{12-20}$$

and

$$V_2 = I_1Z_m + I_2Z_c + (I_1 + I_2)Z_b \tag{12-21}$$

From these equations, a somewhat more useful equivalent circuit may be derived and is shown by Fig. 12-12 just below the schematic circuit of the transistor. It should be noted that the new circuit conveniently permits the lumping of the emitter, collector, and base impedances in corresponding legs of the T section.

The transistor impedances z_{11}, z_{12}, z_{21}, and z_{22} are measured by use of a high-impedance a-c generator providing a small, known alternating current in the audio range. A high-impedance vacuum-tube voltmeter may be used to read the voltages. The necessary readings are indicated by Eqs. 12-10 and 12-11, where open circuit at either output or input

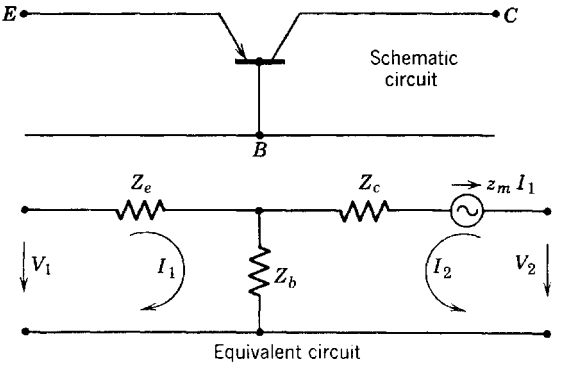

FIG. 12-12. Another equivalent a-c circuit for the transistor.

terminals is assumed. The voltmeter impedance must be sufficiently high. Some average values obtained [9] in this way for the type-A transistor grounded-base amplifier are the following:

D-c operating point $I_e = 0.6$ ma, $v_e = 0.7$ volts

$I_c = -2$ ma, $v_c = -40$ volts

$z_{11} = 530$ ohms, $z_{21} = 34{,}000$ ohms

$z_{12} = 290$ ohms, $z_{22} = 19{,}000$ ohms

$$Z_e = r_e = z_{11} - z_{12} = 240 \text{ ohms}$$

$$Z_c = r_c = z_{22} - z_{12} \cong 19{,}000 \text{ ohms}$$

$$Z_m = r_m = z_{21} - z_{12} \cong 34{,}000 \text{ ohms}$$

$$Z_b = r_b = z_{12} = 290 \text{ ohms}$$

A variation on the equivalent circuit of Fig. 12-12 is possible by converting the voltage generator $Z_m I_1$ to an equivalent-current generator of shunt impedance Z_c and generated current $(Z_m/Z_c)I_1 = aI_1$. The ratio a should be regarded as the ratio of the generated current of the

[9] R. M. Ryder and R. J. Kircher, *BSTJ*, **28**, 367–400 (July, 1949).

indicated current-source generator to the emitter current. The modified circuit is shown in Fig. 12-13.

A condition necessary for the stability of an amplifier circuit is that the circuit determinant of the system of equations must be positive.

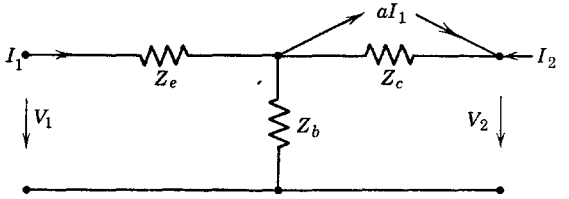

FIG. 12-13. Modification of the equivalent circuit of Fig. 12-12; $a = Z_m/Z_c$.

The circuit determinant as obtained from Fig. 12-11 is

$$\Delta = (z_{11} + Z_g)(z_{22} + Z_L) - z_{12}z_{21} \tag{12-22}$$

Figure 12-14 shows the transistor equivalent circuit of Fig. 12-13 connected as an amplifier. As the given data show, the emitter, collector, and base impedances are resistances in the audio range. The analogous vacuum-tube circuit is the grounded-grid circuit which has been drawn on the same figure for comparison. The circuit equations are

$$E_g = I_1(R_g + r_e + r_b) + I_2 r_b \tag{12-23}$$

$$0 = I_1(r_b + ar_c) + I_2(r_c + R_L + r_b) \tag{12-24}$$

the system determinant may be simplified by use of

$$R_e = R_g + r_e \tag{12-25}$$

$$ar_c = r_m \tag{12-26}$$

$$R_c = r_c + R_L \tag{12-27}$$

and is

$$\begin{aligned} \Delta &= (R_e + r_b)(R_c + r_b) - r_b(r_b + r_m) \\ &= R_eR_c + R_er_b + r_bR_c - r_br_m \end{aligned} \tag{12-28}$$

For stability, then,

$$R_eR_c + R_er_b + r_bR_c > r_br_m$$

or

$$R_e/r_b + R_e/R_c + 1 > r_m/R_c \tag{12-29}$$

The inequality will certainly be satisfied for $r_b = 0$ or for positive values of r_b provided R_c is large enough and r_m small enough. It may be seen from this that the amplifier stability characteristic is improved by the

insertion of high resistances in emitter and collector circuits, but not in the base circuit. The feedback impedance is in the base circuit, and a low value of this impedance is important for amplifier stability.

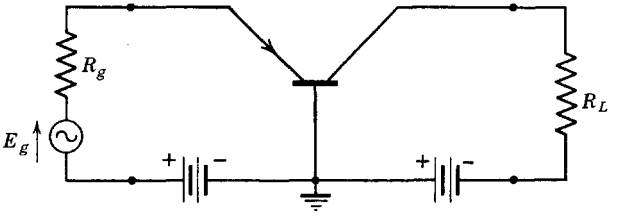

Circuit of grounded-base transistor amplifier

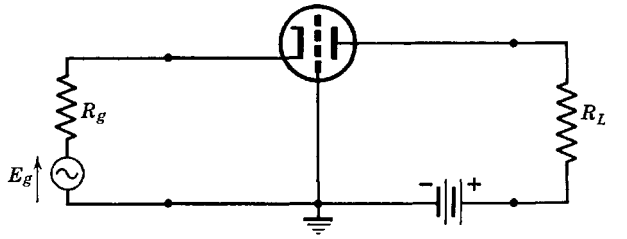

Circuit of grounded-grid tube amplifier

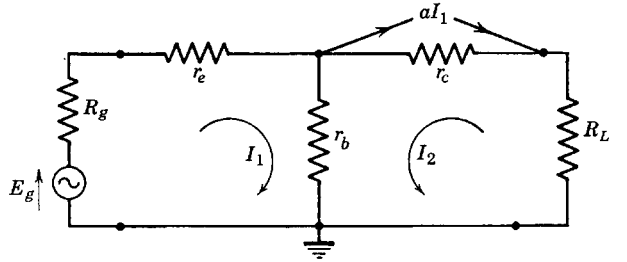

Transistor grounded-base amplifier
Equivalent a-c circuit

FIG. 12-14. Transistor-amplifier grounded-base circuit and tube analogy.

The input and output impedances of the amplifier of Fig. 12-14 follow directly from Eqs. 12-14 and 12-15 with substitution of the appropriate relations between the z's and the r's. The operating power gain, defined as the ratio of the power output to the power available from the driving generator, is easily derived from the equivalent circuit and has been left as a problem exercise. The derivation of an expression for insertion power gain, which is the ratio of the power output to the power that would be delivered to R_L by the driving generator if directly connected

to R_L, has likewise been left as a problem exercise. The operating power gain for the amplifier of Fig. 12-14, G_o, is given by

$$G_o = 4R_gR_L[-(r_b + r_m)/\Delta]^2 \tag{12-30}$$

and the insertion power gain by

$$G_i = (R_g + R_L)^2[-(r_b + r_m)/\Delta]^2 \tag{12-31}$$

12-9. The Grounded-Emitter Type-A Transistor Amplifier

The analogy between grounded-base transistor and grounded-grid tube leads to the search for other analogies. If the analogy is completed, the emitter becomes analogous to the tube cathode, and the collector is analogous to the tube plate. The grounded-emitter circuit is found to have high input and output impedance and provides a phase reversal between input and output provided the quantity $a = 1$. These are the attributes of the grounded-cathode tube, and the analogy is close. However, if $a > 1$, sufficient feedback exists to spoil the analogy to quite an extent. In fact, the output impedance on open circuit is usually negative. Resistance added to the collector lead may be required to provide stability by reducing a to a value of unity.

The grounded-emitter connection is shown in Fig. 12-15. The arrangement of battery sources will require further discussion. The direction of the emitter current I_e of the equivalent circuit should be noted and is taken in the same direction as in the original equivalent circuit. Since

$$I_e = -(I_1 + I_2)$$

the circuit mesh equations are

$$E_g = I_1(R_g + r_b + r_e) + I_2r_e \tag{12-32}$$

$$\begin{aligned} 0 &= I_er_m + I_2(r_c + r_e + R_L) + I_1r_e \\ &= I_1(r_e - r_m) + I_2(r_c + r_e + R_L - r_m) \end{aligned} \tag{12-33}$$

The determinant of the system of equations is

$$\Delta = (R_g + r_b + r_e)(r_c + r_e + R_L - r_m) - r_e(r_e - r_m) \tag{12-34}$$

An application of the fundamental definitions of z_{11}, z_{12}, z_{21}, and z_{22}, to the equivalent circuit of Fig. 12-15 shows that

$$z_{11} = r_b + r_e, \qquad I_2 = 0 \tag{12-35}$$

$$z_{21} = r_e - r_m, \qquad I_2 = 0 \tag{12-36}$$

$$z_{12} = r_e, \qquad I_1 = 0 \tag{12-37}$$

$$z_{22} = r_c + r_e - r_m, \qquad I_1 = 0 \tag{12-38}$$

Then the general four-pole equations 12-14 and 12-15 for the input and output impedances give

$$R_{11} = r_b + r_e - \frac{r_e(r_e - r_m)}{r_c + r_e - r_m + R_L} \tag{12-39}$$

and

$$R_{22} = r_c + r_e - r_m - \frac{r_e(r_e - r_m)}{r_b + r_e + R_g} \tag{12-40}$$

The same relations may be obtained by direct solution for V_1/I_1, and for V_2/I_2 with the generator replaced by its internal impedance.

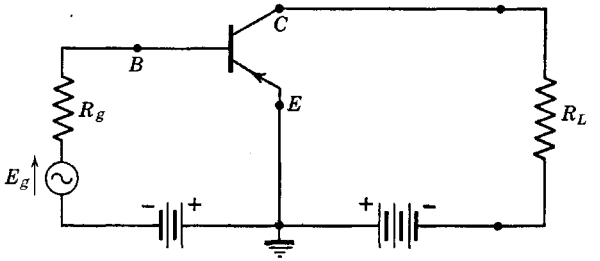

Circuit of the grounded-emitter type-A transistor

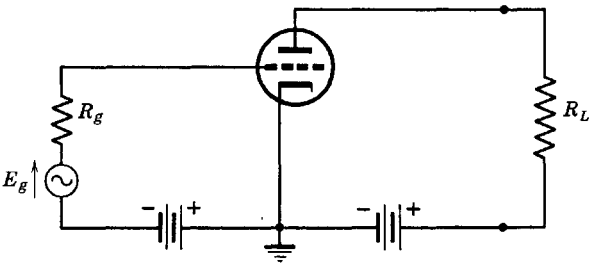

Grounded cathode, analogous tube amplifier

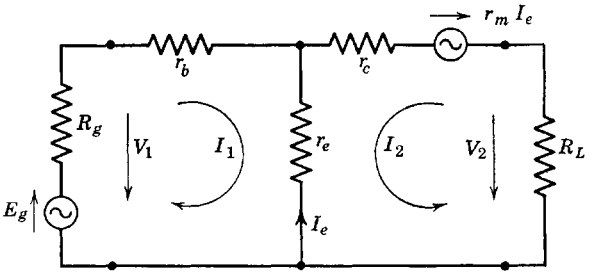

Equivalent a-c circuit of the transistor

FIG. 12-15. Circuit, tube analogy, and equivalent circuit of the grounded-emitter, type-*A* transistor amplifier.

Application of the definition of operating power gain to the equivalent circuit of Fig. 12-15 shows that

$$G_o = 4R_gR_L[(r_m - r_e)/\Delta]^2 \tag{12-41}$$

If a generator of resistance R_L and generated voltage E_L were connected at the emitter-collector terminals, and a load resistance R_g were then connected to the base-emitter terminals, an operating power gain may be derived for this reverse direction and is

$$G_r = 4R_LR_g(r_e/\Delta)^2 \tag{12-42}$$

The properties of the grounded-emitter amplifier as compared with those of the grounded-base circuit are brought out in the solutions to problems 12-10 and 12-13.

12-10. The Grounded-Collector Type-A Transistor Amplifier

Only one tube-connection analogy remains. This is the grounded-plate or cathode follower circuit; the remaining transistor arrangement is grounded collector. The circuit is drawn in Fig. 12-16. It seems desirable to postpone the question of biasing until a later section and to focus attention on the a-c equivalent circuit. Therefore, batteries have not been shown in the transistor circuit of Fig. 12-16.

The analogy between grounded-collector and grounded-plate circuits is fairly close, according to Ryder and Kircher,[9] provided again that $\alpha = 1$. Thus, the grounded-collector transistor circuit is found to have high input and low output impedances, and zero phase shift between input and output circuits. However, it is found [9] that, as α exceeds unity, the grounded-collector transistor becomes bilateral and, at $\alpha = 2$, provides equal operating gains in each direction! For $\alpha > 2$, transmission gain in the direction 2 to 1 exceeds that from 1 to 2 (Fig. 12-16), and a phase inversion occurs 2 to 1 with no phase reversal 1 to 2. Since the device will, under suitable conditions, amplify in either direction, a generator of voltage E_L, internal impedance R_L, has been connected at 2 to provide for the calculations of the 2-to-1 operating power gain, etc.

According to Fig. 12-16, the mesh equations are

$$E_g = I_1(R_g + r_b + r_c) + I_2(r_c - r_m) \tag{12-43}$$

and

$$E_L = I_1r_c + I_2(R_L + r_e + r_c - r_m) \tag{12-44}$$

The system determinant is

$$\Delta = (R_g + r_b + r_c)(R_L + r_e + r_c - r_m) - r_c(r_c - r_m) \tag{12-45}$$

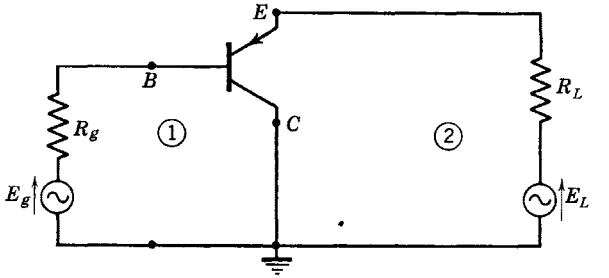

Grounded-collector type-A circuit, batteries omitted

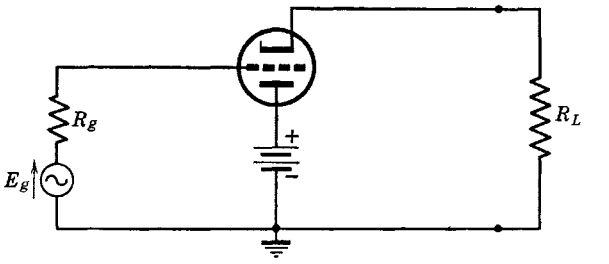

Tube analogy – grounded plate or cathode follower

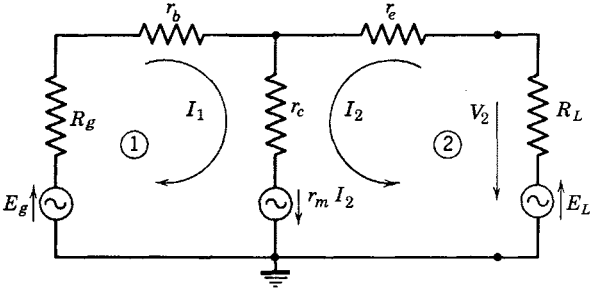

Equivalent a-c circuit

FIG. 12-16. Grounded-collector amplifier circuit of the type-*A* transistor, and grounded-plate tube analogy.

The four-pole open-circuit parameters are:

$$z_{11} = r_b + r_c, \quad \text{with} \quad I_2 = 0 \tag{12-46}$$

$$z_{21} = r_c, \quad \text{with} \quad I_2 = 0 \tag{12-47}$$

$$z_{12} = r_c - r_m, \quad \text{with} \quad I_1 = 0 \tag{12-48}$$

$$z_{22} = r_e + r_c - r_m, \quad \text{with} \quad I_1 = 0 \tag{12-49}$$

Then, the input impedances at 1 and at 2 are, respectively,

$$R_{11} = r_b + r_c - \frac{r_c(r_c - r_m)}{r_e + r_c - r_m + R_L} \tag{12-50}$$

and

$$R_{22} = r_e + r_c - r_m - \frac{r_c(r_c - r_m)}{r_b + r_c + R_g} \tag{12-51}$$

The forward 1-to-2 operating power gain (generator E_L removed) is

$$G_{12} = \frac{I_2^2 R_L}{E_g^2/4R_g} = 4R_g R_L \left(-\frac{r_c}{\Delta}\right)^2 \tag{12-52}$$

and similarly the backward 2-to-1 operating power gain is

$$\begin{aligned} G_{21} &= 4R_L R_g[-(r_c - r_m)/\Delta]^2 \\ &= 4R_L R_g[-r_c(1 - a)/\Delta]^2 \\ &= (1 - a)^2 G_{12} \end{aligned} \tag{12-53}$$

It may be seen from Eq. 12-53 that, as stated before, if $a = 2$, $G_{21} = G_{12}$.

Calculation of the operating characteristics of a grounded-collector amplifier has been assigned as a problem.

The analogy between the various tube and transistor circuit connections has been shown to be close, provided the quantity $a = r_m/r_c = 1$. In cases where $a > 1$, the analogy breaks down, and, in some cases, the transistor circuit performs easily functions that would be impossible for a single vacuum tube.

12-11. Frequency Characteristics of the Type-A Transistor

The equivalent T circuit of resistances r_e, r_b, and r_c is remarkably constant with frequency. Although a small amount of capacitance is found in the collector circuit (chargeable to leads, wiring, and cylindrical case of the unit), capacitance effects are relatively unimportant in setting the upper frequency limit of usefulness of the type-A transistor. The important limitation seems to be the carrier transit time. The important factor which reduces the power gain with increasing frequency has as yet not been adequately defined, but is analogous to the voltage amplification factor μ of vacuum-tube triodes. This quantity, α, is a current amplification factor which is very nearly the same as the quantity $a = r_m/r_c$ already defined.

The definition of α proceeds exactly as does that of μ for vacuum triodes. The functional relation (Eq. 12-5) is

$$v_c = f_2(i_e, i_c)$$

If small changes in i_e and i_c are made, the resulting change in v_c is given by

$$dv_c = \frac{\partial v_c}{\partial i_e} di_e + \frac{\partial v_c}{\partial i_c} di_c$$

If the small changes di_e and di_c are properly proportioned, then no change in the magnitude of v_c will occur. Since v_c remains constant, $dv_c = 0$, and

$$\left(\frac{di_c}{di_e}\right)_{v_c \text{ constant}} = \frac{\partial i_c}{\partial i_e} = -\frac{(\partial v_c/\partial i_e)}{(\partial v_c/\partial i_c)} = -\alpha \tag{12-54}$$

which defines the current amplification factor. The reason for the minus sign is that the slope of the characteristic $i_c = f(i_e)$, with v_c constant is negative. Since

$$\alpha = -\partial i_c/\partial i_e \tag{12-55a}$$

α is positive. This point can be made clear by sketching a typical curve, which has been done in Fig. 12-17 by taking one point at $v_c = -20$ volts from each of the output characteristics of Fig. 12-10. From Eq. 12-54,

$$\alpha = z_{21}/z_{22} = r_{21}/r_{22} \tag{12-55b}$$

as defined by Eq. 12-8. The type-A transistor values previously used were $r_{21} = 34{,}000$ ohms, $r_{22} = 19{,}000$ ohms. Thus $\alpha = 1.76$ as compared with the value of 1.87 obtained by transferring points from the graph of output characteristics (Fig. 12-10). Since

$$a = \frac{r_m}{r_c} = \frac{z_{21} - z_{12}}{z_{22} - z_{12}} = \frac{34{,}000 - 290}{19{,}000 - 290} \cong 1.76$$

there is very little difference in this case between a and α.

The insertion power gain of the grounded-base amplifier is given by the general four-pole formulas

$$G_i = \left| \frac{(Z_g + Z_L)z_{21}}{\Delta} \right|^2 \tag{12-56}$$

where $$\Delta = (z_{11} + Z_g)(z_{22} + Z_L) - z_{12}z_{21}$$

Because of the difficulty of obtaining a load resistance R_L which would be both constant over a wide frequency range and large compared with the collector resistance, a small resistance of 75 ohms constant over a wide range of frequency, has been used [9] to terminate the grounded-base transistor amplifier in frequency tests. Then, for the typical values used, with a constant-current generator of large $Z_g = R_g$, $\Delta = (530 +$

$R_g)(19{,}000 + 75) - 290(34{,}000) \cong R_g z_{22}$ for high enough R_g. Thus

$$G_i \cong \left| \frac{R_g z_{21}}{R_g z_{22}} \right|^2 = \alpha^2 \tag{12-57}$$

for the conditions specified. Curves of current amplification factor α as a function of frequency and with collector voltage constant for

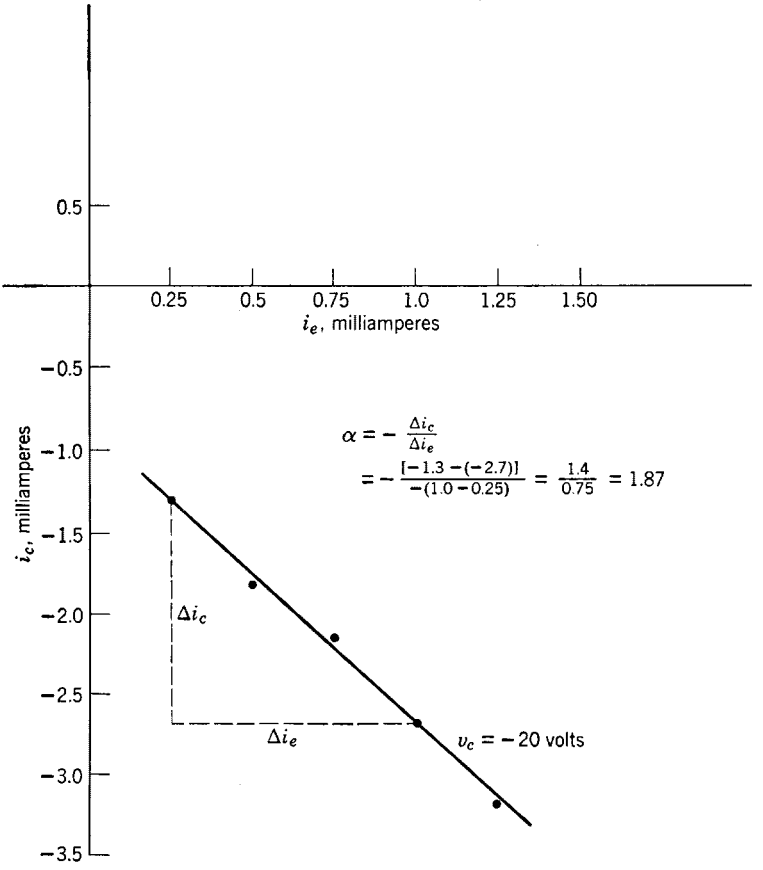

FIG. 12-17. Constant collector-voltage characteristic for a type-A transistor, and the current amplification factor α.

the low R_L, high R_g condition have been obtained by measurement [9] and are shown in Fig. 12-18. The cutoff frequency is defined as the frequency for which α^2 has been reduced to one-half its value at low frequency.

Statistical variation experienced in cutoff frequency of type-A transistors is tabulated in Table 12-4. Both n-type and p-type germanium

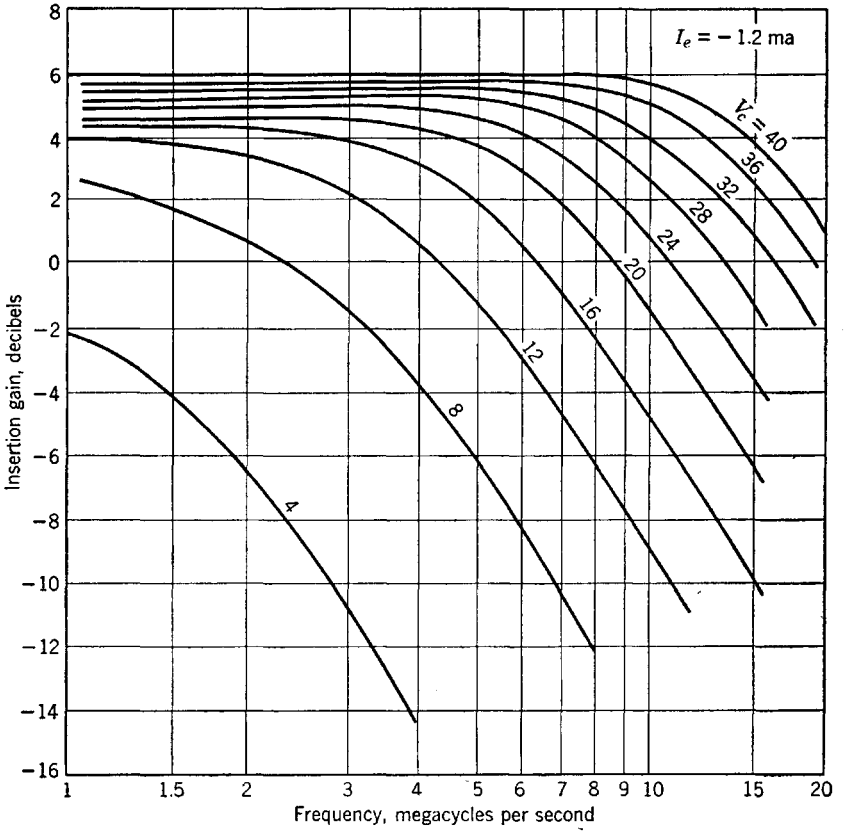

FIG. 12-18. Experimentally determined curves of α versus frequency.[9] (Obtained from curves presented by reference 9, with permission).

TABLE 12-4. STATISTICAL CUTOFF FREQUENCY DATA *

	Per Cent Having Cutoff as Good as f_c	
f_c, Mc per sec	n-Type Ge	p-Type Ge
1	98	100
2	90	99
4	74	94
6	61	86
8	47	75
10	35	63
12	23	51
14	..	37

* Obtained from curves presented by reference 9.

are represented, and the p-type is superior because of greater mobility of the control-(emitter) current carriers which are electrons for p-type Ge. It is found that the cutoff frequency increases with collector voltage and is approximately proportional to collector voltage. It should be remembered that the rapid progress in transistor research and development has, even at the time of this writing, rendered the data of this section more or less obsolete. Any evaluation of the capabilities of transistors for immediate use should utilize the most recent available information. To a large extent, the most important function of this chapter is to present principles of circuit analysis rather than data about transistors.

12-12. Type-A Transistor Amplifiers in Cascade

It is possible to connect any one of the transistor connections previously discussed with any other one in the same multistage amplifier, so that a number of available arrangements exist. Grounded-base

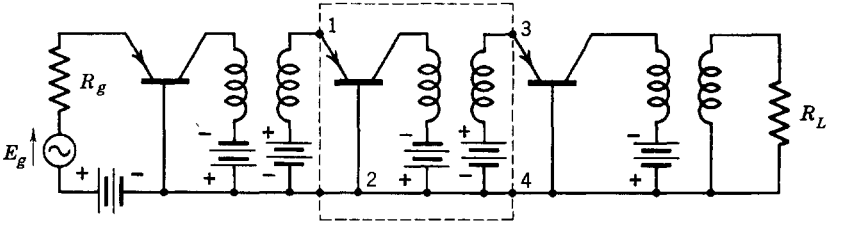

FIG. 12-19. A three-stage, transformer-coupled grounded-base transistor amplifier using type-A transistors.

cascade stages using type-A transistors will provide about 5 db of insertion power gain per stage with feedback neglected and with direct coupling between stages. Transformer-coupled stages, as shown in Fig. 12-19, will provide around 15 to 20 db of power gain per stage. Some mismatch between stages may be required in the interests of stability.

It is possible to use the grounded-base transistors directly connected in a multistage amplifier. Analysis is simple provided the feedback resistance $r_{12} = r_b$ is neglected. An equivalent circuit for the indicated stage (Fig. 12-20) will be analyzed. This stage represents any stage of the amplifier, so that E_g' and R_g' are not the voltage and impedance of an external driving generator, but are the voltage and internal impedance of the generator equivalent of the preceding stage. Similarly, R_L' is the impedance of the following stage. These impedances may be termed

iterative impedances,[10] since in a cascade arrangement of four-poles an impedance terminating any given selected four-pole which replaces the continued cascade of remaining four-poles will allow them to be removed without alteration of the impedance property at the input to the cascade. If the base resistance $r_b = r_{12}$ is neglected in the circuit of Fig. 12-20, then the iterative impedance R_g' would be r_{22} since an impedance and generator identical with that on the right side of Fig. 12-20 has been

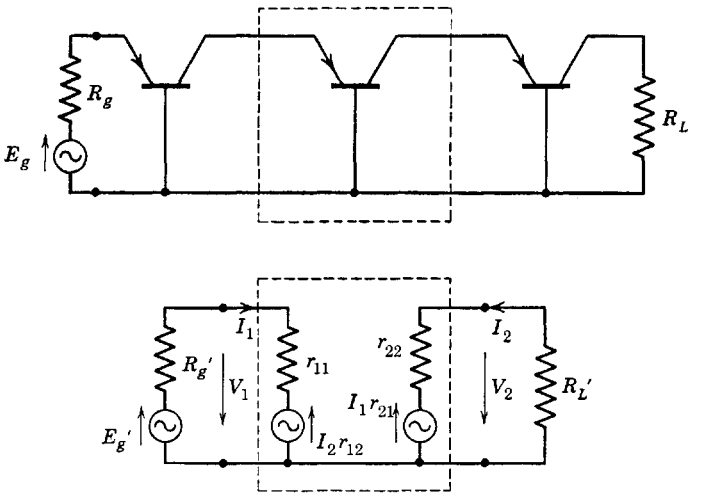

FIG. 12-20. Equivalent circuit of one stage of a multistage grounded-base amplifier.

replaced at the left by R_g' and E_g'. Similarly, $R_L' = r_{11}$. The mesh equations are:

$$E_g' = I_1(R_g' + r_{11}) + I_2 r_{12}$$
$$0 = I_1 r_{21} + I_2(r_{22} + R_L') \tag{12-58}$$

The circuit determinant is

$$\Delta = (R_g' + r_{11})(r_{22} + R_L') - r_{12}r_{21}$$
$$= (r_{22} + r_{11})(r_{22} + r_{11}) \tag{12-59}$$

with the iterative impedances inserted and $r_{12} = 0$. Thus the insertion power gain becomes

[10] E. A. Guillemin, *Communication Networks*, Vol. II, p. 166, John Wiley & Sons.

$$G_i = \frac{I_2^2 R_L'}{[E_g'/(R_g' + R_L')]^2 R_L'}$$

$$= (r_{11} + r_{22})^2 \left[\frac{-r_{21}}{(r_{11} + r_{22})^2}\right]^2$$

$$= \left[\frac{-r_{21}}{r_{11} + r_{22}}\right]^2 = \frac{\alpha^2}{(1 + r_{11}/r_{22})^2} \tag{12-60}$$

The equivalent circuit of a typical stage of the transformer-coupled amplifier of Fig. 12-19 is shown in Fig. 12-21. First, the transistor and the transformer are represented in Fig. 12-21*a* as two four-poles in cascade; second, these two four-poles are combined into one four-pole in the

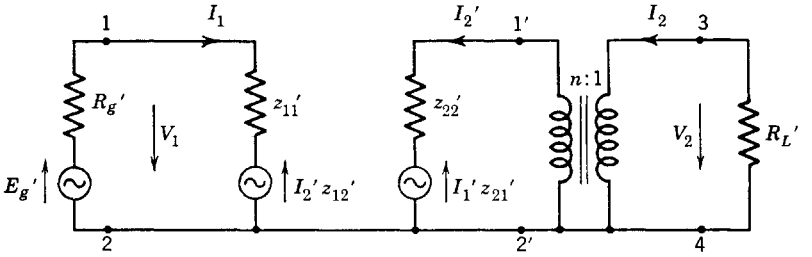

(a) Circuit with two 4-poles in cascade: the transistor, 1-2 to 1'-2', and the ideal transformer, 1'-2' to 3-4

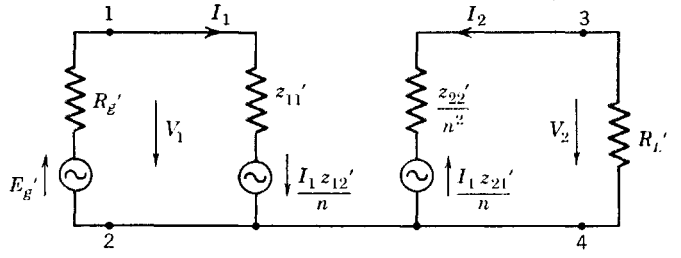

(b) Combination of the two 4-poles into single 4-poles

FIG. 12-21. Equivalent circuit of one stage of Fig. 12-19 and reduction to a single 4-pole.

following manner. Consider the over-all four-pole 1–2 to 3–4, and assume the transformer to be ideal. Then, z_{11}, z_{12}, z_{21}, and z_{22} are the parameters of the over-all four-pole, and the fundamental definitions

may be applied with first $I_2 = 0$, then $I_1 = 0$ to determine the over-all parameters. The results are:

$$z_{11} = z_{11}' \qquad (12\text{-}61)$$

$$z_{21} = z_{21}'/n$$

$$z_{12} = z_{12}'/n \qquad (12\text{-}62)$$

$$z_{22} = z_{22}'/n^2$$

These are shown on the resulting four-pole (Fig. 12-21*b*). The turns ratio of the transformer is n. Again, for simplicity, the impedance $z_{12}' = r_{12}$ is neglected. Thus, the iterative impedances obtained by inspection of Fig. 12-21 are

$$R_L' = z_{11}' = r_{11} \qquad (12\text{-}63)$$

and

$$R_g' = z_{22}'/n^2 = r_{22}/n^2 \qquad (12\text{-}64)$$

The circuit equations may be written from Fig. 12-21 whence, with $r_{12} = 0$, the circuit determinant reduces to

$$\Delta = (r_{11} + r_{22}/n^2)^2 \qquad (12\text{-}65)$$

The insertion power gain is

$$G_i = \frac{I_2^2 R_L'}{[E_g'^2/(R_g' + R_L')^2]R_L'} = \frac{I_2^2(r_{11} + r_{22}/n^2)^2}{E_g'^2}$$

$$= \left(\frac{-r_{21}/n}{r_{11} + r_{22}/n^2}\right)^2 \qquad (12\text{-}66)$$

It is possible to maximize G_i by proper choice of n. Typical computations are suggested in the problems.

The grounded-cathode cascade for vacuum tubes is especially desirable for high-gain amplifiers, and it might be expected that a grounded-emitter cascade would be desirable for high-gain transistor amplifiers. This is true provided precautions are taken to ensure stabilization, which may be accomplished if $a = (r_m/r_c)$ is made equal to unity. The

circuit of Fig. 12-22 shows such an arrangement [9] in which a resistance R_a has been added to the collector such that $a \cong 1$.

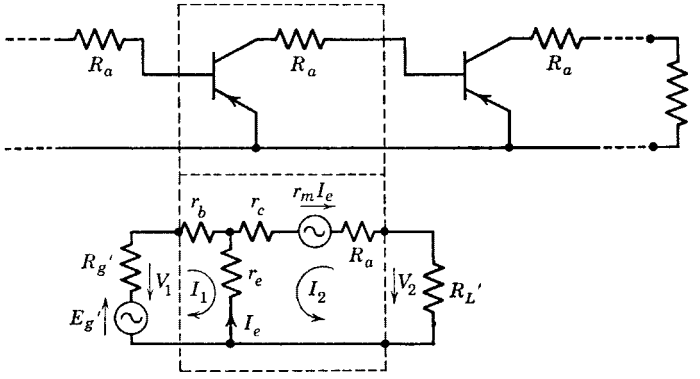

FIG. 12-22. Grounded-emitter cascade, with stabilizing resistance $R_a \cong r_m - r_c$, and equivalent circuit of one stage.

The analysis of Fig. 12-22 is carried out in the usual manner. For convenience, let

$$R_c = r_c + R_a$$

Then, $$E_g' = (R_g + r_b + r_e)I_1 + r_e I_2 \tag{12-67}$$

$$0 = (r_e - r_m)I_1 + (R_c + r_e + R_L' - r_m)I_2 \tag{12-68}$$

and $$\Delta = (R_g + r_b + r_e)(R_c + r_e + R_L' - r_m) - r_e(r_e - r_m) \tag{12-69}$$

Now, in case the feedback impedance r_e is neglected, there results, with $r_e = 0$, the iterative impedance requirements

$$R_L' = r_b \tag{12-70}$$

and, since the internal impedance of the equivalent generator of the collector arm is $r_c + R_a - r_m$,

$$R_g' = r_c + R_a - r_m = R_c - r_m \tag{12-71}$$

Then $$\Delta = (R_c - r_m + r_b)^2 \tag{12-72}$$

and $$G_i = r_m^2/\Delta \tag{12-73}$$

The behavior of this cascade stage is considered in problems 12-17 and 12-18.

An example of noniterative coupling is given by Fig. 12-23 for which the tube analog is a grounded grid followed by a cathode follower. Such a combination [9] has been used to match and feed a 600-ohm line with G_i of 16 db and bandwidth about 1 Mc. Another application

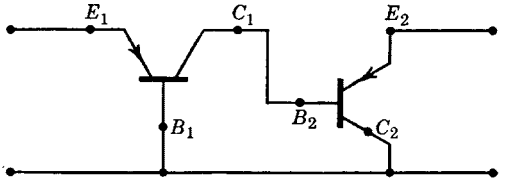

FIG. 12-23. Grounded-base, grounded-collector cascade.

involved a 75-ohm coaxial line and provided a value of G_i of 20 db over the video band of 100 cps to 3.5 Mc.

It has been shown that the grounded-collector stage provides a usable amplification in the reverse direction. This may be utilized as

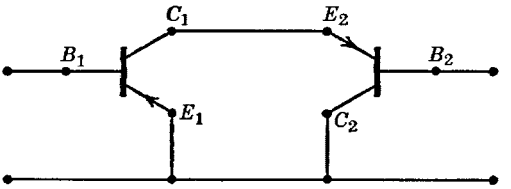

FIG. 12-24. Grounded-emitter, with reversed grounded-collector cascade.

shown in Fig. 12-24 which provides a higher power-output level since the output electrodes involve the base and collector terminals. Stabilization is accomplished by insertion of a resistor in the emitter lead of the first stage.

12-13. The Type-A Transistor Power Stage

Analysis of the large signal properties of the transistor depends upon the use of the static characteristics as in the case of vacuum tubes. The static characteristics are useful, also, in circuit design for maximum power output with minimum distortion. The output characteristics of a type-A power transistor are shown in Fig. 12-25, along with a grounded-base circuit considered as a power stage. According to the circuit (Fig. 12-25)

$$-E_{bb} = V_c + I_c R_L \tag{12-74}$$

which is the equation of the load line on the $(-V_c, -I_c)$ characteristic

sheet. Thus, the intercepts of the load line are given by

$$I_c = 0, \qquad V_c = -E_{bb} \text{ volts}$$

$$V_c = 0, \qquad I_c = -E_{bb}/R_L \text{ amp}$$

If the small-signal operating point be specified as $(-I_{c0}, -V_{c0})$, and the load resistance as R_L, then the necessary voltage of the collector

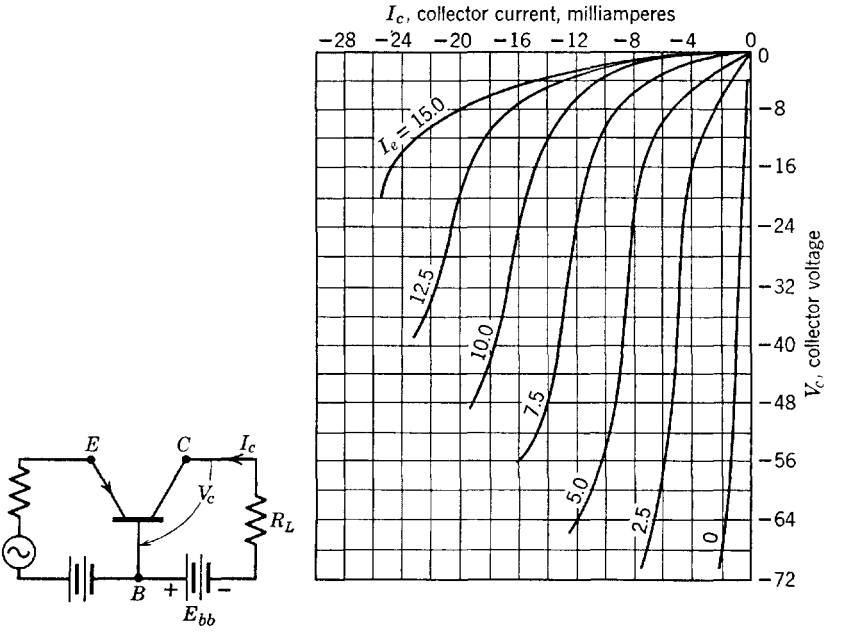

FIG. 12-25. Output characteristics for a type-*A* power transistor. (Courtesy Bell Telephone Laboratories)

voltage source is given by Eq. 12-74, and the load line may be drawn through the operating point in a manner completely analogous to that used for vacuum tubes.

12-14. The *n–p–n* Junction Transistor

The theoretical work of Shockley [11] on the potential distribution and rectification of junctions between *p*- and *n*-type germanium has led to the *n–p–n* junction transistor, a truly amazing device. The behavior [12] of transistors built in accordance with Shockley's theory has been found

[11] W. Shockley, The Theory of *p–n* Junctions in Semiconductors and *p–n* Junction Transistors, *BSTJ*, **28**, 435–489 (July 1949).

[12] W. Shockley, M. Sparks, and G. K. Teal, *p–n* Transistors, *Phys. Rev.*, **83**, 151 (1951).

to be in excellent agreement with the theory. As Shockley [11] has stated, "the p–n–p transistor has the interesting feature of being calculable to a high degree."

The circuit behavior of the junction transistor will be of primary interest here rather than the physical theory which is absorbingly interesting but quite demanding of an extensive background in theory of solid-state physics for its complete appreciation. The circuit behavior has been clearly described by Wallace and Pietenpol [13] whose paper is the source of most of the material to be presented in the following pages.

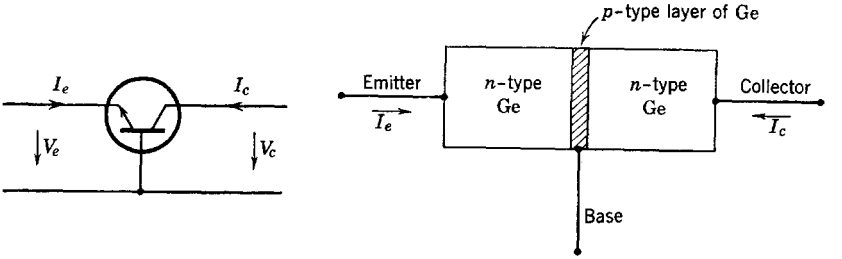

FIG. 12-26. The n–p–n junction transistor.

The n–p–n junction transistor consists of a tiny bar of germanium in which a thin layer of p-type germanium is interposed between much thicker regions of n-type. Ohmic or nonrectifying connections are made to the three regions of the germanium, and contact "cats-whisker" types of emitter and collector as used for type-A transistors are unnecessary. A schematic diagram of the n–p–n transistor is shown in Fig. 12-26. It may be observed that emitter and collector are symmetrically located with respect to the p-type layer. As shown by Shockley,[11] the junction between p- and n-type germanium may behave as an emitter. The entire assembly may be enclosed in a hard plastic bead of about $\frac{3}{16}$ inch in diameter or smaller, with connections brought out as wire terminals. The p layer may be less than 0.001 inch thick. The n–p–n transistor, in contrast with the type A, has complete freedom from short-circuit instability and has positive input impedances, regardless of the connection as grounded base, grounded emitter, or grounded collector. It will provide 40 to 50 db of power gain per stage and operates at class-A efficiencies of 48 or 49 per cent out of a possible 50 per cent. In addition to its small size, the n–p–n junction transistor is extremely rugged, relatively free from microphonics, and has a noise figure in the range 10 to 20 db compared with 60 db for the type A. Probably the

[13] R. L. Wallace, Jr., and W. J. Pietenpol, Some Circuit Properties and Applications of n–p–n Transistors, *BSTJ*, **30**, 530–563 (July 1951).

most striking property of this transistor is its required operating power consumption which is as low as 0.6 microwatt needed from a power supply in order to operate as an audio amplifier. This should be contrasted with the power requirements for heaters alone of the smallest miniature vacuum tubes. Two of the most serious limitations of *n–p–n* junction-type as well as of the type-A transistor are the low upper limits of operating frequency and temperature. These are mentioned in the tabulation of transistor properties given earlier.

12-15. Static Characteristics of the *n–p–n* Transistor

The static characteristics of the *n–p–n* junction transistor differ markedly from those of the type A. The collector or output characteristics of the latter were similar to triode characteristics; junction transistor characteristics resemble static plate characteristics of an ideal pentode. In examining and using the characteristics, it must be kept in mind that the junction *n–p–n* transistor has a *p*-type base, which entails different current signs. The assumed positive sense of current flow for the junction transistor is shown in Fig. 12-26. If currents and voltages have the positive sense indicated by Fig. 12-26, they are called positive. The arrow on the emitter connection has been reversed since the base is *p*-type and requires electron injection from the emitter rather than hole injection as in the type-A transistor. The collector requires a positive supply voltage, and the current flow is in the direction indicated on Fig. 12-26 as shown by the collector characteristics of Fig. 12-27. The emitter current is negative and flows out of the emitter terminal (electrons flow in). Thus the emitter requires a bias such that current can flow from the emitter into a suitable current source. The corresponding collector and emitter currents are almost equal in magnitude. Since they are opposite in sign, the greater part of the current flow in to the collector flows out through the emitter electrode, leaving very little current flowing in the base electrode. The solid portions of the V_e–I_c characteristics represent the range of normal operation. The dotted portions of these curves correspond to cutoff, which for the transistor means zero collector voltage. A very wide range of collector voltages are available, and these may be controlled by minute changes of emitter voltage, producing relatively large changes in emitter current and in collector current. The static characteristics are such that high-voltage amplification may be expected between a low-impedance source and a high-impedance load.

The emitter voltages are so small that the desired bias emitter current can be calculated as

$$I_e = V_{ee}/R$$

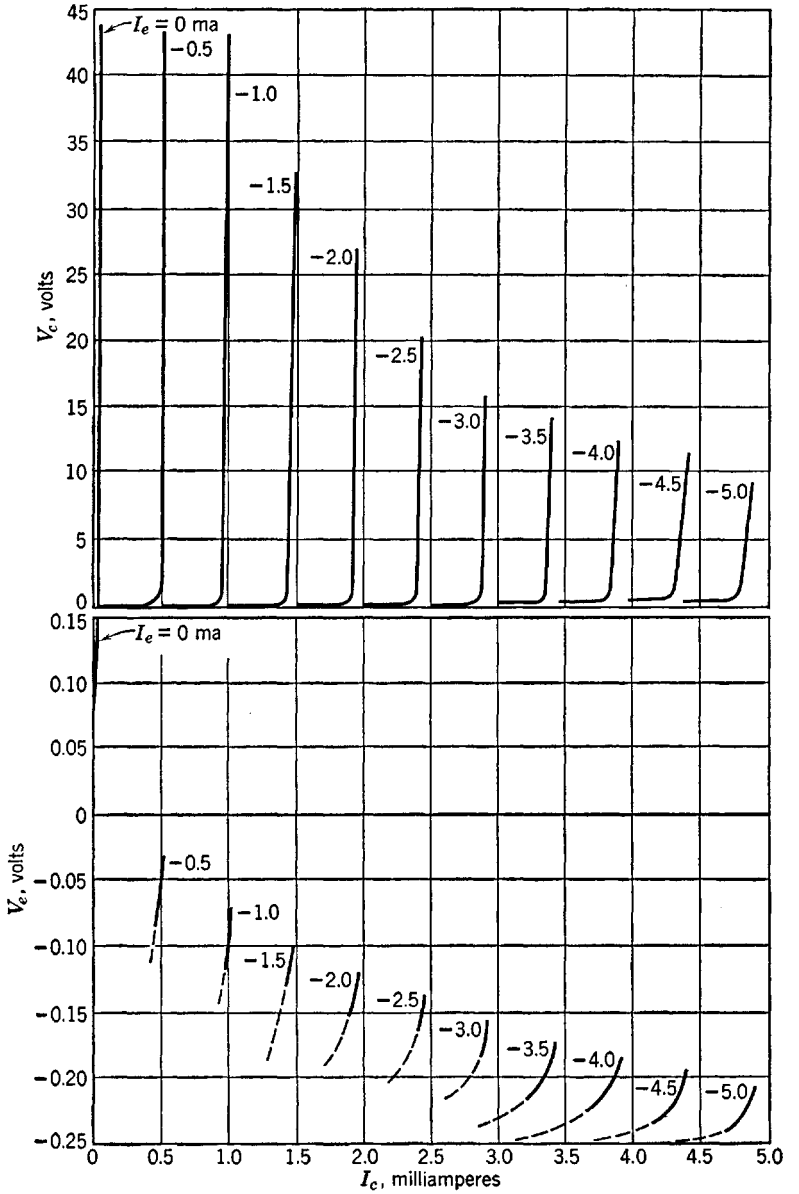

FIG. 12-27. Static characteristics of an n–p–n transistor. (Courtesy Bell Telephone Laboratories)

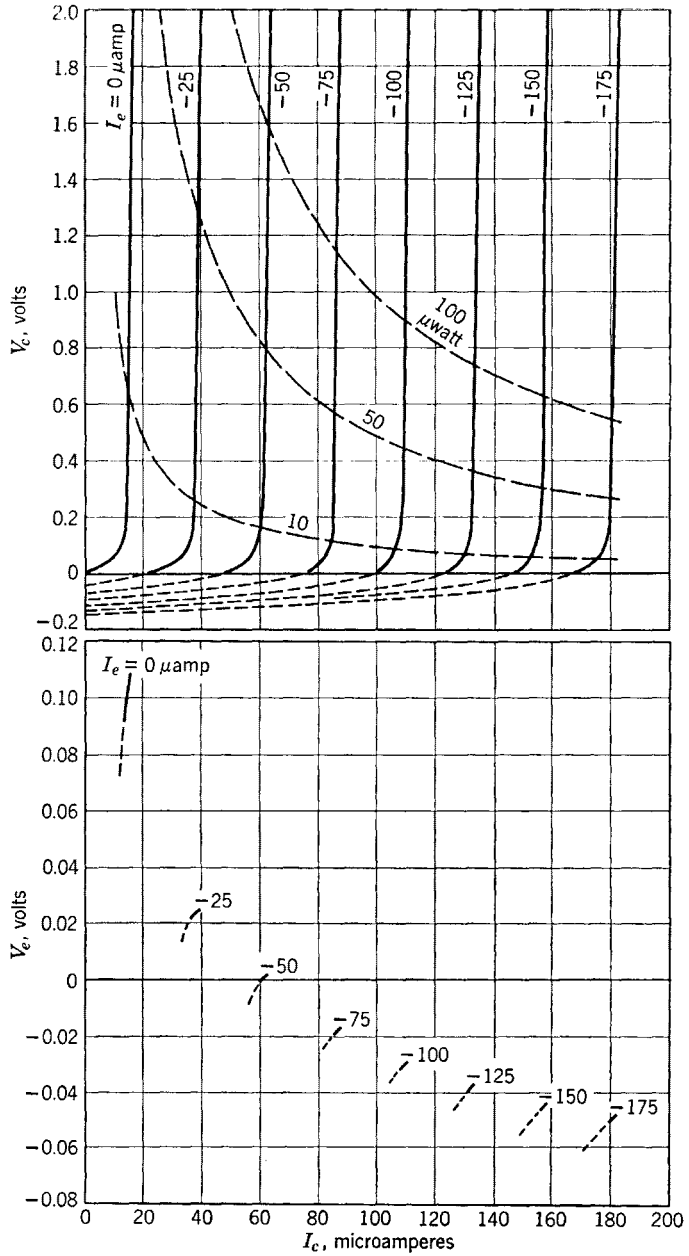

FIG. 12-28. Static n–p–n characteristics for very low-power operation. (Courtesy Bell Telephone Laboratories)

where V_{ee} is the battery voltage used and R is the series resistance between battery and emitter-base circuit.

One of the very striking properties of the n–p–n transistor is its low-power operation. This can be understood more clearly by examining a set of collector characteristics drawn on a scale of I_c and I_e in microamperes and V_e in the voltage range between 0 and 2 volts, as in Fig. 12-28. The transistor can deliver useful gain with very small distortion in this low-power range. Collector power necessary is less than 100 microwatts.

12-16. Circuit Parameters of the n–p–n Transistor

Again the circuit parameters r_{11}, r_{12}, r_{21}, and r_{22} of the four-pole transistor equivalent circuit are determined preferably by a-c measurements as in the type-A case. The same equivalent circuits involving the T of elements r_e, r_b, and r_c with generator of voltage $I_e r_m$ will be used.

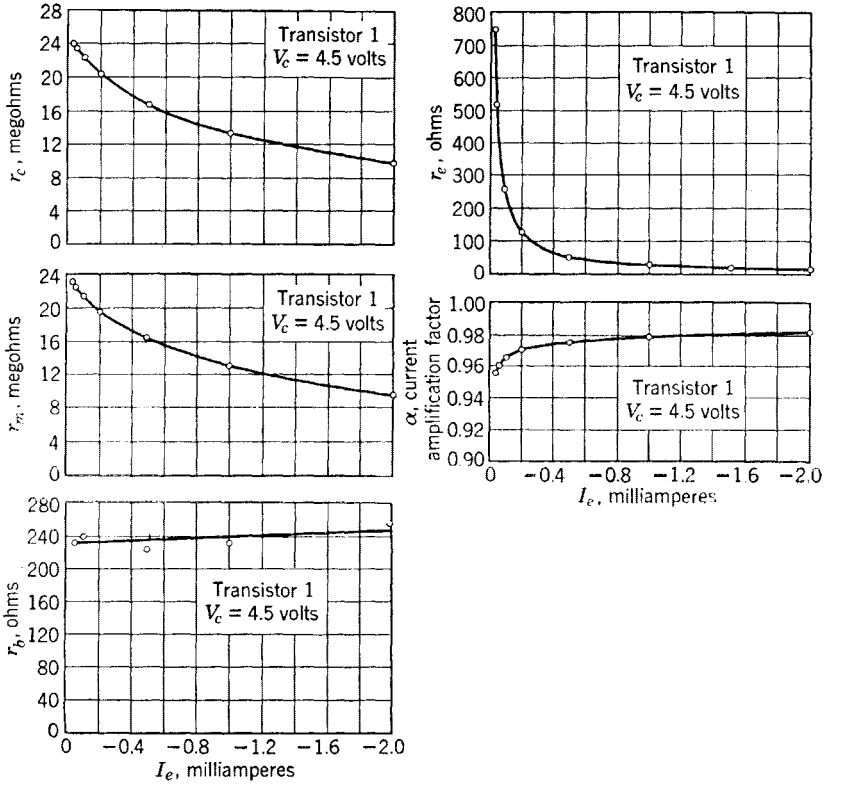

FIG. 12-29. Dependence of T-network parameters on emitter current. (Courtesy Bell Telephone Laboratories)

These parameters, and α as well, depend upon the emitter current as shown in the graphs of Figs. 12-29 from which the magnitudes of the five parameters can be determined. Values plotted in the graphs were determined by measurement,[13] but, in the case of r_e, Shockley [12] has shown that

$$r_e = kT/eI_e \tag{12-75}$$

where k is Boltzmann's constant, T the temperature in degrees Kelvin, e the electronic charge, and I_e the emitter current. At a temperature around 80° F such that $kT/e = 25.9$, values obtained from Eq. 12-75 check well with the curve of r_e as a function of I_e.

12-17. Generalized Circuit Relations for the *n–p–n* Transistor

The various circuit connections such as the grounded base, grounded emitter and grounded collector discussed for the type-A transistor are applicable to the *n–p–n* unit, but the discussion can be shortened in view of the experience already available with the type-A circuit. Since $\alpha < 1$ always for the *n–p–n* transistor, stability problems encountered previously with the type-A units, particularly with respect to impedance matching, will not occur.

The four-pole equations

$$\begin{aligned} V_1 &= I_1 r_{11} + I_2 r_{12} \\ V_2 &= I_1 r_{21} + I_2 r_{22} \end{aligned} \tag{12-76}$$

apply to the circuit of Fig. 12-30, regardless of connection as grounded base, grounded emitter, or grounded collector, provided only that signal amplitudes and operating points are such as to provide linear operation.

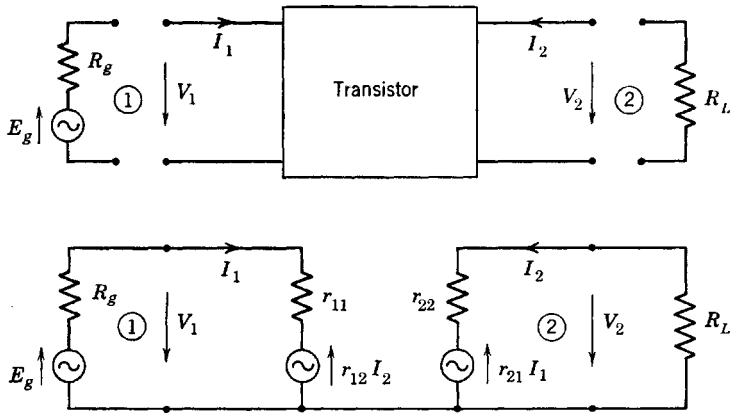

FIG. 12-30. Generalized small-signal circuit of the transistor with terminations.

For the generalized circuit of Fig. 12-30, then, the following relations may be written immediately from the fundamental equations 12-76 and are identical with corresponding relations derived for the type-A transistor (see Eqs. 12-14, 12-15).

The input impedance at terminals 1 is

$$R_{11} = r_{11} - r_{12}r_{21}/(r_{22} + R_L) \tag{12-77}$$

and at 2 is

$$R_{22} = r_{22} - r_{12}r_{21}/(r_{11} + R_g) \tag{12-78}$$

The voltage gain of the four-pole terminated in R_L is

$$A = V_2/V_1 = -I_2R_L/I_1R_{11} \tag{12-79}$$

From the second equation of 12-76, since $V_2 = -I_2R_L$,

$$I_2/I_1 = -r_{21}/(r_{22} + R_L) \tag{12-80}$$

Then,
$$A = \frac{r_{21}R_L}{(r_{22} + R_L)R_{11}} = \frac{r_{21}R_L}{r_{11}(r_{22} + R_L) - r_{12}r_{21}} \tag{12-81}$$

If V_2/E_g is required, it is necessary only to add R_g to r_{11} in Eq. 12-81. Then,

$$\frac{V_2}{E_g} = \frac{r_{21}R_L}{(r_{11} + R_g)(r_{22} + R_L) - r_{12}r_{21}} \tag{12-82}$$

The image impedances of the four-pole (Fig. 12-30) are impedances R_{I1} and R_{I2} of such value that

$$R_{11} = R_{I1} \quad \text{if} \quad R_L = R_{I2}$$

and
$$R_{22} = R_{I2} \quad \text{if} \quad R_g = R_{I1}$$

Thus the proper selection of R_g and R_L will result in an impedance match at both the input and the output. The values of R_{I1} and R_{I2} may be found in terms of the four-pole parameters. If R_L in Eq. 12-77 is replaced by R_{I2}, then R_{11} becomes R_{I1}; thus,

$$R_{I1} = r_{11} - r_{12}r_{21}/(r_{22} + R_{I2}) \tag{12-83}$$

Similarly, in Eq. 12-78, if $R_g = R_{I1}$, then

$$R_{22} = R_{I2} = r_{22} - r_{12}r_{21}/(r_{11} + R_{I1}) \tag{12-84}$$

Equations 12-83 and 12-84 may be solved for R_{I1} and R_{I2}; the results are:

$$R_{I1} = \sqrt{\frac{r_{11}}{r_{22}}(r_{11}r_{22} - r_{12}r_{21})} \tag{12-85}$$

$$R_{I2} = \sqrt{\frac{r_{22}}{r_{11}}(r_{11}r_{22} - r_{12}r_{21})} \tag{12-86}$$

The circuit mesh equations of the circuit of Fig. 12-30 are

$$\begin{aligned} E_g &= I_1(R_g + r_{11}) + I_2 r_{12} \\ 0 &= I_1 r_{21} + I_2(r_{22} + R_L) \end{aligned} \tag{12-87}$$

The determinant of the system is

$$\Delta = (R_g + r_{11})(R_L + r_{22}) - r_{12}r_{21} \tag{12-88}$$

The operating power gain is

$$G_o = \frac{I_2^2 R_L}{E_g^2/4R_g} = 4R_g R_L \left(\frac{-r_{21}}{\Delta}\right)^2 \tag{12-89}$$

The value of G_o becomes maximum for impedance matches at both input and output terminals. Thus, if $R_g = R_{I1}$, and $R_L = R_{I2}$ as defined by Eqs. 12-85 and 12-86 are substituted into Eq. 12-89, the result is the maximum available power gain. The result, after algebraic simplification, is

$$G_{o\,\max} = \frac{r_{21}^2}{r_{11}r_{22}[1 + \sqrt{1 - r_{12}r_{21}/r_{11}r_{22}}]^2} \tag{12-90}$$

12-18. The Grounded-Base Circuit, *n–p–n*

A practical arrangement of the grounded-base circuit and an equivalent a-c circuit are shown in Fig. 12-31. Calculation of the circuit properties of the stage may be carried out in terms of r_e, r_b, r_c, and r_m, or the four-pole equivalents of these may be used in Eqs. 12-76 to 12-90. Application of Eq. 12-76 and the r definitions to the circuit of Fig. 12-31 show that

$$\left.\begin{aligned} r_{11} &= r_e + r_b \\ r_{21} &= r_m + r_b \\ r_{12} &= r_b \\ r_{22} &= r_c + r_b \\ \alpha &= r_{21}/r_{22} = (r_m + r_b)/(r_c + r_b) \end{aligned}\right\} \tag{12-91}$$

from which the four-pole parameters may be computed in case values of the T-network parameters are supplied by the manufacturer.

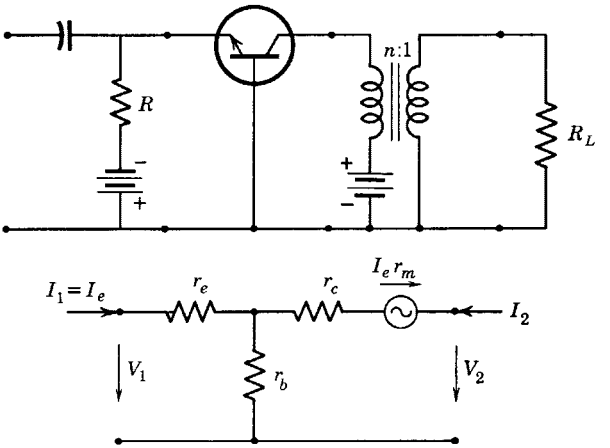

FIG. 12-31. Biasing circuit and n–p–n equivalent a-c circuit, grounded base.

A set of values of circuit parameters for an early development n–p–n unit is given herewith for comparison with the type-A transistor:

$$r_e = 25.9 \text{ ohms}$$

$$r_b = 240 \text{ ohms}$$

$$r_c = 13.4 \cdot 10^6 \text{ ohms}$$

$$r_m = 13.1 \cdot 10^6 \text{ ohms}$$

$$r_c - r_m = 0.288 \cdot 10^6 \text{ ohms}$$

$$\alpha = 0.9785$$

It has been shown [13] that a grounded-base stage using this transistor has the circuit properties listed in Table 12-5. It is suggested that the given results should be computed as an exercise.

TABLE 12-5. CALCULATED CIRCUIT PROPERTIES OF AN *n–p–n* JUNCTION-TYPE GROUNDED-BASE TRANSISTOR

Circuit Property	Terminations, ohms Resistance Tabulations, ohms							
	$R_g = 0$ $R_L = \infty$	$R_g = 0$	$R_L = 0$	$R_g = \infty$	$R_L = \infty$	$R_g = R_{I1}$	$R_L = R_{I2}$	$R_g = 25$ $R_L = 200{,}000$
V_2/E_g	$4.93 \cdot 10^4$							
R_{11}			31.1		266		91	
R_{22}		$1.56 \cdot 10^6$		$13.4 \cdot 10^6$		$4.58 \cdot 10^6$		
G_o								5300 or 37.2 db
G_o max						27,000 or 44.3 db		

Transistor 4-pole parameters:

$r_{11} = 266$ ohms; $r_{12} = 240$ ohms
$r_{21} = 13.1 \cdot 10^6$ ohms; $r_{22} = 13.4 \cdot 10^6$ ohms; $\alpha = 0.9785$

12-19. The Grounded-Emitter Circuit, *n–p–n*

The grounded-emitter circuit shown by Fig. 12-32 provides very high power gains—about 50 db—and has impedances of the order of hundreds

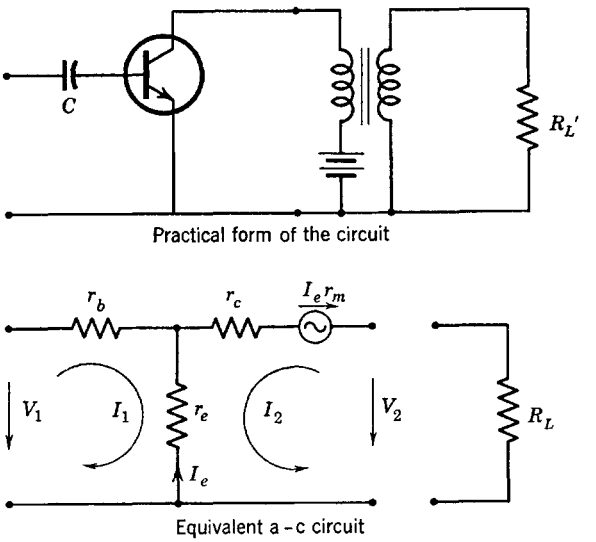

FIG. 12-32. Grounded-emitter circuits of an *n–p–n* transistor.

of ohms at the input and hundreds of thousands of ohms at the output. Voltage phase reversal is experienced, and voltage gain is of the order of 30 db without interstage coupling transformers. The biasing collector voltage may be provided for as shown in Fig. 12-32. The collector bias will be practically the same as the supply voltage since the emitter voltage is in the range 0 to -0.25 volt. The base is shown without d-c bias. Operated in this manner, the base will reach a potential equal in magnitude to that of the emitter. Since the condenser eliminates the d-c component of base current, the d-c components of emitter and collector currents will be exactly the same.

Figure 12-28 shows that I_c is somewhat less than 20 μamp for $I_e = 0$. Suppose that α remains constant as I_c increases. As I_c increases, so does I_e, but, for an increase ΔI_e in emitter current, the increase $\Delta I_c = \alpha\,\Delta I_e$ is somewhat less than ΔI_e since $\alpha < 1$. Therefore, one may compute the value of I_c or of I_e at which the two currents become equal, since, beginning with $I_e = 0$,

$$I_e = \Delta I_e = I_{co} + \Delta I_c = I_{co} + \alpha\,\Delta I_e = I_c$$

whence

$$\Delta I_e = I_{co}/(1 - \alpha) = I_e = I_c \tag{12-92}$$

where I_{co} is the value of I_c for zero emitter current. Thus, Eq. 12-92 permits the calculation of the emitter (and collector) current which will flow in the grounded-emitter circuit if no d-c connection is made to the base. Since α is nearly equal to 1, I_e or I_c for the grounded-emitter connection with floating base change very rapidly with α. It is possible

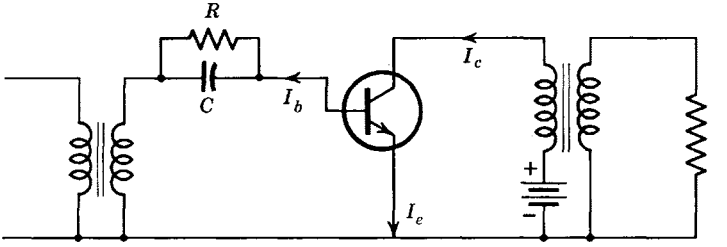

FIG. 12-33. Reduction of collector current by resistance R by-passing C of Fig. 12-32.

to reduce I_e or I_c, which may be desirable in order to reduce power consumption, by providing a path for direct current to flow from the base. If a small current is drawn from the base, the reduction in collector current is $\alpha/(1 - \alpha)$ microamperes per microampere drawn from the base. The reason for this reduction is that the base floats at a small positive potential with respect to ground. Thus, if a resistor is added to the circuit as shown in Fig. 12-33, and the current directions are as

shown, then, in general

$$I_c = I_e + I_b$$

but initially, that is, before the insertion of R,

$$I_{c1} = I_{e1}$$

But

$$I_c = I_{c1} + \Delta I_c = I_{e1} + \Delta I_e + I_b$$

after the insertion of R. Therefore,

$$\Delta I_c = \Delta I_e + I_b$$

Again if it is assumed that α is constant and equal to $\Delta I_c/\Delta I_e$,

$$\alpha\, \Delta I_e = \Delta I_e + I_b$$

and

$$\Delta I_e = -I_b/(1 - \alpha) \tag{12-93}$$

which is a decrease in I_e if I_b is positive. Since initially the collector and emitter currents were equal (before addition of R), Eq. 12-93 is approximately also the change in collector current. More accurately, the change in collector current resulting from the connection of R is

$$\Delta I_c = \alpha\, \Delta I_e = -\frac{\alpha}{1 - \alpha} I_b \tag{12-94}$$

again a decrease for I_b positive. If R is decreased toward zero, the emitter-to-base potential difference becomes zero, and the collector current decreases to the value corresponding to $v_e = 0$ (Fig. 12-28). This result is quite analogous to the flow of grid current through a grid-leak resistor in a vacuum tube resulting in a reduction of plate current be-

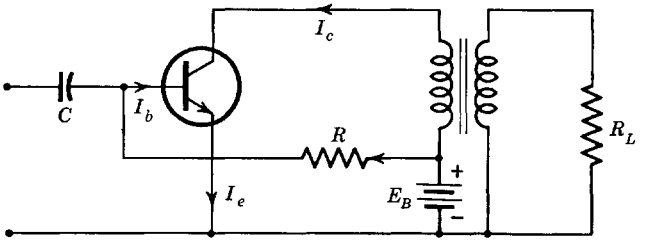

FIG. 12-34. Use of a biasing resistor R to increase the collector current by providing a current through the base in the direction shown.

cause of an increasingly negative grid bias. The insertion of resistance in the emitter circuit would result in the emitter becoming positive with respect to the base, which would still further reduce the collector current, as may be seen by referring to Fig. 12-28.

Another connection of a biasing resistor as shown in Fig. 12-34 produces an increase of v_c with respect to the base equal to the voltage across R. As may be seen from Fig. 12-28, this increase results in an increase in I_c. An analysis based on Fig. 12-34 shows that the increase of I_c is given by

$$\Delta I_c = \frac{\alpha}{1 - \alpha} I_b \tag{12-95}$$

where

$$I_b \cong E_b/R \tag{12-96}$$

The mesh equations for the equivalent a-c circuit of Fig. 12-32 are

$$\begin{aligned} V_1 &= I_1(r_b + r_e) + I_2 r_e \\ V_2 &= I_1(r_e - r_m) + I_2(r_c + r_e - r_m) \end{aligned} \tag{12-97}$$

whence, by inspection,

$$\begin{aligned} r_{11} &= r_b + r_e \\ r_{12} &= r_e \\ r_{21} &= r_e - r_m \\ r_{22} &= r_c + r_e - r_m \end{aligned} \tag{12-98}$$

The same values of r_e and r_m used for the grounded-base stage give

$$r_{21} = 25.9 - 13.1 \cdot 10^6 = -13.1 \cdot 10^6 \text{ ohms}$$

All the remaining four-pole parameters of the grounded-emitter circuit are positive. Thus, from Eq. 12-81 or 12-82, the voltage V_2 is 180° out of phase with V_1 or with E_g, as in the case of the grounded-cathode vacuum tube with resistive load at low frequency.

In case R_L of the equivalent a-c circuit of Fig. 12-32 is infinite, $I_2 = 0$. Then, from Eq. 12-97,

$$V_2/V_1 = (r_e - r_m)/(r_b + r_e) \tag{12-99}$$

If R_L were zero, $V_2 = 0$, and

$$I_2 = \frac{r_m - r_e}{r_c + r_e - r_m} I_1 \tag{12-100}$$

But, with $r_m = 13.1 \cdot 10^6$ ohms, $r_e = 25.9$ ohms, $r_c = 13.4 \cdot 10^6$ ohms, $r_c - r_m = 0.288 \cdot 10^6$ ohms,

$$I_2 \cong \frac{r_m}{r_c - r_m} I_1 = \frac{r_m/r_c}{1 - r_m/r_c} I_1 \cong \frac{\alpha}{1 - \alpha} I_1 = 45.5 I_1 \tag{12-101}$$

which is a measure of the current amplification possibilities of the

grounded-emitter circuit and shows that the current amplification of the amplifier increases rapidly as $\alpha \rightarrow 1$.

Calculated values of the circuit properties of a grounded-emitter transistor amplifier are summarized in Table 12-6.

TABLE 12-6. CALCULATED CIRCUIT PROPERTIES OF AN n–p–n GROUNDED-EMITTER TRANSISTOR

Circuit Property	Terminations, ohms Resistance Tabulations, ohms						
	$R_g = 0$ $R_L = \infty$	$R_g = 0$	$R_L = 0$	$R_g = \infty$	$R_L = \infty$	$R_g = R_{I1}$	$R_L = R_{I2}$
V_2/E_g	$-4.93 \cdot 10^4$						
I_2/I_1			45.5				
R_{11}			1440		266		619
R_{22}		$1.56 \cdot 10^6$		$0.288 \cdot 10^6$		$0.671 \cdot 10^6$	
G_o max						$2.02 \cdot 10^5$ or 53 db	

Transistor 4-pole parameters:

$r_{11} = 266$ ohms; $r_{21} = -13.1 \cdot 10^6$ ohms
$r_{12} = 25.9$ ohms; $r_{22} = 0.288 \cdot 10^6$ ohms; $\alpha = 0.9785$

Since the size of the output image impedance, 671,000 ohms (Table 12-6) is so large compared with that of the input image impedance, 619 ohms, it is evident that impedance matching between stages can be achieved only by using stepdown interstage transformers. A two-stage circuit is shown in Fig. 12-35. Such a circuit enclosed in a transparent

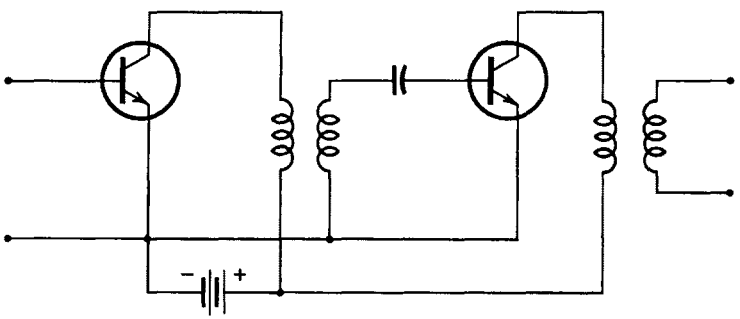

FIG. 12-35. A two-stage, grounded-emitter, transformer-coupled n–p–n transistor amplifier.

plastic similar to lucite and occupying a total volume of less than 1 cubic inch has been constructed [13] and provides an over-all power gain of about 90 db.

12-20. The Grounded-Collector Circuit, *n–p–n*

The grounded-collector transistor, like the vacuum-tube cathode follower as already discussed, will provide high-input and low-output impedances and no phase reversal. The circuits of Fig. 12-36 show the biasing methods, and the equivalent a-c circuit. The base may be allowed to float and will reach a very small positive potential with respect to the emitter as discussed in connection with the grounded-emitter stage. A high resistance connected in such a way as to produce biasing current out of the base, as shown in Fig. 12-36*b*, reduces the collector current but, if connected as in Fig. 12-36*c* to permit the flow of direct biasing current into the base, will increase the collector current.

The circuit equations of Fig. 12-36*d* are

$$\begin{aligned} V_1 &= I_1(r_b + r_c) + I_2(r_c - r_m) \\ V_2 &= I_1 r_c + I_2(r_e + r_c - r_m) \end{aligned} \tag{12-102}$$

whence

$$\begin{aligned} r_{11} &= r_b + r_c \\ r_{12} &= r_c - r_m \\ r_{21} &= r_c \\ r_{22} &= r_e + r_c - r_m \end{aligned} \tag{12-103}$$

If operated between a zero-impedance generator and an infinite-impedance load, $I_2 = 0$, and

$$V_2/V_1 = r_c/(r_b + r_c) \tag{12-104}$$

a gain slightly less than unity. If $R_L = 0$, $V_2 = 0$, and, from Eq. 12-102,

$$\frac{I_2}{I_1} = -\frac{r_c}{r_e + r_c - r_m} = -\frac{1}{1 + r_e/r_c - r_m/r_c} \tag{12-105}$$

The same *n–p–n* transistor values previously used give

$$I_2/I_1 \cong -1/(1 - \alpha) = -46.5 \tag{12-106}$$

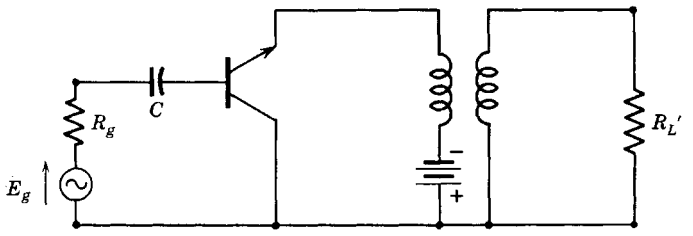

(a) No d-c bias, emitter to base

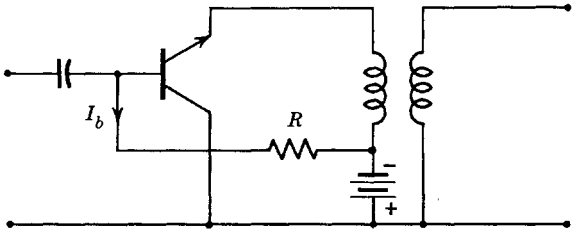

(b) Biasing current I_b reduces collector current

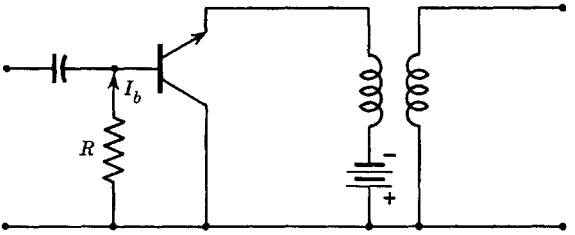

(c) Biasing current I_b increases collector current

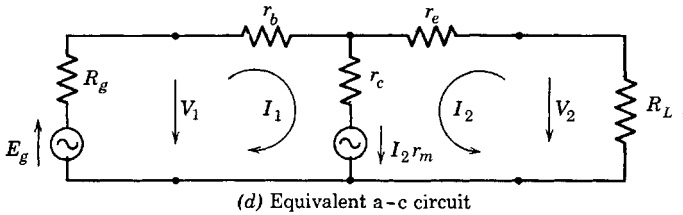

(d) Equivalent a-c circuit

FIG. 12-36. Circuits and biasing of the grounded-collector stage.

Other computed values are listed in Table 12-7.

TABLE 12-7. COMPUTED CIRCUIT PROPERTIES OF A GROUNDED-COLLECTOR *n–p–n* TRANSISTOR AMPLIFIER

Circuit Property	Terminations, ohms Resistance Tabulations, ohms						
	$R_g = 0$ $R_L = \infty$	$R_g = 0$	$R_L = 0$	$R_g = \infty$	$R_L = \infty$	$R_g = R_{I1}$	$R_L = R_{I2}$
V_2/E_g	~1						
I_2/I_1			−46.5				
R_{11}			1445		$13.4 \cdot 10^6$		139,000
R_{22}		31.1		$0.288 \cdot 10^6$		2990	
G_o max						46.5 or 16.7 db	

Transistor 4-pole parameters:

$r_{11} = 13.4 \cdot 10^6$ ohms; $r_{12} = 0.288 \cdot 10^6$ ohms
$r_{21} = 13.4 \cdot 10^6$ ohms; $r_{22} = 0.288 \cdot 10^6$ ohms

12-21. Frequency Limitations of the *n–p–n* Transistor

The frequency limitations of the *n–p–n* transistor seem to be somewhat more severe than those of the type A. The explanations for the observed frequency effects have been given by Shockley in terms of the physics of the transistor as a semiconductor. There are, in brief, three principal effects. The first, explained as a dispersion in transit time of electrons crossing the p layer is measured in terms of a decrease in α with frequency and leads to a frequency cutoff at a frequency for which α^2 is reduced by a factor of one half, as already explained in the case of the type-A transistor. This frequency cutoff is, according to Shockley, inversely proportional to the thickness of the p layer and may be expected to occur at a frequency between 5 and 20 Mc in transistors having parameters as used in example computations of preceding pages.

A second frequency response limitation is dependent upon an effective capacitance at the emitter junction in shunt with r_e. The shunted r_e and r_b are in series with the source impedance so that the cutoff frequency (at which the response is down 3 db) depends upon R_g and r_b but ultimately upon r_b. Thus this cutoff frequency increases as r_b decreases, and is of the same order of magnitude as the α-cutoff frequency.

The third and most important cause of limited frequency response

is the fact that the p and n layers at the collector junction behave as the plates of a capacitance of appreciable magnitude. This capacitance also

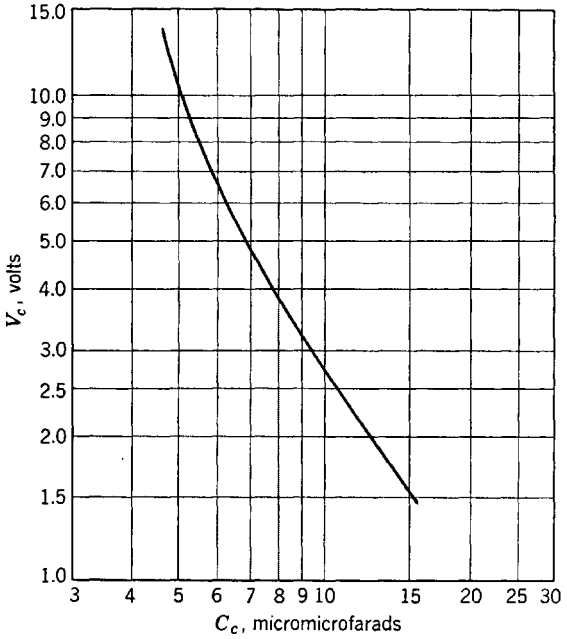

(a) Relation, C_c to V_c, for $I_c = 1$ ma

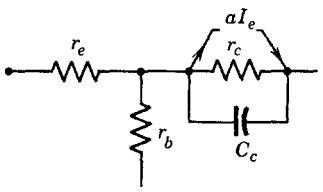

(b) High-frequency circuit

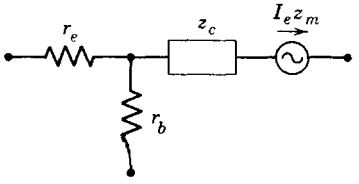

(c) Simplified high-frequency circuit

FIG. 12-37. Collector junction capacitance and its dependence on collector voltage. (Courtesy Bell Telephone Laboratories)

depends upon collector voltage as shown by Fig. 12-37. The cutoff frequency produced by this capacitance is much lower than that produced by either of the other two. The equivalent T circuit with the collector capacitance C_c is shown in Fig. 12-37. The collector arm and its current source may be replaced by a voltage-source generator of impedance

$$z_c = \frac{r_c(1/j\omega C_c)}{r_c + 1/j\omega C_c} = \frac{r_c}{1 + j\omega C_c r_c} \tag{12-107}$$

and generated voltage

$$E_c = aI_e[z_c] = \frac{r_m I_e}{1 + j\omega C_c r_c} = z_m I_e \tag{12-108}$$

The frequency response of the circuit for any of the three connections of interest can then be analyzed by use of z_c and z_m instead of r_c and r_m in the derived equations. The simplified circuit is shown in Fig. 12-37c.

The low-frequency gain $V_2/E_g = A$ (Eq. 12-82) takes the following forms for the indicated transistor connection as expressed in terms of the T-network parameters:

Grounded base:

$$A = \frac{(r_m + r_b)R_L}{(r_e + r_b + R_g)(r_c + r_b + R_L) - r_b(r_m + r_b)} \tag{12-109}$$

Grounded emitter:

$$A = \frac{(r_e - r_m)R_L}{(r_e + r_b + R_g)(r_e + r_c - r_m) - r_e(r_e - r_m)} \tag{12-110}$$

Grounded collector:

$$A = \frac{r_c R_L}{(r_b + r_c + R_g)(r_e + r_c - r_m) - r_c(r_c - r_m)} \tag{12-111}$$

The numerical values given for the T-network parameters are such that the following approximations are justified:

$$(r_m + r_b) \cong r_m$$

$$r_e - r_m \cong -r_m$$

$$r_m/r_c \cong \alpha$$

Then, for the grounded-base connection, the low-frequency gain may be expressed in the form

$$A = \frac{\alpha R_L}{R_0(1 + R_L/r_c) - \alpha r_b} \tag{12-112}$$

where

$$R_0 = r_e + r_b + R_g \tag{12-113}$$

At higher frequencies such that the circuit of Fig. 12-37c must be used, the high-frequency gain as obtained from Eq. 12-112 with the help of Eqs. 12-107 and 12-108 is

$$A_H = \frac{\alpha R_L}{R_0 - \alpha r_b + R_0 R_L / r_c + R_0 R_L j\omega C_c} = \frac{A}{1 + \dfrac{j\omega C_c R_0 R_L}{R_0 - \alpha r_b + R_0 R_L / r_c}} \tag{12-114}$$

Thus, $| A_H/A | = 1/\sqrt{2}$ at a frequency f_c such that

$$f_c = \frac{1}{2\pi C_c}\left(\frac{1}{R_L} + \frac{1}{r_c} - \frac{\alpha r_b}{R_0 R_L}\right) \tag{12-115}$$

which is defined as the collector cutoff frequency. If $R_L = 20{,}000$ ohms, $R_g = 25$ ohms, $C_c = 7$ $\mu\mu$f, and, with $\alpha = 0.9785$, $r_c = 13.4 \cdot 10^6$ ohms, $r_e = 25.9$ ohms, $r_b = 240$ ohms, then $R_0 = 290.9$, and $f_c = 0.227 \cdot 10^6$ cps.

Collector cutoff frequencies for the grounded-emitter and grounded-collector stages may be computed from equations derived in a similar way from the respective four-pole parameters and the voltage gain equations. The results are summarized in Table 12-8.

TABLE 12-8. TABULATION OF COLLECTOR CUTOFF FREQUENCY AND GAIN FOR VARIOUS CIRCUITS AND TERMINATIONS, *n–p–n* TRANSISTOR

Cutoff Frequency and Power Gain		Terminations, ohms						
		$R_g = R_{I1}$ $R_L = R_{I2}$	$R_g = 25$ $R_L = 2 \cdot 10^5$	$R_g = 25$ $R_L = 2 \cdot 10^4$	$R_g = 1000$ $R_L = 10^5$	$R_g = 1000$ $R_L = 10^4$	$R_g = 1000$ $R_L = 1000$	$R_g = 139{,}000$ $R_L = 25$
Grounded base	f_c	3390 cps	23,500 cps	227,000 cps				
	G_o	44.3 db	37.2 db	27.8 db				
Grounded emitter	f_c	3740 cps			11,120 cps	97,900	943,000 cps	
	G_o	53 db			50 db	41.3 db	31.4 db	
Grounded collector	f_c	320,000 cps						$9.77 \cdot 10^6$ cps
	G_o	16.7 db						1.8 db

12-22. Transistor Noise

The problem of noise in transistors has been a difficult one. Noise figures around 60 db were recorded for the earlier forms of the type-A transistor, and measurements [13] of the *n–p–n* units show noise figure values varying from 10 to 17 db for collector voltages between 2 and 16

volts. Additional reductions of noise should accompany continued development of the device as increased knowledge of the factors contributing to noise becomes available through research.

PROBLEMS

12-1. The density of Ge is 5.46 g per cc, its atomic weight 72.60. Find (*a*) the mass of one Ge atom (see mass of the atom of unit atomic weight), (*b*) the number of Ge atoms per cubic centimeter in solid Ge, (*c*) the number of electrons involved in the electron-bond pairs per cubic centimeter.

12-2. Suppose that 4 μg of antimony are thoroughly mixed in molten form with 100 g of pure germanium and that the antimony atoms substitute for Ge atoms uniformly throughout the solid material, after solidification, as indicated in Fig. 12-5. Compute (*a*) the density of antimony atoms, (*b*) the density of donated electrons, assuming uniform distribution.

12-3. If $g_e = 3600$ cm per sec per volt per cm for the carriers of problem 12-2, compute (*a*) the conductivity, (*b*) the total resistance of a bar of such *n*-type germanium 1 inch long and 0.005 by 0.005 inch in cross section.

12-4. Compute the conductivity of *p*-type Ge containing 1 μg of gallium per 100 g of germanium.

12-5. If generator and load are connected to the terminals of the circuit of Fig. 12-11, the determinant of the system of equations is

$$\Delta = (z_{11} + Z_g)(z_{22} + Z_L) - z_{12}z_{21}$$

Derive equations for the input and output impedance of the circuit at terminals 1 with Z_L connected at 2 and at terminals 2 with Z_g connected at 1.

12-6. Derive the expression for the operating power gain of the circuit of Fig. 12-11, and show that it is

$$G_o = 4R_gR_L \left| -z_{21}/\Delta \right|^2$$

12-7. Show that the insertion power gain of the circuit of Fig. 12-11 is

$$G_i = \left| (Z_g + Z_L)z_{21}/\Delta \right|^2$$

12-8. Operating data and parameters for a grounded-base type-A transistor amplifier are as follows:

D-c operating point:	$I_e = 0.6$ ma,	$V_e = 0.7$ volt
	$I_c = -2.0$ ma,	$V_c = -40$ volts
Circuit parameters:	$z_{11} = 530$ ohms $= r_{11}$	
	$r_{12} = 290$ ohms,	$r_{21} = 34{,}000$ ohms
	$r_{22} = 19{,}000$ ohms	

The amplifier is driven by a generator of 500 ohms internal resistance and operates into a load resistor of 20,000 ohms.

(*a*) Compute the input resistance R_{11} and the output resistance R_{22}.

(*b*) Compute the operating power gain G_o.

(*c*) Compute the insertion power gain G_i.

(*d*) Compute the voltage gain A.

12-9. Derive Eqs. 12-39 and 12-40 by direct application of Kirchhoff's laws to the circuit of Fig. 12-15.

12-10. Derive the expressions 12-41 and 12-42 for the forward and backward operating power gains of a grounded-emitter type-A transistor amplifier.

12-11. If the transistor of problem 12-10 is connected grounded emitter between a generator of $R_g = 500$ and a load of $R_L = 20{,}000$ ohms, compute the following: (*a*) the input and output resistances, (*b*) the forward and reverse operating power gains, (*c*) the forward voltage gain, (*d*) the insertion voltage gain (this is the voltage across R_L with the transistor inserted divided by the voltage across R_L if the generator is directly connected to R_L).

12-12. A grounded-collector type-A transistor amplifier has $r_e = 250$ ohms, $r_b = 250$ ohms, $r_c = 20{,}000$ ohms, and $r_m = 40{,}000$ ohms. If $R_g = 20{,}000$ ohms, $R_L = 10{,}000$ ohms, compute (*a*) R_{11} and R_{22}, (*b*) G_{12} and G_{21}, the operating power gains in each direction, (*c*) G_{12} and G_{21} for $R_L = R_g = 20{,}000$ ohms, (*d*) the voltage gain, each direction.

12-13. A four-pole linear active network is composed of a general four-pole in cascade with an ideal transformer. Obtain the over-all four-pole impedance parameters if (*a*) the transformer is connected stepdown with turns ratio n to 1 at the input of the general four-pole, (*b*) the transformer is connected stepdown with turns ratio n to 1 at the output of the general four-pole. In both cases, $n > 1$.

12-14. Determine the conditions for obtaining the maximum insertion power gain per stage of the grounded-base, transformer-coupled amplifier of Fig. 12-21, and compute G_i and $G_{i\,\max}$ for the circuit parameters of problem 12-8.

12-15. Check the stability criterion of the grounded-emitter cascade stage of Fig. 12-22 for $R_a = 17{,}000$ ohms.

12-16. Compute R_{11}, R_{22}, and G_i for the grounded-emitter cascade stage of Fig. 12-22 with $R_a = 17{,}000$ ohms, $r_b = 290$ ohms, $r_m = 34{,}000$ ohms, $r_c = 19{,}000$ ohms, and $r_e = 240$ ohms.

12-17. Assume an operating point of $I_{c0} = -9$ ma, $V_{c0} = -36$ volts for the transistor represented by Fig. 12-25, and determine, from the graph, the values of r_{22}, r_{21}, and α in the vicinity of the operating point.

12-18. Draw a load line corresponding to $R_L = 5000$ ohms on the output characteristic sheet (Fig. 12-25), and determine the following (use the operating point of problem 12-17):

(*a*) Collector source voltage required.

(*b*) Power output corresponding to a variation of emitter current from 0 to 10 ma.

12-19. Sketch a load line corresponding to 6000 ohms on a set of output characteristics for the n–p–n transistor. For an operating point corresponding to an emitter current of -2.5 ma, $V_c = 15$ volts, determine the following:

(*a*) I_c at the operating point.

(*b*) The collector voltage swing corresponding to a variation in emitter current from 0 to -5 ma caused by a sinusoidal a-c signal in the emitter circuit.

(*c*) The a-c power delivered by the transistor.

(*d*) The transistor collector circuit conversion efficiency.

(*e*) The voltage gain.

12-20. Compute the circuit properties of the transistor grounded-base amplifier of Table 12-5, and fill in, in addition, the first three vacancies in the last column.

12-21. The transistor amplifier stage of Fig. 12-31 is required to operate at $I_e = -2$ ma, $V_c = +20$ volts. The turns ratio of the ideal transformer is 4 to 1 stepdown.

(*a*) Determine suitable voltages of the biasing batteries and a value of R.

(*b*) Compute the voltage and operating power gains if the circuit is driven by a generator of internal impedance 500 ohms and $R_L = 500{,}000$ ohms. Compare the phase of input and output voltages.

INDEX

Acceptor, 418
Admittance, cathode follower, 133–134
  four-pole, 36–43
  input, terminated four-pole, 38
    tetrode amplifier, 59
    triode amplifier, 43–44
  output, terminated four-pole, 38
Aiken, C. B., 261
Amplification factor, current, for transistor, 438–440
  definition, voltage, for tube, 11–12, 14
  measurement of, tube, 27
Amplifier—a-f power, 149–167
  class AB push-pull, 161–163
  distortion, class AB, 161–163
    power tetrodes and pentodes, 159–161
  load-coupling circuits, 152–153
  maximum power output from, 155–156
  optimum operation, tetrodes and pentodes, 159–161
  plate dissipation, 150–151
  plate efficiency, 152
    theoretical optimum, triodes, 157–158
  power output, 149–152
Amplifier—a-f vacuum tube, 76
  broad-band (wide-band), 134–144
  cathode follower, 132–134
  circuit, elementary, 15, 17, 23, 31
  classification, 76–77
Amplifier—a-f vacuum tube, class A, 76–77
  broad-band, 134–144
  degenerative, 116–134
  direct coupled, 80–84
  distortion in, 65, 78, 159–161
Amplifier—a-f vacuum tube, dynamic characteristic of, 15–17, 66
  equivalent a-c circuit of, 23, 31
  feedback in, 116–134
  grid-bias voltage for, 14, 15, 22, 25, 49, 50
  inductance-capacitance-coupled, 92
  input admittance of, 43–44
  load line for, 15–17, 74, 153–154
  load resistor for, 15
  output impedance of, 128–129
  phase reversal in, 19–20
  quiescent operating point for, 13, 17, 22, 23
  reactive load, effect of, 21, 29–30
  resistance–capacitance-coupled, 79, 84–92
  transformer-coupled, 80, 93–104
  voltage gain of, definition, 24, 32
Amplifier—r-f class A, 263–285
  see also Tuned amplifier, Single-tuned amplifier, and Double-tuned amplifier.
  cascaded, 280–282
  direct coupled, tuned, 263–267
  double-tuned, transformer-coupled, 272–278
  general requirements for, 263
  grounded grid, 283–285
  single tuned, transformer-coupled, 267–271
  stagger tuning of, 282–283
  tuned circuits for, analysis, 249–262
Amplifier—r-f power, 290–320
  analysis, problem of, 296
  applications of, 292
  circuit for, 291
  class B, algebraic analysis, 297–303

Amplifier—r-f power, class B, equivalent circuit of, 301
graphical analysis, 303–309
linear properties of, 293–294
phase relations, 299
plate dissipation, 302–303
class C, analysis of, 297–303
external characteristics, 293–294
frequency multiplier, 313–314
grid- and plate-current wave forms, 306
grid driving power, 309
grid-modulated, 370
mechanical analogy for, 313
modulator use, 294
phase relations, 291
plate-modulated, 366
synchronous switch, 290
efficiency of, 295, 301
grounded-grid circuit, 318–319
load-coupling analysis, 309–313
neutralization of triode, 314–317
power supplies for, 317–318
secondary emission effects, 294
tank circuit, 291
tank current, 292, 293
Amplifier, transistor, *see* Transistor amplifier.
Amplitude limitation, oscillator, 324
Amplitude modulation, definitions for, 358
degree of, or factor, 362
efficiency, 368–369
frequency spectrum, 363
grid, of class-C amplifier, 370
methods of producing, 365–371
modulated carrier, equation, 363
modulating wave, equation, 360
nature of, reasons for, 356–359
per cent of, 362
plate, of class-C amplifier, 365–368
plate dissipation, 369
power distribution in, 364–365
power relations in, 367–370
receiver for AM waves, 396
sidebands, 363
vector representation of AM waves, 364
Angle modulation, 358, 360
Anode, 2
Arc discharge, 171
Archimbau, L. B., 372
Arc tubes, 177
Armstrong, E. H., 383
Atoms, arrangements of, in germanium, 420
impurity, in germanium, 422–423

Bailey, F. M., 384
Band in energy-level diagram, 416
Band-pass amplifier, 272–278
see also Doubled-tuned transformer-coupled amplifier.
Bandwidth, definition of, 249–250
double-tuned coupled circuit, 261–262
double-tuned transformer-coupled amplifier, 276
expression for, parallel circuit, 251
series circuit, 249
FM requirement, 373–376
single-tuned direct-coupled amplifier, 266
single-tuned transformer-coupled amplifier, 271
Bardeen, J., 423
Barkhausen criterion, oscillators, 327–328
Barrier layer in rectifier, 423–424
Beam tetrode or beam-power tube, 61–63
electrode arrangement, 63
static characteristics, 62
Beat-frequency oscillator, 397–398
Bedford, A. V., 141
Bessel functions, brief table, 373
Bias, grid, 14, 15, 22, 25, 49, 50
Bias control of thyratron, 216
Bias impedance compensation, 143
Biasing resistor, 25, 49, 50
Bias methods, transistors, *see* Transistor amplifier circuits—*n–p–n*.
Bias-stabilized oscillator, 344
Black, H. S., 118
Bleeder resistor, 207–209
Bode, H. W., 128
Boltzmann constant, 419
Brattain, W. H., 423
Bridge connection, three-phase rectifier, 238
Bridge-stabilized oscillator, 343
Broad-band amplifier, 134–144

Broad-band amplifier gain-frequency compensation, 136–144
phase-shift compensation, 138–141
time delay, 138–141
Buffer amplifier, use of, 335
Buss, R. R., 346
By-pass capacitor, 50, 51, 75, 141, 143

Cahill, F. C., 346
Capacitance, interelectrode, 41
effect of, 43–46, 53, 279, 283–285, 314–317
grid plate, 43, 53
of pentode, 64
of tetrode, 59
Capacitance filter, analysis, 199–203
ripple factor, 203
Capacitor, by-pass, 50, 51, 75, 141, 143
Capacitor-input filter, 210–212
ripple factor, 212
Carrier wave, 357
amplitude-modulated, 362
amplitude of, 360
frequency of, 360
Cascaded amplifiers, 280–282
bandwidth, 281
bandwidth reduction factor, 281–282
Cathode, 2
mercury pool, 177
oxide-coated, 177
photosensitive, 46–48
Cathode follower, 132–134
input admittance, 133
output admittance, 134
voltage gain, 133
Cathode spot, 177
Characteristic curves (terminal characteristics), class-B and C amplifiers, 293–294
cold cathode gas diode, 170
composite, diode, resistance load, 8
load line, push–pull, 112
static characteristics, push–pull, beam tetrode, 163
triode, 112, 113, 162
constant current, triode, 11, 305
critical grid voltage, 213
dynamic, 11, 15–17, 30, 66
germanium diode, 425
hot cathode gas diode, 171
Characteristic curves (terminal characteristics), mutual, triode, 11
tetrode, 55
photocell, vacuum, 47
plate, triode, 11, 30, 350
beam tetrode, 62, 163
diode, 5, 169
pentode, 61, 65, 160
rectification, type-6H6 diode, 390
transistor, *n–p–n*, 451, 452
type A, 429, 448
type-FG-33 thyratron, 179
type-WL-631 thyratron, 179
type-WL-632 thyratron, 181
type-6C5 triode, 11
type-6F6 pentode, 61
type-6J7 pentode, 65
type-6L6 beam tetrode, 62
type-24-A tetrode, 55
type-81 diode, 5
Class-A, AB, B, or C amplifier, definitions, 77
Class-B amplifiers, r-f power, *see* Amplifier, r-f power.
Class-C amplifiers, r-f power, *see* Amplifier, r-f power.
Cold-cathode tube, 170
Colpitts oscillator, 334
Commutation in rectifier circuit, 228, 233
Composite (push–pull), dynamic characteristic, 105, 106, 107
equivalent circuit, 110
load line, 114–115
plate current, 106, 107, 109, 112–116
static characteristics, 111–115
tube circuit, 110
Conductance, mutual, *see* Transconductance.
Conduction angle (or period), rectifier, 197, 202, 211, 214, 228
Conductor, energy-level diagram for, 416
Constant-current characteristic curves, 11, 305
Control, of thyratrons, d-c, 181–185
phase shift, 217–221
Control characteristic, thyratron, 179, 181, 213
Control grid, 53
Conversion efficiency, class-A a-f power amplifier, 152, 157–158

Conversion efficiency, class-B r-f power amplifier, 295
class-C r-f power amplifier, 295
rectifier, 192, 193, 196, 198
Conversion transconductance, 399, 400
Conversion transducer, 399
Converter, frequency, 399
Coupling, coefficient, 256, 274, 277
critical, 259–261, 274
tube-to-load, 309–313
Coupling circuits, a-f amplifiers, 79
Critical anode voltage, 213
Critical coupling, 259–261, 274
coefficient, 256, 274, 277
double-tuned circuit, 259
Critical-distance tube, 61
Crosby, M. G., 407
Crystal, piezoelectric, 341
equivalent circuit, 341
oscillator control, 341–343
Current, feedback, 128
grid, *see* Grid current.
plate, *see* Plate current.
space-charge limitation of, 169
Current amplification factor, 438–440
Cutoff, definition, 12
grid voltage, 12, 293
remote, 72
sharp, 72

Day, J. R., 130
De Forest, Lee, 10
Demodulation, *see* Detection.
Detection, definition of, 359
of AM waves, 386
circuit requirements for linear, 392–395
linear diode detector, 386–392
measurement of detector characteristics, 389–390
of FM waves, 403
discriminator, stagger-tuned, 406–407
discriminator circuit, 404–406
discriminator circuit analysis, 407–411
problem of, 386
Detector, 359
Deviation ratio, *see* Frequency modulation.
Diode, circuit symbol, 3
gas, 168–173
anode current ratings for, 172–173
deionization time in, 173
effect of gas in, 168–169
filament heating time, 172
inverse peak voltage rating of, 173
voltage drop in, 170–172
volt-ampere curve for, 170–171
vacuum, as linear detector, 386–392
characteristics of, 5, 8
rectification characteristics of, 390
Direct-coupled a-f amplifiers, 80–84
Direct-coupled r-f amplifier, bandwidth, 266
reduction factor, in cascade, 281
voltage gain, 265, 267
relative, 266
Direct coupling, 79
Discriminator, *see also* Detection of FM waves.
circuit of, 404
definition of, 359
Distortion, 65
class-AB push–pull, 161–163
in amplifiers, 78
in power tetrodes and pentodes, 159–161
phase, 138–141
Donor, 417
Double-tuned amplifier (transformer-coupled), 272–278
bandwidth of, 276
reduction factor, in cascade, 281–282
circuit of, 272
computations, example, 277–278
coupling, critical, 274
equivalent a-c circuit of, 272–273
gain-frequency curve for, 272
voltage gain, 274
relative, 275–276
Double-tuned coupled circuits, 257–262
bandwidth for, 261–262
critical coupling, 259
double peaks, condition for, 259–261
frequencies at peaks, 260
voltage gain, 258–259
Dynamic characteristic, 11, 15–17, 30, 66
Dynatron oscillator, 322–323
negative resistance characteristic, 56

Efficiency, *see* Conversion efficiency.
Equivalent circuit (a-c), applications, 26–27
beam tetrode amplifier, 63
current source, 31–33
four-pole, 34–46
pentode amplifier, 64
tetrode amplifier, 59
transistor amplifier, 429, 431, 432
triode amplifier, 22–25
voltage source, 23–24
Electrode, 2
beam-confining, 63
Electron-coupled oscillator, 336
Electron-volt, 415, 416
Emission limitation of current, 169
Emitter of transistor, 426
Energy-level diagram, conductor, 416
insulator, 416
semiconductor, 416
Everitt, W. L., 97, 292, 296, 395

Feedback, degenerative, 116
direct, 116
inverse, effects of, 116
negative, 116
Nyquist's stability criterion, 127–128
oscillator analysis, 327–328
oscillator basic circuits, 332
oscillators, 324, 337
positive, 116
regenerative, 116
voltage amplifiers, 116–134
Feedback current, 128
Feedback fraction, 118
Feedback network, 118–119
Feedback voltage, 128
Feldkeller, R., 34
Fermi level, 415, 416
Filter circuit, rectifier, 199
capacitor input, 199–203, 210–212
inductor input, 205–210
Firing, of gas diode, 170–171
of thyratron, 178–181
Foot-candle, 47
Fourier analysis, 66
interphase reactor voltage, 242
rectified full-wave, 195
rectified half-wave, 191
Fourier analysis, rectifier output voltage, three-phase double-wye, 242
Four-terminal network theory, 34–36
admittances, 36–37
applications to vacuum tubes, 37–46
generalized equivalent circuit, 46
impedances, 35–36
oscillator application, 325–326
parameters, 35–36
Fredenhall, G. L., 141
Frequency, instantaneous, 358, 361
Frequency compensation, high frequency, 136–141
low frequency, 141–144
wide-band amplifiers, 136–144
Frequency converter, definitions, 399
pentagrid converter, 401, 402
Frequency deviation, fractional, 251–252
in FM, 361
see also Frequency modulation.
Frequency distortion, 78
reduction by inverse feedback, 121–122
Frequency modulation, 358, 361–362
bandwidth required, 373–376
center frequency stability, 380
design of reactance-tube circuit, 379–383
deviation ratio, 359, 371, 374, 375, 376
equation of FM wave, 371
frequency deviation, computation, 381–383
maximum, 371
frequency spectrum, analysis, 372–373
graphical, 374–377
frequency swing, 358, 371
instantaneous frequency, 371
methods of producing, 378–386
phasitron modulator, 384–386
power distribution in sidebands, 377
reactance-tube modulator, 378–384
sideband frequencies, 373–376
transmitter, block diagram, 380
Frequency stability of oscillators, 336
Frequency stabilization of oscillators, 336
see also Oscillators.
Frequency swing, *see* Frequency modulation.
Frequency trippler, 313
Full-wave rectifier, *see* Single-phase rectifier.

Gain, definitions of, insertion power gain, 433–434
operating power gain, 433–434
voltage, 24
of feedback amplifier, 117–118
Gain-band merit figure, tube, 279, 280
Gain-bandwidth product, direct-coupled r-f amplifier, 278–279
double-tuned transformer-coupled r-f amplifier, 280
R–C amplifier stage, 135
single-tuned transformer-coupled r-f amplifier, 279
Gain-frequency curves, for double-tuned transformer-coupled amplifier, 272
for *R–C* amplifier, 92
for shunt-compensated amplifier, 138
for transformer-coupled amplifier, 100
Gas-filled tube, 168
arc voltage drop, 171
classification of, 170–171
cold cathode, 170–171
current–voltage characteristics, 170–171
glow tube, 173, 174
hot cathode, 170–171
inverse peak voltage rating, 173
ratings for, 171–173
relaxation oscillator, 176
thyratron, 173, 174
tube conduction voltage drop, 170–172
voltage regulator, 175
Germanium, 420–423
n-type, 417, 422, 425
p-type, 418, 423
Grid, 2
control, 53
screen, 53
suppressor, 60
Grid control (gas-filled tubes), critical characteristic, 213
ignition angle, 213–215
of rectifiers, 212
trigger action in, 173, 213
Grid-controlled rectifier, bias control, 214, 216
bias-phase control, 214
load-current analysis, resistance load, 214–216
on–off control, 216–217
Grid-controlled rectifier, phase-shift control, 214, 217–221
Grid current, 19, 24, 39–41
Grid driving power, 309
Grid-glow tube, 173
Grid modulation, *see* Amplitude modulation.
Grounded-base transistor, 429
amplifier circuit, 426
equivalent a-c circuits, 429–433
four-pole parameters, 431
insertion power gain, 434
operating power gain, 434
tube analogy, 433
Grounded-collector transistor, 436
amplifier circuit, 437
four-pole parameters, 437
input and output impedances, 438
operating power gain, 438
tube analogy, 437
Grounded-emitter transistor, 434
amplifier circuit, 434–436
four-pole parameters, 434
input and output impedances, 435
operating power gain, 436
tube analogy, 435
Grounded-grid amplifier, 283–285
equivalent a-c circuit, class A, 284
input impedance of, 284
output impedance of, 285
tuned power application, 318–319
voltage gain, 284
Guillemin, E. A., 338, 372, 443

Half-power frequency, 90, 136
for parallel resonant circuit, 251
for series resonant circuit, 249
Hall effect, 419–420
Harmonic amplitudes, 68–70
Harmonic analysis, *p*-anode rectifier, 230–231
Harmonic distortion, reduction by inverse feedback, 120
tetrodes and pentodes, 71–72, 79
triodes, 67–70
Harmonic suppression, push–pull, 106–108
Harries, H. H. D., 61
Hartley oscillator, 333
Hartley, R. V. L., 357

Heising, R. A., 343
Herold, E. W., 400
Heterodyne converter, 399
Heterodyne oscillator, 397–399
Heterodyne principle, 397–399
Hewlett, W. R., 346
Holes in semiconductor, current due to motion of, 421–422
  nature of, 417
  production of, 421–422

Ignition angle, 213–214
Ignitron, 226
Impedance of an amplifier, effect of feedback, 128–130
  input, 43–44
  output, 128–130
Inductance filter, 205–207
  ripple factor, 207
Inductor-input filter, 207, 210
  ripple factor, 210
Information content, 357
Insertion power gain, definition, 433
  of transistor amplifier, 434, 439, 444, 445, 446
Instantaneous forward voltage, maximum, 174
Insulator, energy-level diagram for, 416
Interelectrode capacitance, 41
  effect of on input admittance, 43
  pentode equivalent circuit including, 64
  tetrode equivalent circuit including, 59
  triode equivalent circuit including, 45
Intermediate frequency or i-f, 400
Intermediate-frequency range, *see* Mid-frequency range.
Interphase reactor, 239
  current, 243
  voltage, 242
Interstage coupling circuits, 79
Inverse feedback, cathode-follower circuit, 132–134
  circuit arrangements, 130–132
  current, 128
  effect, on amplifier stability, 125–128
    on frequency and phase distortion, 121–122
    on harmonic distortion, 120
    on output impedance, 128–130
Inverse feedback, effect, on uniformity of operation, 125
    on voltage gain, 117–118
  effects of, 116
  example problem, 123–124
  gain equation, 118
  Nyquist's criterion for stability, 127–128
  plot of $A\beta$, for R–C amplifier, 127
    transformer-coupled amplifier, 127
  push–pull circuit, 131
  voltage, 128
  voltage amplifiers, 116–134
Inverter, parallel, 182, 186
  phase, 111
  series, 185
Ions in gas-filled tubes, 169
IRE standard symbols, 18–19

Jahncke, E. (and Emde, F.), 375
Jen, C. K., 332

Kircher, R. J., 431
Koehler, G., 102
Kozenowski, H. N., 303

L–C-coupled amplifier, 92
Leakage inductance in rectifier transformer, 233
Leakage reactance, effect of, in polyphase rectifier, 233–238
Limitation of current by space charge, 169
Limiter, amplitude, 358
Linear amplifier, class A, 22, 76–77
  class B, 297–303
Linear operation of triode amplifier, 22
Llewellyn, F. B., 337
Load impedance, reactive, 21, 28–30
Load line, 15–17
  composite push–pull, 114–115
  dynamic, 74, 153–154
  static, 74, 153–154
Load resistor, 15
Loftin, E. H. (and White, S. Y.), 81
Lumen, 47

Marti, O. K., 238
Mason, W. P., 343
Maximum instantaneous forward voltage, 174

Maximum power output (class-A amplifier), large signal, undistorted, 155–156
small fixed signal, 154
Mayer, H. F., 129
Meacham, L. A., 343
Meissner oscillator, 335
Mercury-arc rectifier, 177, 226
Mercury-pool tube, 177
ignitron, 226
Merit figure, tube, gain-bandwidth, 279–280
Metal, energy-level diagram for, 416
Mid-frequency range (intermediate-frequency range), 86–87, 90, 98, 100
Miller, J. M., 43
Miller bridge, 26
Miller effect, 43
Millman, Jacob, 238
Mixer, pentagrid, 401
tube, definition, 399
Modulated wave, mathematical formulation, 359–362
Modulation, 355
definition of, 357
nature of, 357, 359
reasons for, 356–357, 359
sidebands, 358
types of, 358–359
Modulator, 294, 357
Morrison, J. F., 383
Morton, J. A., 34, 39, 84, 278, 426
Motor control, d-c, by thyratrons, 221–222
Mouromtseff, I. E., 303
Moyer, E. E., 222
Multielectrode tubes, 72
pentagrid converter, 73
pentagrid mixer, 73
Multivibrator, 347–353
wave forms, 349–353
Mutual conductance, 12, 14
measurement of, 28

Negative feedback, *see* Inverse feedback.
Negative resistance, oscillator theory, 323
tetrode, 56
Neutralization, negative susceptance, 316
Neutralization, neutrodyne, 316–317
of electron space charge, 169
of r-f triode, 314–317
theory, 315
Nottingham, Wayne B., 157
Nyquist, H., 127
stability criterion, 127–128

Operating locus, elliptical, 21, 28–30
Operating power gain, definition, 433
matched, 456, 458, 462, 465
of transistor amplifier, 434, 436, 438, 456, 458
Oscillators, 321–353
amplitude limitation, 324
Barkhausen criterion, 327–328
bias-stabilized circuit, 344
bridge-stabilized circuit, 343
buffer amplifier use, 335
Colpitts, 334
conditions for oscillation, 324
crystal control, 341–343
crystal-controlled tuned-grid, tuned-plate, 342
crystal equivalent circuit, 341
design specifications, 324
dynatron, 322
electron coupling, 336
feedback, basic circuit types, 332
generalized equivalent circuit, 337
use of, 324
frequency stability, 336
frequency stabilization impedances, design of, 336–341
general principles, 321
general theory, simplified, 321–324
Hartley, 333
isolation of tuned circuit, 335
linear analysis, feedback approach, 327–328
four-pole approach, 325–326
Meissner, 335
multivibrator, 347–349
wave forms, free running, 349–353
negative resistance, 323
R–C tuned, 345–346
relaxation, 176
tuned-grid, 333
tuned-plate circuit, 328–331
tuned-plate–tuned-grid, 334

Oscillators, vector diagram of tuned-plate, 330–331
Overlap (polyphase rectifier), 233–238
  angle of, *p*-anode rectifier, 236
    three-phase double-wye, 245
  correction due to, 237–238

Parallel feed, 73
Pearson, G. L., 418
Pentagrid converter, 400, 402
Pentagrid mixer, 401
Pentode, circuit symbol, 3
  connections, 60
  equivalent circuit for amplifier, 64
  in broadband amplifiers, 135, 141
  interelectrode capacitances, 64
  in tuned amplifier, 264–278
  plate characteristics of, 61, 65
  static characteristics, 61, 65
Phase compensation, 138–141
Phase deviation, 358, 361
Phase distortion, 79
  compensation, video amplifier, 138–141
  reduction by inverse feedback, 121–122
Phase-inverter circuit, 111
Phase modulation, 358, 360–361
Phase-shift control of thyratron, 214
  circuits for, 217–222
  use of saturable reactors, 221
Phase-shift curves, shunt-compensated amplifier, 140
Phasitron, 384–386
Photocell, vacuum, 47
    control of relay, 48
Photosensitive devices, 46
  static characteristics, 47
Pietenpol, W. J., 449
Piezoelectric crystal in oscillators, 341–343
Plate (anode), conductance, 5
  resistance, 5, 14
Plate characteristics, *see* Characteristic curves.
Plate dissipation, in a-f amplifiers, 150–151
  in plate modulation, 369–370
  in r-f power amplifiers, 302, 308
Plate efficiency, *see* Conversion efficiency.
Plate modulation, *see* Amplitude modulation.
Polar diagram of feedback amplifier, *R–C*-coupled, 127
  transformer-coupled, 127
Polyphase rectifiers, 226
  commutating voltage, 228
  commutation of current, 228
  harmonic analysis, *p*-anode rectifier, 230–231
  ignitrons, 226
  interphase reactor, 239
  interphase reactor current, 243
  interphase reactor voltage, 242
  load-current wave forms, 231
  overlap, 233–238
    angle of, 236
    correction due to, 237–238
  p-anode rectifier analysis, 229
  ripple factor, 230–231
  secondary current, effective value, 231
  six-phase star, 232–233
  three-phase bridge circuit, 238
  three-phase double-wye circuit, 239–245
  three-phase half-wave circuit, 227
  transformer leakage reactance, effect of, 233–238
  utilization factor, 231–232, 245
Push–pull, advantages of operation in, 104–105
  composite dynamic characteristic, 105–107
  composite equivalent circuit, 110
  composite load line, 114–115
  composite plate current, 106–107, 109, 112–116
  composite static characteristics, 111–115
  input circuits, 110
  operation, 104–116
Push–pull amplifier operation, class A, 104–116
  class AB, 161–163
  class B, 115–116
  optimum class A_1, 164–165
  optimum class AB_1, 164–165

Q of circuit, effective, in tuned amplifier 271, 278, 279, 281

Q of circuit, fundamental definition, 253
loaded, in tuned power amplifiers, 310–313
parallel circuit, 251
series circuit, 250
transformer-coupled amplifier circuit, 271
Quiescent operating point, Q, 7, 9, 13, 17, 22, 23

Rating of gas tube, 171–173
R–C-coupled amplifier, 79, 84–92
plot of $A\beta$ for, 127
push–pull, with phase inverter, 111
R–C tuned feedback oscillator, 345–346
Reactance-tube modulator, 378–384
Receiver, for AM waves, 396
superheterodyne, 396
Rectifier, bleeder resistance, 207
definition, 188
full-wave, gas-filled, 197–198
vacuum, 193–196
grid-controlled, 212
half-wave, circuit, 189
vacuum, 189–193
ripple factor, 189, 191
ripple voltage, 189
tungar, 178
Regulator, voltage, 175
Relaxation oscillator, 175–179
Resonance curve, double-tuned coupled circuit, 255–256
fractional frequency deviation, 251–252
series R, L, C circuit, 250
universal, parallel R, L, C circuit, 252
Ripple factor, 189, 191
capacitor-input filter, 212
inductor-input filter, 210
Russell, J. B., 130
Ryder, R. M., 278, 427, 431

Screen grid, 53
Screen-grid tube, *see* Tetrode.
Secondary emission, 56
in r-f power amplifiers, 294
suppression of, 59–60
Seely, Samuel, 238
Self-bias, 25, 49, 50, 333, 334, 344
Semiconductor, boundary-layer effects in, 423–425
conductivity of, 419
energy-level diagram for, 416
extrinsic, 417
forbidden region, 416, 418, 419
germanium, 420–423
Hall effect in, 419–420
hole-electron pairs in, 421–422
intrinsic, 416
n-type, 417, 422
p-type, 418, 423
Series feed, 333
Shannon, C. E., 357
Sheath, positive ion, 173
Shede, O. H., 61
Shield-grid thyratron, 180
Shockley, W., 419, 448
Shunt feed (parallel feed), 73, 333, 334
Sideband frequencies, *see* Frequency modulation.
Sidebands, *see* Modulation.
Single-phase rectifier circuits, 188–225
bleeder resistance, 207
capacitance filter, 199–203
capacitor-input filter, 210–212
conduction angle, gas-filled tubes, 197, 198
d-c power output, 192, 196, 198
efficiency, full-wave circuit, 196, 198
half-wave circuit, 192
filters, 199
full-wave circuit, advantages, 195
full-wave vacuum-tube circuit, 193–196
half-wave vacuum-tube circuit, 189–193
harmonic current components, 191, 195
inductance filter, 205–207
inductor-input filter, 207–210
ripple factor, 191
voltage doubler circuit, 204
Single-tuned circuit, optimum adjustments, 253–254
Single-tuned transformer-coupled r-f amplifier, 267–271
bandwidth, 271
optimum resonance, conditions for, 269–270, 271

Single-tuned transformer-coupled r-f amplifier, Q, effective, 271
voltage gain, 268–269, 270–271
Space-charge limitation of current, 169
Space-charge neutralization, 169
Sparks, M., 448
Stability, of amplifier, effect of inverse feedback, 125–128
Nyquist's criterion, 127–128
of transistor amplifier, 432
of oscillator, 336–341
Staggered tuning of amplifiers, 282–283
bandwidth of, 283
relative gain, 282
response characteristics of, 283
Standard symbols, IRE, 17–19
definitions, 18–19
Static characteristics, 4
see also Characteristic curves.
beam-power tube or beam tetrode, 62
circuit for obtaining, diode, 4
triode, 14
composite, beam tetrode, 163
diode, 6–9
triode, 112, 162
diode, 5, 8
pentode, 61, 65
tetrode, 55
triode, 11
Strecker, F., 34
Superheterodyne receiver, 396
Suppressor grid, 59–60
Sweep circuit oscillator, *see* Relaxation oscillator.
Synchronous switch, 290

Tang, K. Y., 190
Tank circuit, 290, 291
Tank current, 292, 293
curves for, 293
measurement of, 292
Taylor series, 67, 297
Teal, G. K., 448
Terman, F. E., 100, 104, 121, 130, 144, 266, 346
Tetrode, 53
beam-power, 61-62
circuit symbol, 3
composite push–pull characteristics, 163
Tetrode, equivalent a-c circuit, 57–58
input admittance, 59
static characteristics, 55
Thomas, H. A., 333
Thomas, H. P., 384
Thompson, B. J., 108
Three-phase double-wye circuit, 239–245
Fourier analysis of wave forms, 242
interphase reactor, 239
interphase reactor current, 243
interphase reactor voltage, 242
overlap angle, 245
transition current, 244
voltage regulation, 244
wave forms, load voltage, 241, 243
secondary voltage, 239
Thyratron, 173, 174, 178
control characteristics, 179, 181, 213
d-c control, 181–185
d-c motor control, 221–222
electrode arrangement, 174
ignition angle, 213–215
inverter circuits, 182, 185, 186
phase-shift control, 217–221
shield grid, 180
Time delay on line, 139
of wide-band amplifier, 140–141
Torrey, H. C., 418
Transconductance, 12, 14
measurement of, 28
Transducer, definition of, 358
Transformer-coupled amplifier, 80
audio-frequency voltage, 93–104
plot of $A\beta$, 127
single-tuned r-f, 267–271
Transistor, current amplification factor, 438–440
junction, n–p–n, 448–450
nature of, 425
noise, 468
performance data comparison, 427
type-A point contact, 426
Transistor—n–p–n junction, 448–450
circuit parameters, 453
image impedances, 456
static characteristics, 450–452
Transistor—type A, cascade arrangements, 442–447
equivalent a-c circuit of, 429, 431, 432
frequency characteristics, 438–442

Transistor—type A, power stage, 447
static characteristics, 427–428
Transistor amplifier circuits—*n–p–n*,
biasing, grounded collector, 464
grounded emitter, 459–461
collector current control, 459–460
frequency limitations, 465–468
generalized circuit relations, 454–456
grounded base, 456–458
grounded collector, 463–465
grounded emitter, 458–463
Transistor amplifier circuits—type A, cascade arrangements, 442–447
condition for stability of, 432
general four-pole, 429
grounded base, 429–434
grounded collector, 436–438
grounded emitter, 434–436
power stage, 447
T network, 431, 432
Transmitter, FM, block diagram, 380
Triggering of thyratron, 173, 178, 213–214
Triode, amplification factor, 11–12
circuit symbol, 3
coefficients (or parameters), 10–11, 14
composite push–pull characteristics, 112, 162
constant-current characteristics, 10–11, 305
equivalent a-c circuit, 22–23
load resistance, optimum, 154–156
maximum undistorted power output, 155–156
mutual characteristics, 10–11
plate characteristics, 10–11
plate current, linear approximation for, 298
plate resistance, 11, 14
theoretical plate efficiency, 157–158
transconductance, 11–12, 14
Trippler, frequency, *see* Frequency trippler.
Tube, definitions, 2
vacuum, circuit symbols, 3
Tuned coupled circuits, 253–262
analysis of, 257–259
band-pass characteristic, 256
bandwidth, double-tuned circuit, 261–262
Tuned coupled circuits, double-tuned, 254–256
optimum adjustment, double-tuned, 255
primary, 254
secondary, 253
resonance curves, double-tuned circuit, 256
single-tuned, 253–254
voltage gain, double-tuned circuit, 258–259
Tuned direct-coupled amplifier, bandwidth, 266
voltage gain, 265, 267
relative, 266
Tuned-grid oscillator, 333
Tuned-plate oscillator, 328–331
Tuned-plate, tuned-grid oscillator, 334
crystal-controlled, 342
Tuned r-f power amplifiers, 290–320
analysis of, class B, 297–303
discussion, 296
applications of, 292
circuit for, 291
conversion efficiency of, 295, 301
example solution for, 305–309
external characteristics of, 292–295
graphical analysis of, 303–309
grounded-grid circuit of, 318–319
linear properties of, 292–295
load coupling, analysis of, 309–313
neutralization, triodes, 314–317
phase relations, class B, 299
class C, 291
power supplies and bias for, 317–318
secondary emission effects, 294, 301
variables used in analysis of, 292
Tuned r-f voltage amplifiers, class A, r-f, 263
direct-coupled circuit, analysis, 265–266
impedance characteristic, 263
in cascade, 280–282
requirements for tuned class A, 263
single-tuned direct-coupled, 264–267
single-tuned transformer-coupled r-f, 267–271
typical circuits, 264
Tungar rectifier, 178

Utilization factor, 231–232, 245
six-phase star, 245
three-phase double-wye, 245

Valence electrons, 415–416
Van Dyke, K. S., 342
Variable-mu tubes, 72
Video amplifier, 134–144
frequency compensation, high, 136–141
low, 141–144
phase distortion compensation, 138–141
time delay, 138–141
Voltage amplification factor, 11–12, 14, 27
Voltage doubler, 204
Voltage feedback, 128
Voltage gain, backward, 38
definition, 24
double-tuned amplifier, 274–276
doubled-tuned coupled circuit, 258–259
feedback amplifier, 117–118
forward, 38
grounded-grid amplifier, 284
Voltage gain, transformer-coupled r-f amplifier, 268–269, 270–271
triode amplifier, 43
Voltage regulator tube, 175
Volt-ampere characteristic, *see* Characteristic curves.

Wallace, R. L., Jr., 449
Wave, 139
carrier, 357
definition of, 355–356
equation of, 356
frequency, 139
modulated, mathematical formulation of, 359–362
modulating or modulated, 357, 360, 363, 364
phase of sine, 358, 359
shape, transmitted, 139
velocity of on line, 139
Wheeler, H. A., 278
White, S. Y., 81
Whitmer, C. A., 418
Wilson, A. H., 417
Winograd, Harold, 238
Woods, F. S., 372